

The concentrations, behaviour and fate of polycyclic aromatic hydrocarbons (PAHs) and their oxygenated and nitrated derivatives in the urban atmosphere

by

Ian James Keyte

A thesis submitted to the University of Birmingham for the degree of
Doctor of Philosophy

Division of Environmental Health and Risk Management, School of
Geography, Earth and Environmental Sciences, University of
Birmingham, Edgbaston, B15 2TT, United Kingdom

December 2014

UNIVERSITY OF
BIRMINGHAM

University of Birmingham Research Archive

e-theses repository

This unpublished thesis/dissertation is copyright of the author and/or third parties. The intellectual property rights of the author or third parties in respect of this work are as defined by The Copyright Designs and Patents Act 1988 or as modified by any successor legislation.

Any use made of information contained in this thesis/dissertation must be in accordance with that legislation and must be properly acknowledged. Further distribution or reproduction in any format is prohibited without the permission of the copyright holder.

Abstract

Polycyclic aromatic hydrocarbons (PAHs) play an important role in urban air quality due to the toxic and carcinogenic hazard they present. A class of pollutants receiving increasing interest from researchers are oxygenated (OPAH) and nitrated (NPAH) derivative compounds. There is a need for an improved understanding of the sources, concentrations, behaviour and fate of these pollutants as they can pose a similar public health risk as PAHs and can enter the environment both from primary combustion emissions and secondary formation from atmospheric reactions. This study investigates the airborne concentrations of PAH, OPAH and NPAH compounds in U.K. atmosphere at heavily trafficked and urban background sites. Sampling campaigns were conducted to assess the spatial and temporal trends, primary and/or secondary sources, gas-particle phase partitioning and atmospheric degradation of PAHs, NPAHs and OPAHs. Differences in atmospheric concentrations between trafficked sites and the urban background site indicate a variable influence of road traffic emissions between different PAH, OPAH and NPAH compounds. Seasonal, diurnal and temporal patterns as well as positive matrix factorisation (PMF) source apportionment provide evidence of the key influencing factors governing the concentrations of PAHs, OPAHs and NPAHs in the urban atmosphere, in addition to the strength of road traffic emissions. For example, specific non-traffic sources are identified at these sites including combustion sources such as domestic and non-domestic wood combustion, and non-combustion sources such as temperature-driven volatilisation from surfaces. Evidence for the occurrence of PAH reactivity and atmospheric formation of NPAH and OPAH compounds between traffic and background sites is also observed, with the relative rates of atmospheric degradation shown to play a key role influencing the observed concentrations at these sites. It is also indicated that emissions of NPAHs from road traffic relative to PAHs have increased substantially in the last 20 years, consistent with the increased proportion of diesel passenger vehicles in the U.K. traffic fleet.

Acknowledgements

I would like firstly to say a huge thank you Professor Harrison. It was always going to take careful, considered and wise supervision to guide someone as dense as me though a PhD. Thanks for being up to the challenge. I would also be remiss if I didn't say thanks to Mary for putting up with all my stupid questions and sorting out things like infuriating international order requests and many many other things.

In particular I need to thank Chris, whose guidance, support and infinite patience in the lab has made this project possible. I literally could not have done it without him. I would also like to thank Salim for being a friendly and reassuring presence in the frustrating and often miserable toil of lab work and for being a good companion on our adventures in Munster and Oregon.

I am grateful to Gillian and Eimear for their help in the lab and especially to Richard and Jamie, who have been amazingly helpful and kind and helped me avoid more than a few potential disasters. I also need to thank Duick Young for his help with accessing Elms Cottage weather data and the good folks at Amey for helping with the tunnel sampling,

To my great friends/co-conspirators for the last 4 years - Pallavi, Max, Barbara, Karima, Paul and Anna - you are all truly insane and wonderful - in that order (especially you, Pallavi). There is no way I could have made it through this without laughing so much with and/or at you (you again, Pallavi). Lunchtime will never be as much fun without you. I also say thanks to all the members of the 4th Floor Crew over the years, who it has been a pleasure to know.

Je dis un grand merci à Perrine for being so supportive and patient with me while I have been working on this and for her important guidance on important complex technical issues like how to use a computer.

But above all I want to thank my dad, who has always supported me and never given up on me even during all the times I have given up on myself and even though I sometimes give him every reason to. I am truly grateful. Cheers dad.

“Life is a ball of beauty that makes you want to just cry.....then you die”. – Kurt Vile.

Contents

	Page No.
1. Introduction	
1.1. Polycyclic aromatic hydrocarbons (PAHs), urban air quality and public health	1
1.1.1. Urban air quality and public health	1
1.1.2. The chemical and physical properties of PAHs, OPAHs and NPAHs	2
1.1.3. Policy issues	3
1.2. Sources of PAHs, OPAHs and NPAHs	8
1.2.1. Sources of PAHs	8
1.2.2. Sources of OPAHs and NPAHs	12
1.2.3. Emissions from road traffic	13
1.3. Health effects of PAHs, OPAHs and NPAHs	15
1.3.1. Exposure to PAHs	15
1.3.2. The metabolism and toxicity mechanism of PAHs, NPAHs and OPAHs	16
1.3.3. Health effects of PAHs	17
1.3.4. The role of PAHs in the health effects of urban air	20
1.3.5. The role of atmospheric PAH reactions on toxic effects	23
1.4. Occurrence and behaviour of PAHs in the atmosphere	26
1.4.1. Occurrence in the environment	26
1.4.1.1. <i>PAHs in the environment</i>	26
1.4.1.2. <i>OPAHs and NPAHs in the atmosphere</i>	27
1.4.2. Gas-particle partitioning of PAH, OPAH and NPAH compounds	29
1.4.2.1. Phase partitioning of <i>PAHs</i>	29
1.4.2.2. Phase partitioning of <i>OPAHs and NPAHs</i>	31
1.4.3. Atmospheric transport of PAHs	32
1.4.4. Long-term concentration trends	33
1.4.5. Short term concentration variations	34
1.4.5.1. <i>Seasonal patterns</i>	34
1.4.5.2. <i>Diurnal patterns</i>	35
1.4.6. Ambient sampling of PAH in the U.K. atmosphere	36
1.4.6.1. <i>PAH monitoring in the U.K.</i>	36

1.4.6.2.	<i>PAHs from road traffic</i>	37
1.5.	Fate of PAHs, OPAHs and NPAHs in the atmosphere	37
1.5.1	Wet and dry deposition of PAHs	38
1.5.2.	Photolysis	39
1.5.2.1.	<i>Photolysis of PAHs</i>	39
1.5.2.2.	<i>Photolysis of OPAH and NPAH</i>	41
1.5.3	Atmospheric reactivity of PAHs	42
1.5.3.1.	<i>Gas-phase PAH reactions</i>	43
1.5.3.2.	<i>Heterogeneous reactions</i>	51
1.5.3.3.	<i>Evidence for PAH reactions in ambient air samples</i>	55
1.5.4.	Reactions of OPAH and NPAH	57
1.6.	Project aims and objectives	58
2.	Methodology	61
2.1	Sampling Procedure	61
2.1.1.	Background	61
2.1.1.1.	<i>Overview</i>	61
2.1.1.2.	<i>Particle-phase sampling</i>	62
2.1.1.3.	<i>Gas-phase sampling</i>	62
2.1.2.	Sampling sites	64
2.1.3.	Sampling campaigns	67
2.1.3.1.	<i>Campaign 1 : seasonal 24 hour sampling</i>	67
2.1.3.2.	<i>Campaign 2 : diurnal sampling study</i>	70
2.1.3.3.	<i>Campaign 3: Queensway Road Tunnel sampling study</i>	71
2.1.4.	Meteorological data	72
2.1.5.	Inorganic gaseous pollutants	72
2.1.6.	Quality control : the potential impact of sampling artefacts	73
2.1.6.1.	<i>Gas-phase vs. particle-phase artefacts</i>	73
2.1.6.2.	<i>Chemical reactivity during sampling</i>	73
2.1.6.3.	<i>Artefact sampling experiment</i>	75
2.2.	Sample extraction and clean-up	76

2.2.1. Materials and chemicals	76
2.2.2. Sample preparation	76
2.2.3. Sample extraction	76
2.2.3.1. <i>Extraction background</i>	76
2.2.3.2. <i>Extraction method</i>	78
2.2.4. Clean-up	78
2.2.4.1. <i>Clean-up background</i>	78
2.2.4.2. <i>Clean-up method</i>	79
2.3. Sample analysis	81
2.3.1. Background and analytical development	81
2.3.2. Analysis method for PAHs : GC-MS in EI mode	82
2.3.3. Analysis for OPAH and NPAHs : GC-MS in NICI mode	83
2.4. Sample Quantification	86
2.4.1. Sample concentrations	86
2.4.2. Validating analytical method	92
2.4.2.1. <i>Recoveries</i>	92
2.4.2.2. <i>Standard reference material analysis (SRM)</i>	92
2.4.2.3. <i>Sample blanks</i>	93
2.4.2.4. <i>Detection Limits</i>	93
3. Concentrations, behaviour and fate of PAHs, OPAHs and NPAHs in the ambient urban atmosphere	99
3.1. Measured concentrations of PAH, OPAH and NPAH	99
3.1.1 PAH and OPAH concentrations	99
3.1.2. NPAH concentrations	110
3.1.3. BROS/EROS ratio comparisons	111
3.1.4. Traffic increment	115
3.1.5. Annual BaP concentrations and the UK Air Quality Objective	118
3.2. Influencing factors governing observed concentrations	118
3.2.1. Inter-correlations of PAH, OPAH and NPAH concentrations	119
3.2.2. Correlations with inorganic air pollutants and meteorological parameters	123

3.2.2.1. Correlations of PAH, OPAH and NPAH with TSP	123
3.2.2.2. Correlations of PAH, OPAH and NPAH with NO _x	126
3.2.2.3. Correlations of PAH, OPAH and NPAH with O ₃	127
3.2.2.4. Temperature-dependence of PAH, OPAH and NPAH concentrations	127
3.2.2.5. Rainfall, Wind speed and wind direction	129
3.3. Seasonal variation in PAH, OPAH and NPAH levels	130
3.3.1. PAH seasonality	130
3.3.2. OPAH and NPAH seasonality	134
3.3.3. Factors influencing seasonal trends	137
3.3.3.1. Seasonal variation in source strength	137
3.3.3.2. Seasonality of atmospheric boundary layer height	138
3.3.3.3. Influence of volatilisation from surfaces	139
3.3.4. Seasonal trend in PAH reactivity	141
3.3.5. BROS/EROS ratio seasonality	142
3.4. Temporal trend of PAHs at BROS and EROS	145
3.4.1. Overview	145
3.4.2. Temporal trend in PAH and OPAH concentrations	148
3.4.3. Temporal trend in NPAH concentrations	153
4. Gas-particle partitioning, chemical reactivity and source apportionment of PAHs, OPAHs and NPAHs, and the influence of sampling artefacts	155
4.1. Gas-particle partitioning of PAHs, OPAHs and NPAHs	155
4.1.1. Phase partitioning overview	155
4.1.1.1. Phase partitioning of PAHs	155
4.1.1.2. Phase partitioning of OPAH and NPAH	156
4.1.2. Physicochemical properties influencing partitioning	157
4.1.3. Seasonality in partitioning behaviour	171
4.1.4. Phase partitioning equilibrium behaviour	173

4.2. Assessing the importance of PAH reactivity in the urban atmosphere	178
4.2.1. PAH degradation rates	178
4.2.2. 2NFlt / 1NPyr ratios	179
4.2.3. 2NFlt / 2NPyr ratios	181
4.2.4. Product to reactant ratios	184
4.3. Source apportionment of PAH, OPAH, NPAH compounds using Positive Matrix Factorization (PMF)	188
4.3.1 Introduction	188
4.3.2. Method	191
4.3.3. Results	193
4.3.1. Overview	193
4.3.3.2. Model uncertainty and rotational freedom	193
4.3.3.3. Source contributions	196
4.4. Sampling artefact study	201
4.4.1. Method	201
4.4.1.1. Sampling	201
4.4.1.2. Analysis	202
4.4.1.3. PAH recovery	203
4.4.1.4. OPAH and NPAH formation	203
4.4.2. Results	203
4.4.2.1. Observed PAH losses	203
4.4.2.2. Conversion of PAH to OPAH or NPAH during sampling	210
4.4.3. Summary	215
5. Diurnal profiles of PAH, OPAH and NPAH	216
5.1. BROS and EROS diurnal profiles	216
5.2. NO _x -corrected diurnal profiles	225
5.3. Assessing role of PAH degradation and reactive input of NPAH and OPAH	229
5.3.1. PAH degradation	229
5.3.2. 2NFlt/1NPyr and 2NFlt/2NPyr Ratios	230

5.3.3. Reactant/Parent Ratios	232
6. Concentrations of PAHs, OPAHs and NPAHs in the Queensway Road Tunnel	235
6.1. Tunnel concentrations of PAHs, OPAHs and NPAHs	235
6.1.1. PAH and OPAH concentrations	235
6.1.2. NPAH concentrations	238
6.1.3. Comparison with other Tunnel studies	242
6.1.4. Gas-particle phase partitioning	246
6.2. Temporal trend in PAH and NPAH concentrations	250
6.2.1. Temporal trend of PAHs	250
6.2.2. The driving force behind emission changes	254
6.2.3. Temporal trend of NPAHs	255
6.3. Comparison of tunnel vs. ambient concentrations	258
6.3.1. Overview	258
6.3.2. Tunnel/EROS ratios of PAHs	259
6.3.3. Tunnel/EROS ratios of OPAHs	262
6.3.4. Tunnel/EROS ratios of NPAHs	263
7. Conclusion	267
7.1. Investigation summary	267
7.2. Recommendations for future work	270
References	272
Appendix 1 : Reaction kinetics data for gas phase and heterogeneous PAH reactions	305
Appendix 2 : Sampler calibration and total air flow calculation	320
Appendix 3 : PAH, OPAH and NPAH gas chromatograph peaks	323

List of Figures

Figure 1.1. Estimated emissions of total PAH from key anthropogenic combustion sources, as provided from the NAEI.

Figure 1.2. Relative contributions of different anthropogenic combustion sources to total U.K. PAH emissions, as estimated by the NAEI.

Figure 1.3. Metabolic diol epoxide formation from PAHs via cytochrome P450 enzymes (CYP450) and epoxide hydrolase (EH) enzymes.

Figure 1.4. Metabolic formation of o-quinones from PAHs via dihydrol dehydrogenase (DD) enzymes.

Figure 1.5. Metabolic cation radical formation from PAHs via cytochrome P450 enzymes (CYP450) and peroxidase enzymes.

Figure 1.6. Mechanism for the formation of reactive oxygen species from OPAH quinones (Bolton *et al.*, 2000).

Figure 1.7. Mechanism for the formation of toxic intermediate species from NPAH compounds (Fiedler and Mücke, 1991).

Figure 1.8. The distribution of total PAH burden in the U.K between different environmental compartments (tonnes) as estimated by Wild and Jones (1995).

Figure 1.9. Predicted contribution of different loss mechanisms for PAH compounds in the U.K. based on modelled flux rates.

Figure 1.10. Mechanism for the reaction of gas-phase PAHs with OH radicals ; a) H-atom abstraction; b) OH addition to substituent groups; c) OH addition to the aromatic ring.

Figure 1.11. Potential pathways for the reaction of PAHs with NO_3 .

Figure 1.12. Proposed mechanisms for two possible further reaction pathways of the PAH-OH adduct: a) reaction with NO_2 ; b) reaction with O_2 .

Figure 1.13. Proposed mechanisms for two possible further reaction pathways of the PAH- NO_3 adduct: a) reaction with NO_2 ; b) reaction with O_2 .

Figure 1.14. Suggested mechanisms for the heterogeneous reaction of anthracene with O₃.

Figure 1.15. Suggested mechanisms for the heterogeneous reaction of pyrene with NO₂.

Figure 2.1. Locations of Birmingham sampling and monitoring sites used in the present investigation.

Figure 2.2. Appearance and schematic of high volume samplers used in the present investigation.

Figure 2.3. Comparison between peak separation of MW 247 NPAH compounds using an Agilent DB5-MS column and the Restek® column.

Figure 2.4. Calibration curves for the quantification of all PAH, OPAH and NPAH compounds measured in the present investigation.

Figure 3.1. Box plots of PAH, OPAH and NPAH concentrations measured at BROS and EROS in Campaign 1.

Figure 3.2. Mean concentrations of PAH (P + V) compounds measured at EROS and BROS during Campaign 1.

Figure 3.3. Mean concentrations of OPAH (P + V) compounds measured at EROS and BROS during Campaign 1.

Figure 3.4. Mean concentrations of NPAH (P + V) compounds measured at EROS and BROS during Campaign 1.

Figure 3.5. Correlation of measured PAH, OPAH and NPAH compounds in the Queensway Road Tunnel (Campaign 3) with the BROS-EROS concentration traffic increment (Campaign 1) ; plots are shown including Phe (a) and excluding Phe (b).

Figure 3.6. Mean PAH concentrations (P+V) measured in winter and summer samples only.

Figure 3.7. Mean OPAH concentrations (P+V) measured in winter and summer samples only.

Figure 3.8. Mean NPAH concentrations (P+V) measured in winter and summer samples only.

Figure 3.9. The percentage change of PAH concentrations between mean annual values reported by Harrad and Laurie (2005) and the present study.

Figure 3.10. NAEI estimates of PAH emissions from urban road traffic (tonnes).

Figure 4.1. Mean percentage of PAH, OPAH and NPAH compounds in the particulate (black) and gas (grey) phases at BROS (A) and EROS (B). Compounds are presented with increasing molecular weight from left to right.

Figure 4.2. Plots of %P vs MW for PAH, OPAH and NPAH.

Figure 4.3. Plots of %P vs VP for PAH, OPAH and NPAH.

Figure 4.4. Plots of %P vs log Kow for PAH and NPAH.

Figure 4.5. Plots of %P vs H for PAH and NPAH.

Figure 4.6. Plots of $\log K_p$ vs $\log P_L^\circ$ for PAHs (a), NPAHs (b) and OPAHs (c) in Campaign 1 sample W2 (10/2/12).

Figure 4.7. Relationship between the observed annual mean BROS/EROS concentration ratio for LMW PAHs and the corresponding OH reaction rate coefficient as derived by Reisen and Arey (2002) ; Brubaker and Hites (1998) ; Atkinson et al. (1990).

Figure 4.8. Ratios of measured OPAH or NPAH compounds to the parent PAH at BROS (black dot) and EROS (white dot) in each individual sample in Campaign 1.

Figure 4.9. Results of the 4 factor PMF model displaying the concentration of each species attributed to each factor (blue bar) and the percentage contribution of each factor to the total modelled concentration of each species (red marker).

Figure 4.10. Results of the PMF bootstrapping analysis for each factor.

Figure 4.11. Contributions of each individual factor to the modelled concentrations of each species, as predicted by the PMF model.

Figure 5.1. Diurnal profiles of total PAH concentrations at BROS and EROS, O_3 and NO_x , derived from mean values taken during morning (0700 – 1100), daytime (1100 – 1600), afternoon (1600 – 1900) and night (1900 – 0700).

Figure 5.2. Diurnal profiles of PAHs, OPAHs and NPAHs at BROS and EROS.

Figure 5.3. NO_x -corrected concentration profiles for key PAH, OPAH and NPAH compounds.

Figure 5.4. The diurnal profile of NPAH isomer ratios a) 2NFlt / 1NPyr and b) 2NFlt / 2NPyr measured at BROS and EROS.

Figure 5.5. Mean ratios of 'reaction product' OPAH and (NPAH x10) to 'parent' PAH in diurnal samples at BROS (a) and EROS (b).

Figure 6.1. Mean PAH concentrations measured inside the Queensway Road Tunnel.

Figure 6.2. Concentrations of OPAH compounds measured inside the Queensway Road Tunnel in Campaign 3.

Figure 6.3. Concentrations of NPAH compounds measured inside the Queensway Road Tunnel in Campaign 3.

Figure 6.4. Comparison of measured PAH concentrations inside the Queensway Tunnel in the present study with tunnel emission factors derived by Wingfors et al. (2001).

Figure 6.5. Plots of % of component in the particulate phase vs. molecular weight for a) PAHs, b) OPAHs and c) NPAHs, measured in the tunnel (black dots, solid black line) and at EROS (white dots, dotted line).

Figure 6.6. Contribution of individual PAHs to total PAH burden measured inside the Queensway Road Tunnel in a) 1992 (Smith and Harrison, 1996) and b) 2012 (present study).

Figure 6.7. Total number of gasoline and diesel fuelled passenger cars licensed in Great Britain

Figure 6.8. Mean ratios of concentrations measured in the Queensway Road Tunnel to those measured simultaneously at EROS for samples taken in Campaign 3.

List of Tables

Table 1.1. Names, formulas and structures of the PAH, OPAH and NPAH compounds investigated in this study.

Table 1.2. Mutagenic and/or carcinogenic categorisation of PAH, OPAH and NPAH compounds studies in the present investigation.

Table 1.3. Half lives (hours) of PAH compounds absorbed on various substrates; carbon black (CB), fly ash (FA), silica gel (SG) and alumina (AL), as reported by Behymer and Hites (1988).

Table 2.1. Dates, approximate times and average meteorological parameters, temperature (T), relative humidity (RH), pressure (PRES), solar radiation (SRAD), rainfall (RF), wind speed (WS), wind direction (WD) for all samples taken during this investigation.

Table 2.2. Internal standards, molecular ions and approximate retention times used to identify and quantify target PAH, OPAH and NPAH compounds in sample extracts.

Table 2.3. Calculated recoveries for all internal standards used in the analysis of samples from Campaigns 1, 2 and 3.

Table 2.4. Measured mean and standard deviation for concentrations of PAH, OPAH and NPAH compounds in NIST Standard Reference Material 1649b (urban dust).

Table 2.5. Sample blank concentrations (filters) and comparison with mean annual levels measured at EROS and BROS.

Table 2.5. Sample blank concentrations (PUF) and comparison with mean annual levels measured at EROS and BROS.

Table 2.7. Instrument detection limits (IDLs) and method detection limits (MDLs).

Table 3.1. The mean and (range) of particle-phase (P), vapour-phase (V) and total (T) PAH, OPAH and NPAH concentrations measured during Campaign 1.

Table 3.2. Comparison of total (particulate+gas) OPAH and NPAH concentrations (pg.m³) measured at different locations.

Table 3.3. Annual mean BROS/EROS concentration ratios for all PAH, OPAH and NPAH compounds.

Table 3.4 Inter-correlations of PAH, OPAH and NPAH species at BROS and EROS.

Table 3.5. Correlations of PAH, OPAH and NPAH concentrations with meteorological parameters and concentrations of inorganic air pollutants at BROS and EROS.

Table 3.6. Mean BROS/EROS concentration ratios measured in each sampling season in Campaign 1.

Table 3.7. Mean total (particulate + vapour) NPAH concentrations ($\mu\text{g m}^{-3}$) measured by Dimashki et al. (2000) at Birmingham city centre in Nov 1995-Feb 1996 and in the present study during winter at BROS in 2011-2012.

Table 4.1. Physiochemical properties of the PAH, OPAH and NPAH compounds in the present study.

Table 4.2. Slope (m), intercept (b) and correlation coefficient (R^2) values for the $\log K_p$ vs $\log P_L^o$ plots produced for PAH, OPAH and NPAH sampling data.

Table 4.3. Summary of 2-NFlt/1-NPyr ratios from ambient measurements.

Table 4.4. Summary of 2-NFlt/2-NPyr ratios from ambient measurements.

Table 4.5. Deuterated PAH, OPAH, and NPAH compounds measured in the artefact study

Table 4.6. Mean filter recoveries of PAH compounds measured on sample test filters

Table 4.7. Mean total recoveries of PAHs measured on sample test filters + PUFs

Table 4.8. Mean values for meteorological measurements, temperature (TDRY), relative humidity (RELH), Pressure (PRES) and solar radiation (SRAD) and total rainfall (RTOT) for the sampling campaigns during autumn (A); winter (W); spring (Sp), summer (Su) and the artefact study (ART).

Table 4.9. Mean concentrations of inorganic pollutants ($\mu\text{g/m}^3$) measured during autumn (A); winter (W); spring (Sp), summer (Su) samples in campaign 1 and artefact (ART) study.

Table 6.1. Mean \pm standard deviation of PAH, OPAH and NPAH concentrations measured in the Queensway Road Tunnel and EROS during Campaign 3.

Table 6.2. Comparison of total (P+V) PAH concentrations and percentage of concentration in the particulate phase (%P) in different road tunnel measurements.

Table 6.3. Comparison of total (particulate + vapour) PAH concentrations measured in the Queensway Road Tunnel in 1992 (Smith and Harrison, 1996) and 2012 (present study).

Table 6.4. Comparison of total (particulate + vapour) NPAH concentrations measured in the Queensway Tunnel in 1996 (Dimashki et al., 2000) and 2012 (present study).

List of Abbreviations

BROS – Bristol Road Observatory Site
DCM – dichloromethane
Defra – Department for Environment, Forestry and Rural Affairs
DfT – Department for Transport
EI – electron impact
EROS – Elms Road Observatory Site
FNF – 1-fluoro-7-nitrofluorene
GC-MS – gas chromatography mass spectrometry
HMW – high molecular weight
IDL – instrument detection limit
IS – internal standard
LMW – low molecular weight
MDL – method detection limit
MW – molecular weight
NAEI – National Atmospheric Emissions Inventory
NICI – negative ion chemical ionisation
NIST – National Institute of Standards and Technology
OPAH – oxygenated polycyclic hydrocarbon
NPAH – nitrated polycyclic aromatic hydrocarbon
P – particulate
PAH – polycyclic aromatic hydrocarbon
PFTBA – perfluoro-tri-n-butylamine
PT – p-terphenyl
PUF – polyurethane foam
RF – rainfall
RH – relative humidity
T – temperature
V – vapour
WD – wind direction
WS – wind speed

Chapter 1 : Introduction

1.1. Polycyclic aromatic hydrocarbons (PAHs), urban air quality and public health

1.1.1. Urban air quality and public health

Air pollution is a major threat to public health and failure to adequately tackle this problem could have significant socio-economic consequences (POST, 2014). Poor ambient air quality is projected to be the leading environmental cause of mortality by 2050 (OECD, 2012). In the UK, the potential economic impact of poor air quality is considered to be comparable to that resulting from smoking or obesity, potentially reducing life expectancy on average by 6 months, and costing around £16.4 billion per year (Defra, 2010). This highlights the importance of monitoring major air pollutants in the U.K. atmosphere, in order to improve our understanding of the risks they present and how to reduce these risks.

A specific class of pollutant of considerable interest due to its potential adverse health effects is particulate matter (PM) (Anderson *et al.*, 2012). Indeed, both short-term and long-term exposure to ambient levels of PM is associated with respiratory and cardiovascular illness and mortality (AQEG, 2005). It is estimated that exposure to PM caused up to 51 000 deaths in the U.K. in 2008 (COMEAP, 2010). It is suggested that the harmful effects of PM are predominantly associated with combustion-derived components (AQEG, 2005).

Indeed, Harrison *et al.* (2004) indicated the presence of specific trace metal and organic pollutants such as polycyclic aromatic hydrocarbons (PAHs) may be primarily responsible for lung cancers associated with PM_{2.5}. PAHs are therefore an important class of organic pollutants that require careful monitoring and investigation to understand their concentrations, behaviour and fate in the environment.

Due to the widespread presence of PAHs in the environment, and their potential contribution to poor ambient air quality and public health, these compounds have been the subject to a

considerable amount of research by both toxicologists and atmospheric scientists for over a century. This project focuses on the atmospheric concentrations, behaviour and fate of PAHs as well as their oxygenated (OPAH) and nitrated (NPAH) derivative compounds in the urban atmosphere.

1.1.2. The chemical and physical properties of PAHs, OPAHs and NPAHs

PAHs comprise a large group of persistent organic compounds containing two or more fused aromatic (benzene) rings. These compounds display a wide range of molecular weights (MWs) from 2-ring structures (e.g. naphthalene) to 6+ ring structures (e.g. coronene). Over 100 individual PAH compounds have been identified in urban air (Seinfeld and Pandis, 1998), however research commonly focuses on 16 priority PAHs defined by the USEPA based on their known health risks and environmental occurrence. PAHs are now considered to have a ubiquitous presence in the ambient atmosphere. The names, abbreviated terms (as used throughout this thesis) and structures of the compounds studied in this investigation are presented in Table 1.1.

PAHs are typically generated as by-products from the incomplete combustion and pyrolysis of fossil fuels and wood as well as the release of petroleum products. The physical and chemical properties of PAHs vary considerably between different compounds but are generally characterized by their relatively low water solubility and high lipophilicity (Choi *et al.*, 2010). In general, their volatility, water solubility and biodegradability decrease with increasing molecular weight. Due to their 'semi-volatile' nature, PAHs can be present in the environment in both the gas-phase and associated with particulate matter (EPAQS, 1999).

A range of compounds receiving increasing interest in atmospheric science are PAH derivative compounds such as oxygenated (OPAH) and nitrated (NPAH) polycyclic aromatic hydrocarbons. OPAHs consist of PAH compounds with one or more hydroxyl or carboxylic oxygen groups attached to the aromatic ring e.g. ketone or quinone compounds. NPAH can be defined as a class of aromatic compounds with one or more nitro- (NO_2) functional groups attached to the aromatic

ring. OPAHs and NPAHs are typically characterized by higher molecular weight and lower vapour pressure than their parent PAH, which indicates a stronger tendency to sorb to particulate matter (Walgraeve *et al.*, 2010).

Understanding the atmospheric chemistry of PAHs, OPAHs and NPAHs is particularly important as this will influence the atmospheric lifetime and ultimate distribution of these compounds in the environment and the level of risk posed to human health and wider ecosystems. Individual PAHs, OPAHs and NPAHs vary considerably in their sources, physiochemical properties and environmental behaviour/fate. This is further complicated by the fact that these compounds typically occur in complex, non-uniform mixtures, the composition of which also displays spatial and temporal variations (Albinet *et al.*, 2008a,b).

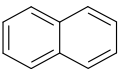
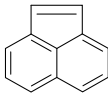
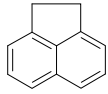
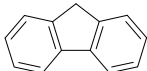
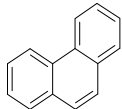
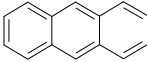
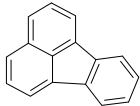
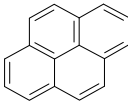
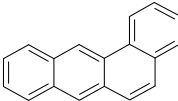
This introductory section outlines the primary sources, health risks, occurrence, behaviour (temporal, seasonal, phase-partitioning, transport) and environmental fate (deposition, photolysis, chemical reactivity) of PAH, OPAH and NPAH compounds and highlights how the understanding of these processes can be enhanced by studies involving atmospheric measurements.

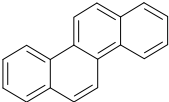
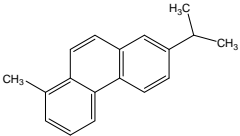
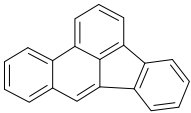
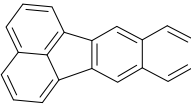
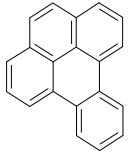
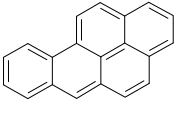
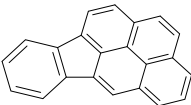
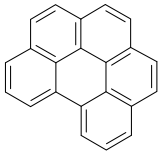
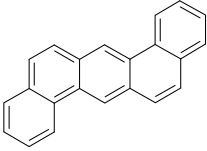
1.1.3. Policy issues

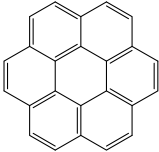
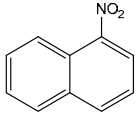
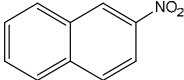
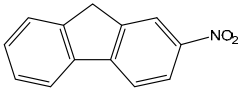
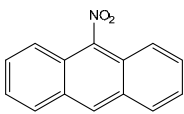
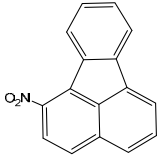
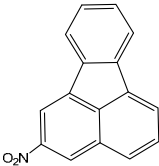
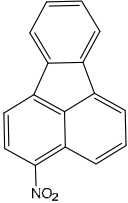
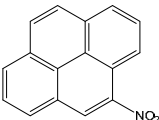
Due to their toxic, persistent and bioaccumulative properties, a number of legislative measures, at national and international levels have been established in an attempt to minimise the levels of PAHs in the atmosphere. The U.K. is a signatory of the 1998 UNECE Protocol on Persistent Organic Pollutants (UNECE, 1998). The protocol contains obligations to reduce emissions of PAHs to below 1990 levels and assess the long-range transport of four specified PAHs (BbF, BkF, BaP and IPy).

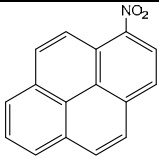
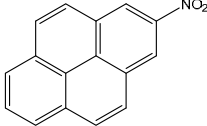
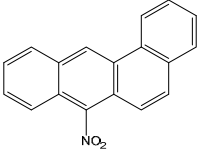
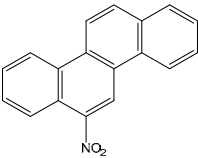
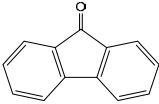
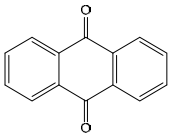
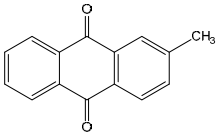
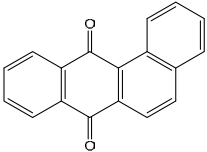
The World Health Organisation (WHO) has recommended concentrations for PAH corresponding to a carcinogenic slope factor. These guidelines indicate concentrations of BaP producing excess lifetime cancer risks of 1/10 000, 1/100 000 and 1/1 000 000 are 1.2, 0.12 and 0.012 ng m⁻³, respectively (WHO, 2000).

Table 1.1. Names, formulas and structures of the PAH, OPAH and NPAH compounds investigated in this study.

Compound Name	Abbrev	Empirical Formula	Chemical Structure	Molecular Weight (g mol ⁻¹)	CAS Number
PAHs					
Naphthalene	Nap	C ₁₀ H ₈		128.2	91-20-3
Acenaphthylene	Acy	C ₁₂ H ₈		152.2	208-96-8
Acenaphthene	Ace	C ₁₂ H ₁₀		154.2	83-32-9
Fluorene	Flo	C ₁₃ H ₁₀		166.2	86-73-7
Phenanthrene	Phe	C ₁₄ H ₁₀		178.2	85-01-8
Anthracene	Ant	C ₁₄ H ₁₀		178.2	120-12-7
Fluoranthene	Flt	C ₁₆ H ₁₀		202.3	206-44-0
Pyrene	Pyr	C ₁₆ H ₁₀		202.3	129-00-0
Benzo(a)anthracene	BaA	C ₁₈ H ₁₂		228.3	56-55-3

Chrysene	Chr	$C_{18}H_{12}$		228.3	218-01-9
Retene (7-Isopropyl-1-methylphenanthrene)	Ret	$C_{18}H_{18}$		234.3	483-65-8
Benzo(b)fluoranthene	BbF	$C_{20}H_{12}$		252.3	205-99-2
Benzo(k)fluoranthene	BkF	$C_{20}H_{12}$		252.3	207-08-9
Benzo(e)pyrene	BeP	$C_{20}H_{12}$		252.3	192-97-2
Benzo(a)pyrene	BaP	$C_{20}H_{12}$		252.3	50-32-8
Indeno[1,2,3-cd]pyrene	IPy	$C_{22}H_{12}$		276.3	193-39-5
Benzo(g,h,i)perylene	Bpy	$C_{22}H_{12}$		276.3	191-24-2
Dibenz(a,h)anthracene	DBA	$C_{22}H_{14}$		278.4	53-70-3

Coronene	Cor	C ₂₄ H ₁₂		300.4	191-07-1
NPAHs					
1-Nitronaphthalene	1NNap	C ₁₀ H ₇ NO ₂		173.2	86-57-7
2-Nitronaphthalene	2NNap	C ₁₀ H ₇ NO ₂		173.2	581-57-7
2-Nitrofluorene	2NFlo	C ₁₃ H ₉ NO ₂		211.2	607-57-8
9-Nitroanthracene	9NAnt	C ₁₄ H ₉ NO ₂		223.2	3586-69-4
1-Nitrofluoranthene	1NFIt	C ₁₆ H ₉ NO ₂		247.3	13177-28-1
2-Nitrofluoranthene	2NFIt	C ₁₆ H ₉ NO ₂		247.3	13177-29-2
3-Nitrofluoranthene	3NFIt	C ₁₆ H ₉ NO ₂		247.3	892-21-7
4-Nitropyrene	4NPyr	C ₁₆ H ₉ NO ₂		247.3	57835-92-4

1-Nitropyrene	1NPyr	C ₁₆ H ₉ NO ₂		247.3	5522-43-0
2-Nitropyrene	2NPyr	C ₁₆ H ₉ NO ₂		247.3	789-07-1
7-Nitrobenz(a)anthracene	7NBaA	C ₁₈ H ₁₁ NO ₂		273.3	20268-51-3
6-Nitrochrysene	6NChr	C ₁₈ H ₁₁ NO ₂		273.3	7496-02-8
OPAHs					
9-Fluorenone	9F	C ₁₃ H ₈ O		180.2	486-25-9
9,10 Anthraquinone	AQ	C ₁₄ H ₈ O ₂		208.2	84-65-1
2-Methyl-Anthraquinone	MAQ	C ₁₅ H ₁₀ O ₂		222.2	84-54-8
Benzo(a)anthracene-7,12-dione	BaAQ	C ₁₈ H ₁₀ O ₂		258.3	2498-66-0

The European Community's fourth Air Quality Daughter Directive (2005/107/EC) set a legally binding target value of 1 ng m^{-3} for the annual mean concentration of BaP as a marker for total PAH levels. BaP is typically used as a representative PAH as it typically constitutes a substantial proportion of the total carcinogenic potential of the PAH mixture present (Delgado-Saborit *et al.*, 2011). It is estimated that 20-29% of the urban population of the EU is exposed to BaP levels higher than the 1 ng m^{-3} EU limit and 93-94% is exposed to levels higher than the 0.12 ng m^{-3} WHO guide level (EEA, 2012).

The National Air Quality Strategy (Defra, 2007) in the U.K. includes an Air Quality Objective for PAHs, stating a maximum annual air concentration average of 0.25 ng m^{-3} BaP (EPAQS, 1999). In order to ensure compliance with the policy drivers described, the levels and trends of PAHs need to be regularly measured and monitored, especially in areas where pollution levels are likely to be highest e.g. busy roads.

No specific obligations or targets are currently in place for OPAHs and NPAHs. However, there is growing concern these compounds may pose a similar threat to public health as their 'parent' PAH compounds. This highlights the need to improve our understanding of the levels and behaviour of PAHs as well as their OPAH and NPAH derivatives in the atmosphere, in order to inform policy makers of new or growing risks relating to these compounds and the potential need for new or amended policies to reduce their negative effects on public health.

1.2. Sources of PAHs, OPAHs and NPAHs

1.2.1. Sources of PAHs

PAHs predominantly result during the burning of fossil fuels and are also found in coal tar, crude oil, creosote and roofing tar, as well as being used in manufacturing dyes, plastics and pesticides (Ravindra *et al.*, 2008). Their specific sources can be divided into the following categories (WHO, 2000 ; Choi *et al.*, 2011 ; Ravindra *et al.*, 2008 and references therein) :

- i) **Natural** e.g. non-anthropogenic fires caused by lightning strikes, volcanic emissions, diagenesis of sedimentary organic material and biosynthesis by microbes and plants.
- ii) **Accidental** e.g. spillage of petroleum products.
- iii) **Domestic** e.g. burning of wood, coal and other fuels for space heating and cooking.
- iv) **Mobile** e.g. exhaust emissions from vehicles including automobiles, trains, ships, aircraft, and machinery.
- v) **Industrial and power plants** e.g. aluminium production, coke production (e.g. in iron and steel works), creosote and wood preservation, cement production, incineration of waste, fossil fuel and biomass burning for commercial heat and electricity production.
- vi) **Agricultural** e.g. open burning of agricultural or forest residues.

A global emissions inventory for PAH has been produced by Zhang and Tao (2009) with total emission of the 16 USEPA PAHs in 2004 estimated to be $\sim 4 \text{ kg km}^{-2} \text{ yr}^{-1}$. Biomass burning and wildfires are the two key contributing sources (57% and 17% respectively) with smaller contributions from traffic (5%), domestic coal combustion (4%) and agricultural waste burning (3%) (Zhang and Tao, 2009).

For the U.K., a preliminary source inventory was provided by Wild and Jones (1995) which suggests the majority of PAH result from anthropogenic activity with negligible contribution from natural sources. Data regarding individual sources of PAHs (both total and individual compounds) in the U.K. are provided by the National Atmospheric Emissions Inventory (NAEI), funded by Defra. Estimated PAH emissions in the U.K. from key combustion sources are presented in Figure 1.1.

It is shown that PAH emissions in the U.K. declined by $\sim 88\%$ between 1990 and 2012. This has resulted due to the almost complete reduction of PAH emissions from anode baking for aluminium production, as a result of production plant closure and improved abatement technologies (Murrells *et al.*, 2010). Emissions reductions have also resulted from reduced domestic coal combustion and

the phasing out of burning agricultural wastes. These changes have resulted in a substantial shift in the relative source contributions for PAHs in the U.K. over this time (see Figure 1.2).

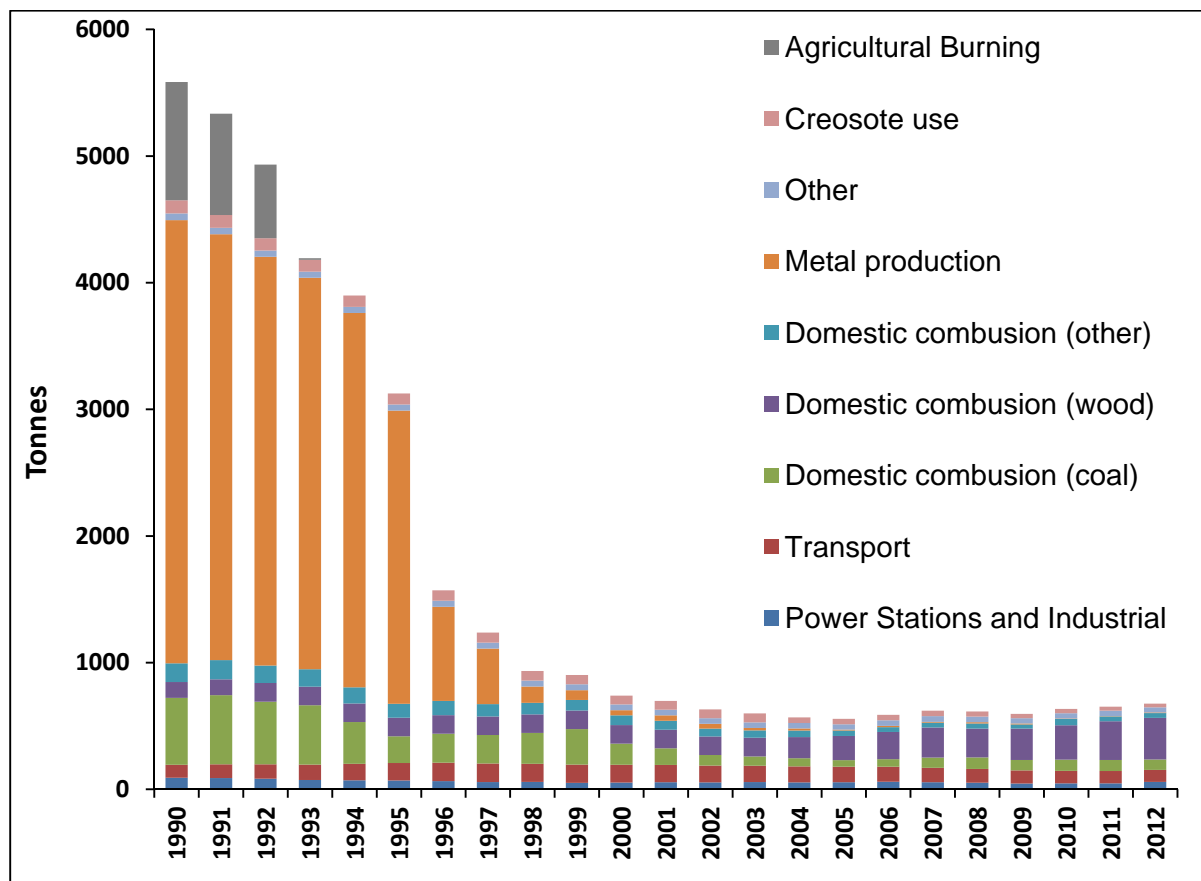


Figure 1.1. Estimated emissions of total PAH from key anthropogenic combustion sources, as provided by the NAEI (<http://naei.defra.gov.uk>). The following distinctions are made regarding these source categories :

- **Power stations/industrial emissions** – dominated by coal burning for public heat and electricity generation, but also includes emissions associated with petroleum refining and manufacturing.
- **Transport emissions** – dominated by gasoline and diesel-fuelled road vehicles.
- **Domestic combustion (other)** – includes combustion of oil, peat and charcoal
- **Metal production** – includes anode baking in aluminium production as well as sinter production in iron and steel plants.
- **Agricultural burning** – for example, the field burning of wheat residues.
- **Other emissions** – includes incineration of waste, accidental fires, emissions from November 5th celebration bonfires, fugitive emissions from coke production and bitumen use in road paving.

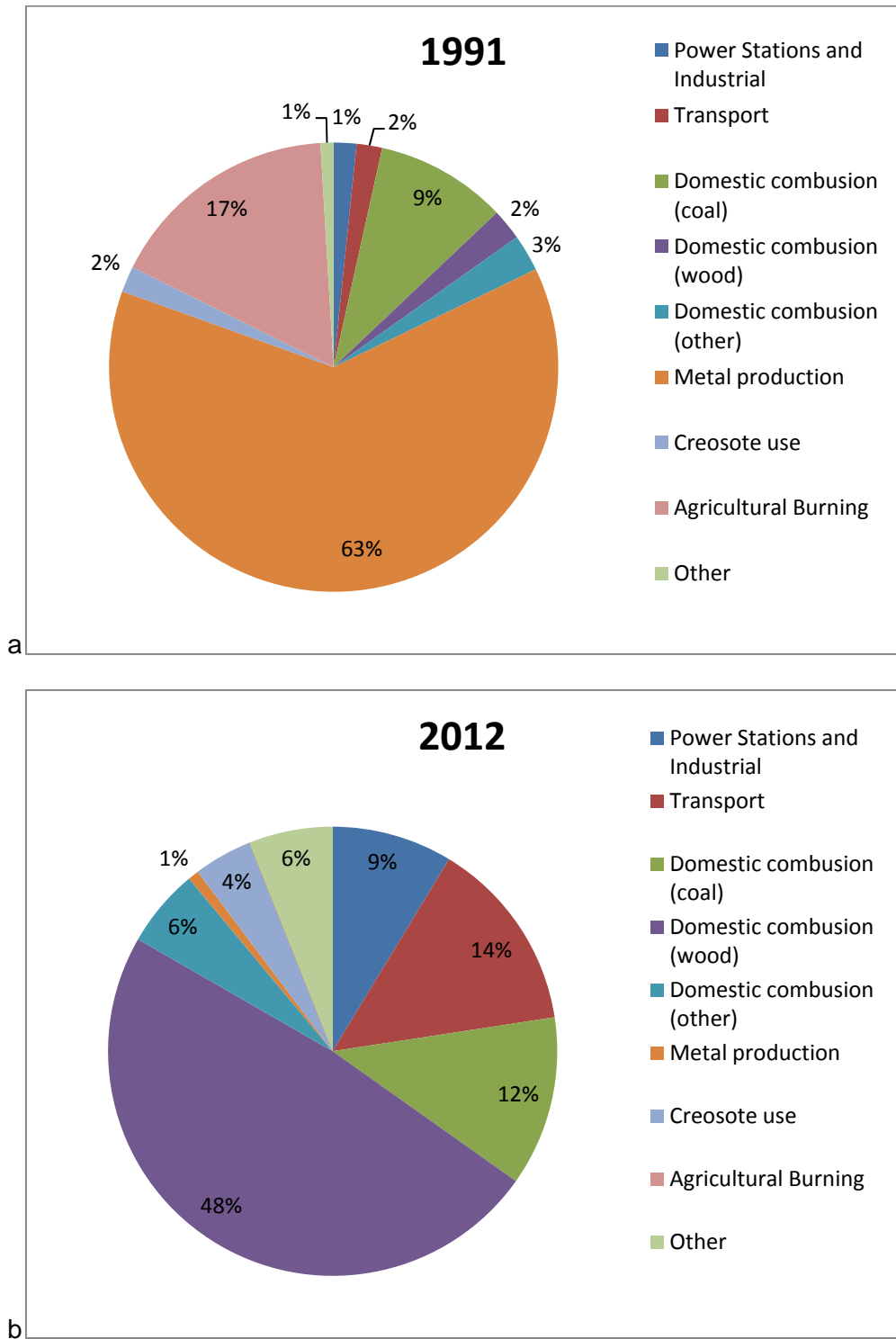


Figure 1.2. Relative contributions of different anthropogenic combustion sources to total U.K. PAH emissions, as estimated by the NAEI (<http://naei.defra.gov.uk>) in 1992 (a) and 2012 (b).

The key contributor of PAHs nationally in the U.K. is domestic combustion of wood (~48%) however vehicular traffic and regional-specific industries frequently dominate in urban and suburban areas (Keyte *et al.*, 2013; WHO, 2000). Indeed, it has been estimated that motor vehicle emissions account for between 46 and 90% of total PAHs in ambient PM in urban areas (Nikolaou *et al.*, 1984).

It should be noted that emissions inventories are likely to be subject to considerable uncertainty and may not be applicable in specific urban areas, where traffic has been shown to be a more dominant source (Harrison *et al.*, 1996; Lim *et al.*, 1999; Nielsen, 1996). Furthermore, emission inventories do not consider evaporative 'recycling' of PAH from vegetation, soils or impermeable surfaces, which can be an important factor and is not possible to quantify (Prevedouros *et al.*, 2004a). It is also noted that certain sources display seasonality (e.g. domestic burning, natural fires), while some do not (e.g. industrial emissions, petroleum refining, road traffic).

It is suggested therefore, that in order to assess the sources of PAH influencing urban or suburban areas, and the processes driving their long- and short-term variability, physical sampling data on atmospheric levels need to be obtained with careful assessment and/or modelling of these data.

1.2.2. Source of OPAHs and NPAHs

OPAHs and NPAHs also result from primary combustion emissions. A comprehensive overview of primary combustion sources for individual OPAH and NPAH compounds is provided in the supplementary information of the Keyte *et al.* (2013) review paper. Compared with 'parent' PAHs, relatively little data are available on primary sources of OPAH and NPAH, and no source inventory or quantitative emission estimates from different sources at national or global scales have yet been provided.

OPAHs can result from burning of domestic waste (Sidhu *et al.*, 2005); coal combustion (Bi *et al.*, 2008; Simoneit *et al.*, 2007), biomass burning (Hays *et al.*, 2005; Iinuma *et al.*, 2007; Shen *et al.*,

2012) , diesel and gasoline vehicle exhaust (Cho *et al.*, 2004; Fraser *et al.*, 1998a; Hays *et al.*, 2005; Iinuma *et al.*, 2007; Jakober *et al.*, 2007; Oda *et al.*, 1998; Rogge *et al.*, 1993a; Shen *et al.*, 2012; Strandell *et al.*, 1994; Zielinska *et al.*, 2004b) ; brake wear from vehicles (Rogge *et al.*, 1993b) ; domestic wood combustion (Fine *et al.*, 2002; Fitzpatrick *et al.*, 2007; Rogge *et al.*, 1998) ; and domestic natural gas burning in home appliances (Rogge *et al.*, 1993c)

NPAH have been measured in vehicular emissions (Dimashki *et al.*, 2000; Gibson, 1982; Hayakawa *et al.*, 1994; Karavalakis *et al.*, 2009; Ratcliff *et al.*, 2010) and are primarily associated with diesel exhaust (Campbell and Lee, 1984; Ciccioli *et al.*, 1989; Draper, 1986; Hayakawa *et al.*, 1994; Murahashi and Hayakawa, 1997; Schuetzle *et al.*, 1981; 1982; Zhu *et al.*, 2003) but have also been observed in gasoline vehicle emissions (Ciccioli *et al.*, 1989; Hayakawa *et al.*, 1992; IARC, 1989) but generally at much lower levels (Zielinska *et al.*, 2004b).

NPAHs are also detected in emissions from carbon electrode manufacture (Liberti and Ciccioli, 1986), stack gases from aluminium smelters and coal-fired power plants (IARC, 1989) as well as emissions of kerosene heaters, fuel gas and liquefied petroleum gas (LPG) burners and coal-fuelled stoves (Tang *et al.*, 2002; WHO, 2000).

However, in addition to these primary combustion emissions, OPAHs and NPAHs can have a secondary input from photochemical atmospheric reactions of PAH (see Section 1.5.3).

1.2.3. Emissions from road traffic

PAHs can be emitted from road vehicles by a number of different pathways (Collier *et al.*, 1995) :

- i) PAHs that survive the combustion process are emitted with unburned fuel components.
- ii) PAHs are formed via pyrolytic or pyrosynthetic reactions of other fuel components in the high temperature, oxygen deficient conditions of the vehicle engine.
- iii) PAHs are emitted via the 'leakage' of unburned fuel into the lubricating oil on the engine walls.

It has been suggested survival of unburned fuel is dominant route of PAH in both gasoline and diesel emissions (Collier *et al.*, 1995; Marr *et al.*, 1999; Tancell *et al.*, 1995a; Williams *et al.*, 1986; 1989). For example, (Tancell *et al.*, 1995b) indicated that fuel survival during combustion was the principal source of BaP in diesel emissions with a lower (<20%) resulting from pyrosynthesis or lubricating oil.

However, studies also indicate the potential importance of PAH formation from aliphatic compounds (Cole *et al.*, 1984) or methyl-PAH (Rhead and Pemberton, 1996) or formation of HMW PAH from LWM PAH during combustion (Williams *et al.*, 1989). Potentially high contribution from lubricating oil has also been indicated (Pedersen *et al.*, 1980; Williams *et al.*, 1989).

For example, Rhead and Pemberton (1996) indicated that 24% of Nap emissions from diesel vehicles resulted from unburned fuel and 76% resulted from pyrosynthesis, possibly from dealkylation from methyl-Nap compounds. Additionally, Westerholm and Egebäck (1994) discussed the key parameters governing the extent and nature of PAH emissions from vehicles and indicated that >50% of PAH emitted are formed during combustion.

For all internal combustion engines of gasoline and diesel vehicles, the emissions may vary considerably. The magnitude of PAH emissions from vehicle exhausts and the relative contributions of these formation mechanisms will be a function of the engine operating conditions (type, load, age, speed and temperature); fuel type (gasoline, diesel), quality (e.g. aromatic content, air/fuel ratio) and mode (direct or indirect injection system) (Collier *et al.*, 1995; Marr *et al.*, 1999; Ravindra *et al.*, 2008; Schauer *et al.*, 2002; Westerholm and Egebäck, 1994; Westerholm and Li, 1994).

Emissions of NPAH from diesel emissions is shown to be much higher than from gasoline emissions (Gibson, 1982; Gorse *et al.*, 1983; Hayakawa *et al.*, 1994; Westerholm and Egebäck, 1994; Westerholm and Li, 1994; Zielinska *et al.*, 2004b) and this route is considered to be the principal source of NPAH in the urban environment (Ciccioli *et al.*, 1989).

More than 200 NPAH have been detected in the diesel exhaust gases and it is suggested that NPAHs are formed via reaction of PAH with NO₂ and/or HNO₃ in the combustion chamber or exhaust system (Fiedler and Mücke, 1991). For example, Sjogren *et al.* (1996) observed a negative correlation between 1NPyr emission rates and the concentrations of NO_x and pyrene, suggesting 1NPyr results from the reaction between pyrene and NO_x.

However, it is suggested that NPAHs are not formed in the engine chamber, but rather in the exhaust system where PAH, NO_x and catalytic acid species will be present together under high temperature and low oxygen conditions (Rosenkranz and Mermelstein, 1983). It is suggested that NO_x present in diesel exhaust contains a higher proportion (30%) of NO₂ compared with gasoline exhaust (<1%), resulting in greater emission of NPAH from diesel-fuelled vehicles relative to gasoline-fuelled vehicles (Schuetzle and Perez, 1983).

1.3. Health effects of PAHs, OPAHs and NPAHs

The exposure, toxicokinetics and health effects of PAHs, OPAHs and NPAHs have been widely discussed and reviewed in the literature (see Finlayson-Pitts and Pitts, 2000 ; WHO, 2000; Choi *et al.*, 2012; IARC, 1983, 1989, 2010; Walgraeve *et al.*, 2010).

1.3.1. Exposure to PAHs

Humans are exposed to PAHs, OPAHs and NPAHs through various routes including consumption of contaminated food or water, inhalation of air and/or re-suspended dust or soil, cigarette smoking, and dermal contact (Choi *et al.*, 2012). It is considered that food ingestion is the principal exposure route for non-smokers, depending on specific diet and cooking mode used (WHO, 2000 ; Choi *et al.*, 2012 and references therein).

For example, the inhalation daily dose of BaP for non-smokers in the homes of industrialised counties has been estimated to be 0.15-21 ng/day compared with estimated dietary intake of 4.2 –

320 ng/day in various European studies (Choi *et al.*, 2012 and referenced therein). However, a significant exposure contribution from outdoor air pollution could occur in heavily polluted urban and industrial areas (WHO, 2000).

1.3.2. The metabolism and toxicity mechanism of PAHs, NPAHs and OPAHs

Gas-phase pollutants are likely to be inhaled and exhaled more easily and will tend to associate with the mucus lining of the lung, while PM is more likely to settle on the lung surface and be absorbed more readily. Hence it is suggested that HMW PAH, associated predominantly with particulates, will pose the greater health risk (Finlayson-Pitts and Pitts, 2000). Upon absorption into the body from the lungs, gut or skin, PAHs can deposit in fatty tissues and have been observed in most internal organs (WHO, 2000).

PAHs are shown to exert toxic effects through oxidative metabolic transformation by enzymes to more polar reactive intermediate species, which can bind covalently to nucleophilic sites in DNA bases to form DNA adducts (Shimada, 2006; WHO, 2000; Xue and Warshawsky, 2005). Three principal enzymatic routes leading to the metabolic activation of PAHs have been proposed (Shimada, 2006; Xue and Warshawsky, 2005) : i) via the formation of diol-epoxide metabolites (see Figure 1.3) ; ii) via radical cation formation (Figure 1.4 ; and iii) via PAH quinone formation (Figure 1.5. DNA adducts can interfere with DNA replication and repair, causing mutations that are fixed after cell division possibly leading to tumour development in various organs including lung, liver, skin and mammary tissues (Choi *et al.*, 2012 and references therein).

NPAH and OPAH can also exert cytotoxicity, immunotoxicity and carcinogenesis, and are a particular concern due to their direct acting mutagenicity (i.e. not requiring external enzymatic activation) (Bolton *et al.*, 2000; Fiedler and Mücke, 1991).

It is expected that NPAH will also undergo metabolism via reduction of the NO₂-group followed by a sequence of reactions that can form N-hydroxylamines or nitrenium ions which yield reactive

DNA-binding species or alternatively to toxic acetylamine species (see Figure 1.6) (Fiedler and Mücke, 1991 ; WHO, 2000).

OPAH quinones can undergo enzymatic and non-enzymatic redox cycling with their semiquinone radicals, leading to the formation of reactive oxidative species (ROS) including superoxide, hydrogen peroxide and ultimately the hydroxyl radical (see Figure 1.7) (Bolton *et al.*, 2000; Kumagai, 2009). ROS can cause severe oxidative stress in cells and cause DNA damage (Walgraeve *et al.*, 2010 and references therein). Kumagai (2009) also details the potential for quinones to cause arylation of cellular proteins resulting in protein adduct formation.

1.3.3. Health effects of PAHs

Data from in vitro and in vivo bioassays using non-mammalian (e.g. bacteria), mammalian non-human (e.g. rodent) and human cells have demonstrated the mutagenicity, immunotoxicity, genotoxicity and carcinogenicity of PAH, OPAH and NPAH exposure (Busby *et al.*, 1994a; 1994b; 1995; Deutschwenzel *et al.*, 1983; Durant *et al.*, 1996; Enya *et al.*, 1997; IARC, 1983 1989; Rosenkranz and Mermelstein, 1983; Ross *et al.*, 1995; Sato *et al.*, 1986; Tokiwa *et al.*, 1987; Wei *et al.*, 1993).

The most significant health effect expected from inhalation exposure to PAHs is excess risk of lung cancer (WHO, 2000). However, PAH exposure is also associated with numerous other negative human health effects including bronchitis, asthma, heart disease and reproductive toxicity (Choi *et al.*, 2012).

The nature and magnitude of health effects caused by PAHs varies between individual compounds and their presence in the atmosphere as mixtures, of varying composition, means evaluating health risks and influence of specific components in the environment is complex (Keyte *et al.*, 2013). The IARC has categorised various PAH and NPAH compounds according to their carcinogenicity (see Table 1.2).

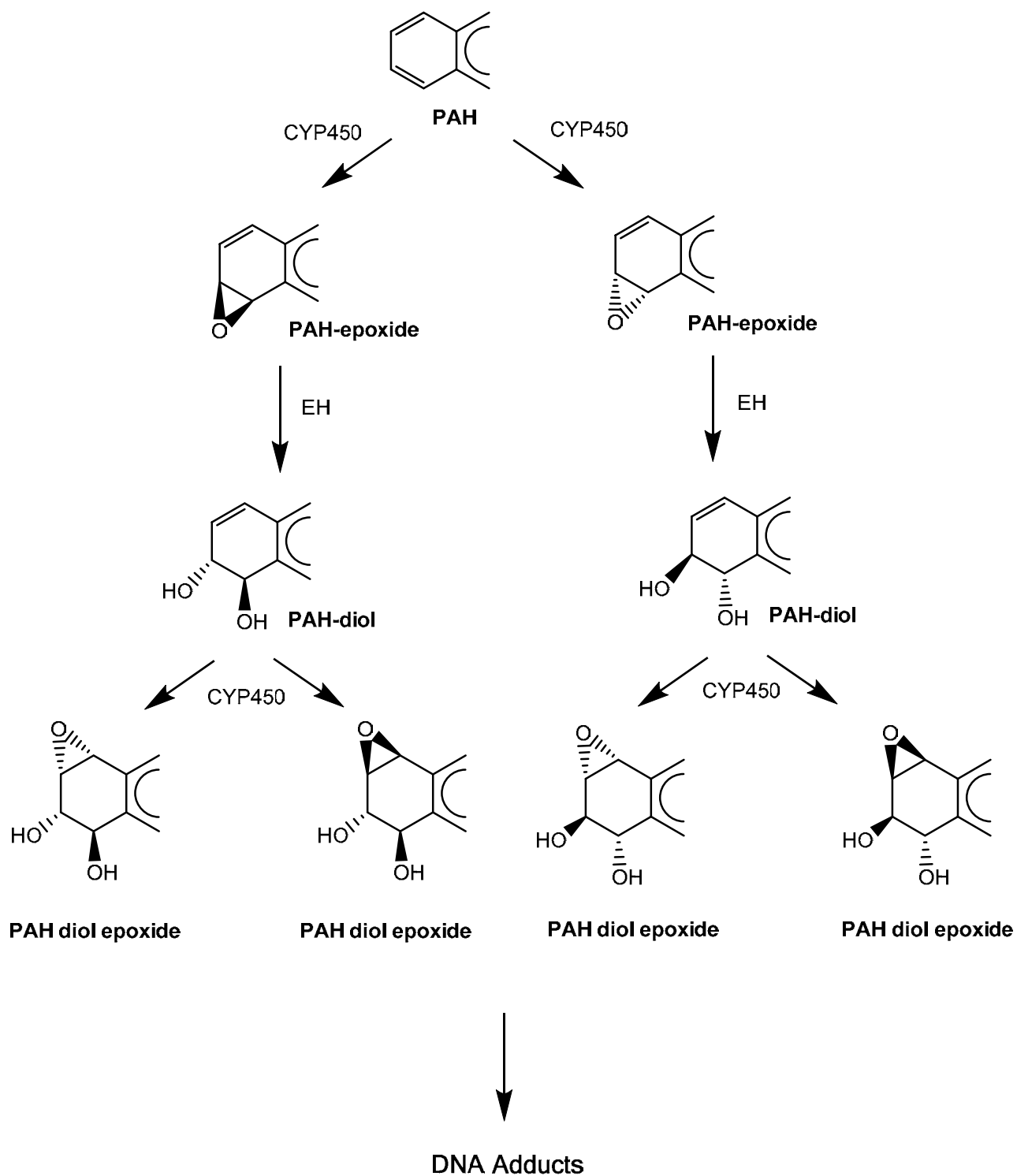


Figure 1.3. Metabolic diol epoxide formation from PAHs via cytochrome P450 enzymes (CYP450) and epoxide hydrolase (EH) enzymes (Shimada, 2006).

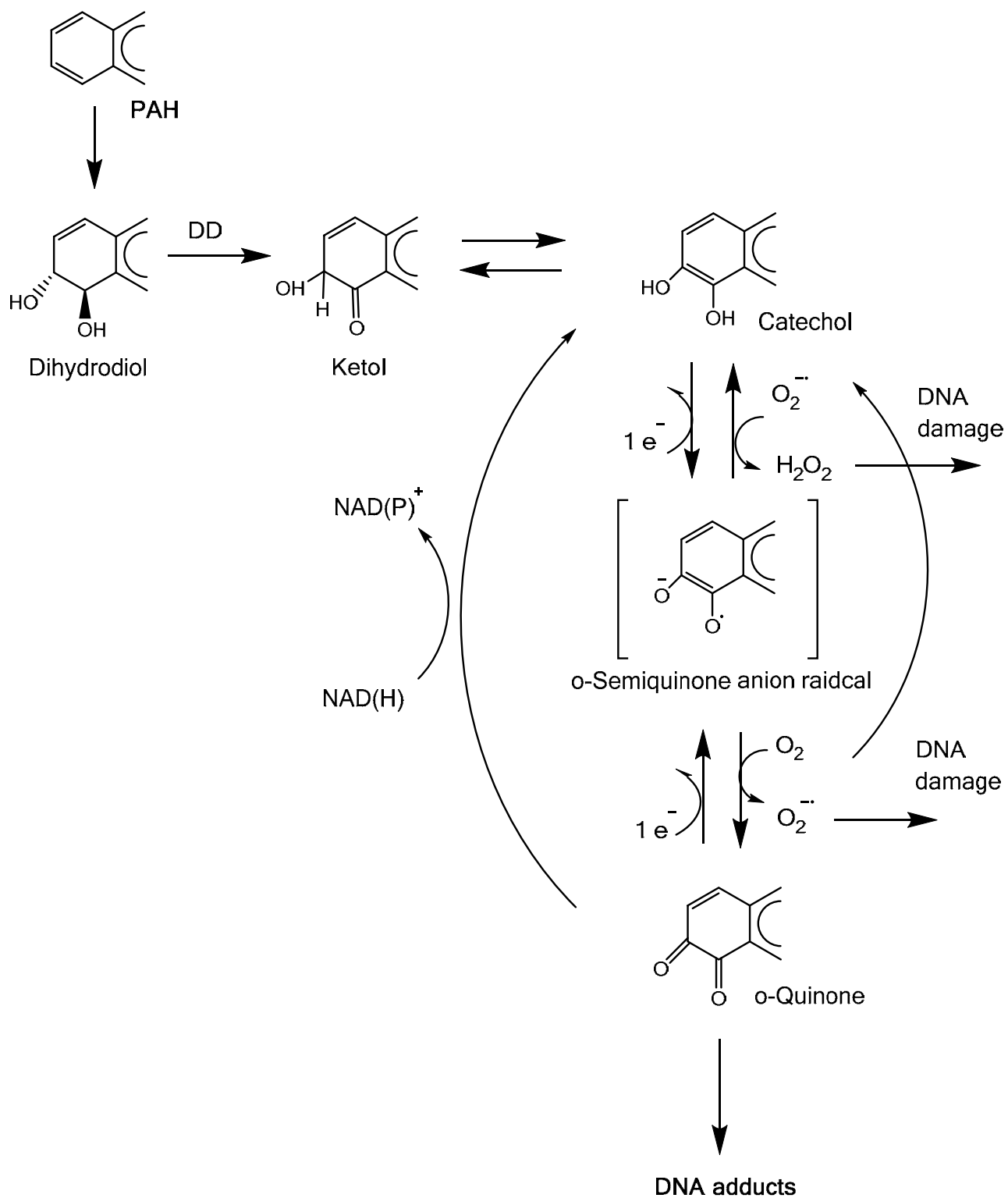


Figure 1.4. Metabolic formation of o-quinones from PAHs via dihydrodiol dehydrogenase (DD) enzymes (Xue and Warshawsky, 2005).

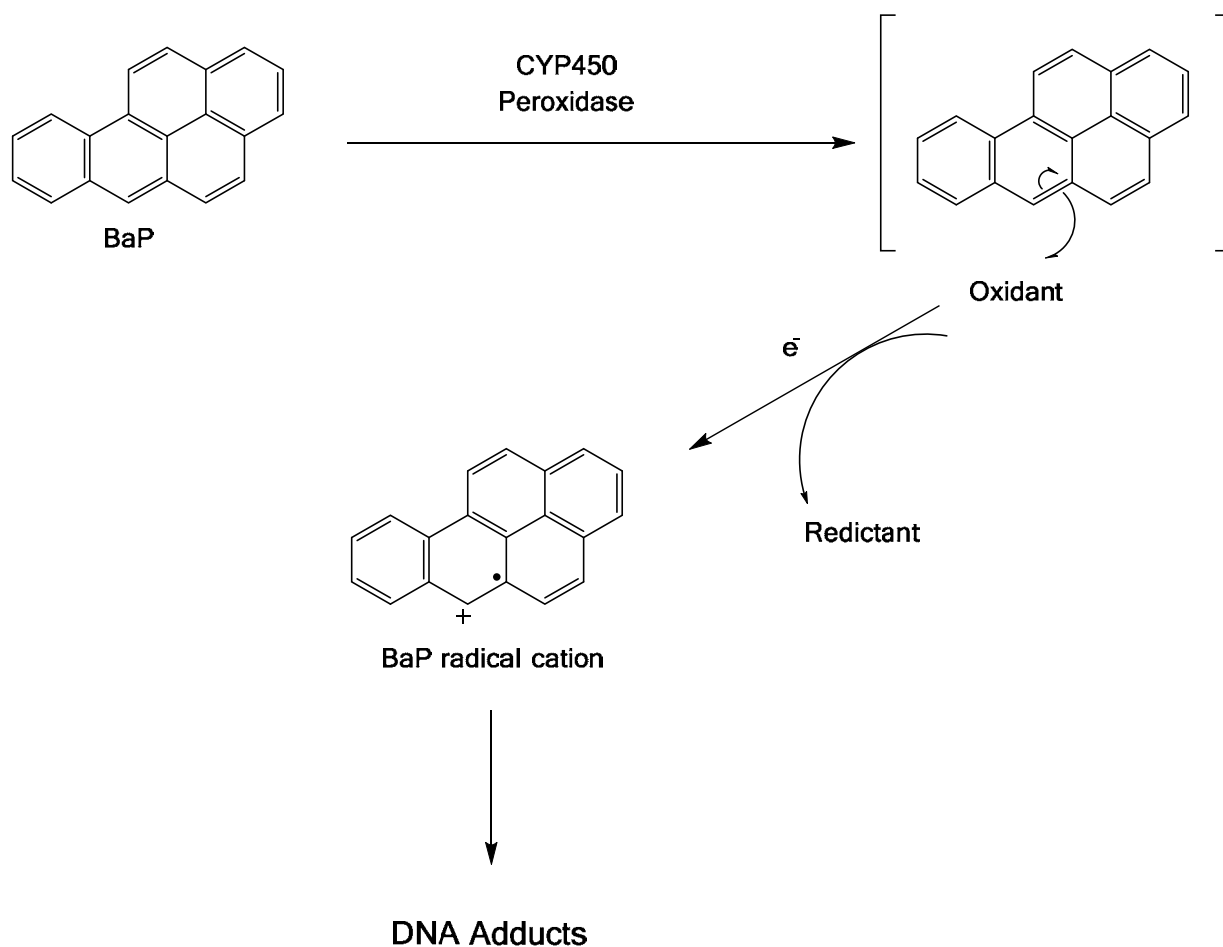


Figure 1.5. Metabolic cation radical formation from PAHs via cytochrome P450 enzymes (CYP450) and peroxidase enzymes.

1.3.4. The role of PAHs in the health effects of urban air

The carcinogenic and/or mutagenic potential of PM in urban air samples has been widely demonstrated (Bayona *et al.*, 1994; Hannigan *et al.*, 1997; Kawanaka *et al.*, 2004; Pitts *et al.*, 1977; Pitts *et al.*, 1982; Tokiwa *et al.*, 1987) and many proven or potentially mutagenic or carcinogenic PAHs, OPAHs and NPAHs are observed in urban air of many countries (see Keyte *et al.*, 2013 for full details).

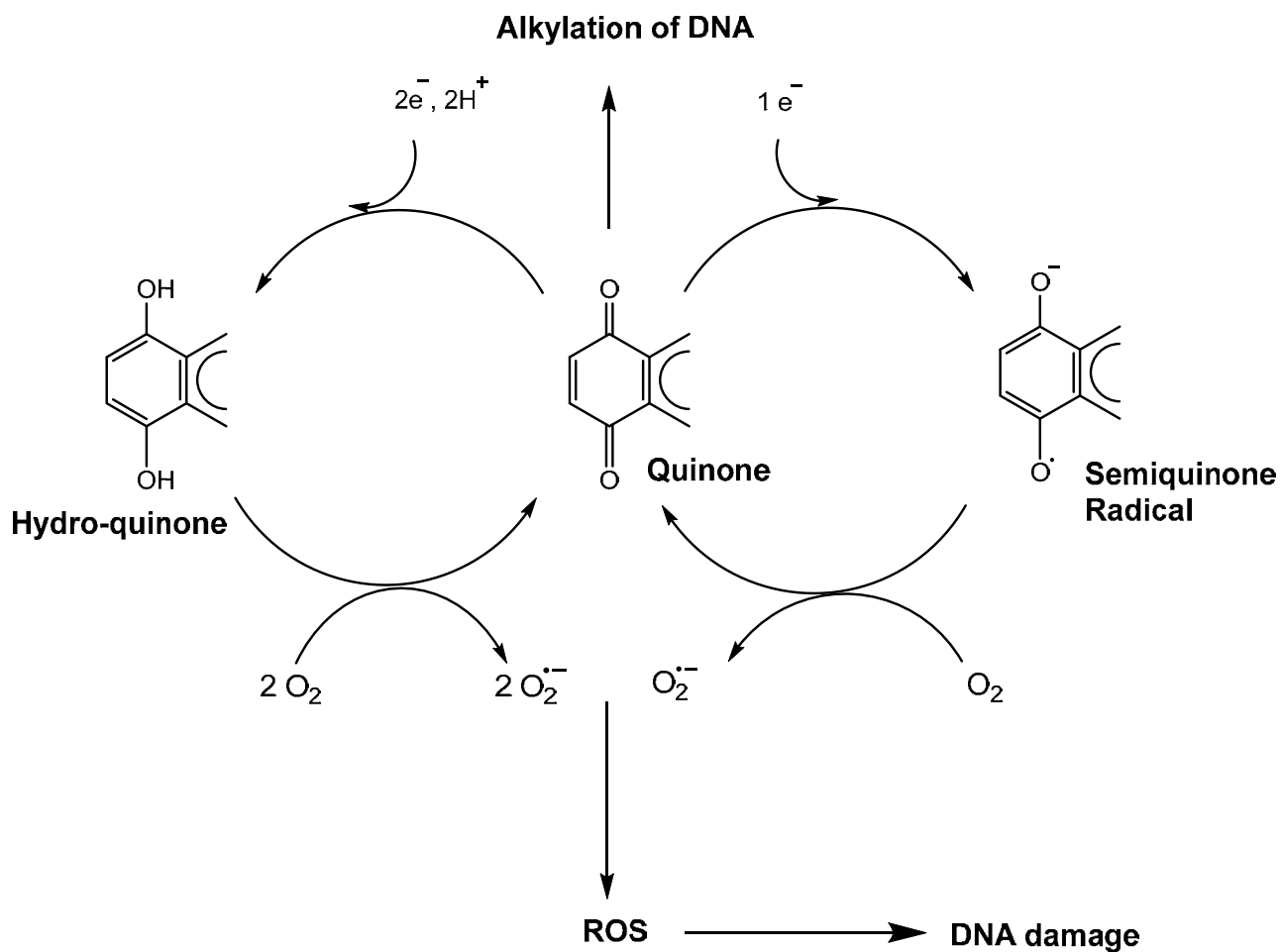


Figure 1.6. Mechanism for the formation of reactive oxygen species from OPAH quinones (Bolton *et al.*, 2000).

Numerous studies have suggested PAHs, OPAHs and NPAHs can contribute significantly to the observed carcinogenicity and/or mutagenicity of ambient air (Bethel *et al.*, 2001; Durant *et al.*, 1998; Gupta *et al.*, 1996; Hannigan *et al.*, 1998; Pedersen *et al.*, 2004; 2005; Tuominen *et al.*, 1988; Umbuzeiro *et al.*, 2008; Wang *et al.*, 2011a) and primary combustion emissions such as diesel exhaust (Arey *et al.*, 1988; Ball and Young, 1992; Bethel *et al.*, 2001; Durant *et al.*, 1998; Enya *et al.*, 1997; Gupta *et al.*, 1996; Hannigan *et al.*, 1998; Hayakawa *et al.*, 1994; IARC, 1989; Pedersen *et al.*, 2004; 2005; Pitts *et al.*, 1982; Rappaport *et al.*, 1980; Salmeen *et al.*, 1982; 1984; Tuominen *et al.*, 1988; Umbuzeiro *et al.*, 2008; Wang *et al.*, 2011a). For example, it has been proposed that

PAHs are a principal contributor to the carcinogenic potential of PM in urban air (Bonfanti *et al.*, 1996; Harrison *et al.*, 2004).

Pedersen *et al.* (2004; 2005) investigated the mutagenicity of individual PAH compounds present in collected airborne PM samples. They indicated that PAH compounds accounted for 13-22% of the mutagenicity potential of the total PM extract, with key contributing compounds including BaP, BbF, BkF, IPy, BPy as well as OPAH ketone 6H-benzo(cd)pyren-6-one.

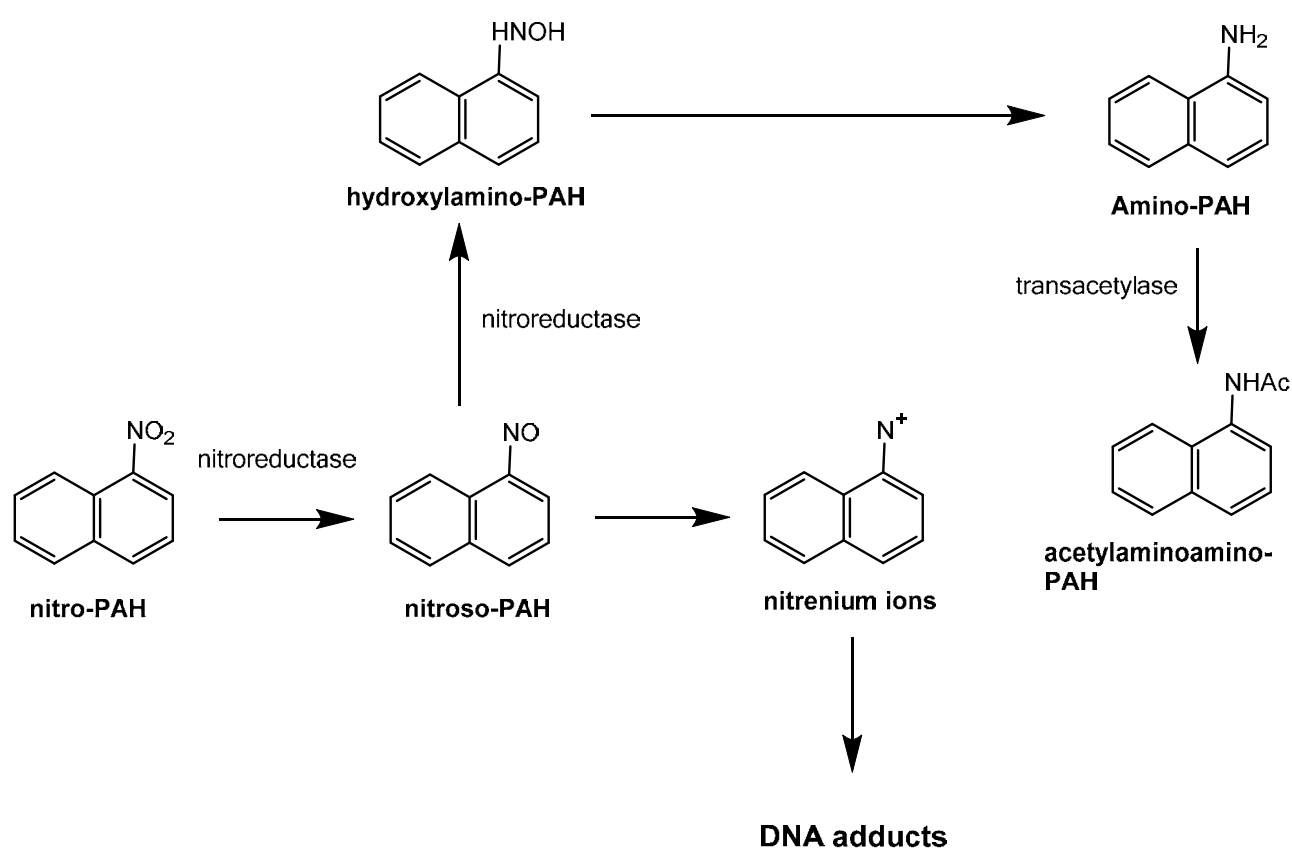


Figure 1.7. Mechanism for the formation of toxic intermediate species from NPAH compounds (Fiedler and Mücke, 1991).

However, a number of studies have indicated that semi-polar fractions or atmospheric PM extracts (likely to contain OPAH and NPAH compounds) display higher direct acting mutagenicity than non-polar extracts (likely to contain PAH compounds) (Lewtas *et al.*, 1990; Nishioka *et al.*, 1985;

Pedersen *et al.*, 2004; Umbuzeiro *et al.*, 2008; Wang *et al.*, 2011a). Furthermore, it has also been demonstrated that ROS generation in airborne PM samples correlates with measured concentrations of OPAH quinones (Chung *et al.*, 2006).

These studies suggest that NPAH and OPAH may pose more toxic hazard in the urban environment than PAH. However it is noted that a significant proportion of compounds potentially responsible for the observed mutagenicity of PM have not yet been identified (Pedersen *et al.*, 2005).

1.3.5. The role of atmospheric PAH reactions on toxic effects

Gas-phase LMW PAHs e.g. Phe, Flo, Pyr and Flt typically dominate the total atmospheric burden of PAHs. While these compounds do not appear to cause significant mutagenicity or carcinogenicity (Durant *et al.*, 1996; Finlayson-Pitts and Pitts, 2000) they may act as precursors to powerful mutagens. PAHs can be transformed in the atmosphere to a wide range of different products including OPAH and NPAH via gas-phase or heterogeneous reactions (see Section 1.5.3).

Albinet *et al.* (2008a) indicate that formation of secondary NPAH from chemical reactions could significantly increase the carcinogenic risk of PM for people exposed far from original sources of direct emissions. For example, 2NFlt is a potent human cell mutagen (Durant *et al.*, 1996 ; Pedersen *et al.*, 2004; 2005) and is typically present in air samples at levels that may contribute to human cell mutagenicity in many areas of the world (Finlayson-Pitts and Pitts, 2000).

Furthermore, it has been demonstrated that products from the OH-initiated reactions of 2-3 ring PAHs such as NPAHs, NPAH lactones and nitrodibenzopyranones identified in experimental gas chamber studies can contribute significantly to the observed mutagenicity of ambient air samples (Helmig *et al.*, 1992a; 1992b; 1992c; Sasaki *et al.*, 1997a).

Table 1.2. Mutagenic and/or carcinogenic categorisation of PAH, OPAH and NPAH compounds studies in the present investigation.

	Human cell mutagenicity^a	IARC classification^b	Relative human cell mutagenicity (ratio to BaP)^a
Acy	(+)	ND	0.00056
Ace	ND	ND	n/a
Flo	ND	ND	n/a
Phe	(-)	ND	n/a
Ant	ND	ND	n/a
Flt	(-)	ND	n/a
Pyr	(-)	ND	n/a
BaA	(+)	2B	0.082
Chr	(+)	3	0.017
BbF	(+)	2B	0.25
BkF	(+)	2B	0.11
BeP	(+)	2B	0.0017
BaP	(+)	2B	1
IPy	(+)	2B	0.31
BPy	(+)	2B	0.19
DBA	(+)	2A	0.29
Cor	(-)	ND	n/a
1NNap	(-)	3	n/a
2NNap	(-)	3	n/a
2NFlo	(+)	2B	n/a
9NAnt	(+)	3	0.0032
1NFlt	ND	ND	n/a
2NFlt	(+) ^c	ND	n/a
3NFlt	(+)	3	0.0026
4NPyr	ND	2B	n/a
1NPyr	(+)	2B	0.025
2NPyr	(-)	ND	n/a
7NBaA	ND	ND	n/a
1,3-DNP	(+)	ND	0.031
1,6-DNP	(+)	2B	0.28
1,8-DNP	(+)	2B	0.046
6NChr	(+)	2B	n/a
9F	ND	ND	n/a
AQ	(-)	ND	n/a
MAQ	(+)	ND	n/a
BaAQ	(-)	ND	n/a

a – Durant et al. (1996) - (+) indicates compound is mutagenic; (-) indicates compound is not mutagenic at the doses tested; ND indicates the compound was not tested.

b – IARC (1983, 1989, 2010) : 1 = carcinogenic to humans ; 2A = probably carcinogenic to humans ; 2B = possibly carcinogenic to humans ; 3 = not possible to classify ; ND = not determined

c – Pedersen et al. (2005)

Gupta *et al.* (1996) demonstrated that ambient concentrations of NNap and MNnap compounds, known to form from atmospheric reactions (Phouongphouang and Arey, 2002,2003b) contributed 18% and 32% of daytime and nighttime vapour phase mutagenicity respectively.

It has also been indicated from sampling in urban and 'receptor' sites that changes in PAH burden are 'mirrored' by changes in observed mutagenicity of the collected PM, (Atkinson and Arey, 1994 and references therein). Indeed, Feilberg *et al.* (2002) indicated that the ratio of BaP concentration to measured mutagenicity of air samples taken in Central Europe rapidly decreased as a function of photochemical age in urban areas. These studies therefore suggest the potential importance of mutagens formed via atmospheric reactions such as OPAH and NPAH.

Jariyasopit *et al.* (2014) also indicated the direct acting mutagenicity of aerosol increased upon laboratory formation of NPAH from PAHs on collected PM exposed to NO₂/NO₃/N₂O₅ in a study simulating long range atmospheric transport.

It is clear that the overall health risk posed by PAH, OPAH and NPAH in urban air will be influenced not only by source strength of primary emissions but also on the atmospheric processes influencing their phase-partitioning, and the secondary input of potentially mutagenic reaction products as well as seasonal, spatial and meteorological variations (Finlayson-Pitts and Pitts, 2000).

This demonstrates the importance of improving our understanding of these processes and the need for interaction between atmospheric chemists and toxicologists in order to provide adequate risk assessments regarding the possible human health effects of PAH, OPAH and NPAH in urban areas (Finlayson-Pitts and Pitts, 2000).

1.4. Occurrence and behaviour of PAHs in the atmosphere

1.4.1. Occurrence in the environment

1.4.1.1. PAHs in the environment

A preliminary budget for PAHs in the U.K. between different environmental compartments was described Wild and Jones (1995). This estimates a total PAH burden (sum of 12 compounds) of ~53 000 tonnes, the vast majority (>90%) of which is found in soils with the bulk of the remainder associated with freshwater sediments (3-5%) (see Figure 1.8).

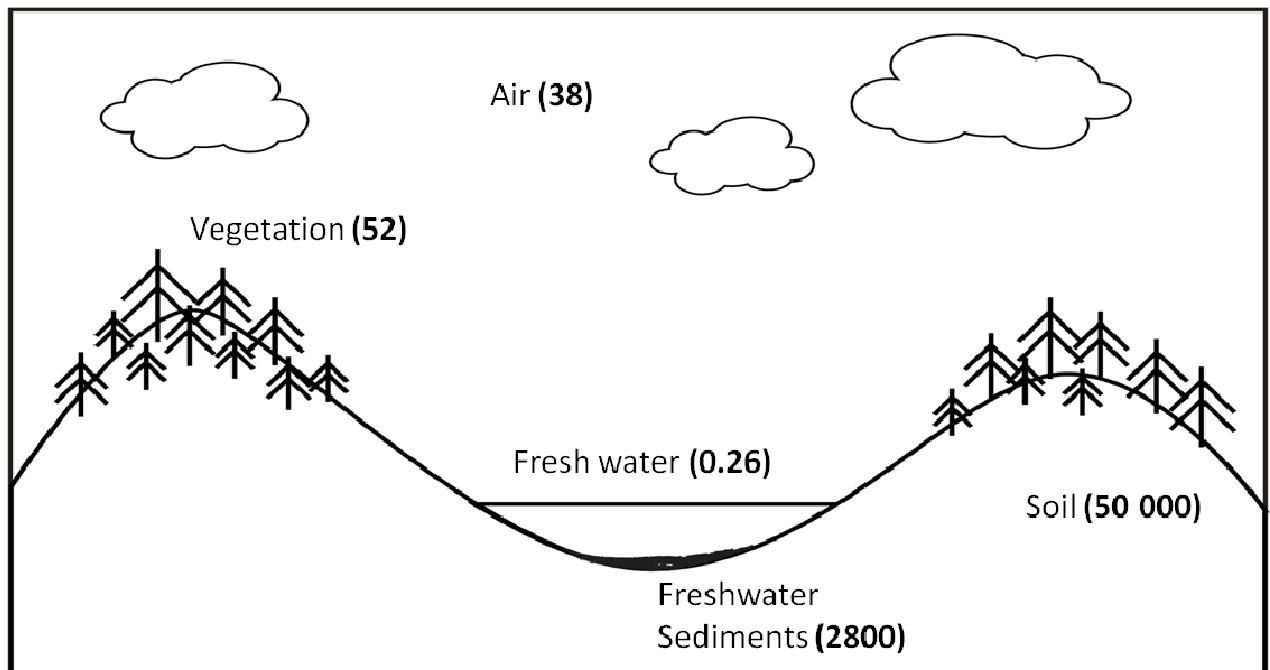


Figure 1.8. The distribution of total PAH burden in the U.K between different environmental compartments (tonnes) as estimated by Wild and Jones (1995).

While only a relatively small (<0.1%) proportion of the total PAH burden is predicted to be present in the atmosphere at a given time, this environmental compartment is important as combustion sources typically emit directly to the atmosphere (Ravindra *et al.*, 2008). The subsequent

atmospheric processing of PAHs will dictate their overall environmental fate and/or transfer to other environmental compartments. For example Jones *et al.* (1989) indicated the PAH concentration in the upper soil level (top 0-23 cm) increased by around four-fold from the 1880s to the 1980s, and attributed this to increased emissions to the atmosphere and subsequent deposition over this time.

Total PAH concentrations in the atmosphere typically range from low (<1 to 10) ng m⁻³ values in remote rural locations to high (10 to >100) ng m⁻³ values in heavy urban and traffic locations, depending on the specific location, nature and strength of primary sources and ambient conditions (Finlayson-Pitts and Pitts, 2000; Liu *et al.*, 2006a; Mastral *et al.*, 2003a; Prevedouros *et al.*, 2004a).

PAHs are typically found within the ultrafine (aerodynamic diameter <0.1 µm) or accumulation (aerodynamic diameter 0.1 to 1 µm) fraction of the particle mass size distribution (Keyte *et al.*, 2013). In urban and rural locations, the median diameter is predominantly found in the accumulation mode, however PAHs may be more associated with the ultrafine mode in closer proximity to primary combustion emissions (Baek *et al.*, 1991; Cancio *et al.*, 2004; Chrysikou *et al.*, 2009; Kawanaka *et al.*, 2004; Kawanaka *et al.*, 2009; Kiss, 1996; Miguel *et al.*, 2004; Schnelle *et al.*, 1995; Venkataraman and Friedlander, 1994).

1.4.1.2. OPAHs and NPAHs in the atmosphere

The presence of NPAHs in air samples has been reported in wide range of urban, suburban, rural and trafficked locations in the U.K. (Dimashki *et al.*, 2000); Continental Europe (Albinet *et al.*, 2006,2007a; 2008a; Bayona *et al.*, 1994; Cecinato, 2003; Di Filippo *et al.*, 2010; Feilberg *et al.*, 2001; Marino *et al.*, 2000; Niederer, 1998; Nielsen, 1984; Ringuet *et al.*, 2012c; Tsapakis and Stephanou, 2007) ; North America (Arey *et al.*, 1987; Arey *et al.*, 1989a; Bamford and Baker, 2003; Ramdahl *et al.*, 1986; Reisen and Arey, 2005; Wilson *et al.*, 1995); South America (Sienra and Rosazza, 2006; Valle-Hernandez *et al.*, 2010); Asia (Dimashki *et al.*, 2000; Hien *et al.*, 2007; Kakimoto *et al.*, 2000; 2001; Murahashi and Hayakawa, 1997; Tang *et al.*, 2002; 2005; Wang *et al.*, 2011a; Wei *et al.*, 2012); Africa (Nassar *et al.*, 2011).

Atmospheric concentration of NPAHs are typically reported to be generally 10-100 times lower than concentrations of PAH (Albinet *et al.*, 2008a; Bamford and Baker, 2003; Feilberg *et al.*, 2001), while OPAHs are typically observed in ambient air at similar concentrations to their parent PAHs (Albinet *et al.*, 2007,2008a; Walgraeve *et al.*, 2010, references and supplementary material therein).

OPAHs have been reported in ambient sampling studies in the U.K. (Alam *et al.*, 2013; 2014; Delgado-Saborit *et al.*, 2013; Harrad *et al.*, 2003; Lewis *et al.*, 1995) ; Continental Europe (Albinet *et al.*, 2006,2007a; Albinet *et al.*, 2008a; Andreou and Rapsomanikis, 2009; Castells *et al.*, 2003; Delhomme *et al.*, 2008; Liu *et al.*, 2006b; Neususs *et al.*, 2000; Schnelle-Kreis *et al.*, 2007; Shimmo *et al.*, 2004b; Valavanidis *et al.*, 2006) ; North America (Allen *et al.*, 1997; Cho *et al.*, 2004; Chung *et al.*, 2006; Eiguren-Fernandez *et al.*, 2008a; Wilson *et al.*, 1995) ; South America (Sienra, 2006; Tsapakis *et al.*, 2002) ; Asia (Lee *et al.*, 2012; Park *et al.*, 2008; Wang *et al.*, 2011a; Wingfors *et al.*, 2001); Africa (Yassaa *et al.*, 2001).

However, relatively few studies have measured both PAH and OPAH or NPAH derivative compounds in the same environmental samples, despite this being necessary in order to gain a clearer understanding of the atmospheric processing of these compounds (Alam *et al.*, 2014).

The majority (>85%) of OPAH and NPAH are shown to be associated with particles with an aerodynamic diameter <0.25 μm (Albinet *et al.*, 2008b; Di Filippo *et al.*, 2010; Kawanaka *et al.*, 2004; 2009; Ringuet *et al.*, 2012c). For example, the mass size distribution of a number of NPAH and OPAH was assessed in various urban, trafficked, suburban and rural locations in France by Albinet and co workers. Albinet *et al.* (2008b) indicated that 60-90% of OPAH and NPAH are associated with the fine (aerodynamic diameter >1.3 μm) mass fraction in both summer and winter. However, Ringuet *et al.* (2012c) noted that, while NPAH compounds are observed in both ultra fine and accumulation mass fractions, OPAHs are predominantly found in the ultra fine mode at traffic (77%) and suburban (64%) sites.

As with unsubstituted PAHs, OPAH and NPAH particle mass size distribution is shown to exhibit seasonal and spatial variations. For example, the extent of particle aging between urban and suburban or rural sites can result in a shift in mass size distribution towards coarser particles (Albinet *et al.*, 2008b; Allen *et al.*, 1997; Ringuet *et al.*, 2012c).

Albinet *et al.* (2008b) indicated fractions in the finest particles (aerodynamic diameter <0.39 µm) were higher for OPAH (56%) and NPAH (63%) than for PAHs (45%) therefore suggesting that these derivative compounds can pose a more toxic threat than PAH as they will penetrate deeper into the human respiratory system (Ringuet *et al.*, 2012c; Walgraeve *et al.*, 2010).

1.4.2. Gas-particle partitioning of PAH, OPAH and NPAH compounds

1.4.2.1. Phase partitioning of PAHs

The wide range of physiochemical properties between compounds mean PAHs can exist in both the free vapour phase and associated with atmospheric particulate matter. In the atmosphere, PAHs range from relatively small 2-ring species (e.g. Nap) that exist almost entirely in the vapour-phase to relatively large molecules with 6 or more rings (e.g. Cor) compounds which are present almost entirely in the particulate phase.

However, the majority of PAH compounds, especially those with 3-4 rings are considered to be semi-volatile and can hence undergo a significant degree of partitioning between these two phases in the atmosphere (Keyte *et al.*, 2013). The dynamics and factors influencing PAH phase partitioning has previously been discussed by Keyte *et al.* (2013) and Finlayson-Pitts and Pitts (2000).

Phase partitioning of PAH can be quantified by defining a gas-particle partitioning coefficient :

$$K_p = C_p / (C_g \times C_m) \quad (1.1)$$

where :

$K_p = \text{partitioning coefficient (m}^3 \mu\text{g}^{-1}\text{)}$

$C_p = \text{concentration in the particulate phase (}\mu\text{g m}^{-3}\text{)}$

$C_g = \text{concentration in the gas phase (}\mu\text{g m}^{-3}\text{)}$

$C_m = \text{particulate matter mass concentration (}\mu\text{g m}^{-3}\text{)}$

The value of K_p can be influenced by the extent and nature both adsorption and adsorption processes and is strongly temperature dependent (Baek *et al.*, 1991; Yamasaki *et al.*, 1982) and can exhibit a pronounced seasonal variation (Baek *et al.*, 1991; Halsall *et al.*, 1993; Keller and Bidleman, 1984; Smith and Harrison, 1996; Yamasaki *et al.*, 1982). The degree of gas-particle partitioning can also be influenced by sampling artefacts (see Sections 2.1.6 and 4.4).

Quantitative analysis suggests PAH phase partitioning can be described by the sum of absorptive (characterised by the octanol-air partitioning coefficient) and adsorptive (characterised by the soot-air partitioning coefficient) contributions (Keyte *et al.*, 2013 and references therein) :

$$K_p = 10^{-12} [f_{OM}/\rho_{oct} K_{oa} + f_{BC}/\rho_{BC} (S_{BC}/S_{soot}) K_{soot-air}] \quad (1.2)$$

where :

f_{BC} and f_{OM} = the mass fraction of soot (black carbon) and organic matter in particulate matter respectively

$K_{soot-air}$ = the soot-air partitioning coefficient

K_{oa} = the octanol-air partition coefficient

ρ_{oct} and ρ_{BC} = the densities of octanol and soot, respectively

S_{BC} and S_{soot} = available specific surface areas

The extent of gas-particle partitioning of PAHs is influenced by a number of physical and chemical factors. As discussed by Baek *et al.* (1991) phase partitioning is a function of : i) the molecular

weight and associated vapour pressure of the compound at ambient temperature; ii) the concentration and nature (e.g. organic matter content) of particulate matter and the available surface area for PAH adsorption ; iii) the affinity of the compound for the organic matrix within particulate matter ; iv) the state of the compound upon emission (e.g. gas-phase, adsorbed at particle surface, or contained within the core particle); v) the reactivity and/or stability of the compound ; vi) meteorological conditions (e.g. temperature, humidity, and precipitation).

1.4.2.2. Phase partitioning of OPAHs and NPAHs

Experimental data regarding the phase partitioning of NPAH and OPAH is relatively lacking compared with unsubstituted PAHs as only a relatively small number of studies have conducted atmospheric measurements in both particulate and vapour phases (Albinet *et al.*, 2007a; Albinet *et al.*, 2008a; Bamford and Baker, 2003; Eiguren-Fernandez *et al.*, 2008a; Lintelmann *et al.*, 2006; Wilson *et al.*, 1995).

OPAH and NPAH typically exhibit higher molecular weight and lower vapour pressures than their 'parent' PAHs, which may lead to a higher tendency to sorb to atmospheric PM (Walgraeve *et al.*, 2010).

Albinet *et al.* (2008a) reported PM associated fractions of a wide range of OPAH and NPAH as a function of molecular weight and sampling season in a French Alpine valley region. It was indicated that 2-3 ring compounds are mainly present in the gas-phase (>50%), while 4+ ring compounds are mostly (>90%) associated with PM. Similar observations have been reported by Liu *et al.*, 2006 and Delgado-Saborit *et al.* (2013).

As with 'parent' PAH, the fraction of OPAH and NPAH in the particle-phase is strongly dependent on the specific physiochemical properties of the molecule e.g. molecular weight and associated vapour pressure, meteorological factors e.g. temperature, and the concentration of particles.

It is indicated that, especially in winter these compounds have a stronger tendency to sorb to PM and the seasonal effects on the extent of gas-particle partitioning is more pronounced for OPAH

and NPAH than for parent PAH (Albinet *et al.*, 2008a). However, the specific partitioning behaviour observed is shown to be highly dependent on sampling site and methodology (Albinet *et al.*, 2008a; Delgado-Saborit *et al.*, 2013; Walgraeve *et al.*, 2010).

Improving the understanding of gas-particle partitioning behaviour is important as this process will influence the extent and nature of potential loss mechanism for PAH, OPAH and NPAH such as chemical reactivity and deposition.

1.4.3. Atmospheric transport of PAHs

Relatively slow photochemical degradation and limited deposition rates can allow PAHs to undergo relatively long range atmospheric transport (LRAT) from their source region (typically the more polluted mid-latitudes in the Northern Hemisphere) to more remote high latitude locations (Keyte *et al.*, 2013 and references therein).

Evidence for LRAT has come from numerous observations of PAHs in air and precipitation/deposition samples at remote continental and mountain sites (Albinet *et al.*, 2008a; Delgado-Saborit *et al.*, 2013; Fernandez *et al.*, 2002; Halse *et al.*, 2011; Klanova *et al.*, 2009; Lammel, 2010; Primbs *et al.*, 2008; Van Drooge *et al.*, 2010; Walgraeve *et al.*, 2010; Xiao *et al.*, 2010); marine sites (Ding *et al.*, 2007; Nizzetto *et al.*, 2008; Tsapakis and Stephanou, 2005) and Arctic or Antarctic sites (EMEP, 2011; Halsall *et al.*, 1997; Halsall *et al.*, 2001; Hung *et al.*, 2005; Jaffrezo *et al.*, 1993; Patton *et al.*, 1991) where local sources are expected to be minimal.

Numerical multimedia modelling has also assessed and in some cases quantified the extent of LRAT (Aulinger *et al.*, 2007; Gusev *et al.*, 2011; Halsall *et al.*, 2001; Prevedouros *et al.*, 2004b; Silibello *et al.*, 2012).

However, investigation of PAH LRAT is hindered by a lack of data on atmospheric processes such as PAH reactivity and volatilisation from surfaces, which are not incorporated into these models (Keyte *et al.*, 2013). For example, volatilisation is estimated to contribute >10% of total global

emissions of Ant and Flt, therefore the gas exchange with vegetation, soils, and surface waters could therefore enhance the LRAT of PAHs (Lammel *et al.*, 2009).

The potential importance of PAH reactivity during long-range transport on the formation of NPAHs and OPAHs has been indicated in ambient sampling (Eiguren-Fernandez *et al.*, 2008b) and experimental (Jariyasopit *et al.*, 2014) studies. However the LRAT behaviour of OPAH and NPAH compounds has not been widely investigated (Yaffe *et al.*, 2001).

1.4.4. Long-term concentration trends

In most developed countries a substantial decline in PAH concentrations has been reported over the last 40 years (WHO, 2000). This downward trend has been observed for most U.K. monitoring sites at urban and suburban locations (Brown *et al.*, 2013; Meijer *et al.*, 2008; Prevedouros *et al.*, 2004a) and at sites in North America (Cortes *et al.*, 2000; Sun *et al.*, 2006) ; Europe (Holoubek *et al.*, 2007) and the Arctic (Becker *et al.*, 2006).

Brown *et al.* (2013) reported that BaP concentrations from monitoring stations in the U.K. have fallen significantly in the last 20 years and that this decline correlates strongly with changes in NAEI-estimated primary emissions (see Figure 1.1). Indeed, a reported decrease in PAH concentrations in Birmingham was attributed to a reduction in emissions as a result of more stringent legislation and cleaner industrial technologies and power generation (Smith and Harrison, 1996).

Specifically, lower PAH concentrations have been linked to the introduction and increased use of catalytic converters for motor vehicles, reduction in coal combustion as an energy source with an increased movement towards oil and natural gas as well as the elimination of emissions from agricultural burning and aluminium production (Murrells *et al.*, 2010; Smith and Harrison, 1996).

There are currently no available data on the long-term concentration trends for OPAH and NPAH compounds in atmospheric samples.

1.4.5. Short term concentration variations

1.4.5.1. Seasonal patterns

PAH, OPAH and NPAH typically exhibit seasonal variations in atmospheric concentration. PAHs have been found at higher concentrations in winter months at urban, suburban and rural sites, particularly for HMW compounds (Brown *et al.*, 2013; Dimashki *et al.*, 2001; Halsall *et al.*, 1993; Harrison *et al.*, 1996; Meijer *et al.*, 2008; Prevedouros *et al.*, 2004a; Smith and Harrison, 1996).

Higher atmospheric concentrations during winter compared to summer at urban sites have also been observed for OPAHs (Albinet *et al.*, 2008a; Andreou and Rapsomanikis, 2009; Brown *et al.*, 2013; Dimashki *et al.*, 2001; Halsall *et al.*, 1993; Harrison *et al.*, 1996; Meijer *et al.*, 2008; Prevedouros *et al.*, 2004a; Schnelle-Kreis *et al.*, 2007; Sienra, 2006; Smith and Harrison, 1996; G Wang *et al.*, 2007) and NPAHs (Albinet *et al.*, 2008a; Bamford and Baker, 2003; Marino *et al.*, 2000; Sienra and Rosazza, 2006; Wei *et al.*, 2012).

Higher winter concentrations can be attributed to increased primary emissions during the colder months when domestic combustion of solid fuels for space heating is expected to be higher (Brown *et al.*, 2013).

The height of the atmospheric boundary layer (ABL) has an important influence on the concentrations of urban air pollutants as this will dictate the extent of dispersion and dilution of atmospheric species (Williams, 2001 ; Holloway and Wayne, 2010). For example, a lower boundary layer will result in pollutants being confined at a higher concentration close to the surface rather than being diluted throughout the free troposphere (Holloway and Wayne, 2010).

It is suggested the colder months will exhibit reduced vertical mixing due to temperature inversion and/or lower atmospheric boundary layer (ABL) height resulting in reduced atmospheric dispersion (Bamford and Baker, 2003; Reisen and Arey, 2005) ; and slower rate of chemical degradation processes (Barbas *et al.*, 1996; Kamens *et al.*, 1989; Prevedouros *et al.*, 2004a).

However, in some instances, higher concentrations of LMW PAHs have been observed in summer, particularly at more remote sites, attributed to local sources due to volatilisation from soil or vegetation sources or sea outgassing (Prevedouros *et al.*, 2004a; Meijer *et al.*, 2008 and references therein). Furthermore, seasonality of NPAH and OPAH concentrations can be influenced by secondary input due to PAH reactivity in the atmosphere (see Section 1.5).

A number of sampling studies have observed enhanced concentrations of NPAH or OPAH compounds at locations downwind of major urban areas, which is more pronounced during summer, suggesting the concentrations of these compounds can increase in the warmer months when levels of atmospheric oxidants (e.g. OH, NO₃, O₃) are higher (Bamford and Baker, 2003; Eiguren-Fernandez *et al.*, 2008a; Reisen and Arey, 2005).

1.4.5.2. Diurnal patterns

Diurnal or nocturnal patterns of PAH, OPAH and NPAH concentrations have been studied in various environments. The diurnal variation of parent PAHs is likely to reflect direct source emission signals e.g. from domestic combustion, biomass burning or road traffic and modification by reactive and/or deposition loss processes as well as the relative height of the ABL (Lee *et al.*, 1998; Reisen and Arey, 2005; Ringuet *et al.*, 2012a; Souza *et al.*, 2014).

In contrast, OPAH and NPAH compounds may display distinct diurnal patterns from those of parent PAH due to the influence of secondary input, for example due to daytime OH and/or nighttime NO₃ reactions, and/or differences in dominant primary sources or photodegradation processes (Arey *et al.*, 1989a; Hien *et al.*, 2007; Reisen and Arey, 2005; Souza *et al.*, 2014; Tsapakis and Stephanou, 2005).

Studies of diurnal patterns commonly focus on 12 hourly 'daytime' and 'nighttime' sampling (Arey *et al.*, 1989a; Hien *et al.*, 2007; Souza *et al.*, 2014). Relatively few studies have investigated shorter-term sampling frequency (Reisen and Arey, 2005 ; Lee *et al.*, 1998 ; Tsapakis and

Stephanou, 2005, which means identifying factors influencing short-term variations in concentration is more difficult. Diurnal sampling over higher resolution time scales is clearly required.

1.4.6. Ambient sampling of PAH in the U.K. atmosphere

1.4.6.1. PAH monitoring in the U.K.

Air sampling campaigns in different locations and over different time scales can provide valuable information regarding the sources, behaviour and fate of PAHs as well as key long-term, short-term and seasonal trends in their concentrations. In the U.K., regular measurements of PAHs have been carried out since 1991, when the Toxic Organic Micropollutants (TOMPS) program was established (Brown *et al.*, 2013).

The TOMPS network began with four sampling locations, but the growing focus and concern over PAHs in the atmosphere led to an expansion of the program in the interceding years, eventually resulting in the establishment of a separate 'PAH Network', funded by the UK Government Department of Farming, Environment and Rural Affairs (Defra). In 2011 there were a total of 36 monitoring sites taking regular measurements of PAHs (Brown *et al.*, 2013), covering a range of location types (including urban, rural, industrial, trafficked and background sites).

These monitoring data have been used to produce publications assessing the concentrations, seasonality, long-term temporal trends and source profiles of PAHs in the UK atmosphere (Jang *et al.*, 2013; Meijer *et al.*, 2008; Prevedouros *et al.*, 2004a) and have been augmented by a number of additional individual sampling studies measuring PAHs (Alam *et al.*, 2013; 2014; Baek *et al.*, 1991; Delgado-Saborit *et al.*, 2013; Dimashki *et al.*, 2000; 2001; Harrad *et al.*, 2003; Harrad and Laurie, 2005; Jang *et al.*, 2013; Jones *et al.*, 1992; Meijer *et al.*, 2008; Prevedouros *et al.*, 2004a; Smith and Harrison, 1996).

Only a very limited data are available for OPAHs and NPAHs in the U.K. atmosphere and no regular or long-term monitoring has been undertaken for these compounds. There is therefore a lack of knowledge regarding the sources, behaviour and fate of OPAH and NPAH in the U.K. atmosphere, or the long- or short-term trends in their atmospheric concentrations.

1.4.6.2. PAHs from road traffic

Road traffic is shown to be a key source of PAHs, OPAHs, NPAHs in urban areas (Fraser *et al.*, 1998a; Jakober *et al.*, 2007; Lim *et al.*, 1999; Oda *et al.*, 1998; Rogge *et al.*, 1993a; Staehelin *et al.*, 1998; Zhu *et al.*, 2003). There is therefore a need accurately assess emission factors of these compounds from vehicle exhausts and to estimate the relative and overall contribution of road traffic to the concentrations of different PAHs, OPAHs and NPAHs present in the ambient urban atmosphere in relation to other combustion sources (e.g. industrial emissions, domestic burning) and influencing factors (e.g. chemical reactivity, volatilisation from surfaces).

However, accurately measuring on-road vehicular emissions of PAHs, OPAHs and NPAHs is complicated by the mixture of engine and fuel types and emission control technologies present. Sampling in road tunnels can provide a more realistic traffic profile than using dynamometer tests (Oda *et al.*, 2001; Wingfors *et al.*, 2001). Experimental studies in a laboratory will only yield data on specific vehicles, engine characteristics and/or fuel formulations, whereas a tunnel will contain a realistic range of different vehicles. Additionally, repeated monitoring in a tunnel environment can assess changes in PAH emission profiles in response to changes in fuel usage or emission control measures (Ravindra *et al.*, 2008).

Road tunnels provide an ideal environment to assess traffic emission profiles as tunnels are assumed to have :

- High traffic density
- Realistic distribution of on-road vehicles

- Relatively low dispersion rate
- Relatively low sunlight and chemical reactivity
- Lack of inputs from other primary sources

1.5. Fate of PAHs, OPAHs and NPAHs in the atmosphere

1.5.1 Wet and dry deposition of PAHs

PAHs can be lost from the atmosphere via direct settling to the surface (dry deposition) or via precipitation in rain droplets or snow fall (wet deposition). This can occur either in the gas-phase or by loss of particulate matter to which the PAH compounds are associated (Bidleman, 1988). The wet and dry deposition processes are discussed in detail by Keyte *et al.* (2013).

The relative rates of wet or dry deposition of PAHs from the atmosphere is dependent on the physiochemical properties of the PAH (solubility in water, Henry's Law constant, vapour pressure), degree of phase partitioning, meteorological parameters (rainfall levels, temperature) and concentration and composition of particulate matter (Keyte *et al.*, 2013).

Wet deposition of PAHs is not expected to be an efficient process unless the substance is associated with PM (Bidleman, 1988; Ligocki *et al.*, 1985). The removal rate of PAH at a Central European site ranged between <2 weeks and >2 weeks for dry and wet deposition respectively (Skrdlikova *et al.*, 2011) indicating dry deposition as the potentially more important process.

Modelling predictions of the relative loss rates of PAHs to various loss processes in the U.K. were made by Prevedouros *et al.* (2004b). The relative percentage loss rates for a number of PAHs predicted are shown in Figure 1.9, which indicate that for LMW (3-4 ring) PAH, wet and dry deposition are minor loss processes relative to OH radical reactivity. However, for HMW (5+ ring) PAHs, which are associated primarily with PM, wet and dry deposition is indicated to be a more important process.

1.5.2. Photolysis

1.5.2.1. Photolysis of PAHs

Direct photolysis is not expected to be a significant sink for PAHs in the gas phase (Atkinson and Arey, 1994 and references therein). However, PAH adsorbed on PM may be susceptible to photolysis due to the wide electron delocalization of PAHs, enabling them to absorb solar radiation and undergo photooxidation (Vione *et al.*, 2006). The chemistry (rates, products and mechanisms) of direct photolytic PAH decomposition has been investigated for PAHs associated with organic aerosols, inorganic substrates, and the air-ice interface (please see Keyte *et al.*, 2013 for full list of references; the reader is directed to Finlayson-Pitts and Pitts, 2000 and Vione *et al.*, 2006 for discussion of PAH photolysis reactions).

Half lives of PAH compounds towards photolysis on various substrates measured by (Behymer and Hites, 1985,1988) are shown in Table 1.3. Degradation rates are influenced strongly by substrate type with relatively faster rates observed on mineral surfaces (e.g. silica gel) than on carbonaceous particles (e.g. fly ash and carbon black). A number of PAHs (e.g. Ace, Acy, Ant, BaA, BaP) are shown to display relatively fast (<5 hr) photolysis on silica and alumina (Behymer and Hites, 1985;1988) while other compounds appear to degrade slowly on all substrates.

It is indicated that PAHs associated with carbonaceous particles (fly ash or carbon black) are less susceptible to photooxidation (Behymer and Hites, 1985,1988; Korfmacher *et al.*, 1980; Yokley *et al.*, 1986) due to higher carbon content and darker colour of the substrate. Kamens *et al.* (1988) also demonstrated that rate of PAH photodegradation is influenced by solar intensity, humidity and pressure.

The ability for carbonaceous particles to shield radiation, means that photo-degradation of PAHs is believed to be minimal relative to gas-phase reaction with OH or NO₃ radicals (Vione *et al.*, 2006). However, it is noted that relatively rapid sensitised photolysis processes can be initiated by compounds such as PAH quinones and carbonyls, either present in direct emissions or partially derived from PAH photooxidation (Vione *et al.*, 2006).

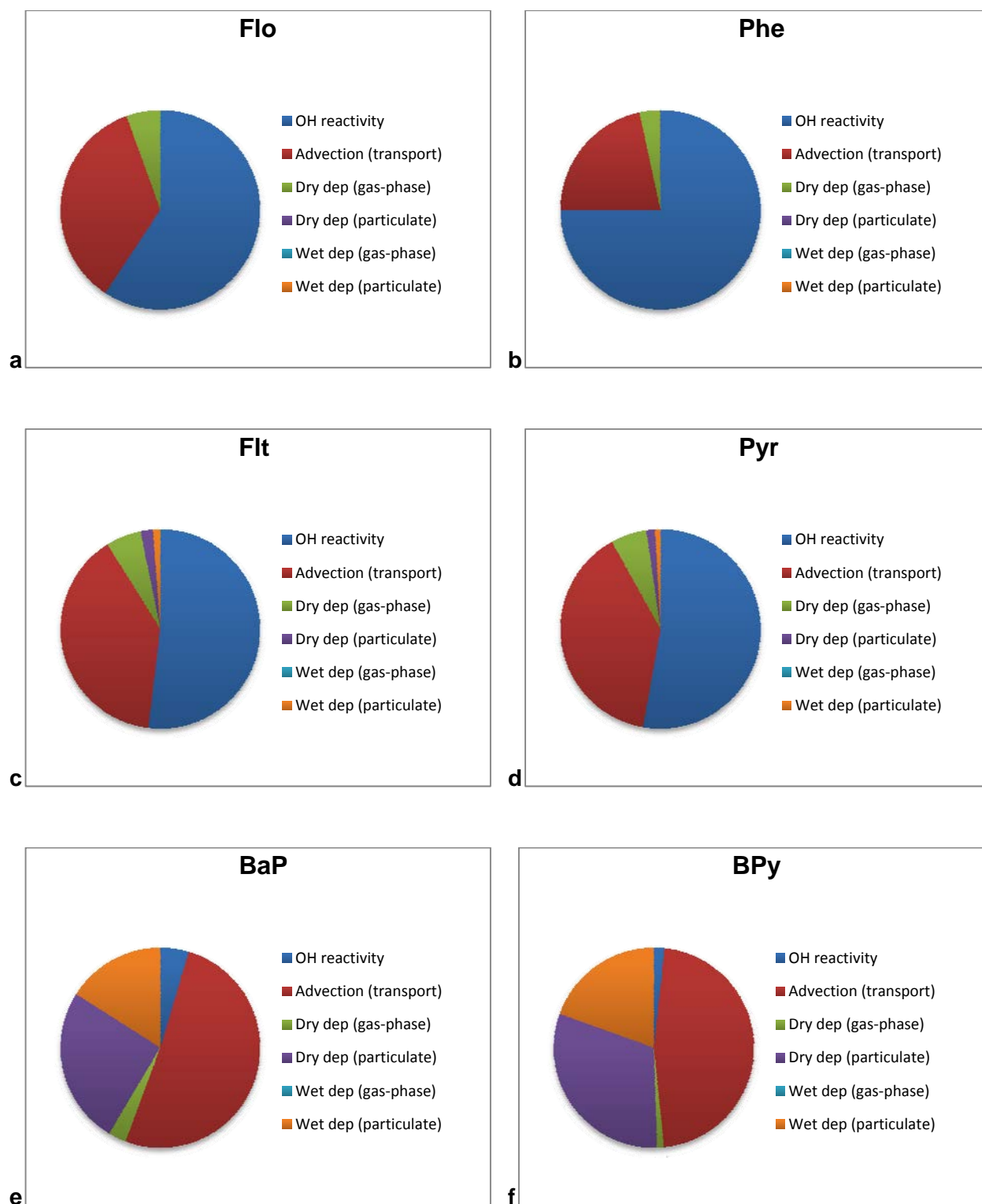


Figure 1.9. Predicted contribution of different loss mechanisms for PAH compounds in the U.K. based on modelled flux rates for a) Flo, b) Phe, c) Flt, d) Pyr, e) BaP and f) BPY (Prevedouros *et al.*, 2004b).

Table 1.3. Half lives (hours) of PAH compounds absorbed on various substrates; carbon back (CB), fly ash (FA), silica gel (SG) and alumina (AL), as reported by Behymer and Hites (1988) for PAH absorbed at 25 µg/g.

	CB	FA ^a	FA ^b	FA ^c	FA ^d	SG	AL
Acy	166	1000	70	89	17	0.6	1.5
Ace	nm	1000	105	76	18	1.6	1.4
Flo	1000	1000	332	500	38	245	55
Phe	1000	1000	500	500	244	268	44.5
Ant	313	608	132	51	19	1.6	0.4
Flt	1000	1000	437	235	330	99.1	22.5
Pyr	1000	1000	357	201	119	35.5	22.5
BaA	651	1000	201	137	19	2.4	1.6
Chr	688	1000	172	334	500	101	59.5
BeP	1000	1000	163	409	338	64.5	79.1
BaP	574	805	125	213	28	2.7	1
IPy	1000	1000	120	304	492	62	38.9
BPy	1000	1000	119	373	224	10.5	20.4
Cor	1000	1000	115	335	487	97.1	104

a – black fly ash, high (59% bulk) carbon content

b – black fly ash, low (22% bulk) carbon content

c – grey fly ash

d – white fly ash

1.5.2.2. Photolysis of OPAH and NPAH

Photolysis of NPAHs has been indicated as a potentially important loss process for both gas-phase and particle-associated compounds (WHO, 2003). The gas-phase N-Nap compounds are shown to be highly susceptible to photolysis with an atmospheric lifetime of <1 to 2 hrs (Atkinson *et al.*, 1989; Feilberg and Nielsen, 2000; Niu *et al.*, 2005; Phousongphouang and Arey, 2003a). For example, Atkinson *et al.* (1989) noted atmospheric lifetimes for NNap compounds due to photolysis were ~38 and ~28 times lower respectively than for their corresponding gas-phase reaction with OH.

Photolysis of NPAHs associated with particles has been studied to assess the mechanisms, products and atmospheric significance of this process (Arce *et al.*, 2008; Chapman *et al.*, 1966; Fan *et al.*, 1995; Fan *et al.*, 1996a; Feilberg and Nielsen, 2000; Healy *et al.*, 2012; Holloway *et al.*, 1987; Ioki, 1977; Kameda, 2011; Pitts, 1983; Stark *et al.*, 1985).

While Holloway *et al.* (1987) noted relatively long photolysis half-lives for 1NPyr and 3NFlt of 1.2 to 6 days and 12.5 to >20 days respectively, other studies suggest this process can be a potentially significant atmospheric sink for particle-bound NPAHs. Fan *et al.* (1996a) derived half-lives due to photolytic decay for 1NPyr, 2NFlt and 2NPyr on diesel soot and wood smoke in an outdoor chamber of 0.8 to 1.2 hr with faster reaction noted for 1NPyr on wood smoke particles.

Photolysis of OPAH has received comparatively little attention in the literature. It is indicated that gas-phase compounds such as 1,4-naphthoquinone are degraded at a comparable rate to gas-phase NNap compounds (Atkinson *et al.*, 1989). However, particle-associated OPAHs are believed to be relatively stable towards solar irradiation (Kamens *et al.*, 1989).

1.5.3 Atmospheric reactivity of PAHs

Chemical reactions represent a key atmospheric loss process for both gas-phase and particle-phase PAH and can be an important secondary source for a number of OPAH and NPAH compounds (Atkinson and Arey, 1994; 2007; Finlayson-Pitts and Pitts, 2000). The reaction kinetics, mechanisms and OPAH or NPAH formation products of gas-phase and heterogeneous PAH reactions has been reviewed by Keyte *et al.* (2013). Included here is a summary of key points discussed in the review. For a more detailed discussion the reader is directed to the specific sections of the review paper.

1.5.3.1. Gas-phase PAH reactions

Atmospheric reactions of gas phase PAHs with key atmospheric oxidants (OH, NO₃ and O₃) and the relative importance of these processes in the removal of PAHs from the atmosphere and conversion to derivative compounds have been widely investigated in laboratory experiments (Arey *et al.*, 1986; 1989b; Atkinson and Aschmann, 1986; Atkinson *et al.*, 1987a; 1988; 1990a; 1990b; 1994; Brubaker and Hites, 1998; Helmig and Harger, 1994; Kwok *et al.*, 1994a,1997; Phouongphouang and Arey, 2002,2003b; Reisen and Arey, 2002).

Rate coefficients have been derived for the gas phase reaction of OH, NO₃ and O₃ with 2-4 ring PAHs (Table A1, A2 and A3 in Appendix 1 respectively) in laboratory investigations. Reactions of PAHs with OH proceed up to 5 orders of magnitude faster than the corresponding reactions with NO₃, suggesting that OH-initiated reactions represent a more important degradation process for PAHs than reactions with NO₃.

There is shown to be considerable variability in reactivity and hence the expected atmospheric lifetime of different PAHs. Acy and Ant are shown exhibit the fastest reactivity towards OH. The rate and products of the reactions are dependent upon the precise reaction mechanism and can be influenced by factors such as steric hindrance of reactive sites (Brubaker and Hites, 1998) and the number and type of substituted groups. For example, the presence of alkyl-groups on Nap and Phe has been shown to increase reactivity towards OH and NO₃ relative to parent PAH, following general order of reactivity dimethyl-PAH > ethyl-PAH > methyl-PAH > PAH (Lee *et al.*, 2003; Phouongphouang and Arey, 2003b).

OH-initiated PAH reactions are considered to be important only during daytime due to the photolytic nature of atmospheric OH formation (Atkinson and Arey, 2007; Krol and Lelieveld, 2003; Prinn *et al.*, 2005). NO₃ radicals are formed via the sequential reactions of NO and NO₂ with O₃ (Atkinson and Lloyd, 1984; Atkinson *et al.*, 1986; Atkinson *et al.*, 1990b; Geyer *et al.*, 2001; Geyer *et al.*, 2003) :

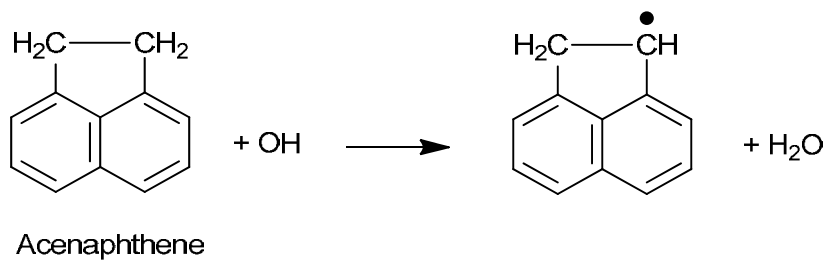


NO_3 can be removed from the troposphere via photolysis by solar radiation (Atkinson and Aschmann, 1986; Atkinson *et al.*, 1990a; Graham and Johnston, 1978) or via reaction with NO.

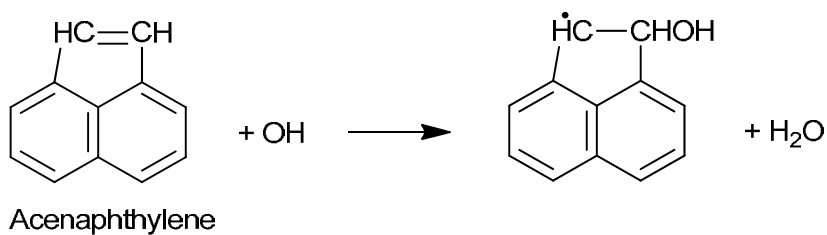


Atmospheric reactions with NO_3 are therefore only expected to occur during evening and night time hours when photolysis is absent and NO levels are low (Atkinson *et al.*, 1984; Atkinson and Arey, 1994; 2007). The reactions of PAHs with OH radicals are shown to proceed via the same initial mechanism, initiated via two pathways (Figure 1.10); (1) OH radical interaction with substituent groups either through H-atom abstraction from C-H groups (1a), or, in the case of Acy which contains an unsaturated cyclopentafused ring, addition to the $>\text{C}=\text{C}<$ bond of this substituent (1b); or (2) OH addition to the aromatic ring, forming an initially energy-rich PAH-radical adduct radical intermediate, which can further react with NO_2 or O_2 , to form products (Atkinson and Arey, 1994).

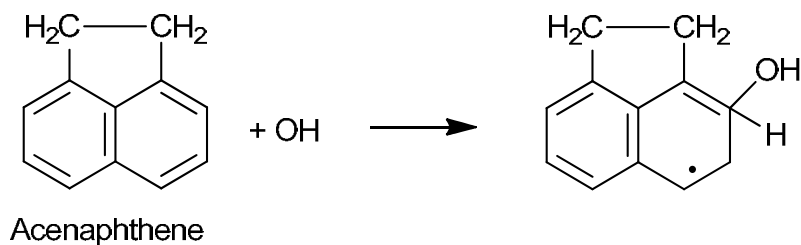
For OH reactions, the radical-addition mechanism is shown to dominate at room temperature, while at elevated temperatures, H-atom abstraction from the C-H bonds will become increasingly important (Ananthula *et al.*, 2006,2007; Atkinson *et al.*, 1987a; Goulay *et al.*, 2005; Lee *et al.*, 2003; Lorenz and Zellner, 1983). It is suggested that reactions of the PAH-OH adduct with NO_2 and O_2 may be competitive for NO_2 mixing ratios down to 60 ppbV (Nishino *et al.*, 2008).



1a.



1b.



1c.

Figure 1.10. Mechanism for the reaction of gas-phase PAHs with OH radicals ; a) H-atom abstraction; b) OH addition to substituent groups; c) OH addition to the aromatic ring (Atkinson and Arey, 1994). Originally presented in Keyte *et al.* (2013).

It is indicated that the NO₃ reaction proceeds via an analogous radical addition or H-atom abstraction mechanism as the OH reaction. The competing reaction pathways of the NO₃-addition mechanism are depicted in Figure 1.11. As discussed by Atkinson and Arey (2007), studies investigating PAH reaction kinetics with NO₃ radicals have used N₂O₅ as a precursor for NO₃ radicals, which will also result in the formation of NO₂ in these systems. Measured second order rate coefficients for the reactions of NO₃ radicals with naphthalene and alkyl-naphthalenes (see Appendix 1) have been shown to be proportional to the NO₂ concentration (Atkinson, 1991), with the rate of reaction described as :

$$-d[\text{PAH}]/dt = k_{\text{obs}}[\text{PAH}][\text{NO}_3][\text{NO}_2] \quad (1.5)$$

The reaction rate of the NO₃ reaction can therefore be defined in terms of the reactions routes in Figure 1.11. (Atkinson and Lloyd, 1984; Atkinson *et al.*, 1994; Pitts *et al.*, 1985a; Wallington *et al.*, 1987) :

$$-d[\text{PAH}]/dt = k_a(k_c[\text{NO}_2] + k_d[\text{O}_2] + k_e) [\text{PAH}] [\text{NO}_3] / (k_b + k_c[\text{NO}_2] + k_d[\text{O}_2] + k_e) \quad (1.6)$$

where :

k_a = rate coefficient of of PAH-NO₃ adduct formation

k_b = rate coefficient of PAH- NO₃ adduct dissociation

k_c = rate coefficient of PAH- NO₃ adduct reaction with NO₂ to form products

k_d = rate coefficient of PAH- NO₃ adduct reaction with O₃ to form products

k_e = rate coefficient of PAH- NO₃ unimolecular decomposition to form products

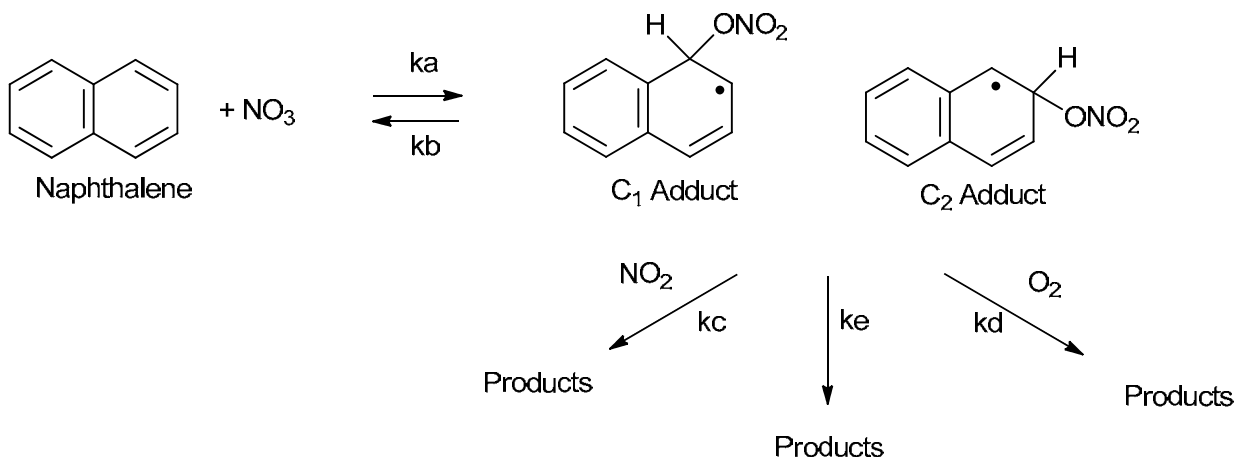


Figure 1.11. Potential pathways for the reaction of PAHs with NO_3 (Atkinson and Arey, 2007). Originally presented in Keyte *et al.* (2013).

It is indicated from experimental data (Atkinson *et al.*, 1987a; Atkinson *et al.*, 1990b; Atkinson, 1991; Atkinson *et al.*, 1994; Kwok *et al.*, 1994a; Phousongphouang and Arey, 2003b; Pitts *et al.*, 1985c), that under conditions used in reaction studies and in the ambient troposphere :

$$k_b \gg (k_c[\text{NO}_2]) \quad \text{and} \quad k_c[\text{NO}_2] > (k_d[\text{O}_2] + k_e)$$

Hence :

$$-d[\text{PAH}]/dt = k_a k_c[\text{NO}_2][\text{PAH}][\text{NO}_3]/k_b \quad (1.7)$$

The observed second order rate coefficient (k_{obs}) for the reactions of LMW PAHs with NO_3 (as presented in Appendix 1) can therefore be derived by simplified equation (Atkinson and Arey, 2007) :

$$k_{\text{obs}} = k_a k_c / k_b \quad (1.8)$$

The rate coefficient of PAH reactions with NO_3 will therefore be proportional to NO_2 concentration, if the reaction involves formation of the PAH- NO_3 adduct. (Atkinson *et al.*, 1994) indicate the reaction Nap- NO_3 adduct with NO_2 is expected to dominate relative to the reaction with O_2 down to a NO_2 mixing ratio of at least 80 ppbV and possibly much lower (Atkinson and Arey, 2007).

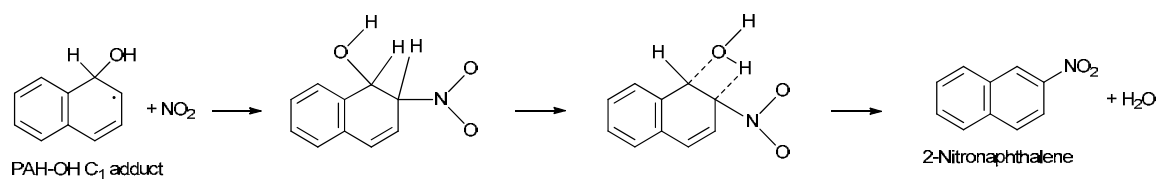
Both ring-retaining compounds (e.g. hydroxy-PAHs, NPAHs and OPAHs such as quinones and ketones) and ring-opened products (e.g. 2-formylcinnamaldehyde, phthalic acid and phthalaldehyde) have been identified from OH and NO_3 reactions of PAHs (Arey *et al.*, 1986; 1989b; Atkinson *et al.*, 1987a, 1990a; Bunce *et al.*, 1997; Kautzman *et al.*, 2010; Kwok *et al.*, 1997; Lee and Lane, 2009; Nishino *et al.*, 2008; Reisen and Arey, 2002; Sasaki *et al.*, 1997b; L Wang *et al.*, 2007a).

Several studies have proposed reaction pathways for the formation of these products. For example, Qu and co workers conducted theoretical predictions for the mechanism of Nap-OH and Nap- NO_3 adducts reactions with NO_2 and/or O_2 using molecular orbital calculations. Pathways to NPAH and OPAH from OH- and NO_3 PAH adducts were derived (see Figure 1.12 and 1.13 respectively; further examples in Keyte *et al.*, 2013).

Reactions of NO_3 with a number of PAHs (e.g. Nap, Ace, Flt) yield NPAH products at higher NPAH yields than OH reactions. For example the yield of 1NNap, 2NNap and 2NFlt from OH reaction is reported to be 0.3%, 0.3% and 3% respectively, compared with yields of 17%, 7% and 24% respectively for NO_3 reactions (Atkinson and Arey, 1994). This suggests that while NO_3 reactions appear to be less significant than OH reactions as a PAH degradation process, night-time reactions of PAHs with NO_3 may be a significant contributor atmospheric NPAH, in addition to daytime OH reactions.

Experimental studies indicate reactions of PAH with O_3 are much slower than OH and NO_3 and this process is generally considered to be of negligible importance (Atkinson and Arey, 1994). The reaction of Acy is shown to be faster (~3 orders of magnitude) than other PAHs due to interaction of ozone with the $>\text{C}=\text{C}<$ bond of the cyclopenta-fused ring (Reisen and Arey, 2002).

a)



b)

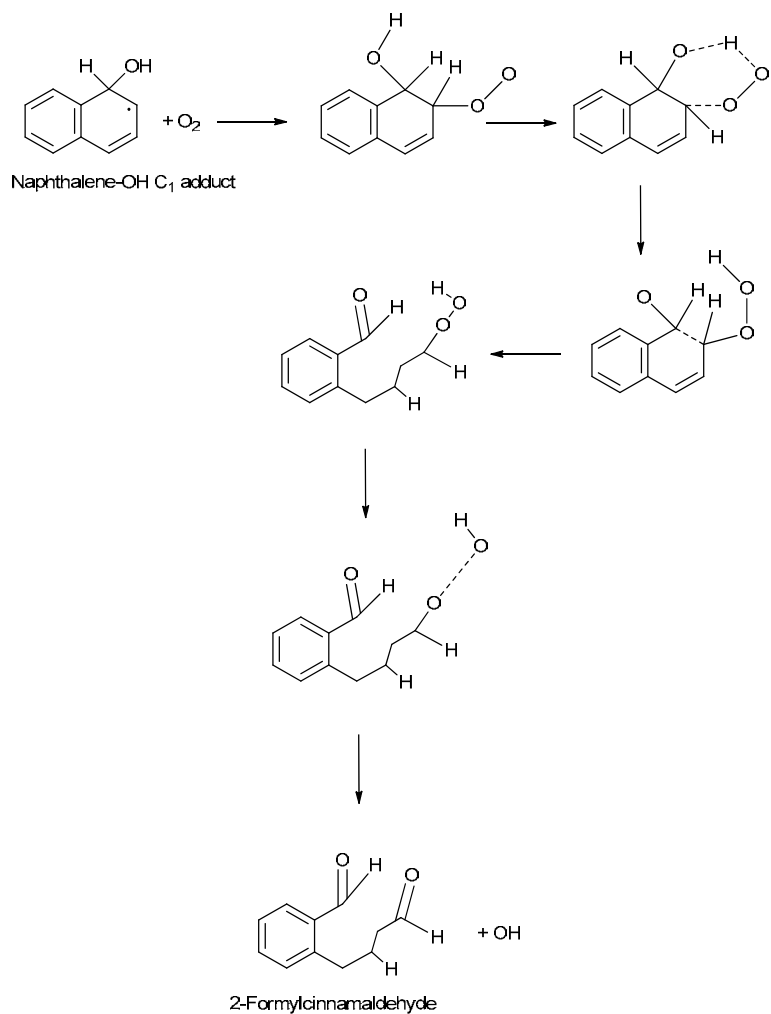


Figure 1.12. Proposed mechanisms for two possible further reaction pathways of the PAH-OH adduct: a) reaction with NO₂; b) reaction with O₂ (Qu *et al.*, 2006b). Originally presented in Keyte *et al.* (2013).

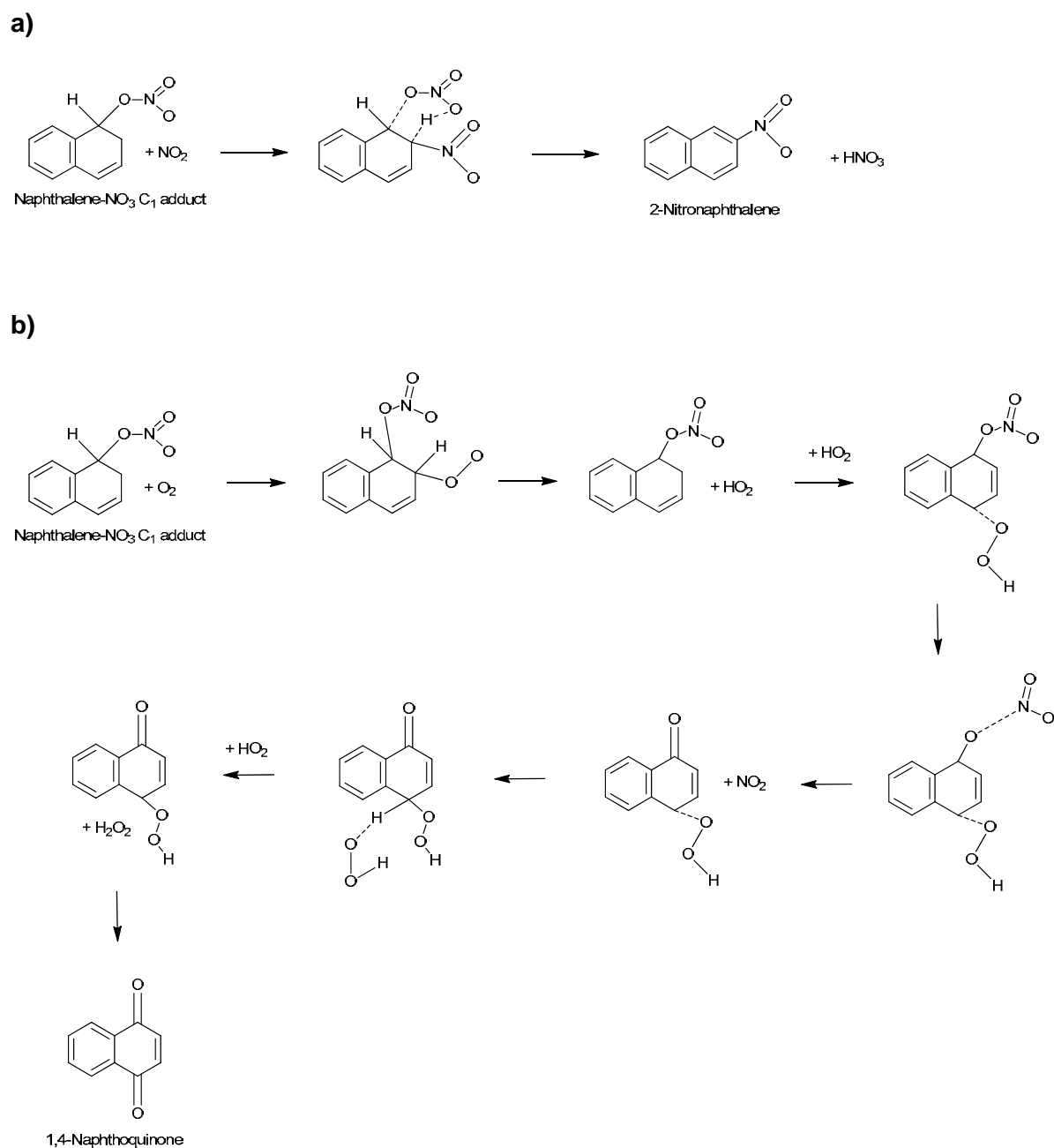


Figure 1.13. Proposed mechanisms for two possible further reaction pathways of the PAH-NO₃ adduct: a) reaction with NO₂; b) reaction with O₂ (Qu *et al.*, 2006a) . Originally presented in Keyte *et al.* (2013).

1.5.3.2. Heterogeneous reactions

The reaction kinetics, mechanisms and products of PAHs on solid substrates has been studied extensively in laboratory experiments.

Substrate surfaces studied include both carbonaceous (graphite, soot, and diesel exhaust) and mineral (silica, MgO) particles for reactions with OH (Bedjanian *et al.*, 2010; Bertram *et al.*, 2001; Estéve *et al.*, 2003,2004,2006; Jariyasopit *et al.*, 2014; Miet *et al.*, 2009a; Ringuet *et al.*, 2012b), NO₃/N₂O₅ (Karagulian and Rossi, 2007; Liu *et al.*, 2012; Mak *et al.*, 2007; Pitts *et al.*, 1985a; 1985b; 1985c; Zimmermann *et al.*, 2013) , NO₂ (Brorstrom-Lunden and Lindskog, 1985; Butler and Crossley, 1981; Guo and Kamens, 1991; Inazu *et al.*, 1997; Jariyasopit *et al.*, 2011; 2014; Ma *et al.*, 2011; Miet *et al.*, 2009c; Nguyen *et al.*, 2009; Perraudin *et al.*, 2005; Pitts *et al.*, 1978; Ramdahl *et al.*, 1984; Tokiwa *et al.*, 1981; Wang *et al.*, 2000; Zimmermann *et al.*, 2013), , O₃ (Brorstrom *et al.*, 1983; Kahan *et al.*, 2006; Katz *et al.*, 1979; 2004; Kwamena *et al.*, 2006; Lane and Katz, 1977; Lindskog *et al.*, 1985; Miet *et al.*, 2009b; Mmereki and Donaldson, 2003; Mmereki *et al.*, 2004; Perraudin *et al.*, 2007; Pitts *et al.*, 1977; 1980). Derived rate coefficients for these processes are presented in Table A4 in Appendix 1.

The rate, mechanism and products of atmospheric gas-particle PAH reactions are shown to depend strongly on the structure and UV-vis absorption spectra of the PAH compound as well as the physical and chemical nature of the particle surface to which they are associated (Finlayson-Pitts and Pitts, 2000; Keyte *et al.*, 2013). Reactions with OH and NO₃/N₂O₅ are indicated to be the dominant pathway for heterogeneous degradation of PAHs compared with reactions with NO₂ and O₃. However, loss rates are shown to be more comparable when expected atmospheric concentrations of the oxidants are considered (Keyte *et al.*, 2013).

Particles are shown to exhibit an 'inhibiting factor' on PAH reactivity (Estéve *et al.*, 2004,2006; E. Perraudin *et al.*, 2007). For example OH reactions on carbonaceous particles are shown to proceed 1-3 orders of magnitude lower than corresponding gas-phase reactions. This stabilisation is shown to be variable between species and substrates and has been attributed to the relatively

slow diffusion of the oxidant or inaccessibility of PAHs in the bulk particle (Jariyasopit *et al.*, 2014; Zimmermann *et al.*, 2013).

A wide variety of ring-opened and ring-retaining products have been identified from heterogeneous reactions of PAH including OPAH and NPAH compounds.

In some cases, a distinction is noted between the products of gas-phase and particle-phase reactions. For example 1NPyr has been observed as a reaction product in the reaction of particle-bound PAH (Miet *et al.*, 2009c; Ramdahl *et al.*, 1984; Wang *et al.*, 2000), which is not observed in gas-phase reactions.

However, other OPAH and NPAH e.g. 2NFlt, 2NPyr have been observed in both gas-phase and particle-phase reactions (Arey *et al.*, 1986; Atkinson *et al.*, 1990a; Inazu *et al.*, 1997; Ringuet *et al.*, 2012b). Reaction pathways in the formation OPAH (Figure 1.14) and NPAH (Figure 1.15) products have been proposed for reactions of NO₂ and O₃ respectively (Keyte *et al.*, 2013).

Heterogeneous PAH reactivity with atmospheric oxidants is complex and is influenced by a number of factors including the PAH molecule, the nature (chemical composition, surface area, porosity) of the matrix, presence of other species (e.g. nitric acid, water or other organic species), oxidant concentration, and PAH surface concentration (Keyte *et al.*, 2013 and references therein). For example, the reactivity of PAHs towards NO₂ is shown to be enhanced by the presence of nitric acid and/or HNO₂ gas on the particle surface (see Figure 1.15).

It is suggested from these studies that particle-phase reaction can contribute to PAH degradation and OPAH or NPAH formation in the atmosphere. However, the wide diversity in chemical composition (organic, mineral, biogenic), sources (combustion, erosion, gas phase condensation), origin (natural, anthropogenic), formation conditions (temperature, pressure), physical properties (size, porosity, specific surface area) and surface coatings (water, nitric acid, organic molecules) of particles mean heterogeneous PAH reactivity will be extremely difficult to predict or assess in the

ambient atmosphere and the relative importance of these factors will be highly variable across different environments (Keyte *et al.*, 2013).

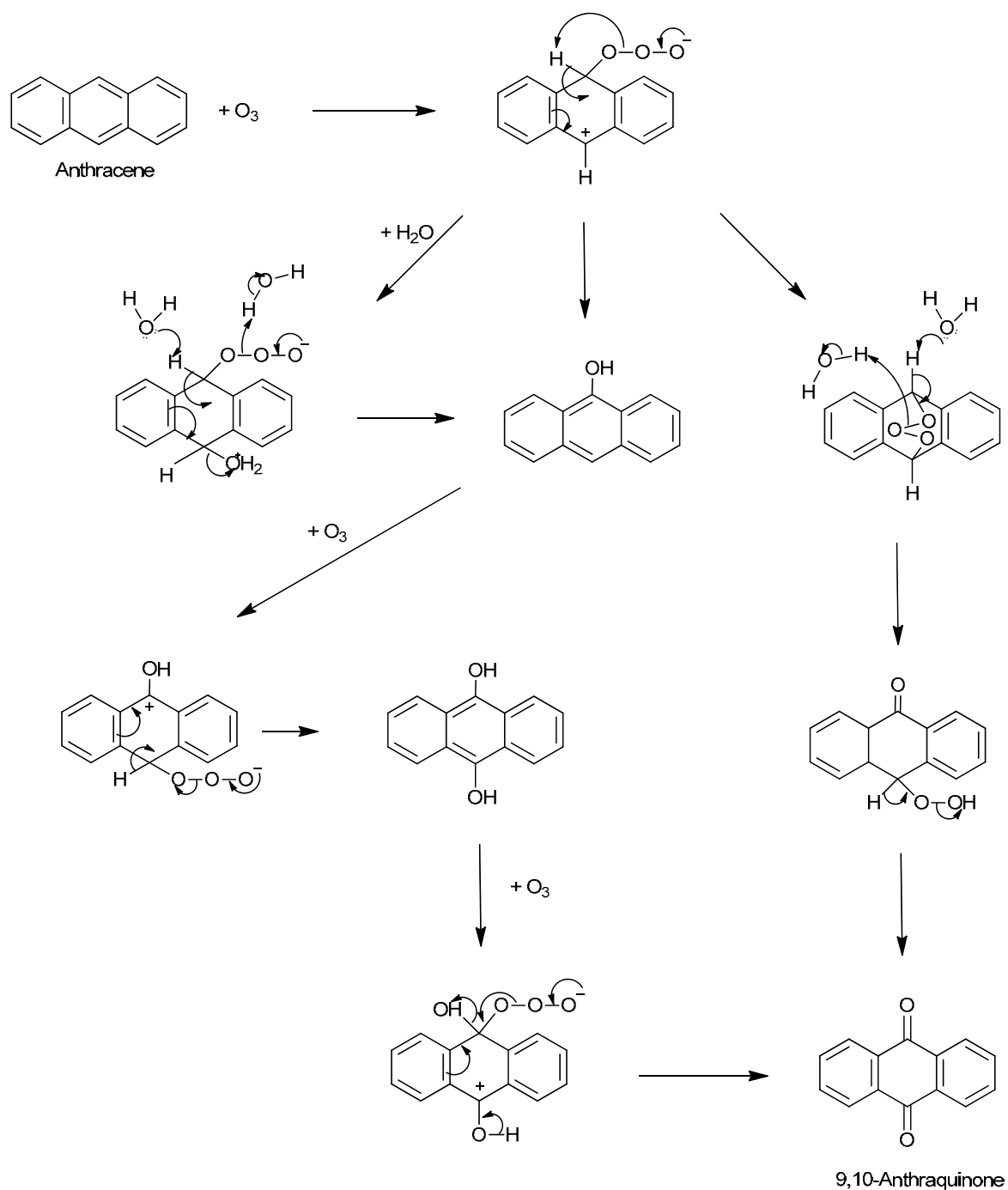


Figure 1.14. Suggested mechanisms for the heterogeneous reaction of anthracene with O_3 (Mmereki *et al.*, 2004). Originally presented in Keyte *et al.* (2013).

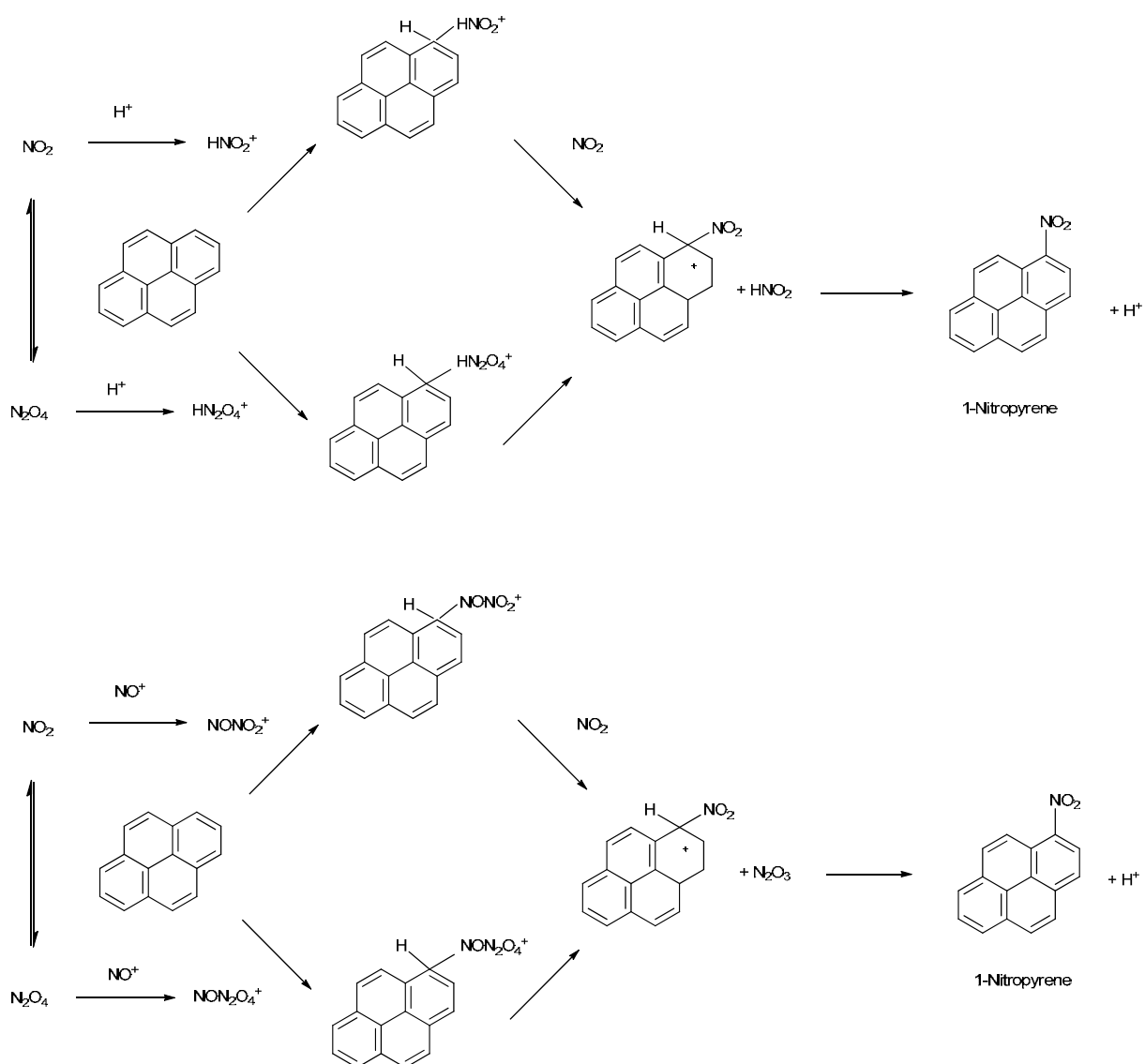


Figure 1.15. Suggested mechanisms for the heterogeneous reaction of pyrene with NO₂ (Wang *et al.*, 1999,2000). Originally presented in Keyte *et al.* (2013).

1.5.3.3. Evidence for PAH reactions in ambient air samples

Laboratory investigations strongly indicate that gas- and particle-phase atmospheric reactions of PAHs can contribute to observed atmospheric levels of NPAH and OPAH. However, the applicability of laboratory data in the ambient environment is uncertain. For example recent studies observing heterogeneous formation of NPAHs on atmospheric PM from reactions of PAH with $\text{NO}_3/\text{NO}_2/\text{N}_2\text{O}_5$ have used oxidant concentrations that are >100 times higher than typically observed in the ambient atmosphere (Jariyasopit *et al.*, 2014; Zimmermann *et al.*, 2013).

A number of ambient sampling approaches, in addition to or in conjunction with, laboratory reaction kinetics data, have been conducted to answer the key questions : i) To what extent do PAH reactions occur under ambient atmospheric conditions? ii) What is the relative contribution of reactions to observed atmospheric levels of OPAH and NPAH compared with primary combustion emissions?

As discussed by Keyte *et al.* (2013), the position on the aromatic ring where PAH oxidation or nitration occurs will determine the specific OPAH or NPAH isomer formed. Differences in NPAH formation mechanism between combustion and atmospheric photoreaction processes are observed leading to distinct NPAH isomer distributions. Assessing the relative levels of these different NPAH isomers in the ambient atmosphere could therefore indicate the relative contribution of primary and secondary inputs.

For example, in the case of Pyr and Flt, electrophilic nitration, expected to occur during primary combustion processes (Nielsen, 1984; Ruehle, 1985) is shown to produce 1NPyr and 3NFlt. 1NPyr has been identified in a number of combustion sources but is not observed as a gas phase reaction product, making it suitable as a marker for direct emissions (IARC, 1989). Conversely, the products of the gas phase OH and/or NO_3 radical initiated reactions are 2NPyr and 2NFlt (Atkinson and Arey, 1994), which are typically not observed in primary combustion emissions.

2NFlt has been observed in a direct industrial emission from carbon electrode manufacture (Liberti and Ciccioli, 1986) but this is not considered to be a major contributor on a large scale. (Zhu *et al.*, 2003) also identified 2NFlt in diesel vehicle emissions but with an emission rate significantly lower (~0.2%) than that of 1NPyr.

Due to their distinct origins, the ratio of 2NFlt to 1NPyr concentration ratio can be used to assess the relative contributions of atmospheric reactions (OH and/or NO₃) and direct emissions (Ciccioli *et al.*, 1989; Ciccioli *et al.*, 1996; Feilberg *et al.*, 2001; Marino *et al.*, 2000; Wang *et al.*, 2011a). Similarly, isomer profiles of NPAH products of Nap, methyl-Naps and ethyl-Naps (Reisen and Arey, 2005; Wang *et al.*, 2010) as well as nitro-triphenylenes (Kameda, 2011) have also been used to assess the relative importance of daytime OH and nighttime NO₃ reactions and primary emissions. The ratios of OPAH or NPAH to their parent PAH in ambient samples and the temporal or seasonal trend in these ratios have also been used to assess the relative importance of atmospheric reactions (Alam *et al.*, 2013; 2014; Reisen and Arey, 2005; Walgraeve *et al.*, 2010).

Diurnal profiles of NPAH and OPAH have been shown to be distinct from those of PAH (Hien *et al.*, 2007; Reisen and Arey, 2005; Tsapakis and Stephanou, 2005). Studies suggest that profiles of PAH and 1NPyr are driven by emission strength and losses due to reactivity, while 2NFlt and 2NPyr are driven by atmospheric formation and loss processes.

(Kojima *et al.*, 2010) observed strong correlations between OPAH concentrations and primary emissions such as PAHs and CO in Tokyo in winter, while a much weaker correlation was observed in summer. Concentration ratios in summer:winter were shown to be higher for 2NFlt (0.36) than for 1NPyr (0.19-0.27), indicating the relative dominance of direct emissions in winter and a greater importance of atmospheric reactivity in summer.

The ratio of 'night time' to 'daytime' PAH concentrations measured in the atmosphere have been shown to correlate with OH radical reaction rate coefficients, with the largest ratios being observed for PAHs most reactive towards OH radicals (Arey *et al.*, 1989a; Phousongphouang and Arey, 2002).

Atmospheric levels of NPAHs have been predicted based on calculations using experimental data (OH reaction rate coefficients, NPAH formation yields, measured parent PAH concentrations and NPAH photolysis rate) and have been observed to be in good agreement with concentrations in ambient air samples (Arey *et al.*, 1990; Atkinson and Arey, 2007). Furthermore, the concentration profile of NNAp, methyl-NNAp, dimethyl-NNAp and ethyl-NNAp isomer product profiles observed in laboratory OH and NO₃ reaction experiments have been shown to closely resemble those of daytime (Reisen *et al.*, 2003) and nighttime (Gupta *et al.*, 1996) profiles from ambient sampling respectively.

While PAH levels are shown to be higher in urban areas during winter compared to summer, OPAH and NPAH levels have been observed at higher levels downwind of an urban source area in summer (Reisen and Arey, 2005) indicating the influence of photochemical reactions. Eiguren-Fernandez *et al.* (2008b) investigated the changes in phenanthrenequinone (PQ) concentration with increasing distance downwind of the highly polluted Los Angeles basin. A significant increase in PQ concentration was observed along this trajectory with an estimated ~90% of PQ at the receptor site resulting from photochemical reactions.

1.5.4. Reactions of OPAH and NPAH

It is indicated that reaction with OH, NO₃ and O₃ is not a significant loss process for gas-phase NPAHs or OPAHs (Atkinson *et al.*, 1989). Photodegradation is considered to be the primary loss process for NPAH in the atmosphere in both gas- and particle-phases (Atkinson *et al.*, 1989; Fan *et al.*, 1995; Fan *et al.*, 1996a; Feilberg and Nielsen, 2000; Phouongphouang and Arey, 2003a).

While photolysis is expected to be the major loss process for during daylight hours, particle-bound NPAHs are shown to react with O₃, which could present an additional degradation pathway at night (Fan *et al.*, 1996b; Miet *et al.*, 2009b; Ringuet *et al.*, 2012b).

Heterogeneous formation and decay have been observed for NPAHs due to reactions of OH, and O₃/NO₂ on natural aerosol particles (Ringuet *et al.*, 2012b). The reaction particle-associated NPAH

and OPAH compounds with NO₃ have been observed and product identification has been noted (Zhang *et al.*, 2011) but this has not been investigated in terms of a potential atmospheric loss process.

Relatively few data are available on the reaction processes of OPAHs in the atmosphere. Kamens *et al.* (1989) indicated that OPAHs such as AQ on wood smoke particles are relatively stable towards photolysis but are shown to decay when exposed to O₃. (Ringuet *et al.*, 2012b) demonstrated OPAHs are also degraded by OH radicals on natural aerosol particles. However, the kinetics of these processes are yet to be fully investigated.

1.6. Project aims and objectives

This introductory section has highlighted the following issues :

PAHs, OPAHs and NPAHs are important pollutants influencing ambient air quality and public health, particularly in urban areas where source strength and population density is greatest. These compounds are likely to present a substantial toxic hazard, comprising a potentially important proportion of the mutagenicity and/or carcinogenicity of ambient air. An appropriate understanding of their sources, behaviour and fate is required in order to assess the exposure and risk presented to humans and the wider environment.

PAHs, OPAHs and NPAHs display a wide range of physiochemical properties and can exist in both gas-phase and associated with atmospheric particulate matter. The nature and extent of their atmospheric processing will largely dictate their overall fate in the environment and the extent of human exposure.

PAHs are emitted to the atmosphere via incomplete combustion of organic materials, mainly due to anthropogenic activities. The concentration of PAHs in the U.K. has declined significantly in the past 25 years, which has resulted in a shift in relative source profile. Current emissions are dominated by domestic wood combustion and vehicular traffic.

OPAH and NPAH can result both from primary combustion emissions and secondary input from gas-phase and heterogeneous reactions of PAH with atmospheric oxidants (e.g. OH, NO₃, and O₃) Therefore assessing the sources and behaviour of these compounds is rather more complex.

PAH atmospheric reactivity is dependent on the specific PAH molecule, the concentration of atmospheric oxidants, the concentration and nature of particulate matter and the degree of phase partitioning. While the extent to which reactions can produce OPAH and NPAH compounds has been widely investigated in laboratory studies, limited work has been done in terms of field studies of the ambient atmosphere.

While, PAHs have been monitored in the UK atmosphere for over 25 years, and much has been learned regarding their long- and short-term trends, much less is known regarding the levels of OPAH and NPAH in the U.K. atmosphere and the factors influencing their input and loss.

The overall aim of this project was to investigate the concentrations of PAHs as well as key OPAH and NPAH derivative compounds in the U.K. urban atmosphere, and to interpret their observed levels and atmospheric behaviour to assess the importance of different primary (e.g. emissions from road traffic or other combustion activities) or secondary (e.g. reactive formation) sources and atmospheric sinks of these compounds.

The specific objectives of the project were to :

- Measure concentrations of PAHs, OPAHs and NPAHs at urban background and trafficked sites and investigate their sources, behaviour and trends and the factors governing these processes.
- Investigate temporal trends and assess potential factors affecting long- and short-term variations in observed concentrations, with particular reference to changes in overall and relative source profiles.
- Obtain a 'traffic profile' for target compounds from a trafficked environment to compare with ambient locations in order to gain a clearer understanding of the influence of primary traffic

sources to observed atmospheric concentrations in comparison with other input and loss mechanisms.

- Obtain a diurnal profile for target compounds to provide more insight into the sources, meteorological factors and degradation processes influencing observed concentrations.
- Investigate the potential influence of atmospheric reactions on the levels of OPAH and NPAH in comparison with primary combustion emissions.
- Carry out a source apportionment analysis of PAH, OPAH and NPAH compounds using positive matrix factorisation (PMF).

Chapter 2 : Methodology

2.1. Sampling Procedure

2.1.1. Background

2.1.1.1. Overview

PAHs, OPAHs and NPAHs are present in the atmosphere in both particulate and gaseous phases and have the propensity to partition between the two phases (as discussed in Section 1.4.2). It is desirable, therefore, to collect samples of both gas-phase and particle-phase PAH simultaneously to gain clearer insights into key processes driving their atmospheric behaviour and fate (e.g. phase partitioning, chemical reactivity and/or wet and dry deposition).

It is now common for air samples to be collected using high-volume air samplers adapted to collect both particle-phase and gas-phase pollutants separately (Finlayson-Pitts and Pitts, 2000). In this method, a motor-driven pump draws air through the inlet at the top of the sampler; the air passes first through a filter where airborne particulates are deposited, followed by an absorbent material to collect gas-phase components downstream (Finlayson-Pitts and Pitts, 2000 ; see Figure 2.2b).

This approach has been utilised in a large number of ambient sampling studies for PAHs (Dimashki *et al.*, 2000; 2001; Harrad and Laurie, 2005; Harrison *et al.*, 2003; Keller and Bidleman, 1984; Smith and Harrison, 1996; Wilson *et al.*, 1995) as well as OPAHs and NPAHs (Albinet *et al.*, 2007a; 2008a; Bamford and Baker, 2003; Liu *et al.*, 2006b; Wilson *et al.*, 1995). This sampling approach was utilised in the present investigation.

2.1.1.2. Particle-phase sampling

Particle-bound PAH compounds have been collected on a variety of different filter types (Liu *et al.*, 2007) including :

- Glass fibre filters (GFFs) (Bamford and Baker, 2003; Barrado *et al.*, 2012; Bi *et al.*, 2005; Feilberg *et al.*, 2001; Kim *et al.*, 2012; Lin *et al.*, 2002; Simcik *et al.*, 1998);
- Polytetrafluoroethylene (Teflon) membrane filters (TMFs) (Alam *et al.*, 2013; Delgado-Saborit *et al.*, 2013; Ligocki and Pankow, 1989; Smith and Harrison, 1996) ;
- Teflon coated glass fibre filters (TGFFs) (Alam *et al.*, 2013; Allen *et al.*, 1997; Arey *et al.*, 1987; Delgado-Saborit *et al.*, 2013; Dimashki *et al.*, 2000; 2001; Feilberg *et al.*, 1999; Harrad *et al.*, 2003; Harrad and Laurie, 2005; Harrison *et al.*, 2003; Ligocki and Pankow, 1989; Lim *et al.*, 1999; Reisen and Arey, 2005; Smith and Harrison, 1996);
- Quartz fibre filter (QFFs) (Fraser *et al.*, 1998b; Lee *et al.*, 2012; Nassar *et al.*, 2011; Ringuet *et al.*, 2012a; 2012c; Sienra, 2006; Wilson *et al.*, 1995).

Quartz fibre filters were chosen in the present study due to their relative cheapness and availability as well as their high retention efficiency and compatibility with available sampling equipment.

2.1.1.3. Gas-phase sampling

The desired sorbent material for collecting the gas-phase component should have large absorption capacity, low airflow resistance, reasonable chemical stability and ease of preparation and handling (Liu *et al.*, 2007). Common sorbent materials used to collect gaseous PAHs include :

- Tenax-GC and Tenax-TA solid absorbents (Arey *et al.*, 1989a; Baek *et al.*, 1991; Hart and Pankow, 1994);
- XAD material (Alam *et al.*, 2013; Delgado-Saborit *et al.*, 2013; 2014; Eiguren-Fernandez *et al.*, 2008a; Wilson *et al.*, 1995);

- Polyurethane foams (PUFs) (Albinet *et al.*, 2008a; Bamford and Baker, 2003; Dimashki *et al.*, 2000; 2001; Harrad and Laurie, 2005; Harrison *et al.*, 1996; Kim *et al.*, 2012; Reisen and Arey, 2005; Yamasaki *et al.*, 1982).

PUF are commonly used due to their advantages of low-cost, ease of preparation and handling. Flame retardant (FR)-free PUF material is preferable as this will reduce air flow resistance and content of impurities in sample extracts. However, some breakthrough of LMW through PUFs can occur (Arey *et al.*, 1989a). As noted by Finlayson-Pitts and Pitts (2000), PUFs may not be suitable for sampling highly volatile 2-ring PAH e.g. Nap and methyl-Nap (MNap) isomers. Indeed, evidence of significant evaporative losses of Nap, 1MNap and 2MNap was observed during the present study (see Section 6.1 for a discussion) therefore the concentrations of these compounds were not included in the results of this study.

A number of studies have utilised diffusive denuders for the sampling of PAH, OPAH and NPAH (Delgado-Saborit *et al.*, 2013; 2014; Eiguren-Fernandez *et al.*, 2003; Goriaux *et al.*, 2006; Liu *et al.*, 2006b; Tsapakis and Stephanou, 2003). Denuders collect the gas-phase component using a solid sorbent coated on the surface of the trap, with the particulate-phase component collected on a filter downstream. These can therefore provide the dual function of separating out the gas- and particle-phase components of semi-volatile species (e.g. PAHs) and removing reactive oxidant species (e.g. O₃) to prevent transformation of species during sampling (Delgado-Saborit *et al.*, 2014).

For example, the design of sampling system utilising a micro orifice uniform deposit impactor (MOUDI) to collect the particulate phase with upstream multi-parallel denuder plates coated with XAD-4 to collect the gas phase component has been described (Delgado-Saborit *et al.*, 2014; Eiguren-Fernandez *et al.*, 2003). This approach has been demonstrated to perform accurate, repeatable sampling with low-denuder breakthrough. However it has been noted that artefact formation (see Section 2.1.6) occurred during both denuded and un-denuded sampling (Delgado-Saborit *et al.*, 2014; Eiguren-Fernandez *et al.*, 2003).

Liu et al. (2006b) measured atmospheric PAH and OPAH concentrations using samplers with and without a MnO₂ denuder. The undenuded sampler was shown to underestimate PAH concentrations and overestimate HMW OPAH concentrations. The authors attributed this to the occurrence of PAH reactivity with oxidants such as O₃ during sampling. However, higher concentration of LMW OPAH e.g. 9F and AQ were found on the filters of denuded samplers, suggesting catalytic formation on the denuder surface. Therefore OPAH artefact can be formed in both denuded and undenuded samplers.

Furthermore, the flow rate achieved by a MOUDI sampler would sample <50 m³ of air in a 24 hour period. While this would be adequate to obtain a sample large enough to provide analytically detectable levels of PAH and OPAH (Alam *et al.*, 2013; Delgado-Saborit *et al.*, 2014), this may not provide detectable concentrations of some NPAH compounds, which are typically observed at much lower (~1-2 orders of magnitude) concentrations. Therefore a non-denuded sampling system was used in the present study.

2.1.2. Sampling sites

The sampling locations for the principal campaigns in this study were situated on the University of Birmingham campus (Latitude: 52.4797; Longitude: -1.8965). The University is located approximately 3 km south of Birmingham city centre (see Figure 2.1).

Air sampling was conducted at two sites termed the Bristol Road Observatory Site (BROS) and the Elms Road Observatory Site (EROS). BROS is located on the south edge of the University adjacent to the A38 main road (Bristol Road). This road is a major commuting route to Birmingham city centre, with approximately 27,000 vehicles passing by per day, as estimated by the Department of Transport (<http://www.dft.gov.uk/traffic-counts>).

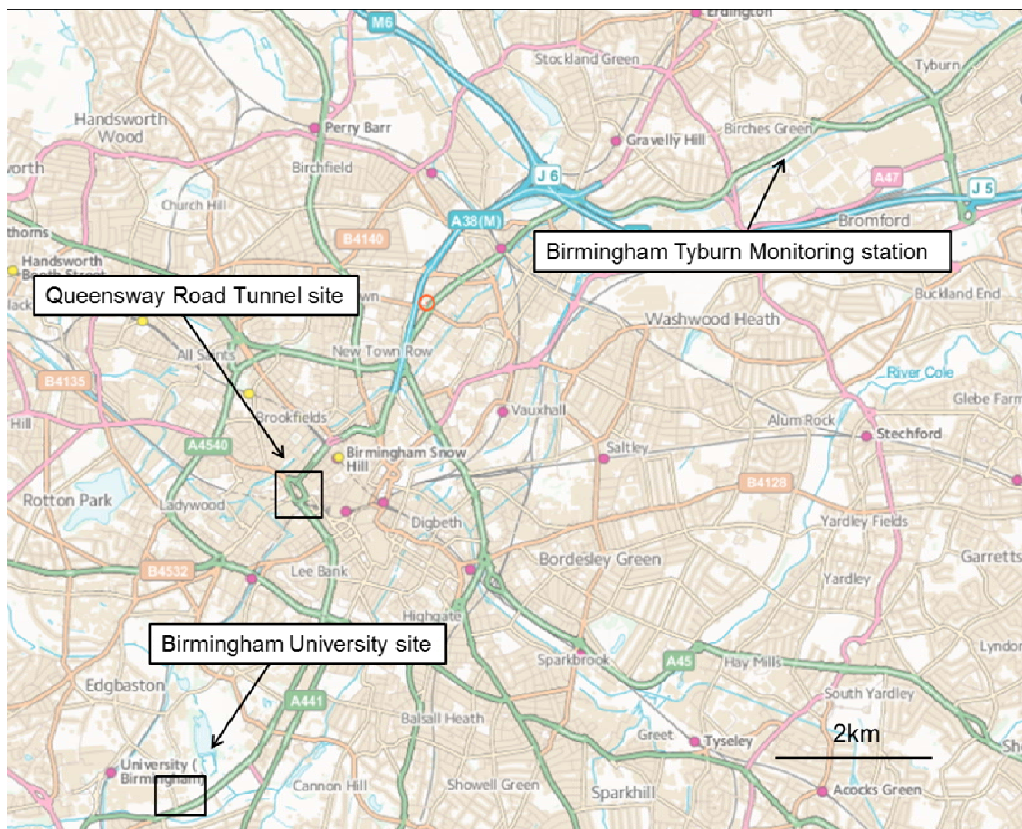
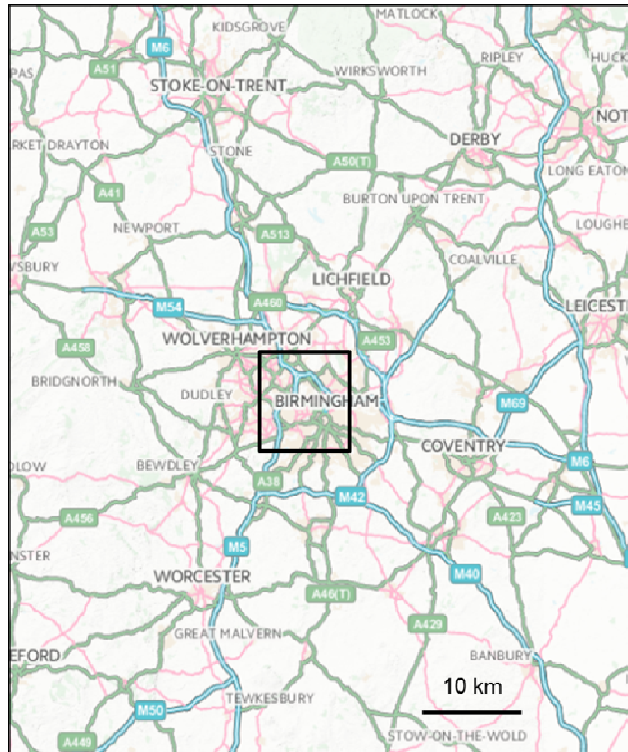


Figure 2.1a. Locations of Birmingham sampling and monitoring sites used in the present investigation. West Midlands conurbation (upper) and central Birmingham (lower). Obtained from Ordnance Survey Getamap online resource.



Figure 2.1b. Locations of Birmingham sampling and monitoring sites used in the present investigation BROS and EROS at the University site (upper) and the Queensway Road Tunnel (lower). Obtained from Ordnance Survey Getamap online resource.

It is assumed that, due to the proximity of this site to a major traffic emission source, this site acts as a 'polluted' site. EROS is located on the north-west side of the campus in an open field ~1km north of BROS. The lack of major primary pollution sources in close proximity allows EROS to act as an 'urban background' site.

2.1.3. Sampling campaigns

The project consisted of a number of individual sampling campaigns at the sites described in Section 2.1.2. Details (e.g. dates, times, meteorological conditions) for all individual samples taken during these campaigns are presented in Table 2.1 and a description of the different campaigns is provided below.

2.1.3.1. Campaign 1 : seasonal 24 hour sampling

For the principal period of this study, sampling was conducted during specific seasonal campaigns in October 2011 (autumn) ; Jan-Feb 2012 (winter) ; April-May 2012 (spring) ; and July 2012 (summer). ~24 hour air samples were collected simultaneously at the BROS and EROS sites on weekdays during these campaigns. Samples were taken using high volume air samplers (Tisch Environmental Inc., Cleves, Ohio, USA) adapted to sample both particle-phase and gas-phase pollutants. The appearance and design of these samplers is shown in Figure 2.2.

Total particulate matter was collected on quartz fibre filters (Whatman Int. Ltd, UK, obtained from VWR International Ltd, Lutterworth, Leicestershire, UK ; dimensions, 8" x 10"; retention efficiency >99%), loaded inside a slotted metal filter plate (filter holder). Gas-phase sample was collected using cylindrical PUF plugs (dimensions 3" x 3 3/8", FR-free, Tisch Environmental Inc., Cleves, Ohio, USA). Two PUF plugs were loaded in series inside a cylindrical metal tube (PUF holder) fitted below the filter holder. This sampling apparatus was enclosed inside an aluminium casing to shelter equipment from sunlight and rainfall.

Table 2.1. Dates, approximate times and average meteorological parameters, temperature (T), relative humidity (RH), pressure (PRES), solar radiation (SRAD), rainfall (RF), wind speed (WS), wind direction (WD) for all samples taken during this investigation.

	Start Date	Start Time approx.	End Date	End Time approx.	T (°C)	RH (%)	PRES (hPa)	SRAD (W/m ²)	RF (mm)	WS (m/s)	WD (deg)
Campaign 1											
A1	18/10/11	11:58	19/10/11	12:30	7.6	69.8	1013	200	0.0	1.9	256
A2	19/10/11	14:10	20/10/11	14:20	6.2	74.7	1023	222	0.2	1.2	269
A3	01/11/11	11:30	02/11/11	11:46	9.7	87.1	1009	170	0.2	1.3	190
A4	03/11/11	11:35	04/11/11	11:39	12.6	92.4	995	79	7.0	1.1	173
W1	08/02/12	13:34	09/02/12	09:30	-1.4	81.6	1035	91	0.0	1.1	162
W2	09/02/12	15:55	10/02/12	16:07	-0.4	91.8	1033	33	1.2	1.0	157
W3	15/02/12	13:31	16/02/12	13:55	7.5	71.9	1026	111	0.0	1.8	290
W4	20/02/12	10:00	21/02/12	10:14	6.2	78.4	1025	93	0.0	2.6	221
W5	21/02/12	12:10	22/02/12	12:49	8.2	82.4	1022	43	0.8	3.7	215
W6	22/02/12	14:48	23/02/12	15:19	12.0	85.0	1019	181	0.4	2.4	234
W7	27/02/12	08:55	28/02/12	09:27	9.9	87.6	1021	57	1.0	1.6	246
Sp1	30/04/12	09:07	01/05/12	09:30	12.1	72.9	999	145	8.4	2.9	41
Sp2	01/05/12	09:45	02/05/12	09:55	8.7	94.7	1003	46	3.2	1.6	43
Sp3	02/05/12	10:18	03/05/12	10:22	9.9	74.9	1000	127	1.4	2.5	33
Sp4	03/05/12	10:43	04/05/12	11:22	6.4	93.8	994	34	7.6	0.9	37
Sp5	07/05/12	10:11	08/05/12	10:25	11.9	62.4	991	219	0.0	1.4	118
Sp6	08/05/12	10:44	09/05/12	10:52	11.9	62.4	991	219	0.0	1.4	118
Sp7	16/05/12	10:31	17/05/12	11:00	8.6	65.1	1004	167	0.0	0.9	90
Su1	05/07/12	13:33	06/07/12	13:47	17.5	77.6	993	106	0.4	0.9	86
Su2	09/07/12	09:53	10/07/12	09:54	14.5	82.7	995	113	1.8	1.0	130
Su3	12/07/12	13:17	13/07/12	13:30	13.6	88.7	989	107	12.8	1.0	76
Su4	17/07/12	09:50	18/07/12	10:22	17.2	80.9	1001	160	0.6	2.8	115
Su5	23/07/12	10:02	24/07/12	09:59	19.2	65.9	1003	324	0.0	1.6	118
Su6	26/07/12	11:50	27/07/12	12:10	20.0	66.1	999	265	0.0	1.1	105
Su7	30/07/12	11:08	31/07/12	11:13	13.5	72.5	998	205	4.6	1.3	116
Campaign 2											
D1	07/08/12	07:08	07/08/12	11:11	15.1	84.1	1002	232	0.2	1.9	117
D2	07/08/12	11:25	07/08/12	15:29	18.5	60.5	1003	536	0.0	2.5	117
D3	07/08/12	15:44	07/08/12	18:36	16.3	74.3	1003	141	0.0	2.5	111
D4	07/08/12	18:50	07/08/12	06:57	14.6	94.0	1004	15	1.8	0.5	89
D5	08/08/12	07:13	08/08/12	10:46	17.1	78.2	1005	274	0.0	0.8	95
D6	08/08/12	11:01	08/08/12	15:05	19.6	59.2	1006	417	0.0	1.1	115
D7	08/08/12	15:21	08/08/12	18:37	20.8	50.2	1006	286	0.0	0.8	131
D8	08/08/12	18:52	08/08/12	06:50	13.9	89.2	1007	18	0.0	0.3	45
D9	09/08/12	06:55	09/08/12	10:48	18.6	60.4	1009	508	0.0	1.1	69
D10	09/08/12	11:02	09/08/12	14:52	22.1	44.9	1009	622	0.0	1.2	109
D11	09/08/12	15:07	09/08/12	18:51	22.3	42.0	1008	287	0.0	0.9	89
Campaign 3											
Q1	11/09/12	07:36	12/09/12	07:34	10.5	70.9	998	152	0.6	1.6	126
Q2	12/09/12	07:44	13/09/12	07:36	10.8	80.3	999	118	3.0	1.6	133
Q3	13/09/12	07:45	14/09/12	unk	14.7	69.2	998	179	0.0	2.7	121
Q4	18/09/12	09:22	19/09/12	09:10	9.8	68.6	1001	155	0.2	1.6	136
Artefact Campaign											
AR1	01/10/13	10:20	02/10/13	10:35	14.4	81.3	1000	90	0.0	0.9	130
AR2	04/10/13	16:40	05/10/13	17:00	14.1	78.7	993	43	0.8	1.3	63
AR3	08/10/13	09:30	09/10/13	09:30	14.9	74.4	1006	100	0.0	1.3	133

unk = unknown



Figure 2.2a. High volume sampler at the EROS location.

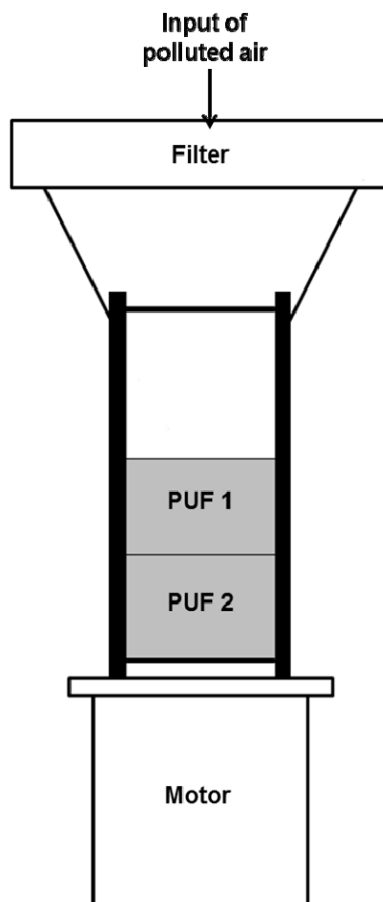


Figure 2.2b. Schematic diagram of a high volume sampler used in the present investigation. Adapted from Finlayson-Pitts and Pitts (2000).

PUF and filter holders were pre-rinsed with solvent prior to loading PUFs and filter. Filters were pre-treated by heating at 450°C for 24 hours and were accurately weighed before and after sampling in order to obtain TSP concentration for collected samples. PUFs were pre-cleaned by ultrasonication twice (30 minutes) in a solvent mixture of DCM, hexane and methanol (1:1:1 by volume) followed by ultrasonication in hexane only (60 minutes).

Sampler flow rates were calibrated according to manufacturer guidelines (Tisch TE-5000 Operations Manual). Sampler calibrations were carried out each time a sampler motor was changed. The procedure for sampler calibration is described in detail in Appendix 2. Air flow rates during sampling were measured using a flow chart recorder and manometer readings were taken at the beginning and ending of sampling duration to assess change in flow rate during sampling. Total air volume sampled during ~24 hour sampling periods during this study varied from ~800-1200 m³.

After sampling, filters and PUFs were removed from the filter plate or PUF holder using pre-cleaned stainless steel forceps, wrapped in aluminium foil and transported to the laboratory in a cool box. Samples were contained inside a sealed polythene bag and stored at -10°C prior to extraction and analysis.

2.1.3.2. Campaign 2 : diurnal sampling study

A diurnal sampling study was conducted at the BROS and EROS sites on August 7th, 8th and 9th 2012. Sampling during this campaign was conducted following the procedure detailed in Section 2.1.3.1.

Multiple samples were collected on these days to assess how concentrations of target pollutants vary throughout the day in response to different factors (variations in primary emission strength, levels of other gaseous pollutants, and meteorological conditions). The sampling times in this campaign were as follows (specific times of each sample are presented in Table 2.1) :

07:00 – 11:00 (morning) – period of ‘rush hour’ with maximum traffic flow

11:00 – 15:00 (daytime) – period of maximum sunlight/radiation levels, lower traffic flow

15:00 – 19:00 (afternoon) – period of temperature maxima and afternoon traffic input

19:00 – 07:00 (night-time) – period of low traffic and absence of sunlight

2.1.3.3. Campaign 3: Queensway Road Tunnel sampling study

As discussed in Section 1.4.6.2, it is important to obtain an accurate traffic profile of traffic-related PAH emissions in order to assess the relative importance of these compounds in the urban atmosphere. Road tunnels are expected to provide an ideal environment to assess traffic emissions of PAHs as the tunnel is assumed to be an ‘enclosed’ atmosphere containing only diluted exhausts from a realistic mixture of on-road vehicles.

The aims of this campaign were to :

- Measure levels of selected PAHs, OPAHs and NPAHs in a road tunnel.
- Obtain a ‘traffic signature’ for these compounds for comparison with ambient measurements.
- Assess the temporal trend of these compounds in the tunnel and relate this to observed changes in traffic characteristics.

A sampling campaign was conducted inside the Queensway Road Tunnel (see Figure 2.1b) in central Birmingham in September 2012. The tunnel passes under Birmingham city centre, providing a main through route for the A38 dual carriageway, which constitutes part of the A4400 inner city ring road. The tunnel is approximately 544m long with natural ventilation (Amey, *pers.comm.*). The speed limit in the tunnel is 30 mph. The average number of vehicles passing

through the tunnel per day is estimated to be 89,000. This value is an estimate for 2010 extrapolated from Birmingham City Council data from 2005 (Amey, pers. comm.).

24 hour air samples were collected during this campaign, following the procedure detailed in Campaign 1. The sampler was set up in an emergency breakdown lay-by in the southbound section of the tunnel. The two carriageways were separated by a concrete dividing wall. Concurrent sampling was conducted at EROS to provide 'background' concentrations to be subtracted from the tunnel concentrations to calculate a 'traffic' concentration.

2.1.4. Meteorological data

For sampling periods during each campaign, mean values for key meteorological parameters (temperature, pressure, relative humidity, wind speed, wind direction, solar radiation), as well as total rainfall, were measured. These data were obtained from the Elms Cottage Automated Weather Station, which is located adjacent to the EROS sampling site. These data are used for both EROS and BROS samples.

2.1.5. Inorganic gaseous pollutants

For each sampling period during each campaign, mean concentrations of key gaseous pollutants (NO_x , O_3 and SO_2) were obtained. These data were derived from measurements at the Birmingham Tyburn monitoring site (UKA00479), operated as part of the Defra Automatic Urban and Rural Network (AURN) (<http://uk-air.defra.gov.uk/networks>). Birmingham Tyburn is located to the north-west of Birmingham city centre (see Figure 2.1a) and is designated an 'urban background' site.

2.1.6. Quality control : the potential impact of sampling artefacts

Ambient sampling of PAHs using the filter/sorbent technique, as performed in the present study, can be subject to positive or negative 'artefacts' that may lead to significant deviations away from 'true' concentrations present in the atmosphere, particularly for semi-volatile 3-4 ring compounds (Finlayson-Pitts and Pitts, 2000 and references therein). This can be caused by disruptions in gas-particle partitioning equilibrium or by chemical reactivity of adsorbed PAHs during sampling.

2.1.6.1. Gas-phase vs. particle-phase artefacts

Two key phenomena can occur during a relatively long (i.e. 24 hr) sampling study to disrupt 'natural' gas-particle phase equilibrium conditions, thus creating sampling artefacts (Finlayson-Pitts and Pitts, 2000 and references therein) :

i) Vapour-phase PAH can adsorb to the filter or adsorbed particles due to either a decrease in temperature or increase in pollutant concentration during sampling (Finlayson-Pitts and Pitts, 2000 and references therein). This would therefore overestimate particle-phase concentrations and underestimate gas-phase concentrations. For example, Hart and Pankow (1994) demonstrated that the use of quartz fibre filters can lead to gas-phase adsorption leading to an overestimation of the particle-phase component by a factor of 1.3 to 1.6.

ii) Volatilisation ("blow off") of PAH collected on filter and/or breakthrough of ultrafine particles through the filter and collection by the absorbent can occur (Kavouras *et al.*, 1999; Wilson *et al.*, 1995). This may result from temperature increase, concentration decrease or drop in pressure during sampling. This would result in an underestimate of particle-phase PAH and an overestimate of gas-phase PAH concentrations (Finlayson-Pitts and Pitts, 2000 and references therein).

2.1.6.2. Chemical reactivity during sampling

As discussed in Section 1.5.3 PAH degradation and OPAH or NPAH formation on solid surfaces in laboratory experiments has been observed to occur due to chemical reactions, for example with O₃

(Brorstrom *et al.*, 1983; Katz *et al.*, 1979; Lane and Katz, 1977; Lindskog *et al.*, 1985; Pitts *et al.*, 1978; 1980; 1986; Van Vaeck and Van Cauwenberghe, 1984) or NO₂-N₂O₅-HNO₃ (Jariyasopit *et al.*, 2014; Pitts *et al.*, 1985b; Pitts *et al.*, 1985c; Zimmermann *et al.*, 2013).

If such chemical reactivity of filter-bound PAHs occurred during sampling, this could lead to underestimation of PAH concentrations and overestimation of observed levels of OPAHs and NPAHs formed. The occurrence and extent of this artefact formation during sampling experiments has been investigated but is subject to a number of conflicting observations in the literature.

For example, several studies have reported contrasting or inconclusive results from O₃ exposure studies for PAHs deposited on glass filters, diesel exhaust particles and ambient particles (Brorstrom *et al.*, 1983; Grosjean, 1983). Coutant *et al.* (1988) reported that PAHs reacted readily with O₃ in laboratory studies, but no evidence was found for reaction of O₃ with particulate matter during the field sampling experiments.

In more recent studies (Goriaux *et al.*, 2006; Liu *et al.*, 2006b; Schauer *et al.*, 2003; Tsapakis and Stephanou, 2003) the impact of oxidation reactions during sampling on the concentrations filter-bound PAHs and OPAHs has been investigated by sampling with and without an upstream denuder to remove atmospheric oxidants.

These studies indicate ozonation reactions could result in an underestimation of particulate-phase PAH concentrations by up to a factor 2. Furthermore, Liu *et al.* (2006) indicated particle-bound concentrations of certain OPAHs (e.g. AQ and BaAQ) were 10-40% higher without a denuder, indicating artefact formation of OPAHs due to the reaction of collected PAHs with ozone during sampling.

Arey *et al.* (1988) observed formation of deuterated NPAHs on particulate samples deposited on glass fibre filter surfaces pre-spiked with deuterated PAHs, collected in a sampling study for 7-10 h with an NO₂ concentration of ~160 ppb. However, the maximum NPAH formation rates observed were generally very low (<3% for 1-nitropyrene-d₉; 0.1% for 3-nitroperylene-d₁₂) and no formation of NFlt isomers was observed. It was concluded that formation of nitro-pyrenes and nitro-

fluoranthenes during high volume sampling does not significantly affect the measured concentrations.

Similarly, Dimashki *et al.* (2000) carried out an artefact study in a road tunnel in Birmingham, UK. It was observed that, even in this high NO₂ environment (~0.2 ppmv) the maximum NPAHs artefact formation during sampling was <0.1%. Formation of NPAH artefacts generally does not seem problematic in high volume sampling studies.

Albinet *et al.* (2007b) measured concentrations of PAH, OPAH and NPAH using two different samplers (cascade impactor and conventional hi-vol) during summer and winter periods. It was shown that during winter, the sampler 'underestimated' concentrations of NPAHs by a factor of 3-4. This was attributed to the heating of the sampler PM₁₀ head during winter, causing enhanced chemical degradation of particle-bound NPAHs collected on filters. No external heating was used in the present study so it is assumed this level of degradation did not occur during sampling.

2.1.6.3. Artefact sampling experiment

An experiment to assess the potential influence of sampling artefacts on the results obtained in this project was carried out. The aim of this experiment was to assess the extent to which sampling artefacts may have affected the measured concentrations of PAHs, OPAH and NPAH compounds during the sampling campaigns carried out in this project. This involved conducting a sampling campaign to monitor the possible loss of PAHs from the filter and the formation of OPAH and NPAH derivatives during sampling.

Details of the methodology and a discussion of observed results from this experiment can be found in Section 4.4.

2.2. Sample extraction and clean-up

2.2.1. Materials and chemicals

All solvents (DCM, hexane, methanol) used in this study were HPLC grade (purity >98%), obtained from Fisher Scientific UK Ltd. Sodium sulphate absorbent and aminopropyl solid phase extraction tubes were obtained from Sigma-Aldrich Company Ltd., Gillingham, UK. Standards of perdeuterated and native PAH and NPAH compounds (>98% purity in toluene or isooctane) and p-terphenyl-d14 recovery standard (>99% purity, in toluene) were obtained from Greyhound Chromatography, Merseyside, UK, as pre-prepared solutions by Chiron AS, Trondheim, Norway. Perdeuterated and native OPAH internal standards and 1-fluoro-7-nitrofluorene recovery standard (purity >98%) were obtained initially as solids from Sigma-Aldrich Company Ltd., Gillingham, UK and solutions prepared by dilution with hexane. Methane gas (99.9% purity) was obtained from Argo International Ltd, UK.

2.2.2. Sample preparation

The extraction, clean-up and preparation of samples prior to analysis was conducted according to a standard operating procedure, previously produced by members of this research group (Delgado-Saborit and Baker, 2006) incorporating a solid phase extraction step developed from methods described by Albinet *et al.* (2006) and Cochran *et al.* (2012). All glassware was cleaned using this procedure; soaked and cleaned in Lipsol detergent (SciLabware Ltd), rinsing with deionised water and drying for >2 hr at 100 °C in a glass oven.

2.2.3. Sample extraction

2.2.3.1. Extraction background

Extraction of PAH and related compounds from environmental samples is commonly achieved using an organic solvent such as dichloromethane (DCM), acetonitrile, benzene, toluene or cyclohexane (Liu *et al.*, 2007).

Soxhlet extraction using DCM or other solvents (e.g. acetonitrile/acetone/benzene) is a common method (Becker *et al.*, 2006; Dachs *et al.*, 2002; Dimashki *et al.*, 2001; Harrad *et al.*, 2003; Harrad and Laurie, 2005; Harrison *et al.*, 2003; Kim *et al.*, 2012; Lim *et al.*, 1999) and NPAH and OPAH derivatives (Andreou and Rapsomanikis, 2009; Arey *et al.*, 1987; Bamford and Baker, 2003; Bamford *et al.*, 2003; Dimashki *et al.*, 2000; Gibson, 1982; Marino *et al.*, 2000; Sienna, 2006; Wilson *et al.*, 1995). This method is favoured due to high extraction efficiency (Yang, 1999), however, this approach is time-consuming and solvent- and energy-intensive, requiring considerable sample concentration prior to analysis (Liu *et al.*, 2007).

Ultrasonication offers reduced extraction time (0.25 – 1.5 hr), and utilises less solvent (15-20 mL) while maintaining satisfactory analyte recovery. This method has been utilised for PAH extraction using DCM (Bi *et al.*, 2003; 2005; Chetwittayachan *et al.*, 2002; Guo *et al.*, 2003; Hayakawa *et al.*, 2002; Ohura *et al.*, 2004; 2005; Park *et al.*, 2002; Schnelle-Kreis *et al.*, 2001; Tang *et al.*, 2005). as well as toluene (Sharma *et al.*, 2007) and dimethylformamide (DMF) (Mastral *et al.*, 2003b)

Ultrasonication has also been used for the extraction of OPAHs and NPAHs using DCM (Allen *et al.*, 1997; Castells *et al.*, 2003; Delgado-Saborit *et al.*, 2013; Feilberg *et al.*, 2001; Nielsen *et al.*, 1984; Schnelle-Kreis *et al.*, 2001; Wei *et al.*, 2012) as well as benzene/ethanol (3/1, v/v) (Hien *et al.*, 2007; Murahashi and Hayakawa, 1997; Nassar *et al.*, 2011; Tang *et al.*, 2002; 2005), dichloromethane:acetonitrile (2:1 v/v) (Eiguren-Fernandez *et al.*, 2008a) and methanol (Kishikawa *et al.*, 2006).

Pressurised liquid extraction has also been investigated for PAHs (Hien *et al.*, 2007; Murahashi and Hayakawa, 1997; Nassar *et al.*, 2011; Tang *et al.*, 2002; 2005) and OPAHs and NPAHs (Albinet *et al.*, 2006,2007a; 2008a; Wang *et al.*, 2011a). However, this approach may lead to chemical degradation or rearrangement (Lintelmann *et al.*, 2006) and the reproducibility of this method has been questioned (Walgraeve *et al.*, 2010). Microwave-assisted extraction has also been applied for PAH and OPAH compounds (Barrado *et al.*, 2012; McDonald *et al.*, 2002) but this method is expensive and requires specific instrumentation.

Supercritical fluid extraction (SFE) has been shown to exhibit high extraction efficiency and good selectivity (Peltonen and Kuljukka, 1995) and has been applied for extraction of PAHs (Jonker *et al.*, 2005; Romero *et al.*, 2002; Shimmo *et al.*, 2002; 2004a), OPAH and NPAH (Castells *et al.*, 2003). However, it has been noted that SFE displays poor recovery of polar compounds if CO₂ is used, so requires a multi-step process involving solvent modifiers (Shimmo *et al.*, 2004a; 2004b).

2.2.3.2. *Extraction method*

In accordance with Delgado-Saborit and Baker (2006), one quarter of the filter from each sample was used for extraction and analysis. Filters were cut into small pieces with a stainless steel scalpel, placed inside a glass flask and spiked with a known amount of internal standard (IS) mixture (deuterated PAH, NPAH and OPAH compounds; see Table 2.2 for details). Approximately 15 mL DCM was added and the flask was covered with aluminium foil to prevent any evaporative loss of analyte and standard. PUFs were placed and compressed inside a large glass beaker and spiked with a known amount of IS mixture. Approximately 300 mL dichloromethane was added for PUF extraction.

Filter and PUF samples were extracted by ultrasonication in a water bath (~20°C, 30 minutes). Due to the larger volume of solvent used in PUF extractions, samples were initially transferred to Turbovap apparatus (Biotage Ltd, Uppsala, Sweden) and blown down under a gentle stream of nitrogen (~20°C) to reduce sample volume ~5 mL prior to sample clean-up.

2.2.4. Clean-up

2.2.4.1. *Clean-up background*

Sample pre-treatment is a crucial step in order to remove impurities that may interfere with analysis of target compounds and/or create a high GC baseline. Preliminary clean-up methods for PAH compounds have been reviewed and discussed previously (Liu *et al.*, 2007). PAHs can generally undergo analysis without substantial clean-up, however, polar derivatives, particularly NPAH often

require several purification steps due to their relatively low concentrations in atmospheric samples (pg m^{-3} range) (Albinet *et al.*, 2006). Pre-treatment is usually achieved through solid phase extraction (SPE) or normal phase liquid chromatography techniques which can isolate specific classes of compounds (Cochran *et al.*, 2012).

2.2.4.2. Clean-up method

In accordance with Delgado-Saborit and Baker (2006), sample extracts were initially eluted through an absorption chromatography column. Filter samples were passed through a Pasteur pipette containing ~1g anhydrous sodium sulphate in order to remove any macromolecules and water present in the sample extract. The column was pre-eluted with ~5 mL DCM before the crude solvent extracts were introduced to the head of the column with DCM washings from the flask or Turbovap tube. The column was finally eluted with ~5 mL DCM.

In accordance with Delgado-Saborit and Baker (2006), all samples were then concentrated under a gentle stream of nitrogen to almost dryness and made up to 1mL with hexane. Sample extracts were then subject to a solid phase extraction step, based on the methodology described by Cochran *et al.*, (2012). An aminopropyl solid phase extraction tube was pre-eluted with 3x 1mL aliquots of DCM followed by the same measure of hexane.

The sample was then passed through the column and target compounds were eluted by the sequential DCM/hexane solvent gradient (3 x 1mL) of 20/80%, 35/65%, 50/50%. This resulted in optimum recovery of PAH, NPAH and OPAH compounds in one sample extract to undergo analysis for PAH and OPAH/NPAH separately. Extracts were further reduced under nitrogen to almost dryness.

In accordance with Delgado-Saborit and Baker (2006), prior to analysis, a known amount of recovery standard was added to the sample. For this purpose, p-terphenyl-d14 was used for the analysis of PAHs and 1-fluoro-7-nitrofluorene (FNF) was used for the analysis of OPAH and NPAHs. Samples were made up to a final volume of 100 μL with nonane inside a glass vial insert.

Table 2.2. Internal standards, molecular ions and approximate retention times used to identify and quantify target PAH, OPAH and NPAH compounds in sample extracts.

PAH Internal Standard	M⁺	Retention time (min)	Target compounds	M⁺	Retention time (min)
p-Terphenyl-d14	244	31.2	n/a		
Acenaphylene-d8	160	12.7	Acenaphthylene	152	12.8
Acenaphthene-d10	162	13.6	Acenaphthene	153	13.6
Fluorene-d10	176	16.8	Fluorene	166	16.9
Phenanthrene-d10	188	21.5	Phenanthrene	178	21.6
Anthracene-d10	188	21.7	Anthracene	178	21.8
Fluoranthene-d10	212	28.2	Fluoranthene	202	28.3
			Pyrene	202	29.5
Pyrene-d10	212	29.4	Retene	219	
Benzo(a)anthracene-d12	240	36.5	Benzo(a)anthracene	228	36.6
Chrysene-d12	240	36.6	Chrysene	228	36.7
Benzo(b)fluoranthene-d12	264	42.3	Benzo(b)fluoranthene	252	42.4
Benzo(k)fluoranthene-d12	264	42.4	Benzo(k)fluoranthene	252	42.5
Benzo(e)pyrene-d12	264	43.5	Benzo(e)pyrene	252	43.6
Benzo(a)pyrene-d12	264	43.8	Benzo(a)pyrene	252	43.9
Indeno(1,2,3-cd)pyrene-d12	288	48.8	Indeno(1,2,3-cd)pyrene	276	48.9
Dibenz(a,h)anthracene-d12	292	49.1	Dibenz(a,h)anthracene	278	49.3
Benzo(ghi)perylene-d12	288	49.9	Benzo(ghi)perylene	276	50.2
Coronene-d12	312	56.2	Coronene	300	56.4
NPAH Internal Standard	M⁺		Target compounds	M⁺	
1-Fluoro-Nitro-Fluorene	229	29.8	n/a		
			1-Nitronaphthalene	173	17.8
1-Nitronaphthalene-d7	180	17.7	2-Nitronaphthalene	173	18.8
2-Nitrofluorene-d8	220	30.7	2-Nitrofluorene	211	30.9
			1-Nitrofluoranthene	247	39.5
			2-Nitrofluoranthene	247	40.5
3-Nitrofluoranthene-d9	256	40.8	3-Nitrofluoranthene	247	40.9
			4-Nitropyrene	247	41.4
		42.3	1-Nitropyrene	247	42.4
1-Nitropyrene-d9	256		2-Nitropyrene	247	42.8
6-Nitrochrysene-d11	284	47.2	6-Nitrochrysene	273	47.4
OPAH Internal Standard	M⁺		Target compounds	M⁺	
9-Fluorenone-d8	188	21.0	9-Fluorenone	180	21.1
			Anthraquinone	208	27.7
		27.6	Methyl-anthraquinone	222	30.7
Anthraquinone-d8	216		Benzo(a)anthracene-7,12-dione	258	41.7

2.3. Sample analysis

2.3.1. Background and analytical development

Sample analysis during this study was conducted using gas chromatography-mass spectrometry (GC-MS) techniques, developed according to a standard operating procedure previously produced by members of this research group (Delgado-Saborit and Baker, 2006). GC-MS has been established as method of PAH detection and quantification for over 50 years and remains a widely used method for the analysis of environmental samples for PAH (Lee, 1995; Liu *et al.*, 2007; Poster *et al.*, 2006); OPAHs (Walgraeve *et al.*, 2010) and NPAHs (Dimashki *et al.*, 2000; Albinet *et al.*, 2006, 2007a, 2008a).

GC-MS analysis of PAH is commonly achieved operating in electron impact (EI) mode. As discussed by (Rood, 2001), this process involves the collision between relatively high energy electrons (~70 eV) and sample molecules, removing their outer shell electron(s) producing primarily positive molecular ions $[M^+]$:



However, the energy imparted by this ionization can result in molecular ion disintegration to a number of smaller fragmented ions, the nature and extent being dependent on the structure of parent molecule:



An alternative technique has been adopted using negative ion chemical ionisation (NICI). This method involves the utilisation of a large amount of reagent gas (e.g. methane) in the ion source, which acts as a moderator to the high-energy electrons. In this process, methane is introduced to the ionisation chamber and collisions occur between methane molecules and high energy electron stream forming the CH_4 molecular ion (CH_4^+) and low-energy (thermal) electrons:



Molecules with high electron affinities (e.g. those containing electronegative substituent groups) such as oxy- or nitro- groups efficiently capture the electrons produced, forming negative ions:



Because NICI formation involves a much lower energy transfer, this usually results in less molecular ion fragmentation so molecular ions (M⁻) are predominantly produced. Furthermore, no negative reagent gas ions are formed, reducing the number of background peaks. The collision rate of sample molecules with these low energy electrons is much faster than the rate of ion-molecule collisions. Therefore this 'softer' ionization method allows lower detection limits for target compounds, with sensitivity up 10-1000 times higher than other CI and EI techniques (Albinet *et al.*, 2006 ; Cochran *et al.*, 2012).

This is particularly pertinent for the analysis of NPAH which requires low detection limits to analyse levels in environmental samples. NICI methods have been widely used to analyse atmospheric samples for both OPAH and NPAH compounds (Dimashki *et al.*, 2000; Cochran *et al.*, 2012; Albinet *et al.*, 2006, 2007a, 2008a ; Bezabeh *et al.*, 1997 ; 2003 ; Bonfanati *et al.*, 1996 ; Bamford *et al.*, 2003 ; Dušek *et al.*, 2003 ; Siegmund *et al.*, 2003 ; Ramdahl and Urdal, 1982 ; Newton *et al.*, 1982). This method also allows direct analysis of these compounds without requiring additional modifications e.g. conversion to diacetyl derivatives that has previously been required (Cho *et al.*, 2004; Delgado-Saborit *et al.*, 2013).

2.3.2. Analysis method for PAHs : GC-MS in EI mode

This method was used for the analysis of PAH compounds in extracts of filter and PUF samples, in accordance with Delgado-Saborit and Baker (2006). GC-MS analysis was carried out using an Agilent 5973 Network Mass Selective Detector (MSD) coupled to an Agilent 6890N Network GC system, operated in electron impact (EI) mode. 1 uL of sample was injected in splitless mode and

non-pulsed injection. Separation was carried out using an Agilent HP-5MS (5% phenyl methyl siloxane) capillary column (30m x 0.25 mm i.d. x 0.25 um film thickness).

The ion source, inlet and transfer line temperatures were 230°C, 300°C and 280°C respectively. Helium was used as a carrier gas with a set flow rate of 1.0 mL min⁻¹. The oven temperature was programmed as follows : starting temperature 100°C (held for 2 minutes), increased with a temperature gradient of 4°C min⁻¹ to a final temperature of 300°C (held for 7 minutes). The total run time was 59.0 minutes.

The mass selective detector was operated in Selective Ion Monitoring (SIM) mode, allowing detection of specific ions in set time windows, allowing optimum selectivity and sensitivity of the method. The molecular weight (MW) values of each peak used to identify PAH compounds and internal standards are shown in Table 2.2. Examples of the gas-chromatograph peaks for each target and internal standard compound, detected in prepared standards and sample extracts are shown in Appendix 3.

In accordance with Delgado-Saborit and Baker (2006), before and after sample runs, a quantification standard containing all target compounds, internal standards and the recovery standard p-terphenyl-d14 was analysed to assess any changes in GC-MS performance. Tuning checks were also carried out with the reference compound perfluoro-tri-n-butylamine (PFTBA) on a regular basis and after any GC-MS maintenance was performed in order to maintain optimum detector response. Calibrations were routinely carried out for all target compounds and method adjustments made as required.

2.3.3. Analysis for OPAH and NPAHs : GC-MS in NICI mode

This method was used for the analysis of OPAH and NPAH in extracts of filter and PUF samples.

GC-MS analysis was carried out using an Agilent 5973 Network Mass Selective Detector (MSD) coupled to an Agilent 6890N Network GC system operated in negative ion chemical ionisation (NICI) mode. The GC-MS configuration utilised a Gerstel Multipurpose auto sampler MPSL.

Compound separation was carried out using an Rxi®-PAH GC (Restek Ltd, UK) column (60m, 0.25 mm i.d., 0.10 µm film thickness). This column displayed notably improved separation of 2-NFlt and 3-NFlt compound peaks, which previous studies have failed to achieve (Albinet et al., 2007).

Improved peak separation achieved by the Restek®column was attributed to the narrower bore column and higher phenyl content of the column stationary phase. A comparison of the 2NFlt and 3NFlt peak separation on the Restek®column and a conventional Agilent DB5-MS 60m column can be seen in Figure 2.3.

The ion source, inlet and transfer line temperatures were 250°C, 300°C and 280°C respectively. Helium was used as a carrier gas with a set flow rate of 1.0 mL min⁻¹. Methane was used as the reagent gas with a set flow rate of 2 mL min⁻¹. The oven temperature was programmed as follows : starting temperature 60°C (held for 2 minutes), increased with a temperature gradient of 45°C min⁻¹ to 150 (held for 2 minutes) and further increased with a temperature gradient of 4°C min⁻¹ to a final temperature of 320°C (held for 11 minutes). The total run time was 59.5 minutes.

As with the EI GC-MS method, the mass selective detector was operated in SI mode. The molecular weight (MW) values of each peak used to identify OPAH and NPAH compounds and internal standards are shown in Table 2.1. Examples of the gas-chromatograph peaks for each target and internal standard compound, detected in prepared standards and sample extracts are shown in Appendix 3.

As detailed above, in accordance with Delgado-Saborit and Baker (2006), tuning checks were also carried out with the reference compound perfluoro-tri-n-butylamine (PFTBA) on a regular basis and after any GC-MS maintenance was performed in order to maintain optimum detector response. Before and after sample runs, a quantification standard containing all target compounds, internal standards and the recovery standard 1-fluoro-7-nitrofluorene (FNF) was analysed to assess any changes in GC-MS performance. Calibrations were routinely carried out for all target compounds and method adjustments made as required.

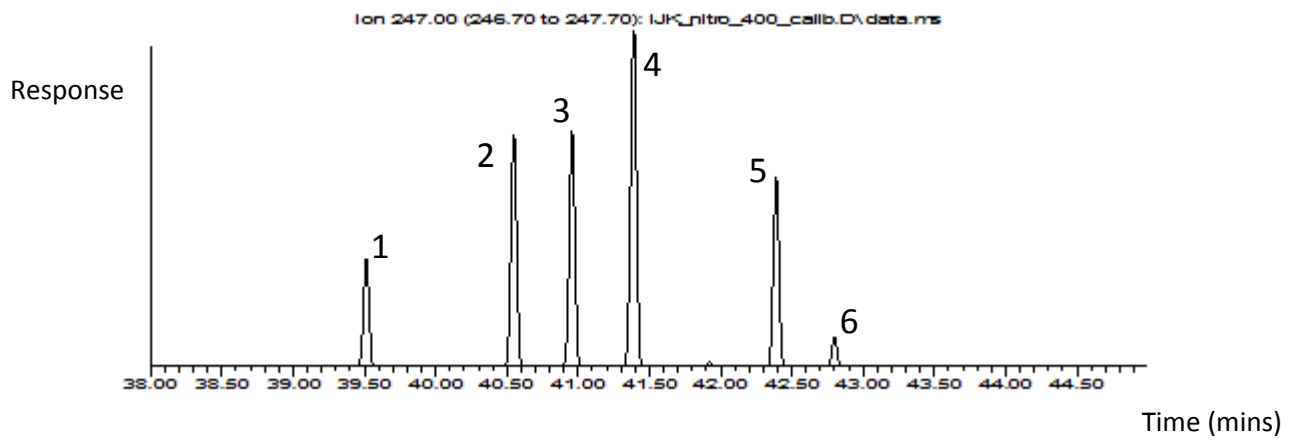
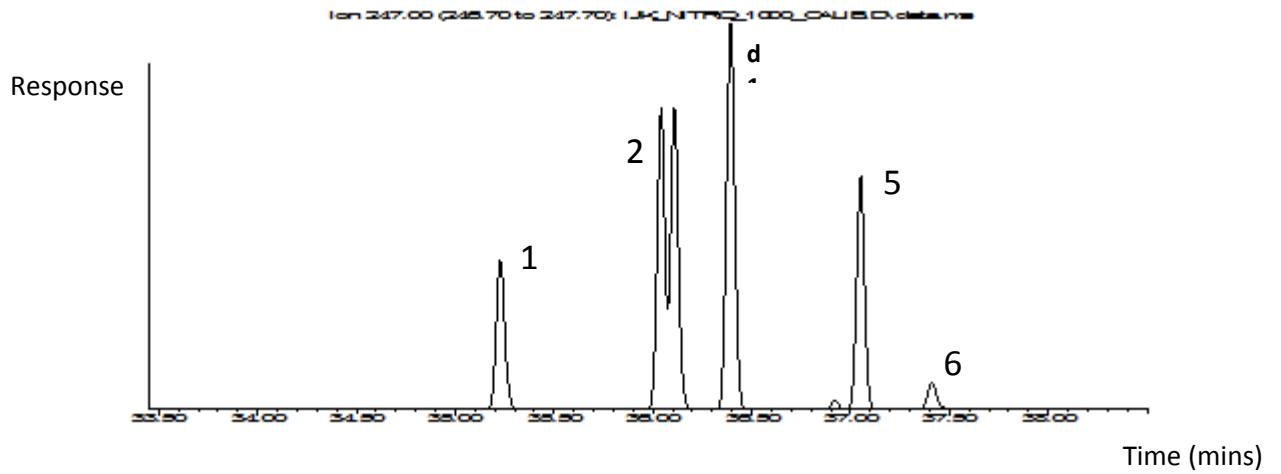


Figure 2.3. Comparison between peak separation of MW 247 NPAH compounds using an Agilent DB5-MS 60m column (upper) and the Restek® 60m column (lower). 1 = 1NFit, 2 = 2NFit, 3= 3NFit, 4 = 4NPyr, 5 = 1NPyr, 6 = 2NPyr.

2.4. Sample Quantification

2.4.1. Sample concentrations

Quantification of all target compounds in collected samples was based upon the ratios of analyte response peak area to that of an appropriate deuterated internal standard (IS) (Laurie, 2003) (Table 2.1).

Calibrations curves for each target compound were plotted using prepared standards of varying concentrations (10 – 1000 pg). Calibration plots for each compound quantified are shown in Figure 2.4. It should be noted that in the case of 9-NANt and 7-NBaA, quantification based on this calibration method were not valid due to peak fractionation of their natural and/or IS compound during GC-MS (NICI) analysis. In the case of these compounds, quantification was based on an external calibration, utilising a simple response to concentration relationship.

The internal standards were used to calculate relative response factors (RRFs) for each target compound. RRFs are defined as ‘the instrument response for a unit amount of target pollutant relative to that obtained for the same amount of the internal standard’ (Laurie, 2003).

$$\text{RRF} = (A_{\text{nat}} / A_{\text{is}}) \times (C_{\text{s}} \times C_{\text{nat}}) \quad (2.5)$$

A_{nat} = peak area of the ‘native’ compound in the standard

A_{is} = peak area of the internal standard in the standard

C_{s} = concentration of the ‘native’ compound in the standard

C_{nat} = concentration of the ‘native’ compound in the standard

Concentrations in samples are calculated using the following equation (Laurie, 2003) :

$$\text{Conc (pg/ul)} = (A_{\text{nat}} / A_{\text{is}}) \times (1/\text{RRF}) \times (M_{\text{is}}/\text{SS}) \times 1/\text{Er} \quad (2.6)$$

Where :

A_{nat} = peak area of the 'native' compound in the standard

A_{is} = peak area of the internal standard in the standard

RRF = relative response factor

M_{is} = mass of internal standard added to sample (pg)

SS = air sample volume (m^3)

Er = recovery

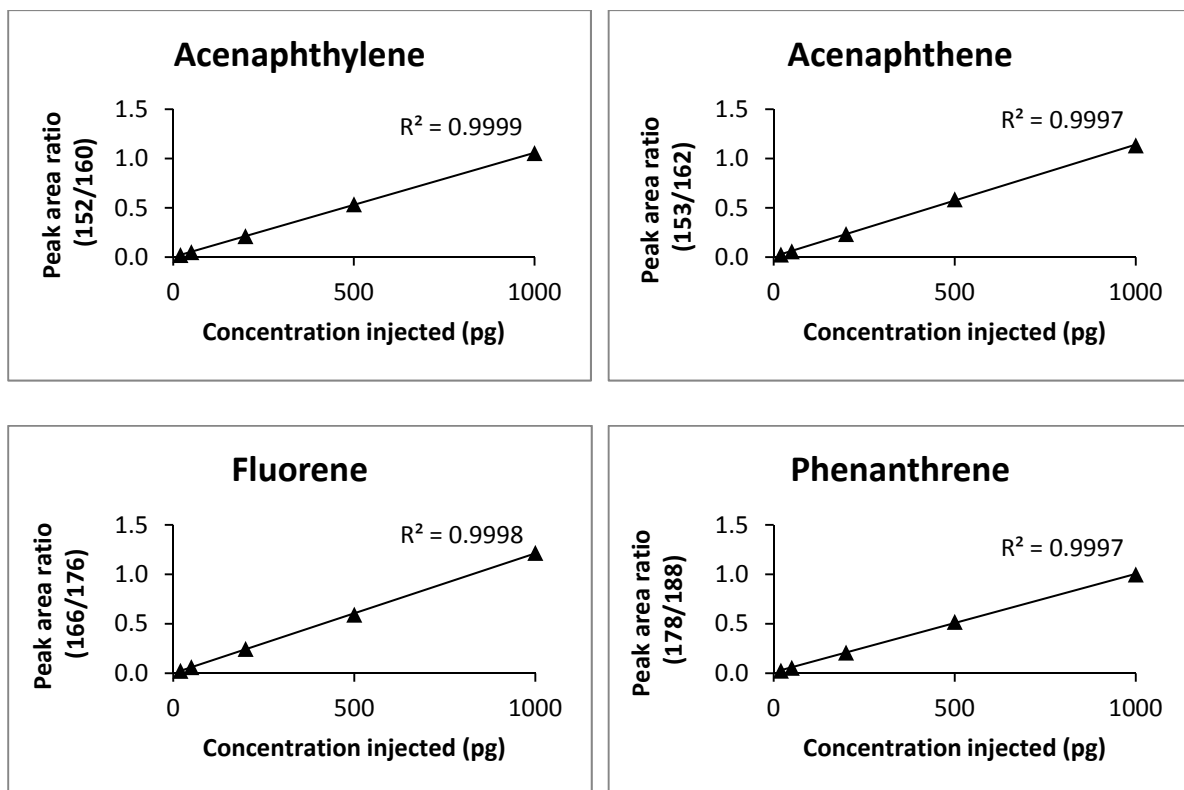


Figure 2.4. Calibration curves for the quantification of all PAH, OPAH and NPAH compounds measured in the present investigation.

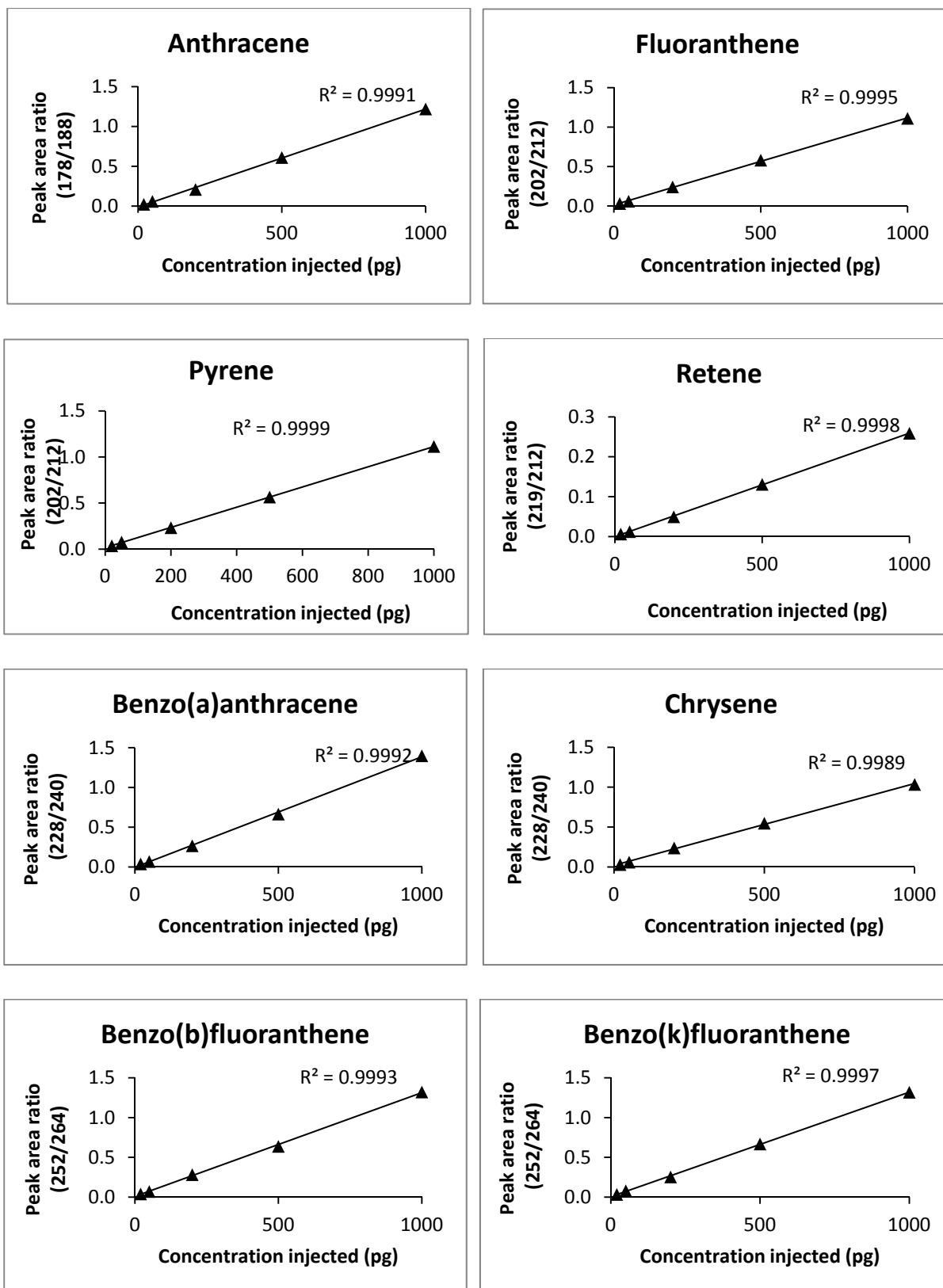


Figure 2.4(cont). Calibration curves for the quantification of all PAH, OPAH and NPAH compounds measured in the present investigation.

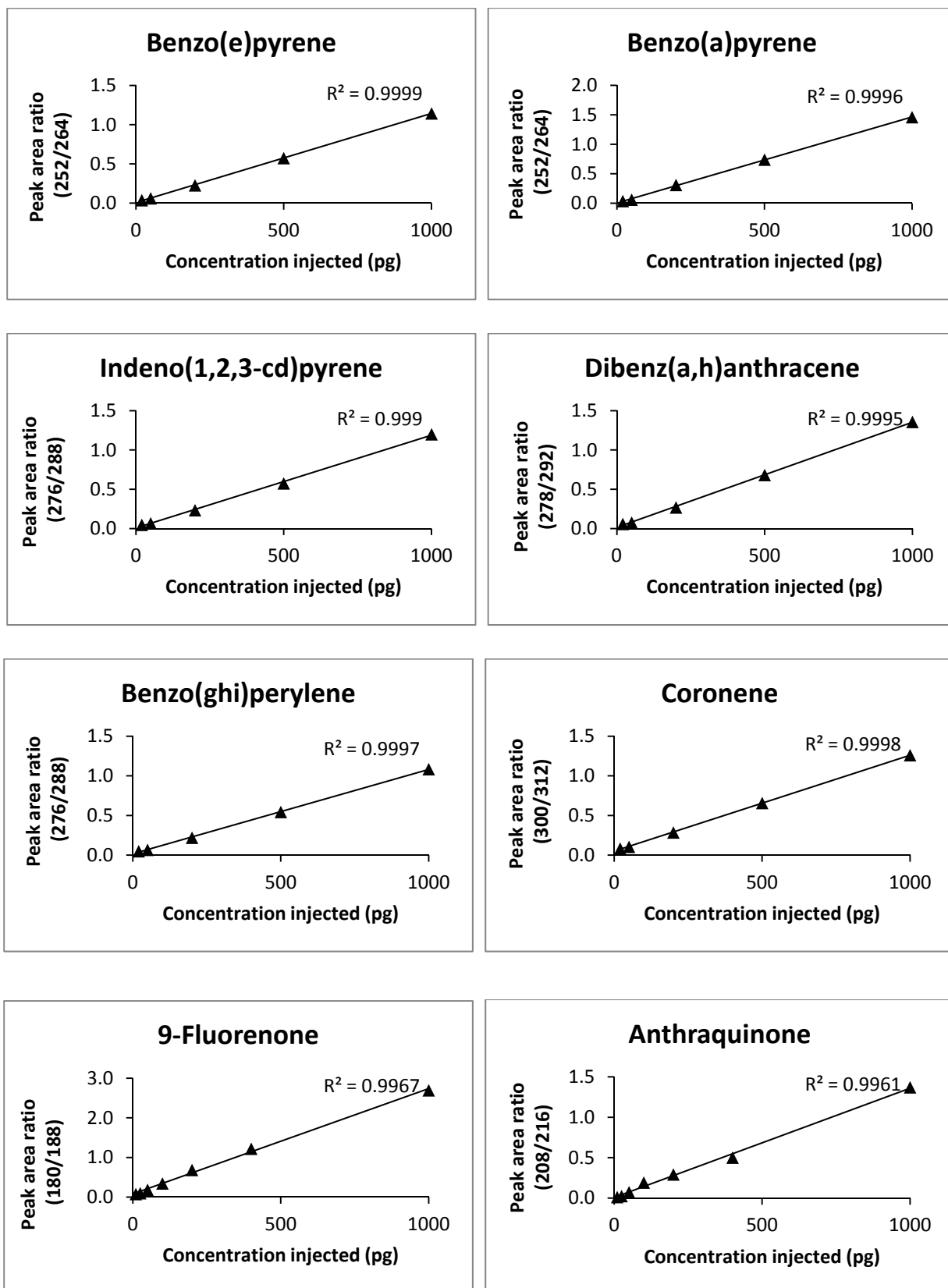


Figure 2.4(cont). Calibration curves for the quantification of all PAH, OPAH and NPAH compounds measured in the present investigation.

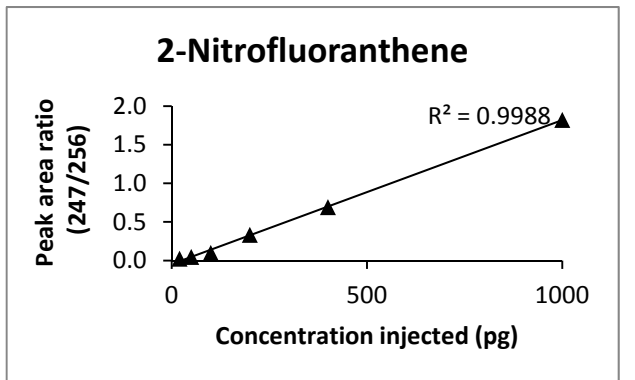
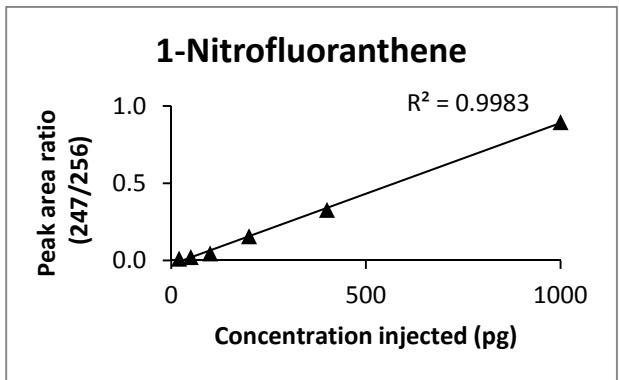
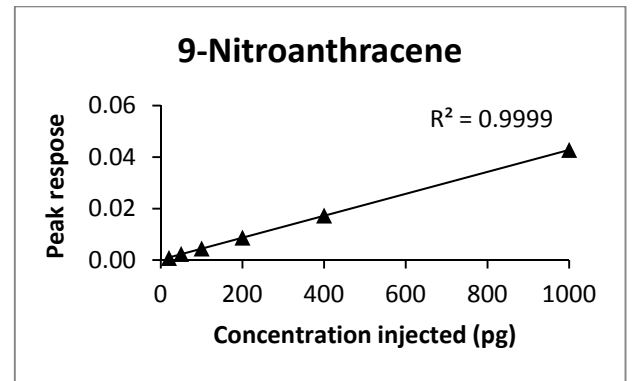
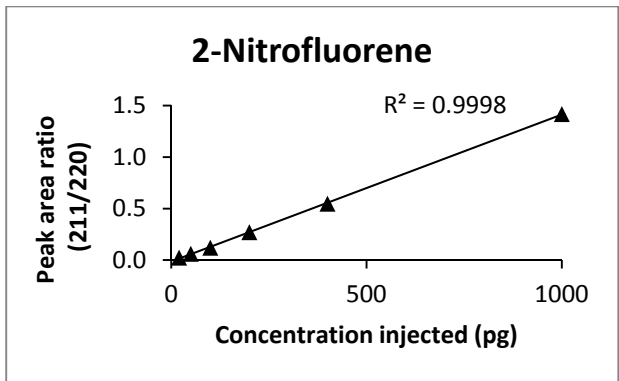
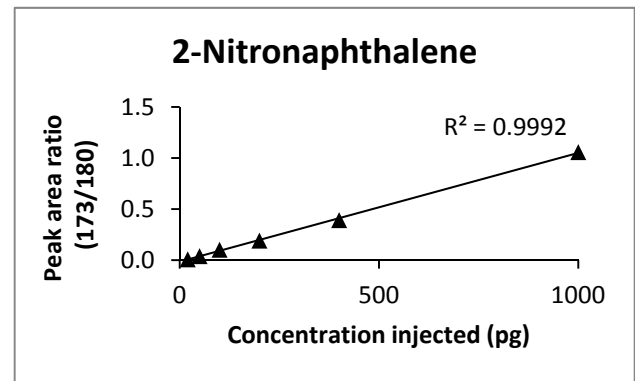
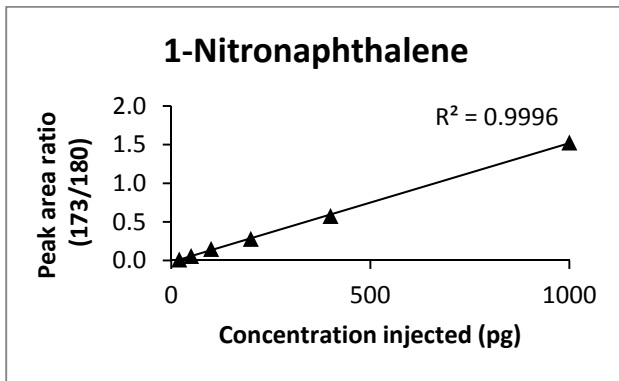
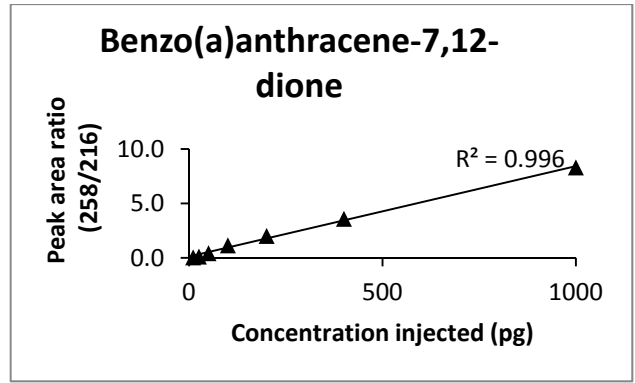
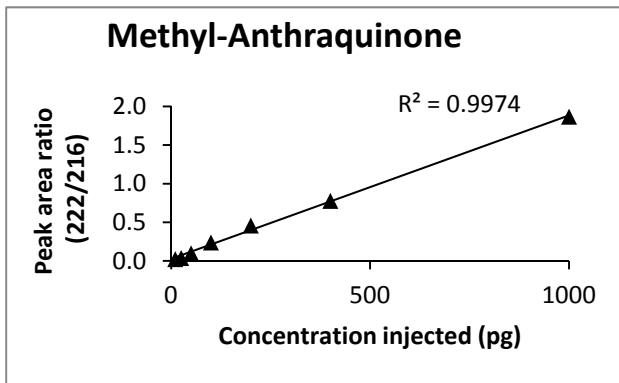


Figure 2.4(cont). Calibration curves for the quantification of all PAH, OPAH and NPAH compounds measured in the present investigation.

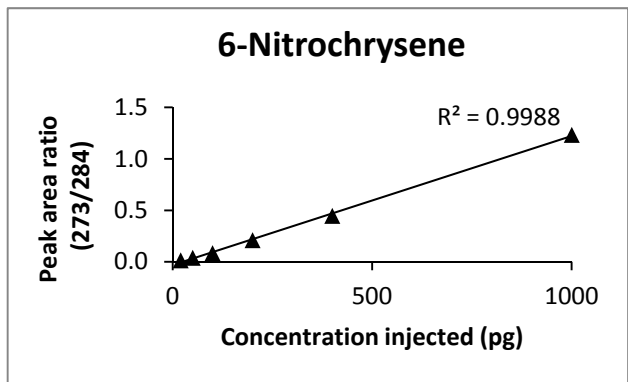
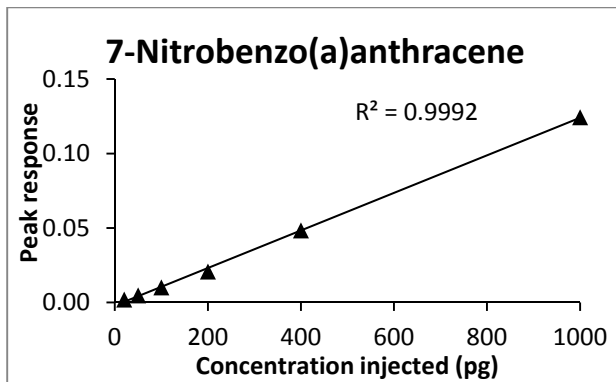
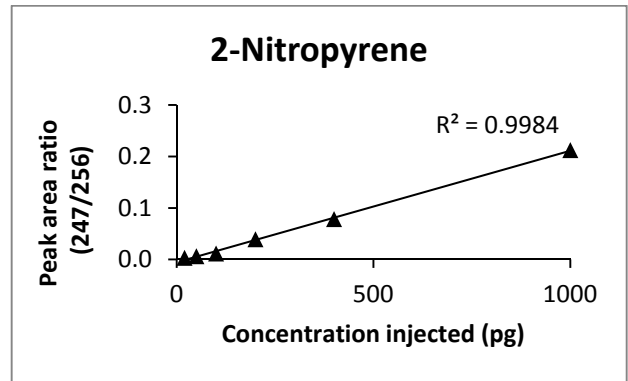
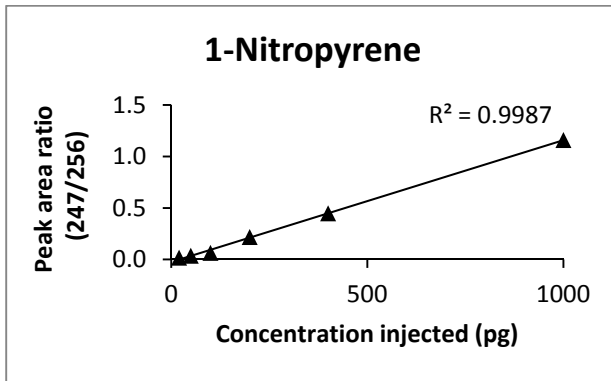
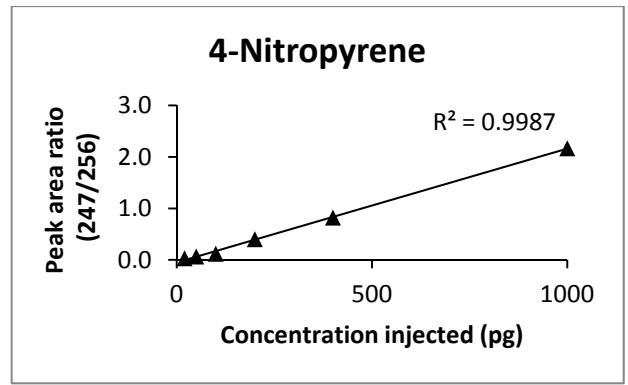
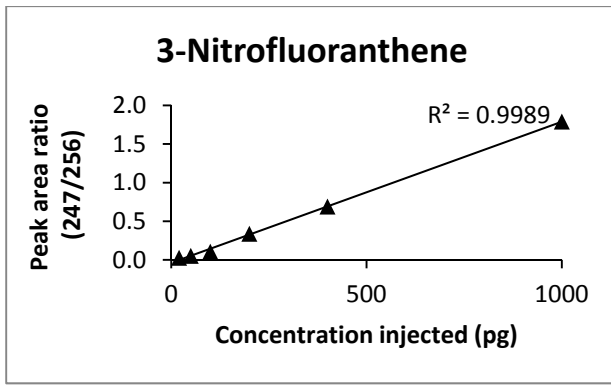


Figure 2.4(cont). Calibration curves for the quantification of all PAH, OPAH and NPAH compounds measured in the present investigation.

2.4.2. Validating analytical method

2.4.2.1. Recoveries

Percentage recoveries of internal standards were calculated to assess loss of target compounds during extraction and clean-up procedure (Table 2.3). This was based on the calculation (Laurie, 2003) :

$$\% \text{ Recovery} = [(A_{is} / A_{rds})_s \times (A_{rds} / A_{is})_{std}] \times [(C_{is} / C_{rds})_{std} \times (C_{rds} / C_{is})_s] \times 100 \quad (2.7)$$

Where :

$(A_{is}/A_{rs})_s$ = response ratio of internal standard to recovery standard (sample)

$(A_{rs}/A_{is})_{std}$ = response ratio of recovery standard to internal standard (standard)

$(C_{is}/C_{rs})_{std}$ = the concentration ratio of recovery standard to internal standard (standard)

$(C_{rs}/C_{is})_s$ = the concentration ratio of internal standard to recovery standard (sample)

Acceptable recoveries were considered to be in the range 30-150%. In some cases where recoveries fell outside of this range, the analyte concentration for the IS compound in question was removed when calculating the mean of this compound.

2.4.2.2. Standard reference material analysis (SRM)

In order to test the accuracy, precision and reproducibility of the extraction, clean-up and analysis methods, a validation experiment was carried out by performing replicate analysis of NIST Standard Reference Material 1649b (urban dust). 10 samples of ~10mg SRM 1649b material were weighed and extracted, cleaned up and analysed for all target compounds using the procedure described above.

Table 2.4. shows the mean concentrations measured in these samples and, where available, these are compared with the certified or reference concentrations provided by NIST. It can be seen that in all cases, the mean concentration measured with this method fell within or close to one standard deviation of the certified value. Therefore we can be reasonably confident of the precision and accuracy of the applied method in this investigation.

2.4.2.3. *Sample blanks*

In order to provide 'blank' field samples, filters and PUFs were prepared for sampling, as described in Section 1.3.1, transported to the sampling site(s) and installed inside the sampler. In these cases, the sampler was not run and the filters and PUFs were immediately transported to the laboratory. As these 'samples' had not been exposed to ambient air, they were used as sample blanks, representing concentrations of compounds resulting from contamination that may have occurred during preparation and transport of filters and PUFs.

A total of eight sample blanks (filters and PUFs) were prepared in this way during the campaigns. Blank concentrations were calculated assuming a sampling volume of 1043 m³, the mean air volume of all air samples measured. The mean concentrations of target compounds in sample blanks in filters and PUFs, and their relative levels to annual mean measured concentrations, is shown in Table 2.4 and Table 2.5 respectively. These mean values were then subtracted from measured sample concentrations to take into account this background contamination.

2.4.2.4. Detection Limits

Instrument detection limits (IDLs) (i.e. the minimum analyte concentration required to obtain an instrument response) were calculated for each target compound for a signal to noise ratio of 5:1. Method Detection Limits (MDLs) (i.e. the minimum detectable atmospheric concentration in the for each target compound) were calculated assuming a final sample volume of 100uL and an air

sample volume of 1043 m³, the mean air volume of all air samples measured. IDL and MDL values are shown in Table 2.6.

Table 2.3. Calculated recoveries for all internal standards used in the analysis of samples from Campaigns 1, 2 and 3.

Internal Standard	Filter			PUF		
	mean Recovery (%)	# of samples >150%	# of samples <30%	mean Recovery (%)	# of samples >150%	# of samples <30%
Acenaphylene-d8	74	2	2	48	1	3
Acenaphthene-d10	66	1	2	50	2	5
Fluorene-d10	78	2	3	57	2	4
Phenanthrene-d10	70	1	2	54	1	3
Anthracene-d10	68	1	3	60	3	4
Fluoranthene-d10	73	2	2	51	3	5
Pyrene-d10	74	1	3	57	2	4
Benzo(a)anthracene-d12	68	1	2	61	1	3
Chrysene-d12	78	1	2	63	1	3
Benzo(b)fluoranthene-d12	69	1	3	57	0	2
Benzo(k)fluoranthene-d12	72	1	2	52	1	3
Benzo(e)pyrene-d12	56	0	4	41	0	2
Benzo(a)pyrene-d12	75	3	2	43	0	2
Indeno(1,2,3-cd)pyrene-d12	77	3	2	59	1	1
Dibenz(a,h)anthracene-d12	79	2	3	56	2	2
Benzo(ghi)perylene-d12	80	3	3	56	2	3
Coronene-d12	69	0	4	43	1	3
1-Nitronaphthalene-d7	71	2	2	72	3	2
2-Nitrofluorene-d8	66	1	1	50	0	3
3-Nitrofluoranthene-d9	62	0	2	49	1	3
1-Nitropyrene-d9	58	0	2	52	1	3
6-Nitrochrysene-d11	61	1	2	45	0	2
9-Fluorenone-d8	80	3	2	70	3	1
Anthraquinone-d8	76	2	1	60	3	1

Table 2.4. Measured mean and standard deviation for concentrations of PAH, OPAH and NPAH compounds in NIST Standard Reference Material 1649b (urban dust).

PAHs	Mean (mg/kg)	SD (mg/kg)	NIST value (mg/kg)
Acenaphthylene	0.3	0.1	0.2±0.036 ^b
Acenaphthene	0.2	0.05	0.2±0.026 ^b
Fluorene	0.3	0.05	0.2±0.02 ^b
Phenanthrene	4	0.5	3.9±0.05 ^a
Anthracene	0.4	0.1	0.4±0.002 ^b
Fluoranthene	6	1	6.1±0.1 ^a
Pyrene	5	0.7	4.8±0.03 ^a
Retene	0.3	0.05	0.3±0.04 ^a
Benzo(a)anthracene	2	0.4	2.1±0.05 ^a
Chrysene	3	0.5	3.01±0.04 ^a
Benzo(b)fluoranthene	6	0.6	6±0.2 ^a
Benzo(k)fluoranthene	2	0.4	1.8±0.08 ^a
Benzo(e)pyrene	3	1	3±0.04 ^a
Benzo(a)pyrene	3	0.5	2.5±0.2 ^a
Indeno(1,2,3-cd)pyrene	1	0.1	1.1±0.4 ^a
Dibenz(a,h)anthracene	0.3	0.04	0.3±0.004 ^a
Benzo(ghi)perylene	4	0.2	3.9±0.05 ^a
Coronene	3	0.3	2.8±0.5 ^b
OPAHs	Measured mean (mg/kg)	Measured SD (mg/kg)	NIST value (mg/kg)
9-Fluorenone	1	0.2	1.4 ^b
Anthraquinone	2	0.2	1.8 ^b
2-Methyl-Anthraquinone	1	0.1	n/a
Benzo(a)anthracene-7,12-dione	3	0.4	3.6 ^b
NPAHs	Measured mean (ug/kg)	Measured SD (ug/kg)	NIST value (ug/kg)
1-Nitronaphthalene	8	4	7.2±0.1 ^b
2-Nitronaphthalene	12	5	11.4±0.3 ^b
2-Nitrofluorene	59	12	n/a
9-Nitroanthracene	39	11	34.6±0.7 ^b
1-Nitrofluoranthene	29	14	n/a
2-Nitrofluoranthene	311	21	311±5 ^b
3-Nitrofluoranthene	6	2	4.6±0.1 ^b
4-Nitropyrene	7	4	5.5±0.1 ^b
1-Nitropyrene	68	9	71.8±1.3 ^b
2-Nitropyrene	17	7	10.8±0.3 ^b
7-Nitrobenzo(a)anthracene	25	4	24.2±0.7 ^b
6-Nitrochrysene	4	3	3.8±0.1 ^b

n/a = no value available; a = certified value; b = reference value

Table 2.5. Sample blank concentrations (filters) and comparison with mean annual levels measured at EROS and BROS.

	Mean Blank ($\mu\text{g m}^{-3}$)	Standard deviation	EROS Mean ($\mu\text{g m}^{-3}$) ^a	% Blank (EROS)	BROS Mean ($\mu\text{g m}^{-3}$) ^a	% Blank (BROS)
Acy	0.4	0.3	7	5	17	2
Ace	0.4	0.2	45	1	52	0.7
Flo	0.9	0.4	12	8	27	3
Phe	4	0.8	192	2	411	0.9
Ant	0.1	0.0	21	0.7	47	0.3
Flt	3	0.6	233	1	544	0.5
Pyr	2	0.4	167	1	479	0.4
Ret	2	1.1	132	1	187	1
BaA	0.7	0.2	101	0.7	176	0.4
Chr	1	0.2	239	0.5	354	0.3
BbF	0.9	0.1	176	0.5	239	0.4
BkF	0.6	0.3	171	0.3	238	0.2
BeP	1	0.5	120	0.9	162	0.7
BaP	0.8	0.4	102	0.8	167	0.5
IPy	0.7	0.3	137	0.5	184	0.4
DBA	0.6	0.3	33	2	42	1
BPy	0.8	0.4	164	0.5	243	0.3
Cor	2	0.5	83	2	98	2
1NNap	0.03	0.01	2	1.8	5	0.7
2NNap	0.02	0.01	1	1.8	4	0.6
2NFlo	0.05	0.08	1	4	3	2
9NAnt	0.1	0.3	11	1.1	20	0.7
1NFlt	0.03	0.02	4	0.8	9	0.3
2NFlt	0.03	0.01	25	0.1	37	0.1
3NFlt	0.01	0.003	2	0.5	3	0.1
4NPyr	0.01	0.003	3	0.2	4	0.2
1NPyr	0.03	0.02	7	0.4	19	0.2
4NPyr	0.06	0.04	10	0.6	15	0.4
7NBaA	0.02	0.02	5	0.5	8	0.3
6NChr	0.01	0.002	0.7	1	1	0.3
9F	0.3	0.2	72	0.4	156	0.2
AQ	1.6	1.0	430	0.4	721	0.2
MAQ	1	0.4	278	0.3	433	0.2
BaAQ	0.6	0.5	78	0.5	111	0.5

a : mean particle-phase concentration measured in samples from Campaign 1 (Section 3)

Table 2.6. Sample blank concentrations (PUF) and comparison with mean annual levels measured at EROS and BROS.

	Mean Blank (pg m ⁻³)	Standard deviation	EROS Mean (pg m ⁻³) ^a	% Blank (EROS)	BROS Mean (pg m ⁻³) ^a	% Blank (BROS)
Acy	6	1	444	1.4	1775	0.4
Ace	21.5	5	1609	1.3	1747	1
Flo	41	5.5	2336	1.8	3708	1
Phe	303	39	5839	5.2	9569	3
Ant	16	3	579	2.7	1382	1
Flt	56	7	2295	2.4	3798	1.5
Pyr	60	11	1749	3.4	3058	2
Ret	80	13	802	10.0	1209	7
BaA	4.5	0.6	39	11.5	73	6
Chr	10	1.5	72	13.7	131	8
BbF	6	1	69	9.0	95	7
BkF	4	0.8	74	5.7	86	5
BeP	3	0.8	30	10.6	38	8
BaP	3	1	19	18.1	32	11
IPy	7	1	36	19.7	38	19
DBA	1	0.4	4	27.3	14	8
BPy	4	2	32	11.6	39	9
Cor	1	0.2	7	14.5	6	18
1NNap	0.5	0.4	90	0.5	233	0.2
2NNap	0.3	0.1	61	0.6	110	0.3
2NFlo	0.2	0.1	1	12	2	7
9NAnt	0.04	0.02	7	0.5	9.5	0.4
1NFlt	0.2	0.3	0.9	19	1	13
2NFlt	0.1	0.1	4	2.5	4	2
3NFlt	0.03	0.1	1	4	0.3	16
4NPyr	0.1	0.1	1	24	0.6	25
1NPyr	0.3	0.3	1	39	1	26
4NPyr	0.3	0.5	2	17	2	18
7NBaA	0.001	0.003	0.1	3	0.02	20
6NChr	0.002	0.01	0.04	0.04	0.04	21
9F	13	1	1394	1	2248	0.6
AQ	12	2	274	3	395	3
MAQ	1	0.7	76	1	81	2
BaAQ	0.3	0.2	4	7.5	7	4

a : mean gas-phase concentration measured in samples from Campaign 1 (Section 3)

Table 2.7. Instrument detection limits (IDLs) and method detection limits (MDLs).

	Instrument Detection Limit (IDL), pg	Filter Method Detection Limit (MDL), pg/m³	PUF Method Detection Limit (MDL), pg/m³
PAH			
Acenaphthylene	1.87	0.72	0.07
Acenaphthene	1.11	0.42	0.04
Fluorene	2.35	0.9	0.09
Phenanthrene	2.18	0.84	0.08
Anthracene	2.89	1.11	0.11
Fluoranthene	1.79	0.69	0.07
Pyrene	2.18	0.84	0.08
Retene	1.41	0.54	0.05
Benzo(a)anthracene	2.68	1.03	0.1
Chrysene	2.49	0.95	0.09
Benzo(b)fluoranthene	2.44	0.94	0.09
Benzo(k)fluoranthene	1.8	0.69	0.07
Benzo(e)pyrene	1.47	0.56	0.05
Benzo(a)pyrene	1.31	0.5	0.05
Indeno(1,2,3-cd)pyrene	3.01	1.16	0.11
Dibenz(a,h)anthracene	2.51	0.96	0.09
Benzo(ghi)perylene	2.25	0.86	0.08
Coronene	1.72	0.66	0.06
OPAH			
9-Fluorenone	0.05	0.02	0.003
Aceanthraquinone	0.16	0.06	0.01
Methyl-Anthraquinone	0.14	0.05	0.004
Benzo(a)anthracene-7,12-dione	0.04	0.01	0.003
NPAH			
1-Nitronaphthalene	0.11	0.04	0.003
2-Nitronaphthalene	0.25	0.1	0.01
2-Nitrofluorene	0.06	0.02	0.002
9-Nitroanthracene	4.69	1.8	0.17
1-Nitrofluoranthene	0.5	0.19	0.02
2-Nitrofluoranthene	0.18	0.07	0.01
3-Nitrofluoranthene	0.16	0.06	0.01
4-Nitropyrene	0.06	0.02	0.006
1-Nitropyrene	0.17	0.06	0.01
2-Nitropyrene	0.54	0.21	0.02
7-Nitrobenzo(a)anthracene	0.42	0.16	0.02
6-Nitrochrysene	0.06	0.02	0.004

Chapter 3 : Concentrations and trends of PAHs, OPAHs and NPAHs in the ambient urban atmosphere

3.1. Measured concentrations of PAH, OPAH and NPAH

Details of the samples taken in Campaign 1 are provided in Table 2.1. The mean concentrations for all PAH, OPAH and NPAH compounds measured in Campaign 1 are presented in Table 3.1. Box plots of the measured concentrations for all compounds during this campaign are presented in Figure 3.1. Because sampling was conducted during all four seasons of the year, the mean concentrations measured are assumed to represent an 'annual mean' concentration.

3.1.1 PAH and OPAH concentrations

Annual mean concentrations (sum of particulate and vapour phases) of PAHs measured in Campaign 1 at BROS and EROS are shown in Figure 3.2. Annual mean total PAH concentrations (sum of 18 compounds measured) were 30.5 ng m^{-3} and 18.2 ng m^{-3} at BROS and EROS respectively. The most abundant PAHs at both sites were the 3- or 4-ring compounds Phe, Flo, Flu and Pyr. These compounds are shown to contribute >70% to the total PAH load at both sites.

PAH concentrations observed at these sites are broadly of the same magnitude as levels typically observed in the UK atmosphere at urban, suburban and roadside locations (Brown *et al.*, 2013; Halsall *et al.*, 1993; Meijer *et al.*, 2008; Prevedouros *et al.*, 2004a). LMW (3-4 ring) PAHs, present predominantly in the gas-phase, dominate the total PAH load compared with HMW (5+ ring) PAHs, which are present mostly in the particulate phase. The average gas-phase/particulate-phase ratio for total PAH measured in this campaign was 8.8 and 9.6 for BROS and EROS respectively. The higher ratio at EROS may indicate an influence of phase-partitioning to the gas-phase occurred between sites (discussed further in Section 3.5).

Table 3.1. The mean and (range) of particle-phase (P), vapour-phase (V) and total (T) PAH, OPAH and NPAH concentrations measured during Campaign 1 at BROS and EROS (n=24).

	BROS			EROS		
	P (pg m ⁻³)	V (pg m ⁻³)	T (pg m ⁻³)	P (pg m ⁻³)	V (pg m ⁻³)	T (pg m ⁻³)
Acy	17 (2 – 54)	1775 (172 – 11700)	1792 (190 – 11755)	7 (<MDL – 18)	443 (404 – 1723)	450 (76 – 2390)
Ace	52 (17 – 138)	1747 (329 – 5280)	1800 (432 – 5343)	45 (8-74)	1609 (418 – 4039)	1653 (433 – 4085)
Flo	27 (7 – 65)	3708 (1556 – 12570)	3735 (1560 – 12636)	12 (6-31)	2336 (1047 – 4135)	2348 (1054 – 4157)
Phe	411 (100 – 1602)	9569 (2462 – 21850)	9980 (2632 – 22173)	192 (73 – 490)	5839 (2083 – 17497)	6031 (2220 – 17728)
Ant	47(3 –142)	1382 (319 – 2713)	1429 (415 – 2801)	21 (5 – 72)	579 (153 – 1281)	599 (160 – 1046)
Flt	544(112 – 1276)	3798 (1421 – 7362)	4342 (1558 – 7008)	233 (75 – 658)	2295 (709 – 4075)	2528 (823 – 4150)
Pyr	479 (87 – 1155)	3058 (1700- 7972)	3537 (1959 – 5528)	167 (64 – 513)	1749 (626 – 5468)	1916 (712 – 3531)
Ret	187 (69 – 724)	1209 (104 – 2426)	1395 (216 – 2756)	132 (42 – 407)	802 (58 – 1604)	934 (132 – 1597)
BaA	176 (27 – 696)	73 (5 – 235)	249 (64 – 828)	101 (19 – 373)	39 (8 – 174)	140 (39 – 548)
Chr	354 (77 – 1502)	131 (<MDL – 420)	485 (158 – 1922)	239 (28 – 1006)	72 (9 – 240)	311(50 – 1246)
BbF	239 (68 – 971)	95 (<MDL – 633)	333 (100 – 1180)	176 (38 – 634)	69 (<MDL – 249)	245 (61 – 764)
BkF	238 (65 – 991)	86 (<MDL – 463)	324 (95 – 1454)	171 (45 – 670)	74 (<MDL – 295)	244 (60 – 870)
BeP	162 (49 – 594)	38 (5 – 125)	200 (77 – 645)	120 (34 – 436)	30 (1 – 71)	151 (46 – 507)
BaP	167 (29 – 668)	32 (<MDL – 99)	200 (37 – 698)	102 (19 – 377)	19 (1 – 67)	121 (35 – 404)
IPy	184 (52 – 670)	38 (0.7 – 100)	222 (89 – 770)	137 (38 – 473)	36 (6 – 106)	173 (68 – 579)
DBA	42 (9 – 150)	14 (<MDL – 71)	56 (12 – 150)	33 (8 – 96)	4 (<MDL – 25)	37 (8 – 96)
BPy	243 (54 – 841)	38 (<MDL – 123)	282 (61 – 837)	164 (50 – 544)	32 (<MDL – 84)	195 (84 – 563)
Cor	98 (50 – 269)	6 (0 – 22)	104 (42 – 284)	83 (24 – 172)	7 (<MDL – 61)	90 (34 – 252)
9F	156 (11 – 740)	2248 (833 – 4943)	2404 (890 – 5680)	72 (10 – 330)	1394 (481 – 2821)	1466 (512– 2973)
AQ	721 (113 – 1742)	395 (132 – 983)	1086 (632 – 2013)	430 (90 – 984)	274 (72 – 821)	704 (451 – 1023)
MAQ	433 (203 – 743)	81 (23 – 193)	514 (253 – 794)	278 (121 – 453)	76 (<MDL – 174)	354 (183 – 573)
BaAQ	111 (32 – 314)	7 (<MDL – 23)	118 (32 – 312)	78 (34 – 204)	4 (<MDL – 10)	82 (32 – 203)
1NNap	5 (0.4 – 11)	233 (78 – 676)	238 (81 – 686)	2 (<MDL – 7)	90 (41 – 261)	92 (42 – 264)
2NNap	4 (0.7 – 10)	110 (51 – 214)	113 (53 – 224)	1 (0.6 – 3)	60 (32 – 168)	61 (32 – 169)
2NFlo	3 (0.6 – 8)	2 (0.8 – 5)	5 (2 – 10)	1 (0.6 – 4)	1 (0.5 – 3)	3 (1.3 – 5)
9NAnt	20 (3 – 49)	10 (2 – 18)	30 (6 – 56)	11 (2 – 26)	7 (2 – 15)	18 (5 – 32)
1NFlt	9 (0.6 – 17)	1 (<MDL – 7)	10 (0.7 – 18)	4 (0.4 – 8)	1 (<MDL – 4)	4 (1 – 9)
2NFlt	37 (4 – 163)	4 (0.7 – 14)	41 (9 – 169)	25 (4 – 94)	4 (<MDL – 23)	30 (5 – 94)
3NFlt	3 (0.1 – 12)	0.3 (<MDL – 1)	3 (0.1 – 12)	2 (0.1 – 7)	0.5 (<MDL – 3)	2 (0.1 – 7)
4NPyr	4 (0.8 – 20)	0.6 (<MDL – 2)	5 (0.9 – 20)	3 (0.2 – 13)	0.6 (<MDL – 4)	4 (0.4 – 13)
1NPyr	19 (6 – 67)	1 (<MDL – 5)	20 (7 – 67)	7 (1 – 31)	0.9 (<MDL – 6)	8 (2 – 31)
2NPyr	15 (4 – 11)	2 (4 – 6)	16 (5 – 107)	10 (<MDL – 62)	2 (<MDL – 6)	12 (2 – 62)
7NBaA	8 (1 – 28)	0.02 (<MDL – 0.2)	8 (1 – 28)	5 (0.6 – 14)	0.1 (<MDL – 3)	5 (0.7 – 14)
6NChr	1 (0.1 – 4)	0.04 (<MDL – 0.5)	1 (0.1 – 4)	0.7 (<MDL – 2)	0.02 (<MDL – 0.2)	0.7 (<MDL – 2)

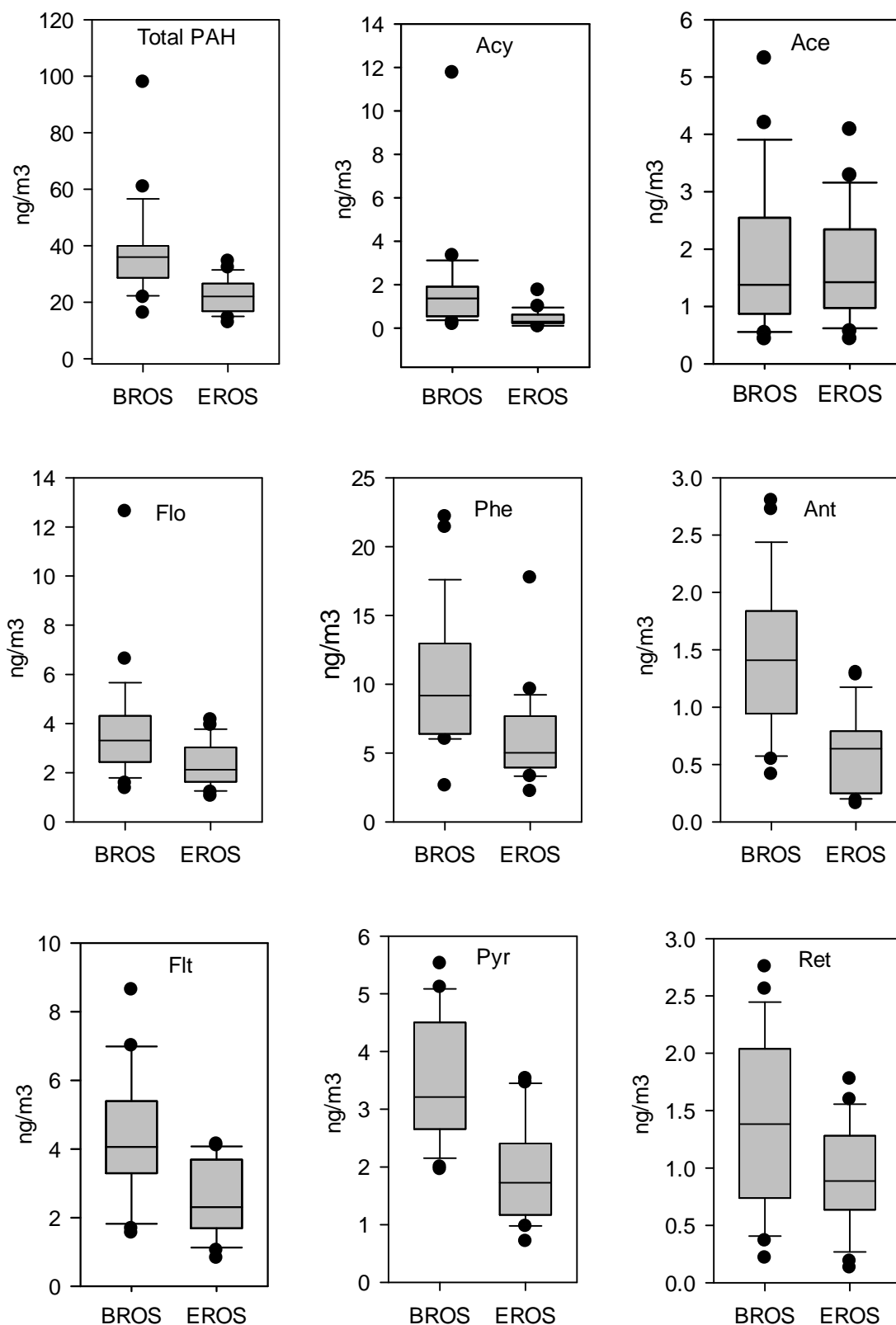


Figure 3.1. Box plots of PAH concentrations measured at BROS and EROS in Campaign 1 (n=24). The upper and lower boundaries of the box represent the 75th and 25th percentile values respectively. The upper and lower boundaries of the whiskers represent the 90th and 10th percentile values respectively. The median value is represented by the vertical line within the box. Black dots represent outlier values.

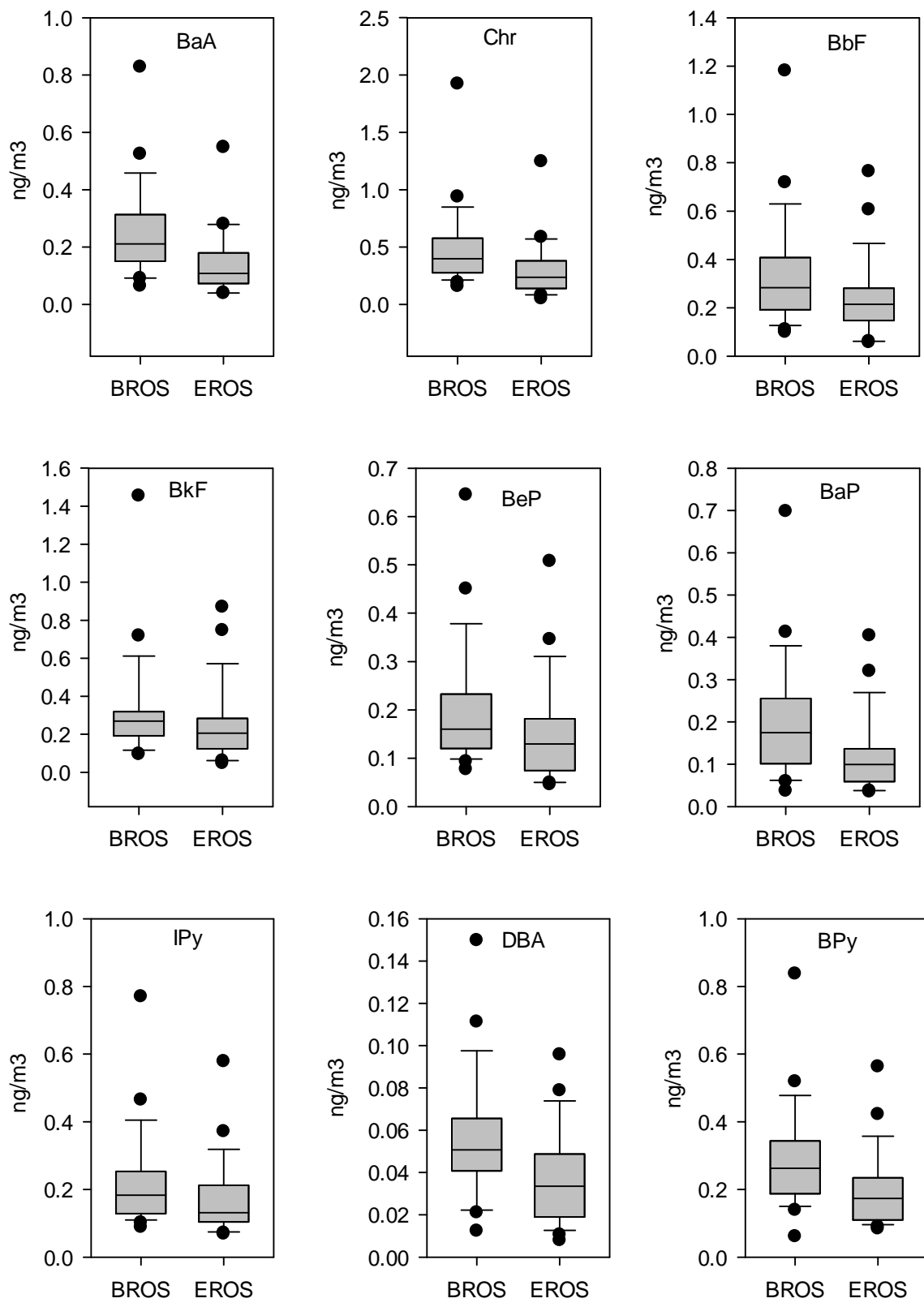


Figure 3.1(cont). Box plots of PAH, OPAH and NPAH concentrations measured at BROS and EROS in Campaign 1 (n=24).

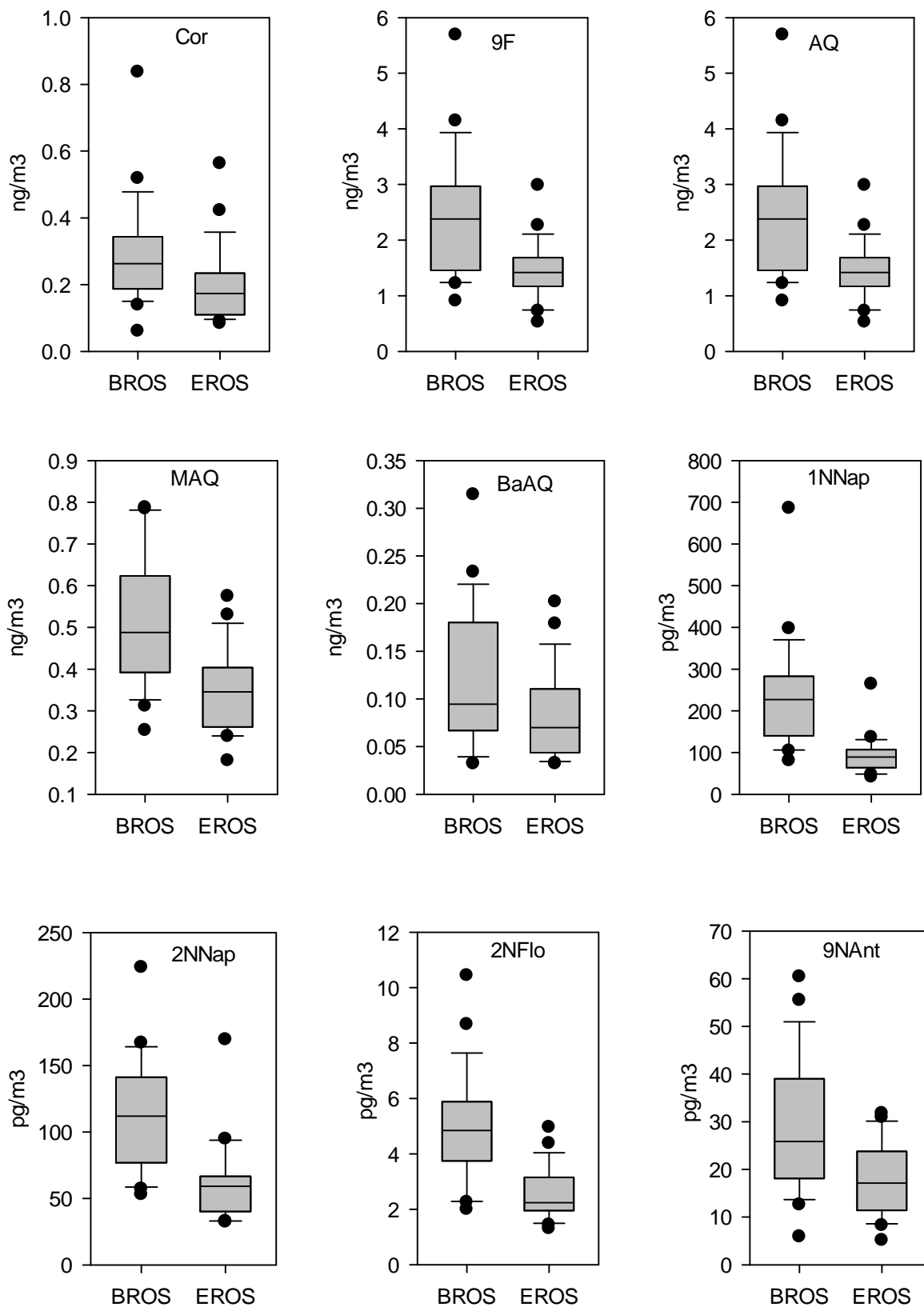


Figure 3.1(cont). Box plots of PAH, OPAH and NPAH concentrations measured at BROS and EROS in Campaign 1 (n=24).

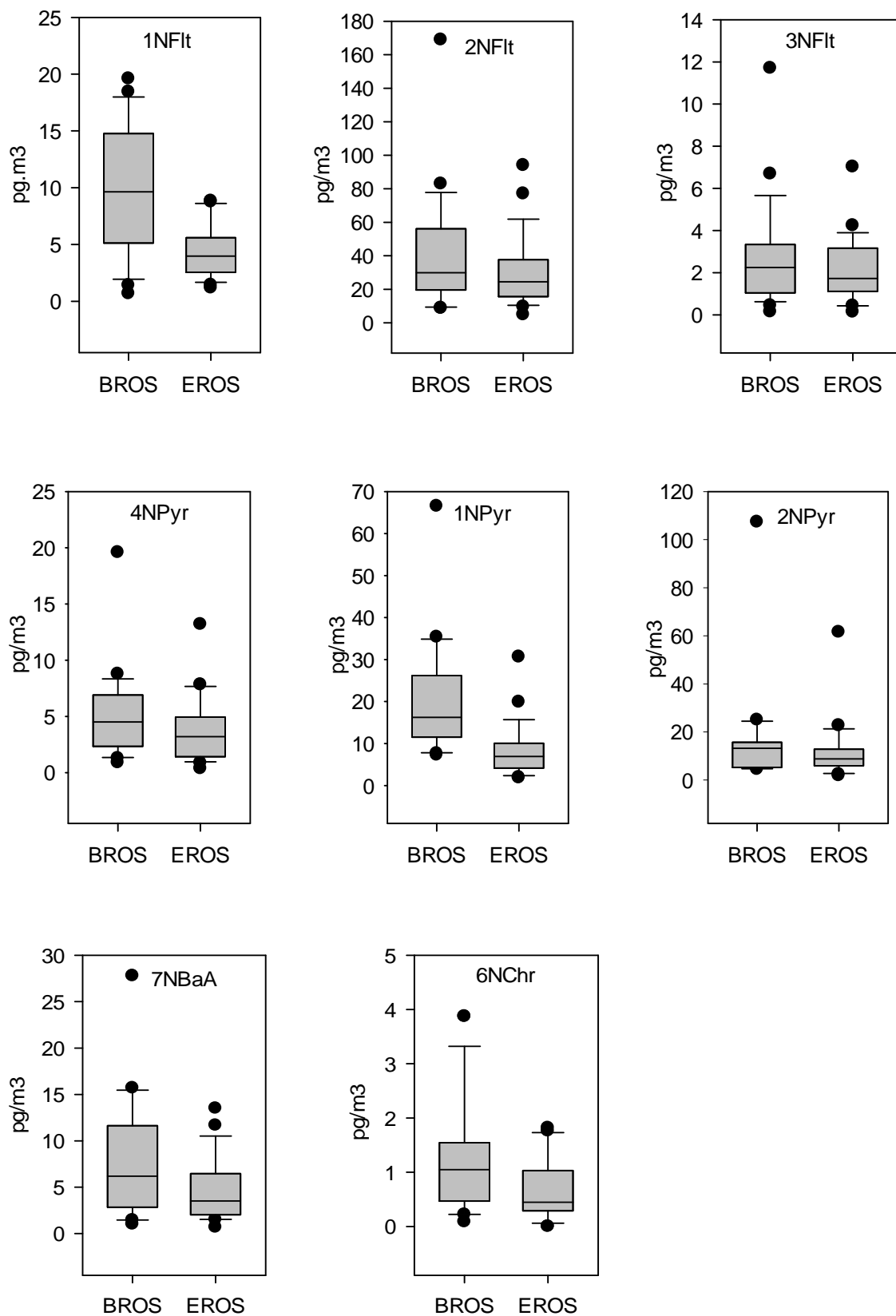


Figure 3.1(cont). Box plots of PAH, OPAH and NPAH concentrations measured at BROS and EROS in Campaign 1 (n=24).

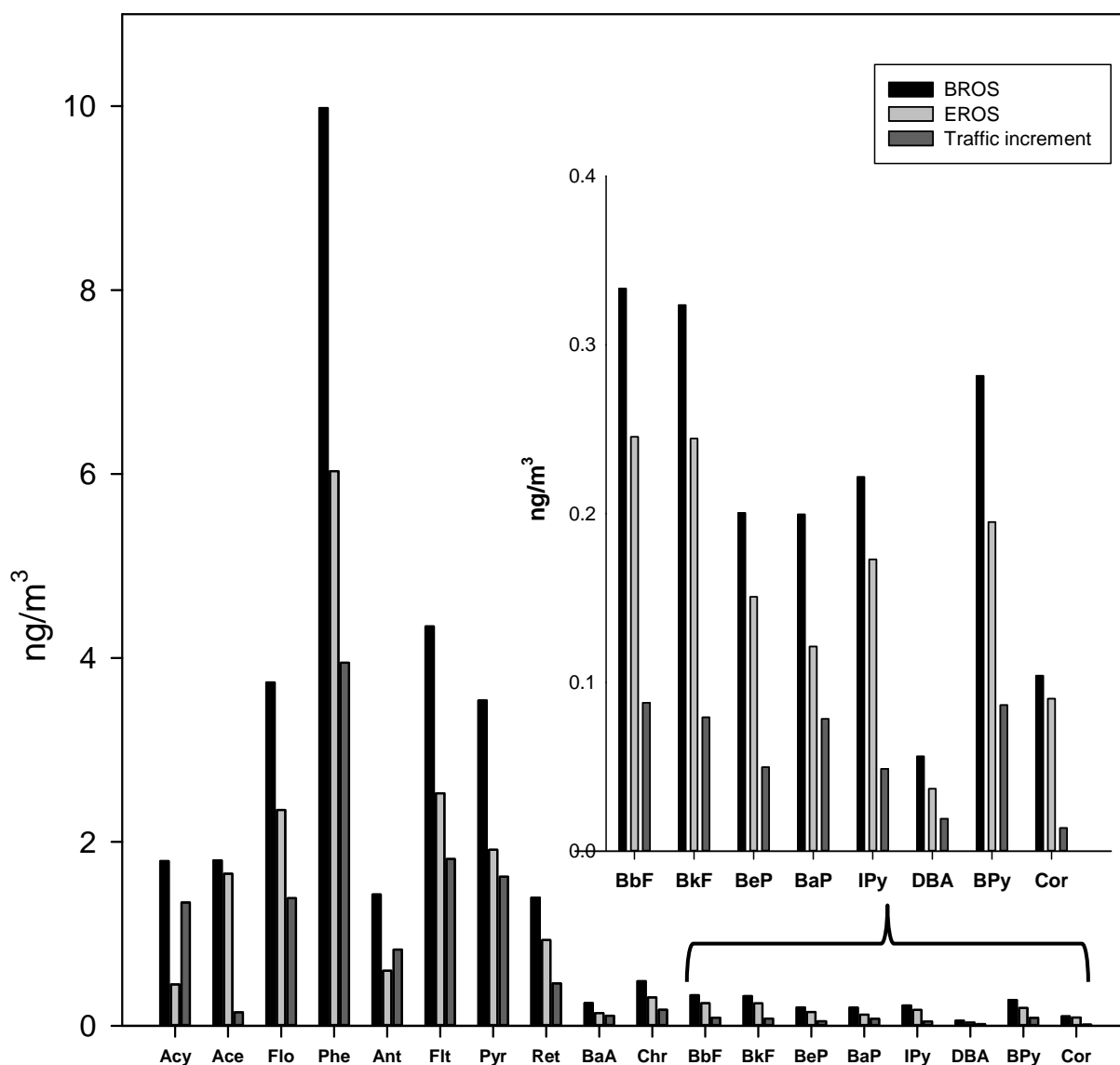


Figure 3.2. Mean concentrations (P + V) of PAH compounds measured at BROS and EROS and the ‘traffic increment’ (i.e. the BROS – EROS concentration) during Campaign 1 (n=24).

The relative distribution of compounds is very similar at BROS and EROS, suggesting a common emission source is dominating both sites. These observations are in good agreement with the typical species distribution of PAHs observed previously at these sites (Alam *et al.*, 2013; Delgado-Saborit *et al.*, 2013; Harrad and Laurie, 2005; Harrison *et al.*, 2003), at other sites in the Birmingham area (Dimashki *et al.*, 2001; Smith and Harrison, 1996), and at other urban and

suburban sampling locations in the UK (Eiguren-Fernandez *et al.*, 2003; Halsall *et al.*, 1993; Meijer *et al.*, 2008; Prevedouros *et al.*, 2004a).

Annual mean concentrations (sum of particulate- and vapour- phases) of the four OPAH measured in campaign 1 are shown in Figure 3.3.

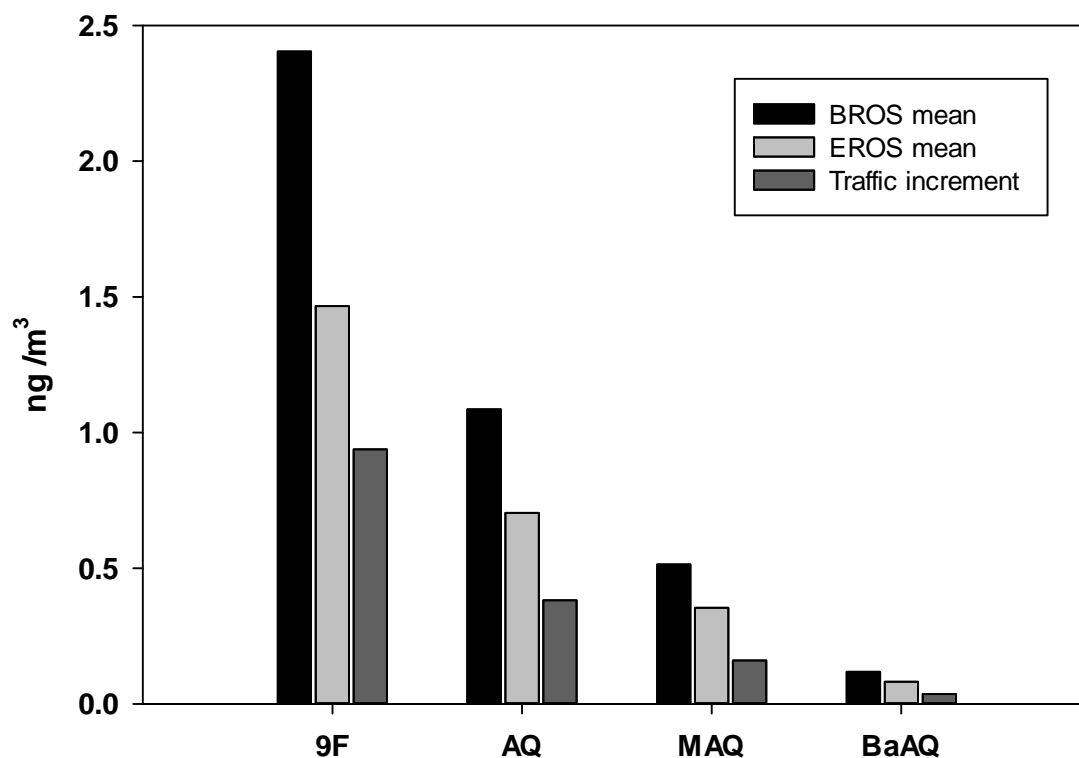


Figure 3.3. Mean concentrations (P + V) of OPAH compounds measured at BROS and EROS and the 'traffic increment' (i.e. the BROS – EROS concentration) during Campaign 1 (n=24).

9F was the most abundant OPAH, present predominantly in the gas phase. AQ was present at levels a factor ~2 lower than 9F at both sites and is shown to undergo considerable partitioning between phases. MAQ is present at levels 2-3 times lower than AQ. MAQ was present mostly in the particulate phase, in contrast to previous measurements at these sites (Alam *et al.*, 2013; Delgado-Saborit *et al.*, 2013), which suggested this OPAH was present mainly in the gas-phase.

Table 3.2 provides a comparison between measured OPAH and NPAH concentrations with those reported in previous studies. Relatively few previous studies have measured OPAHs and NPAHs in the ambient atmosphere in both particulate and gas phases. Furthermore, many previous measurements have been carried out as seasonal campaigns, collecting samples in summer and winter months only so comparisons must be made with caution.

Concentrations of 9F, AQ and BaAQ (P+V) concentrations measured at BROS in this study fall within the range of concentrations measured by (Albinet *et al.*, 2008a) during winter and summer months in two Alpine valley locations in France. When just particulate-phase is considered, OPAH concentrations measured at BROS are generally similar to those measured previously in Paris, France (Nicol *et al.*, 2001) ; Basel, Switzerland (Niederer, 1998) ; Munich, Germany (Schnelle-Kreis *et al.*, 2001); Augsburg, Germany (Liu *et al.*, 2006b; Schnelle-Kreis *et al.*, 2005; Sklorz *et al.*, 2007) ; Santiago, Chile (Sienra, 2006; Tsapakis *et al.*, 2002); Finokalia, Crete (Tsapakis and Stephanou, 2007); Helsinki, Finland (Kallio *et al.*, 2003; Shimmo *et al.*, 2004a); Southern California, USA (Cho *et al.*, 2004; Chung *et al.*, 2006); Athens, Greece (Andreou and Rapsomanikis, 2009; Valavanidis *et al.*, 2006); Tempe, Arizona, USA (Delhomme *et al.*, 2008); and southern China (Wei *et al.*, 2012; Yassaa *et al.*, 2001). OPAH concentrations were lower than in more heavily polluted cities of less developed countries e.g. Algiers, Algeria (Yassaa *et al.*, 2001) and in road tunnel studies (Oda *et al.*, 2001).

PAHs and OPAHs have been measured at these sites previously (Alam *et al.*, 2013; Delgado-Saborit *et al.*, 2013; Harrad and Laurie, 2005). Concentrations of individual PAHs measured in the present study are shown to exhibit a strong ($R^2 > 0.9$) correlation with concentrations measured by Harrad and Laurie (2005) at both BROS and EROS in 1999-2001. Similarly there is a strong correlation ($R^2 = 0.94$ and 0.98 for BROS and EROS respectively) between the mean winter concentrations measured in this study and those measured during the same period by (Alam *et al.*, 2013). This suggests the dominant sources and processes governing the observed levels of PAH and OPAH at these sites have not changed significantly in the last 15 years.

Table 3.2. Comparison of total (particulate + gas) OPAH and NPAH concentrations (pg/m³) measured at different locations.

	Chamonix valley, France ^a	Houston, Texas ^b	Marseilles, France ^c	Baltimore, Maryland ^d	Birmingham, U.K. ^e
NPAHs					
1NNap	186 56	113 403	208	59 8	238 (81- 686)
2NNap	66 21	20 67	120	39 12	113 (53 – 224)
2NFlo	1 4.3	nm	21	0.4 0.1	5 (2 – 10)
9NAnt	85 22	6 60	107	64 53	30 (6 – 56)
1NFIt	nm	nm	nm	0.2 0.03	10 (0.7 – 18)
2NFIt	168	20 49		60 99	41 (9 – 169)
3NFIt	30	nm	90	0.5 0.3	3 (0.1 – 12)
4NPyr	21 3	nm	1.4	2 0.5	5 (0.9 – 20)
1NPyr	54 8	11 6	61	27 8	20 (7 – 67)
2NPyr	186 28	nm	34	7 3	16 (5 – 107)
7NBaA	13 2	nm	4	23 3	8 (1 – 28)
6NChr	0.5 1	<1 1.5	33	0.4 0.1	1 (0.1 – 4)
OPAHs					
9F	11123 1770	nm	3577	nm	2404 (890 – 5680)
AQ	3600 970	nm	1398	nm	1086 (632 – 2013)
MAQ	nm	nm	nm	nm	514 (253 – 794)
BaAQ	550 150	77 66	120	nm	118 (32 – 312)

a Albinet et al 2008, Traffic area, winter 2002-2003, n = 14 (upper) ; summer 2003 (2), n = 14 (lower)

b Wilson et al., 1995, Suburban area, Nov 1990 - Feb 1991, n=5 (upper) ; Aug-Sep 1990, n=7 (lower)

c Albinet et al 2007, Urban area, July 2004, n=12

d Bamford and Baker, 2003, city centre , Winter (Jan) n =4(upper) ; Summer (July) n=5 (lower)

e This study, Traffic site (BROS), July 2011 – May 2012, annual mean and (range) n=24

PAH and OPAH concentrations were measured at these sites most recently in January 2010 (Alam *et al.*, 2013; Delgado-Saborit *et al.*, 2013). The concentrations of LWM (3-4 ring) PAH measured in these previous studies were a factor of 2-11 higher, and HMW (5+ ring) PAHs 0.7 - 4 times higher, compared with the mean concentrations measured during the winter months in the present study. The OPAHs MAQ and BaAQ were 1.2-5.1 times higher in the previous studies. In contrast AQ was measured at higher levels in the present study. This may be due to a greater proportion of AQ observed in the particle-phase in the present study which may protect it from photo degradation processes. Higher levels of AQ could also have resulted due to inputs from atmospheric reactivity or volatilisation from soil, vegetation or road surfaces.

It should be noted that the range of ambient temperature during sampling was narrower (1°C to 4°C) in the studies by Alam *et al.* (2013) and Delgado-Saborit *et al.* (2013) compared to the winter sampling in the present study (-1 °C to 12°C). The higher concentrations of PAH and OPAH observed in the previous studies may therefore be partly explained by lower temperatures and associated lower mixing height resulting in slower advective dispersion. However, if the differences in concentrations were governed by temperature-driven variation in mixing height it may be expected that higher proportion of PAHs and OPAHs would be observed in the particle-phase than in this study. In contrast the proportion of particle-phase component for most PAH and OPAH is lower than in the present study.

As noted in Section 2.1.6, Alam and co-workers utilised a deduced sampling system, with upstream collection of the gas-phase component with XAD-4 (Delgado-Saborit *et al.*, 2014). The results of the present study may therefore not be directly comparable with those of Alam *et al.* (2013) and Delgado-Saborit *et al.* (2013) as the differences in concentrations of, and overall contribution from, gas-phase PAH and OPAH compounds in these studies may have resulted due to differences in the sampling technique used to collect the gas-phase component.

3.1.2. NPAH concentrations

Annual mean concentrations (sum of particulate- and vapour- phases) of NPAH compounds measured in this campaign at BROS and EROS are shown in Figure 3.4. 1NNap and 2NNap are the most abundant NPAHs at both sites, present almost completely in the gas-phase. These compounds are shown to result from both direct emissions and gas-phase reactions.

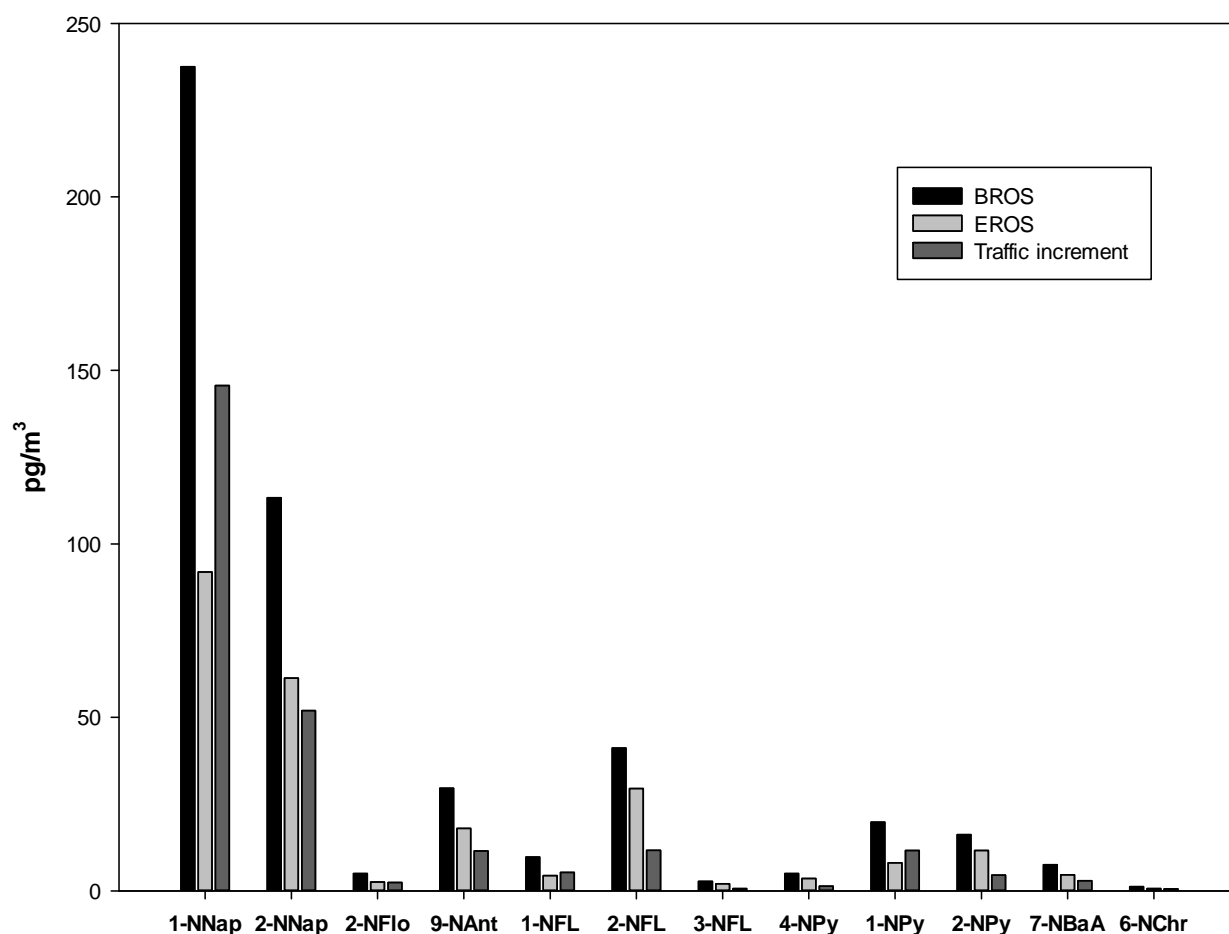


Figure 3.4. Mean concentrations (P + V) of NPAH compounds measured at BROS and EROS and the 'traffic increment' (i.e. the BROS – EROS concentration) during Campaign 1.

2NFlt is the dominant particle-bound NPAH measured, in agreement with other studies in the USA (Arey *et al.*, 1987; Bamford and Baker, 2003; Chuang *et al.*, 1991; Zielinska *et al.*, 1989) and Europe (Cecinato, 2003; Ciccioli *et al.*, 1996; Dimashki *et al.*, 2000; Feilberg *et al.*, 2001; Marino *et*

al., 2000). 2NPyr is also present, mostly in the particulate-phase at lower levels than 2NFlt. Both of these compounds are expected to be present solely as a result of gas-phase PAH reactions in the atmosphere (Atkinson and Arey, 1994).

1NPyr and 9NAnt, which result primarily from diesel exhaust emissions, were also observed in relatively high concentrations, predominantly in the particulate phase at both sites.

NPAH concentrations have previously been measured simultaneously in gas- and particulate phases in urban, suburban or traffic locations in Maryland, USA (Bamford and Baker, 2003) the Chamonix Valley, France (Albinet *et al.*, 2008a) Los Angeles and Riverside, USA (Reisen and Arey, 2005) Houston, USA (Wilson *et al.*, 1995) in both summer and winter months (see Table 3.3). Concentrations measured at BROS in this study were within the range or of the same order of magnitude of those reported in these previous studies.

NPAH concentrations in the present study were lower than observed during photochemical smog events in California, USA (Arey *et al.*, 1987, 1989) and those reported in more highly polluted urban centres or high traffic areas such as Copenhagen, Denmark (Feilberg *et al.*, 2001); Ho Chi Minh City, Vietnam (Hien *et al.*, 2007); Tokyo, Japan (Kakimoto *et al.*, 2000; 2001; Kojima *et al.*, 2010); Beijing, China (Wang *et al.*, 2011b) and Cairo, Egypt (Nassar *et al.*, 2011).

The presence of NPAH compounds that result from gas-phase reactions (2NFlt, 2NPyr), direct emissions (1NPyr) and a combination of both (1NNap, 2NNap) indicates that concentrations of OPAH (e.g. 9F, AQ) and NPAH compounds at these sites will be influenced by both direct emissions from traffic and secondary reactions of parent PAH with atmospheric oxidants e.g. OH, NO₃, O₃.

3.1.3. BROS/EROS ratio comparisons

The relative magnitude and seasonal variability of BROS/EROS concentration is dependent on a number of factors : the emission source strength from traffic, the influence of other non-traffic

combustion or non-combustion sources, levels of mobility and/or reactivity in the atmosphere, and the relative input of some NPAH and OPAH compounds from atmospheric PAH reactions.

The mean BROS/EROS ratios for each compound measured in Campaign 1 are presented in Table 3.3. The annual mean concentrations of all PAH, OPAH and NPAH compounds measured were higher at BROS than at EROS. This is consistent with BROS being in closer proximity to the major local emission source (i.e. road traffic) and levels at EROS being depleted to a greater degree due to dispersion, deposition and/or chemical reactivity.

Statistical analysis of results indicates a significant ($p < 0.01$) correlation exists between the measured concentrations at BROS and EROS for all compounds (with the exception of Ant and Cor). A paired t-test of the BROS and EROS samples indicates that concentrations at BROS are significantly ($p < 0.01$) higher at BROS for nearly all measured compounds. This is in agreement with the work of Alam et al. (2013) Alam *et al.* (2013) and Harrad and Laurie (2005) where significant inter-site differences were also reported. These results strongly indicate that traffic is the dominant source influencing the observed concentrations of most compounds measured at these sites.

However, no significant difference between sites was observed for Ace and Cor. Cor is typically used as a marker for traffic emissions, so higher levels at BROS may be expected. However, the lack of a statistical difference between sites may be explained by the relatively low volatility and reactivity of this compound, which may result in relatively low inter-site difference in concentration. For Ace, this may indicate a relatively low traffic input at these sites and the possibility of a non-traffic input that is more prominent at EROS masking a traffic-related input.

The magnitude of BROS/EROS ratios varies considerably between compounds. For PAHs, BROS/EROS ratios are generally higher for the LMW PAHs with 3-4 rings (1.1-3.8) compared to HMW PAH with 5+ rings (1.3 – 2.0). These ratios are broadly in good agreement those observed previously by Harrad and Laurie (2005) and Alam *et al.* (2013).

Table 3.3. Annual mean BROS/EROS concentration ratios for all PAH, OPAH and NPAH compounds.

	Annual mean BROS/EROS ratio
Acy	3.8
Ace	1.1
Flo	1.6
Phe	1.7
Ant	3.1
Flu	1.8
Pyr	2.1
Ret	1.6
BaA	2.0
Chr	1.9
BbF	1.4
BkF	1.5
BeP	1.5
BaP	1.7
Ipy	1.4
DBA	2.0
BPy	1.5
Cor	1.3
9F	1.7
AQ	1.5
MAQ	1.5
BaAQ	1.6
1NNap	2.7
2NNap	2.0
2NFlo	2.0
9NAnt	1.7
1NFlt	2.3
2NFlt	1.6
3NFlt	1.6
4NPyr	1.7
1NPyr	2.9
2NPyr	1.7
7NBaA	1.6
6NChr	1.7

The higher ratios observed for LWM PAHs may reflect the higher proportion of these compounds in the gas-phase and their subsequent susceptibility to reactive losses and more rapid dispersion. The relative magnitude of BROS/EROS ratios for different compounds may be due to their relative reactivity towards atmospheric oxidants (see Section 4.2).

The lower ratios observed for HMW PAH are expected due their greater association with the particulate phase and greater stability towards degradation. Ace displays a relatively low ratio, possibly indicating a minor traffic input and/or additional source influencing predominantly at EROS. Ret is not expected to result from a traffic emission source, being a typical marker for wood combustion (Ramdahl, 1983). However, the BROS/EROS ratio observed for Ret is similar to those of other semi-volatile PAHs. This may indicate a non-traffic combustion source that displays a similar high input in close proximity to BROS relative to EROS.

OPAHs generally display BROS/EROS ratios similar to those of semi-volatile 3-4 ring PAHs, suggesting the levels of these derivative compounds are governed by similar emission source and inter-site processing as 'parent' PAHs.

For many NPAHs e.g. 1NNap, 2NNap, 2NFlo and 1NPyr, the BROS/EROS ratios are relatively high compared with corresponding semi-volatile 3-4 ring PAHs. This may be attributed to the prominence of these compounds in diesel exhaust emissions and relatively low proportions in other combustion sources and/or more rapid degradation in the atmosphere relative to 'parent' PAHs.

It is expected that photolysis will be the dominant loss process for most gas-phase and particle-phase NPAHs (Atkinson *et al.*, 1989; Fan *et al.*, 1996a; Feilberg *et al.*, 1999; Nassar *et al.*, 2011; Phouongphouang and Arey, 2003a). Indeed it has been indicated that the atmospheric lifetime of gas-phase NNaps towards photolytic degradation is comparable or faster than that of gas-phase PAH towards OH reactions (Atkinson and Arey, 1994).

The mean inter-site ratio is shown to be larger for 1NNap than for 2-NNap. Experimental studies indicate 1NNap exhibits a rate of photolysis ~1.3 – 8 times higher than that of 2NNap (Atkinson *et al.*, 1989; Niu *et al.*, 2005; Phouongphouang and Arey, 2003a), which may partly explain this

observation. However, there is relatively little quantitative data on the rate of loss for particle-phase NPAH towards photolysis or other reactive loss processes.

Gas-phase reaction products 2NFlt and 2NPyr exhibit lower ratios than primary emission-related 1NPyr. This may indicate the possible input of the former two compounds between sites, while the latter is enhanced considerably at the roadside location and is expected to undergo relatively rapid degradation (see following sections for further discussion). A similar observation was made by Feilberg *et al.* (2001) where the ratios between urban and suburban areas were reported to be higher for 1NPyr than for 2NPyr, 2NFlt and 9NAnt which the authors attributed to direct emissions dominating the former and reactivity influencing the latter.

3.1.4. Traffic increment

It is assumed that if road traffic is the main emission source of PAHs, OPAHs and NPAHs measured in this campaign, the [BROS] – [EROS] value will represent a ‘traffic increment’ concentration for each compound (Alam *et al.*, 2013). Analysis of these [BROS] – [EROS] values will therefore help to assess the potential influence of additional input from either primary or secondary sources and/or losses due to deposition or reactivity between sites. The traffic increment of PAH, OPAH and PAH compounds in the present study are shown in Figures 3.2, 3.3 and 3.4 respectively.

The highest traffic increments were observed for Phe, Flu and Pyr, in agreement with the results of Alam *et al.* (2013) and Harrad and Laurie (2005). Concentrations of all compounds measured in BROS and EROS were also measured in the Queensway Road Tunnel in Campaign 3 (see Section 5). The levels measured in the tunnel represent those expected from on-road vehicle emissions only, with losses due to dispersion, inputs from other combustion sources and losses due to chemical reactivity or photolysis all assumed to be minimal.

There is shown to be a strong positive correlation between the annual mean [BROS]-[EROS] traffic increment measured in Campaign1 and the mean concentrations measured in the Queensway Road Tunnel (see Figure 3.5). This indicates that for most compounds, observed concentrations are governed by traffic source input. This is in agreement with previous assessments of source contributions at the Birmingham University sampling sites (Harrad and Laurie, 2005; Harrison *et al.*, 2003; Mari *et al.*, 2010).

Interestingly, the correlation is much stronger when Phe is removed from the regression analysis (see Figure 3.5). It is indicated that the traffic increment of Phe is a factor ~3 lower than expected, based on linear regression of the mean tunnel concentrations against the mean [BROS]-[EROS] plot. This result could possibly indicate a substantial input of Phe at EROS from non-traffic source, thus driving the observed B-E value lower than would be predicted. It has been suggested previously that this could be due to volatilisation of Phe previously deposited on soils/vegetation (Harrad and Laurie, 2005; Dimashki *et al.*, 2001). This is discussed further in Section 3.3.

There are other notable outliers to this 'traffic increment' regression. Ret displays a higher-than-expected BROS-EROS traffic increment. Ret is typically used as a marker for wood combustion (Fine *et al.*, 2002; McDonald *et al.*, 2000; Ramdahl, 1983; Simoneit *et al.*, 1993). These results indicate input from wood combustion activity may be higher at BROS than EROS. This is consistent with BROS being in relatively close proximity to local houses that may use wood as a domestic heating fuel or have greater frequency of fires to dispose of garden waste.

Ace displays a lower-than-expected BROS-EROS traffic increment. This suggests there is a relatively high non-traffic related input at EROS. This is consistent with the relatively low BROS/EROS ratio that is observed for Ace. The higher input of this compound at EROS relative to BROS suggests the source may not be wood combustion related as the converse is observed for Ret.

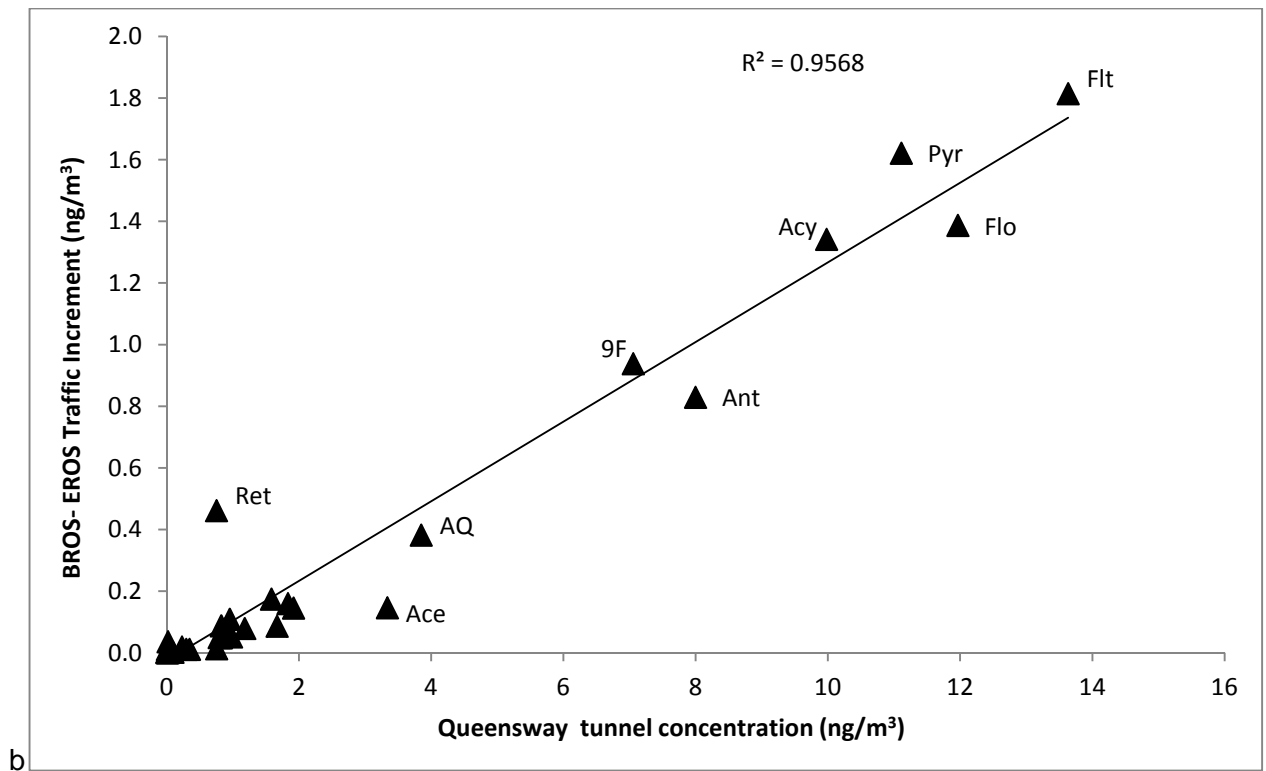
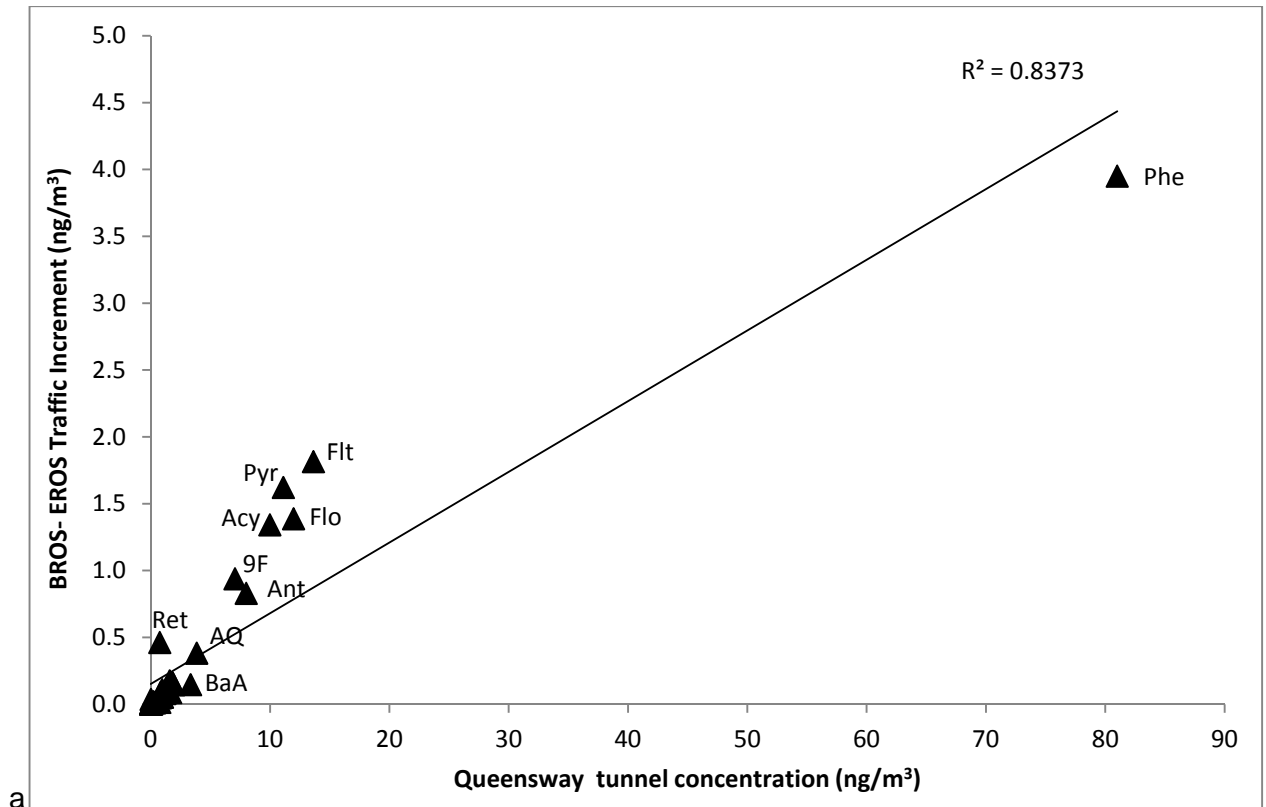


Figure 3.5. Correlation of measured PAH, OPAH and NPAH compounds in the Queensway Road Tunnel (Campaign 3) with the BROS-EROS concentration traffic increment (Campaign 1) ; plots are shown including Phe (a) and excluding Phe (b).

3.1.5. Annual BaP concentrations and the UK Air Quality Objective

The annual mean concentrations of BaP measured at BROS and EROS were 0.2 and 0.12 ng m⁻³ respectively. These concentrations are of the same magnitude as reported for other sampling sites in urban and suburban locations in the UK in 2011 (Brown *et al.*, 2013).

Annual mean BaP levels in Birmingham therefore appear to be in compliance with the UK's PAH Air Quality Objective of 0.25 ng m⁻³ annual mean for BaP. However, samples in the autumn and winter months at BROS and winter months at EROS display concentrations that often exceed 0.25 ng m⁻³. It is suggested, therefore that areas of higher traffic flow and/or areas influenced significantly by other primary sources in the Birmingham area may exceed the objective value for BaP.

However, monitoring data from other heavily trafficked areas in 2013 (e.g. Birmingham Tyburn and London Marylebone Road) display a similar seasonal pattern to that observed at the sites in this study. BaP concentrations tend to exceed 0.25 ng m⁻³ in winter months but tend to fall well below this value during spring and summer. Overall, annual mean concentrations appear to comply with the annual objective value in most urban and heavy traffic locations.

3.2. Influencing factors governing observed concentrations

Assessing how the measured concentrations of PAHs, OPAHs and NPAHs relate to each other as well as with other atmospheric species and meteorological variables can help gain further insight into the origins, behaviour and fate of these compounds. This section presents a statistical analysis of measured concentrations and atmospheric parameters from samples in Campaign 1 at both sites.

3.2.1. Inter-correlations of PAH, OPAH and NPAH concentrations

Table 3.4a and 3.4b present the Pearson coefficients for the correlations between individual PAH, OPAH and NPAH compounds measured during Campaign 1 at BROS and EROS locations respectively. It is noted that Ret does not correlate significantly with other compounds at BROS. This is consistent with Ret resulting predominantly from a wood combustion-related source rather than a traffic-related source, with the latter expected for most other compounds. However it is also noted that Ant does not correlate with other compounds, possibly indicating the presence of a different source in addition to vehicle exhaust for this compound.

Phe correlates significantly at BROS with Flu and Pyr, which display a common diesel source, as well as Acy, Flo, BbF and BkF. Correlation between Phe and gasoline-related HMW PAH e.g, BaP, IPy, DBA, BPy, Cor as well as most OPAH and NPAH compounds is weaker or absent. At EROS, Phe does not display a significant correlation with other compounds, consistent with the deviation of Phe away from expected 'traffic profile', suggesting the influence of a different source at this site.

Acy, Ace, Flo, BaA, Chr, BbF, BkF, BeP, BaP, IPy, DBA, BPy and Cor display significant ($p < 0.05$) inter-correlations at both sites, suggesting a common source amongst these compounds. This is consistent with road traffic being the dominant emission source for these compounds at both BROS and EROS. Similar inter-correlations were noted by Kakimoto *et al.* (2001) in highly trafficked urban areas in Japan.

Ace, Acy and Flo display stronger correlation with gasoline related HMW PAH such as Cor and BPy than for diesel-related compounds Phe, Flu and Pyr at both sites, as well as correlating strongly with each other. Pyr, Flth and Ret correlate strongly at EROS but do not correlate with other PAH, OPAH and NPAH compounds, suggesting Pyr and Flth may be influenced by a similar wood combustion-related source at this site.

For each of the four OPAH measured, relatively weak or absent correlations are noted with diesel related Phe, Flt, Pyr. Stronger and more significant correlations are noted with gasoline-related

Table 3.4a. Inter-correlations of PAH, OPAH and NPAH species at BROS.

Pearson Correlation	Acy	Ace	Flo	Phen	Anth	Fith	Pyr	Ret	B(a)A	Chry	B(b)F	B(k)F	B(e)P	B(a)P	IPy	D(ah)A	B(ghi)P	Cor	9-F	AQ	MAQ	BaQ	1-NNap	2-NNap	DNN	2-NFlo	9-NAnt	1-NFL	2-NFL	3-NFL	4-NPy	1-NPy	2-NPy	7-NBaA	6-NChr
Acy		.766**	.930**	.570**	0.05	.564**	0.36	-0.04	.877**	.937**	.807**	.945**	.878**	.843**	.901**	.679**	.855**	.831**	.662**	.568**	.465*	0.38	.827**	.682**	.570**	0.20	.636**	0.21	.877**	.817**	.841**	.839**	.956**	.771**	0.13
Ace	.766**		.840**	.412*	0.01	.514*	.422*	-0.14	.840**	.886**	.613**	.787**	.862**	.828**	.814**	.625**	.825**	.813**	.592**	.626**	.497*	.444*	.759**	.678**	.540**	.427*	.710**	0.36	.725**	.557**	.661**	.779**	.724**	.630**	0.36
Flo	.930**	.840**		.556**	0.15	.546**	0.40	-0.04	.866**	.902**	.733**	.860**	.827**	.796**	.814**	.544**	.794**	.775**	.552**	.466*	0.39	0.30	.748**	.669**	.543**	0.14	.602**	0.18	.847**	.685**	.750**	.813**	.898**	.701**	0.14
Phen	.570**	.412*	.556**		0.00	.552**	.539**	0.07	.450*	.476*	.729**	.609**	.508*	0.38	.480*	.480*	0.32	0.32	0.33	0.21	0.18	-0.03	.467*	.409*	0.16	0.22	0.29	0.14	.469*	0.39	.407*	0.40	.518**	0.38	-0.01
Anth	0.05	0.01	0.15	0.00		0.35	0.28	0.33	-0.06	0.01	-0.18	-0.03	-0.04	0.07	-0.07	-0.25	-0.02	0.02	0.01	-0.03	-0.06	-0.21	0.09	0.19	0.12	-0.09	-0.02	-0.03	0.21	0.07	0.14	0.00	0.08	-0.03	-0.15
Fith	.564**	.514*	.546**	.552**	0.35		.654**	0.23	0.35	.534**	.429**	.530**	.471*	.457*	.467*	0.39	.423**	.452*	.421*	0.20	.416*	0.14	.564**	.639**	0.14	0.22	0.38	0.31	.585**	.623**	.620**	.488**	.587**	0.37	0.05
Pyr	0.36	.422*	0.40	.539**	0.28	.654**		.411*	0.30	0.33	0.30	0.33	0.36	0.29	0.29	0.27	0.27	0.29	0.39	0.20	0.40	0.16	.583**	.609**	0.20	0.33	.466*	.573**	.507*	0.25	0.37	0.35	0.29	0.33	0.18
Ret	-0.04	-0.14	-0.04	0.07	0.33	0.23	.411*		-0.17	-0.12	-0.25	-0.11	-0.14	-0.17	-0.18	-0.26	-0.10	-0.14	0.14	-0.09	-0.05	-0.16	0.09	0.21	-0.19	0.00	0.03	0.26	-0.03	-0.12	-0.01	-0.18	-0.11	-0.12	-0.26
B(a)A	.877**	.840**	.866**	.450*	-0.06	0.35	0.30	-0.17		.925**	.739**	.904**	.925**	.917**	.919**	.664**	.893**	.848**	.627**	.680**	.433*	.494*	.767**	.561**	.559**	0.28	.695**	0.16	.778**	.648**	.681**	.766**	.813**	.820**	0.29
Chry	.937**	.886**	.902**	.476*	0.01	.534**	0.33	-0.12	.925**		.788**	.961**	.961**	.939**	.969**	.754**	.949**	.914**	.722**	.692**	.522**	.523**	.853**	.692**	.594**	0.30	.745**	0.22	.840**	.751**	.830**	.872**	.909**	.829**	0.28
B(b)F	.807**	.613**	.733**	.729**	-0.18	.429**	0.30	-0.25	.739**	.788**		.885**	.794**	.759**	.832**	.796**	.730**	.693**	.526**	.425*	0.25	0.26	.647**	.422**	.543**	0.15	.561**	0.20	.680**	.625**	.676**	.678**	.768**	.737**	0.10
B(k)F	.945**	.787**	.860**	.609**	-0.03	.530**	0.33	-0.11	.904**	.961**	.885**		.948**	.920**	.975**	.806**	.921**	.879**	.683**	.667**	.457*	.463*	.807**	.619**	.566**	0.29	.710**	0.21	.816**	.773**	.833**	.804**	.906**	.856**	0.16
B(e)P	.878**	.862**	.827**	.508*	-0.04	.471*	0.36	-0.14	.925**	.961**	.794**	.948**		.935**	.964**	.748**	.933**	.896**	.649**	.749**	.514*	.537**	.808**	.623**	.620**	0.35	.755**	0.28	.821**	.676**	.789**	.841**	.843**	.821**	0.35
B(a)P	.843**	.828**	.796**	0.38	0.07	.457*	0.29	-0.17	.917**	.939**	.759**	.920**	.935**		.964**	.765**	.967**	.913**	.680**	.709**	.462*	.535**	.780**	.526**	.631**	0.35	.775**	0.23	.753**	.687**	.742**	.757**	.802**	.877**	0.26
IPy	.901**	.814**	.814**	.480*	-0.07	.467*	0.29	-0.18	.919**	.969**	.832**	.975**	.964**	.964**		.836**	.966**	.923**	.708**	.723**	.510*	.573**	.820**	.580**	.579**	0.36	.769**	0.21	.779**	.746**	.797**	.804**	.866**	.891**	0.27
D(ah)A	.679**	.625**	.544**	.480*	-0.25	0.39	0.27	-0.26	.664**	.754**	.796**	.806**	.748**	.765**	.836**		.771**	.732**	.653**	.517**	.463*	.506**	.694**	.429**	.443**	.412*	.638**	0.21	.546**	.574**	.617**	.583**	.672**	.742**	0.12
B(ghi)P	.855**	.825**	.794**	0.32	-0.02	.423**	0.27	-0.10	.893**	.949**	.730**	.921**	.933**	.967**	.966**	.771**		.940**	.703**	.730**	.486**	.561**	.807**	.600**	.636**	0.36	.849**	0.30	.762**	.697**	.780**	.750**	.806**	.876**	0.22
Cor	.831**	.813**	.775**	0.32	0.02	.452*	0.29	-0.14	.848**	.914**	.693**	.879**	.896**	.913**	.923**	.732**	.940**		.698**	.667**	.430*	.481**	.827**	.650**	.702**	0.27	.758**	0.23	.773**	.704**	.839**	.756**	.830**	.879**	0.21
9-F	.662**	.592**	.552**	0.33	0.01	.421*	0.39	-0.14	.627**	.722**	.526**	.683**	.649**	.680**	.708**	.653**	.703**	.698**		.648**	.611**	.472*	.877**	.681**	.525**	0.29	.685**	0.25	.596**	.630**	.692**	.643**	.646**	.617**	0.29
AQ	.568**	.526**	.466**	0.21	-0.03	0.20	0.20	-0.09	.680**	.692**	.425*	.667**	.749**	.709**	.723**	.517**	.730**	.667**	.648**		.675**	.706**	.609**	.478**	.525**	.451**	.701**	0.34	.572**	.573**	.622**	.584**	.521**	.569**	.456*
MAQ	.465*	.497*	0.39	0.18	-0.06	.416*	0.40	-0.05	.433**	.522**	0.25	.457*	.514*	.462*	.510*	.463**	.486**	.430*	.611**	.675**		.797**	.569**	.482**	0.26	0.33	.516**	0.32	.530**	.553**	.554**	.552**	.502**	.445*	0.37
BaQ	0.38	.444*	0.30	-0.03	-0.21	0.14	0.16	-0.16	.494**	.523**	0.26	.463**	.537**	.535**	.573**	.506**	.561**	.481**	.472**	.706**	.797**		.455*	0.30	0.18	0.25	.500**	0.15	.404*	.406**	.449**	.465**	0.40	.583**	0.36
1-NNap	.827**	.759**	.748**	.467*	0.09	.564**	.583**	0.09	.767**	.853**	.647**	.807**	.808**	.780**	.820**	.694**	.807**	.827**	.877**	.609**	.569**	.455*		.850**	.602**	0.33	.760**	0.36	.824**	.649**	.785**	.783**	.775**	.728**	0.30
2-NNap	.682**	.678**	.669**	.409*	0.19	.639**	.609**	0.21	.561**	.692**	.422**	.619**	.623**	.526**	.580**	.429**	.600**	.650**	.681**	.478**	.482**	0.30	.850**		.478*	0.20	.630**	0.39	.775**	.556**	.741**	.670**	.641**	.472*	0.18
DNN	.570**	.540**	.543**	0.16	0.12	0.14	0.20	-0.19	.559**	.594**	.543**	.566**	.620**	.631**	.579**	.443**	.636**	.702**	.525**	.525**	0.26	0.18	.602**	.478*		0.01	.586**	.419**	.697**	.440**	.669**	.579**	.559**	.435*	0.17
2-NFlo	0.20	.427*	0.14	0.22	-0.09	0.22	0.33	0.00	0.28	0.30	0.15	0.29	0.35	0.35	0.36	.412*	0.36	0.27	0.29	.451**	0.33	0.25	0.33	0.20	0.01		.489**	.487**	0.13	0.12	0.05	0.21	0.06	0.35	0.39
9-NAnt	.636**	.710**	.602**	0.29	-0.02	0.38	.466**	0.03	.695**	.745**	.561**	.710**	.755**	.775**	.769**	.638**	.849**	.758**	.685**	.701**	.516**	.500**	.760**	.630**	.586**	.489**		.547**	.648**	.558**	.607**	.526**	.522**	.752**	0.31
1-NFL	0.21	0.36	0.18	0.14	-0.03	0.31	.573**	0.26	0.16	0.22	0.20	0.21	0.28	0.23	0.21	0.21	0.30	0.23	0.25	0.34	0.32	0.15	0.36	0.39	.419**	.487**		.547**	.415**	0.16	0.31	0.20	0.08	0.18	0.19
2-NFL	.877**	.725**	.847**	.469*	0.21	.585**	.507*	-0.03	.778**	.840**	.680**	.816**	.821**	.753**	.779**	.546**	.762**	.773**	.596**	.572**	.530**	.404*	.824**	.775**	.697**	0.13	.648**	.415**		.709**	.880**	.788**	.853**	.675**	0.20
3-NFL	.817**	.557**	.685**	0.39	0.07	.623**	0.25	-0.12	.648**	.751**	.625**	.773**	.676**	.687**	.746**	.574**	.697**	.704**	.630**	.573**	.553**	.406*	.649**	.556**	.440**	0.12	.558**	0.16	.709**		.831**	.670**	.835**	.600**	0.22
4-NPy	.841**	.661**	.750**	.407*	0.14	.620**	0.37	-0.01	.681**	.830**	.676**	.833**	.789**	.742**	.797**	.617**	.780**	.839**	.692**	.622**	.554**	.449*	.785**	.741**	.669**	0.05	.607**	0.31	.880**	.831**		.770**	.893**	.640**	0.10
1-NPy	.839**	.779**	.813**	0.40	0.00	.488**	0.35	-0.18	.766**	.872**	.678**	.804**	.841**	.757**	.804**	.583**	.750**	.756**	.643**	.584**	.552**	.465**	.783**	.670**	.579**	0.21	.526**	0.20	.788**	.670**	.770**		.854**	.680**	.461*
2-NPy	.956**	.724**	.898**	.518**	0.08	.587**	0.29	-0.11	.813**	.909**	.768**	.906**	.843**	.802**	.866**	.672**	.806**	.830**	.646**	.521**	.502*	0.40	.775**	.641**	.559**	0.06	.522**	0.08	.853**	.835**	.893**	.854**		.704**	0.11
7-NBaA	.771**	.630**	.701**	0.38	-0.03	0.37	0.33	-0.12	.820**	.829**	.737**	.856**	.821**	.877**	.8																				

Table 3.4b. Inter-correlations of PAH, OPAH and NPAH species at EROS.

Pearson Correlation	Acy	Ace	Flo	Phen	Anth	Flth	Pyr	Ret	B(a)A	Chry	B(b)F	B(k)F	B(e)P	B(a)P	IPy	D(ah)A	B(ghi)P	Cor	9-F	AQ	MAQ	BaQ	1-NNap	2-NNap	DNN	2-NFlo	9-NAnt	1-NFL	2-NFL	3-NFL	4-NPy	1-NPy	2-NPy	7-NBaA	6-NChr
Acy		.636**	.716**	.058	-.036	.249	-.007	-.026	.826**	.873**	.709**	.679**	.782**	.743**	.837**	.709**	.695**	.509**	.594**	.472**	.575**	.018	.828**	.755**	.416*	.274	.656**	.397	.641**	.554**	.579**	.755**	.786**	.564**	.488**
Ace	.636**		.834**	-.029	-.140	.311	-.067	-.128	.640**	.612**	.659**	.632**	.685**	.727**	.729**	.427**	.402	.325	.235	.479**	.366	.041	.472**	.394	.143	.261	.572**	.355	.413*	.298	.260	.401	.504**	.375	.525**
Flo	.716**	.834**		-.087	-.086	.250	.011	-.050	.599**	.604**	.512*	.531**	.657**	.608**	.667**	.533**	.452*	.383	.326	.327	.384	.017	.488**	.415*	.191	.218	.684**	.312	.517**	.236	.243	.447**	.508**	.423*	.455**
Phen	.058	-.029	-.087		.249	.377	.217	.332	-.033	.001	.106	-.058	-.046	-.085	.038	-.083	-.120	-.187	-.008	-.214	.046	-.205	.076	.107	.044	.256	-.193	.095	.067	.140	.057	.167	.235	-.120	-.078
Anth	.036	-.140	-.086	.249		.034	.108	.115	.230	.201	.091	-.009	.131	.190	.119	.246	.118	-.017	.398	.034	-.028	-.128	.061	.153	.225	.110	-.003	-.043	.209	.182	.013	.007	.162	.381	.225
Flth	.249	.311	.250	.377	.034		.743**	.629**	.052	.136	.218	.167	.195	.155	.124	.171	-.055	-.006	-.126	.040	.299	.253	.093	.017	.057	.394	.146	.440*	.186	.235	.158	.144	.059	.104	.428**
Pyr	-.007	-.067	.011	.217	.108	.743**		.810**	-.204	-.074	-.141	-.116	-.144	-.163	-.111	.159	-.142	.070	-.146	-.221	.164	.121	-.085	-.122	-.119	.286	-.033	.133	-.036	.055	-.047	-.148	-.188	.011	.336
Ret	-.026	-.128	-.050	.332	.115	.629**	.810**		-.103	-.004	.016	.053	-.033	-.081	-.031	.147	.056	.187	-.239	-.198	.020	.145	-.040	-.079	.194	.126	-.117	.063	.045	.098	.068	-.085	-.136	-.051	.176
B(a)A	.826**	.640**	.599**	-.033	.230	.052	-.204	-.103		.973**	.860**	.822**	.915**	.926**	.935**	.793**	.888**	.657**	.658**	.670**	.483*	.117	.763**	.750**	.535**	.206	.646**	.173	.663**	.540**	.601**	.749**	.740**	.716**	.366
Chry	.873**	.612**	.604**	.001	.201	.136	-.074	-.004	.973**		.852**	.822**	.887**	.895**	.935**	.825**	.881**	.664**	.671**	.673**	.539**	.158	.801**	.759**	.567**	.219	.655**	.205	.641**	.558**	.657**	.798**	.762**	.727**	.436*
B(b)F	.709**	.659**	.512*	.106	.091	.218	-.141	.016	.860**	.852**		.944**	.926**	.925**	.915**	.675**	.777**	.531**	.415*	.568**	.421*	.269	.729**	.664**	.542**	.291	.553**	.134	.647**	.558**	.625**	.659**	.709**	.661**	.320
B(k)F	.679**	.632**	.531**	-.058	-.009	.167	-.116	.053	.822**	.822**	.944**		.924**	.909**	.895**	.701**	.791**	.550**	.378	.570**	.338	.346	.752**	.637**	.591**	.218	.576**	.083	.687**	.596**	.706**	.614**	.666**	.719**	.293
B(e)P	.782**	.685**	.657**	-.046	.131	.195	-.144	-.033	.915**	.887**	.926**	.924**		.951**	.913**	.735**	.816**	.521**	.518**	.554**	.371	.204	.760**	.685**	.573**	.214	.669**	.116	.752**	.601**	.646**	.715**	.721**	.764**	.343
B(a)P	.743**	.727**	.608**	-.085	.190	.155	-.163	-.081	.926**	.895**	.925**	.909**	.951**		.912**	.708**	.771**	.540**	.529**	.659**	.374	.155	.687**	.601**	.525**	.303	.616**	.175	.601**	.584**	.559**	.624**	.663**	.763**	.425*
IPy	.837**	.729**	.667**	.038	.119	.124	-.111	-.031	.935**	.935**	.915**	.895**	.913**	.912**		.828**	.859**	.658**	.553**	.610**	.506*	.171	.828**	.791**	.497*	.305	.674**	.219	.716**	.536**	.612**	.671**	.777**	.682**	.422*
D(ah)A	.709**	.427**	.533**	-.083	.246	.171	.159	.147	.793**	.825**	.675**	.701**	.735**	.708**	.828**		.875**	.772**	.606**	.559**	.523**	.310	.708**	.729**	.450*	.389	.736**	.236	.667**	.391	.484*	.515**	.519**	.745**	.370
B(ghi)P	.695**	.402	.452*	-.120	.118	-.055	-.142	.056	.888**	.881**	.777**	.791**	.816**	.771**	.859**	.875**		.794**	.584**	.596**	.400	.257	.727**	.755**	.617**	.115	.658**	.045	.665**	.397	.572**	.640**	.608**	.660**	.172
Cor	.509**	.325	.383	-.187	-.017	-.006	.070	.187	.657**	.664**	.531**	.550**	.521**	.540**	.658**	.772**	.794**		.271	.573**	.496*	.183	.482**	.571**	.270	.310	.577**	.103	.349	.227	.347	.348	.286	.408**	.114
9-F	.594**	.235	.326	-.008	.398	-.126	-.146	-.239	.658**	.671**	.415*	.378	.518**	.529**	.553**	.606**	.584**	.271		.486**	.433*	.084	.600**	.576**	.360	.140	.515**	-.008	.370	.195	.270	.458**	.567**	.591**	.332
AQ	.472**	.479**	.327	-.214	.034	.040	-.221	-.198	.670**	.673**	.568**	.570**	.554**	.659**	.610**	.559**	.596**	.573**	.486**		.433*	.316	.479**	.456**	.439**	.223	.663**	.311	.235	.208	.418**	.378	.386	.469**	.345
MAQ	.575**	.366	.384	.046	-.028	.299	.164	.020	.483**	.539**	.421*	.338	.371	.374	.506**	.523**	.400	.496*	.433*		.464*	.487**	.507**	-.100	.372	.360	.311	.282	.075	.250	.413*	.413*	.218	.378	
BaQ	.018	.041	.017	-.205	-.128	.253	.121	.145	.117	.158	.269	.346	.204	.155	.171	.310	.257	.183	.084	.316	.464*		.132	.076	.132	-.057	.197	.021	.256	-.194	.212	.091	.009	.247	.166
1-NNap	.828**	.472**	.488**	.076	.061	.093	-.085	-.040	.763**	.801**	.729**	.752**	.760**	.687**	.828**	.708**	.727**	.482**	.600**	.479**	.487**	.132		.938**	.581**	.158	.588**	.244	.762**	.683**	.794**	.685**	.879**	.533**	.324
2-NNap	.755**	.394	.415*	.107	.153	.017	-.122	-.079	.750**	.759**	.664**	.637**	.685**	.601**	.791**	.729**	.755**	.571**	.576**	.456**	.507**	.076	.938**		.488**	.151	.597**	.210	.770**	.600**	.715**	.633**	.842**	.467*	.174
DNN	.416*	.143	.191	.044	.225	.057	-.119	-.194	.535**	.567**	.542**	.591**	.573**	.525**	.497**	.450**	.617**	.270	.360	.439**	-.100	.132	.581**	.488**		-.129	.337	.092	.504**	.484**	.631**	.469**	.545**	.408**	.130
2-NFlo	.274	.261	.218	.256	.110	.394	.286	.126	.206	.219	.291	.218	.214	.303	.305	.389	.115	.310	.140	.223	.372	-.057	.158	.151	-.129		.208	.396	-.003	.198	-.053	-.040	.001	.200	.180
9-NAnt	.656**	.572**	.684**	-.193	-.003	.146	-.033	-.117	.646**	.655**	.553**	.576**	.669**	.616**	.674**	.736**	.658**	.577**	.515**	.663**	.360	.197	.588**	.597**	.337	.208		.269	.576**	.230	.370	.414**	.478**	.639**	.353
1-NFL	.397	.355	.312	.095	-.043	.440*	.133	.063	.173	.205	.134	.083	.116	.175	.219	.236	.045	.103	-.008	.311	.311	.021	.244	.210	.092	.396	.269		.199	.259	.137	.132	.156	-.052	.489**
2-NFL	.641**	.413*	.517**	.067	.209	.186	-.036	.045	.663**	.641**	.647**	.687**	.752**	.601**	.716**	.667**	.665**	.349	.370	.235	.282	.256	.762**	.770**	.504**	-.003	.576**	.199		.594**	.714**	.594**	.748**	.595**	.223
3-NFL	.554**	.298	.236	.140	.182	.235	.055	.098	.540**	.558**	.558**	.596**	.601**	.584**	.536**	.391	.397	.227	.195	.208	.075	-.194	.683**	.600**	.484	.198	.230	.259	.594**		.809**	.605**	.624**	.498**	.151
4-NPy	.579**	.260	.243	.057	.013	.158	-.047	.068	.601**	.657**	.625**	.706**	.646**	.559**	.612**	.484*	.572**	.347	.270	.418**	.250	.212	.794**	.715**	.631**	-.053	.370	.137	.714**	.809**		.748**	.722**	.506**	.129
1-NPy	.755**	.401	.447**	.167	.007	.144	-.148	-.085	.749**	.798**	.659**	.614**	.715**	.624**	.671**	.515**	.640**	.348	.458**	.378	.413*	.091	.685**	.633**	.469**	-.040	.414**	.132	.594**	.605**	.748**		.724**	.552**	.168
2-NPy	.786**	.504**	.508**	.235	.162	.059	-.188	-.136	.740**	.762**	.709**	.666**	.721**	.663**	.777**	.519**	.608**	.286	.567**	.386	.413*	.009	.879**	.842**	.545**	.001	.478**	.156	.748**	.624**	.722**	.724**		.472**	.250
7-NBaA	.564**	.375	.423*	-.120	.381	.104	.011	-.051	.716**	.727**	.661**	.719**	.764**	.763**	.682**	.745**	.660**	.408**	.591**	.469**	.218	.247	.533**	.467**	.408**	.200	.639**	-.052	.595**	.498**	.506**	.552**	.472**		.295
6-NChr	.488**	.525**	.455**	-.078	.225	.428**	.336	.176	.366	.436*	.320	.293	.343	.425**	.422**	.370	.172	.114	.332	.345	.3														

PAHs such as Cor, BPy and IPy, especially in the case of 9F and AQ. This may indicate the strong traffic input of AQ and 9F, more predominantly from gasoline-fuelled vehicles, with a relatively lower input of MAQ and BaAQ from traffic. This is in contrast to the study of Alam *et al.* (2013) which suggested MAQ as a possible marker for traffic-related emissions.

BaAQ and MAQ are shown to be very strongly correlated, possibly indicating the presence of a common source for these compounds. At EROS, BaAQ shows no significant correlation with other PAH, OPAH and NPAH compounds, possibly suggesting the presence of a non-traffic source of this compound influencing predominantly at EROS.

At both sites, 2NFlo, 6NChr and 1NFlu do not display significant correlation with most other compounds, possibly indicating the presence of a non-traffic source for these compounds. 1NNap, 2NNap, 9NAnt, 1NPyr, 7NBaA are shown to be significantly inter-correlated at both sites and also strongly correlated with traffic-related HMW PAHs, such as Cor and BPy, consistent with traffic being the main source of these NPAHs at both sites. The strongest NPAH inter-correlations at BROS and EROS are for 2NFIt and 2NPyr, possibly reflecting their common reactive input. This is in agreement with Feilberg *et al.* (2001) who measured NPAH concentrations in the urban atmosphere in Copenhagen, Denmark. 4NPyr also displays strong correlations with 2NFIt and 2NPyr, possibly also indicating reactive input of this compound.

Interestingly, 2NFIt and 2NPyr, do not display a correlation with their parent PAH. However, they do display strong correlations with compounds associated with primary emission sources e.g. 1NPyr, BeP and IPy. Feilberg *et al.* (2001) also noted a significant correlation between 2NFIt and primary PAHs BeP and BPy at a rural site in Denmark. The authors suggested that the level of NPAHs formed via atmospheric reactions are also dependent on the PAH levels and that these compounds act as a better marker than the actual parent PAHs as they are present almost entirely in the particle-phase like the 2NFIt and 2NPyr while Flt and Pyr observed predominantly in the gas-phase and are subject to temperature-dependent phase partitioning.

3.2.2. Correlations with inorganic air pollutants and meteorological parameters

The relationship between measured PAH, OPAHs and NPAH concentrations and the levels of inorganic air pollutants such as TSP, NO_x, O₃ and SO₂, as well as meteorological factors such as temperature, wind speed, wind direction, pressure and intensity of solar radiation, may also provide insight into the sources, behaviour and fate of these compounds.

Table 3.5a and 3.5b provide Pearson correlation coefficients for the measured PAH, OPAH and NPAH compounds with these key parameters. It should be noted that the values for meteorological variables are provided for Birmingham University sampling site as a whole so may only be of limited usefulness for assessing differences in compound behaviour between sites. The concentrations of NO_x, O₃ and SO₂ were obtained from the Birmingham Tyburn monitoring site, located ~6-7km away from BROS and EROS, therefore these relationships need to be viewed with caution as these may not adequately represent the levels observed at the sampling sites but offer the most representative values available.

3.2.2.1. Correlations of PAH, OPAH and NPAH with TSP

Most compounds at BROS correlate strongly with measured TSP concentration. This suggests that most compounds are associated strongly with freshly emitted local sources from Bristol Road traffic. The exceptions to this include LWM compounds Phe, Ant, Flth, Pyr, Ret and 2NFlo, possibly indicating the influence of additional/alternative sources dominating for these compounds. At EROS, the correlation with TSP appears to be weaker, although still statistically significant for most compounds, consistent with the traffic source dominating at both sites and the greater distance of EROS from the road traffic source.

Interestingly, for OPAH compounds, while significant correlations with TSP are seen at BROS, indicating a close association with primary emissions, no significant correlations are observed for these compounds at EROS. In the case of 9F and AQ, this may suggest the influence of increased partitioning into the gas-phase and/or secondary input from photooxidation reactions or local

Table 3.5a. Correlations of PAH, OPAH and NPAH concentrations with meteorological parameters and concentrations of inorganic air pollutants at BROS.

	TSP	T(degC)	T(degC) - NOx Corr	Hum (%)	Pres (hPa)	SR (W/m2)	Rain (mm)	WS (m/s)	COS(WD) (deg)	SIN(WD) (deg)	NOx	O3	SO2
Acy	.706**	-.631**	.267	.321	.446*	-.437*	-.076	-.148	.320	-.142	.488*	-.366	.338
Ace	.758**	-.708**	.385	.530**	.447*	-.482*	.020	-.112	.319	-.085	.623**	-.400	.189
Flo	.678**	-.562**	.525**	.334	.293	-.375	-.011	-.247	.194	-.239	.546**	-.384	.256
Phen	.274	-.283	.778**	-.014	.020	-.112	-.096	-.201	.196	-.335	.258	-.205	.034
Anth	-.186	.223	.405*	.093	-.120	.265	.119	-.111	.036	.014	.142	-.314	-.192
Flth	.382	-.192	.692**	.193	.181	-.087	.007	.078	.439*	.021	.270	-.135	.098
Pyr	.117	-.302	.751**	.195	.130	-.183	.007	.039	.188	.117	.469*	-.282	-.211
Ret	-.269	.349	.268	.045	-.036	.049	-.117	.108	-.229	.044	.093	-.234	-.241
B(a)A	.763**	-.780**	.172	.364	.563**	-.475*	-.166	-.219	.259	-.103	.659**	-.458*	.281
Chry	.810**	-.743**	.297	.447*	.582**	-.488*	-.099	-.182	.396	-.135	.618**	-.441*	.294
B(b)F	.535**	-.661**	.555**	.083	.408*	-.209	-.285	-.241	.352	-.299	.467*	-.309	.205
B(k)F	.740**	-.747**	.348	.280	.581**	-.386	-.200	-.222	.407*	-.200	.578**	-.402	.278
B(e)P	.829**	-.828**	.380	.444*	.601**	-.514*	-.094	-.230	.349	-.167	.606**	-.461*	.232
B(a)P	.714**	-.824**	.131	.376	.716**	-.373	-.195	-.117	.406*	-.046	.687**	-.509*	.202
IPy	.765**	-.831**	.320	.355	.689**	-.453*	-.180	-.154	.446*	-.091	.627**	-.446*	.262
D(ah)A	.480*	-.727**	.472*	.289	.616**	-.371	-.209	-.010	.605**	.103	.556**	-.400	.398
B(ghi)P	.751**	-.812**	.163	.412*	.707**	-.433*	-.144	-.139	.374	-.092	.680**	-.470*	.219
Cor	.733**	-.727**	.387	.398	.611**	-.396	-.058	-.174	.288	.045	.681**	-.449*	.191
9-F	.483*	-.475*	.576**	.375	.664**	-.388	-.247	.178	.322	.224	.618**	-.328	.079
AQ	.719**	-.700**	.566**	.446*	.725**	-.505*	-.235	-.043	.400	-.108	.379	-.294	-.010
MAQ	.575**	-.500**	.687**	.372	.521**	-.519**	-.011	.332	.384	.234	.135	.000	.138
BaQ	.556**	-.615**	.164	.335	.656**	-.504*	-.203	.076	.458*	.197	.254	-.192	.163
1-NNap	.604**	-.605**	.566**	.478*	.507*	-.488*	-.015	-.016	.333	.146	.691**	-.452*	.182
2-NNap	.565**	-.299	.628**	.532**	.161	-.457*	.162	-.202	.265	-.022	.556**	-.307	.224
DNN	.479*	-.499*	.273	.379	.319	-.253	-.020	-.120	-.024	-.036	.452*	-.340	.073
2-NFlo	.282	-.563**	.789**	.203	.456*	-.301	.015	.330	.493*	.029	.262	-.097	-.098
9-NAnt	.596**	-.727**	.238	.416*	.617**	-.454*	-.124	.020	.321	-.108	.696**	-.377	.014
1-NFL	.258	-.365	.534**	.173	.219	-.146	-.155	.286	.152	-.085	.142	.014	-.194
2-NFL	.737**	-.563**	.365	.359	.296	-.381	-.044	-.179	.246	-.119	.449*	-.301	.288
3-NFL	.625**	-.487*	.377	.179	.536**	-.354	-.238	.091	.477*	.000	.291	-.080	.262
4-NPy	.714**	-.506*	.379	.251	.459*	-.263	-.169	-.169	.302	-.064	.417*	-.197	.197
1-NPy	.744**	-.666**	.557**	.455*	.451*	-.546**	.072	-.162	.345	-.085	.450*	-.286	.214
2-NPy	.707**	-.561**	.287	.292	.425*	-.369	-.055	-.183	.304	-.074	.426*	-.307	.355
7-NBaA	.588**	-.810**	.061	.143	.667**	-.334	-.218	-.139	.404	-.076	.681**	-.369	.181
6-NChr	.449*	-.464*	.384	.401	.370	-.578**	-.027	.198	.311	.071	.168	-.042	-.115
TOT PAH	.653**	-.594**		.278	.299	-.328	-.029	-.161	.296	-.221	.514*	-.325	.169
TSP		-.639**		.379	.423*	-.497*	-.018	-.139	.237	-.249	.255	-.041	.265
degC	-.639**			-.257	-.733**	.451*	.151	.031			-.540**	.307	-.052
%	.379	-.257			.174	-.769**	.418*	-.064			.344	-.638**	.388
hPa	.423*	-.733**		.174		-.277	-.467*	.240			.476*	-.286	-.102
W/m2	-.497*	.451*		-.769**	-.277		-.294	-.085			-.256	.384	-.462*
mm	-.018	.151		.418*	-.467*	-.294		-.120			-.128	-.058	.177
m/s	-.139	.031		-.064	.240	-.085	-.120				-.268	.305	-.049
deg	-.208	-.309		-.029	.701**	.072	-.470*	.166			.330	-.312	-.359
NOx	.255	-.540**		.344	.476*	-.256	-.128	-.268				-.643**	.025
O3	-.041	.307		-.638**	-.286	.384	-.058	.305			-.643**		-.195
SO2	.265	-.052		.388	-.102	-.462*	.177	-.049			.025	-.195	

Key : ** Correlation is significant at the 0.01 level (2-tailed) (green) ; *Correlation is significant at the 0.05 level (2-tailed) (yellow); no statistically significant correlation (red)

Table 3.5b. Correlations of PAH, OPAH and NPAH concentrations with meteorological parameters and concentrations of inorganic air pollutants at EROS.

	TSP	T(degC)	T(degC)-NOx Corr	Hum (%)	Pres (hPa)	SR (W/m2)	Rain (mm)	WS (m/s)	COS WD (deg)	SIN WD (deg)	NOx	O3	SO2
Acy	.407*	-.589**	.512*	.416*	.354	-.580**	-.087	-.110	.464*	-.212	.463*	-.305	.334
Ace	.724**	-.657**	.338	.338	.416*	-.416*	-.089	.006	.281	-.120	.373	-.136	.115
Flo	.526**	-.520**	.684**	.429*	.283	-.555**	.078	.024	.122	-.046	.488*	-.217	.150
Phen	-.175	.095	.688**	-.169	-.200	.120	-.102	.033	.161	-.070	-.011	-.102	-.023
Anth	-.013	-.006	.752**	.247	.185	-.049	-.072	.156	.242	.097	.222	-.372	.007
Flth	.062	-.296	.361	.072	.196	-.157	-.162	.163	.471*	.126	.173	-.021	-.128
Pyr	-.150	.034	.783**	.000	.200	-.084	-.070	.272	.355	.304	.081	.018	-.276
Ret	-.106	.021	.576**	.008	.188	-.043	-.131	.014	.099	.038	.118	-.207	-.452*
B(a)A	.527**	-.630**	.510*	.418*	.478*	-.481*	-.150	-.286	.329	-.255	.546**	-.428*	.336
Chry	.475*	-.640**	.144	.427*	.548**	-.529**	-.181	-.227	.442*	-.194	.548**	-.411*	.319
B(b)F	.632**	-.770**	.158	.196	.582**	-.352	-.350	-.267	.372	-.294	.463*	-.341	.238
B(k)F	.665**	-.807**	.395	.183	.652**	-.375	-.298	-.290	.313	-.194	.519**	-.379	.187
B(e)P	.641**	-.799**	.106	.373	.540**	-.484*	-.145	-.317	.312	-.222	.618**	-.448*	.311
B(a)P	.657**	-.817**	.140	.338	.656**	-.405*	-.240	-.195	.392	-.236	.551**	-.404	.225
IPy	.640**	-.686**	.174	.371	.543**	-.527**	-.231	-.223	.386	-.189	.546**	-.428*	.333
D(ah)A	.320	-.496*	.298	.380	.490*	-.581**	-.174	-.128	.343	.003	.629**	-.431*	.313
B(ghi)P	.362	-.486*	-.013	.332	.432*	-.442*	-.186	-.401	.137	-.232	.604**	-.471*	.274
Cor	.307	-.217	-.041	.176	.286	-.336	-.126	-.283	.088	-.312	.324	-.141	.098
9-F	.147	-.285	.139	.326	.367	-.344	-.222	-.023	.282	-.002	.478*	-.331	.342
AQ	.383	-.393	.479*	.275	.443*	-.206	-.342	-.278	.390	-.228	.413*	-.202	.201
MAQ	.227	-.108	.596**	.233	.067	-.435*	-.141	-.035	.396	-.148	-.078	.039	.364
BaQ	.027	-.172	.719**	-.065	.194	-.107	-.311	-.214	.108	.125	.090	-.069	-.005
1-NNap	.540**	-.530**	.287	.338	.380	-.495*	-.136	-.216	.337	-.080	.435*	-.322	.389
2-NNap	.487*	-.324	.430*	.315	.194	-.431*	-.090	-.261	.245	-.140	.370	-.258	.472*
DNN	.169	-.463*	.488*	.330	.495*	-.182	-.216	-.249	.109	.060	.658**	-.603**	.002
2-NFlo	.124	-.245	-.224	-.020	.278	-.244	-.314	.440*	.382	.039	.060	.021	.274
9-NAnt	.421*	-.458*	.660**	.249	.297	-.352	-.173	-.308	.236	-.247	.678**	-.179	.200
1-NFL	.041	-.177	.321	.295	-.022	-.318	-.078	.228	.285	.008	.020	-.055	.085
2-NFL	.454*	-.455*	.603**	.258	.169	-.380	-.042	-.351	.136	-.005	.522**	-.424*	.333
3-NFL	.453*	-.559**	.233	.168	.355	-.266	.078	-.048	.337	-.031	.217	-.165	.234
4-NPy	.430*	-.478*	.439*	.162	.333	-.302	-.061	-.333	.324	-.011	.289	-.211	.320
1-NPy	.228	-.518**	.287	.341	.199	-.486*	.150	-.323	.340	-.154	.332	-.244	.431*
2-NPy	.485*	-.425*	.558**	.293	.254	-.279	-.106	-.254	.343	-.120	.396	-.362	.380
7-NBaA	.349	-.698**	.380	.189	.592**	-.350	-.098	-.166	.431*	-.056	.634**	-.355	.206
6-NChr	.362	-.490*	.065	.454*	.522**	-.485*	-.270	.154	.576**	.069	.287	-.248	-.120
TSP		-.549**		.262	.439*	-.331	-.112	-.150	.177	-.232	.155	-.084	.149
degC				-.257	-.733**	.451*	.151	.031	1	.072	-.540**	.307	-.052
%		-.257			.174	-.769**	.418*	-.064	.072	1	.344	-.638**	.388
hPa		-.733**		.174		-.277	-.467*	.240			.476*	-.286	-.102
W/m2		.451*		-.769**	-.277		-.294	-.085			-.256	.384	-.462*
mm		.151		.418*	-.467*	-.294		-.120			-.128	-.058	.177
m/s		.031		-.064	.240	-.085	-.120				-.268	.305	-.049
deg		-.309		-.029	.701**	.072	-.470*	.166			.330	-.312	-.359
NOx		-.540**		.344	.476*	-.256	-.128	-.268				-.643**	.025
O3		.307		-.638**	-.286	.384	-.058	.305			-.643**		-.195
SO2		-.052		.388	-.102	-.462*	.177	-.049			.025	-.195	

Key : ** Correlation is significant at the 0.01 level (2-tailed) (green) ; *Correlation is significant at the 0.05 level (2-tailed) (yellow); no statistically significant correlation (red)

volatilisation between the two sites. In the case of MAQ and BaAQ this may indicate an additional source that influences EROS to a higher degree than BROS.

3.2.2.2. Correlations of PAH, OPAH and NPAH with NO_x

Most compounds in this study display a significant positive correlation with NO_x. This can be interpreted in a number of ways:

Firstly, NO_x is expected to result predominantly from local road traffic in this area (Lim *et al.*, 1999) therefore this relationship may reflect the intensity of vehicle exhaust input. For example, Feilberg *et al.* (2001) indicated that at an urban location in Copenhagen, 1NPyr and 9NAnt correlated with traffic gas NO while 2NFlt and 2NPyr did not, reflecting the importance of direct vehicle emissions over atmospheric formation. However, in the present study 1NPty, 9NAnt, 2NFlt and 2NPyr were shown to correlate with NO_x at BROS and/or EROS. A number of compounds (e.g. Phe, Ant, Flt, Pyr, Ret, AQ, MAQ, BaQ, 2NFlo, 1NFlt, 3NFlt, 6NChr) display weaker or no correlation with NO_x, possibly indicating different primary sources and/or processes governing their concentrations.

It has also been suggested that NPAH may be formed (in the particle-phase) from direct reaction of PAH with NO₂ (Inazu *et al.*, 1997; Kwok *et al.*, 1995; Ma *et al.*, 2011; Miet *et al.*, 2009c; Wang *et al.*, 2000) therefore it has been suggested a positive correlation could reflect secondary NPAH input in this way (Feilberg *et al.* 2001). This was observed for a number of NPAHs at BROS. The compounds for which a significant correlation remains at EROS include 9NAnt, 2NFlt and 7NBaA which have been observed as NO₂ heterogeneous reaction products (Inazu *et al.*, 1997; Liu *et al.*, 2012; Ma *et al.*, 2011; Zhang *et al.*, 2011).

However, NO_x also displays a significant ($p < 0.01$) negative correlation with temperature. Since NO_x is expected to result primarily from local road traffic in this area, this relationship indicates that the relationship observed between PAH, OPAH and NPAH with NO_x may be more reflective of the temperature-dependence of the atmospheric boundary layer (ABL) height rather than the magnitude of primary or secondary input.

3.2.2.3. Correlations of PAH, OPAH and NPAH with O₃

A number of compounds display a weak (yet statistically significant) negative correlation with O₃ concentrations. This was observed more commonly for compounds found predominantly in the particulate phase (e.g. BaA, Chr, IPy, BeP, BaP, DBA, BPy and Cor).

It has been shown that these compounds can undergo heterogeneous reactions with O₃ on particle surfaces (Kwamena *et al.*, 2004; 2006; Perraudin *et al.*, 2007). Relatively weak negative correlations between NPAHs with O₃ were previously reported by Feilberg *et al.* (2001) possibly indicating O₃ reactions as a possible nighttime degradation pathway. However, this was not indicated to be a significant process for NPAHs in this study with only a small number of compounds displaying weak negative correlation with O₃.

It is expected that heterogeneous reactivity is not the cause of the negative correlation observed in the present study as this is more consistent with the strong negative correlation observed between O₃ and NO_x which is likely to be due to reactions occurring between O₃ and NO.

3.2.2.4. Temperature-dependence of PAH, OPAH and NPAH concentrations

Most compounds (with the exception of Phe, Ant, Flt, Pyr, Ret, 2NNap and 1NFlt) display a significant negative correlation with temperature. This is more prevalent at BROS with weaker or absent correlations present for some compounds at EROS. A similar observation was made for PAH, OPAH and NPAH in southern China (Wei *et al.*, 2012). This could indicate the primary sources influencing the levels of these compounds are seasonal in nature, with higher emission strength occurring in winter, for example due to domestic combustion of solid fuels for space heating.

However, the negative correlation between temperature and NO_x highlights the possible importance of the ABL height on pollutant concentrations. To test this theory, measured PAH, OPAH and NPAH concentrations were 'corrected' by dividing the observed concentrations by the

corresponding NO_x concentration at Birmingham Tyburn (see Section 2) for each sampling period to reflect the seasonal variation in ABL height, so variations caused only by source strength can be assessed. It should be noted that CO has been previously used for PAH 'corrections' as it is considered a more appropriate traffic-marker compound (Reisen and Arey, 2005). However, CO measurements were not available as this species is no longer measured at the Birmingham Tyburn site. The NO_x-corrected concentrations were then correlated with temperature. This method has been utilised at this site previously by Dimashki *et al.* (2001). The authors hypothesised that following correlation behaviour could be interpreted in terms of the prevailing emissions sources as follows :

- i) **a significant negative correlation** would indicate seasonally modulated space heating as a dominant source
- ii) **no significant correlation** would indicate the dominance of road traffic as an emission source
- iii) **a significant positive correlation** would indicate the influence of volatilisation from surfaces.

It is shown (Table 3.6) that the correlation of most NO_x-corrected compounds with temperature is not significant, consistent with traffic being the dominant emission source at both sites. It is expected, therefore that highest concentrations of most compounds occur under relatively cold, stable conditions when vertical transport is restricted, leading to relatively slow dispersion. This is also consistent with a significant positive correlation observed for most compounds with atmospheric pressure.

For a number of compounds, a significant positive correlation is observed between NO_x-corrected concentrations and temperature (Table 3.6). This positive correlation could be indicative of input via volatilisation from road, pavement, vegetation or soil surfaces at these sites, which is likely to be enhanced during warmer conditions.

This behaviour is observed mostly for LMW 3-4 ring species (e.g. Flo, Phe, Ant, Flt, Pyr, Ret, 9F, AQ, 1NNap, 2NNap, 2NFlo) and relatively few HMW compounds (1NFlt, 1NPyr, MAQ, BaQ). This is consistent with higher volatility of these lighter compounds, possibly facilitating a higher tendency towards evaporation from surfaces or soil.

Dimashki *et al.* (2001) also found no correlation with temperature for most NO_x corrected PAHs in Birmingham, consistent with a non-seasonal traffic source dominating, but observed positive correlations for LMW PAHs Phe, Flo and Flu, indicating the possible input of these compounds from surface volatilisation. Similarly, Harrad and Laurie (2005) observed no correlation between 'non-corrected' PAH concentrations and temperature at these sites, which the authors attributed to a seasonal pattern (higher emissions in winter) being buffered by volatilization during summer.

Interestingly, positive correlations of 'corrected' concentrations of 9NAnt, 2NFlt, 4NPyr and 2NPyr are observed at EROS but not BROS. These compounds are formed, partly or entirely, by photochemical reactions, which may be higher during the warmer summer conditions. However, no correlation was noted for these compounds with solar radiation intensity so the nature of apparent the temperature-dependence of these compounds is unclear.

3.2.2.5. Correlations of PAH, OPAH and NPAH with rainfall, wind speed and wind direction

No correlation was observed for PAH, OPAH or NPAH concentrations with rainfall. This is consistent with previous studies at these sites (Laurie, 2003). Prevedouros *et al.* (2004b) also indicated that the influence of scavenging by rainfall will have minor influence on atmospheric PAH concentrations.

Furthermore, no correlation was noted between any measured compound and wind speed at either site. This is in contrast to the findings of Harrad and Laurie (2005) where a significant negative correlation was observed for most PAHs at both sites, the authors suggesting higher concentrations were therefore observed under relatively still, calm conditions.

The measurement $\sin(\text{WD})$ is an indication of east-west wind direction. No significant correlation was observed between compound concentrations and $\sin(\text{WD})$, suggesting the absence of a significant emission source to the east or west of the sampling sites. This is broadly consistent with the findings of Harrad and Laurie (2005)

$\cos(\text{WD})$ is an indication of the north-south wind direction. Weak yet significant negative correlation between concentrations and $\cos(\text{WD})$ was observed for only for a small number of compounds (BkF, BaP, DBA, BaAQ, 2NFlo, 3NFlu at BROS ; Acy, Flu, Chr, 7BaA, 6NChr at EROS). Harrad and Laurie (2005) previously reported a significant negative correlation for most LMW PAHs with $\cos\text{WD}$ at BROS but not at EROS. This suggested the levels of LMW PAHs were higher during periods of low wind and air arriving from the south (Bristol Road) but were not influenced to a large degree by wind direction at EROS. Most HMW PAH did not show a significant correlation with $\cos\text{WD}$.

3.3. Seasonal variation in PAH, OPAH and NPAH levels

3.3.1. PAH seasonality

The mean concentrations (particulate + vapour) of PAHs measured only in summer and winter samples are compared in Figure 3.6a and 3.6b for BROS and EROS respectively. It should be noted that these 'seasonal' concentrations are based on a relatively small number of samples ($n=7$) taken during the summer and winter months respectively.

It assumed that these values are representative of concentrations for the full season, which may not be the case so results need to be interpreted with caution. The mean temperature measured on the 'winter' sampling days was ~ 6 °C while the mean temperature on 'summer' sampling days was ~ 15 °C. Interestingly, the mean temperature measured at Birmingham Tyburn during all winter days (Dec 2011 – Feb 2012) was 4.8 °C while the mean summer temperature (June 2012 – Aug 2012) was 14.9 °C.

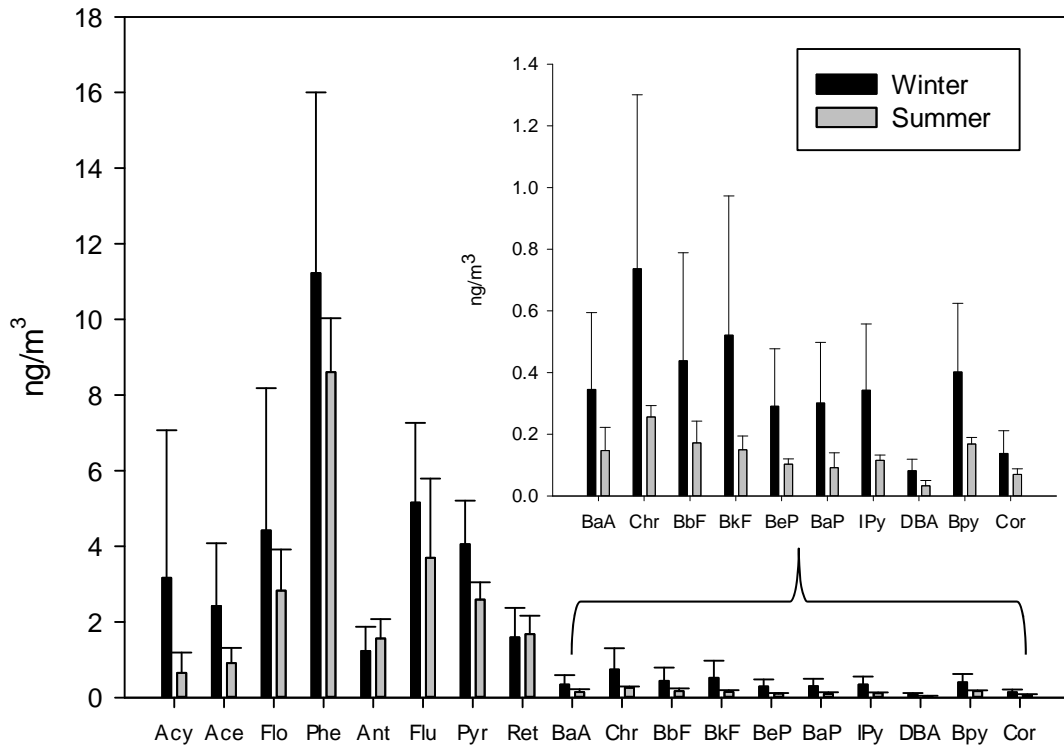
Mean NO_x concentrations measured at Tyburn were 55 µg/m³ and 38 µg/m³ during the winter and summer sampling days respectively. The mean NO_x concentration measured at Tyburn for the whole seasons was 76 µg/m³ for winter months and 33 µg/m³ for summer months. This may therefore suggest that the observed concentrations and conditions in this campaign may be representative of the respective seasons.

Generally, higher concentrations are observed in winter at both sites for most compounds compared with summer samples. However the nature and extent of the observed seasonal profile is highly variable between species and between the two sites. The observed winter (W) to summer (S) ratio of >1 could be caused by an increased concentration in winter and/or reduced concentration in summer.

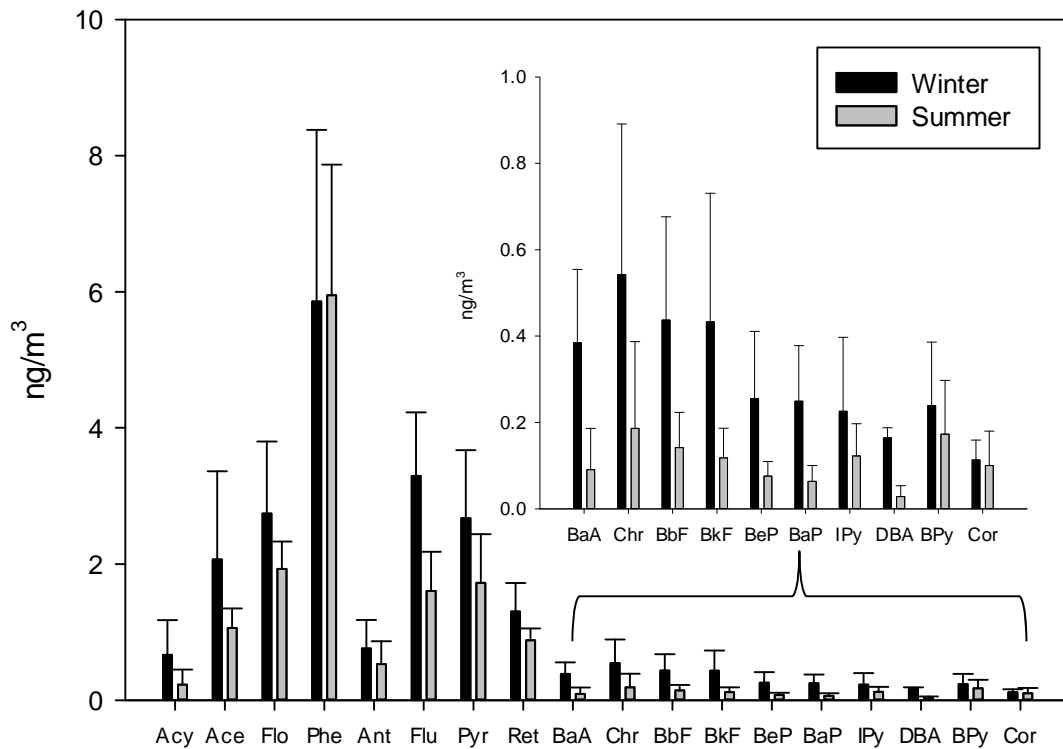
This seasonal trend has been observed for PAHs in previous air sampling studies (Cortes *et al.*, 2000; Cortes and Hites, 2000; Dimashki *et al.*, 2001; Holoubek *et al.*, 2007; Meijer *et al.*, 2008; Smith and Harrison, 1996; Sun *et al.*, 2006).

The key factors that govern the observed seasonal profiles are i) differences in source strength and/or relative contributions from different sources, and ii) changes in the meteorological conditions influencing the rate of dispersion or deposition and the changes in the oxidative capacity of the atmosphere controlling the rate of loss for PAH and/or input of OPAH and NPAH.

Acy is shown to display the highest W:S ratio of the LWM (3-ring) PAH compounds at both sites. This is consistent with the relatively high reactivity towards OH radicals (Atkinson and Arey, 1994), which is likely to cause significant depletion during summer months when photochemical activity is enhanced. This ratio is more pronounced at BROS, possibly due to the closer proximity to the traffic source and the relatively low mixing heights in winter but might also suggest an additional local input influencing the levels of this compound primarily at EROS.



a)



b)

Figure 3.6. Mean PAH concentrations (P+V) measured in winter (n=7) and summer (n=7) samples only at BROS (a) and EROS (b).

A similar profile could be expected for Ant which is also highly reactive towards OH (Brubaker and Hites, 1998). However, relatively low W:S ratios of 0.8 and 1.4 were observed at BROS and EROS respectively. This may suggest that concentrations of Ant are being 'buffered' by a non-traffic related source at these sites during summer.

Phe also displays relatively low seasonal variation with W:S ratios of 1.3 and <1 at BROS and EROS respectively. Analysis of the PAH traffic profile (Section 3.1) indicated the presence of a non-traffic source of Phe, primarily influencing EROS.

It was indicated from the observed traffic profile that concentrations of Ace and Ret are not dominated by traffic inputs and may originate from other combustion sources. Ace displays relatively high W:S ratios. This may result from higher emission rates in winter due seasonally variable activities such as solid fuel combustion for space heating. However, Ret does not display the same profile. This compound is associated with wood combustion but does not display a pronounced seasonal profile. This may suggest that Ret levels observed at these sites are influenced primarily by a non-seasonal wood combustion source.

HMW PAH compounds IPy, BPy and Cor are commonly associated with road traffic emissions (Ravindra *et al.*, 2008). W:S ratios of these compounds are relatively high at BROS, which is consistent with traffic dominating the source profile of these compounds and a seasonal profile resulting due to the colder, more stable conditions prevailing during winter, resulting in reduced vertical transport and dispersion relative to summer months. Ratios at EROS are lower for these compounds, presumably due to a dilution effect caused by greater distance from the local emission source.

Other PAHs such as BaA, BbF, BkF, BeP, BaP and DBA display higher W:S ratios at EROS possibly indicating the presence of an additional seasonally-dependent source of these compounds that may influence EROS more than BROS. This is notably most pronounced for DBA, suggesting this compound is not strongly emitted from road traffic and is predominantly associated with a seasonally-mediated combustion source. This is consistent with the study by

Jang *et al.* (2013) which demonstrated a relatively small input of DBA from 'net traffic' relative to 'net urban' profiles at monitoring sites in London.

Prevedouros *et al.* (2004b) modelled the predicated seasonal variation in PAH concentrations when emissions are constant but environmental conditions (e.g. temperature rainfall, wind speed, TSP concentration, OH reaction rate and boundary layer height) are variable. It was predicted that this would result in relatively high W:S ratios (~4-6) for LMW PAHs and lower ratios (1.5-2) for HMW PAHs.

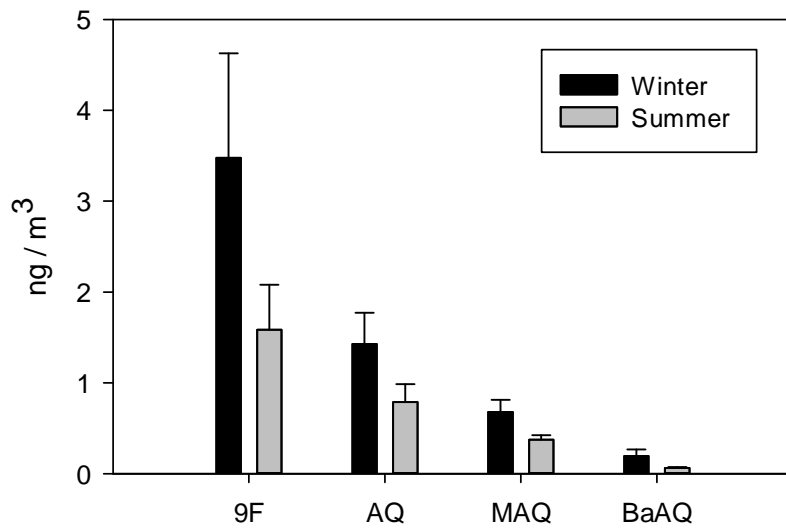
However this trend was not observed in the present study or in previous urban air sampling studies in the U.K. (Baek *et al.*, 1991; Halsall *et al.*, 1993; Prevedouros *et al.*, 2004b). While in the present study, the W:S ratios of HMW PAHs are broadly consistent with modelling predictions, the seasonality of LMW PAHs is shown to be much lower than predicted.

Prevedouros *et al.* (2004b) suggest summer emissions would need to be 1-16 times higher than winter emissions in order to account for the discrepancy between modelled and measured PAH concentrations. The authors highlight a number of potential summer PAH sources that may be responsible, including volatilisation from soil, vegetation, water or impermeable urban surfaces, burning of garden residues and microbially-mediated natural input, and caution that these sources are extremely difficult to characterise and quantify.

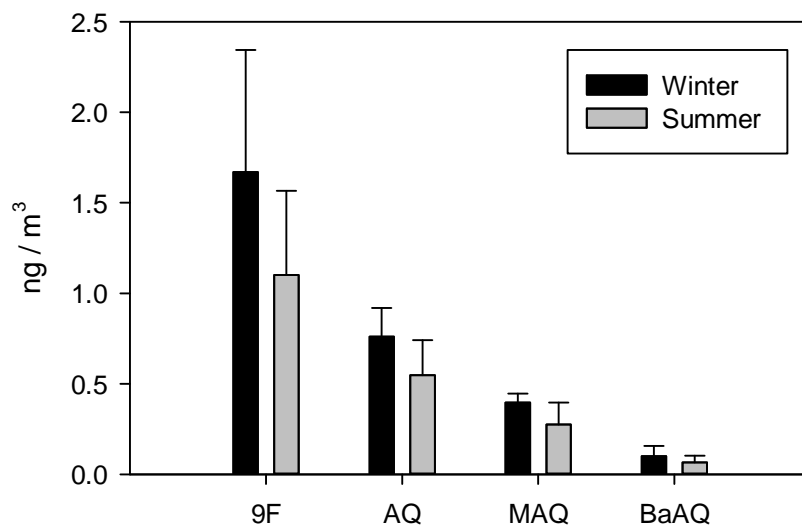
3.3.2. OPAH and NPAH seasonality

OPAH and NPAH seasonal profiles are displayed in Figure 3.7 and 3.6 respectively

OPAH compounds 9F, AQ and MAQ display similar W:S ratios of 1.8-2.2 at BROS and 1.4-1.5 at EROS. This suggests these compounds are subject to similar seasonal variability in input and/or loss processes. The lower W:S ratios observed at EROS may suggest a more enhanced input of these compounds at this site during summer.



a)



b)

Figure 3.7. Mean OPAH concentrations (P+V) measured in winter (n=7) and summer samples (n=7) only at BROS (a) and EROS (b).

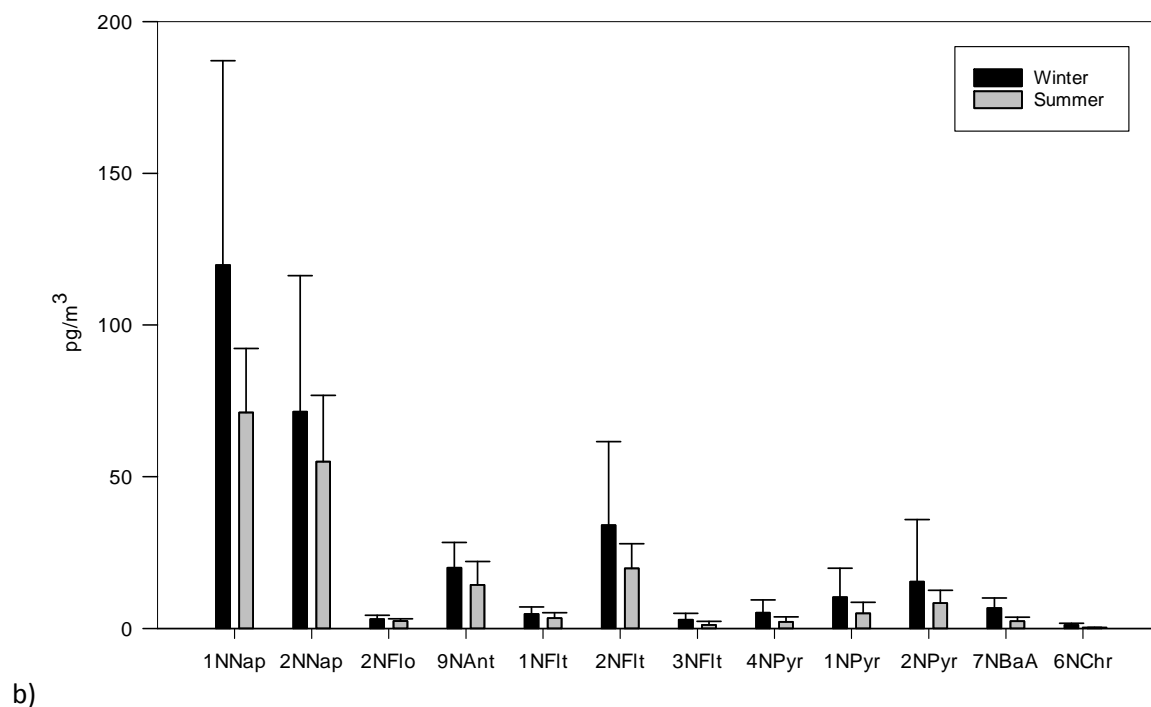
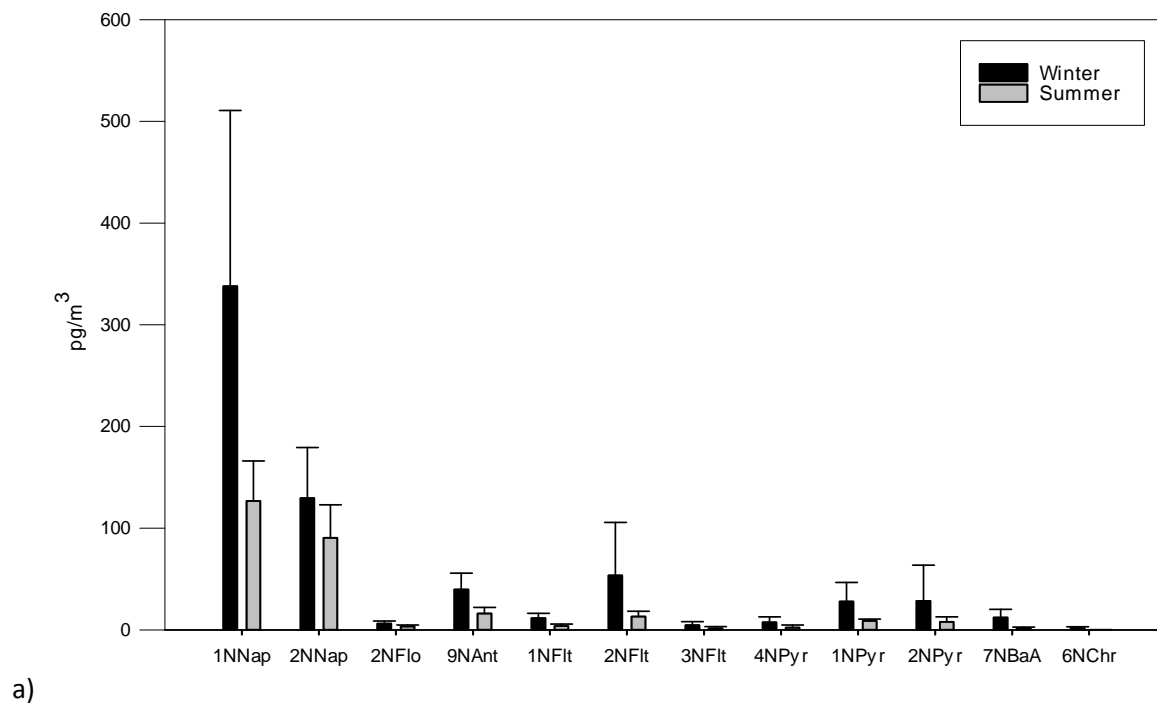


Figure 3.8. Mean NPAH concentrations (P+V) measured in winter (n=7) and summer samples (n=7) only at BROS (a) and EROS (b).

Walgraeve *et al.* (2010) reviewed a large number of OPAH sampling studies from different locations, and reported that median concentrations are 3-4 times higher during winter than during summer. The relatively lower W:S values observed in the present study may therefore reflect the dominance of non-seasonal road traffic as a primary emission source and the possible additional input of OPAHs due to non-traffic related sources during summer.

NPAHs display relatively high W:S ratios at BROS compared with most PAH and OPAH. This may be attributed to photolysis being the primary loss process for these compounds, with rates of degradation being relatively suppressed during the colder winter months and higher during summer. It is noted that the 1NNap W:S ratio is ~2 times higher at BROS than that of 2NNap, which may be attributed to the faster rate of photolysis observed for 1NNap relative to 2NNap (Atkinson *et al.*, 1989; Niu *et al.*, 2005; Phousongphouang and Arey, 2003a).

The relatively high ratios observed for 7NBaA and 6NChr at BROS may indicate the more dominant influence of a seasonally-dependent combustion source for these compounds. To date, no data on non-traffic emissions of these compounds has been provided. The lower W:S ratios observed for NPAHs at EROS may reflect the relatively more 'aged' air mass at this site and/or the influence of secondary input from non-traffic sources such as surface volatilisation or atmospheric reactions.

3.3.3. Factors influencing seasonal trends

3.3.3.1. Seasonal variation in source strength

Previously, relatively high W:S ratios of PAH, NPAH and OPAH observed in urban areas has been associated with a stronger seasonal source strength, with higher concentrations in winter associated, for example with higher emissions from space heating (Andreou and Rapsomanikis, 2009; Coleman *et al.*, 1997; Eiguren-Fernandez *et al.*, 2008a; Harrison *et al.*, 1996; Smith and Harrison, 1996). However, the dominant emission source at the University of Birmingham sites is expected to be road traffic with a much lower contribution from domestic emission sources.

The seasonal variability of traffic-related PAH, NPAH and OPAH emissions is difficult to predict and the lack of data on the seasonal variability of traffic flow at the sampling sites means there is uncertainty regarding this trend. As discussed by Prevedouros *et al.* (2004b), the level of vehicle usage may be higher during summer (for example due to a greater number of people taking vacations and the longer average length of 'daytime'). However, the contribution due to 'cold start' emissions is likely to be higher in winter.

Based on the lack of significant correlation between temperature and PAH/NO_x for traffic marker compounds such as Cor, BeP and BPy (see Section 3.2), it is assumed that traffic emissions do not display significant seasonality and that variability in the emission source strength will not influence the seasonal concentration variation at these sites. Reisen and Arey (2005) noted the seasonal variation of 1NPyr (normalised to CO) was lower than for reaction products 2NFlt and 2NPyr, and suggested this indicated traffic sources were relatively non-seasonal .

A lack of seasonality in emission sources would partly account for the relatively low W:S variability between seasons observed in this study in relation to sampling studies, for example close to Birmingham city centre (Smith and Harrison, 1996).

3.3.3.2. Seasonality of atmospheric boundary layer height

The height of the ABL can influence the concentrations of air pollutants as this will dictate the degree of atmospheric stability and rate of dispersion (Williams, 2001 ; Holloway and Wayne, 2010). The height of the ABL exhibits seasonal and diurnal patterns with daytime summer heights of ~1000m and nighttime winter heights of ~100m (Williams, 2001). It has been indicated, based on the significant ($p < 0.01$) negative correlation between temperature and NO_x concentration, that the ABL height displays seasonality at these sites.

Higher levels of OPAH and NPAH in urban areas where higher emissions from space heating are not likely to occur have been attributed to colder temperature resulting in lower ABL height, less

rapid photooxidation and associated accumulation of pollutants (Albinet *et al.*, 2008a; Bamford and Baker, 2003; Kakimoto *et al.*, 2000; Kakimoto *et al.*, 2001; Marino *et al.*, 2000; Wei *et al.*, 2012).

It is suggested, therefore that seasonality in temperature may be the dominant factor governing observed seasonal PAH, OPAH and NPAH concentration variations at these sites. It should be noted, however that the annual variation in temperature was relatively narrow. Mean ambient temperature from the winter samples was 6°C compared with ~15°C in summer samples.

Albinet *et al.* (2008a) measured concentrations of OPAH and NPAH at a traffic site in France during winter and summer, observing higher W:S ratios than were observed in the present study. In summer, Albinet *et al.* (2008a) reported a concentration of BaP of 0.12 ng m⁻³ in very good agreement with the summer mean concentration observed at BROS. This suggests the rate of primary pollutant input is broadly similar in the two studies. The seasonal temperature trend reported by Albinet *et al.* (2008a) varied from a mean winter temperature of -3°C to a mean summer temperature of 17°C.

This much wider range of temperature may therefore account for the observed differences in OPAH and NPAH seasonality between these two studies, with higher accumulation in the colder winter caused by a lower ABL height and slower photodegradation, and more rapid loss in the much warmer summer months. Indeed Albinet and co-workers report a winter BaP concentration ~9 times higher that was observed at BROS, therefore indicating the influence of a lower mixing height during winter in the previous study.

3.3.3.3. *Influence of volatilisation from surfaces*

It has been previously been indicated that PAH concentrations measured in the U.K. atmosphere can be influenced by the secondary input due to volatilisation from soil, vegetation and/or road surfaces in urban areas (Dimashki *et al.*, 2001; Harrad and Laurie, 2005; Lee and Jones, 1999) or from the sea in coastal areas (Meijer *et al.*, 2008).

Vegetation can represent an important compartment in the scavenging of atmospheric PAH (Simonich and Hites, 1994). For example, it has been demonstrated that PAHs can accumulate in leaf foliage (Keyte *et al.*, 2009; Wild *et al.*, 2006) particularly the waxy cuticle layer on the vegetation surface (Wild *et al.*, 2007). It has been suggested in multimedia modelling study that semi-volatile organic compounds like PAHs can be subsequently released from this compartment to the atmosphere (Diamond *et al.*, 2001). It has also been suggested that volatilisation from soil to air can also occur for LMW organic pesticides (Harner *et al.*, 2001) and PAHs (Wei *et al.*, 2014).

Lee and Jones (1999) noted a significant positive correlation between 3 and 4 ring compounds Phe, Flt and Pyr concentration and temperature in a semi rural site in northern England, indicating the possibility of temperature-driven evaporation from vegetation and/or soils, contributing to observed ambient concentrations in summer. In contrast HMW 5 ring PAHs BbF and BkF were negatively correlated with temperature.

In the present study, the trend between temperature and NO_x-corrected concentrations was investigated to account for the seasonal trend in ABL height (see Section 3.2). Significant ($p < 0.05$) positive correlations were noted at BROS for Flo, Phe, Ant, Flt, Pyr, BbF, DBA, 9F, AQ, MAQ, 1NNap, 2NNap, 2NFlo, 1NFlt and 1NPyr; and at EROS for Acy, Flo, Phe, Ant, Pyr, Ret, BaA, AQ, MAQ, BaAQ, 2NNap, 9NAnt, 2NFlt, 4NPyr, 2NPyr. While this trend does not necessarily indicate the influence of volatilisation from surfaces at these sites, nor the relative significance of this source, it may suggest that a local temperature-driven secondary input may contribute to the observed concentrations of PAH, OPAH and NPAH, particularly in summer for LMW compounds.

Dimashki *et al.* (2001) and Lim *et al.* (1999) indicated that volatilisation from surfaces was more significant in the city centre than at the University site. It was hypothesised that the greater area of impermeable surfaces and density of primary sources would mean road surfaces would represent an area with a greater 'reservoir' of previously deposited PAH compounds than the background site.

In the present study, however, it is unclear as to whether volatilisation is more significant at BROS or EROS. For example, the traffic increment profiles (Section 3.1) indicate a more distinct input of Phe from additional source exists at EROS, however the correlation between temperature and Phe/NO_x is stronger at BROS. Similarly, it was indicated that a stronger additional source of Ret is present at BROS, however a significant trend between Ret/NO_x and temperature is only indicated at EROS.

3.3.4. Seasonal trend in PAH reactivity

It is expected that during summer, higher concentrations of atmospheric oxidants will result in higher reactive input of OPAH and NPAH compounds. For example, Reisen and Arey (2005) observed S:W ratios for 1NNap, 2NFlt and 2NPyr were 2.3, 5.2 and 1.5 respectively at the receptor suburban site Riverside, USA. The authors noted that NPAHs formed by OH reactions only (e.g. 2NPyr) displayed lower summer/winter ratios than those formed by both OH and NO₃ reactions (1NNap, 2NNap and 2NFlt) suggesting significant summer input from NO₃ reactions.

In the present study, mean 2NFlt/2NPyr ratios were relatively low (<6) at both BROS and EROS in all seasons, indicating minimal impact of NO₃ reactivity relative to OH reactions. However, 2NFlt/1NPyr ratios were higher at EROS relative to BROS in all sampling seasons. Ratios were a factor ~3.5 higher at EROS in summer, compared with an inter-site difference of factor ~2.3 in winter. This highlights the potential importance of OH reactions between sites and suggests this is more pronounced during the warmer summer months.

The greater prominence of atmospheric reactivity during summer may be expected to cause NPAH/PAH and OPAH/PAH ratios to display similar seasonality. For example, Walgraeve *et al.* (2010) assessed the ratio of OPAH/ 'parent' PAH in a number of ambient sampling studies in the literature. It was shown that during winter, 50% of these ratios were between 0.006 and 0.16. In summer ratios were reported to be about 20 times higher, with 50% of ratios between 0.54 and 3.6 (Keyte *et al.*, 2013).

OPAH or NPAH 'product' / PAH ratios (see Section 3.6) were shown to be highly variable and no distinct seasonal trend in ratio values or in the significance of atmospheric reactivity to the measured atmospheric concentrations of OPAH and NPAH could be observed.

Other seasonal factors may occur which will also influence the relative value of these ratios. This includes differences phase partitioning, which can lead to protection of PAH, NPAH or OPAH from photolytic or reactive losses as well as possible influence of temperature-dependent volatilisation of compounds from surfaces, which may occur at differing levels of significance and occur at different rates for different PAH, OPAH and NPAH compounds.

Similarly, Wei *et al.* (2012) showed that at sampling sites in southern China, NPAH/PAH and OPAH/PAH ratios displayed considerable spatial, seasonal and diurnal variations, likely influenced by a number of competing factors including changes in emission strength, reactivity rates and degree of phase partitioning.

3.3.5. BROS/EROS ratio seasonality

Table 3.6. presents the mean ratios of BROS/EROS concentrations measured for all compounds during each sampling season during Campaign 1.

HMW (5+ ring) PAHs exhibit relatively small seasonal variation in BROS/EROS ratios, attributed to their relatively high stability, low volatility and strong association with PM expected in all sampling seasons. LMW PAHs may be expected to display higher BROS/EROS ratios during summer due to enhanced chemical reactivity between sites. However, this is not observed for most compounds.

For PAHs, the highest ratios in all seasons are observed for the most reactive PAHs, Acy and Ant. However, opposing seasonal trends are observed for these compounds. Ant displays higher BROS/EROS ratios in spring and summer compared to autumn and winter, consistent with higher reactive losses between sites in the warmer months.

It is indicated above that the seasonal profile of Ant may be influenced by non-traffic sources during summer. These results suggest this if this phenomenon occurs, it is primarily influencing at BROS. Conversely, Acy displays higher BROS/EROS ratios in winter. This may indicate that levels of Acy may be 'buffered' to a certain degree by evaporative input from surfaces, primarily influencing EROS, as indicated by the significant ($P < 0.05$) correlation between Acy/NO_x and temperature at this site.

Flt and Pyr display similar ratios in winter, indicating similar input and loss processes are affecting both compounds. However, in summer Flt displays higher BROS/EROS ratio while Pyr appears to show minimal seasonal variability. It has been indicated above that both Pyr and Flt may be influenced by an additional source at both sites (as suggested by their observed association with Ret; see Section 3.2). However, while both Flt/NO_x and Pyr/NO_x are shown to correlate significantly with temperature at BROS, only Pyr displays this trend at EROS. This may partly account for the discrepancy in the seasonal behaviour of the BROS/EROS ratios of these compounds.

BROS/EROS ratios of Flo and Phe are highest in autumn and winter respectively and lower in summer. As indicated in the present and previous (Dimashki *et al.*, 2001) studies, these compounds may be influenced by local input due to temperature-driven volatilisation from surfaces. These results would suggest this phenomenon is more prevalent at EROS than at BROS.

Ret exhibits a higher BROS/EROS ratio in summer, suggesting the concentrations of Ret at these sites is not controlled by seasonally-mediated domestic wood combustion for space heating but rather a source that may be more prevalent at BROS in summer such as incineration of garden wastes. Ace displays ratios of < 1 in spring and summer and > 1 in winter, possibly indicating the influence of a seasonally-mediated combustion source that is more prevalent at BROS and/or a local input at EROS in summer, which masks the influence of a traffic related pattern.

Table 3.6. Mean BROS/EROS concentration ratios measured in each sampling season in Campaign 1.

	Autumn	Winter	Spring	Summer
Acy	4.4	4.0	3.8	3.3
Ace	1.6	1.2	0.9	0.9
Flo	1.8	1.6	1.6	1.5
Phe	1.5	1.9	1.9	1.5
Ant	2.3	2.2	3.3	4.6
Flu	1.9	1.7	1.6	2.2
Pyr	2.9	1.7	2.2	1.7
Ret	1.6	1.2	1.8	2.0
BaA	1.8	1.9	2.0	2.3
Chr	1.7	1.5	1.8	2.4
BbF	1.5	1.3	1.6	1.4
BkF	1.4	1.3	1.7	1.5
BeP	1.3	1.5	1.5	1.6
BaP	1.9	1.8	1.6	1.8
Ipy	1.6	1.4	1.3	1.2
DBA	1.7	1.5	2.9	1.8
Bpy	1.6	1.6	1.6	1.3
Cor	1.6	1.2	1.4	1.0
9F	1.9	2.2	1.5	1.3
AQ	1.6	1.9	1.4	1.3
MAQ	1.8	1.7	1.4	1.1
BaAQ	1.3	2.3	1.4	1.1
1NNap	3.2	3.1	2.9	1.9
2NNap	2.2	2.1	2.0	1.7
2NFlo	2.2	2.2	2.2	1.5
9NAnt	2.4	2.0	1.4	1.2
1NFit	3.6	2.6	2.2	1.3
2NFit	1.9	1.5	2.2	0.7
3NFit	1.0	1.7	1.4	2.0
4NPyr	1.6	2.0	1.6	1.6
1NPyr	2.5	3.4	2.7	2.7
2NPyr	1.2	2.1	2.0	1.2
7NBaA	1.9	1.8	1.8	1.0
6NChr	1.4	1.5	2.4	1.2

OPAHs and NPAHs generally display lower inter-site ratios during summer compared with other times of the year. For NPAHs, this observation is unexpected as relatively rapid photolytic degradation of these compounds would be expected to produce relatively large BROS/EROS ratios during summer, assuming a predominant traffic source from BROS.

The observation of relatively lower BROS/EROS ratios may therefore reflect a greater influence of non-traffic related sources of these compounds during summer months e.g. input from garden bonfires, or volatilisation/resuspension.

It is also suggested that NPAH and OPAH concentrations (for compounds such as 1NNap, 2NNap, 2NFlt, 2NPyr, AQ and 9F) at EROS may be enhanced during summer due to higher input from atmospheric reactions between sites (see Section 3.6 and 4.3). For example a ratio of <1 is noted for 2NFlt during summer, suggests the more enhanced reactivity in the atmosphere during the warmer months.

3.4. Temporal trend of PAHs at BROS and EROS

3.4.1. Overview

PAH concentrations have previously been measured at the University of Birmingham sites in 1997 (Dimashki *et al.*, 2001) and 1999-2001 (Harrad *et al.*, 2003; Harrad and Laurie, 2005). A comparison between the annual mean concentrations of PAH and OPAH compound 9F measured in the present study and those reported in the previous studies is shown in Figure 3.9. It should be noted that this comparison is made based on a relatively small number of individual samples taken at these sites in the present and previous studies, used as representative 'annual mean' concentrations. Differences in specific conditions (e.g. traffic flow, meteorological variables, analytical methods) may mean the annual concentration values derived may not be directly comparable. The interpretation of temporal pattern at these sites must therefore be made with caution.

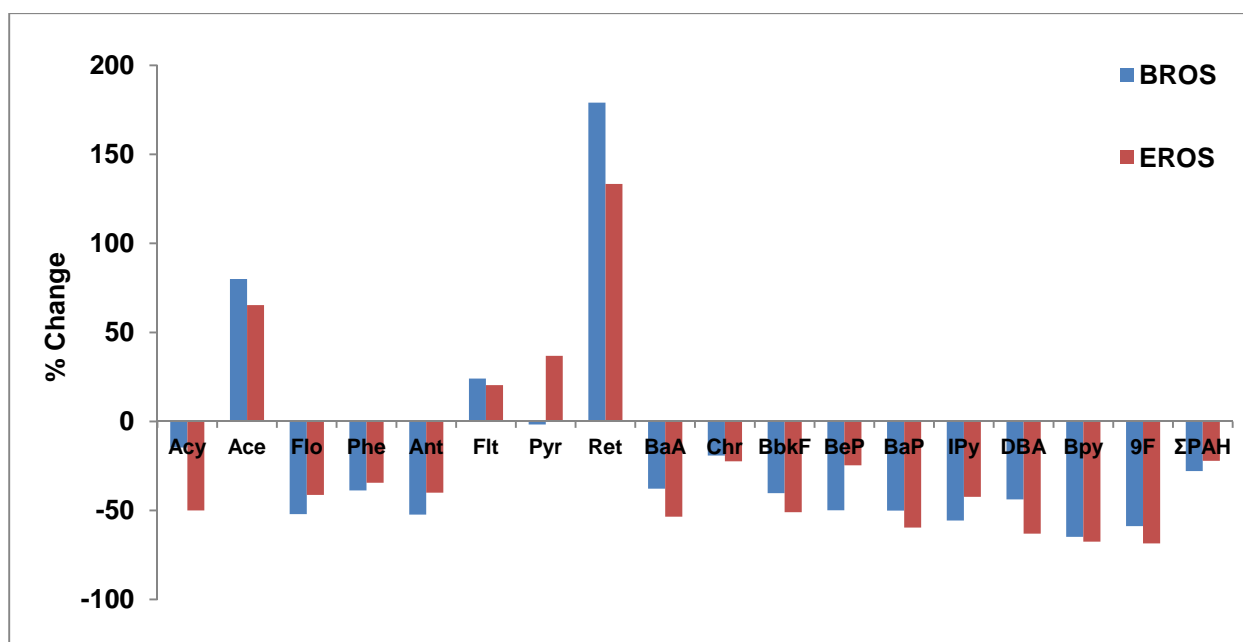


Figure 3.9. The percentage change of PAH concentrations between mean annual values reported by Harrad and Laurie (2005) and the present study.

Decreases in concentration are noted for most compounds at both sites. For BaP a decline of 51% and 61% is observed at BROS and EROS respectively. This is consistent with observed decreases in BaP concentrations at monitoring stations in similar urban locations across the U.K. over the same timescale (Brown *et al.*, 2013). The reductions noted for most PAHs measured at BROS and EROS over the last decade are consistent with the ongoing downward trend in PAH concentrations observed at urban sites in the UK over the past century.

As discussed by (Brown *et al.*, 2013), the first PAH monitoring data in the U.K. was produced in 1949-50 with levels of BaP reported to be over 60 ng m^{-3} , approximately 300 times higher than the annual mean measured at BROS in this study. Monitoring of PAH levels in central London showed that BaP concentration declined by around 90% from 1949 to 1973 (Lawther and Waller, 1976). Jones *et al.* (1992) used plant foliage as a monitor of PAHs at the Rothemstead Experimental Station in Hertfordshire, U.K. and reported concentrations measured in the period 1985 to 1989 were up to 4 times lower than those measured in the period 1965 to 1969.

Smith and Harrison (1996) indicated that PAH concentrations measured at sites in Birmingham in 1992 were 2 to 10 times lower than levels observed in 1976-1978 by Butler and Crossley (1979). Further decline of ambient PAH levels were noted during sampling studies in different urban locations in the UK during the 1990s (Coleman *et al.*, 1997; Meijer *et al.*, 2008). Dimashki *et al.* (2001) noted a 56% decrease in total PAH concentrations at the University of Birmingham campus in the period 1992-1997. Harrad and Laurie (2005) reported a further decrease of 31% at the University site between the 1997 and 1999-2001.

The observed decline in PAH concentrations reported in ambient air measurements has been shown to correlate with reductions in estimated primary combustion emissions (Brown *et al.*, 2013). These historical emission reductions have therefore been attributed to the introduction of the Clean Air Acts of 1956 and 1968 as well as the implantation of the Environmental Protection Act in 1990, which enforced emission reduction measures (Brown *et al.*, 2013).

Indeed, as discussed in Section 1.4.4, data from the NAEI indicates that the reductions in PAH concentrations observed over the last 20 years can be attributed largely to the almost complete reduction of PAH emissions from industrial metal processing and banning the burning of agricultural waste (Murrells *et al.*, 2010). Additionally, the decline in PAH concentrations in Birmingham specifically have been attributed to the establishment of 'smokeless zones' in West Midlands area as well as reduction in use of coal movement towards natural gas heating (Smith and Harrison, 1996). More recent decreases in PAH concentrations in the U.K. have been associated with the introduction of catalytic converters in 1993 and the associated reduction in emissions from on-road vehicles (Smith and Harrison, 1996 ; Dimashki *et al.*, 2001).

It is suggested, therefore, that the observed changes in concentrations and relative contributions of PAHs in the period 2000 to 2012 can be attributed to changes in local emission source profiles.

3.4.2. Temporal trend in PAH and OPAH concentrations

As shown in Figure 1.1, the total emission of PAHs in the UK, as estimated by the NAEI, declined <10% between 2000 and 2012. The observed decline in concentrations for most PAH compounds at BROS and EROS over this period would therefore seem to be quite large in relation to this national trend.

Figure 3.10 shows NAEI emission estimates for different individual PAHs resulting only from 'urban traffic', which is expected to be the primary source of PAHs at both sites in this study for most compounds. The observed decline in Σ PAH concentration was 28% and 22% for BROS and EROS respectively, while the estimated decline in total PAHs emissions from urban traffic over this period was 37%. This discrepancy may therefore suggest that PAH concentrations at these sites are being influenced by other non-traffic sources, either primary (e.g. other primary combustion sources) or secondary (e.g. resuspension or volatilisation from soil, vegetation or road surfaces).

There is clearly considerable variability in the temporal trends of individual PAH compounds at these sites, which requires careful consideration. For many PAHs (e.g. Phe, Ant, BaA, BaP, IPy, DBA and BPy), the observed magnitude of atmospheric concentration decline appears to resemble the estimated national reduction in urban traffic emissions. This is consistent with traffic being the dominant source of most PAHs, OPAHs and NPAHs at both sites, as suggested by the observed 'traffic profiles' (see Section 3.1).

Exceptions to this include BbF, BkF, Chr which show lower concentration decreases than expected from their traffic emission behaviour, and Flo which displays a higher decrease than suggested by estimated traffic emissions. This may be due to relative changes in the contribution of non-traffic sources e.g. an increase in contribution from coal combustion (Khalili *et al.*, 1995; Ravindra *et al.*, 2008) or a decrease in surface volatilisation contribution (Dimashki *et al.*, 2001). More significant differences from the expected 'traffic decrease' were observed for Ace, Ret, Flt and Pyr which may reflect a relatively large contribution from non-traffic sources.

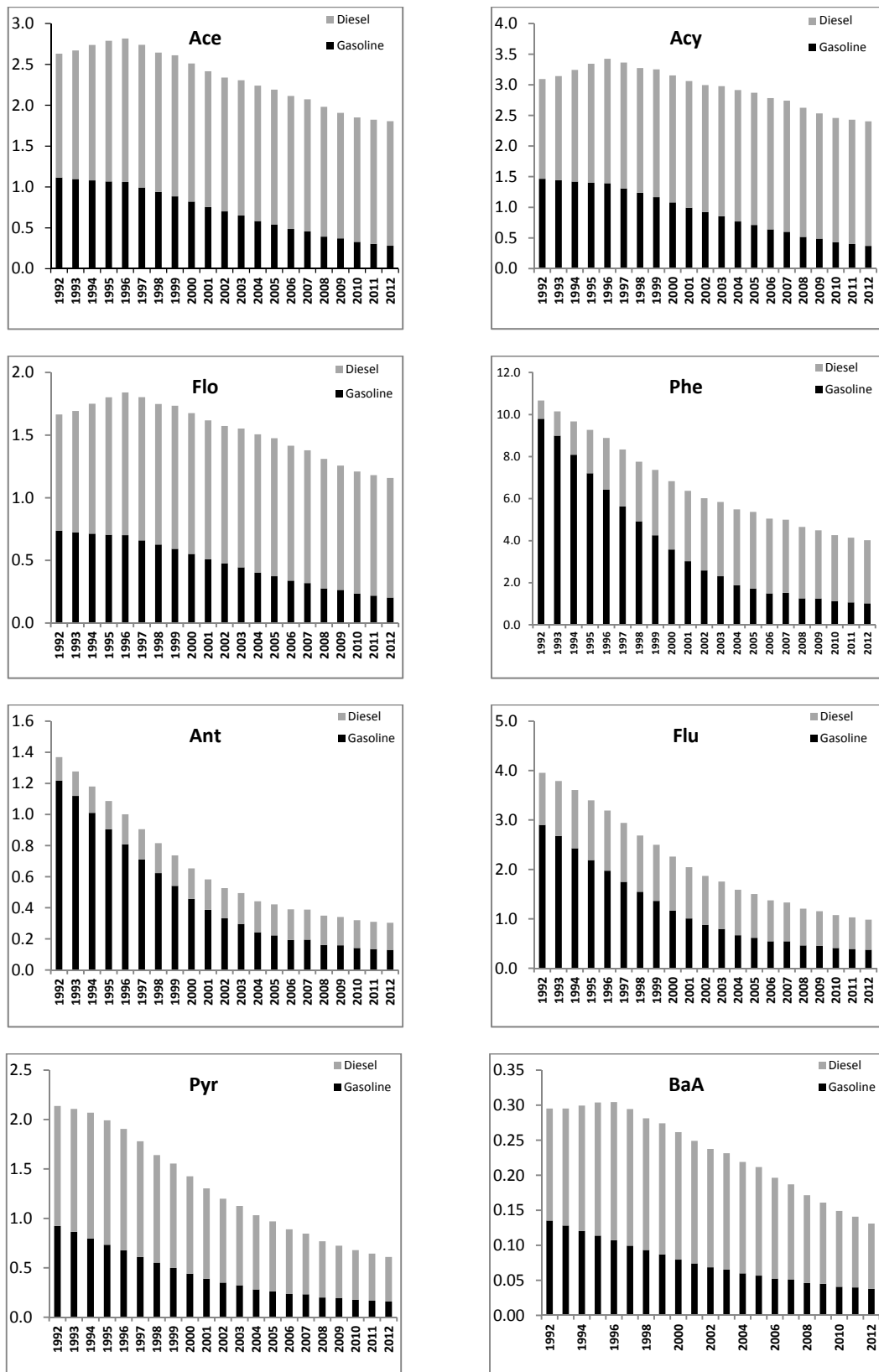


Figure 3.10. NAEI estimates for PAH emissions from urban road traffic (tonnes)

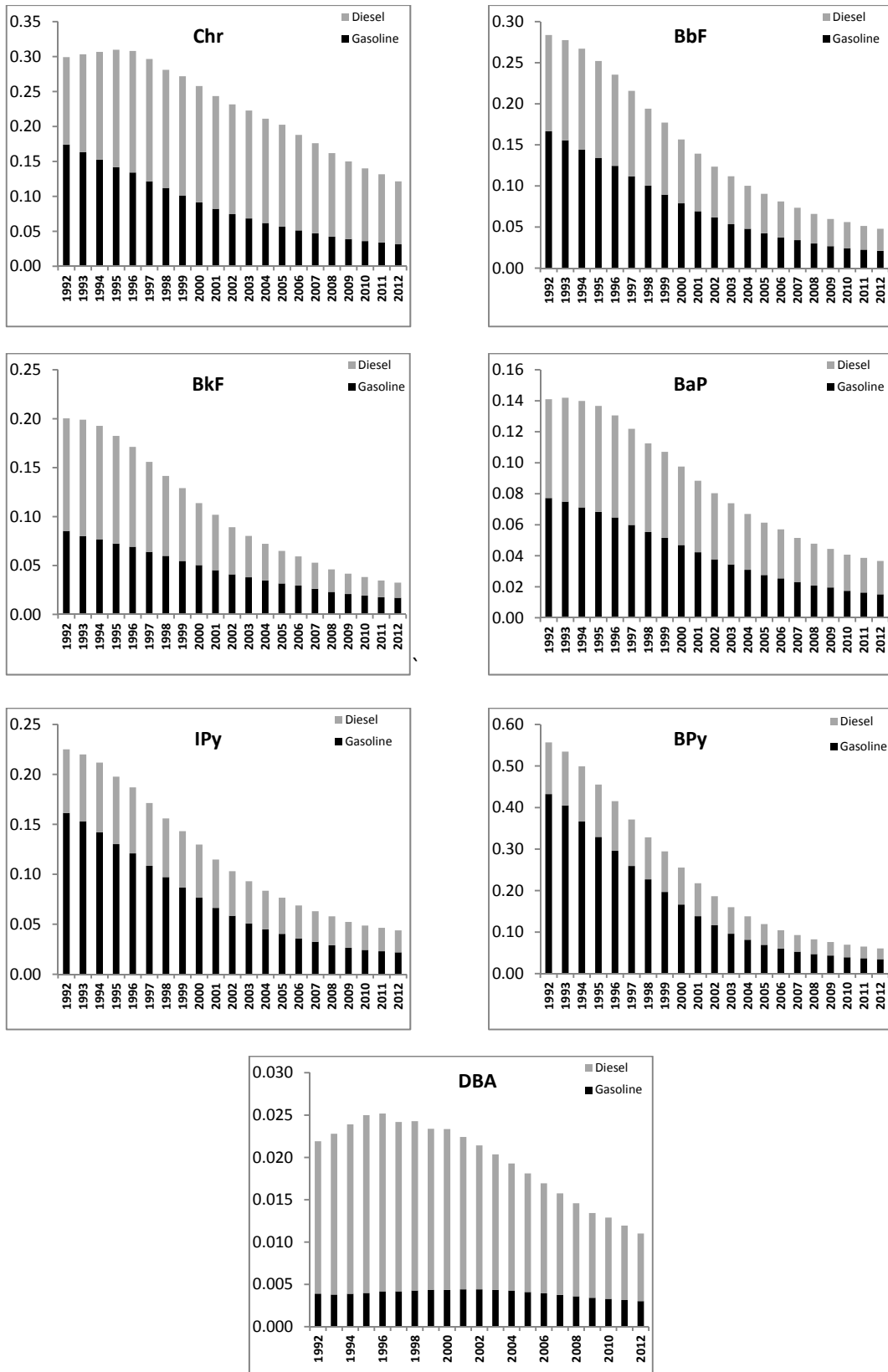


Figure 3.10. NAEI estimates for PAH emissions from urban road traffic (tonnes)

Ace and Ret both display substantial increases in annual concentration at both sites, in contrast to most other PAHs. Harrad and Laurie (2005) also noted an increase in Ace concentration between 1997 and 1999-2001. As noted above, these compounds displayed a deviation away from the expected 'traffic profile' correlation observed between road tunnel concentrations and [BROS – EROS] increment, indicating the possible influence of non-traffic source(s).

Ret is commonly associated with wood combustion (McDonald *et al.*, 2000; Ramdahl, 1983) and shown to display elevated concentrations during 'bonfire night' celebrations (Harrad and Laurie, 2005 ; Mari *et al.*, 2010). The increase in Ret concentrations of 179% and 133% at BROS and EROS respectively would appear to be consistent with NAEI emissions data indicating a 123% national increase in PAH emissions from domestic wood combustion over this period.

However, seasonal (Section 3.3) and diurnal (Section 5) profiles of Ret suggest domestic combustion may not be the dominant source for this compound. PMF analysis (Section 4.3) suggests Ret concentrations are dominated by a non-traffic source attributed to wood combustion but it is suggested the specific source is more likely to be the periodic combustion of wood material for example in garden bonfires rather than a seasonal domestic source.

A similar though smaller increase in concentration of Ace also indicates a strong influence from a non-traffic source. Furthermore, Flt and Pyr also do not display expected decreases in concentrations based on estimated traffic emission reductions, with levels either similar or higher than those measured in 1999-2001.

Inter-correlations of species (Section 3.2) indicate Pyr and Flth are strongly associated at both sites and both are correlated with Phe at BROS. These compounds are commonly associated with diesel emissions so this may suggest the levels of these compounds at BROS may be influenced by a common diesel source. However, Flt and Pyr are not correlated with other PAHs at EROS with the exception of Ret. This suggests a common non-traffic source may influence Flt, Pyr and Ret at EROS and to a lesser degree at BROS.

Indeed, PMF analysis (see Section 4.3) suggests Phe, Flt and Pyr concentrations are strongly associated with the same source factor at Ret, suggesting the influence of wood combustion for these compounds. This is consistent with the observation that Pyr and Flt display relatively high levels in emissions from incineration (Ravindra *et al.*, 2008). The temperature dependence of Flt/NO_x, Pyr/NO_x and Ret/NO_x indicates the possible additional influence of evaporative input of Pyr and Flt at BROS and Pyr and Ret at EROS.

Ace was not strongly associated with Pyr, Flu or Ret at EROS but displays a weak (though significant) correlation with Pyr and Flt at BROS. This could indicate that these compounds are influenced to a degree by the common traffic source at BROS, but also influenced by separate non-traffic sources at both sites. PMF analysis indicated a strong association of Ace with a factor attributed mostly to volatilisation from road surfaces. However, this would not account for the relatively high increase in concentrations since 1999-2001 or the observed seasonal pattern for Ace (see Section 3.3). It is possible therefore that a domestic combustion source may also influence Ace concentrations at these sites.

The observed decrease in concentrations of 9F at BROS and EROS, compared with measurements in 1999-2000 is higher than those observed for semi-volatile PAH compounds. No emission estimates are available for OPAH compounds in the NAEI database but 9F has been observed in relatively high concentrations in gasoline and diesel exhaust emissions (Jakober *et al.*, 2007; Oda *et al.*, 1998; Oda *et al.*, 2001; Zielinska *et al.*, 2004b). Inter-correlations of 9F with other PAHs at these sites suggest a stronger with gasoline emissions than diesel. Therefore a relative decline in concentration similar to other gasoline-related PAH compounds e.g. BPy and IPy would appear sensible.

9F has also been shown to result from atmospheric reactions (Wang *et al.*, 2007b). Therefore, it might have been expected that while direct emissions decline, the levels of such compounds may be 'buffered' to a degree by reactive input, as observed for 2NFlt by Kojima *et al.* (2010) and Wang *et al.* (2011a) in urban areas where emission control measures were implemented. The relatively

substantial decline may indicate, therefore that reactivity (and volatilisation from surfaces) has not influenced the temporal trend of this compound.

3.4.3. Temporal trend in NPAH concentrations

The relative lack of NPAH measurements carried out in the UK prior this study makes an assessment of temporal variation difficult. However, NPAH concentrations were previously measured in Birmingham city centre in 1995/6 in the period Nov to Feb (Dimashki *et al.*, 2000). Table 3.7 provides a comparison between the NPAH concentrations measured in the previous study and those measured in the present study at BROS. The mean of winter samples is used and BROS chosen for comparison due to its close proximity to relatively high traffic levels.

The levels of gas-phase NNAp compounds in the present study are a factor ~4 and ~2 higher than measured by Dimashki *et al.* (2000) in 1995/6 for 1NNAp and 2NNAp respectively. In contrast, concentrations of compounds associated primarily with particulate matter (e.g. 1NPy, 9NAn and 2NFIt) are 2.5 to 5 times lower at BROS compared with concentrations in the previous study. The sampling sites in the present study are ~3km south of the city centre so measurements may not be directly comparable so assessment of relative levels needs to be made with caution.

Indeed, traffic counts adjacent to the city centre sampling site are estimated to be 3-4 times higher than at BROS (DfT figures). Also, the contribution of traffic to the observed PAH levels have been estimated to be higher at the city centre (80-82%) compared to the University campus site (61-67%) (Lim *et al.*, 1999). Therefore, the lower concentrations of particulate-phase NPAH observed in this study may not be entirely associated with reduction in NPAH concentrations over time.

Table 3.7. Mean total (particulate + vapour) NPAH concentrations (pg m³) measured by Dimashki *et al.* (2000) at Birmingham city centre in Nov 1995-Feb 1996 and in the present study during winter at BROS in 2011-2012.

NPAH Compound	Birmingham City Centre, winter 1996 (pg m³)	BROS, winter 2012 (pg m³)
1-NNap	90	338
2-NNap	70	130
9-NAnt	190	40
1-NPyr	90	28
2-NFlth	220	54
7-NBaA	30	12

These results are difficult to interpret definitively. It is unclear why gas-phase NNAp compounds display higher concentrations in the present study compared to the previous study. If the relative increase in diesel emissions over this time had dictated observed NPAH concentrations, a corresponding increase should be noted for 1NPyr and 9NAnt. Conversely, if the campus site(s) experienced higher input from photochemical reactivity, this should also be observed for 2NFlt. The lower levels of particulate-phase NPAHs may partly indicate a temporal decline in concentrations but this may also simply reflect differences in emission strength at two different sites. It is not possible to conclude the level of temporal change for NPAH at these sites relative to the trend for PAH.

Chapter 4 : Gas-particle partitioning, chemical reactivity and source apportionment of PAHs, OPAHs and NPAHs, and the influence of sampling artefacts

4.1. Gas-particle partitioning of PAHs, OPAHs and NPAHs

4.1.1. Phase partitioning overview

The distinction between the gas-phase and particulate-phase fraction was taken by the proportion present in the PUF material and filter respectively. The mean percentages of PAH, OPAH and NPAH compounds in the gas- and particulate-phases in the samples from Campaign 1 are presented in Figure 4.1. It is expected that sampling artefact has not influenced gas-particle partitioning to a significant degree in this study (see Section 4.4).

4.1.1.1. Phase partitioning of PAHs

The PAH phase distribution observed in the present study is generally consistent with previous sampling studies from the urban locations such as Tokyo, Japan (Yamasaki *et al.*, 1982), London, U.K. (Baek *et al.*, 1991) and Chicago, USA (Simcik *et al.*, 1998). LMW PAHs (MW<228) are shown to be present predominantly in the gas-phase while HMW PAHs (MW>228) are mainly associated with the particulate-phase. This partitioning behaviour is also similar to measurements previously reported at the Birmingham University site in 1999-2001 (Laurie, 2003) and by Harrison and co workers in 1992.

There is only a very modest difference in average gas-particle profiles for most compounds between BROS and EROS locations, suggesting a limited degree of partitioning is occurring between the 'polluted' site and the 'background' site. This is also consistent with previous work at these sampling sites (Laurie, 2003).

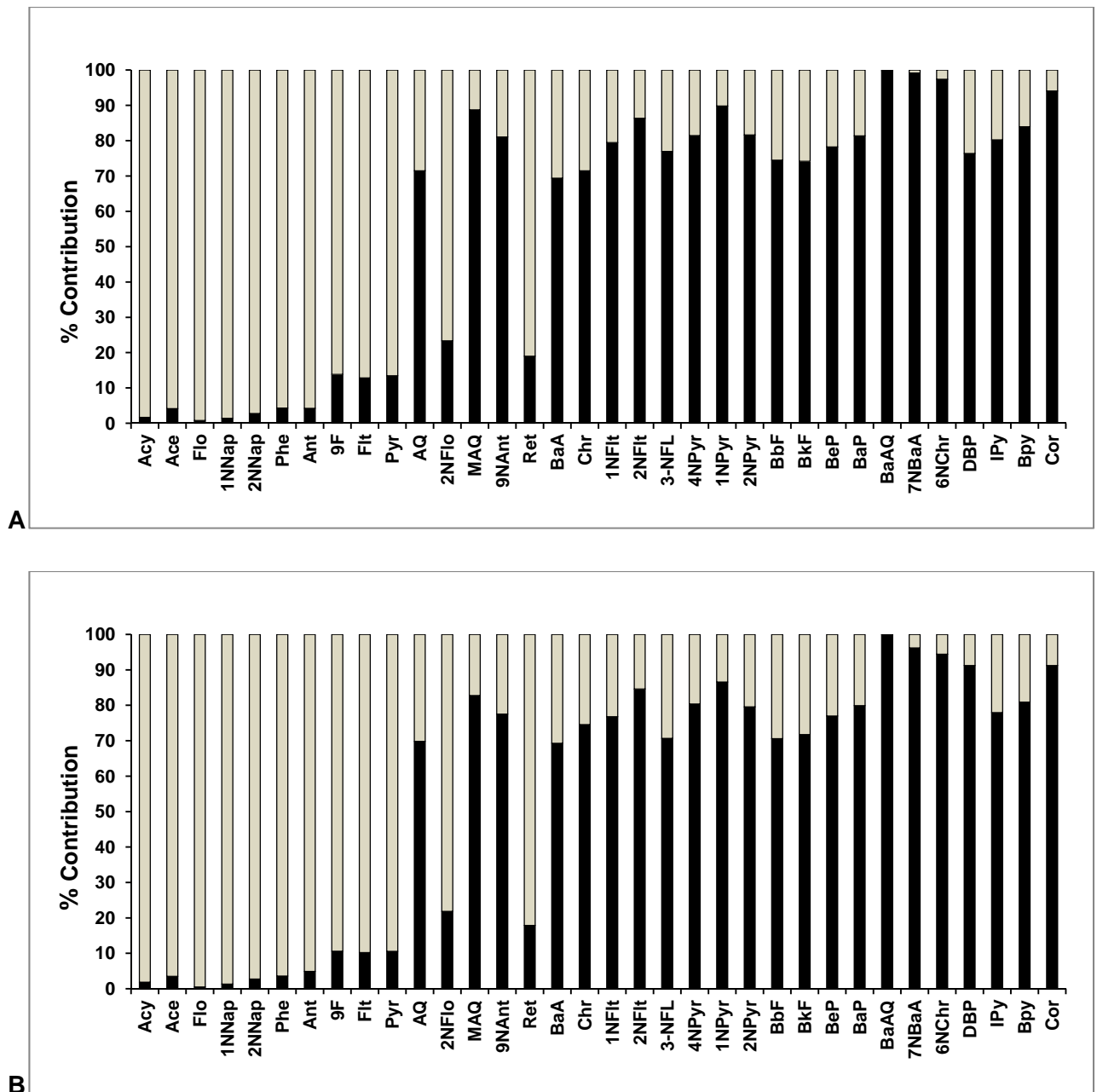


Figure 4.1. Mean percentage of PAH, OPAH and NPAH compounds in the particulate (black) and gas (grey) phases at BROS (A) and EROS (B). Compounds are presented with increasing molecular weight from left to right.

4.1.1.2. Phase partitioning of OPAHs and NPAHs

There have been relatively few studies measuring OPAH and NPAH compounds in both particulate- and gas-phases (Alam *et al.*, 2013; 2014; Albinet *et al.*, 2008a; Bamford and Baker, 2003; Delgado-Saborit *et al.*, 2013). The partitioning profiles of OPAH and NPAH compounds in

the present study are broadly similar with that observed by Albinet *et al.* (2008a), Bamford and Baker (2003), Huang *et al.* (2014) and Delgado-Saborit *et al.* (2013). As with unsubstituted PAHs, more volatile compounds (MW < 207) are predominantly present in the gas-phase while HMW compounds (MW > 247) are mainly associated with the particle-phase.

Previously, Dimashki *et al.* (2000) measured NPAH concentrations in central Birmingham during winter. NNAp isomers were shown to exist almost entirely in the gas-phase while HMW compounds 2NFIt, 1NPyr and 7NBaA were shown to be almost entirely in the particulate phase. The more semi-volatile 9NAnt was shown to exhibit a particle-phase contribution of ~77%. This NPAH phase distribution is very similar to that observed in the winter samples of the present study.

The phase-partitioning behaviour of individual PAH, OPAH and NPAH compounds, particularly those of intermediate size (234 > MW > 207) is highly dependent on the specific sampling location, ambient conditions, and the sampling method used (Baek *et al.*, 1991; Yamasaki *et al.*, 1982 ; Delgado-Saborit *et al.*, 2013), and can display significant seasonal differences (see below).

It is clear from Figure 3.10 that while molecular weight is a good predictor of PAH gas-particle partitioning, intermediate MW PAH, OPAH and NPAH compounds display very different partitioning behaviour, suggesting other/additional factors play an important role. For example, the particle-phase fraction of Ret, AQ, 2NFlo and 9NAnt are shown to display very different values despite relatively small differences in MW between these compounds.

4.1.2. Physiochemical properties influencing partitioning

The percentage proportion of PAH, OPAH and NPAH compounds in atmospheric measurements (%P) have previously been plotted with respect to their respective molecular weights by Albinet *et al.* (2008a), who observed a distinct pattern for the distribution of these compound classes for winter and summer sampling.

Delgado-Saborit *et al.* (2013) have also characterised PAH and OPAH phase partitioning based on molecular weight (MW) as well as other physiochemical properties including vapour pressure, VP (to represent compound volatility); octanol-water partitioning coefficient, Log K_{ow} (to represent compound polarity); and Henry's Law Constant, H (to represent a compound's tendency to partition to the aqueous phase).

This approach was applied to the sampling data from Campaign 1 of the present study, in order to compare observations with those of previous studies and extend the approach of Delgado-Saborit *et al.* (2013) to include NPAH compounds. Plots of percentage particulate-phase contribution against MW, VP, $\log K_{ow}$ and H are shown in Figure 4.2, 4.3, 4.4 and 4.5 respectively, with different plots shown for each individual compound class. These include distributions for the mean %P value for all samples in the campaign as well as those for averages of winter and summer samples. Details of the sources for physiochemical metrics used in these plots can be found in Table 4.1.

Experimental data were not available for all compounds and it should be noted that due to relatively few OPAH compounds measured in the study, curves could not be adequately fitted for certain parameters (e.g. $\log K_{ow}$ and H) and plots for OPAH should be interpreted with caution. Delgado-Saborit *et al.* (2013) provide plots using a more expansive range of measured OPAH compounds and a more detailed discussion of partitioning behaviour.

Delgado-Saborit *et al.* (2013) demonstrated that a sigmoidal logistic curve using 4 parameters (Eq 4.1) provides a good fit for the plots of %P vs MW, %P vs VP and %P vs $\log K_{ow}$ and an exponential curve fitted for %P vs H for PAHs and OPAHs in samples collected at these sites.

$$y = y_0 + \frac{a}{1 + e^{-\left(\frac{x-x_0}{b}\right)}} \quad (4.1)$$

This approach was used in the present study to provide comparable results to those of the Delgado-Saborit *et al.* (2013) study as to assess the suitability of this approach for NPAH compounds.

Table 4.1. Physiochemical properties (at 25 °C unless stated) of the PAH, OPAH and NPAH compounds in the present study, molecular weight (MW) ; vapour pressure (VP) ; vapour pressure of the subcooled liquid, (P[°]_L), solubility in water (S), octanol-water partition coefficient (K_{OW}), octanol-air partition coefficient (K_{OA}), Henry's Law coefficient (H).

PAH	MW (g mol ⁻¹)	VP ^a (Pa)	P [°] _L (Pa) ^b	S (mg/L) ^a	Log K _{OW} ^c	Log K _{OA} ^c	H (Pa m ³ mol ⁻¹) ^a
Acy	152.2	9 x 10 ⁻¹	4.2	16.1	3.9	6.5	8.4
Ace	154.2	3 x 10 ⁻¹	1.4	3.8	4	6.4	12.2
Flo	166.2	9 x 10 ⁻²	6 x 10 ⁻¹	1.9	4.1	6.9	7.9
Phe	178.2	2 x 10 ⁻²	9 x 10 ⁻²	1.1	4.5	7.6	3.2
Ant	178.2	1 x 10 ⁻³	7 x 10 ⁻²	5 x 10 ⁻²	4.6	7.7	4
Pyr	202.3	6 x 10 ⁻⁴	1 x 10 ⁻²	1 x 10 ⁻¹	5	8.9	0.9
Flt	202.3	1 x 10 ⁻³	8 x 10 ⁻³	3 x 10 ⁻¹	5	8.8	1
Chr	228.3	6 x 10 ⁻⁷	2 x 10 ⁻⁴	2 x 10 ⁻³	5.7	10.3	0.01
BaA	228.3	3 x 10 ⁻⁵	1 x 10 ⁻⁴	1 x 10 ⁻²	5.8	10.3	0.6
Ret	234.3	na	na	na	na	na	na
BbF	252.3	5 x 10 ⁻⁸	2 x 10 ⁻⁴	1.5 x 10 ⁻³	5.9	11.3	na
BkF	252.3	5 x 10 ⁻⁸	1 x 10 ⁻⁵	8 x 10 ⁻⁴	5.9	11.4	0.02
BeP	252.3	7 x 10 ⁻⁷	2 x 10 ⁻⁵	4 x 10 ⁻³	6.4	11.1 ^a	0.02
BaP	252.3	7 x 10 ⁻⁷	4 x 10 ⁻³	4 x 10 ⁻³	6.1	11.5	0.05
DBA	278.4	4 x 10 ⁻¹⁰	3 x 10 ⁻⁵	6 x 10 ⁻⁴	6.8 ^b	11.2 ^b	0.0002
Bpy	276.3	7 x 10 ⁻⁸	8 x 10 ⁻⁶	3 x 10 ⁻⁴	6.6	12.6	0.075
IPy	276.3	1 x 10 ⁻⁸	9 x 10 ⁻⁴		6.6	12.4	na
Cor	300.4	2 x 10 ⁻¹⁰	5 x 10 ⁻⁶	1 x 10 ⁻⁴	6.5 ^b	12.7 ^b	na
OPAH	MW (g mol ⁻¹)	VP (Pa) ^d	P [°] _L (Pa) ^b	S (mg/L) ^d	Log K _{OW} ^d	Log K _{OA}	H (Pa m ³ mol ⁻¹) ^d
9F	180.2	8 x 10 ⁻³	3 x 10 ⁻²	25	3.6	na	7 x 10 ⁻²
AQ	208.2	2 x 10 ⁻⁵	6 x 10 ⁻³	1	3.4	na	2 x 10 ⁻³
MAQ	222.2	10 x 10 ⁻⁵	4 x 10 ⁻³	0.7	3.8	na	3 x 10 ⁻²
BaAQ	258.3	5 x 10 ⁻⁶	2 x 10 ⁻⁴	0.3	4.4	na	3 x 10 ⁻⁵
NPAH	MW (g mol ⁻¹)	VP (Pa) ^e	P [°] _L (Pa) ^b	S (mg/L) ^e	Log K _{OW} ^e	Log K _{OA}	H (Pa m ³ mol ⁻¹) ^e
1NNap	173.2	3 x 10 ⁻²	2 x 10 ⁻⁷	34	3.2	na	6 x 10 ⁻¹
2NNap	173.2	3 x 10 ⁻²	3 x 10 ⁻⁷	26	3.2	na	6 x 10 ⁻¹
2NFlo	211.2	10 x 10 ⁻⁵	3 x 10 ⁻⁸	2	4.1	na	9.5 x 10 ⁻²
9NAnt	223.2	na	1 x 10 ⁻⁹	na	4.2	na	na
1NFlt	247.3	na	5 x 10 ⁻¹¹	na	4.7	na	na
2NFlt	247.3	10 x 10 ⁻⁷	5 x 10 ⁻¹¹	2 x 10 ⁻³	na	na	1 x 10 ⁻²
3NFlt	247.3	na	5 x 10 ⁻¹¹	na	5.2	na	na
4NPyr	247.3	4 x 10 ⁻⁶	5 x 10 ⁻¹¹	2 x 10 ⁻³	na	na	6 x 10 ⁻²
1NPyr	247.3	4 x 10 ⁻⁶	5 x 10 ⁻¹¹	2 x 10 ⁻³	4.7	na	6 x 10 ⁻²
2NPyr	247.3	4 x 10 ⁻⁶	5 x 10 ⁻¹¹	2 x 10 ⁻³	na	na	6 x 10 ⁻²
7NBaA	273.3	na	7 x 10 ⁻¹²	na	5.3	na	na
6NChr	273.3	na	7 x 10 ⁻¹²	na	5.4	na	na

a Finlayson-Pitts and Pitts, 2000 unless stated. ; b Estimated values (EPIWIN; USEPA) ; c Ma et al., 2010; d Walgeave et al., 2010 ;

e WHO, 2000; na= not available

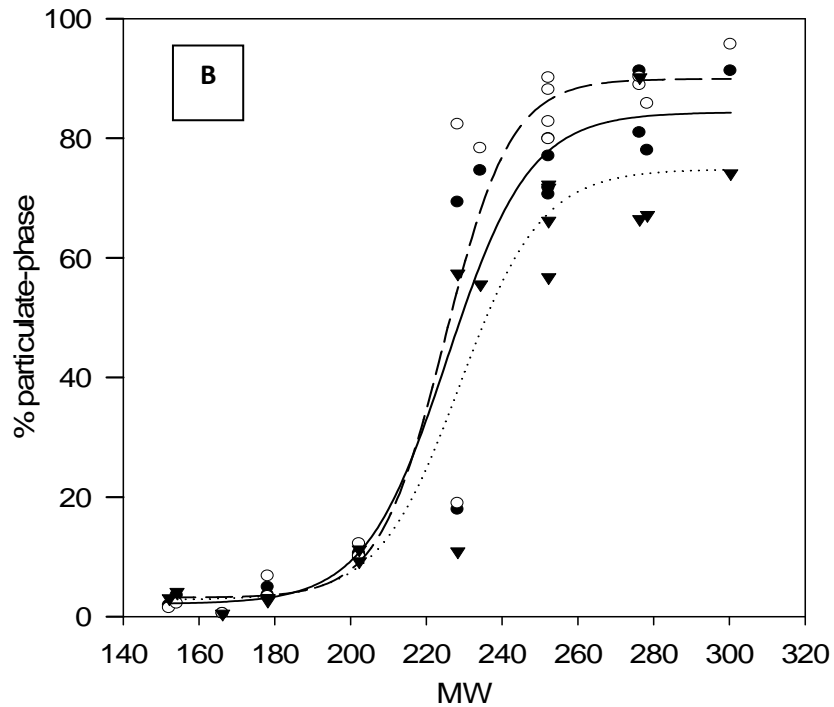
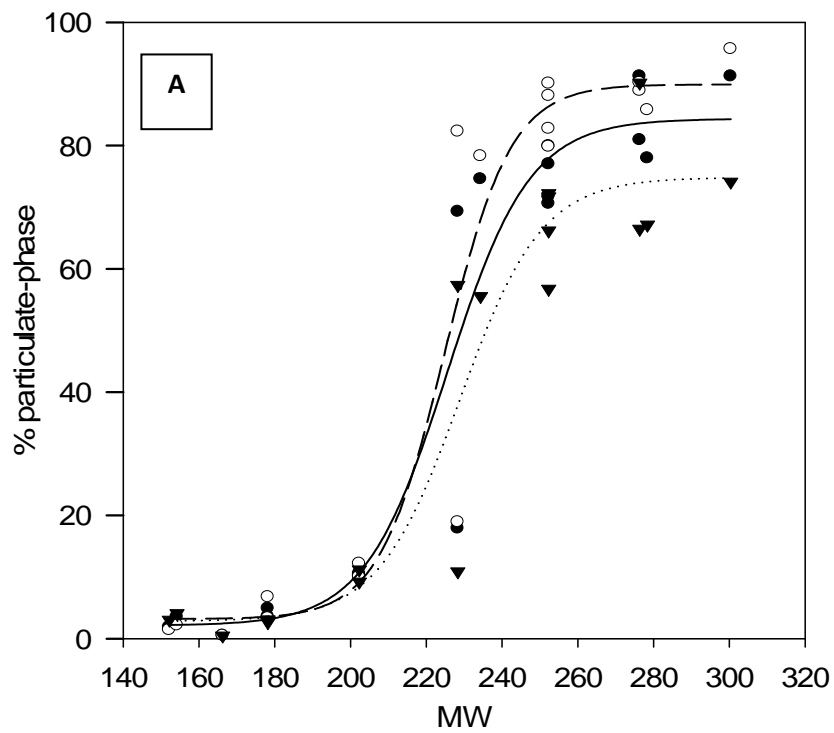


Figure 4.2a. Plots of %P vs MW for PAH at A) BROS and B) EROS for annual mean (black circles, solid black line) ; winter (white circles, dashed line) ; and summer (black triangle, dotted line). Data are fitted with a sigmoidal curve with 4 parameters (see Eq 4.1).

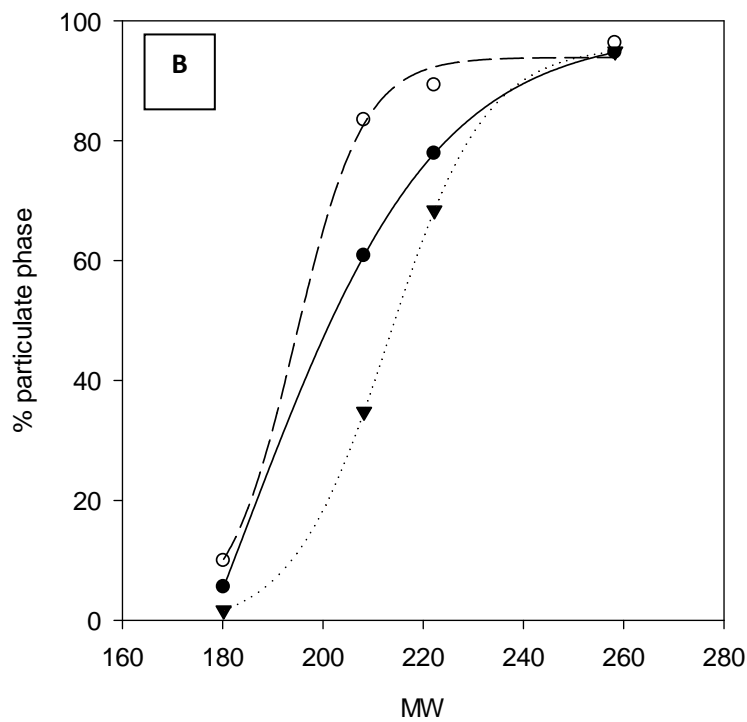
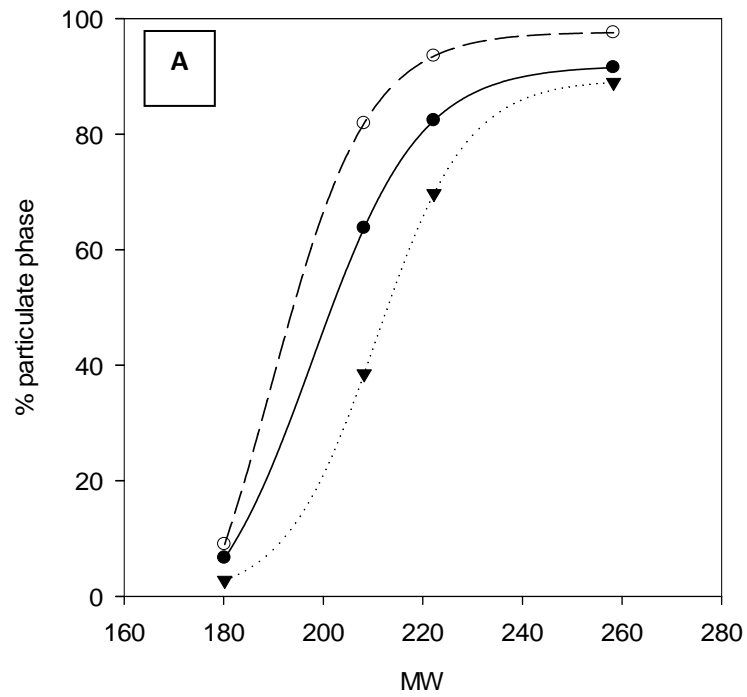


Figure 4.2b. Plots of %P vs MW for OPAH at A) BROS and B) EROS for annual mean (black circles, solid black line) ; winter (white circles, dashed line) ; and summer (black triangle, dotted line). Data are fitted with a sigmoidal curve with 4 parameters (see Eq 4.1).

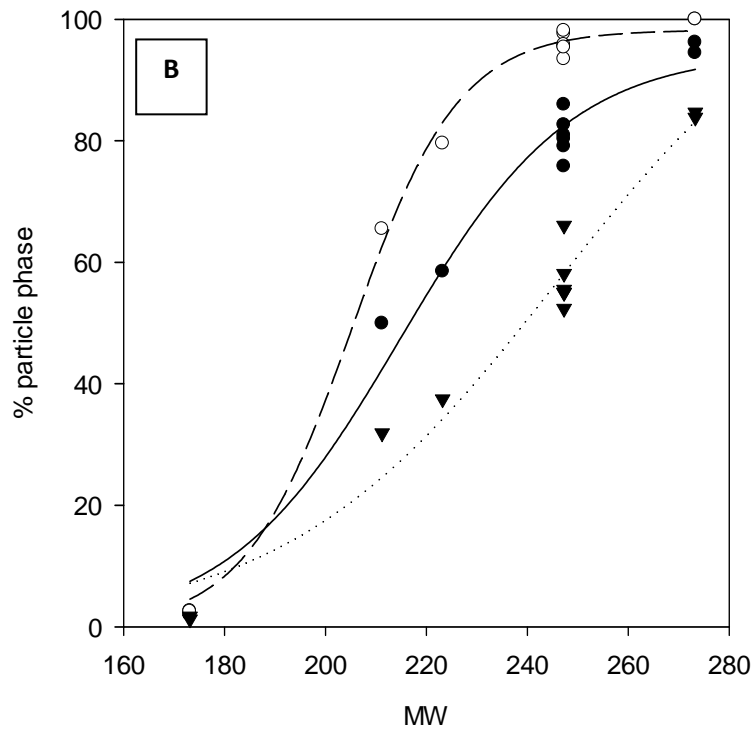
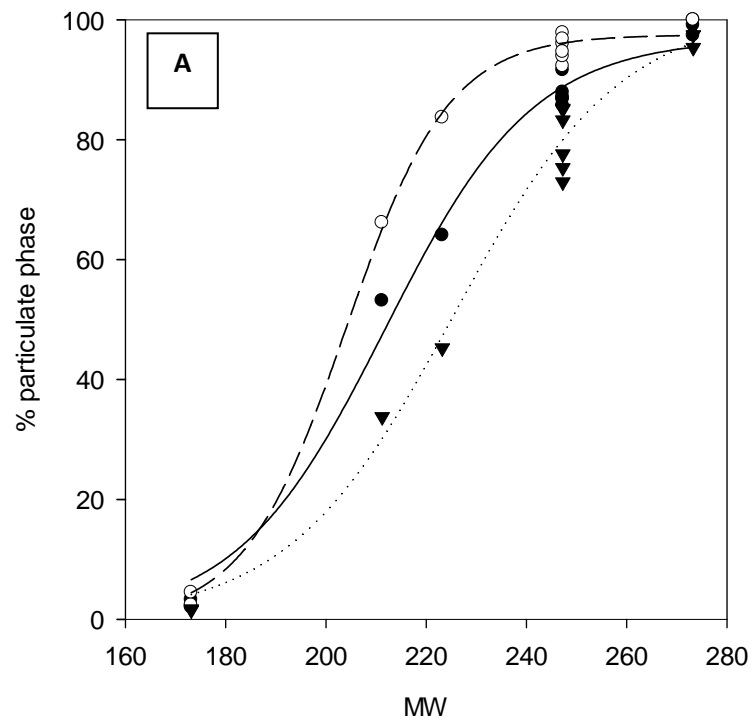


Figure 4.2c. Plots of %P vs MW for NPAH at A) BROS and B) EROS for annual mean (black circles, solid black line) ; winter (white circles, dashed line) ; and summer (black triangle, dotted line). Data are fitted with a sigmoidal curve with 4 parameters (see Eq 4.1).

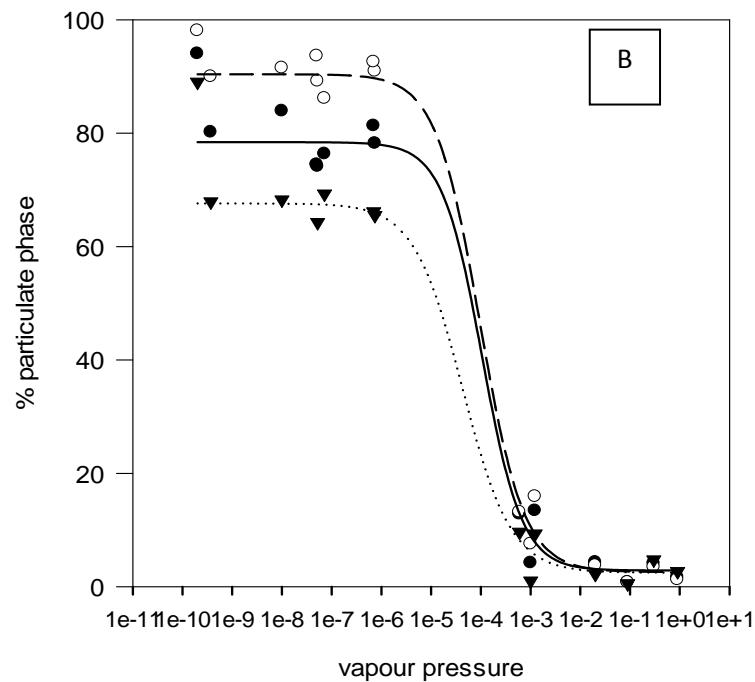
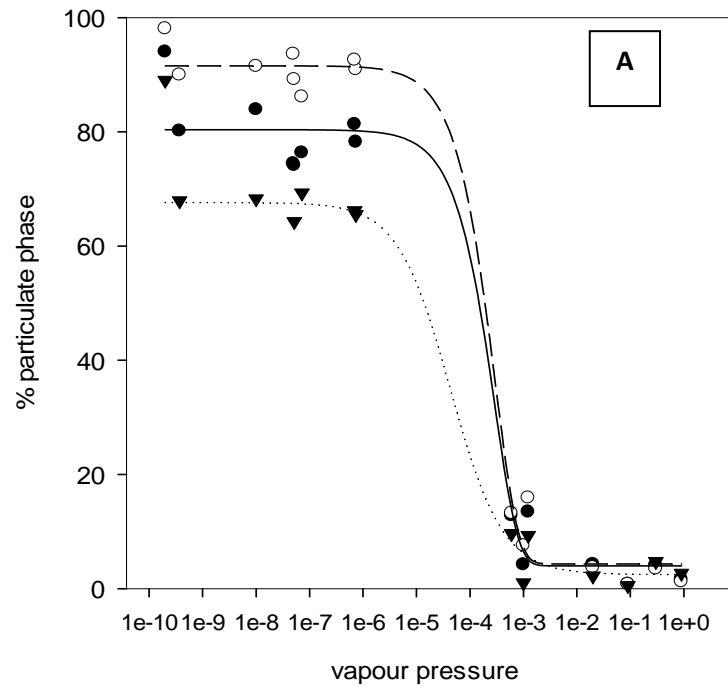


Figure 4.3a. Plots of %P vs VP for PAH at A) BROS and B) EROS for annual mean (black circles, solid black line) ; winter (white circles, dashed line) ; and summer (black triangle, dotted line). Data are fitted with a sigmoidal curve with 4 parameters (see Eq 4.1).

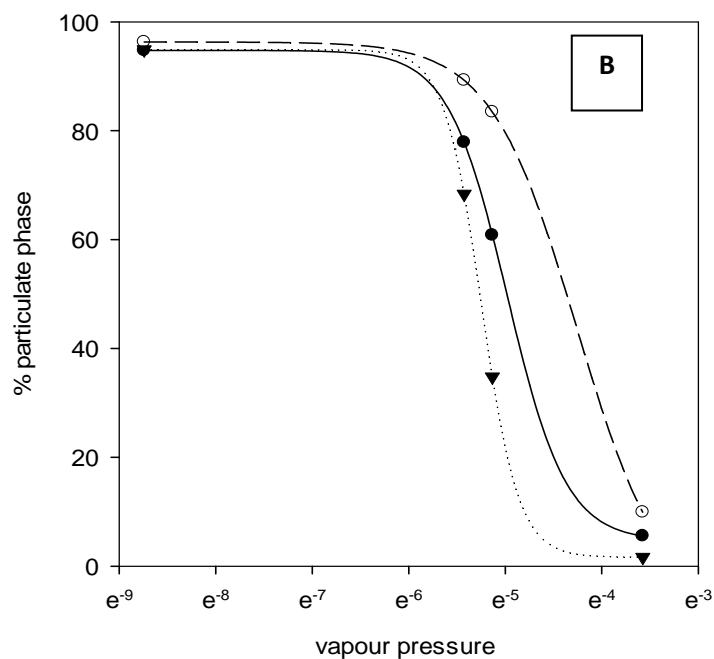
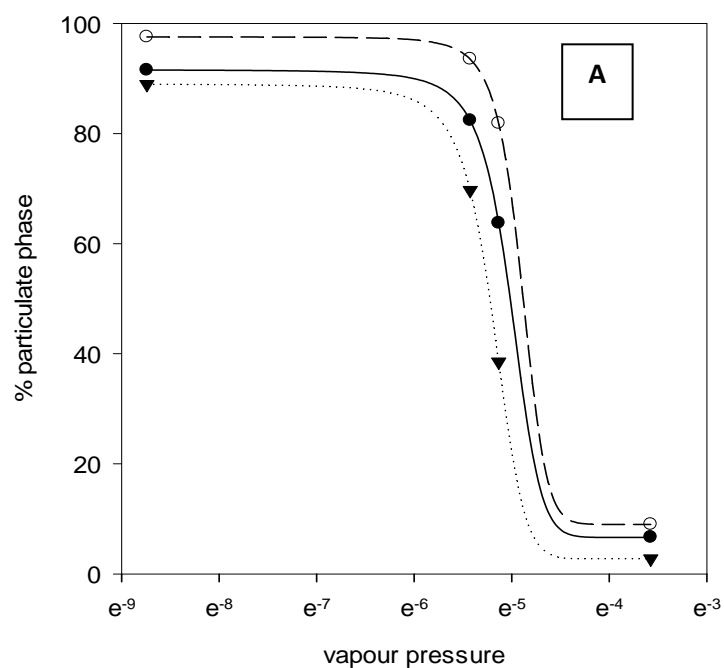


Figure 4.3b. Plots of %P vs VP for OPAH at (A) BROS and (B) EROS for annual mean (black circles, solid black line) ; winter (white circles, dashed line) ; and summer (black triangle, dotted line). Data are fitted with a sigmoidal curve with 4 parameters (see Eq 4.1).

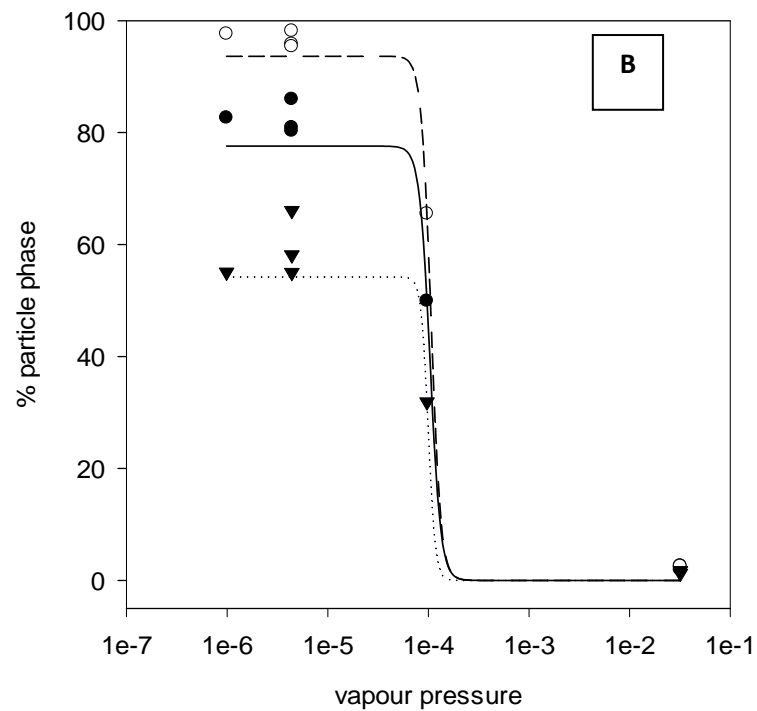
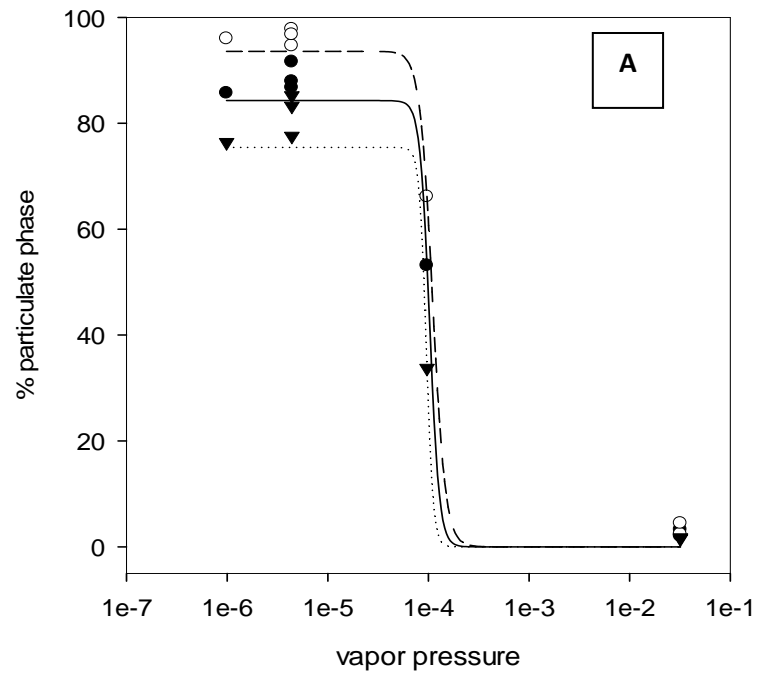


Figure 4.3c. Plots of %P vs VP for NPAH at (A) BROS and (B) EROS for annual mean (black circles, solid black line) ; winter (white circles, dashed line) ; and summer (black triangle, dotted line). Data are fitted with a sigmoidal curve with 4 parameters (see Eq 4.1).

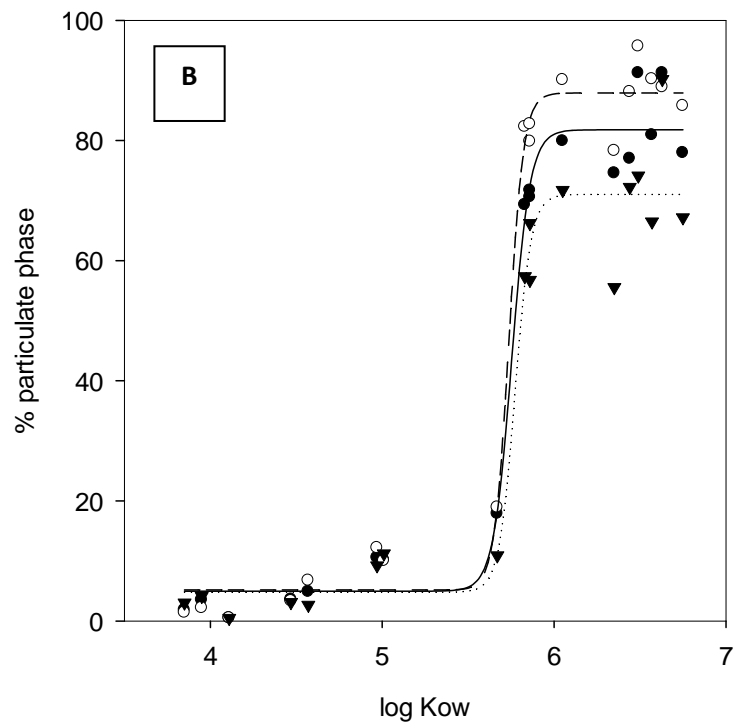
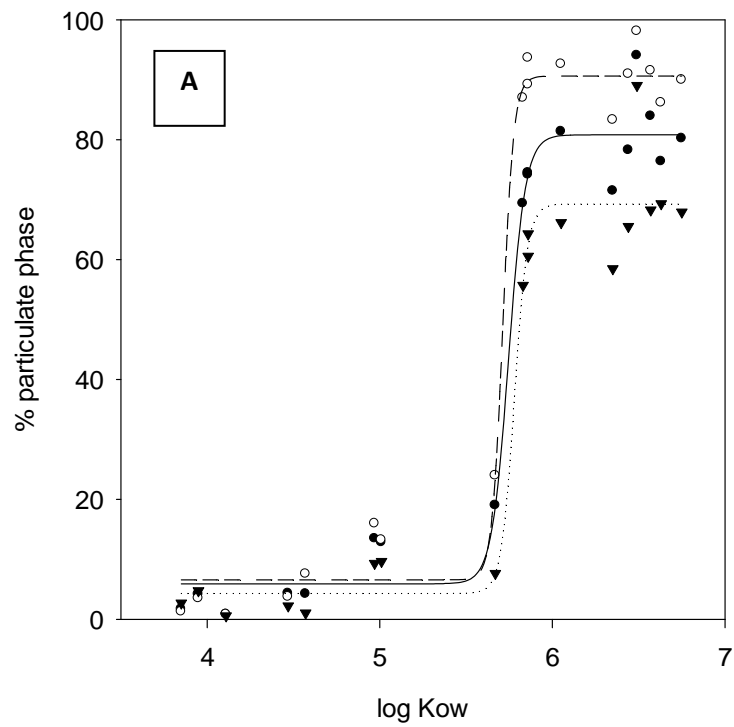


Figure 4.4a. Plots of %P vs log K_{ow} for PAH at (A) BROS and (B) EROS for annual mean (black circles, solid black line) ; winter (white circles, dashed line) ; and summer (black triangle, dotted line). Data are fitted with a sigmoidal curve with 4 parameters (see Eq 4.1).

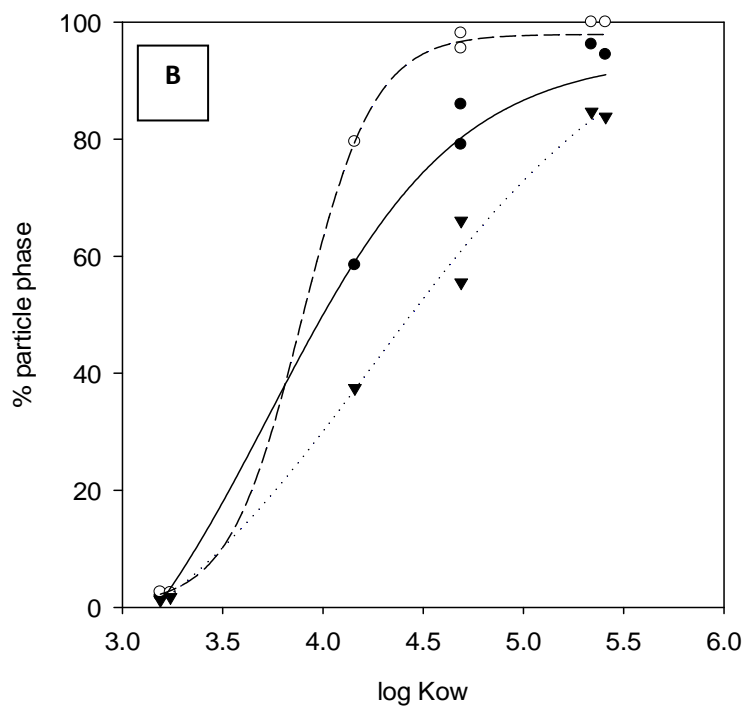
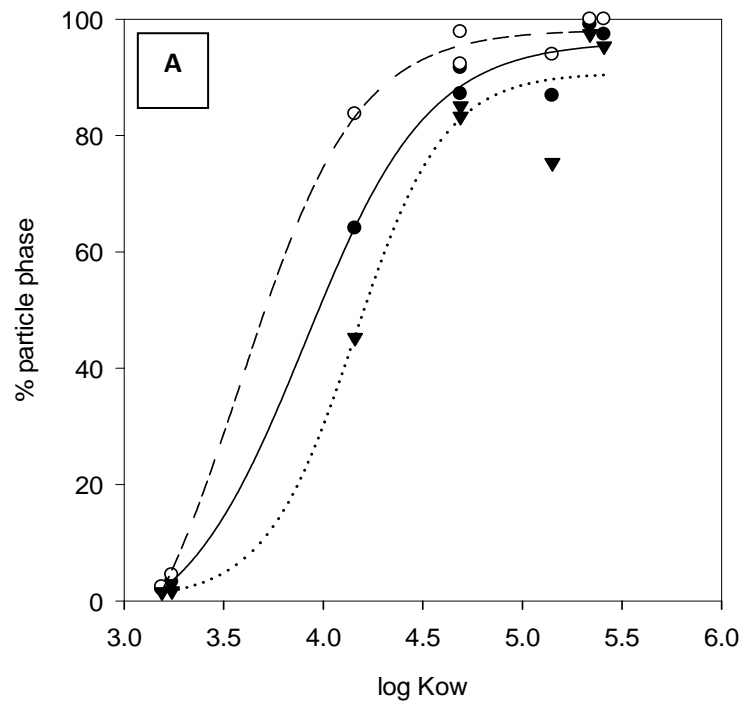


Figure 4.4b. Plots of %P vs $\log K_{ow}$ for PAH at (A) BROS and (B) EROS for annual mean (black circles, solid black line) ; winter (white circles, dashed line) ; and summer (black triangle, dotted line). Data are fitted with a sigmoidal curve with 4 parameters (see Eq 4.1).

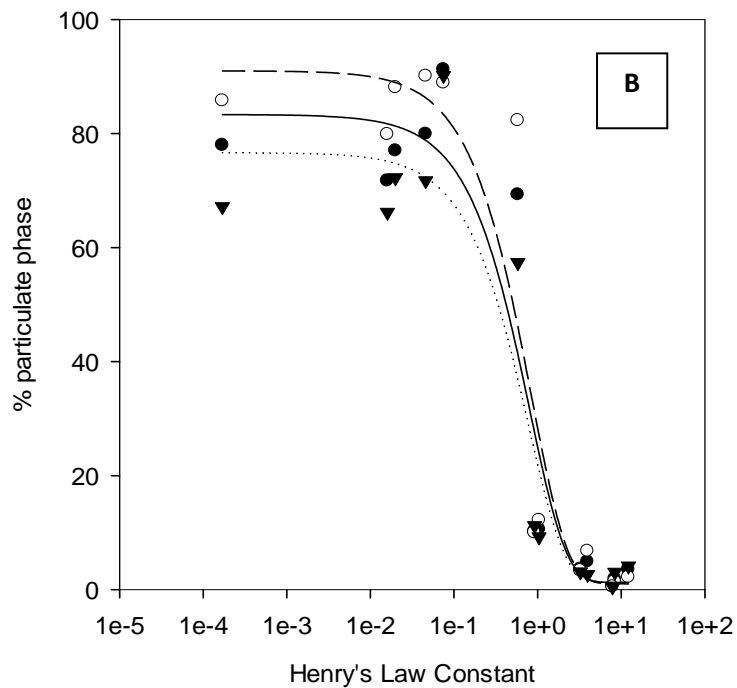
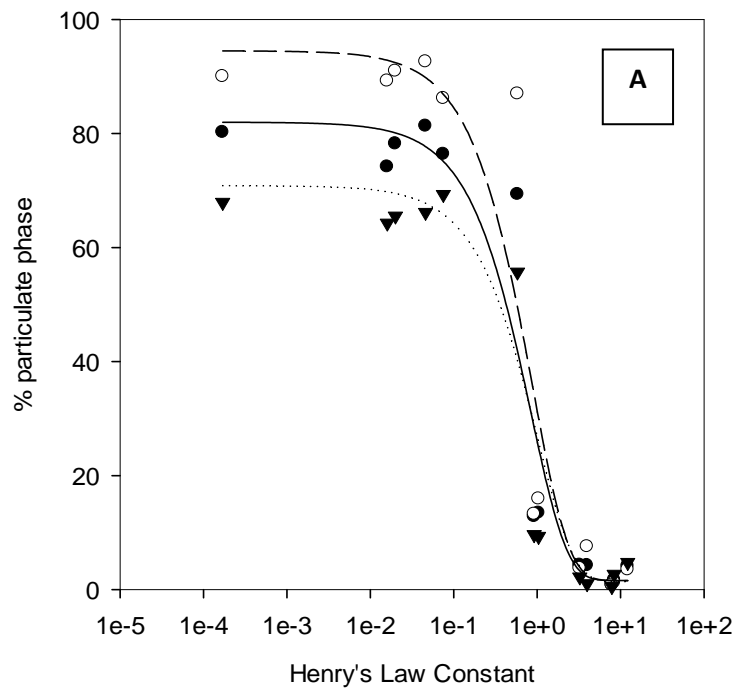


Figure 4.5a. Plots of %P vs H for PAH at A) BROS and B) EROS for annual mean (black circles, solid black line) ; winter (white circles, dashed line) ; and summer (black triangle, dotted line). Data are fitted with a sigmoidal curve with 4 parameters (see Eq 4.1).

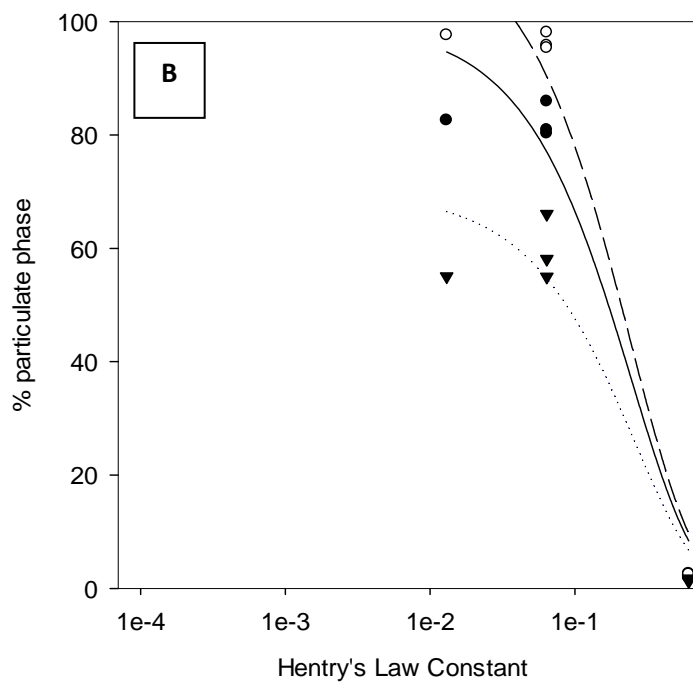
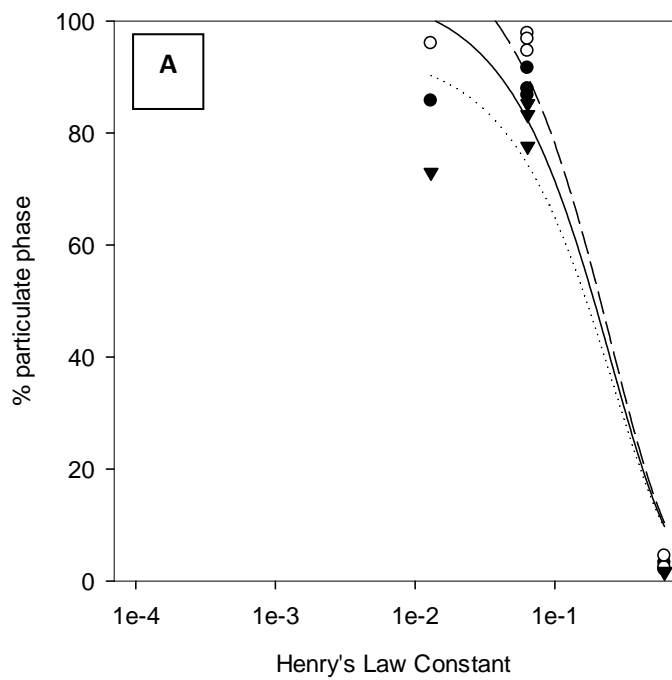


Figure 4.5b. Plots of %P vs H for NPAH at A) BROS and B) EROS for annual mean (black circles, solid black line) ; winter (white circles, dashed line) ; and summer (black triangle, dotted line). Data are fitted with a sigmoidal curve with 4 parameters (see Eq 4.1).

It is shown in Figures 4.2, 4.3, 4.4 and 4.5 that the slopes of these plots are broadly similar between BROS and EROS, suggesting very similar partitioning behaviour for these compound classes at the two sites.

Plots of %P vs MW display similar curves to those observed by Albinet *et al.* (2008a). Interestingly, Delgado-Saborit *et al.* (2013) observed a shallower slope for OPAH compared with PAH, in contrast to the work present here and by Albinet *et al.* (2008a). It should be noted, however that relatively fewer data were used in the plots in the present study compared with the Delgado-Saborit *et al.* (2013) study.

The seasonality of partitioning for semi-volatile ($240 > MW > 200$) compounds is apparent from these plots. As with the plots of %P vs MW produced by Albinet *et al.* (2008a), a notable shift in curve position is observed for PAH, OPAH and NPAH. As reported by Albinet *et al.* (2008) a relatively large seasonal shift in proportion of compounds present in the particulate phase is observed for OPAH and NPAH compared with PAH. However it is noted that HMW PAH compounds display relatively higher seasonal change compared with LMW species.

PAHs, OPAH and NPAHs display broadly similar %P vs VP curves, which is expected due to similar relationships between MW and VP for these compound classes (see Table 3.9). Plots of %P vs Log K_{ow} for PAH are generally in agreement with that reported by Delgado-Saborit *et al.* (2013) with a similar although slightly steeper curve than that observed for the %P vs MW plot. The plot for NPAH compounds displays a similar pattern to this. The plots of %P vs H for PAH are fitted by an exponential curve, in agreement with Delgado-Saborit *et al.* (2013) with NPAH compounds displaying a similar pattern.

It is perhaps surprising that different physiochemical properties display similar curves defining the partitioning behaviour of PAHs, OPAHs and NPAHs. The similar influence of these different physiochemical variables for both PAH and OPAH compounds was observed previously (Delgado-Saborit *et al.*, 2013). It is shown that good correlations exist between these different properties for both PAH and OPAH compounds, which may explain why similar curves are observed between

%P and these different properties Delgado-Saborit *et al.* (2013). Correlations are also noted for the NPAHs included in the present study, however it should be noted that relatively few experimental data are available for NPAH compounds.

OPAH and NPAH display lower log K_{ow} and H values than unsubstituted PAH. This would indicate these compounds will exhibit a higher affinity towards aqueous atmospheric droplets or water on or within atmospheric particles. This is expected due to the higher polarity of these $-NO_2$ or $=O$ containing compounds Delgado-Saborit *et al.* (2013). This behaviour may partly explain the differences in partitioning behaviour for OPAH and NPAH compounds compared with PAHs of similar MW.

More work is clearly required to investigate differences in phase-partitioning of PAHs and their OPAH and NPAH derivatives. A further property that could be investigated as a predictor for partitioning behaviour is the octanol-air partitioning coefficient (K_{oa}) (Harner and Bidleman, 1998; Huang *et al.*, 2014). For example, investigating the partitioning behaviour of PAHs with respect to K_{oa} would allow researchers to assess the importance of absorption into the organic fraction of atmospheric PM on this process. However, limited experimental data are available on K_{oa} values for OPAH and NPAH compounds.

4.1.3. Seasonality in partitioning behaviour

Despite a considerable number of studies measuring both particle- and gas-phases of PAHs and (to a lesser extent) OPAHs and NPAHs, relatively little discussion in the literature exists regarding the seasonal variation in partitioning behaviour of these compounds (Yamaski *et al.*, 1982 ; Baek *et al.*, 1991 ; Smith and Harrison, 1996 ; Albinet *et al.*, 2008a). As demonstrated in Figure 3.10, the PAH, OPAH and NPAH compounds measured in the present study display seasonally-dependent behaviour, likely to be driven by temperature differences between warmer summer and colder winter months .

Clearly, the proportion of compounds present in the particulate phase is reduced in summer relative to winter, in agreement previous sampling studies in urban or trafficked sites for PAHs

(Baek *et al.*, 1991 ; Yamasaki *et al.*, 1982), NPAHs and OPAHs (Bamford and Baker, 2003; Albinet *et al.*, 2008a). However Smith and Harrison (1996) reported a higher proportion of 3-4 ring PAH in the particulate-phase during summer in Birmingham in contrast to the present study. This would suggest a temperature-driven partitioning of species is occurring, with low temperatures in winter facilitating more pronounced association with particulate matter in winter and higher temperatures resulting in more enhanced partitioning to the gas-phase in summer. However, it should be noted that, similar to the observation of Albinet *et al.* (2008a), no correlation was found between the percentage of compound in the particulate phase and ambient temperature in the present study.

The TSP concentration was also shown to be higher in winter samples compared with summer samples in the present study. The mean TSP concentration in only winter and summer samples were $\sim 32 \mu\text{g m}^{-3}$ and $\sim 17 \mu\text{g m}^{-3}$ respectively at BROS and $\sim 24 \mu\text{g m}^{-3}$ and $\sim 13 \mu\text{g m}^{-3}$ respectively at EROS. A higher concentration of TSP in winter relative to summer could therefore be an important driver to higher particle-phase fraction of PAHs and derivatives in these samples.

The observed seasonality of %P for intermediate MW compounds is much less pronounced than has been reported in previous studies. For example, Albinet *et al.* (2008a) reported a much greater winter/summer differential in the partitioning behaviour for intermediate molecular weight NPAH compounds such as 2NFlo and 9Ant and OPAH compounds such as 9F and AQ in a trafficked site in a French Alpine valley. A similar observation was reported by Bamford and Baker (2003) for Flt, Pyr, 2NFlo and 9NAnt in Baltimore, USA.

As mentioned above, the difference in average seasonal temperature could partly explain this discrepancy. For example, the mean ambient temperature measured for the winter and summer samples in the present study were 6°C and 15°C respectively. In the study by Albinet *et al.* (2008) the mean winter and summer temperatures were -3°C and 17°C respectively. The relatively cold winter temperatures in the previous study could facilitate a higher association with the particulate phase.

4.1.4. Phase partitioning equilibrium behaviour

For all compounds measured in each individual sample in Campaign 1, K_p values were calculated according to (Equation 1, Section 1). The values of K_p are shown to be a function of the compound's subcooled liquid vapour pressure (P_L°) (Pankow, 1987; Pankow and Bidleman, 1992), as described by the formula:

$$\log K_p = m \log P_L^\circ + b \quad (4.2)$$

Plots of $\log K_p$ vs $\log P_L^\circ$ were produced, where slope gradient = m and intercept = b . Separate plots were made for the PAH, NPAH and OPAH species in each sample. Summaries of the results of these plots are shown in Table 4.2 and an example plot of these data is shown in Figure 4.6. P_L° values were obtained from (Finlayson-Pitts and Pitts, 2000). Experimental data were only available for PAH compounds. For NPAH and OPAH compounds, experimental values of P_L° values were not available and were derived from estimates using the USEPA EPISUITE MPBPWIN v1.42 model.

When phase-partitioning equilibrium prevails, it is expected that the value of m will approach -1 (Pankow and Bidleman, 1992) assuming a) partitioning behaviour is governed by adsorption processes; b) the difference between the enthalpies of desorption and volatilisation and the number of available adsorption sites remain constant over a compound class; c) activity coefficients remain constant over a compound class (Simick *et al.*, 1998 and references therein).

Table 4.2. Slope (m), intercept (b) and correlation coefficient (R²) values for the log K_p vs log P_L^o plots produced for PAH, OPAH and NPAH sampling data

	PAH						NPAH						OPAH					
	BROS			EROS			BROS			EROS			BROS			EROS		
	R ²	m	b	R ²	m	b	R ²	m	b	R ²	m	b	R ²	m	b	R ²	m	b
A1	0.75	-0.45	-2.79	0.76	-1.59	-4.70	0.61	-0.60	-6.55	0.76	-0.66	-6.78	0.73	-0.62	-2.41	0.94	-1.01	-3.22
A2	0.74	-0.54	-2.90	0.77	-0.56	-2.84	0.81	-0.98	-9.55	0.82	-0.79	-8.07	0.66	-0.78	-3.14	0.79	-0.87	-3.36
A3	0.79	-0.61	-3.10	0.80	-1.36	-4.57	0.85	-0.74	-7.80	0.83	-0.74	-7.59	0.76	-0.89	-3.42	0.76	-1.11	-3.79
A4	0.62	-0.51	-2.94	0.68	-1.12	-4.33	0.85	-0.75	-7.78	0.59	-0.71	-7.27	0.50	-0.78	-3.22	0.71	-1.13	-4.02
W1	0.75	-0.67	-3.48	0.68	-1.01	-4.38	0.80	-0.73	-7.76	0.83	-0.98	-9.69	0.81	-1.09	-3.56	0.97	-1.02	-3.44
W2	0.73	-0.69	-3.64	0.72	-0.98	-4.08	0.71	-1.01	-9.86	0.80	-1.10	-10.3	0.82	-1.11	-3.95	0.56	-0.83	-3.37
W3	0.75	-0.68	-2.99	0.61	-1.01	-3.87	0.79	-0.75	-7.38	0.83	-0.77	-7.36	0.78	-1.11	-3.46	0.81	-0.91	-2.74
W4	0.76	-0.53	-3.13	0.73	-1.29	-4.72	0.84	-0.84	-8.38	0.72	-0.78	-7.77	0.60	-0.98	-3.35	0.75	-0.84	-8.38
W5	0.67	-0.84	-3.30	0.68	-0.75	-3.61	0.86	-0.96	-9.33	0.80	-0.80	-7.87	0.59	-1.09	-3.54	0.75	-1.28	-3.54
W6	0.67	-0.71	-2.97	0.71	-0.94	-3.67	0.83	-0.81	-7.98	0.83	-0.82	-7.64	0.64	-1.16	-3.67	0.96	-2.53	-6.10
W7	0.69	-0.89	-3.14	0.65	-0.98	-3.93	0.83	-0.79	-7.88	0.87	-0.87	-8.26	0.36	-0.67	0.41	0.41	-1.00	-0.40
Sp1	0.81	-0.53	-3.22	0.74	-1.04	-4.32	0.76	-0.66	-7.17	0.42	-0.49	-5.64	0.92	-1.15	-4.23	0.99	-0.85	-3.28
Sp2	0.84	-0.55	-3.41	0.78	-1.13	-4.57	0.78	-0.78	-8.30	0.71	-0.96	-9.74	0.66	-0.95	-3.78	0.73	-1.10	-4.16
Sp3	0.65	-0.48	-3.14	0.75	-1.09	-4.23	0.84	-0.72	-7.74	0.72	-0.73	-7.82	0.30	-0.55	-2.78	0.37	-0.69	-2.94
Sp4	0.72	-0.72	-3.49	0.74	-1.07	-3.77	0.84	-0.76	-8.25	0.82	-0.88	-8.51	0.97	-1.60	-4.63	0.82	-1.20	-3.54
Sp5	0.55	-0.53	-0.30	0.61	-0.99	-3.94	0.74	-0.64	-0.74	0.71	-0.62	-6.66	0.98	-1.21	-3.79	0.98	-1.32	-4.15
Sp6	0.13	-0.31	-1.98	0.62	-1.04	-4.01	0.81	-0.65	-6.75	0.86	-0.74	-7.56	0.83	-1.17	-3.77	0.92	-1.60	-4.56
Sp7	0.48	-0.57	-2.90	0.54	-1.06	-4.31	0.69	-0.66	-7.05	0.68	-0.65	-7.13	0.70	-0.86	-3.16	0.68	-1.12	-3.60
Su1	0.62	-0.62	-3.66	0.73	-1.36	-3.96	0.89	-0.77	-8.31	0.86	-0.66	-8.31	0.84	-1.23	-4.75	0.85	-1.14	-3.77
Su2	0.53	-0.50	-0.31	0.57	-1.53	-5.10	0.76	-0.60	-6.65	0.80	-0.55	-6.39	0.67	-1.02	-3.66	0.73	-1.23	-4.28
Su3	0.70	-0.46	-2.53	0.66	-1.42	-4.87	0.80	-0.80	-8.07	0.27	-0.26	-4.15	0.96	-1.43	-4.12	1.00	-1.99	-5.55
Su4	0.73	-0.48	-3.01	0.79	-1.29	-4.58	0.81	-0.60	-6.58	0.78	-0.52	-6.24	0.71	-0.90	-3.53	0.81	-1.17	-4.28
Su5	0.56	-0.49	-3.19	0.80	-1.13	-4.21	0.87	-0.70	8.10	0.70	-0.68	-7.99	0.75	-1.23	-5.00	0.94	-1.71	-5.81
Su6	0.75	-0.45	-2.79	0.80	-1.13	-4.21	0.74	-0.58	-6.28	0.74	-0.48	-5.58	0.75	-0.84	-3.37	0.73	-1.25	-4.28
Mean	0.67	-0.58	-2.85	0.70	-1.12	-4.20	0.80	-0.75	-6.84	0.74	-0.72	-7.51	0.72	-1.02	-3.49	0.79	-1.20	-4.02

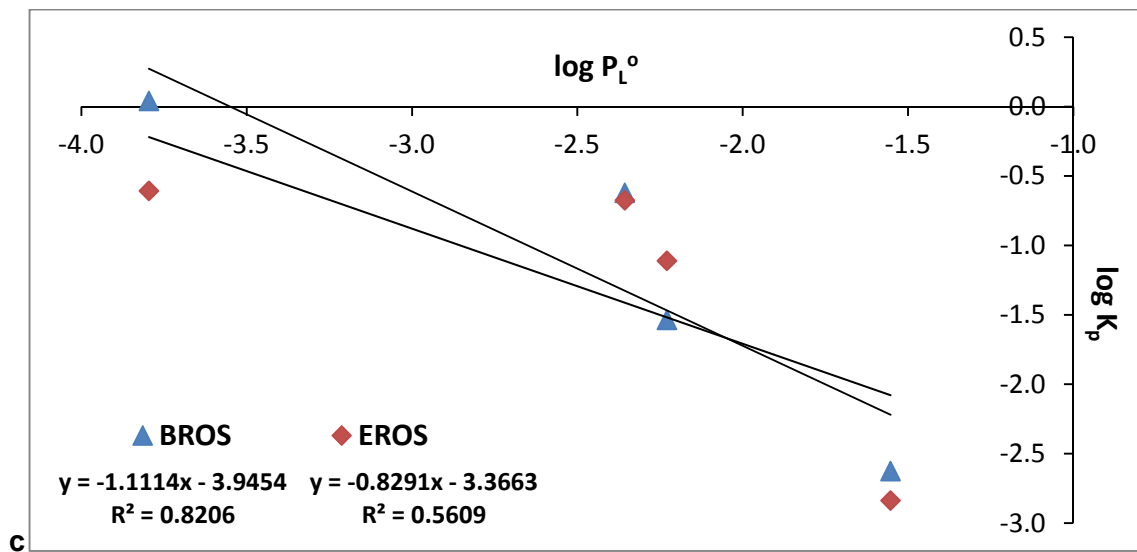
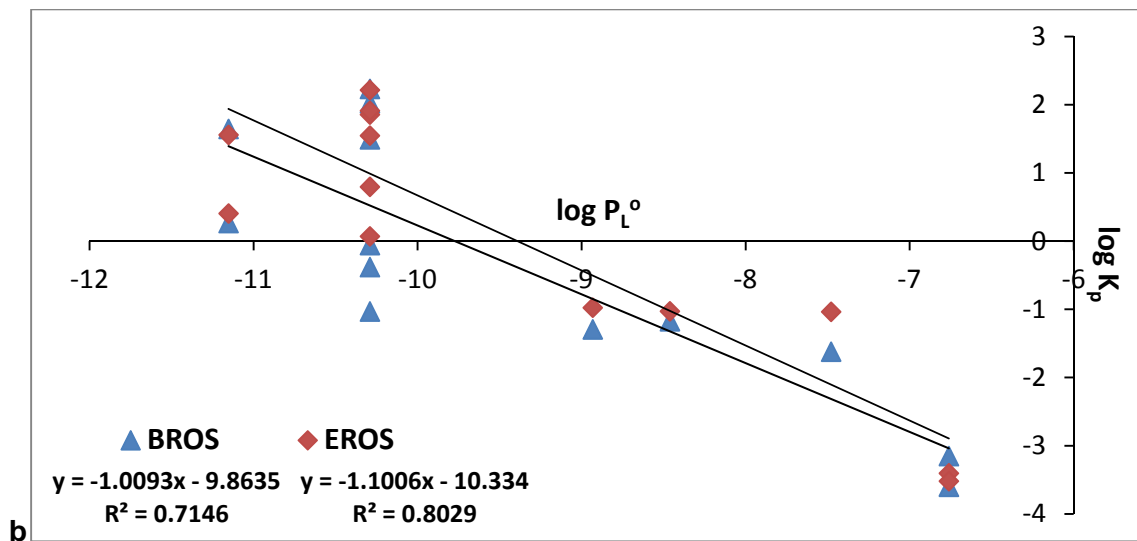
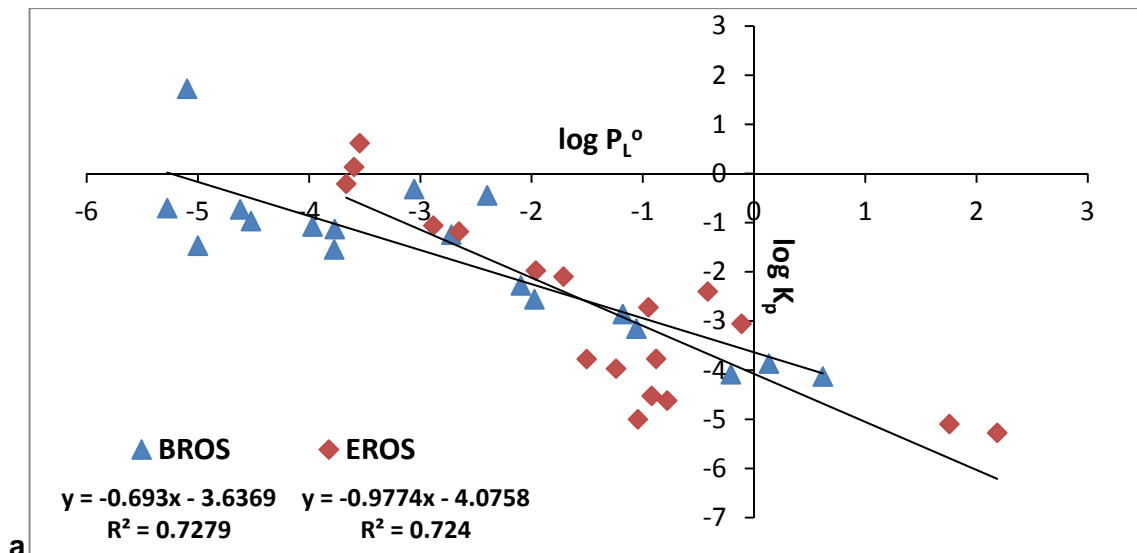


Figure 4.6. Plots of $\log K_p$ ($\text{m}^3 \text{ng}^{-1}$, x axis) vs $\log P_L^0$ (Pa, y axis) for PAHs (a), NPAHs (b) and OPAHs (c) in Campaign 1 sample W2 (10/2/12).

For PAHs, strong correlations are noted for most samples. In all samples the slope of these plots were steeper for EROS samples than the corresponding sample at BROS with m values approaching or exceeding -1, despite the relatively minor overall partitioning pattern observed between the two sites indicated in Figure 4.6.

This can be attributed to the closer proximity of BROS to freshly emitted PAHs from road traffic and suggests the PAHs measured at this site have not reached partitioning equilibrium. Samples at EROS are expected to have had a longer exposure time and display partitioning values that are much closer to equilibrium due to a temperature-driven partitioning from the particle-phase to the gas-phase.

The difference in gradient of these plots is notably higher for summer samples relative to winter samples, which may be due to higher ambient temperature during summer leading to a relatively larger degree of PAH phase partitioning occurring between sites.

A similar observation was made by Cotham and Bidleman (1995) where PAH concentrations were measured at the urban location Chicago and rural location Green Bay, USA. The authors reported relatively shallow $\log K_p$ vs $\log P_L^0$ slopes at the Chicago location with steep slopes, approaching -1, at Green Bay. It was suggested this could be attributed to PAHs moving further towards equilibrium with increasing distance (and hence increasing aerosol ageing) from source region to remote region.

In contrast, Simick *et al.* (1998) did not observe notable changes in slope values for PAHs between the urban Chicago area and the adjacent coastal area. The authors therefore suggested the necessity of the slope approaching a value of -1 to describe equilibrium conditions does not always hold true in all environments.

As noted in Keyte *et al.*, 2013 interpreting variation in m and b values from these plots is complex and can be influenced by myriad factors such as :

- Changes in temperature or compound concentrations during sampling

- Differences and variation in sorption kinetics between gas and solid surfaces, mediated by a number of factors e.g. adsorption to OM, enthalpy of desorption and volatilization
- Kinetic constraints (e.g. introduction of fresh particles) or presence of non-exchangeable compounds on or within the particle matrix.
- The occurrence of sampling artefacts (see Section 4.4).

Therefore results need to be interpreted with caution as many of these factors are extremely difficult to fully characterize or quantify. The concentration of PAH, OPAH and NPAH are shown to vary during the 24hr sampling period due to the diurnal traffic pattern (see Section 4) and temperatures during sampling typically changed by up to 10°C during summer with lower (~4°C) changes observed in winter. However, it is unclear how these factors influence partitioning behaviour.

Slope and intercept values for OPAH and NPAH are shown to be more variable between different samples, with more modest differences observed between the two sampling sites. There are a number of possible explanations for the similar slopes of NPAH and OPAH plots : i) the OPAH and NPAH derivatives are approaching equilibrium relatively rapidly upon emission ; ii) the OPAH and NPAH derivatives are approaching equilibrium relatively slowly upon emission; iii) OPAH and NPAH equilibrium behaviour is not well defined by the slope of the $\log K_p$ vs $\log P_L^\circ$ plot and/or the data is not complete enough to produce appropriate plots; iv) the partitioning of OPAHs and NPAHs is governed by different mechanisms and/or influencing factors (see above) .

This approach has not been applied to OPAH or NPAH compounds previously. Albinet *et al.* (2008a) measured OPAH and NPAH concentrations in the particulate- and gas-phases in trafficked, suburban and rural locations. Using the data reported from this previous study, $\log K_p$ vs $\log P_L^\circ$ plots for NPAH compounds were derived for the traffic, suburban and rural sites. The slopes from all three location types were approximately -1. This suggests the equilibrium conditions for NPAHs are not greatly influenced by proximity to local sources, in agreement with observations in the present study.

However, the relatively small number of OPAH and NPAH compounds used to produce the plots in Figure 4.6 compared with PAHs, as well as the lack of experimentally derived P_L^0 values for these compounds, mean the plots should be viewed with caution and it is not possible to gain definitive insight into the main factors driving the partitioning behaviour of these compounds from this investigation.

4.2. Assessing the importance of PAH reactivity in the urban atmosphere

4.2.1. PAH degradation rates

Atmospheric reactivity, predominantly due to daytime reaction with OH or O₃ can result in atmospheric lifetimes for LWM PAHs of the order of hours (Atkinson and Arey, 1994; 2007; Keyte *et al.*, 2013). Therefore, the effect of reactive losses on the relative PAH concentrations between BROS and EROS may be observed during 24hr sampling. The ratio between observed BROS and EROS concentrations can therefore be interpreted in terms of differences in the relative chemical reactivity of individual PAHs.

Alam *et al.* (2013) previously noted the good agreement between observed BROS/EROS concentration ratios of LWM PAHs and their respective reaction rate coefficient with respect to OH in the gas phase. The relationship between annual mean BROS/EROS ratio (particle- + vapour-phases) and experimentally derived reaction rate coefficient with respect to OH is shown in Figure 4.7. Ace was not included because, as discussed in Section 3.1, this compound did not appear to display the same traffic-related profile at these sites in contrast to the other LWM PAH compounds.

The order of observed BROS/EROS ratios, Acy > Ant > Pyr > Flth > Phe > Flo is broadly reflected in the gas-phase reactivity rates towards OH. This is in agreement with the observations of Alam *et al.* (2013) where samples were only taken during winter months. It is notable that the BROS/EROS ratio for Ant is lower than might be expected based on its relatively high OH reactivity, possibly indicating the presence of an additional source of Ant at EROS.

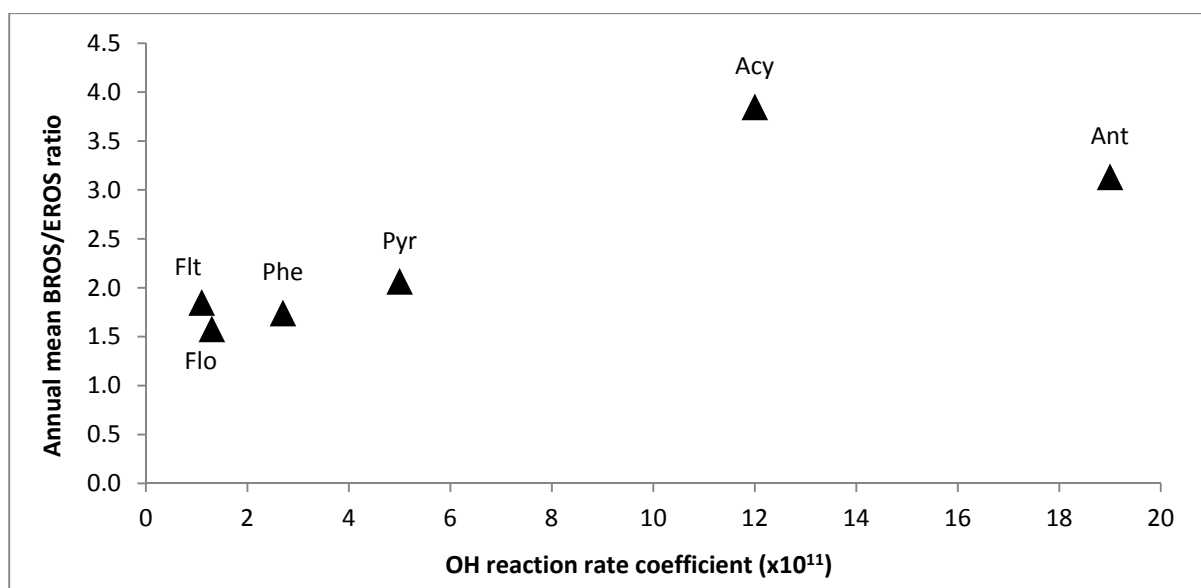


Figure 4.7. Relationship between the observed annual mean BROS/EROS concentration ratio for LMW PAHs and the corresponding OH reaction rate coefficient as derived by Reisen and Arey (2002) ; Brubaker and Hites (1998) ; Atkinson et al. (1990)

In contrast to the relationship with OH reaction rate coefficient, no relationship between BROS/EROS ratio and rate coefficients for gas-phase reaction with NO_3 was observed. This indicates that NO_3 reactivity has a minimal impact on PAH loss and the inter-site variability of LMW PAHs is driven mainly by gas-phase reactions with OH, as previously indicated in urban and traffic locations (Wang *et al.*, 2011 ; Mario *et al.*, 2000 ; Feilberg *et al.*, 2001).

4.2.2. 2NFlt / 1NPyr ratios

As discussed in Section 1.3.3.3, the concentration ratio of 2NFlt to 1NPyr in ambient samples is commonly used to assess the relative importance of primary combustion emissions and secondary input from photochemical (OH and NO_3) reactions, with 1NPyr representing a marker for the former and 2NFlt a marker for the latter (Bamford and Baker, 2003; Ciccioli *et al.*, 1989; 1996; Feilberg *et al.*, 2001; Marino *et al.*, 2000; Wang *et al.*, 2011a).

It is suggested that, assuming comparable emission rates and atmospheric concentrations of Flt and Pyr and comparable dispersion and photolytic loss rates of 2NFlt and 1NPyr, a 2NFlt/1NPyr ratio of >5 indicates the dominance of atmospheric reactions while a ratio of <5 indicates the dominance of direct combustion emissions (Albinet *et al.*, 2008a; Ciccioli *et al.*, 1996).

These ratios were highly variable between sampling days at both the BROS and EROS locations, ranging from 0.7 to ~13 over the full sampling period. The annual mean 2NF/1NP ratio at BROS and EROS measured during Campaign 1 was 2.1 and 4.6 respectively. A comparison between 2NFlt/2NPyr ratios observed in this study and other sampling studies in different locations is provided in Table 4.3.

2NFlt /1NPyr values of >5 is more commonly observed (Bamford and Baker, 2003; Ciccioli *et al.*, 1996; Reisen *et al.*, 2003; Wang *et al.*, 2011a), indicative of atmospheric formation dominating in these environments. Lower (<5) ratios, are commonly observed in heavily trafficked areas (Dimashki *et al.*, 2000; Feilberg *et al.*, 2001; Hien *et al.*, 2007) and large urban centres (Bamford and Baker, 2003; Murahashi and Hayakawa, 1997; Reisen and Arey, 2005).

Observations in the present study are therefore broadly consistent with previous observations in trafficked and urban locations. The relatively low ratios, particularly at BROS are likely to have resulted by virtue of the close proximity to a traffic source, which contributes a fresh source of 1NPyr throughout the year.

2NFlt /1NPyr ratios are generally higher at suburban sites relative to their proximate urban site (Bamford and Baker, 2003; Feilberg *et al.*, 2001; Marino *et al.*, 2000). In this study, ratios are consistently higher at EROS than at BROS. A paired t-test revealed the difference in ratios between the two sites was statistically significant ($p < 0.01$). This could be attributed to a longer exposure time of the air mass to photochemical oxidants (OH and/or NO₃) at EROS relative to BROS (Ciccioli *et al.*, 1996).

Table 4.3. Summary of 2NFlt/1NPyr ratios from ambient measurements (Keyte et al., 2013).

	Details	2NFlt/1NPyr	Reference
Birmingham, UK	Traffic site (BROS)	2.1	This study
Birmingham, UK	Background site (EROS)	4.6	This study
Marseilles area, France	Urban and suburban	<5	Albinet et al.(2007a)
Marseilles area, France	Rural	>10	Albinet et al. (2007a)
Alpine Valley locations, South France	Mean summer value (one location)	>20	Albinet et al.(2008a)
Alpine Valley locations, South France	Mean winter value (all locations)	<10	Albinet et al. (2008a)
Baltimore, USA	Urban, winter	1 – 3	Bamford and Baker (2003)
Baltimore, USA	Urban, summer	6 – 24	Bamford and Baker (2003)
Baltimore, USA	Suburban	1 – 10	Bamford and Baker (2003)
Baltimore, USA	Urban	8 – 30	Bamford and Baker (2003)
Barcelona, Spain	Residential area	4	Bayona et al. (1994)
Milan, Italy	Residential area	6.1	Cecinato et al.(2003)
Rome, Italy	Residential area	1.4	Cecinato et al.(2003)
Columbus, USA	Residential area	2.5	Chuang et al. (2006)
Rome, Italy	Urban	6.7	Ciccioli et al. (1996)
Milan, Italy	Urban	5.2	Ciccioli et al. (1996)
Naples, Italy	Residential area	1	Ciccioli et al. (1996)
Montelibretti, Italy	Suburban	9	Ciccioli et al. (1996)
Madrid, Spain	Suburban	7	Ciccioli et al. (1996)
C.Porziano, Italy	Suburban	12	Ciccioli et al. (1996)
Birmingham, UK	Roadway tunnel	2.5	Dimashki et al.(2000)
Ho Chi Minh City, Vietnam	Urban	21	Hien et al. (2007)
Ho Chi Minh City, Vietnam	Traffic site	2.7	Hien et al. (2007)
Copenhagen, Denmark	Traffic site	0.72	Feilberg et al. (2001)
Tokyo, Japan	Urban (summer)	8.9	Kojima et al. (2010)
Tokyo, Japan	Urban (winter)	5.4	Kojima et al. (2010)
Kanazawa, Japan	Urban	1.8	Murahashi and Hayakawa (1997)
Athens, Greece	Urban	2.1	Marino et al. (2000)
Riverside, USA	Urban background	8.75	Pitts et al. (1985c)
Los Angeles, USA	Urban	3.9	Reisen and Arey (2005)
Claremont, USA	Urban background	7.8	Ramdahl et al. (1986)
St Louis, USA	SRM (1648)	3.5	Ramdahl et al. (1986)
Washington DC, USA	SRM (1649)	3	Ramdahl et al. (1986)
Aurskog, Norway	Rural residential	3.7	Ramdahl et al. (1986)
Beijing, China	2008 Olympic Games	25-46	Wang et al. (2011)
Houston, USA	Suburban	4.2	Wilson et al. (1995)
Claremont, USA	Urban	21	Zielinska et al. (1989)

4.2.3. 2NFlt/2NPyr ratios

Laboratory studies indicate that 2N-Flt are formed via both OH and NO₃ initiated reactions (Arey *et al.*, 1986; Atkinson *et al.*, 1990a), while 2N-Pyr is formed from OH-initiated reactions only (Atkinson *et al.*, 1990a; Zielinska *et al.*, 1986). The ratio between these two isomers can therefore be used as

an indicator for the relative importance of OH (daytime) and NO₃ (night time) reaction pathways (Bamford and Baker, 2003; Feilberg *et al.*, 2001; Tsapakis and Stephanou, 2007). A ratio value of between 5 and 10 indicates the dominance of OH reactions, while a value of above 100 suggests the enhanced importance of NO₃ reactions (Albinet *et al.*, 2008a).

The mean 2NFIt/2NPyr ratio at BROS and EROS measured in samples during Campaign 1 was 2.1 and 3.3 respectively. These ratios were shown to be relatively low (<8) in all samples and display low inter-site and inter-season variability. Higher mean ratio at EROS compared to BROS may indicate the occurrence of NO₃ reactivity between sites. However, a paired sample t-test revealed no significant difference in ratios between sites.

A comparison between the 2NFIt/2NPyr ratios observed in this study and other sampling studies in different locations is provided in Table 4.4. The relatively low (<10) 2NFIt /2NPyr ratios observed in most urban and trafficked locations (Cecinato, 2003; Ciccioli *et al.*, 1996; Marino *et al.*, 2000; Wang *et al.*, 2011a), are in agreement with the ratios observed in the present study, and are indicative of daytime OH-initiated reactions dominating over NO₃-initiated reactions.

It is commonly considered that NO₃ levels (and by extension PAH reactions with NO₃) will be minimal during the day due to the photolytic loss of NO₃ in sunlight (Atkinson *et al.*, 1990a; Graham and Johnston, 1978; Magnotta and Johnston, 1980) :



However, NO₃ can also be removed from the atmosphere by reaction with nitrogen oxide (NO) :



NO is primarily associated with traffic emissions, therefore the close proximity of a traffic source to the sampling locations in this study may lead to relatively low NO₃ concentrations throughout the year. Higher 2NFIt / 2NPyr ratios have been noted in rural areas compared to urban areas (Albinet

et al., 2007a; Albinet *et al.*, 2008a), and suburban areas downwind of polluted urban sites (Reisen and Arey, 2005) suggesting increased importance of NO₃ reactions, which may be attributed to lack of fresh inputs of NO (Albinet *et al.*, 2008a; Bamford and Baker, 2003).

Table 4.4. Summary of 2NFI/2NPyr ratios from ambient measurements (Keyte *et al.*, 2013).

Location	Details	2NFI/2NPyr	Reference
Birmingham, UK	Traffic site (BROS)	2	This study
Birmingham, UK	Background site (EROS)	3.3	This study
Marseilles area, France	Rural	3.7	Albinet <i>et al.</i> (2007a)
Alpine Valley locations, France	Mean summer value (one location)	<60	Albinet <i>et al.</i> (2008a)
Alpine Valley locations, France	Mean winter value (all locations)	<10	Albinet <i>et al.</i> (2008a)
Baltimore, USA	Urban	5 – 57	Bamford and Baker (2003)
Baltimore, USA	Suburban	7 – 60	Bamford and Baker ³⁶⁴
Barcelona, Spain	Residential area	6	Bayona <i>et al.</i> (1994)
Rome, Italy	Residential area	2.2	Cecinato <i>et al.</i> (2003)
Milan, Italy	Residential area	4.6	Cecinato <i>et al.</i> (2003)
Naples, Italy	Residential area	1.7	Ciccioli <i>et al.</i> (1996)
Montelibretti, Italy	Suburban	4.5	Ciccioli <i>et al.</i> (1996)
Madrid, Spain	Suburban	3.5	Ciccioli <i>et al.</i> (1996)
C.Porziano, Italy	Suburban	6	Ciccioli <i>et al.</i> (1996)
Copenhagen, Denmark	Urban and Suburban	< 10	Feilberg <i>et al.</i> (2001)
Copenhagen, Denmark	Urban and Suburban	14.2	Feilberg <i>et al.</i> (2001)
Athens, Greece	Urban	1.9	Marino <i>et al.</i> (2000)
Riverside, USA	Ambient POM	23.3	Pitts <i>et al.</i> (1985c)
Claremont, USA	Urban background	35	Ramdahl <i>et al.</i> (1986)
St Louis, USA	SRM (1648)	9.3	Ramdahl <i>et al.</i> (1986)
Washington DC, USA	SRM (1649)	12	Ramdahl <i>et al.</i> (1986)
Aurskog, Norway	Rural residential	3.3	Ramdahl <i>et al.</i> (1986)
Los Angeles and Riverside, USA	Winter	16±7	Reisen and Arey (2005)
Los Angeles and Riverside, USA	Summer	>35	Reisen and Arey (2005)
Finokalia, Crete	Mean value from a diurnal study, marine background location	3.5	Tsapakis and Stephanou (2007)
Beijing, China	2008 Olympic games	3.4 – 4.8	Wang <i>et al.</i> (2011)

Results of 2NFI/2NPyr analysis from other sampling studies have been subject to conflicting conclusions. While studies (Feilberg *et al.*, 2001 ; Bamford and Baker, 2003) have concluded that the contribution of the OH mechanism is generally dominant (>90%) in relation to NO₃ reactions, it

is suggested the NO₃ mechanism may be important in some circumstances. However, while Feilberg *et al.* (2001) indicate NO₃ reactivity may be more important during wintertime when OH is relatively low, Bamford and Baker (2003) and Reisen and Arey (2005) suggest the NO₃ mechanism can become more significant in summer.

It should be noted that the 2NFlt /1NPyr and 2NFlt /2NPyr ratios reflect simply the relative levels of these isomers in the atmosphere and while they can be used as a reasonable marker for OH and/or NO₃ initiated reactions in the atmosphere, these ratios can be influenced by other factors such as the relative input and removal rates of particulate matter and meteorological factors such as changes in mixing height or intensity of solar irradiation, which can influence the degree of their dispersion and photolytic loss respectively (Keyte *et al.*, 2013). The use of these ratios should therefore be used with caution when assessing the relative importance of OH and/or NO₃-induced PAH reactivity.

4.2.4. Product to reactant ratios

The relative levels of 'product' compounds (i.e. OPAH and NPAH species) to 'reactant' compounds (i.e. parent PAH compounds) observed in ambient samples can be used as an indicator for the extent to which reactivity is influencing the OPAH or NPAH concentrations in ambient samples (Alam *et al.*, 2013; Nassar *et al.*, 2011; Wei *et al.*, 2012).

There are relatively few studies that have used this metric to assess the importance of PAH reactivity on the observed concentrations of OPAH and NPAH. This method assumes that the rate of primary input (i.e. from traffic or other combustion sources), atmospheric behaviour (i.e. phase partitioning) and loss (i.e. reactive, photolytic or deposition) is similar for both parent and product, with secondary input of OPAH or NPAH driving the variability in observed ratios. However, it should be noted that results from the present investigation e.g. tunnel/ambient ratios (Section 6.3) ;

phase partitioning (Section 4.1) and source apportionment (Section 4.4) may suggest this assumption may not hold for these product/parent ratios.

However it must be considered that the rate of primary input from traffic may be different and more variable for parent and product, the rate of phase partitioning and loss may not be the same for these compounds, and the ratios may be influenced by input of both parent and product from additional sources. Therefore, while product/parent ratios can be used as a tentative assessment of PAH reactivity in ambient samples, these values must be viewed with caution.

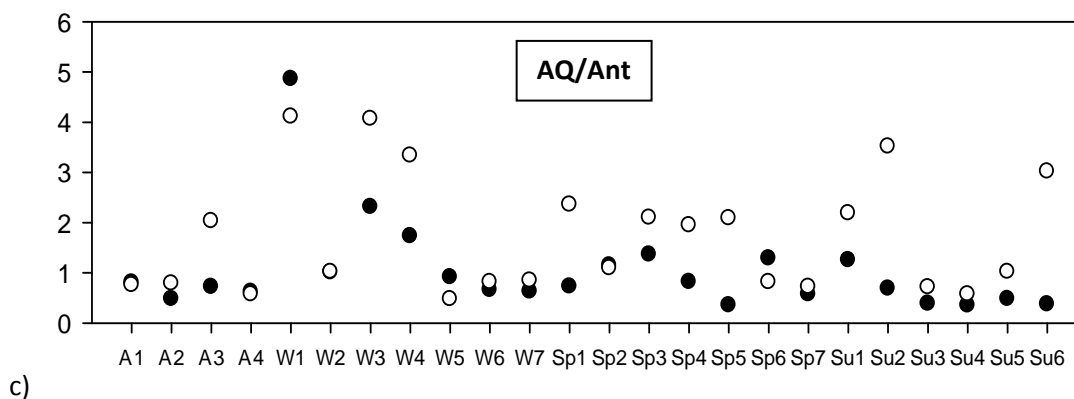
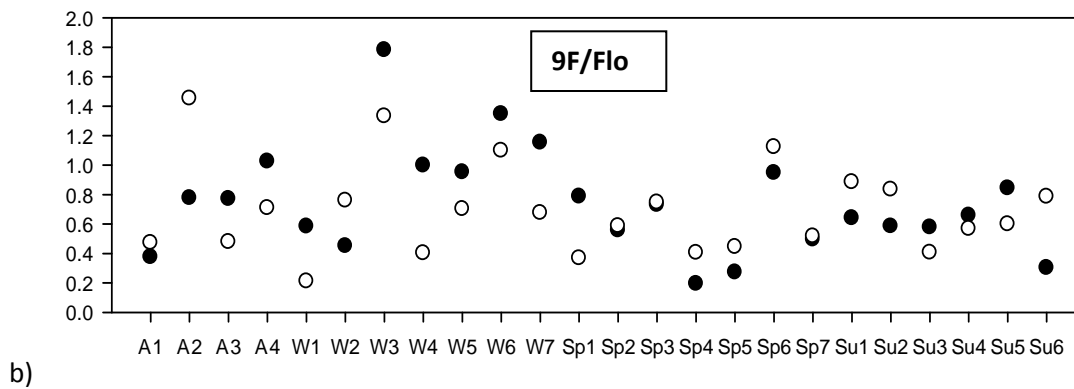
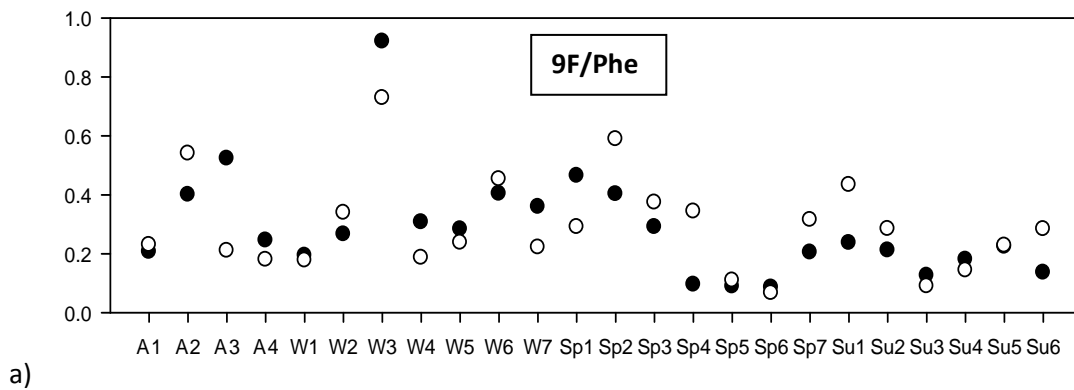
The ratios chosen for assessment in this study are 9F/Flo, AQ/Ant, BaAQ/BaA, 9NAnt/Ant, 2NFIt/FIt and 2NPyr/Pyr. 9F has been identified as gas-phase reaction products of both Flo (Helmig *et al.*, 1992a; Kwok *et al.*, 1997) and Phe (Lee and Lane, 2010; L Wang *et al.*, 2007b). The formation yield of 9F from OH reactions is shown to be higher from Flo (~9% ; Helmig *et al.*, 1992) compared with Phe (~0.3% ; Wang *et al.*, 2007).

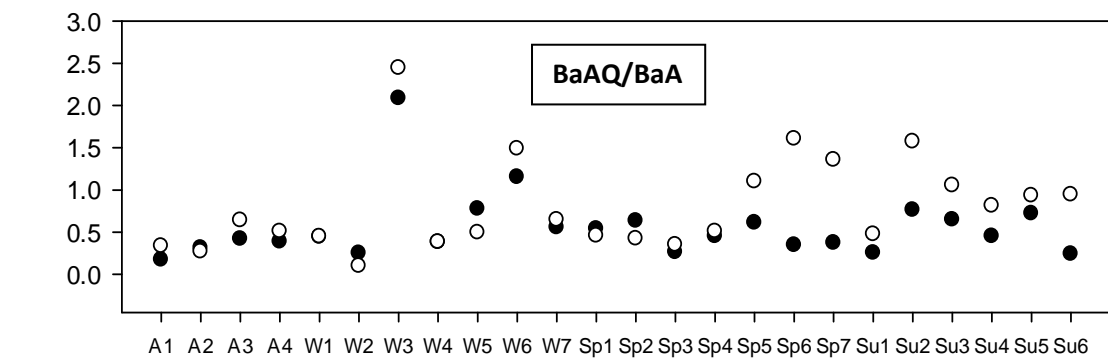
AQ has been identified as a reaction product of Ant in heterogeneous reactions with O₃ (Kwamena *et al.*, 2006; Mmereki *et al.*, 2004; Perraudin *et al.*, 2007), NO₂ (Ma *et al.*, 2011) and NO₃ (Zhang *et al.*, 2011). BaAQ has been identified as a product if the heterogeneous reaction of BaA with NO₃ (Liu *et al.*, 2012; Zhang *et al.*, 2011).

2NFIt and 2NPyr have been identified from both gas-phase (Atkinson and Arey, 1994) and heterogeneous (Inazu *et al.*, 1997; Ringuet *et al.*, 2012b) reactions of FIt and Pyr respectively. There is not expected to be a primary input of these compounds so these ratios are rather simpler to interpret.

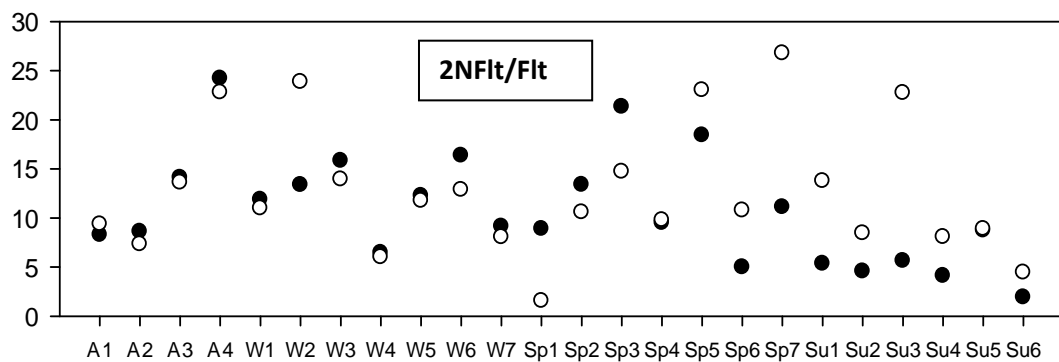
The ratios of OPAH/PAH and NPAH/PAH for individual samples throughout Campaign 1 are shown in Figure 4.8. It can be seen in these plots, that there is considerable variability in ratios between individual samples and it is not possible to draw definitive conclusions regarding trends in, and contribution of chemical reactivity to the levels of OPAH or NPAH in the collected samples based on these ratios.

It is interesting to note, however, that OPAH/PAH and NPAH/PAH ratios are generally higher at EROS than at BROS, as noted by Alam *et al.* (2013), and this was particularly distinct in the spring and summer samples. While these ratios may suggest that atmospheric reactivity may not dominate the overall input of OPAH and NPAH compounds relative to direct emissions, they do suggest the influence of reactivity occurring between sampling sites.

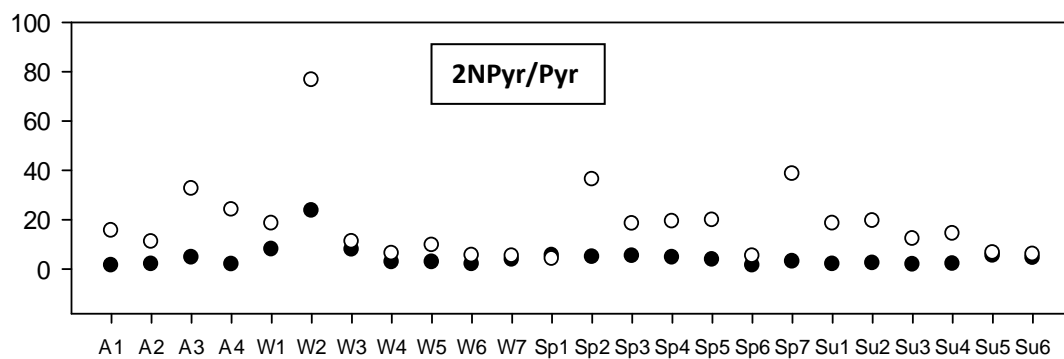




d)



e)



f)

Figure 4.8. Ratios of measured OPAH or NPAH compounds to the parent PAH at BROS (black dot) and EROS (white dot) in each individual sample in Campaign 1. a) 9F/Phe ; b) 9F/Flo ; c) AQ/Ant ; d)BaAQ/BaA; e) 2NFlt/Flt (x1000); f) 2NPyr/Pyr (x 1000) .

Ratios of OPAH/PAH compounds have been measured by Alam *et al.* (2013) at the BROS and EROS samples during the winter months. The authors noted higher ratios at EROS compared to BROS. The results of this study are broadly in agreement with this observation, with a more pronounced difference in ratios noted for spring and summer samples. This may indicate the possible influence of inter-site chemical reactivity influencing the concentrations of OPAH and NPAH, particularly during the warmer summer months

Alam *et al.* (2013) reported BaAQ/BaA ratios ranging from <0.05 to ~0.5 in a winter sampling campaign. Most of the winter samples in the present study displayed similar ratios to the previous study, with higher values (up to a factor 3) observed in spring and summer, particularly at EROS.

AQ/Ant ratio values are shown to be much higher (up to >10 times) and more variable in this study than previously measured by Alam *et al.* (2013). This could indicate a greater role of reactive input is influencing the samples in the present study, However, it should also be noted that the fraction of AQ in the particulate phase in the previous study was ~50%, which is lower than the fraction notes in the present study during autumn (65%), winter (82%) and spring (67%). This could indicate that AQ in the present study was more protected towards reactive and/or photolytic losses than in the previous study, which could also contribute towards higher observed ratios.

4.3. Source apportionment of PAH, OPAH, NPAH compounds using Positive Matrix Factorization (PMF)

4.3.1 Introduction

Positive Matrix Factorization (PMF) is a multivariate factor analysis tool that can resolve the identities and contributions of the components in a mixture of unknown composition (Reff *et al.*, 2007). The model assumes p source types (factors) contribute linearly to the observed concentrations of defined species at a specific receptor site.

This method treats factor analysis as a true least squares problem i.e. a data set denoted by a matrix, X where:

$$X = G F + E \quad (4.4)$$

Where : G = factor contribution matrix

 F = factor profile matrix

 E = residual matrix

This equation can be written in an index notation (Reff *et al.*, 2007) :

$$x_{ij} = \sum_{k=1}^p g_{ik} f_{kj} + e_{ij}$$

(4.5)

Where x_{ij} = concentration of species j in sample i

p = number of factors contributing to the samples

f_{kj} = concentration of species j in factor profile k

g_{ik} = relative contribution of source k to sample i

e_{ij} = the error of the model for species j measured in sample i

The objective of the PMF model is to derive suitable values for f_{kj} , g_{ik} and p that can best reproduce x_{ij} . To do this the model produces a value of Q, an object function of the residual matrix :

$$Q = \sum_{i=1}^n \sum_{j=1}^m (e_{ij}/u_{ij})^2$$

(4.6)

e_{ij} = error of the PMF model (residuals) for species j measured in sample i

u_{ij} = uncertainty of the j^{th} species concentration in sample i

n = number of samples

m = number of species

The Q value must be minimised to derive the most appropriate factor contributions and profiles.

The values of f_{kj} and g_{ik} are adjusted until a minimum Q value for a defined p value is obtained.

PMF is considered to be a suitable method for modelling environmental data because it : a) incorporates variable uncertainties commonly found in environmental samples; and b) constrains the solution profiles (F) and concentrations (G) to be non-negative (Reff *et al.*, 2007). This method has been applied previously to source apportionment of atmospheric PAHs (Hanedar *et al.*, 2014; Jang *et al.*, 2013; Okuda *et al.*, 2010; Prevedouros *et al.*, 2004a; Sofowote *et al.*, 2011). Previously, principal component analysis (PCA) has been a popular technique for carrying out source apportionment for PAH (Harrison *et al.*, 1996; Harrison *et al.*, 2003; Mari *et al.*, 2010; Ravindra *et al.*, 2008) and NPAH (Bamford and Baker, 2003).

However, PMF is preferable over PCA because it allows each sample and variable to be weighted individually, unlike PCA where all are equally weighted (Park *et al.*, 2012). Furthermore, PMF can identify factor contributions directly without requiring further multiple regression analysis (Jang *et al.*, 2013). While PMF has been applied to PAHs, it has yet to be used for NPAH and OPAHs for atmospheric source apportionment.

The initial data analysis of samples collected from the Queensway Road Tunnel and ambient sites BROS and EROS suggest traffic is the dominant source to the Birmingham University sites but

other potential sources may also influence the observed concentrations (e.g. non-traffic combustion sources, volatilisation or chemical reactivity). In the present study, PMF was applied for source apportionment of selected PAH, OPAH and NPAH compounds to assess potential source profiles.

4.3.2. Method

The model was run using EPA PMF 5.0. Model input data files were produced using 'receptor' concentration (C) and uncertainty (U) matrices, as previously described by Jang *et al.* (2013).

For measured concentration above the MDL, the input values c and u were calculated as follows :

$$C_i = C_m \quad (4.7a)$$

$$U_i = 0.1C_m + MDL/3 \quad (4.7b)$$

For measured concentrations below the MDL, the input values C and U were calculated :

$$C_i = MDL/2 \quad (4.8a)$$

$$U_i = 0.2 C_i + MDL/3 \quad (4.8b)$$

where :

C_i = input concentration

C_m = measured concentration

U_i = input uncertainty

MDL = method detection limit (calculated separately for filter and PUF components)

Total concentration (particulate + vapour) values from BROS, EROS and the Queensway Road Tunnel samples obtained in campaigns 1, 2 and 3 were combined in the model input to ensure there was sufficient number of samples to obtain adequate model performance. The total number of 60 samples was included.

Due to the relatively low number of samples collected in this study, not all target compounds measured in this investigation could be considered in the model. Base model data was assessed prior to running the model to select the most appropriate compounds to include. Significant correlations between compounds at each sampling site (see Section 3.2) allowed certain compounds to be excluded from the model and assumed to display similar prevailing sources and atmospheric behaviour patterns.

For example species IPy, BPy and Cor were shown to correlate strongly at both sites and are all assumed to result predominantly from gasoline fuel combustion (Marr *et al.*, 1999; Ravindra *et al.*, 2008; Staehelin *et al.*, 1998). Similarly, 1NNap and 2NNap are assumed to display similar sources and atmospheric behaviour.

Since both BROS and EROS samples were used in this analysis, both Acy and Ace were not included as these have been shown to be the most reactive PAHs (Atkinson and Arey, 1994; Brubaker and Hites, 1998; Reisen and Arey, 2002). Similarly, 2NFlt and 2NPyr were not included in the analysis as the presence of these compounds is known to result entirely from atmospheric reactions.

Some compounds and a small number of individual samples, where modelled data points were shown to deviate significantly from observed data, were excluded from the analysis in order to achieve optimal model performance. All included species displayed a correlation coefficient of >0.7 for the plot of observed vs. modelled concentrations. The final model runs included 9 PAHs, 1 OPAH and 3 NPAHs : Ace, Phe, Flt, Pyr, Ret, Chy, BbF, BaP, IPy, AQ, 1NNap, 9NAnt and 1NPyr.

The PMF model was run in 'robust mode', where model outliers are not allowed to overly influence the fitting of the contributions and profiles. To achieve this, uncertainties for species or samples

with uncertainty-scaled residual values greater than an outlier distance of four, $(e_{ij} / u_{ij})^2 > 4$, are increased to downweight their influence on the PMF solution.

The distribution of intra-run residuals was analysed for each species, with all included species displaying normally distributed residuals between values of -3 and +3, considered to be an adequate range to provide reliable model results. The optimal number of factors required to obtain an adequate model fit was investigated with a 4 factor found to be the best fit for modelled data. The model also allows an additional percentage of uncertainty to be added. A varying degree of additional uncertainty was tested, with a value of 3% found to result in optimal model performance.

4.3.3. Results

4.3.3.1. Overview

The distribution of species concentration between the 4 model factors and the percentage contribution of each factor to the modelled PAH, OPAH and NPAH concentrations is shown in Figure 4.9. This section discusses the model performance/uncertainty and the possible sources attributed to each factor.

4.3.3.2. Model uncertainty and rotational freedom

Uncertainty in the PMF model was estimated using a bootstrap technique. This involved performing 250 bootstrap model runs with a correlation set at 0.75. The estimated uncertainty, in terms of the percentage contribution of each factor for the modelled species', derived in this study is shown in Figure 4.10. The bootstrapping output estimated the percentage of 'factor swaps' in this study was <20% for all factors. The results of the PMF model can therefore be considered sufficiently robust for source interpretation.

PMF analysis is complicated by the fact that there can theoretically exist multiple F and G values that can produce the same minimum Q value (Reff *et al.*, 2007). This is known as rotational freedom. This phenomenon can be assessed and reduced by the parameter F_{peak}, where new

matrices are produced by forcing rows and columns of F and G matrices to be added or subtracted to or from each other (depending on the positive or negative F_{peak} value).

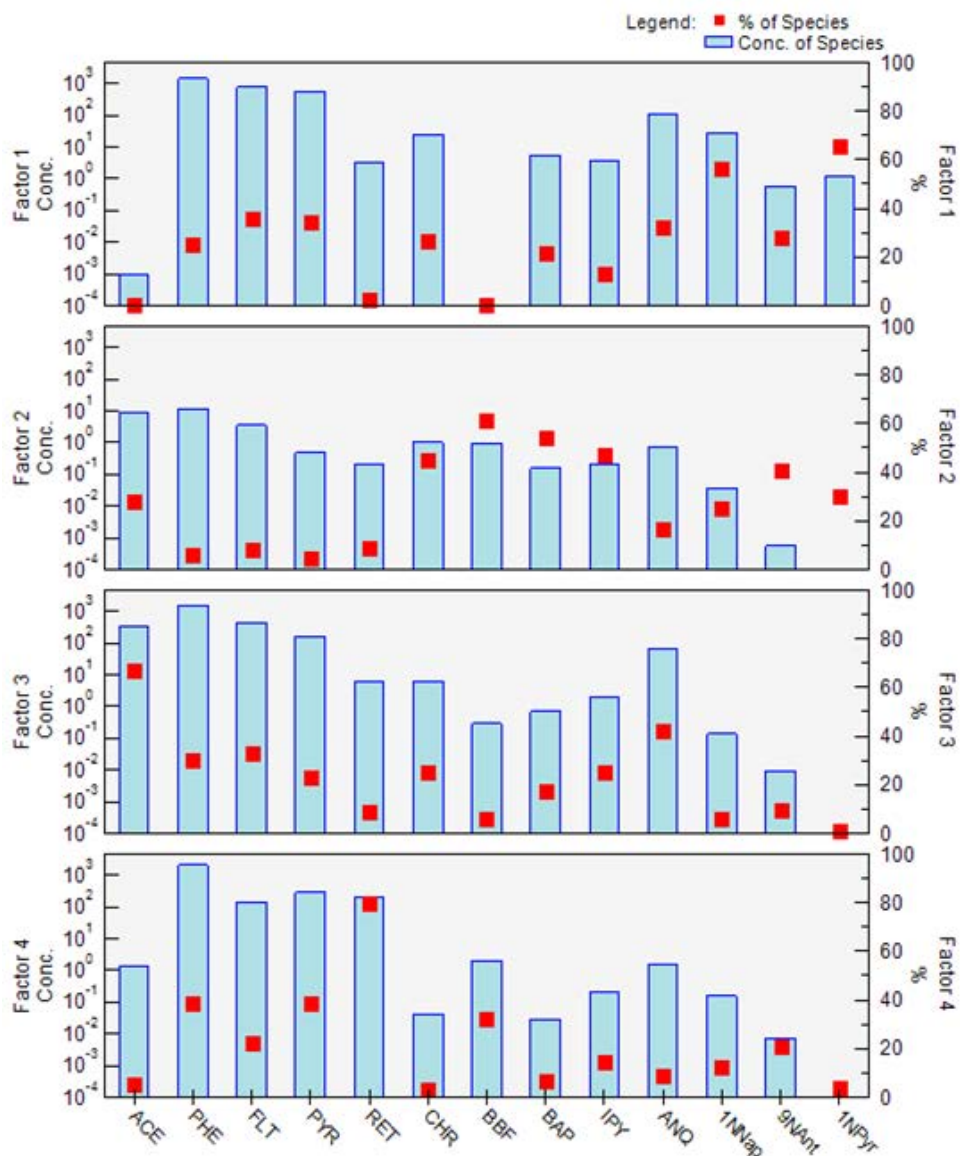


Figure 4.9. Results of the 4 factor PMF model displaying the concentration of each species attributed to each factor (blue bar) and the percentage contribution of each factor to the total modelled concentration of each species (red marker).

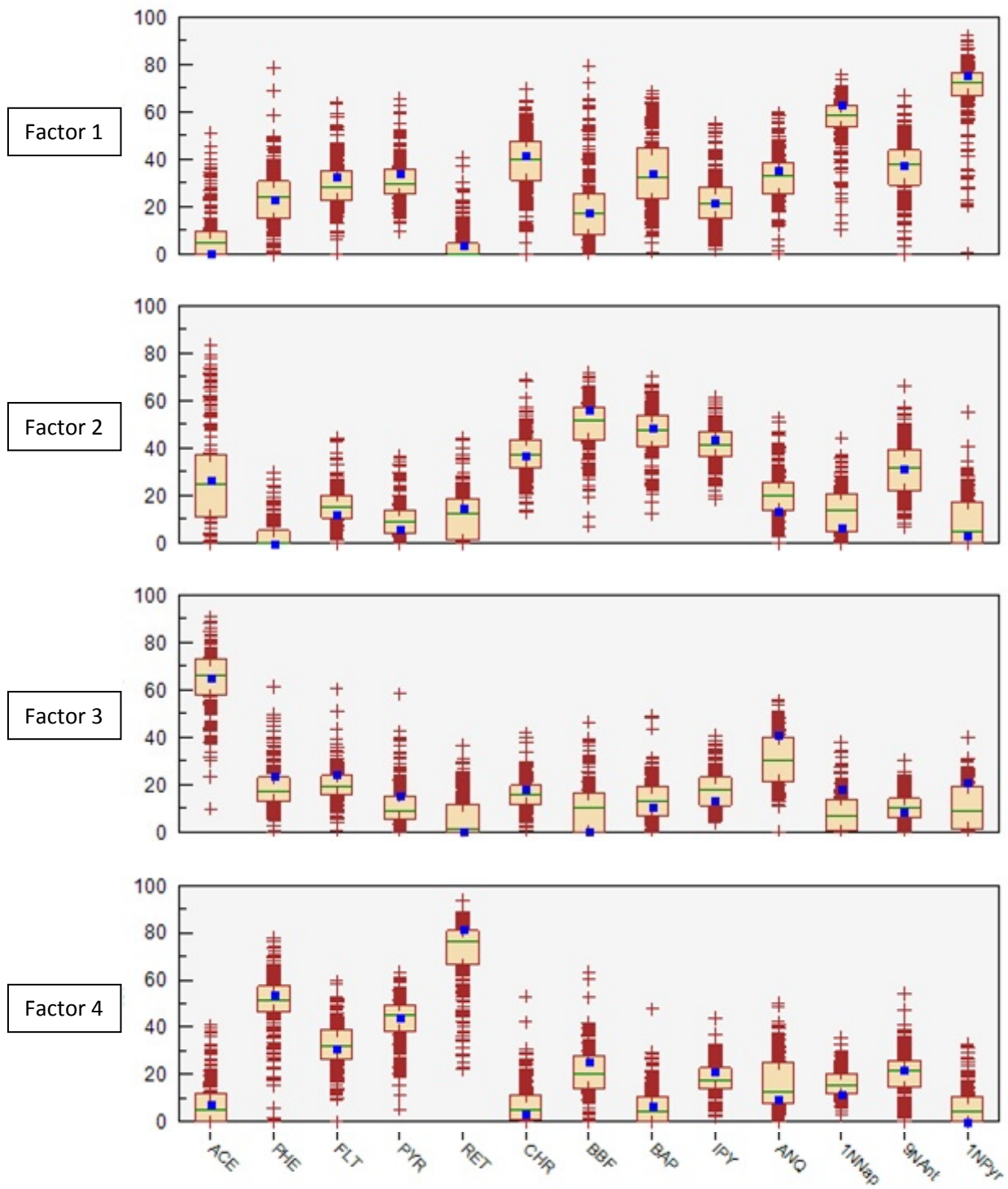


Figure 4.10. Results of the PMF bootstrapping analysis for each factor. Box plots display the median percentage contribution (green line) and the upper and lower edges of the box denote the 75th and 25th percentile values respectively. The percentage contribution predicted in the original base run is denoted by a blue square.

Fpeak values from -1 to +1 were investigated in this study. A final Fpeak value of -0.1 was selected as the most appropriate, based on relatively large change in Q observed from Fpeak values tested either side of this value (Reff *et al.*, 2007). Only modest changes in the factor profiles, scaled residuals and correlations of observed and modelled data were observed compared with original base runs. The factor profiles in Figure 4.9 were derived using this 'rotated' analysis.

4.4.3.3. Source contributions

The distribution of factor contributions for each individual compound measured is shown in Figure 4.11. Primary emission sources have been attributed to each of the factors as follows :

Factor 1 is shown to display high percentage contributions for 1NPyr and 1NNap with this factor contributing 65% and 57% of their modelled concentrations respectively.

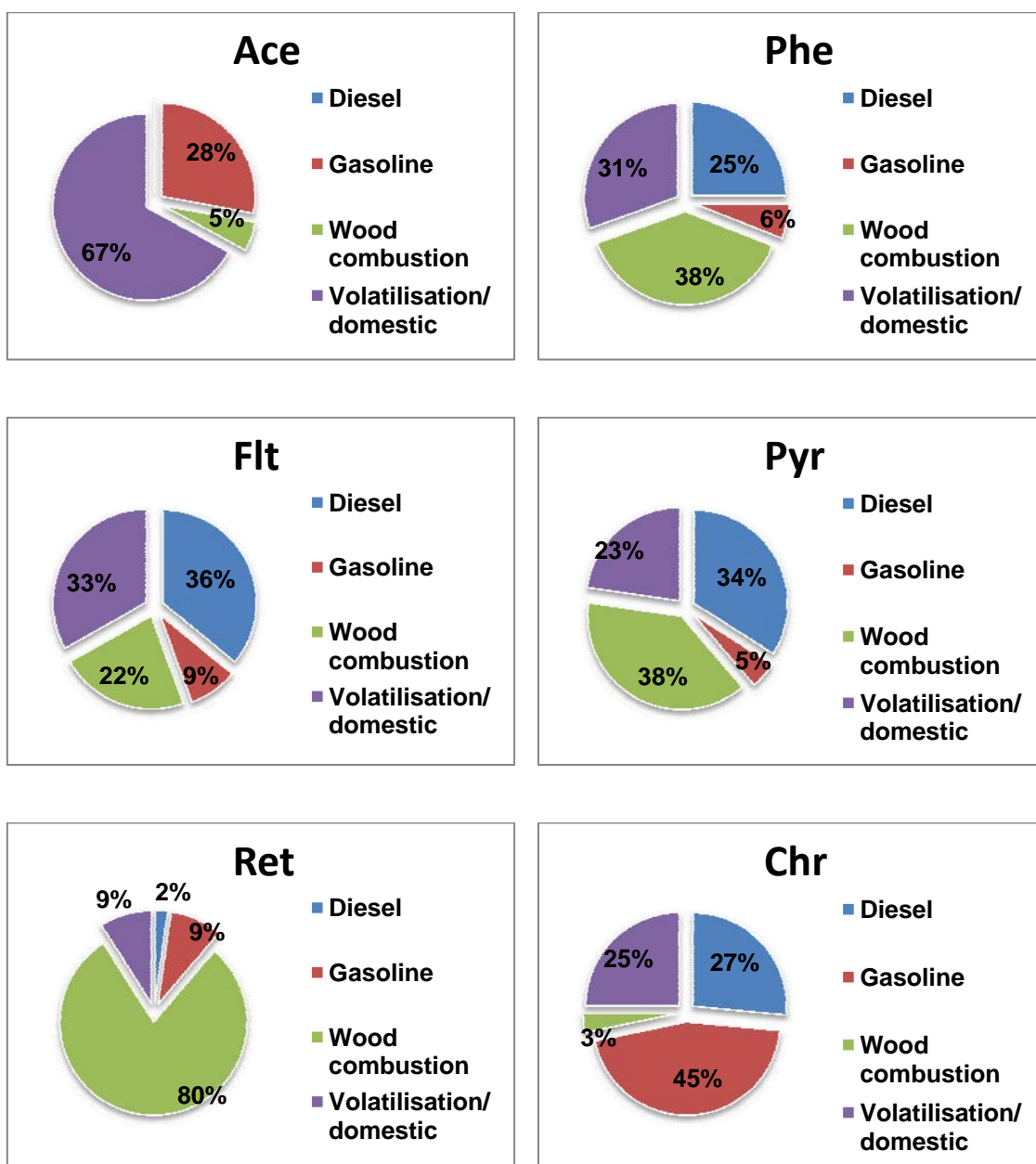
These two compounds are shown to be present predominantly diesel emissions (Draper, 1986; IARC, 1989; Reff *et al.*, 2007; Schuetzle *et al.*, 1981; 1982; Schuetzle and Perez, 1983; Zhu *et al.*, 2003). This factor can therefore reasonably be attributed to emissions from diesel vehicles.

It is interesting to note that 9NAnt is also strongly associated with diesel exhaust, however PMF analysis in the present study associates only ~28% of 9NAnt concentrations to this factor. Other potential combustion sources of this compound have not been characterised (Keyte *et al.*, 2013).

PAH compounds Phe, Flu and Pyr are emitted from diesel vehicles in relative high concentrations (Oda *et al.*, 1998; Staehelin *et al.*, 1998) and have been previously observed contributing relatively high loadings to factors in PCA analysis attributed to diesel emissions (Harrison *et al.*, 2003; Mari *et al.*, 2010). The relatively low loading of Phe, Flt and Pyr (25%, 36%, 34% respectively) is somewhat unexpected and suggests other sources influence levels of these compounds.

Factor 2 displays relatively high loadings for HMW PAH compounds. The contribution of this factor to modelled concentrations of Chr, BbF, BaP, IPy was 45%, 62%, 54% and 47% respectively. These compounds found at relatively high levels in vehicular emission (Fraser *et al.*, 1998a; Oda *et*

al., 1998). It is considered that HMW 5 ring PAH compounds are a marker for gasoline emissions, while LMW 3 ring PAH are more associated with diesel emissions (Miguel *et al.*, 1998; Perrone *et al.*, 2014; Phuleria *et al.*, 2006; Schauer *et al.*, 2003; Schauer *et al.*, 1999). This factor can therefore be attributed to gasoline vehicle emissions. This is in agreement with PCA analysis previously conducted at these sites (Mari *et al.*, 2010).



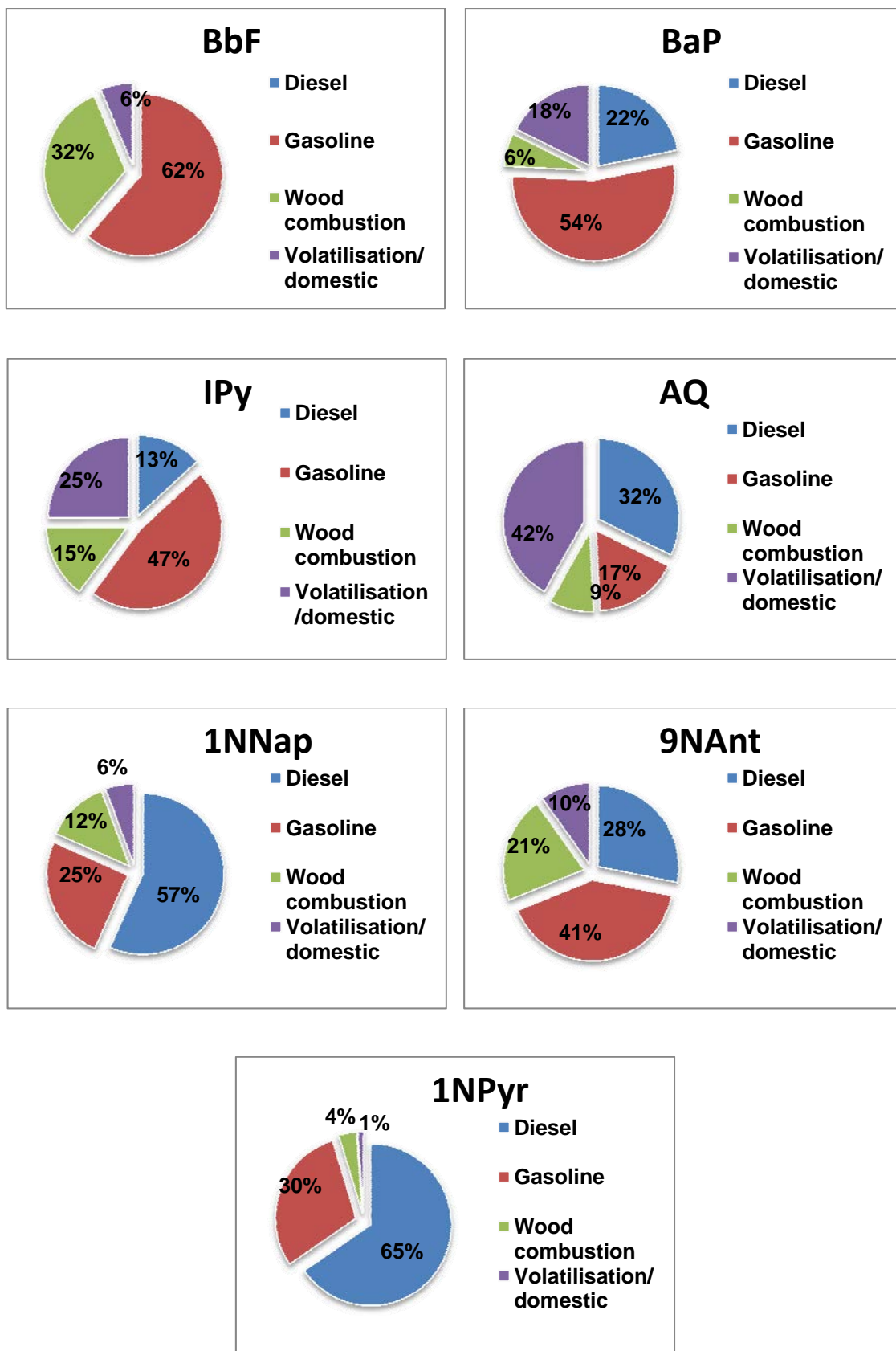


Figure 4.11. Contributions of each individual factor to the modelled concentrations of each species, as predicted by the PMF model.

AQ is emitted from both gasoline and diesel vehicles (Jakober *et al.*, 2007; Oda *et al.*, 2001; Rogge *et al.*, 1993a; Sidhu *et al.*, 2005; Strandell *et al.*, 1994; Zielinska *et al.*, 2004b). PMF results in the present study indicate an equal contribution of gasoline and diesel emissions, with a total traffic input contributing ~50% of AQ concentrations to the Birmingham University sites.

Factor 3 is characterised by a high loading of Ace (67%) with relatively smaller contributions for other PAHs.

It has been suggested in previous sections and by Dimashki *et al.* (2001), that concentrations of PAHs at these sites may be influenced by localised resuspension or volatilisation of components from the ground surface. This may result from unburned components in vehicle exhausts being deposited on the road surface (Rogge *et al.*, 1993b), then undergoing temperature-driven volatilisation to the atmosphere. PAHs can also be volatilised from soil or vegetation surfaces (Diamond *et al.*, 2001; Lee and Jones, 1999).

However, this does account for the relatively high loading of Ace in this factor. As discussed in Section 3.4, a relatively large increase in Ace concentration has been indicated at these sites since 1999-2001. Furthermore, the seasonal profile (Section 3.3) suggests levels of Ace at the University sites are much higher during the winter, suggesting the influence of a seasonally-mediated source.

Previously, a PCA factor containing high loading of Ace was attributed to “a specific fuel combustion source” (Mari *et al.*, 2010). This factor is therefore attributed to domestic wood combustion.

This would seem consistent with the increase in NAIE estimated emissions of PAH from domestic wood in the last 10 years, however it is unclear why this source produces elevated Ace concentrations but this is not observed for other LMW PAHs that are also associated with domestic wood combustion.

Factor 4 is characterised by a very high (80%) contribution to Ret concentration. Ret is typically associated with wood combustion (Bari *et al.*, 2010; Fine *et al.*, 2002; McDonald *et al.*, 2000;

Ramdahl, 1983). Mari *et al.* (2010) previously conducted PCA source apportionment to BROS and EROS sampling data. The authors reported a PCA factor with a very high loading of Ret, which displayed high contribution around November 5th 'bonfire night' celebrations.

Phe, Flt, Pyr also have relatively high (38%, 22%, 38% respectively) contribution from this factor. While these compounds have been observed in traffic emissions (see Section 5.1), particularly diesel (Zhu *et al.*, 2003), these results suggest non-traffic sources such as wood combustion significantly influence the levels of these compounds at BROS and EROS. This could provide an explanation for the lack of substantial temporal decrease in Flt and Pyr concentrations observed at these sites (Section 3.4).

The seasonal profile (Section 3.3) of Ret, Phe, Flt and Pyr, with relatively small differences observed between summer and winter concentrations may suggest the dominant source of these compounds is not seasonally mediated. These compounds have been shown to exhibit high levels in emissions from incineration (Harrison *et al.*, 1996; Ravindra *et al.*, 2008). This factor may therefore be associated with localised emissions from burning garden waste, which may be more prominent in summer. Indeed Ret displays higher concentrations in summer relative to winter at BROS, which may be explained by the close proximity of this site to local houses.

Jang *et al.* (2013) previously applied PMF source apportionment to airborne PAH concentration data from various U.K. urban monitoring sites. The authors identified four source factors for these data assigning the source contribution for urban sites ; unburned gasoline fuel (50.5%), diesel fuel (21.4%), coal combustion (15.0%) and wood combustion (13.1%).

Coal combustion was more strongly associated with locations of known industrial activity, with 48.5% of total PAH associated with this factor compared with 34.1% and 17.5% for unburned petroleum and diesel respectively at industrial locations (Jang *et al.*, 2013).

Clearly, different urban locations will exhibit different source profiles so comparison between the analysis of these combined 14 urban sites and the present study are not directly applicable. It is not expected that coal combustion has influenced the Birmingham University site to a significant

degree. Indeed PCA analysis of measured PAH concentrations by Mari *et al.* (2010) did not attribute any of the identified source factors to an industrial emission source.

It has previously been estimated that traffic is the main contributor of PAHs to the urban atmosphere in Birmingham (Harrison *et al.*, 1996; Lim *et al.*, 1999). However, the results of the present study indicate PAH concentrations at these sites are also influenced by other sources.

This work has demonstrates that PMF source apportionment analysis can be applied to OPAHs and NPAHs in air samples, suggesting the possible application of this tool for more extensive studies with greater numbers of samples and species.

4.4. Sampling artefact study

As discussed in Section 2.1 atmospheric sampling of PAHs can be influenced by the occurrence of sampling artefacts, which can alter both the measured concentrations of collected PAHs, OPAHs and NPAHs and the observed gas-particle partitioning behaviour of these compounds. In order to examine the potential influence of sampling artefacts under the sampling conditions and methods used in the present study, and determine if the results obtained in the present investigation are sufficiently robust, a quality control sampling experiment was conducted.

4.4.1. Methodology

4.4.1.1 Sampling

A sampling study was conducted for three sampling days in October 2013 at EROS. Two high volume samplers were operated at the site simultaneously, one acting as a 'sample test' sampler the other as a 'sample blank' sampler. The sampling materials were prepared, and the samplers calibrated and operated as described in Section 2.1.

Briefly, both 'sample test' and 'sample blank' samplers used quartz fibre filters to collect particulate matter (PM₁₀) with two PUF plugs downstream to collect the gas-phase component. Both samplers

were run for ~12-24 hours prior to the artefact experiment to pre-load the filters with ambient particulate matter.

Prior to the start of the experiment the 'sample test' filter was spiked with 250uL of PAH internal standard, a solution of deuterated PAH mixture made up with hexane (1000 pg/uL). The deuterated PAH compounds that were present in this mixture are shown in Table 4.5. These compounds are synthetic and are not found naturally in the environment. However, they display identical physiochemical properties as 'natural' PAH in collected samples.

There is assumed to be no natural addition of these deuterated compounds during sampling so their presence can be used to monitor possible PAH losses, due to volatilisation, breakthrough from the filter and/or chemical reactions. Monitoring the levels of the equivalent OPAH and NPAH deuterated internal standards (which are also not naturally present in the atmosphere) will also help to assess to what extent reactions of filter-bound PAH may have occurred during sampling and hence influenced the measured levels of PAH, OPAH and NPAH compounds. The 'sample blank' filter was not spiked and acted as a control sample. Both samplers were then run for a ~24 hours sampling period.

4.4.1.2. Analysis

Collected filter and PUF samples were prepared, extracted and analysed as described in Section 2.3. Briefly, samples were extracted in DCM using ultrasonication, blown to almost dryness by a gentle stream of nitrogen gas and made up to ~1mL volume in hexane. Sample extracts were cleaned up using an aminopropyl solid phase extraction column and finally made up to a final volume of 250uL in nonane for GC-MS analysis. In addition to 'sample test' and 'sample blank' samples, 'lab blank' filters was analysed for comparison with collected samples. These were filters spiked with the PAH IS mix but these were not exposed to sampling conditions, but immediately extracted and analysed.

4.4.1.3. PAH recovery

Collected filter and PUF samples were analysed for deuterated PAH concentrations using GC-MS operated in EI mode (see Section 2 for full instrumental details) to assess the recovery of PAH compounds during sampling, based on comparison with levels measured in lab blank filters. Calibration curves for each compound were produced from prepared standard solutions based on response ratios relative to the internal standard p-terphenyl-d14. A known amount of the p-terphenyl-d14 internal standard was spiked on to samples prior to extraction and analysis. Concentrations were calculated as described in Section 2.3.

4.4.1.4. OPAH and NPAH formation

Concentrations of deuterated OPAHs and NPAHs, corresponding to appropriate deuterated PAH compounds (see Table 1) were analysed by GC-MS operated in NICI mode (see Section 2 for full instrumental details). Concentrations were calculated based on calibration standards, prepared using 2-fluoronitrofluorene (FNF) as an internal standard. A known amount of FNF internal standard was spiked on to filter and PUF samples prior to analysis.

4.4.2. Results

4.4.2.1. Observed PAH losses

Deuterated PAH concentrations in sample blank extracts were very low (0 to 1.5%) relative the lab blank extracts. Therefore, we can reasonably conclude that levels of these deuterated PAH compounds observed in sample test extracts have resulted from the initial spike of PAH internal standard mixture prior to sampling.

The recoveries of deuterated PAHs from the internal standard mixture, measured in sample test filter extracts were based on the calculation :

$$\text{Filter Recovery (\%)} = [(C_{ST} - C_{SB})_{FILT} / (C_{LB})_{FILT}] \times 100 \quad (4.9)$$

Where : C_{ST} = concentration in 'sample test'

C_{SB} = concentration in 'sample blank'

C_{LB} = concentration in 'lab blank'

FILT denotes filter concentration

Table 4.5. Deuterated PAH, OPAH, and NPAH compounds measured in the artefact study

Spiked IS mixture compounds	Associated target OPAH and NPAH compounds
Acenaphthylene-d8	
Acenaphthene-d10	
Fluorene-d10	2-Nitrofluorene-d8 9-Fluorenone-d8
Phenanthrene-d10	9-Fluorenone-d8
Anthracene-d10	9-Anthraquinone-d8
Fluoranthene-d10	3-Nitrofluoranthene-d9
Pyrene-d10	1-Nitropyrene-d9
Chrysene-d12	6-Nitrochrysene-d11
Benz[a]anthracene-d12	
Benzo[a]pyrene-d12	
Benzo[b]fluoranthene-d12	
Benzo[k]fluoranthene-d12	
Benzo[ghi]perylene-d12	
Indeno[1,2,3-cd]pyrene-d12	
Dibenz[a,h]anthracene-d14	

The mean filter recoveries for the PAH compounds calculated in this study are shown in Table 4.6. For HMW (5+ ring) compounds, which are predominantly found in the particulate-phase in the atmosphere (Smith and Harrison, 1996 ; Alam *et al.*, 2013; Delgado-Saborit *et al.*, 2013), the recoveries were generally high (77 to 100%). This suggests the minimal losses from the filter during sampling and the levels of these HMW compounds measured with these samplers are in reasonable agreement with 'true' levels present in the atmosphere. This is consistent with the relatively high vapour pressures and subsequent low volatility of these compounds.

Recoveries of more volatile (3-4 ring) compounds were much lower (15-50%) suggesting these compounds may be subject to losses from the filter during sampling and hence their levels may be underestimated. This may have resulted due to volatilization, filter break-through or chemical reaction during sampling. It is assumed that the use of a relatively non-volatile solvent (hexane) for the IS spike prior to sampling meant that loss of PAH compounds prior to sampling was minimal. However, it is possible some loss of more volatile compounds may have occurred prior to the beginning of sampling .

Previously, Delgado-Saborit *et al.* (2013) collected PAH and OPAH at the BROS location using a denuder system which collected the gas-phase component using XAD-4 upstream of a MOUDI collecting the particulate-phase component on PTFE filters. This sampling system also used a PUF plug downstream to monitor the amount of blow-off from the filter. The authors noted more volatile 3-ring PAHs displayed relatively high (18-63%) artefact levels compared with PAHs with 4+ rings (0-10%).

The volatilisation artefact in the present study is relatively high for most compounds in relation to this previous study, however the general trend of higher loss for LMW (3-4 ring) compounds relative to HMW (5+ ring) compounds is consistent with the observation made by Delgado-Saborit *et al.* (2013).

Kavouras *et al.* (1999) also utilised a denuded sampling system, observing particle-phase losses for 3-4 ring PAH of 56-97% with much lower losses of 5+ ring PAH, which is also consistent with losses during the present study.

It has been noted in studies utilising denuded sampling systems, that volatilisation from particles can be enhanced in a denuded system as, by removing the gas-phase component upstream of the particle component, the phase-partitioning equilibrium of the PAH compounds will be disrupted, leading for a higher tendency for particle-bound fraction to partition to the gas-phase to move towards equilibrium (Delgado-Saborit *et al.*, 2014; Kavouras *et al.*, 1999)

This study therefore demonstrates the loss of particle-phase component during sampling is a phenomenon that influences both denuded and undenuded systems. The relatively high loss rates of 3-4 ring PAH indicates that volatilisation/breakthrough from the filter and/or chemical reaction of PAH with atmospheric oxidants are more significant processes influencing these PAHs than adsorption of gas-phase components to the filter.

In order to assess whether loss of particle-associated semi-volatile PAH is predominantly due to blow off/breakthrough or reactivity during sampling, the PAH levels present in the PUF material downstream of the filter were also taken into account. The 'total' PAH recovery was calculated and these recoveries are shown in Table 4.7 derived using the formula :

$$\text{Total Recovery (\%)} = [(C_{ST} - C_{SB})_{FILT} + (C_{ST} - C_{SB})_{PUF} / (C_{LB})_{FILT}] \times 100 \quad (4.10)$$

Where : C_{ST} = concentration in 'sample test'

C_{SB} = concentration in 'sample blank'

C_{LB} = concentration in 'lab blank'

FILT – denotes filter concentration

PUF – denotes PUF concentration

Table 4.6. Mean filter recoveries of PAH compounds measured on sample test filters

Compound	Mean	SD
Acenaphylene-d8	51.6	23.9
Acenaphthene-d10	46.8	3.1
Fluorene-d10	21.8	10.4
Phenanthrene-d10	15.5	6.9
Anthracene-d10	23.4	10.6
Fluoranthene-d10	22.5	6.7
Pyrene-d10	27.9	2.4
Benzo(a)anthracene-d12	26.0	7.9
Chrysene-d12	31.7	10.2
Benzo(b)fluoranthene-d12	79.4	12.7
Benzo(k)fluoranthene-d12	77.1	5.1
Benzo(a)pyrene-d12	94.1	2.7
Indeno(1,2,3-cd)pyrene-d12	103.3	9.8
Dibenz(a,h)anthracene-d12	102.4	11.0
Benzo(ghi)perylene-d12	103.4	7.3

When the concentrations measured in PUFs is taken into account, total recoveries for most compounds are generally high (>75%). These results suggest that in cases where filter recovery was low, it is as a result of volatilisation/breakthrough from the filter to the PUF. If this behaviour indeed occurred during sampling, this may influence the gas-particle partitioning behaviour of the semi-volatile PAHs as the 'real' concentration of the compound in the particulate phase may have been higher than reported.

This behaviour is likely to influence the semi-volatile PAHs, Pyr and Flt (and Ret which may be assumed to display similar behaviour) primarily as the partitioning behaviour of these compounds

may to be subject to variability, driven by changes in temperature. The annual average contribution of the particulate-phase to the concentrations of these compounds is 10%, 11% and 18% respectively.

Table 4.7. Mean total recoveries of PAHs measured on sample test filters + PUFs

Compound	Mean (%)	SD (%)
Acenaphylene-d8	76.5	15.2
Acenaphthene-d10	66.9	3.5
Fluorene-d10	53.5	23.6
Phenanthrene-d10	68.8	7.5
Anthracene-d10	88.5	8.7
Fluoranthene-d10	96.7	17.4
Pyrene-d10	98.1	9.4
Benzo(a)anthracene-d12	102.3	24.4
Chrysene-d12	86.8	13.9
Benzo(b)fluoranthene-d12	100.6	8.9
Benzo(k)fluoranthene-d12	94.8	13.9
Benzo(a)pyrene-d12	100.6	4.1
Indeno(1,2,3-cd)pyrene-d12	103.4	9.7
Dibenz(a,h)anthracene-d12	102.6	10.9
Benzo(ghi)perylene-d12	103.5	7.3

The results of this experiment suggest the particle-phase contribution of these compounds may have been up to a factor 4 higher than reported in the present study.

However, for purposes of assessing total PAH concentrations, total recoveries were relatively high, therefore subsequent analysis of concentration trends and correlations using 'total' concentrations

will be valid. A number of LMW compounds (Ace, Acy, Flo, Phe) have lower (<77%) total filter recoveries. This indicates these compounds are subject to losses from the filter and not recovered by PUFs. This will result in overall loss and underestimation of total PAH concentration.

For 3-ring PAHs, which are typically found predominantly in the gas-phase, the influence of observed loss rates from the filter is not likely to influence their partitioning or total concentrations significantly. Considering the mean total (gas+particle) concentrations of PAHs measured in campaign 1, the calculated loss of particle-phase 3-ring PAHs from filters during this artefact experiment is likely to represent <1% decrease in total concentration.

While NPAH and OPAH losses were not directly monitored in this study, it is suggested that more volatile compounds (MW<200) e.g. 1NNap, 2NNap and 9Flo may exhibit a similar level of loss as more volatile PAHs

It is assumed that gas-phase loss from PUFs is minimal during sampling. PUFs have been widely used in previous sampling studies collecting gas-phase 3-4 ring PAH, OPAH and NPAH (Yamasaki *et al.*, 1982 ; Keller and Bidleman, 1984; Harrison *et al.*, 1996; Dimashki *et al.*, 2000; 2001, Bamford and Baker, 2003; Harrad and Laurie, 2005; Reisen and Arey, 2005; Albinet *et al.*, 2008a, Kim *et al.*, 2012).

Keller and Bidleman (1984) demonstrated that PUF plugs of similar dimensions to those used in this study, 3-ring PAH displayed <15% and 4-ring PAH <10% breakthrough during 24 hour sampling studies. The use of 2 plugs in series therefore means we can be reasonably confident that minimal loss of gas-phase species occurred during sampling in the present study.

Because the artefact sampling experiment was conducted for a specific period of the year in early autumn, the meteorological conditions observed during this period were compared with those during Campaign 1 to assess whether the results observed are likely to be representative for other periods of Campaign 1, 2 and 3 (see Section 2) Meteorological data measured during the artefact study are shown in Tables 4.8, along with mean values for each seasonal period of sampling campaign 1.

Table 4.8. Mean values for meteorological measurements, temperature (TDRY), relative humidity (RELH), Pressure (PRES) and solar radiation (SRAD) and total rainfall (RTOT) for the sampling campaigns during autumn (A); winter (W); spring (Sp), summer (Su) and the artefact study (ART).

	TDRY (°C)	RELH (%)	PRES (hPa)	SRAD (W/m ²)	RTOT (mm)
A	10.5	82.3	1012.2	156.1	3.5
W	6.0	82.7	1025.9	87.0	0.5
Sp	9.9	75.2	997.5	136.7	2.9
Su	16.5	76.3	996.7	183.1	2.9
ART	14.5	78.1	999.7	78.0	0.3

It can be seen that mean temperature during the artefact study was higher than that during the autumn, winter and spring periods of Campaign 1, and slightly lower than measured during summer. Other meteorological parameters (relative humidity, pressure) measured during the artefact study and those measured in spring/summer were broadly comparable. However, solar radiation levels during the artefact study were considerably lower. It is possible, therefore that volatile losses of PAH compounds may have been more pronounced during the summer periods when temperature and solar radiation levels were higher.

4.4.2.2. Conversion of PAH to OPAH or NPAH during sampling

Peaks on the gas chromatograph were identified corresponding at times consistent with the OPAH and NPAH compounds. However these were noted in both 'sample test' and 'sample blank' extracts. This suggests that these peaks may not be attributable solely to the presence of deuterated OPAH and NPAH compounds.

However, peak area of 'sample test' peaks were consistently much greater than those in 'sample blanks' and only very minor peaks corresponding to deuterated OPAH and NPAH compounds was observed in lab blank extracts. It is suggested, therefore that the presence of gas chromatograph peaks for sample test extracts is predominantly due to reaction products of deuterated PAH compounds spiked to the test filter, with minor amounts of interference contaminant species transferred to the filter during sampling and/or analysis.

Total conversion of PAH to OPAH and NPAH derivatives was calculated for each compound based on the calculation :

Total Conversion (%) =

$$\frac{[(C_{DER})_{ST} - (C_{DER})_{SB}]_{FILT} + [(C_{DER})_{ST} - (C_{DER})_{SB}]_{PUF}}{(C_{PAH})_{LB}} \times 100 \quad (4.11)$$

Where :

C = concentration

PAH = concentration of deuterated PAH compound

DER= concentration of deuterated oxy/nitro derivative compound

ST = concentration in 'sample test'

SB = concentration in 'sample blank'

LB = concentration in 'lab blank'

FILT – denotes filter concentration

PUF – denotes PUF concentration

For all tested OPAH and NPAH compounds (Table 1) total conversion for the 24 hour sampling period was <1%. The conversion to 9-Fluorenone-d8 ; Anthraquinone-d8 ; 2-Nitrofluorene-d8; 3-Nitrofluoranthene-d9 ; 1-Nitropyrene-d9 ; 6-Nitrochrysene-d11 were 0.67%, 0.95%, 0.76%, 0.34%, 0.00%, 0.05% respectively.

This suggests that the measured levels of OPAH and NPAH compounds measured in this investigation are not significantly influenced by artefact formation on the filter so the concentrations measured during this investigation are broadly an accurate reflection of 'true' levels in the atmosphere

It should be noted for most compounds the majority of observed detuterated OPAH or NPAH (with the exception of 6NChr-d11) were detected in PUFs, suggesting formation had occurred on the filter surface followed by volatilisation and/or break through to the PUF downstream.

Taking into account the mean particulate concentrations of PAH, OPAH and NPAH measured at BROS and EROS in campaign 1, it is clear that a <1% conversion of PAH to their associated derivatives will have a negligible influence of the overall concentrations of most PAH, OPAH and NPAH measured during this study.

However, relatively low annual mean concentrations of 3NFlt and 6NChr suggest even minimal artefact formation could influence these compounds. Indeed, considering the annual mean particulate concentrations the conversion rates of 0.34% and 0.05% respectively of Flt and Chr could lead to an overestimate of 3NFlt and 6NChr concentrations of >100%.

The extent of PAH reactivity towards oxidants during sampling will be highly dependent on the oxidant concentration in the atmosphere. For example, Schauer *et al.* (2003) observed a correlation between the denuded : undenuded PAH concentrations and the mixing ratio of O₃.

In order to assess how the potential for oxidation reaction may vary during the sampling campaigns in this project, and to compare the results of the present artefact study with previous studies, mean

concentrations of O₃ and NO_x concentrations measured at Birmingham Tyburn during both campaign 1 and the artefact study are shown in Table 4.9.

Table 4.9. Mean concentrations of inorganic pollutants (ug/m³) measured during autumn (A); winter (W); spring (Sp), summer (Su) samples in campaign 1 and artefact (ART) study.

	NO _x	O ₃
Mean A	61.4	27.2
Mean W	54.8	32.1
Mean Sp	40.2	52.0
Mean Su	37.6	36.5
Mean ART	36.5	29.2

Arey *et al.* (1988) investigated the formation of NPAH artefacts during high-volume air sampling by exposing perdeuterated Flt, Pyr and BaP compounds spiked on a filter. While it was shown that 6NBaP was formed from BaP during sampling, no formation of NFlt and <3% formation of 1NPyr was observed. It should be noted that Arey *et al.* (1988) conducted sampling during a high pollution episode, where NO₂ concentrations were reported to be 4 to >10 times higher than the average concentration in the present artefact study. The results of the present study suggest, in agreement with Dimashki *et al.* (2000), that reactivity with NO₂ was not a significant sink for PAH, nor a source of NPAH artefact formation during the sampling campaigns of this project.

Previous studies have indicated that on undenuded samplers, O₃ reactivity can result in an underestimation of particulate-phase PAH concentrations by up to a factor 2 (Goriaux *et al.*, 2006; Schauer *et al.*, 2003; Tsapakis and Stephanou, 2003). However, Brown and Brown (2013) noted a

relatively small (~6%) underestimation in BaP concentrations due to reactive loss during 24 hr sampling studies.

It is interesting to note that negligible loss of BaP is noted in this study, while previous studies have noted this compound as one of the most reactive PAHs on the filter surface (Goriaux *et al.*, 2006; Liu *et al.*, 2006; Tsapakis and Stephanou, 2003). This observation, in addition to the very low conversion rates of PAHs to OPAH in this study suggest O₃ reactivity on the filter surface was not a significant process during this sampling experiment.

Furthermore, during the study of Tsapakis and Stephanou (2003) the O₃ mixing ratio was >50ppb, more than 3 times higher than was observed during the present study. Similarly, Liu *et al.* (2006) noted 20% loss of BaP during sampling in an experiment where O₃ mixing ratio was reported to be 70 µg/m³, over a factor 2 higher than the present study. It is suggested, therefore that the occurrence of artefact formation during sampling in these previous studies, and relative absence of such an effect in the present study was as a result of much lower concentrations of reactant species.

It can be seen in Table 4.9 that levels of NO_x during the artefact study were similar to those observed during spring and summer campaigns with higher levels observed during autumn and winter. It is possible therefore, that while negligible levels of chemical conversion were indicated in the artefact study, reactions of filter-bound PAH towards NO_x may have been more enhanced during winter.

The converse situation is true for O₃ concentrations, for which levels during the artefact study are similar to the autumn and winter concentrations but much lower than spring and summer concentrations. It is possible therefore, that while negligible levels of chemical conversion were indicated in the artefact study, reactions of filter-bound PAH towards O₃ may have been more enhanced during spring and summer.

4.4.3. Summary

The results of this quality control experiment suggest that sampling artefacts did not significantly influence the total concentrations of target PAH or derivative compounds measured in the three campaigns of this investigation.

Breakthrough and/or volatilisation of LMW 3-4 ring PAH was shown to occur, which resulted in either loss of particulate component of these compounds to the atmosphere or to the downstream PUF plug. However, because it is expected that vast majority of these 3-4 ring compounds will be present in the atmosphere the gas-phase, the influence of this process on total concentration and phase partitioning behaviour of these compounds is not expected to be significant.

It was shown that reactivity of PAH on the filter results in negligible levels of PAH loss and NPAH or OPAH formation during sampling for most compounds. Based on these results, we can be confident of the validity of assessments made using 'total' (vapour + particulate) concentrations as total loss of PAH and derivatives is likely to be minimal.

Chapter 5. Diurnal profiles of PAH, OPAH and NPAH

5.1. BROS and EROS diurnal profiles

Diurnal profiles of PAHs, NPAHs and OPAHs compounds at BROS and EROS were derived from sampling in Campaign 2. Details of the samples taken in Campaign 2 are provided in Table 2.1. The profiles of Σ PAH concentrations at BROS and EROS, as well as the concentrations of O_3 and NO_x are shown in Figure 5.1. It should be noted that the nighttime samples BD12 and ED12 taken on 9/8/2012 displayed unusual behaviour. These samples were characterised by very high ($>100 \mu\text{g}/\text{m}^3$) average nighttime NO_x concentration at Tyburn and unexpectedly high concentrations of HMW particle-phase PAHs. However the observed concentrations of LMW gas-phase compounds and OPAH and NPAH compounds did not appear higher than expected. This could possibly suggest the occurrence of external pollution 'episode' influencing the Birmingham area during this time or an error in extraction/analysis for these samples. These samples are excluded from the calculation of mean diurnal patterns and any statistical analyses performed.

These profiles are based on mean values from each time period during the three sampling days of this campaign during the summer months and therefore represent concentrations at these sites and on these specific days. Given the spatial and temporal variation PAH, OPAH and NPAH concentrations can exhibit, these diurnal profiles must be viewed with caution and may not be representative of the wider area throughout other times of the year.

For Σ PAH at BROS, the highest concentrations are observed in the morning (0700 – 1100). This is consistent with traffic being the principal source of compounds at these sites and emission strength being strongest during the morning 'rush hour' period. Indeed, the profile for Σ PAH at BROS appears to follow a distinct PAH 'traffic' pattern (Nielsen *et al.*, 1999). The concentration peak in the morning is followed by a sharp decline during daytime (1100 – 1600), possibly due to reduced

traffic flow and maximum reactive loss of compounds with higher levels of atmospheric oxidants, as indicated by increased O₃ concentrations.

Concentrations are shown to increase during the afternoon (1600 – 1900), possibly in response to increased traffic flow during the evening rush hour, although this may also be due to temperature-driven local input e.g. volatilisation from road and/or vegetation and soil surfaces. Lowest concentrations are observed during the nighttime (1900 – 0700) period when the emission source strength from road traffic is likely to be lowest. ΣPAH at EROS is shown to follow a similar, but much weaker trend, consistent with the greater distance of this site from the traffic emission source. A similar traffic pattern has been observed for PAHs at these sites previously (Laurie, 2003).

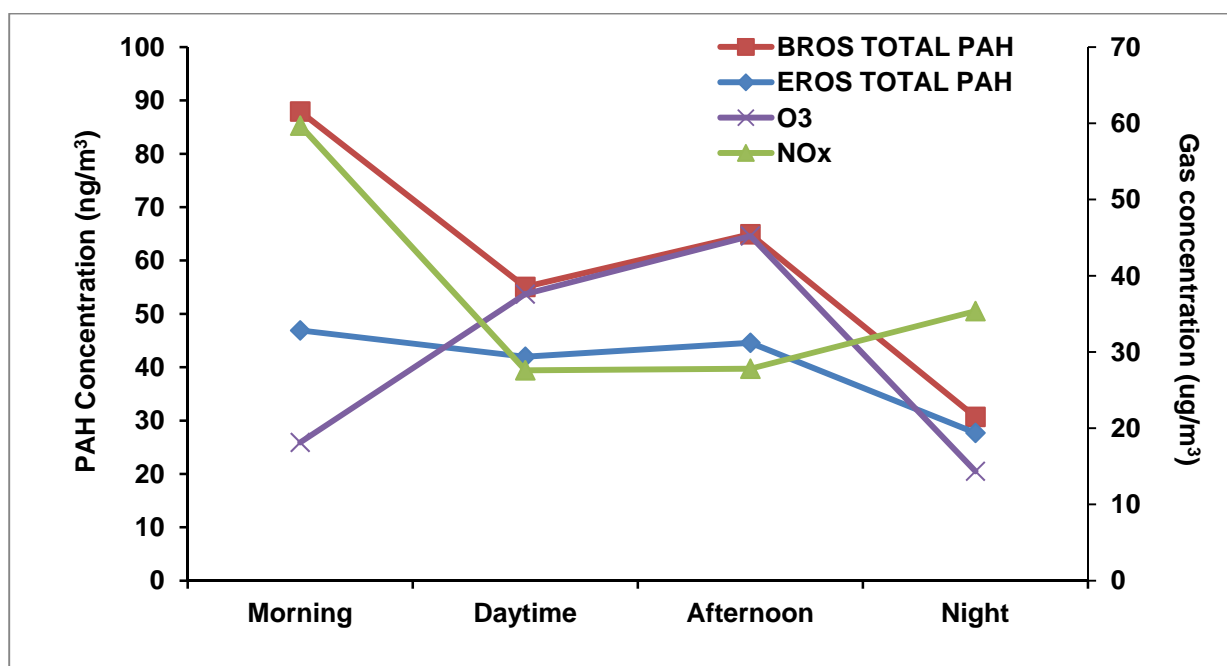


Figure 5.1. Diurnal profiles of total PAH concentrations at BROS and EROS, O₃ and NO_x, derived from mean values taken during morning (0700 – 1100), daytime (1100 – 1600), afternoon (1600 – 1900) and night (1900 – 0700).

The PAH trend at BROS, and to a lesser extent at EROS is followed, at least partially by the trend in NO_x concentrations. The close association of PAHs and traffic-related gases such as NO_x and CO have previously been observed by Nielsen (1996). This indicates NO_x levels are predominantly governed by road traffic input. The observed increase in NO_x concentration in nighttime samples is therefore somewhat unexpected and may indicate the influence of non-traffic related combustion sources at night and/or lower atmospheric losses of NO_x resulting from reaction with OH.

Concentrations of NO_x are shown to correlate significantly ($p > 0.05$) with ambient temperature, indicating the height of atmospheric mixing layer varies during the day, which will also influence the observed diurnal patterns. For example, relatively high nighttime PAH concentrations have previously been observed at night, attributed to thermal inversions in mixing height (Ringuet *et al.*, 2012a; Wu *et al.*, 2010).

The diurnal profiles for individual PAH, OPAH and NPAH compounds at BROS and EROS are presented in Figure 5.2. The relative distribution of PAH, OPAH and NPAH compounds, throughout the diurnal cycle is shown to be broadly similar to that of seasonal samples collected in Campaign 1.

While the characteristic traffic-related pattern is observed for Phe at BROS, the daytime and afternoon concentrations are higher at EROS than may be expected from traffic input. As discussed in previous sections, this may be due to relatively high evaporative input from surfaces causing a considerable variation from a traffic-mediated pattern, influencing more significantly at EROS.

Ant displays highest concentrations during the afternoon at both sites. Ant displays high reactivity towards OH (Atkinson and Arey, 1994; Brubaker and Hites, 1998) so might be expected to display a relatively large decline in concentration during the daytime. Similarly, Acy, which is shown to be the most reactive PAH towards OH (Reisen and Arey, 2002) does not display relatively steep decline in daytime concentrations. Furthermore, while Flo follows a traffic-related pattern at both sites, the trend is much weaker than observed for other compounds. The observed diurnal

behaviour of these LMW compounds suggests possible influence of an additional source during the daytime, possibly due to volatilisation from soil, vegetation and/or road surfaces, as indicated by the positive correlation between temperature and NO_x-corrected concentrations at both sites (although this is not observed for Acy at BROS).

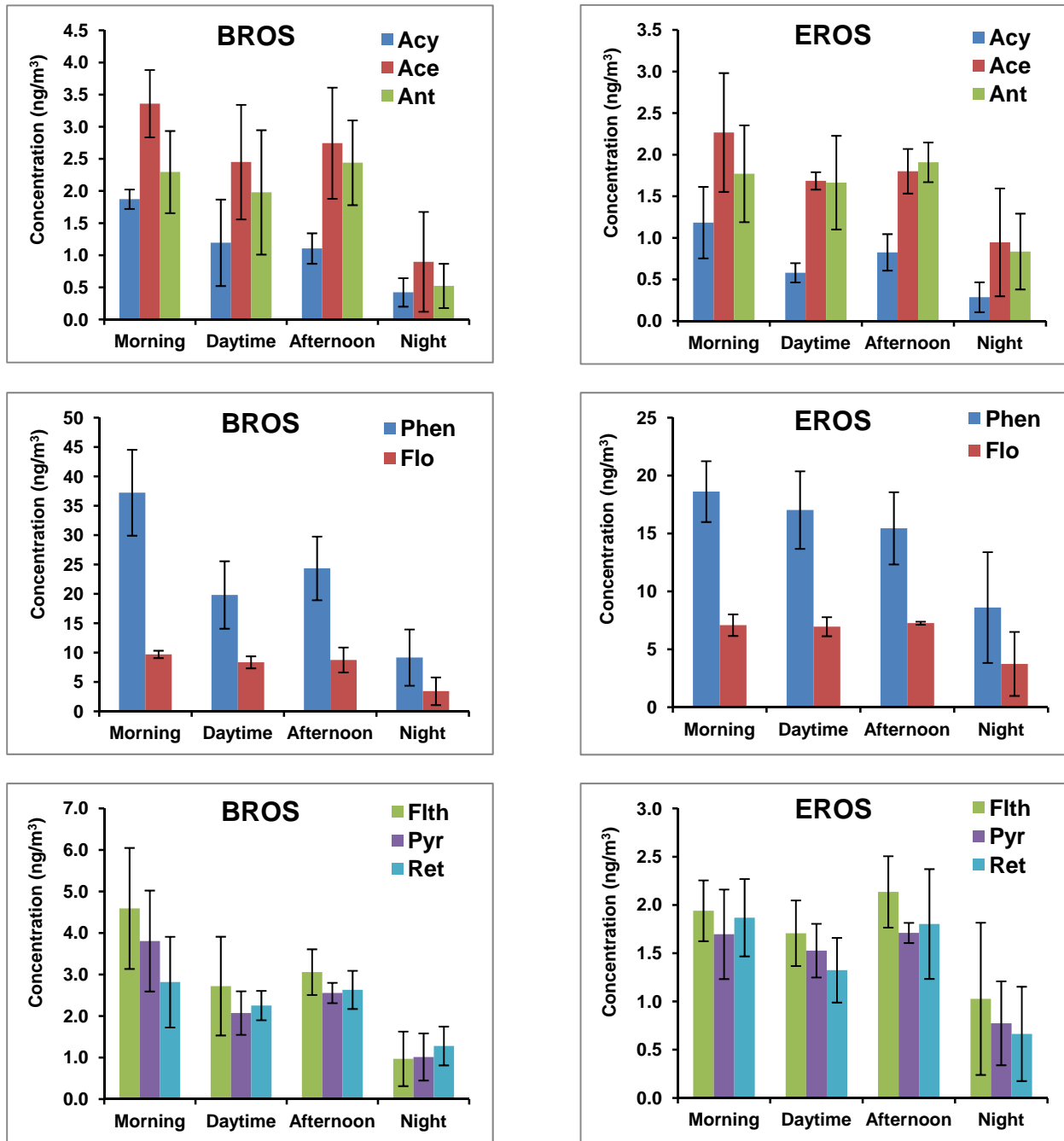


Figure 5.2. Diurnal profiles of PAHs, OPAHs and NPAHs at BROS and EROS. Morning = 0700 – 1100; Daytime = 1100 – 1500; Afternoon = 1500 – 1900; Night = 1900 – 0700.

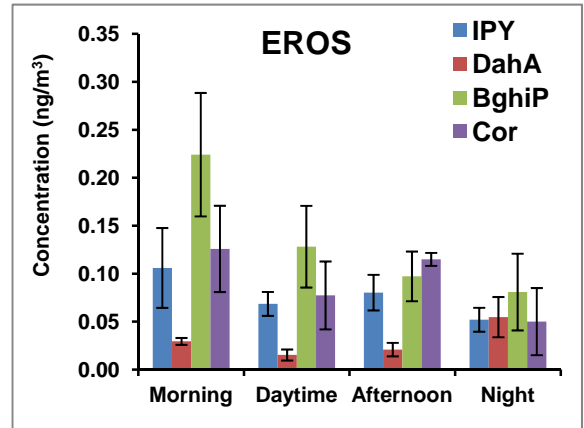
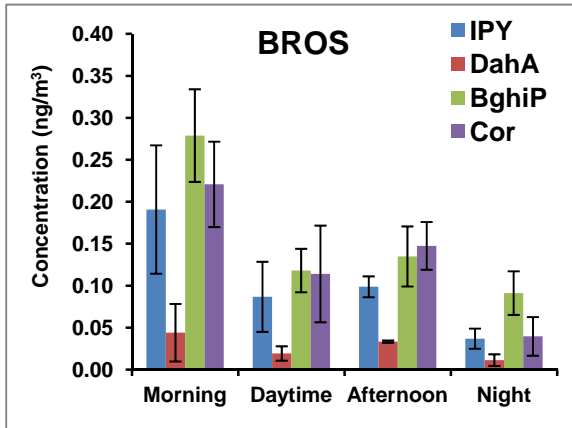
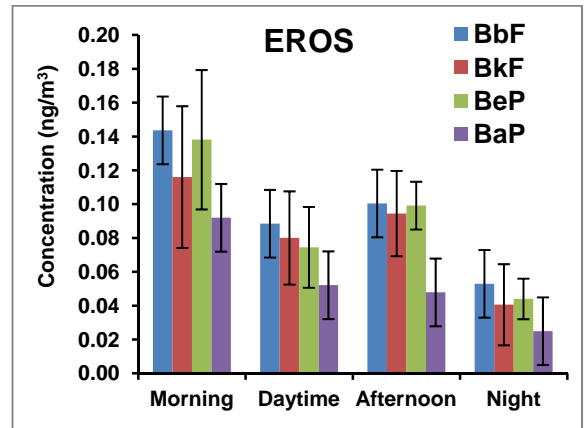
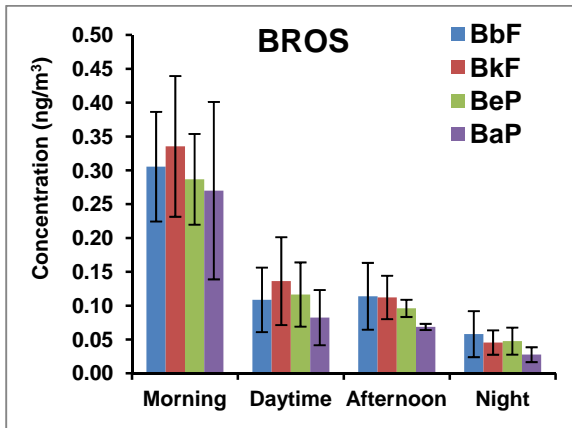
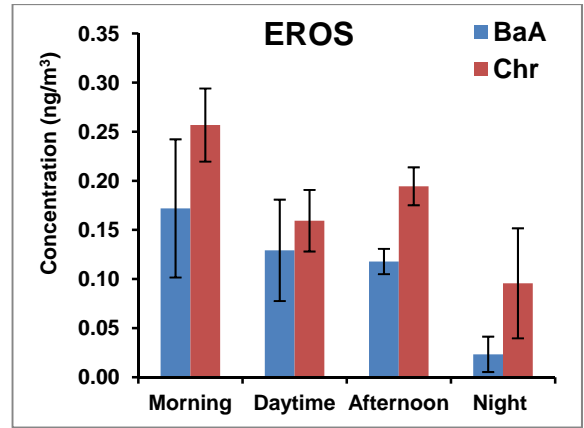
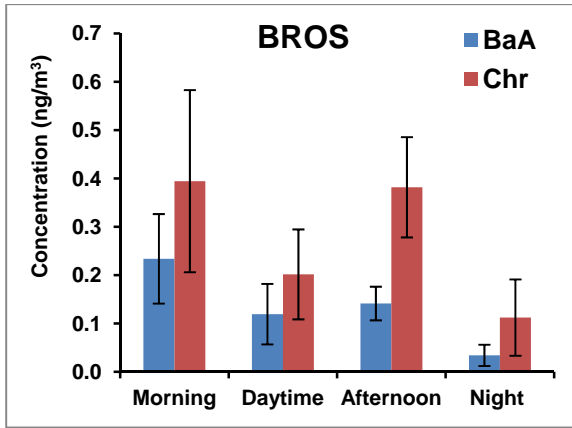


Figure 5.2 (cont) . Diurnal profiles of PAHs, OPAHs and NPAHs at BROS and EROS. Morning = 0700 – 1100; Daytime = 1100 – 1500; Afternoon = 1500 – 1900; Night = 1900 – 0700.

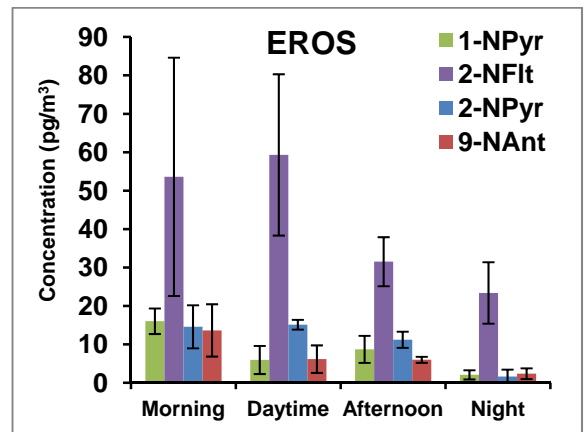
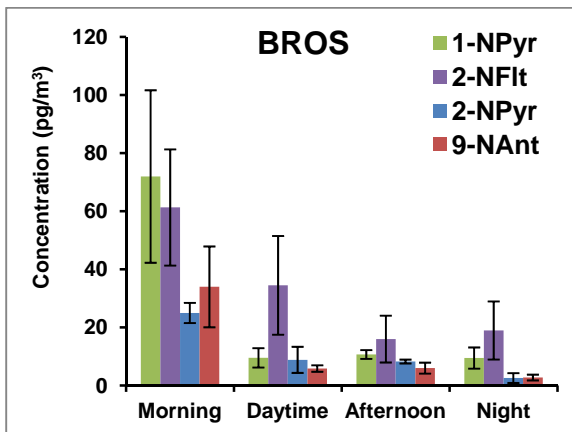
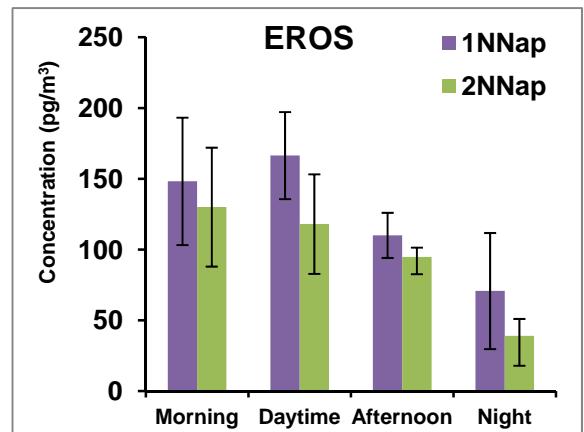
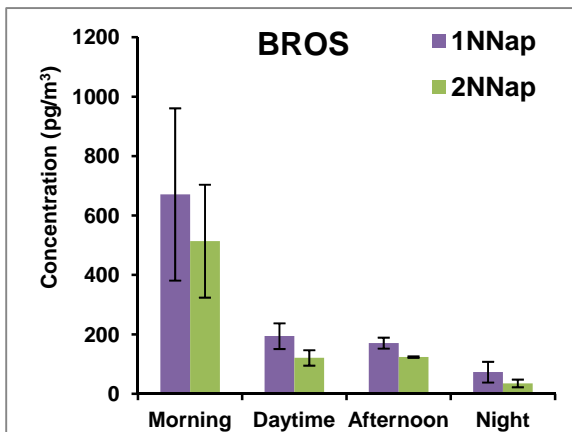
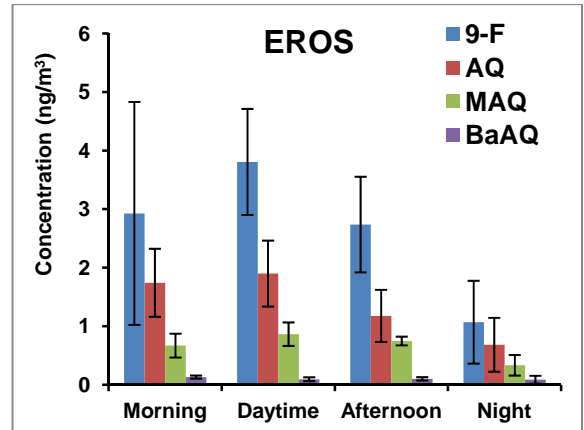
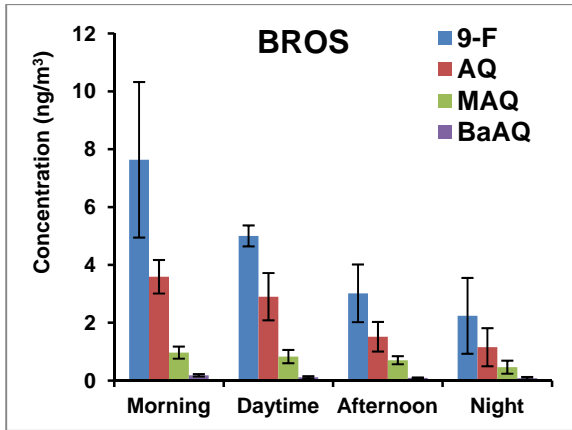


Figure 5.2 (cont) . Diurnal profiles of PAHs, OPAHs and NPAHs at BROS and EROS. Morning = 0700 – 1100; Daytime = 1100 – 1500; Afternoon = 1500 – 1900; Night = 1900 – 0700.

It is interesting to note that Ace displays a characteristic traffic pattern at both BROS and EROS, despite seasonal (Section 3) and tunnel (Section 6) measurements suggesting a deviation away from this behaviour. This may suggest measured concentrations in Campaign 1 are influenced by a number of relatively isolated episodic emissions of Ace that mask the influence of traffic at these sites.

Ret also displays a profile similar to a traffic-pattern, although relatively weakly, which is unexpected because this compound has a relatively minor traffic input. It is suggested this profile is primarily governed by variation in mixing layer height, with afternoon levels influenced by evaporative input, particularly at EROS, as indicated by temperature-dependent behaviour of NO_x-corrected concentration (see Section 3.2).

At BROS, Flt and Pyr seem to follow a characteristic traffic pattern. However, at EROS, the relatively shallow decline during the daytime, and rapid increase during the afternoon from these compounds suggests the influence of an additional local daytime source, possibly volatilisation from surfaces.

HMW PAHs (5+ ring) are shown to display the most pronounced morning rush hour peaks and daytime declines of the PAHs measured. Since these compounds are not expected to display significant reactive losses, this trend is expected to mostly indicate the impact of traffic flow variation between morning and daytime.

However, afternoon concentrations are not shown to increase in correspondence with afternoon rush hour, suggesting that afternoon traffic may have a minimal impact on the PAH profile and afternoon increases observed for more volatile LMW compounds is due to contribution from evaporative input. Fine *et al.* (2004) observed a diurnal profile for particle-bound BPy in Los Angeles and Riverside, USA very similar to that of this study.

Reisen and Arey (2005) investigated diurnal variations of PAH and NPAH levels to assess atmospheric reactivity by sampling over four time periods (morning, day, evening and night) in

California, USA. It was shown that, in summer, PAH concentrations clearly decrease during the day and evening periods, in agreement with the observation in the present study.

While the diurnal pattern of PAH is likely to reflect relative source strength and photostability of compounds (Dachs *et al.*, 2002; Souza *et al.*, 2014; Wu *et al.*, 2010), the interpretation of OPAH and NPAH diurnal patterns is more complex, due to the potential influence of secondary input from atmospheric reactivity for some compounds. For example Souza *et al.* (2014) measured the diurnal profile PAH, OPAH and NPAH in PM in Sao Paulo and indicated that direct emission from vehicles influence concentrations of these compounds, but photochemical production contributes to levels of NPAH and OPAH and photolysis of NPAH is also a significant loss process.

All for OPAH compounds measured concentrations display a morning peak in concentrations and a decline throughout the day at BROS. However, it should be noted that this daytime decline is less pronounced than for HMW PAHs and NPAH compounds. The relatively low concentrations during the afternoon may be consistent with the relatively low impact of afternoon traffic at these sites but may also indicate daytime concentrations are higher than expected due to additional input from reactivity and/or volatilisation. The temperature dependence of NO_x-corrected concentrations might suggest the latter for 9F, AQ, MAQ (Section 3.2).

For 9F, AQ and MAQ, highest levels at EROS are observed during the daytime period, suggesting a deviation away from a traffic-mediated profile. While NO_x-corrected MAQ displays positive correlation with temperature, this relationship is not observed for 9F and AQ. This might suggest MAQ concentrations are influenced by volatilisation during the day at EROS while reactive input is a more important factor contributing to 9F and AQ levels at EROS during the day.

1NNap and 2NNap levels display a morning rush hour peak at BROS with a relatively steep decline in concentrations during the day. The decline is notably more pronounced for 1NNap than 2NNap, which is attributed the faster rate of photolysis for 1NNap.

At EROS, the profiles display an increase (1NNap) and relatively low decrease (2NNap) in concentration between morning and daytime, which may indicate an additional source, possibly

from reactive or evaporative input, is influencing the concentrations of these compounds. A positive correlation between temperature and NO_x-corrected concentration is noted for 1NNap but not 2NNap at EROS.

1NPyr and 9NAnt are expected to be most prevalent in diesel exhaust emissions and are likely to represent a traffic-related pattern for particle-phase NPAHs. These compounds display similar patterns at BROS and EROS with a peak in the morning period followed by a steep decline during daytime.

Kameda *et al.* (2004) investigated the diurnal pattern of 1NPyr concentration in Osaka, Japan and observed higher concentrations during the morning and late evening, when traffic levels were higher. The lack of a significant increase in concentrations during the afternoon may be due to a minimal afternoon traffic impact at these sites, as observed with HMW PAHs. 1NFIt, 3NFIt, 6NChr and 7NBaA display similar trend, indicating a similar traffic-related behaviour.

At BROS, reaction product compounds 2NFIt and 2NPyr display a similar traffic-related pattern to other NPAH, indicating that levels of these reaction product compounds is dictated predominantly by the primary input of precursor PAH compounds and reactive input is not significant that this site relative to the strength of primary emissions. However, the daytime decline in concentration is lower than observed for 1NPyr or 3NFIt, possibly indicating the impact or reactive or evaporative input of these compounds at BROS.

At EROS, highest 2NFIt and 2NPyr concentrations are observed during the daytime period, when OH radical concentration is expected to be highest, suggesting reactive input is an important factor. The diurnal profile of 2NFIt and 2NPyr have been shown to closely follow the measured concentration of OH, with highest concentrations observed during the daytime (1100-1500) period (Tsapakis and Stephanou, 2007). Kameda *et al.* (2004) also observed a significant ($p < 0.05$) correlation between 2NFIt and estimated OH concentrations during a diurnal study.

A number of studies have noted lower levels of PAH, OPAH and NPAH during the day compared with nighttime levels or a rapid decline during the daytime or afternoon, which is attributed to rapid

photodecomposition (Ciccioli *et al.*, 1996; Hien *et al.*, 2007; Ringuet *et al.*, 2012a; Tsapakis and Stephanou, 2007; Wu *et al.*, 2010; Zielinska *et al.*, 1989). The relatively steep decline in NPAH concentrations during the day, in comparison with PAH and OPAH during the day, may indicate the relatively rapid photolytic loss for these compounds.

4.2. NO_x-corrected diurnal profiles

In an investigation of PAH and NPAH diurnal patterns in California, USA by Reisen and Arey (2005) normalised observed concentrations to CO levels (used as a traffic marker) to compensate for variation in ABL height during the diurnal cycle and the dilution of traffic-generated emissions between urban and suburban sites. It was shown that normalising the PAH and NPAH levels removed much of the traffic- or mixing height- mediated profile and allowed closer insight into the processes driving the short term variations in concentrations. In this study NO_x was used as a traffic marker to normalise the PAH, OPAH and NPAH concentrations as data for CO were not available. Normalised diurnal profiles for a number of selected PAH, OPAH and NPAH are presented in Figure 5.3.

It is notable that highest normalised concentrations of the LWM (3-4 ring) PAHs (e.g. Phe, Flo, Acy, Pyr and Flt) are highest during the daytime and/or afternoon periods at both sites, when temperature is shown to be highest. This indicates the potential importance of temperature-driven volatilisation from soil, vegetation or road surfaces on the concentrations of these compounds at these sites. It is suggested, therefore, that while direct emissions of road traffic is likely to govern the concentrations of these LMW PAHs, local input will also be an important factor, particularly in warmer conditions.

For HMW compounds, the observed diurnal trend is either removed (e.g. IPy, BPy) or unchanged (e.g. BaP, BeP) suggesting these compounds are not influenced significantly by reactive loss or evaporative input. Interestingly, for OPAH compounds, highest normalised concentrations are observed during the daytime period, when the intensity of solar radiation is highest. This indicates

the influence of surface volatilisation and/or input from atmospheric reactions of PAH with OH radicals or O₃, consistent with the un-normalised traffic pattern observed for these compounds.

For NPAH, compounds more closely associated with diesel exhaust (e.g. 1NPyr and 9NAnt) show highest normalised concentrations at BROS during the morning rush hour period, with much lower levels at EROS and during other periods of the day. This indicates the diurnal behaviour of these compounds is governed predominantly by the strength of road traffic source and relatively rapid photodegradation during the day, with minimal impact of other sources such as heterogeneous reactivity of parent PAH.

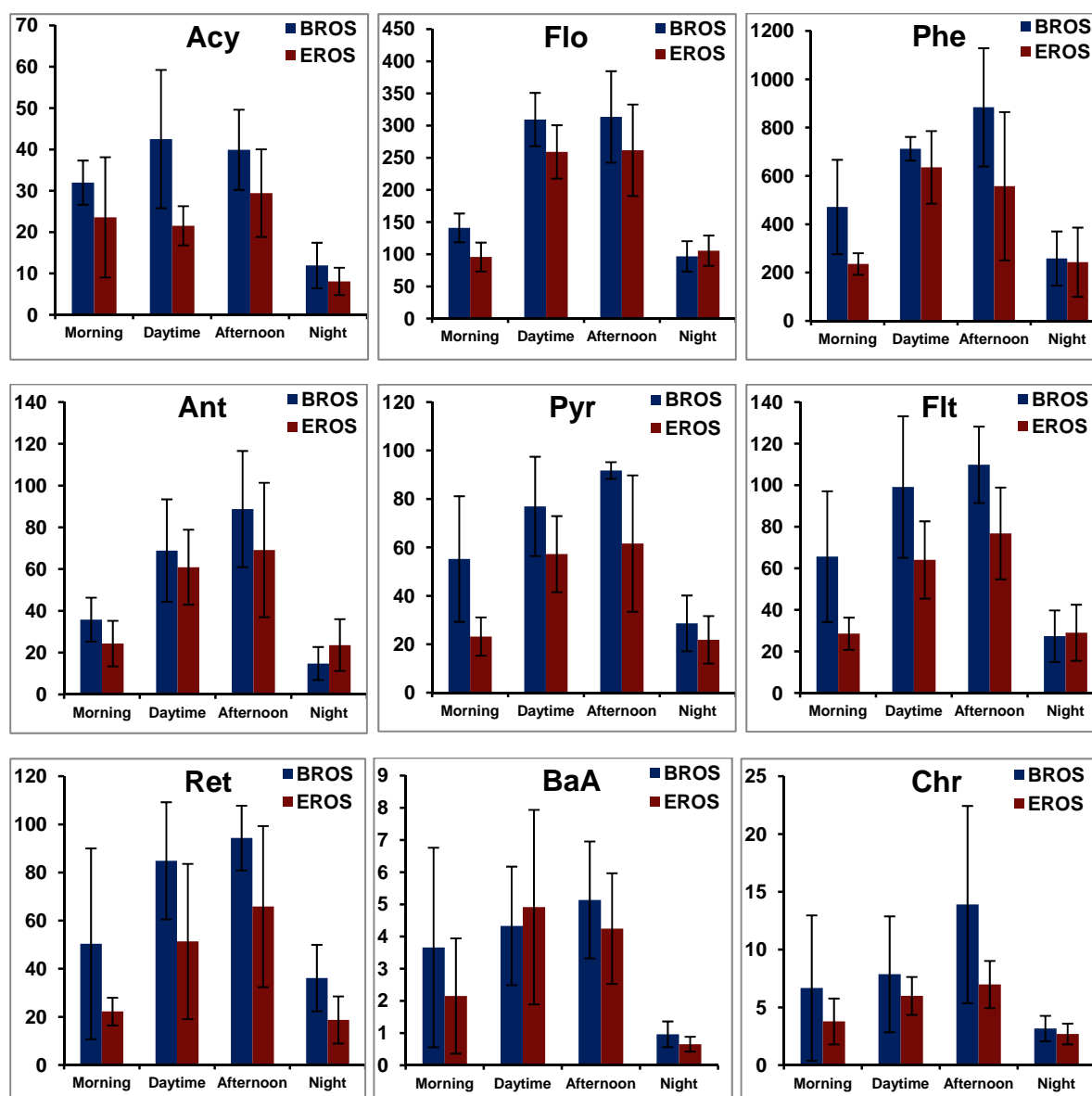


Figure 5.3. NO_x-corrected diurnal concentration profiles for key PAH, OPAH and NPAH compounds.

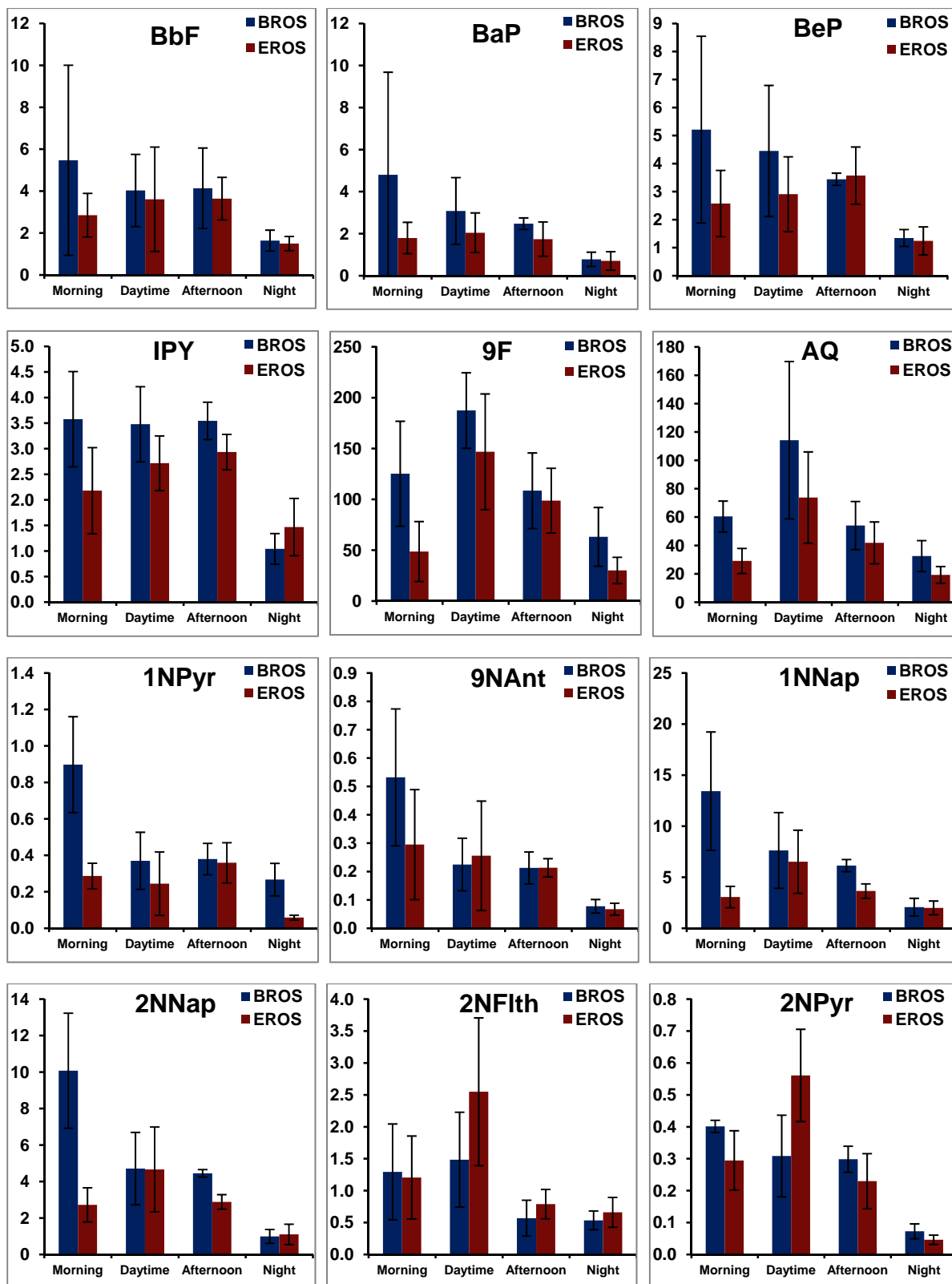


Figure 5.3 (cont). NO_x-corrected diurnal concentration profiles for key PAH, OPAH and NPAH compounds.

A broadly similar trend in the normalised profile of 1NPyr was observed by Reisen and Arey (2005) in Los Angeles and Riverside, USA, suggesting urban and suburban areas display similar behaviour for marker compounds of diesel traffic emissions.

NNap compounds display a similar normalised profile to those of 1NPyr and 9NAnt, with peak concentrations during the morning rush hour and lower concentrations during the daytime and afternoon. This would suggest the profiles of these compounds are more dominated by traffic-generated input and photolytic loss, with a minor contribution from atmospheric reactions. However, it should be noted that at EROS, while concentrations of 1NPyr and 9NAnt decrease between morning and daytime, an increase in concentration is observed for NNap compounds over this period. This may indicate an influence of OH reactivity between sites influencing the concentrations of 1NNap and 2NNap at the background site.

Normalised concentrations of 2NFIt and 2NPyr are highest at EROS during the daytime period, consistent with the profiles in Figure 5.2. This suggests that while reactive input from OH-initiated input is not significant at the traffic site, the contribution of reactions between sites leads to relatively high 2NFIt and 2NPyr concentrations at EROS. However, it should also be noted that temperature-driven volatilization may also influence concentrations of these compounds at EROS. The normalised concentrations of 2NFIt and 2NPyr are relatively low at both sites at night. This suggests that the influence of NO₃ reactions on the levels of these compounds at night may be minimal.

It is interesting to note that Reisen and Arey (2005) observed peaks in NNap, 2NFIt and 2NPyr normalised concentrations in Riverside during the night, indicating NO₃ reactivity was occurring between Los Angeles and this background site. This may be due to the much greater distance between 'polluted' and 'background' sites in this previous (~90km) and present (~1km) study, allowing increased time for reactions to occur and a much greater reduction in NO concentrations in the atmosphere.

4.3. Assessing role of PAH degradation and reactive input of NPAH and OPAH

4.3.1. PAH degradation

It is considered that OH reactions will be the dominant loss process influencing LMW PAHs in the atmosphere (Atkinson and Arey, 1994; 2007; Keyte *et al.*, 2013).

Arey *et al.* (1989a) measured 12-hr daytime and night time concentrations of LMW PAHs during a photochemical air pollution episode in the Los Angeles Basin. The nighttime/daytime concentration ratios were shown to correlate with the laboratory-derived second order OH radical reaction rate coefficients (see Appendix 1), for example with the largest ratios being observed for PAHs that display the highest rate coefficients for OH reactions, such as Acy and Ace. This indicates the occurrence of OH-induced reactions occurring in the atmosphere at similar rates to those predicted by laboratory-derived kinetics data. Furthermore, Dachs *et al.* (2002) estimated OH rate coefficient values based on daytime and nighttime PAH profiles, which were in good agreement with literature values.

Similarly, a linear correlation has been observed between the OH reaction rate coefficients for Nap, methyl-Nap, ethyl-Nap and dimethyl-Nap compounds and both corresponding nighttime/daytime concentration ratios measured in Riverside, USA (Phouongphouang and Arey, 2003b) and morning/daytime concentration ratios measured in Los Angeles, USA (Reisen and Arey, 2005). The slope of the latter trend was shown to be steeper in summer compared to winter, providing further evidence for the dominant role of OH reaction chemistry on the observed degradation of PAHs in the atmosphere.

While the annual mean BROS/EROS concentration ratios have been shown to agree well with OH reactivity rates (Section 3.6), no correlation was observed between OH reaction rate coefficients and nighttime/daytime or morning/daytime concentration ratios at either site for the diurnal samples. This may partly be explained by the close proximity of these sites to a local traffic source which dominates the observed PAH diurnal profiles. Additionally, as discussed above, the levels of LMW PAHs may be influenced by local input from local temperature-driven volatilisation from surfaces at

both sites. This may affect the concentrations of compounds during the day to differing degrees and potentially mask the influence of OH-initiated degradation.

It should also be noted that the previous studies were conducted in California, where the meteorological conditions are likely to be more conducive to atmospheric reactivity. For example the study by Arey *et al.* (1989) was conducted during a photochemical pollution 'episode' and other O₃ concentrations in previous studies ranged between 40-140 ppb (Phousongphouang and Arey, 2003b; Reisen and Arey, 2005) compared to a maximum level of 40 ppb in the present study. The oxidising potential of the atmosphere in these previous studies is therefore likely to have been much higher than in the present study.

4.3.2. 2NFlt/1NPyr and 2NFlt/2NPyr Ratios

The reaction source marker ratios of 2NFlt/1NPyr and 2NFlt/2NPyr were calculated for the samples in Campaign 3 to assess the potential influence of OH and NO₃ reactivity over the diurnal cycle. The mean ratios for each time period are shown in Figure 5.4.

The 2NFlt/1NPyr ratio at BROS is shown to be low (<5) throughout the diurnal cycle, indicative of vehicular traffic emissions dominating over secondary input at this site. However, at EROS, the ratio was shown to be relatively high (>9) during the daytime (1100 – 1600) and night (1900 – 0700) periods, possibly indicating the greater influence of both OH and NO₃ reactivity at the background site. Similarly, noted 2NFlt/1NPyr values <5 at a traffic site and >5 at a suburban site in both daytime and nighttime samples.

2NFlt/2NPyr ratios are low (<7) at both sites during morning, daytime and afternoon periods. This is consistent with negligible influence of NO₃ reactivity during daylight hours. This is also consistent with the yield ratio from OH reactivity (assuming identical levels of Flu and Pyr in the air) of 2NFlt/2NPyr = 6 (Atkinson and Arey, 1994).

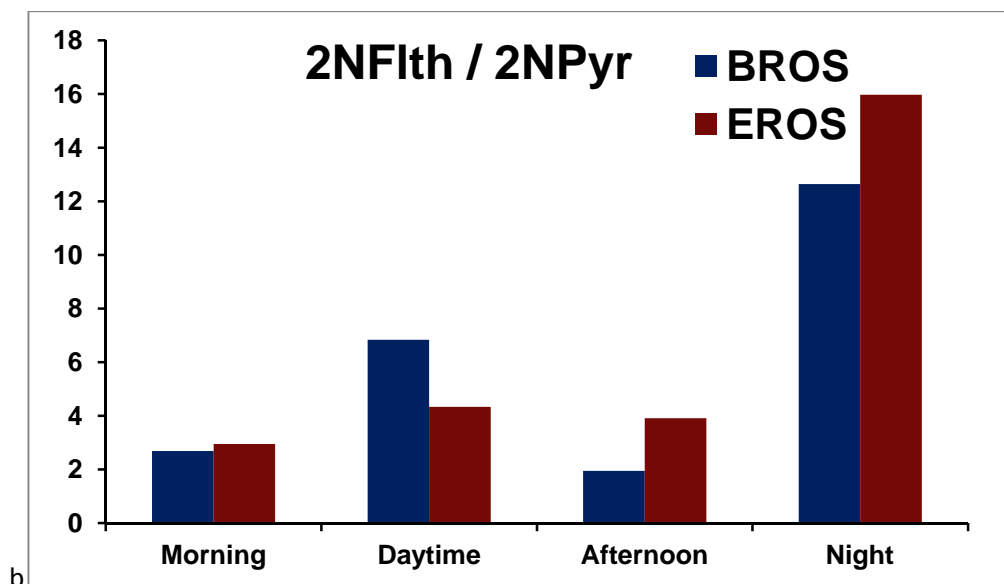
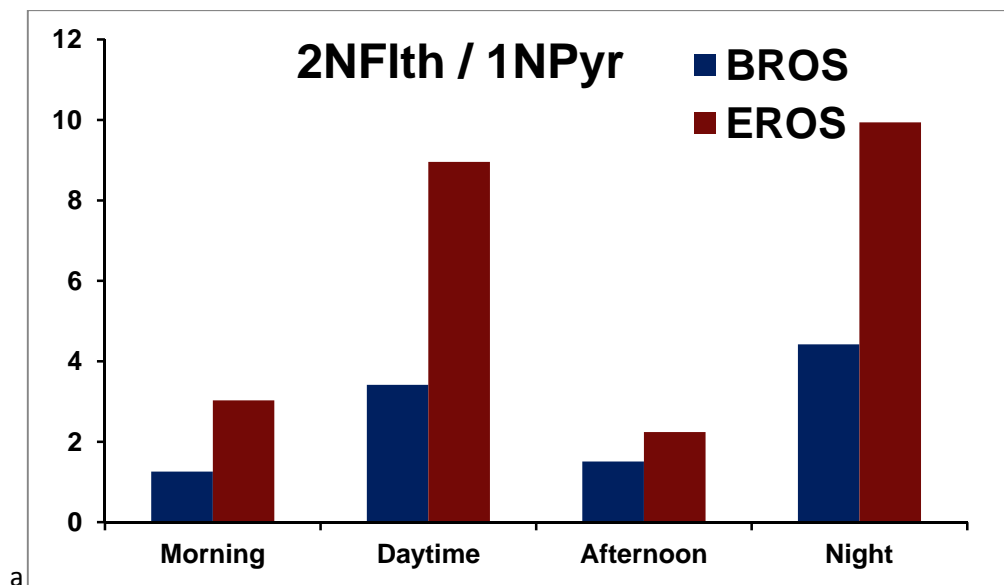


Figure 5.4. The diurnal profile of NPAH isomer ratios a) 2NFIth / 1NPyr and b) 2NFIth / 2NPyr measured at BROS and EROS.

The ratio is higher (>12) at both sites during the night indicating NO₃ reactivity can play a more important role at night when the concentrations of this species will be higher due to absence of sunlight and lower levels of NO. The higher ratio at EROS relative to BROS may indicate the occurrence of NO₃ reactivity between sites.

However, overall the role of NO_3 is not significant at these sites, as indicated previously in urban (Feilberg *et al.*, 2001; Marino *et al.*, 2000; Wang *et al.*, 2011a), suburban (Ciccioli *et al.*, 1996) and background (Tsapakis and Stephanou, 2007) sites. However, much higher ratios have been noted in other studies during summer months in urban and suburban sites (Albinet *et al.*, 2008a; Bamford and Baker, 2003; Reisen and Arey, 2005; Ringuet *et al.*, 2012a).

5.3.3. Reactant/Parent Ratios

The ratios of OPAH or NPAH 'product' to PAH 'parent' for the diurnal samples were also assessed. The ratios calculated during each time period at the two sites are presented in Figure 5.5. OPAH/PAH ratios are generally higher at BROS relative to EROS during most time periods indicating 9F and AQ are more strongly associated with primary vehicular emissions at the traffic site than at the background site.

The decline in 9F/Flo ratio from morning rush hour peak throughout the daytime period at BROS is likely to reflect the traffic-related profile of both compounds. The increases in 9F/Flo, 9F/Phe and AQ/Ant during the daytime period at EROS may be a reflection of OH-generated input (and/or reaction with O_3 in the case of AQ) during the period of maximum solar radiation and high O_3 concentrations.

However, AQ/ NO_x and 9F/ NO_x displayed a significant ($p > 0.01$) correlation with temperature, indicating the possible input from resuspension or volatilisation from surfaces at this site. However it should be noted that Flo, Phe and Ant also displayed this trend. The distinction between reactive and evaporative input at BROS is therefore unclear from these profiles.

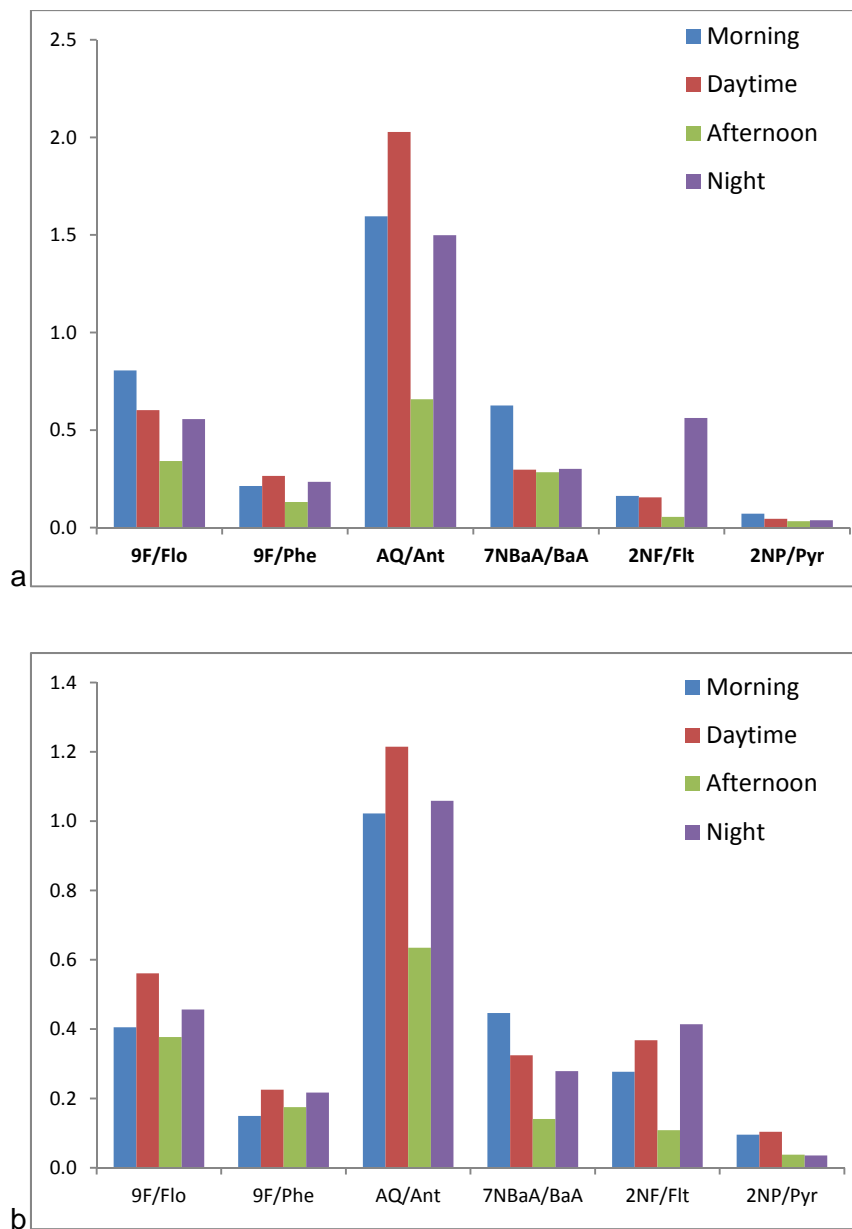


Figure 5.5. Mean ratios of ‘reaction product’ OPAH and (NPAH x10) to ‘parent’ PAH in diurnal samples at BROS (a) and EROS (b).

Observed nighttime increases in OPAH/PAH ratios at both sites may indicate the influence of NO_3 reactions which have been shown to produce 9F from Phe (L Wang *et al.*, 2007b) and Flo (Kwok *et al.*, 1997) in the gas phase and AQ from Ant (Zhang *et al.*, 2011) in the particle phase.

The NPAH/PAH ratios are shown to be higher at EROS than BROS during the daytime, indicating a greater reactive input at the background site, consistent with samples at this site representing a

more 'aged' air mass. The lack of an increase in NPAH/PAH ratio between morning and daytime at BROS indicates a less significant input from OH-initiated reactions at the traffic site.

At EROS, ratios were higher during daytime than morning, indicating the formation of 2NFlt and 2NPyr during the period when OH concentrations are likely to be highest. However, as with OPAH/PAH, the ratios at EROS are likely to be influenced by volatilization of PAH and NPAH compounds from surfaces making the distinction between reactive and evaporative input more complex.

At both BROS and EROS 2NFlt/Flt ratios display a marked increase at night, indicating the influence of NO₃-initiated input of 2NFlt during this period. The lack of increase in 2NP/Pyr during the night is consistent with the observation that 2NPyr does not result from NO₃ reactions, in contrast to 2NFlt. Similar diurnal variability in these NPAH/PAH ratios was observed by (Wei *et al.*, 2012) at sampling sites in southern China where 2NFlt/Flt shown to be higher during the night than during the day in summer and the converse trend was noted for 2NPyr/Pyr.

Interestingly, Wei *et al.* (2012) noted much higher 7NBaA/BaA ratios at night than during the day. The authors indicated this may be due to a strong night-time emission source of 7NBaA rather than due to atmospheric reactivity. In this study, this ratio strongly indicated the dominance of morning emissions of 7NBaA, suggesting this compound is primarily emitted from road traffic, in contrast to the seasonal (Section 3.3) and traffic (Section 3.1) patterns. The origin of this NPAH compound is therefore rather unclear.

Chapter 6. Concentrations of PAHs, OPAHs and NPAHs in the Queensway Road Tunnel

6.1. Tunnel concentrations of PAHs, OPAHs and NPAHs

Details of the samples taken in Campaign 3 are provided in Table 2.1. Mean concentrations of PAHs, OPAHs and NPAHs measured in the Queensway Road Tunnel during Campaign 3 (calculated by subtracted corresponding EROS concentration from measured tunnel concentration), and the proportion of each compound present in the particle-phase, are presented in Table 6.1. A comparison with concentrations measured simultaneously at EROS is provided.

The relative proportions of PAHs, OPAHs and NPAHs present in the tunnel were broadly similar to those measured at the ambient roadside location BROS (see Section 3). Since it is assumed that road traffic is the only source influencing levels in the road tunnel, this indicates that traffic is the dominant source of most of these compounds at BROS also.

6.1.1. PAH and OPAH concentrations

EROS-corrected tunnel concentrations of PAHs and OPAHs in the Queensway Road Tunnel, and their distribution between the gas-phase and particle-phase are shown in Figure 6.1 and 6.2 respectively. LMW PAHs (MW<203) comprised ~93% of total PAH mass, with concentrations ranging from 3.3 ng m⁻³ (Ace) to 81 ng m⁻³ (Phe). HMW (MW>228) PAHs were present at much lower levels, with concentrations ranging from 0.1 ng m⁻³ (DBA) to 0.9 ng m⁻³ (BPy).

Concentrations of the OPAHs measured in the tunnel were lower than their corresponding semi-volatile 3-4 ring PAHs. 9F was the dominant OPAH compound measured with lower levels of AQ and MAQ. BaAQ was present at very low concentration, indicating a relatively low traffic input of this compound. 9F was observed predominantly in the gas phase, while AQ, MAQ and BaAQ were present mainly in the particulate-phase.

Table 6.1. Mean±standard deviation of PAH, OPAH and NPAH concentrations measured in the Queensway Road Tunnel and EROS during Campaign 3 (n=4)

PAHs	Mean Tunnel (ng/m³)	% particle-phase	Mean EROS (ng/m³)	% particle-phase
Acy	10±4	1	0.2±0.1	2
Ace	3±2	3	0.4±0.2	4
Flo	12±13	1	4±1.1	1
Phe	81±26	5	26±1.3	4
Ant	8±3	7	2±1	5
Flt	14±4	49	3±1	10
Pyr	11±4	67	4±0.6	11
Ret	0.8±0.3	67	2±0.3	18
BaA	1±0.3	72	0.1±0.01	69
Chr	2±0.7	70	0.1±0.03	75
BbF	0.8±0.4	88	0.4±0.2	71
BkF	1±0.5	79	0.2±0.04	72
BeP	0.8±0.3	90	0.1±0.04	77
BaP	0.9±0.4	91	0.1±0.02	80
IPy	0.8±0.4	95	0.2±0.1	78
DBA	0.2±0.2	65	0.1±0.1	91
Bpy	2±0.7	95	0.3±0.1	81
Cor	0.8±0.2	99	0.1±0.01	91
OPAHs	Mean Tunnel (ng/m³)	% particle-phase	Mean EROS (ng/m³)	% particle-phase
9F	7±3	18	0.3±0.1	6
AQ	4±1	94	0.3±0.1	61
MAQ	2±0.3	100	0.2±0.02	78
BaAQ	0.02±0.02	100	0.1±0.04	95
NPAHs	Mean Tunnel (pg/m³)	% particle-phase	Mean EROS (pg/m³)	% particle-phase
1NNap	1918±461	2	118±58	2
2NNap	980±820	3	135±103	2
2NFlo	94±85	95	13±10	50
9NAnt	294±165	88	34±16	59
1NFlt	19±24	75	13±15	79
2NFlt	9±11	100	11±4	83
3NFlt	18±16	95	1±0.4	76
4NPyr	8±1	89	2±1	80
1NPyr	343±157	96	5±3	86
2NPyr	15.2±8	86	6±5	81
7NBaA	2±3	94	1±1	96
6NChr	5±3	88	0.4±0.3	94

The high proportion of gas-phase LWM PAH (3-4 rings) relative to particulate phase HMW PAH (5+ rings) has been observed in previous tunnel air samples (Fraser *et al.*, 1998a; Khalili *et al.*, 1995) and emission studies of gasoline and diesel vehicles (Schauer *et al.*, 1999,2002; Zhu *et al.*,

2003; Zielinska *et al.*, 2004a; 2004b). However, previous studies have noted much higher proportions of 3-ring compounds Ace, Acy and Flo in gasoline and diesel emissions (Fraser *et al.*, 1998a; Khalili *et al.*, 1995; Zielinska *et al.*, 2004b), relative to 4-ring PAHs such as Flt and Pyr, than were measured in the present tunnel samples. In contrast, Schauer and co workers observed that levels of Ace, Acy and Flo were much higher than Flt and Pyr in gasoline emissions but were relatively lower in diesel emissions.

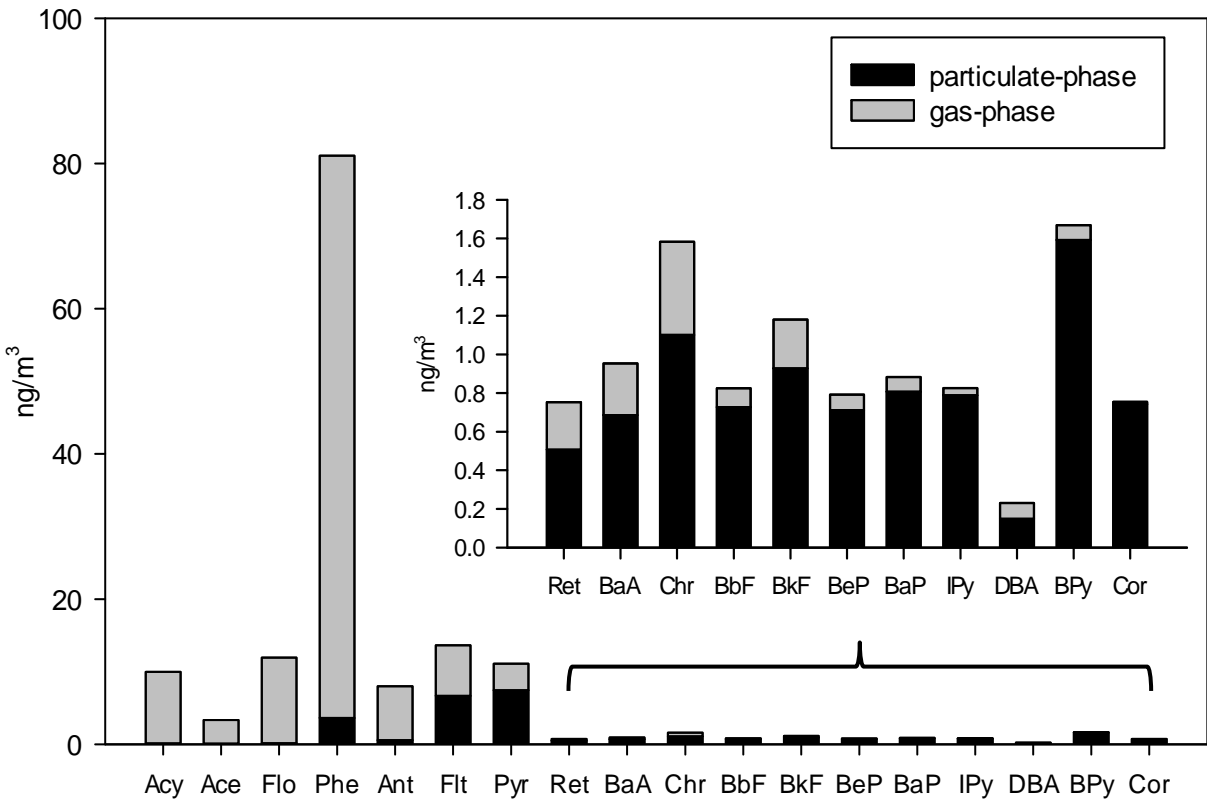


Figure 6.1. Mean PAH concentrations measured inside the Queensway Road Tunnel

Emission rates of OPAHs have also been measured previously in tunnel sampling studies (Fraser *et al.*, 1998; Oda *et al.*, 1998) and dynamometer studies of gasoline and diesel vehicles. Zielinska *et al.* (2004b) indicated that gasoline emissions produce higher levels of AQ and 9F than diesel

emissions. However, other emission studies have indicated that diesel emissions can produce higher levels of 9F than catalyst-equipped gasoline emissions (Schauer *et al.*, 1999, 2002).

Oda *et al.* (1998) measured particulate-phase emission factors for OPAHs from traffic in a road tunnel. They indicated that particulate-phase emissions of AQ were a factor ~2 higher than 9F and MAQ. This is consistent with the findings in the present study when only the particle phase sample is considered. It has been shown that 9F is present mainly in the gas-phase in tunnel samples (Fraser *et al.*, 1998), diesel emissions (Schauer *et al.*, 1999) and gasoline emissions (Schauer *et al.*, 2002), consistent with the Queensway Tunnel samples.

When gas-phase contribution is considered, the ratio of 9F to AQ in the present study was ~1.8. Other studies indicate higher ratios (~5-50) have been observed in tunnel measurements (Fraser *et al.*, 1998) and gasoline emission studies (Rogge *et al.*, 1993a; Schauer *et al.*, 2002; Zielinska *et al.*, 2004b). However it should be noted that lower 9F:AQ ratios have been noted for diesel emissions relative to gasoline emissions (Rogge *et al.*, 1993a; Zielinska *et al.*, 2004b). The relatively low 9F:AQ ratio measured in this study could therefore indicate a relatively higher contribution from diesel vehicles in the tunnel.

The parent PAH to OPAH ratio for Flo / 9F and Ant / AQ in the tunnel were ~1.7 and ~2 respectively. Lower ratios have been observed in gasoline and diesel emissions for both Flo / 9F (Rogge *et al.*, 1993a; Schauer *et al.*, 1999,2002; Zielinska *et al.*, 2004b) and Ant / AQ (Zielinska *et al.*, 2004b). However, much higher ratios have been noted in other tunnel studies where a mixture of vehicles is present (Fraser *et al.*, 1998a). It has been observed that PAH/OPAH ratios are higher for diesel emissions than gasoline emissions (Schauer *et al.*, 1999,2002; Zielinska *et al.*, 2004b).

6.1.2. NPAH concentrations

Measured concentrations of NPAH compounds in the Queensway Road Tunnel, and their distribution between the gas-phase and particle-phase are shown in Figure 6.3. 1 and 2NNAp

isomers were the most abundant NPAHs compounds measured, predominantly present in the gas-phase. The observed ratio of 1NNap/2NNap was ~1.8. This ratio is slightly higher than previously observed in the same tunnel by Dimashki *et al.* (2000).

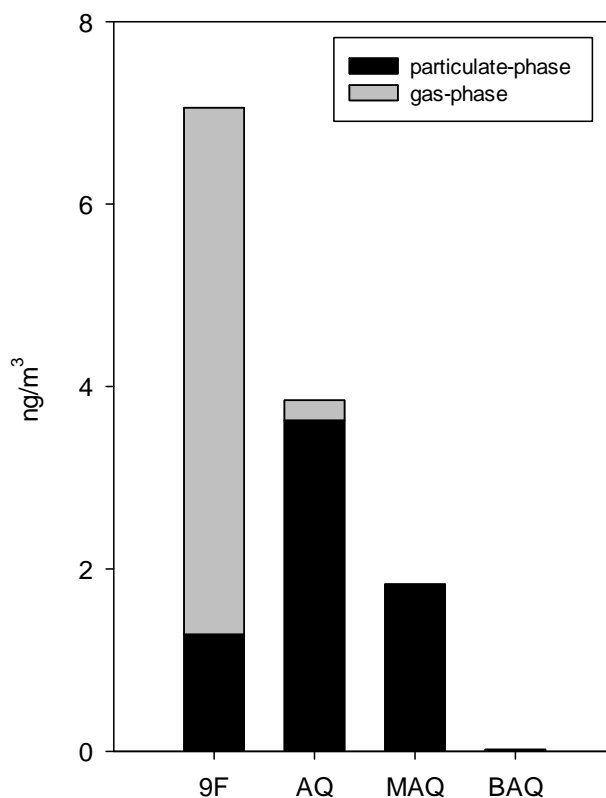


Figure 6.2. Concentrations of OPAH compounds measured inside the Queensway Road Tunnel in Campaign 3.

Direct vehicular emission data for NNAp compounds, and relative production of 1- and 2- isomers is lacking and is typically only available for particulate-phase emissions (Draper, 1986; Zhu *et al.*, 2003; Zielinska *et al.*, 2004b). Electrophillic nitration of Nap, likely to occur during the combustion process is expected to produce 1- and 2NNap at yields of 95% and 5% respectively (Ruehle, 1985). Therefore it would be expected for 1NNap to be present at much higher levels than 2NNap in diesel emissions. It is indicated by some studies that the 1NNap isomer is dominant in diesel

emissions (Zielinska *et al.*, 2004b) while others indicate emissions of 2NNap isomer can be higher (Ratcliff *et al.*, 2010).

1NPyr and 9NAnt are the dominant particle-phase NPAHs measured in the tunnel. These compounds have been identified as the two principal NPAHs present in diesel emissions (Campbell and Lee, 1984; Newton *et al.*, 1982; Paputa-Peck *et al.*, 1983; Ratcliff *et al.*, 2010; Schuetzle *et al.*, 1981; Schuetzle *et al.*, 1982; Zhu *et al.*, 2003; Zielinska *et al.*, 2004b).

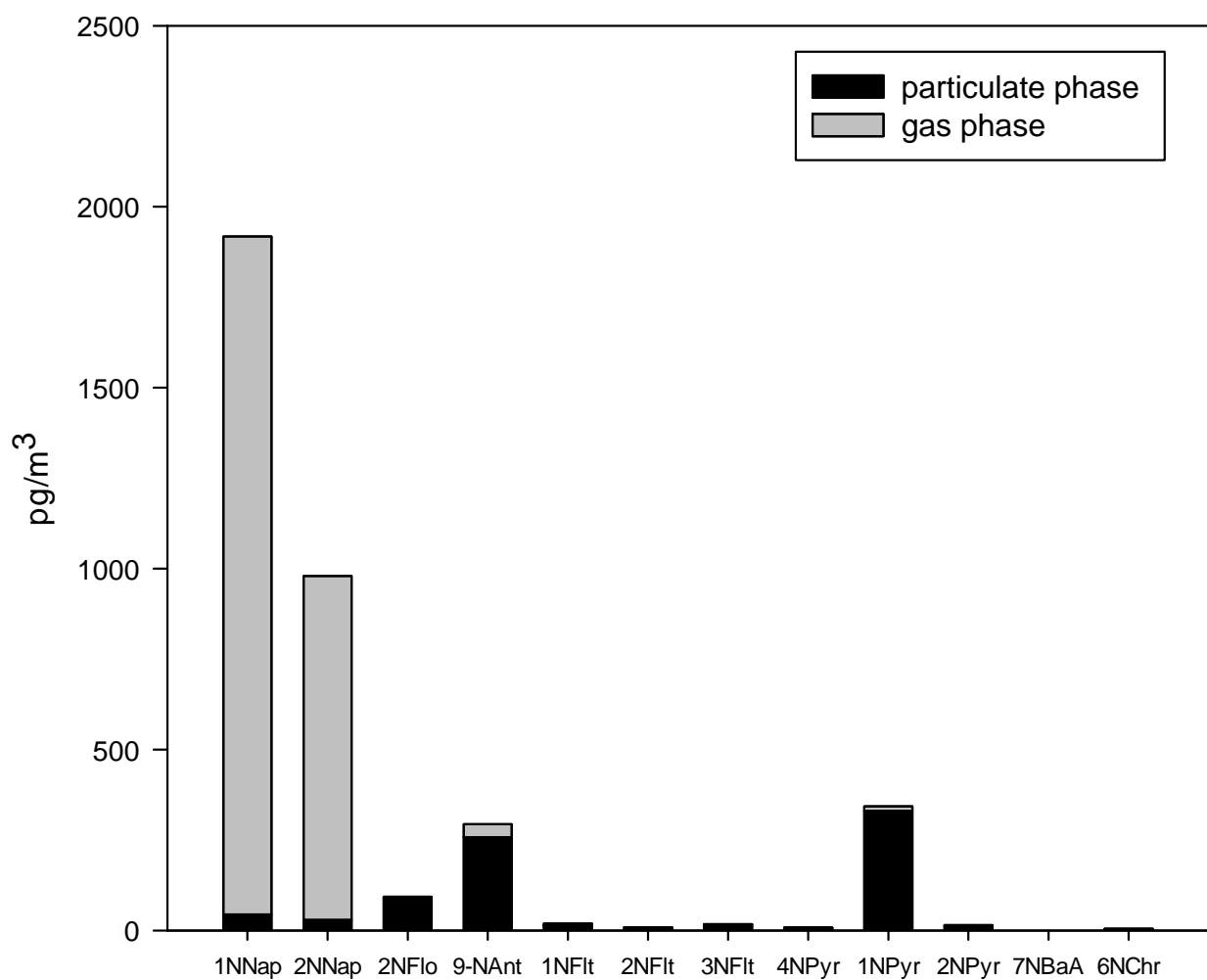


Figure 6.3. Concentrations of NPAH compounds measured inside the Queensway Road Tunnel in Campaign 3.

Dynamometer studies indicate diesel vehicles produce 1NPyr at levels a factor ~2 to 6 higher than 9NAnt (Zhu *et al.*, 2003; Zielinska *et al.*, 2004b). However in the present study, the two compounds are present at similar levels. This is consistent with samples previously collected in the same tunnel by Dimashki *et al.* (2000). Furthermore, 9NAnt has been observed at higher concentration than 1NPyr at high traffic locations in the ambient atmosphere (Albinet *et al.*, 2008a; Valle-Hernandez *et al.*, 2010).

2NFlo was present in the tunnel at levels a factor ~3 lower than 1NPyr and 9NAnt. No previous data on emission rates of 2-NFlo from vehicular traffic are available for comparison. Other NPAH compounds 1NFlt, 3NFlt, 4NPyr, 7NBaA and 6NChr were identified in the tunnel at much lower concentrations. These compounds are typically found in relatively low concentrations in diesel emissions (Zhu *et al.*, 2003; Zielinska *et al.*, 2004b).

2NPyr and 2NFlt are found in relatively low levels in the tunnel. These compounds are generally not observed in vehicular emissions and are the principal products of gas-phase (OH and/or NO₃ initiated) reactions of Pyr and Flth respectively (Atkinson and Arey, 1994). The low concentration of these compounds found in the tunnel is in agreement with previous measurements by Dimashki *et al.* (2000) and is consistent with the absence of direct sunlight and low oxidant concentrations resulting in negligible photochemical reactivity inside the tunnel. The relatively small amounts of these compounds observed in the tunnel can probably be attributed to the migration of air from outside of the tunnel.

However, the possible formation of gas-phase reaction products, 2NFlt and 2NPyr, as well as 1-NNap and 2-NNap inside the tunnel has been proposed (Dimashki *et al.*, 2000). This involves the possible dark formation of OH radicals via the rapid conversion of NO to NO₂ in diluted diesel exhaust (Shi and Harrison, 1997). This is further discussed in Section 6.3.

6.1.3. Comparison with other Tunnel studies

Many previous on-road emission studies have sampled only particle-phase PAH (Chen *et al.*, 2013; Eiguren-Fernandez and Miguel, 2012; Marr *et al.*, 1999; Miguel *et al.*, 1998; Phuleria *et al.*, 2006). Furthermore, a large number of studies report results in terms of PAH emission factors i.e. mass emitted per unit volume/weight of fuel consumed (Marr *et al.*, 1999; Miguel *et al.*, 1998) or unit distance of vehicle travel (Fraser *et al.*, 1998a; Kam *et al.*, 2012; Staehelin *et al.*, 1998).

Table 6.2 provides a comparison between PAH levels observed in the present study with three previous investigations that measured total (particulate- + gas-phase) PAH concentrations in road tunnel studies.

Pollutant concentrations in different locations can vary considerably due to differences in traffic fleet composition (e.g. relative level of gasoline- and diesel-fuelled vehicles), level of traffic congestion, fuel formulations, emission control measures (e.g. legislative requirements), tunnel characteristics (e.g. dimensions, level of ventilation) and meteorological conditions (e.g. relative humidity, temperature).

Benner *et al.* (1989) measured considerably higher levels of HMW (5+ ring) PAHs than in the present study and the other studies. This is consistent with the relatively higher proportion of gasoline-fuelled vehicles present in the vehicle fleet. Indeed, it was estimated that the vehicle fleet in the Baltimore Harbour Tunnel comprised >80% gasoline-fuelled light duty vehicles. Semi-volatile 3-4 ring PAHs were also present in high relatively high concentrations in this previous study, possibly due to the presence of a considerable proportion (>20%) of un-catalysed vehicles.

The levels of HMW PAHs are relatively low in the other studies. This suggests a lesser proportion of gasoline-fuelled vehicles and/or similar emission control technologies being utilized in these locations. However there is considerable variation in the relative levels of LMW (3-4 ring) species between studies.

Wingfors *et al.* (2001) indicated that levels of Phe and Ant measured in a road tunnel correlated with the proportion of diesel-fuelled HDVs present in the vehicle fleet. The estimated proportions of diesel HDVs in the relevant studies were <3% (this study; Amey pers. comm) ; 9% (Benner *et al.*, 1989); 8-24% (Wingfors *et al.*, 2001); and 47% (Ho *et al.*, 2009). This could therefore partly provide an explanation for the observed differences in the levels of Phe and Ant between these tunnel studies.

Table 6.2. Comparison of total (P+V) PAH concentrations and percentage of concentration in the particulate phase (%P) in different road tunnel measurements.

	This study ^a		Ho <i>et al.</i> (2009) ^b		Benner <i>et al.</i> (1989) ^c		Wingfors <i>et al.</i> (2001) ^d	
	ng/m ³	%P	ng/m ³	%P	ng/m ³	%P	ng/m ³	%P
Acy	10	1.2	645	0	nm	nm	12	4
Ace	3	3	1748	0	nm	nm	8	15
Flo	12	1.2	209	0.7	nm	nm	46	3
Phe	81	5	205	4	209	12	179	21
Ant	8	7	32	4	38	14	15	51
Flt	14	49	45	46	56	55	73	84
Pyr	11	67	45	59	58	51	87	87
Ret	0.8	67	nm	nm	nm	nm	0.3	100
BaA	1	72	5	99	8	99	3	100
Chr	2	70	8	74	14	85	4	97
BbF	0.8	88	1	100	11	100	1	100
BkF	1	79	0.3	100	11	100	0.1	100
BeP	0.8	90	0	n	5	100	1	100
BaP	0.9	91	1	100	6	100	1	100
IPy	0.8	95	0.2	100	5	100	0.5	100
DBA	0.2	65	0.3	100	nm	nm	0.2	100
BPy	2	95	0	nm	8	100	2	100
Cor	0.8	99	nm	nm	nm	nm	0.5	100

a – Queensway Road Tunnel, Birmingham; Sept 2012; estimated 89 000 vehicles per day

b – Shing Mun Tunnel, Hong Kong; Weekday noon samples; summer 2003; 53 000 vehicles per day.

c – Baltimore Harbor Tunnel, USA; 1985-86; mechanical ventilation; traffic flow unknown

d – Ludby Road Tunnel in Gothenberg, Sweden; April 2000; 20 000 vehicles per day

nm – not measured

No correlation with proportion of HDVs was found for other 3-4 ring species Ace, Acy, Flo, Flt and Pyr, which have been observed in relatively high concentrations in diesel emissions (Ratcliff *et al.*, 2010; Rogge *et al.*, 1993a; Schauer *et al.*, 1999; Zhu *et al.*, 2003; Zielinska *et al.*, 2004b). Differences in traffic numbers could potentially account for differences in observed concentrations of these PAHs.

It should be noted that estimated traffic flow for Queensway tunnel, as provided by engineering consultancy Amey, was ~4-5 and ~1.7 times higher than the tunnel studies by Wingfors *et al.* (2001) and Ho *et al.* (2009) respectively. The observation of lower concentrations of 3-4 ring species in this study compared with the other studies is therefore somewhat unexpected.

This could indicate the traffic flow in the Queensway Tunnel has been overestimated. Accurate daily traffic data is not available for the tunnel itself and traffic counts were not performed during sampling. Traffic counts, supplied by the Department of Transport are available for sites on the same road approximately 200m away at either end of the tunnel, Daily traffic counts in 2012 at these sites were ~75 000 and ~25 000 for roads to the south and north east of the tunnel respectively. Only an unknown proportion of the traffic at these sites is expected to have passed through the tunnel. It is assumed, based on the number of potential traffic routes/origins available, that the lower of these traffic counts will be a better approximation of tunnel traffic flow, thus strongly suggesting that the traffic count supplied by Amey is an overestimate.

Total PAH concentrations measured by Ho *et al.* (2009) were ~7 and ~20 times higher than the Wingfors *et al.* (2001) study and the present study respectively. Specifically, levels of Ace and Acy were considerably (60-600 times) higher. This was attributed to the high ratio of HDV diesel vehicles to gasoline vehicles present in the Ho *et al.* (2009) study, Indeed, the diesel emission factor was shown to be ~5 times higher than gasoline vehicles.

Wingfors *et al.* (2001) and Ho *et al.* (2009) derived emission factors for PAHs in road tunnels, based on measured PAH concentrations, traffic numbers, tunnel dimensions and wind speed. It can be seen in Figure 5.4 that a very good correlation ($R^2 > 0.9$) is observed between measured

concentrations in this study and the emission factors calculated by Wingfors *et al.* (2001). This is largely driven by high concentration and estimated emission factors for Phe. Correlation between these two data sets was weaker when Phe was removed ($R^2 \sim 0.77$).

It should be noted that, when the measured concentrations of Nap, 1MNap and 2MNap were included in this plot, a substantial discrepancy was observed between measured tunnel concentrations and the emission factors derived by Wingfors *et al.* (2001). This suggested the occurrence of significant evaporative loss of these 2-ring PAH compounds during sampling, as previously suggested by Atkinson and Arey (*pers. comm*). Therefore, these compounds are not considered in the results of this investigation, as detailed in Section 2.1.

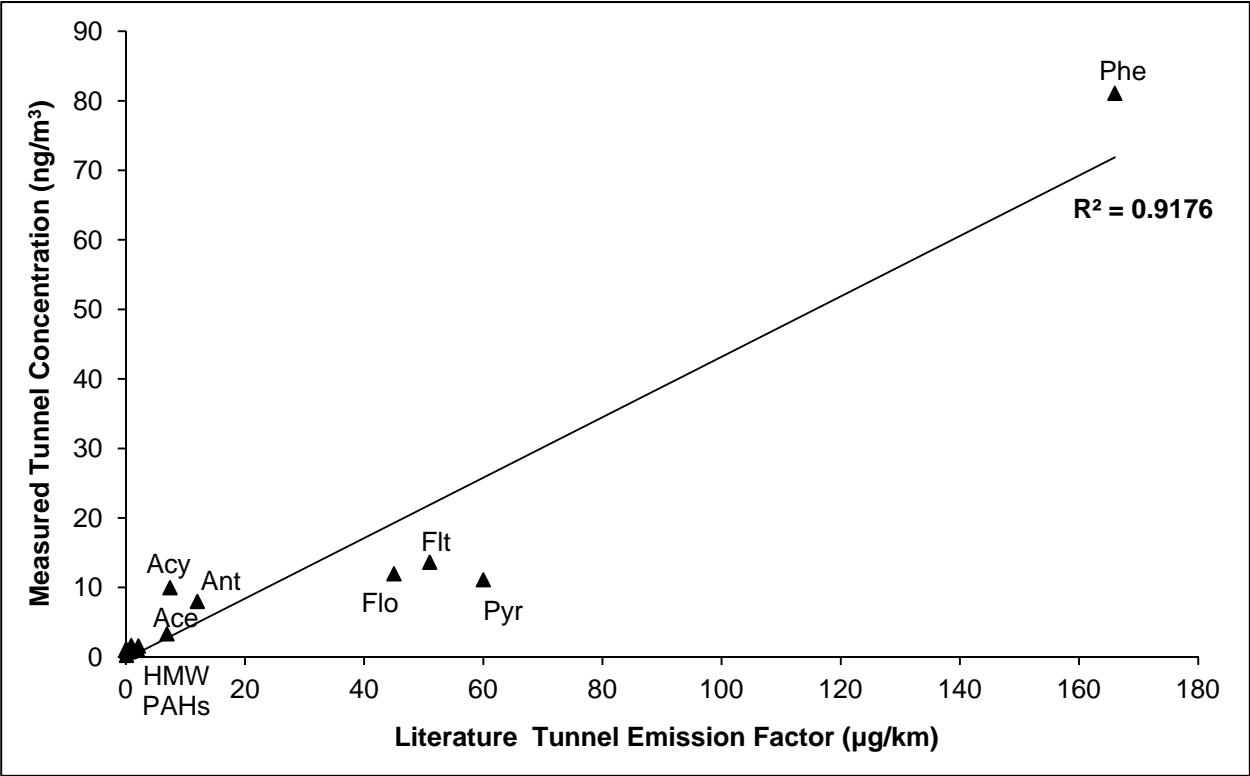


Figure 6.4. Comparison of measured PAH concentrations inside the Queensway Tunnel in the present study with tunnel emission factors derived by Wingfors *et al.* (2001)

The two tunnels were similar (vehicle speed limit of $\sim 70 \text{ km hr}^{-1}$, natural ventilation), and sampling techniques were identical. The good agreement between measured concentrations and previous emission factors indicates broadly similar traffic characteristics (vehicle types and fuel compositions) and emission controls measures are influencing both tunnels.

However, it can be seen that concentrations of Flo, Flt and Pyr measured in the present study fall below the expected level based on emission factors. This may be due to the higher proportion of diesel HDVs present in the Swedish tunnel. No correlation was found between measured concentrations in the Queensway Tunnel and the emission factors derived by Ho *et al.* (2009). This suggests very different traffic fleet composition, emission control measures and/or fuel formulations exist between the two location and this causes considerable differences in PAH emission profiles.

Measured concentrations of OPAHs and NPAHs in road tunnels are lacking in the literature. NPAHs were measured previously in the Queensway Road Tunnel in 1996 by Dismashki *et al.* (2000). Comparison between the two studies is discussed in detail below as this will provide an assessment of temporal changes in traffic sources.

Gorse *et al.* (1983) measured 1NPyr concentrations in the Allegheny Mountain Tunnel in Pennsylvania, USA in 1981. The maximum reported concentration was ~ 3 times lower than the mean concentration measured in the present investigation. Benner (1988) measured mean concentrations of $\sim 0.3 \text{ ng/m}^3$ for 1NPyr and 9NAnt in the Baltimore Harbour Tunnel in 1985, in good agreement with the levels observed in the present study. Given that the Baltimore Harbour Tunnel was artificially ventilated, while the Queensway Road Tunnel is not, the similar levels may result from a higher overall traffic flow in the previous study, differences in the relative proportion of diesel-fuelled vehicles and/or improved emission control technologies in the present study.

6.1.4. Gas-particle phase partitioning

Gas-phase compounds are shown to dominate the PAH burden in the tunnel environment, comprising $\sim 82\%$ of the total PAH mass. This is broadly consistent with ambient measurements at

roadside locations and in other tunnel measurements (see Section 3 ; Harrad and Laurie, 2005; Smith and Harrison, 1996; Benner *et al.*, 1989 ; Ho *et al.*, 2009; Fraser *et al.*, 1998, Khalili *et al.*, 1995).

For example, Wingfors *et al.* (2001) indicated that ~81% of PAHs in a road tunnel were emitted in the gas-phase. Zielinska *et al.* (2004b) also showed that the bulk of PAH emissions from gasoline and diesel vehicles are in the gas-phase. Furthermore, Khalili *et al.* (1995) observed that 92% of the measured PAH in a road tunnel in Chicago were 2-3 ring PAHs present in the gas-phase.

The relative level of PAH, OPAH and NPAH phase partitioning varies between tunnel and ambient measurements (see Table 6.1). For most LMW 3-ring compounds and HMW 5+ ring compounds, the proportion of compounds in the particle-phase in the tunnel is only slightly higher than that observed at EROS. However, semi-volatile compounds (e.g. Pyr, Flt, Ret, 9F, AQ, MAQ, 2NFlo) display markedly higher proportions in the particle-phase in the tunnel than in the ambient atmosphere. The phase partitioning behaviour of PAH, OPAH and NPAH as a function of compound MW is therefore markedly different for the tunnel and ambient samples (see Figure 6.5) with greater proportions of each compound class present in the particulate phase.

Higher particulate-phase contributions may reflect more dominant role of direct emissions from vehicles in the tunnel, which may be associated to a greater extent with fine particles (Albinet *et al.*, 2008b; Zielinska *et al.*, 2004a). Zielinska *et al.* (2004a) investigated phase partitioning of PAHs from diesel and gasoline vehicles. They found that Flt and Pyr were predominantly in the gas-phase when vehicles were idle or at low engine loads but at higher vehicle load, a much larger proportion of these compounds were present in the particulate phase, particularly for diesel vehicles. This could indicate vehicles in the tunnel were operating under relatively higher load, thus contributing to higher particulate concentrations of these compounds.

However, Ret has been shown to display an emission factor >250 times smaller than Flt and Pyr in a road tunnel (Wingfors *et al.*, 2001), and is typically a marker for wood combustion (Ramdahl, 1983). In this study Ret concentrations in the tunnel were lower than observed at EROS (see

Section 5.3). This indicates the dominant source of Ret is not road traffic and transportation of Ret from the ambient atmosphere outside the tunnel may be responsible for observed concentrations.

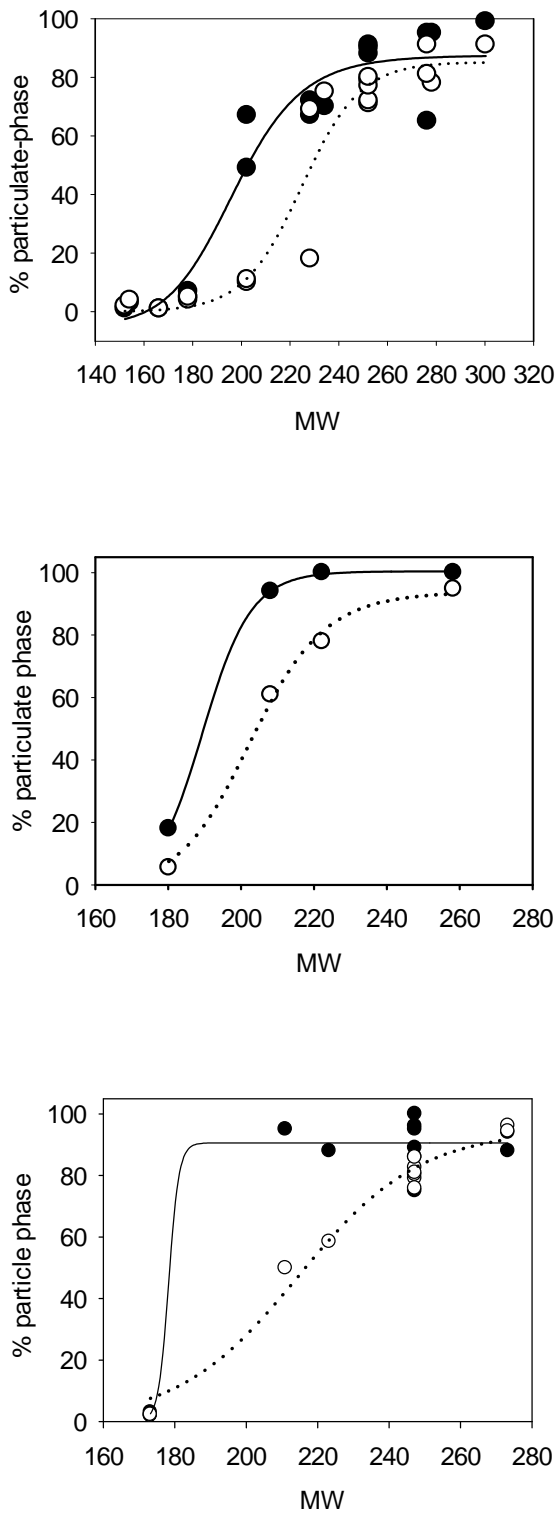


Figure 6.5. Plots of % of component in the particulate phase vs. molecular weigh for a) PAHs, b) OPAHs and c) NPAHs, measured in the tunnel (black dots, solid black line) and at EROS (white dots, dotted line).

If this is the case, it would suggest the tunnel environment (enclosed location, low ventilation rate and an assumed low, constant temperature) facilitates a more rapid partitioning of semi-volatile species to the particulate-phase than the ambient atmosphere (Kam *et al.*, 2012). Furthermore it is noted that the concentration TSP in the tunnel was ~4-5 times higher than the annual mean at EROS. Ambient measurements will represent a more 'aged' PAH profile with contributions from other combustion sources and variations in meteorological conditions (e.g. temperature) which may drive partitioning into the gas-phase.

Ho *et al.* (2009) and Benner *et al.* (1989) measured similar distribution of partitioning for 4-ring PAH in tunnel sampling studies. Wingfors *et al.* (2001), utilizing the same sampling technique as used in this study, found higher relative concentrations in the particle-phase for Flt and Pyr, with ~84% and ~89% measured in the particulate phase respectively, compared with 49% and 67% in the present study. This may be attributed to higher levels of TSP, which were ~6 times higher in the Swedish tunnel than in the present study.

As indicated in Section 4.1, PAH partitioning at EROS appears to be approaching equilibrium behaviour. However, the situation was more unclear in the case of NPAH and OPAH compounds.

The difference in partitioning behaviour between tunnel and ambient environments could possibly be attributed to compounds in the tunnel atmosphere representing a freshly emitted air mass where compounds have not reached partitioning equilibrium. To test this theory, as in Section 4.1, plots of $\log K_p$ vs $\log P_L^\circ$ were produced for both tunnel and EROS samples. While the slopes for EROS plots were each approximately -1, the plots for tunnel samples produced more variable slopes, ranging from -0.5 to -1.1. This variation in slope values and the relatively small number of samples taken in this campaign mean is unclear how the difference in equilibrium conditions influences the gas-particle partitioning of PAHs in the tunnel.

6.2. Temporal trend in PAH and NPAH concentrations

Previously sampling studies have measured concentrations of PAHs (Smith and Harrison, 1996) and NPAHs (Dimashki *et al.*, 2000) in the Queensway Road Tunnel. Comparing the results of these previous studies with the current study can therefore provide an assessment of changes in emission profiles and possible reasons for observed changes over time. Concentrations of OPAHs have not previously been measured in the tunnel.

6.2.1. Temporal trend of PAHs

A comparison of PAH levels measured in the tunnel in 2012 and 1992 and the relative decline in compound concentrations is shown in Table 6.3. It should be noted that both studies were based on a relatively small number of samples and Smith and Harrison (1996) collected ~2 hr samples at unspecified times so comparisons should be made with caution.

Table 6.3. Comparison of mean total (particulate + vapour) PAH concentrations measured in the Queensway Road Tunnel in 1992 (Smith and Harrison, 1996) and 2012 (present study).

	Tunnel concentration (ng/m ³)		% Decline
	1992 (n=8)	2012 (n=4)	
Acy	95	10	90
Ace	114	3	97
Flo	167	12	93
Phe	333	81	76
Ant	51	8	84
Flt	48	14	71
Pyr	55	11	80
BaA	14	1	93
Chr	26	2	94
BbF	13	0.8	93
BkF	5	1	88
BaP	13	0.9	93
IPy	22	0.8	96
DBA	4	0.2	95
BPy	35	2	95
Cor	12	1	94
ΣPAH	1122	158	86

The concentration of total PAH (comparing only the compounds measured in both studies) in 2012 was ~85% lower than that reported in 1992. The magnitude of concentration reduction varies considerably between individual PAH compounds. The majority of compounds (Ace, Flo and HMW compounds) exhibit a decline of >90% while Phe, Flt and Pyr exhibit a decline of <80%. The differences in relative concentration decline decrease between compounds has resulted in a notable change in relative contributions of individual compounds to the total PAH burden inside the tunnel (see Figure 6.6).

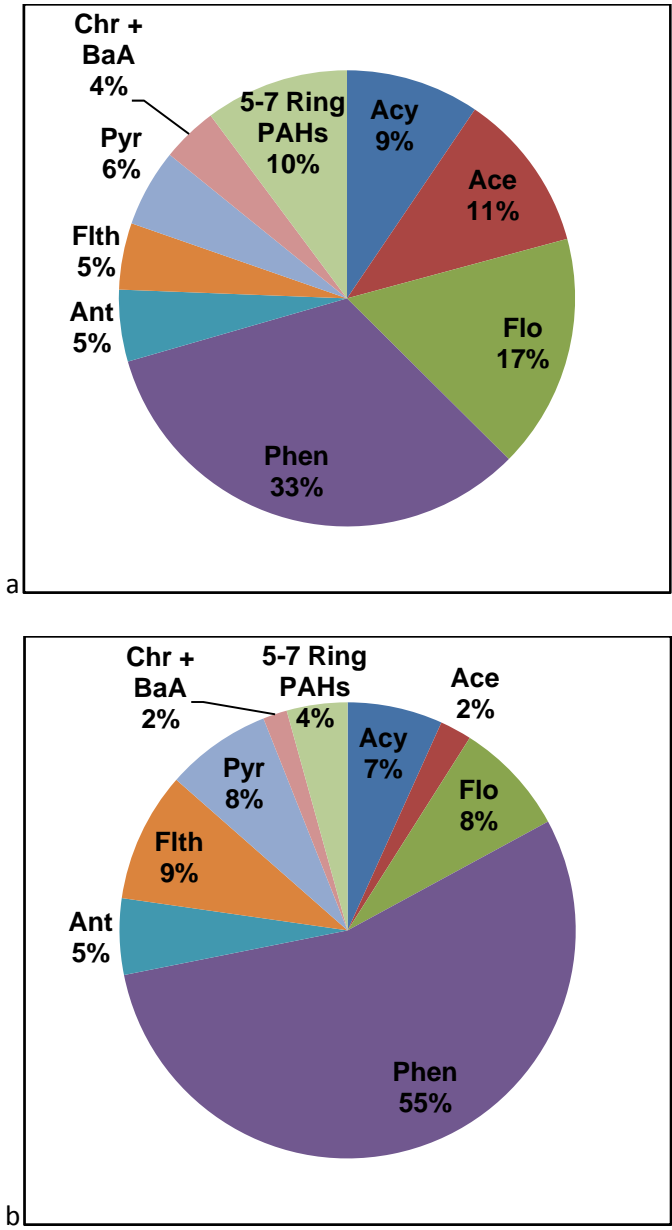


Figure 6.6. Contribution of individual PAHs to total PAH burden measured inside the Queensway Road Tunnel in a) 1992 (Smith and Harrison, 1996) and b) 2012 (present study).

The NAEI provides an estimate for emissions of individual PAH compounds from both gasoline- and diesel-fuelled urban vehicular traffic (Figure 3.9, Section 3.4). Estimated total emission decline from urban traffic over this time are shown to range from 23% and 70% for different PAHs with HMW compounds displaying more pronounced decreases than LMW compounds. It is indicated that the observed decline in PAH concentrations in the Queensway Road Tunnel between 1992 and 2012 is generally higher than predicted by the NAEI emission estimates.

However, emissions from gasoline vehicles only are shown to be relatively high (>65%) for most compounds over this time period. The relative reduction in diesel-fuel emissions over this time is shown to be generally lower and more variable between species. It should be noted that the emission inventory estimates are subject to a degree of uncertainty and that a national estimate may not be directly comparable with measurements in a specific traffic location.

Historical reduction in PAH levels have been reported previously in road tunnel studies (Benner *et al.*, 1989; Eiguren-Fernandez and Miguel, 2012). A number of factors have been shown to be responsible for reduction of PAHs from road vehicles. These include changes to fuel formulations (Westerholm and Egebäck, 1994) e.g. uses of biofuels (Ratcliff *et al.*, 2010) or use of additives to enhance the cetane or octane number (Williams *et al.*, 1986; Zhu *et al.*, 2003); innovations in engine design e.g. use of three-way catalysts (Rogge *et al.*, 1993a; Schauer *et al.*, 2002; Westerholm and Egebäck, 1994; Zielinska *et al.*, 2004b) and improvement in exhaust emission control measures e.g. particulate filters (Hu *et al.*, 2013), with their implementation being principally driven by increasingly strict government legislation (Perrone *et al.*, 2014). Other factors e.g. state of vehicle maintenance and ambient conditions (temperature) of the vehicle are also shown to influence PAH emissions from road traffic (Zielinska *et al.*, 2004b).

For example, Eiguren-Fernandez and Miguel (2012) calculated emission factors (EFs) for particle-phase PAH in the Caldecott Tunnel in Berkeley, California, where emissions from gasoline-fuelled LDVs and diesel-fuelled HDVs could be measured separately. EFs calculated were 9 and 17 times lower in 2004 than had been measured in the same tunnel in 1997 (Marr *et al.*, 1999) for HDV and

LDV vehicles respectively. This was attributed to reformulated gasoline fuel and removal of older, higher-emitting vehicles from the fleet over this period (Phuleria *et al.*, 2006).

The reduction of PAH levels on the Queensway Road Tunnel can be attributed, to a large degree, to the introduction of mandatory catalytic converters to the UK in 1993. Catalytic converters have been shown to reduce the emissions of PAHs in gasoline-fuelled vehicles by 92-99% and reductions in OPAHs by ~79-97% (Rogge *et al.*, 1993a; Schauer *et al.*, 2002; Westerholm and Egebäck, 1994; Zielinska *et al.*, 2004b). For example, Benner *et al.* (1989) measured PAH concentrations in the Baltimore Harbour Tunnel, USA, a factor 5-10 lower than a study conducted 10 years earlier (Fox and Stanley, 1976). This was attributed to the introduction of catalytic converters which were first used in the USA in 1974.

Figure 6.6 indicates that three compounds display an increase in relative contribution to total PAH burden in the tunnel; Pyr and Flt show relatively small increases while Phe which displays a larger increase. Other PAHs have reduced contributions compared with 1992 levels. The combined contribution of (Phe + Flt + Pyr) to Σ PAH burden has increased from ~44% in 1992 to ~72% in 2012.

The composition of the vehicle fleet has a major influence on the PAH emission profile. As discussed in previous sections, a large number of tunnel sampling and chassis dynamometer studies have identified the differences in PAH emission profiles for gasoline and diesel fuelled vehicles (Westerholm and Egebäck, 1994; Zielinska *et al.*, 2004b).

Gasoline-fuelled vehicles shown to emit higher levels of HMW compounds e.g. BaP, IPy, BPy, Cor (Marr *et al.*, 1999; Miguel and Pereira, 1989; Miguel *et al.*, 1998; Perrone *et al.*, 2014), while diesel is generally shown to be a greater source of semi-volatile compounds such as Phe, Flt, and Pyr (Chen *et al.*, 2013; Harrison *et al.*, 1996; Miguel *et al.*, 1998; Perrone *et al.*, 2014). The results presented here may therefore be indicative of a more important role of diesel emissions to the total PAH burden than was observed in 1992.

However, it has been indicated that different stages of EU legislation on new vehicle emission limits (91/441/EEC) has resulted in progressively reduced PAH emissions from both gasoline and diesel since 1993 (Perrone *et al.*, 2014). This may explain why, despite the stronger association with diesel exhaust, concentrations of LMW PAHs such as Phe have also decreased significantly, albeit to a lesser degree than gasoline-related compounds.

6.2.2. The driving force behind emission changes

The number of vehicles on the road in Great Britain increased by over 10 million between 1992 and 2012, mostly due to passenger cars, taxis and vans (DfT, 2014).

This period has also seen a notable shift in the relative distribution of gasoline- and diesel-fuelled vehicles in the traffic fleet (Figure 6.7). While there has been a modest (~500,000) decrease in the number of gasoline-fuelled cars in Great Britain since 1994, the number of diesel-fuelled passenger cars has increased by ~7.8 million. This trend has seen the relative proportion of diesel cars in the traffic fleet increase from ~7% in 1994 to ~33% in 2012 (DfT, 2014).

This change has largely come about because diesel-fuelled vehicles have become more popular. Diesel vehicles tend to display a superior fuel economy, therefore making them cheaper to run, as well as producing lower emission CO₂. Cars with lower CO₂ emissions fall into cheaper Vehicle Excise Duty (car tax) bands. This provides the consumer with a financial incentive to purchase diesel cars. Furthermore, the legally binding EU CO₂ emission targets give the car manufacturers further incentive to bring lower emission vehicles, such as diesel cars into the market at competitive prices.

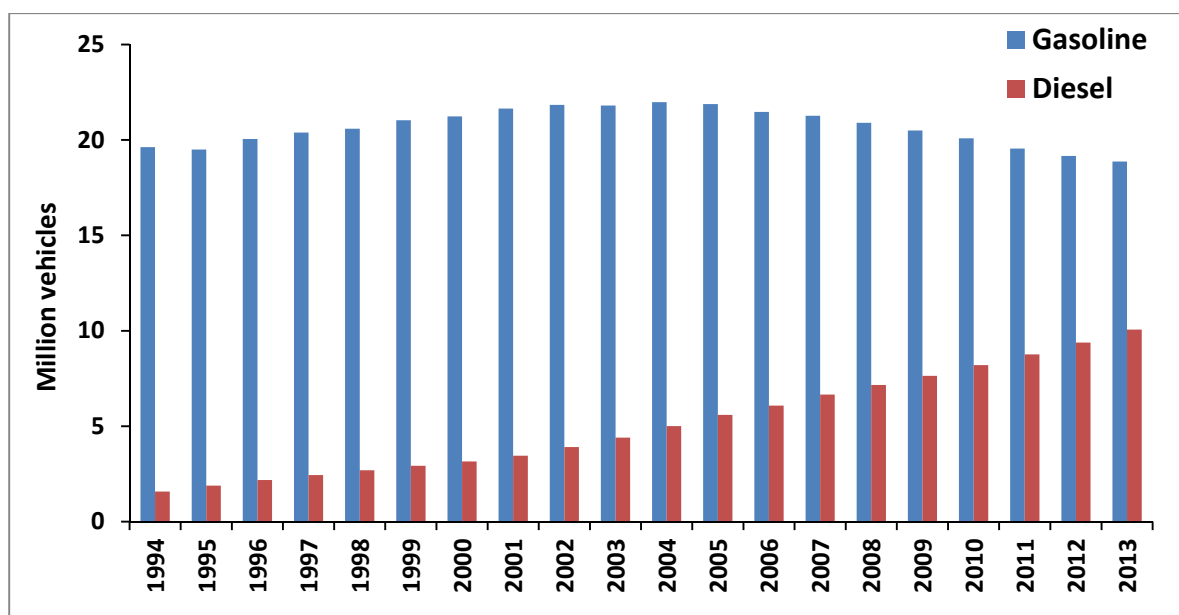


Figure 6.7. Total number of gasoline and diesel fuelled passenger cars licensed in Great Britain (Dft, 2014).

The trend in the number of gasoline and diesel vehicles on the road is reflected in national fuel sales. In the UK, sales of gasoline fuel decreased by ~43% between 1990 and 2011, from 33 billion litres to 19 billion litres. Meanwhile the sales of diesel fuel more than doubled over this period, from ~12 billion litres in 1992 to ~25 billion litres in 2011 (UKPIA, 2012). The results of the present study therefore indicate the increased role of diesel emissions on the overall and relative levels of different PAHs in the urban atmosphere. For example this may provide an explanation for the change in relative contribution of individual compounds such as Phe, Pyr and Flt to the observed in the Queensway Road Tunnel.

6.2.3. Temporal trend of NPAHs

A comparison in concentrations of four NPAHs measured in the present study and those measured by Dimashki *et al.* (2000) in 1996 is shown in Table 6.4. In contrast to the significant decline noted for PAH concentrations, little or no decline in concentration is noted for NPAHs. The mean levels of

NNap isomers measured in the tunnel in 2012 fall within the range of concentrations measured in 1996. The concentrations of 9NAnt and 1NPyr display levels only slightly lower (within 1 standard deviation) than the lower range of concentrations measured by Dimashki *et al.* (2000). The previous measurements were made on only one sampling day, while the current study is the average of four separate sampling days so comparison of results must be done with caution. Nevertheless, this observation is striking.

Table 6.4. Comparison of total (particulate + vapour) NPAH concentrations measured in the Queensway Tunnel in 1996 (Dimashki *et al.*, 2000) and 2012 (present study).

	Tunnel concentration (pg/m ³)	
	2012 (This Study)	1996 (Dimashki <i>et al.</i> , 2000)
1NNap	1918±461	560-2120
2NNap	980±820	620-1570
9NAnt	294±165	370-760
1NPyr	343±157	440-690

To our knowledge, this is the first study to investigate temporal variations in traffic profiles of NPAHs. 1NNap, 2NNap, 9NAnt and 1NPyr are all present in diesel exhaust emissions in relatively high levels (Campbell and Lee, 1984; Draper, 1986; Paputa-Peck *et al.*, 1983; Zhu *et al.*, 2003) and are present in low/negligible emissions from gasoline vehicles (Zielinska *et al.*, 2004b).

The difference between the temporal trends observed for NPAH compared with PAH may therefore be associated with the greater contribution of diesel vehicles to NPAH compounds. The overall and relative increase in diesel vehicles in the traffic fleet since 1996 may therefore account for a lack of decrease in NPAH concentrations.

Evidence for the increased importance of NPAH over time in urban air has been indicated previously. For example, Matsumoto *et al.* (1998) noted the concentration of BaP declined

significantly in the period 1975 to 1992 in the heavily trafficked region of Sapporo, Japan, while the mutagenicity of collected particles remained unchanged. The authors suggested this could be attributed to an increase in diesel traffic and the possible associated increase in NPAH concentrations.

The lack of increase in observed NPAH levels in the tunnel over this time may suggest that while the volume of diesel traffic has increased, the net emissions of NPAHs from diesel vehicles may have declined. Indeed, improved engine design (e.g. use of catalytic devices or particulate traps) and fuel formulation has been shown to reduce NPAH and OPAH concentrations as well as PAH (Fiedler and Mücke, 1991; Marinov *et al.*, 2009; Nielsen *et al.*, 1999; Ratcliff *et al.*, 2010; Westerholm and Egebäck, 1994; Zhu *et al.*, 2003).

Perrone *et al.* (2014) indicated that increasingly stringent EU legislation on exhaust emissions of new vehicles (91/441/EEC) since 1993 has led to decreases in PAH emissions from both gasoline and diesel vehicles. Therefore, it may be expected that a decrease in NPAH emissions may have also resulted. However, as yet emission studies on NPAH have not been conducted to confirm this.

The results of the present study suggest the temporal variation in NPAH concentrations in the Queensway Road Tunnel have been influenced by competing factors : i) an increase in the number of diesel vehicles on U.K roads, and ii) a net reduction in emissions from individual diesel vehicles in response to changes in fuel formulation and engine/exhaust system design.

Despite these observations being based on a small number of relatively small sampling campaigns, it is indicated that the relative concentration of NPAH in vehicular emissions relative to PAHs has increased considerably in the past 20 years. For example, the ratio of 1NPyr to BPy in Queensway Tunnel samples in the present study (~0.16) is an order of magnitude higher than the ratio using the concentrations of 1NPyr and BPy reported by Dimashki *et al.* (2000) and Smith and Harrison (1996) for concentrations in 1996 and 1992 (0.016).

6.3. Comparison of tunnel vs. ambient concentrations

6.3.1. Overview

It is assumed that concentrations of PAHs, OPAHs and NPAHs measured in the tunnel will result entirely from the emissions of gasoline and diesel traffic. Comparing levels of compounds measured in the tunnel with those observed in the ambient atmosphere (tunnel/ambient ratios) will allow the assessment of other influences (e.g. non-traffic sources, relative rates of loss processes) potentially affecting their overall and relative concentrations in the urban atmosphere.

The ratios between mean concentrations measured in samples from the Queensway Road Tunnel to those measured simultaneously at EROS are shown in Figure 6.8. It can be seen that these ratios vary considerably for different individual compounds. This section discusses these differences and the possible explanations for the observed variations. It should be noted that these ratios represent the mean concentrations measured on only 4 individual sampling days, therefore may not necessarily be representative of compound behaviour over longer time scales.

For most PAHs, OPAHs and NPAHs, concentrations are higher in the tunnel environment than were measured at the ambient background location. Total PAH concentration was ~4.5 times higher in the tunnel than the mean concentration at ambient EROS. This is generally consistent with the lower rate of dispersion and lower chemical reactivity expected in the tunnel environment.

Similar observations have been noted in previous studies. Kim *et al.* (2012) noted that PAH concentrations were ~6 and 10 times higher in the Bukak Tunnel in Seoul, South Korea, than were measured at an ambient roadside location during spring and winter respectively. Similarly, Wingfors *et al.* (2001) also noted total PAH concentrations in the Ludby Tunnel in Gothenburg, Sweden were an order of magnitude higher than those measured in heavily trafficked urban areas.

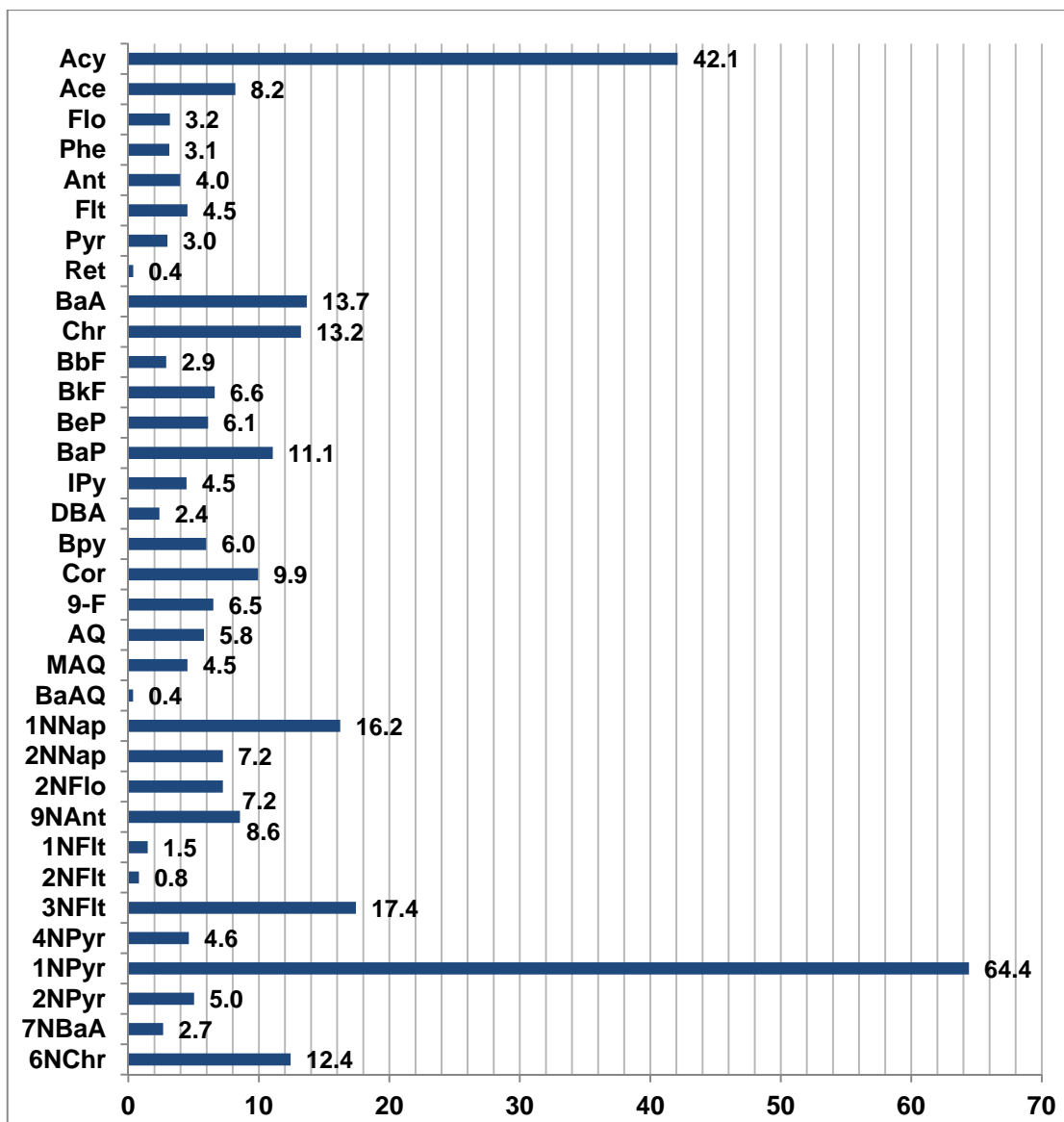


Figure 6.8. Mean ratios of concentrations measured in the Queensway Road Tunnel to those measured simultaneously at EROS for samples taken in Campaign 3.

6.3.2. Tunnel/EROS ratios of PAHs

It can be seen that ratios for most PAH and OPAH compounds are in the range 2.5-8.5, however there is considerable variability between compounds, which can be attributed to differences in source contribution at the ambient site, physiochemical properties, and/or relative reactivity rates of individual PAHs.

Reaction with OH is expected to be the dominant loss process for gas-phase LMW PAHs in the ambient atmosphere (Atkinson and Arey, 1994; Brubaker and Hites, 1998). However, as was observed with the diurnal pattern of these compounds, no trend was observed between [tunnel] / [ambient] concentration ratios and experimentally derived rate coefficients for gas-phase reaction towards OH. This suggests the ambient concentrations at BROS and EROS are influenced by other potential input and/or loss factors.

The only PAH compound to exhibit a tunnel/ambient ratio of <1 was Ret. This is consistent with this compound resulting primarily from wood combustion rather than road traffic (Bari *et al.*, 2010; Fine *et al.*, 2002; McDonald *et al.*, 2000; Ramdahl, 1983). Indeed, PMF analysis (see Section 3.7) suggested this Ret concentrations at the ambient sites result primarily from this source. Ret has not been measured in traffic exhaust emissions, however Wingfors *et al.* (2001) did measure very low levels of Ret in a road tunnel, suggesting a small contribution from vehicle emissions or transfer of air from outside of the tunnel.

LMW (3-4 ring) compounds Flo, Phe, Ant, Flth, Pyr display relatively low (3 – 4.5) tunnel/ambient ratios. Given that these compounds, are expected to be relatively abundant in traffic emissions this observation is somewhat surprising. For example, Phe, Flt and Pyr are the dominant PAHs in diesel exhaust (Ratcliff *et al.*, 2010 ; Zhu *et al.* , 2003) and therefore may be expected to display enhanced ratios.

However, PMF analysis indicated that <45% of Phe, Flt and Pyr measured at the ambient sites result from traffic. The abundance of non-traffic sources at the ambient sites e.g. wood combustion or revolatilisation of pollutants from road and or soil/vegetation surfaces, may therefore explain the relatively low ratios of these compounds.

Interestingly, the tunnel/ambient ratio of Flt is higher than that of Pyr, despite higher OH reactivity noted for Pyr relative to Flt (Atkinson *et al.*, 1990a; Bari *et al.*, 2010; Brubaker and Hites, 1998; Fine *et al.*, 2002; McDonald *et al.*, 2000; Ramdahl, 1983).

It was noted in Section 3.2 that the positive correlation between NO_x-corrected concentration and temperature was observed for Pyr but not Flt, suggesting Pyr concentrations at EROS may be 'buffered' by volatilisation from soil or vegetation surfaces to a much greater degree than Flt resulting in lower tunnel/ambient ratio. This may account for lower tunnel/ambient ratios for Pyr relative to Flt.

The tunnel/ambient ratio of Acy was considerably higher than those of other PAHs. This is consistent with relatively high gas-phase OH reactivity of this compound (Brubaker and Hites, 1998; Reisen and Arey, 2002). The lack of direct sunlight inside the tunnel is likely to result in minimal reactivity, leading to enhanced ratios.

However, while Ant is shown to display similarly fast reactivity towards OH (Brubaker and Hites, 1998), the observed tunnel/ambient ratio is relatively lower than expected. This may suggest the ambient concentration of these PAHs is influenced by non-traffic sources, either primary or non-combustion related, as indicated by the seasonal (Section 3.3) and diurnal (Section 5) profiles of this compound.

Ace displays relatively high tunnel/ambient ratios compared with other semi-volatile PAHs. This observation indicates a dominant traffic input at the ambient sites in these samples. This is consistent with the diurnal pattern observed for of Ace (Section 5). However the [BROS] – [EROS] traffic profile (Section 3.1) and temporal trend (Section 3.4) suggests the Ace concentration at the ambient sites is influenced significantly by a non-traffic seasonally-mediated source. PMF analysis suggested Ace concentrations are dominated by a specific source attributed to volatilisation from road surfaces, however it was noted that this does not account for the seasonal profile in Ace concentrations, suggesting a possible additional contribution from a domestic combustion source.

Most HMW PAHs (MW>228) display relatively high tunnel/ambient ratios compared with most LMW PAHs. BaA and Chy display particularly high ratios compared with other PAHs. Which may reflect a relatively low contribution of non-traffic related source of these compounds at the ambient

sites, as indicated by PMF analysis for Chr (see Section 3.7), and/or the additional influence of heterogeneous reactivity influencing these compounds.

The relative differences in tunnel/ambient ratios between these compounds may be attributed to the relative stability of these compounds and/or the relative contribution of non-traffic sources to their ambient concentrations. For example, BaP displays a relatively higher ratio compared with other 5 ring PAH compound, despite PMF analysis attributing a significant proportion of BaP concentration to ambient concentrations at these sites (Section 4.3). This may be attributed to greater susceptibility of BaP to heterogeneous reactivity in the ambient atmosphere (Perraudin *et al.*, 2007).

DBA displays a relatively low tunnel/ambient ratio. This is consistent with a relatively low input from road traffic, as indicated by Jang *et al.* (2013) who assessed a 'traffic' profile at London monitoring sites, and may indicate an alternative seasonally-dependent combustion source influencing the ambient sites. BbF also displays a relatively low tunnel/ambient ratio despite PMF analysis suggesting a relatively high (~62%) contribution from traffic at the ambient sites. This observation is therefore somewhat unexpected.

6.3.3. Tunnel/EROS ratios of OPAHs

The OPAHs 9F, AQ and MAQ display higher tunnel/ambient ratios than those of most semi-volatile 3-4 ring PAH compounds.

It has been indicated in Section 3, 4 and 5, that concentrations of 9F, AQ and MAQ may be influenced by secondary input due to volatilisation from surfaces, wood combustion and/or chemical reactivity between sites. Indeed, the PMF analysis performed for AQ indicates a contribution from traffic of ~50% at these sites. However, the relatively high ratios suggest that concentrations at the ambient sites are dominated by traffic emissions and that non-traffic sources (both primary and secondary) do not control the concentrations of these compounds.

It has been demonstrated that particulate-phase OPAH are relatively stable towards photolysis but are shown to decay when exposed to ozone with half lives on wood smoke particles of 80-200 mins (Kamens *et al.*, 1989). However, it is noted that O₃ concentrations used in this experiment were >10 times higher than the atmospheric O₃ concentration observed in this study. It is suggested, therefore that OPAH concentrations are not influenced significantly by photolytic or reactive losses between BROS and EROS.

The low (<1) ratios observed for BaAQ indicate that this compound is not emitted to a significant degree by road vehicles and is present in much higher levels in the ambient atmosphere. This suggests levels of this compound observed at BROS and EROS result primarily from a non-traffic combustion source such as natural gas home appliances (Rogge *et al.*, 1993c) or uncontrolled domestic waste combustion (Sidhu *et al.*, 2005). However, it should also be noted that a statistically significant 'traffic increment' was observed for this compound.

6.3.4. Tunnel/EROS ratios of NPAHs

NPAHs generally display higher tunnel/ambient ratios than unsubstituted PAHs, although, as noted with PAHs there is wide variability between individual compounds.

Relatively high ratios were observed for 1NNap, 2NNap, 2NFlo, 9NAnt, 3NFIt, 1NPyr and 6NChy. These compounds are expected to be predominantly associated with diesel exhaust emissions (Ball and Young, 1992; Campbell and Lee, 1984; IARC, 1983 ; Paputa-Peck *et al.*, 1983; Rappaport *et al.*, 1982; Schuetzle *et al.*, 1982; Schuetzle and Perez, 1983; Zhu *et al.*, 2003; Zielinska *et al.*, 2004a; 2004b) with lower input from other combustion sources (WHO, 2000).

The principal atmospheric loss process for NPAHs is expected to be photolysis (Atkinson *et al.*, 1989; Fan *et al.*, 1995; 1996a; 1996b; Phousongphouang and Arey, 2003a). This process is not expected to occur significantly in the tunnel environment where direct sunlight is absent. The high

ratios may therefore reflect the relative lack of non-traffic input of these compounds in the ambient atmosphere and the rapid photolytic and/or reactive losses in the ambient atmosphere.

Indeed, both PMF analysis of 1NPyr and 1NNAp concentrations indicate the strong influence of diesel emissions for these compounds at the ambient sites and the relatively low (3% and 18% respectively) from non-traffic sources. The extremely high tunnel/ambient ratio observed for 1NPyr in summer at EROS suggests this compound is the most susceptible to photolytic degradation. Relatively few quantitative data are available for NPAH loss rates due to photolysis.

While Fan *et al.* (1996a) indicated the structure of particle-associated NPAH compounds does not influence the rate of degradation, it has been suggested elsewhere that the isomeric structure of the compound does influence the rate of photolytic decay (Pitts, 1983). For example, Holloway *et al.* (1987) and Feilberg and Nielsen (2000) have indicated 1NPyr decays up to 10 times more rapidly than other MW 247 NPAHs.

Previously, Dimashki *et al.* (2000) observed levels of 1NPyr and 9NAnt in the tunnel were ~6 and ~2 times higher in the Queensway Road Tunnel than in the ambient atmosphere of Birmingham respectively. The ambient sampling in this previous study was conducted in central Birmingham during winter.

The Tunnel/EROS ratio in the present study is shown to be a factor ~10 and ~4.5 higher than the previous study for 1NPyr and 9NAnt respectively. This may partly be attributed to higher input of pollutants in the city centre compared to the background University site and the fact that sampling in the present study was conducted in the late summer/early autumn with associated higher temperatures leading to potentially higher degradation rates in the ambient atmosphere.

The tunnel/ambient ratio of 1NNAp is a factor ~2.2 higher than 2NNAp. Experimental studies indicate 1NNAp will exhibit a rate of photolysis ~1.3 – 8 times higher than that of 2NNAp (Atkinson *et al.*, 1989; Niu *et al.*, 2005; Phouongphouang and Arey, 2003a). This would suggest the observed difference in ratios for the two NNAp isomers is due to differences in the rates of photolytic degradation and the relatively long exposure time of air samples collected at EROS.

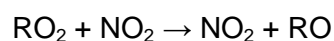
NNap isomers are also shown to originate from secondary reactions from OH and NO₃ reactions. The yield of 1NNap resulting from NO₃ reactions with Nap has been shown to be higher (17%) than for 2NNap (7%) (Atkinson *et al.*, 1989). However, it is indicated from diurnal profiles (see Section 4) that NO₃ reactivity is of minor importance to these compounds at these sampling sites. NNap photolysis is rate is likely to be much faster than the reaction rate of Nap with OH (Atkinson and Arey, 1994) so it is suggested this process is not likely to have a substantial impact on observed tunnel/ambient ratios.

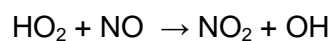
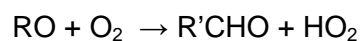
The relatively low ratios observed for 1NFlt and 7NBaA indicate only a minor contribution from traffic for these compounds at the ambient sites. There is almost a complete absence of previous sampling (Bamford and Baker, 2003) and source emissions data available for 1NFlt. 7NBaA has been measured in vehicular emissions (Karavalakis *et al.*, 2009; Zhu *et al.*, 2003). However, the previous study in Birmingham did not detect this compound in the Queensway Road Tunnel but did observe measureable levels in the city centre (Dimashki *et al.*, 2000).

2NFlt and 2NPyr are expected to result from atmospheric reactions with minor input from road traffic (Atkinson and Arey, 1994). A tunnel/ambient ratio of <1 was observed for 2NFlt, consistent with low reactivity chemical in the tunnel. However, 2NPyr displays a ratio of ~5 which is unexpected. While relatively higher concentrations inside the tunnel may have been caused by transport of pollutants from outside the tunnel, this may not account for the relatively high ratio observed for 2NPyr

It has been suggested that OH can be generated in-situ via the rapid conversion of NO to NO₂, that can take place in the absence of light in dilute vehicle emissions (Shi and Harrison, 1997).

The proposed sequence of reactions would be initiated by diene components found in gasoline vehicle exhaust reacting with oxygen :





It is possible, therefore, that OH reactivity may occur inside the tunnel despite the absence of direct sunlight. However, more work is clearly required to establish if these reactions do indeed result in NPAH formation.

It is not expected that gas-phase reactivity will not contribute significantly to the levels of 1NNap and 2NNap present in the tunnel, even if significant in-situ OH formation occurred as formation yields from OH-initiated reactions are relatively low (~1%) compared with NO₃-initiated reactions (7-24%) (Atkinson and Arey, 1994). The high NO levels expected in the tunnel would result in very low NO₃ concentrations.

Chapter 7. Summary and conclusions

7.1. Investigation summary

In this investigation the airborne concentrations of PAH, OPAH and NPAH compounds have been measured at ambient sites in trafficked and urban background locations and inside a road traffic tunnel. High volume air samplers were used to collect both particulate- and gas-phase air samples in a number of different sampling campaigns, designed to investigate different aspects of PAH behaviour and fate such as traffic source profiles, seasonality, phase partitioning, diurnal patterns and chemical degradation and/or formation.

The difference in traffic source profiles, as well as spatial and temporal variations for individual PAH, OPAH and NPAH compounds has allowed an assessment of the factors governing their concentrations, behaviour and fate in the urban atmosphere. The following conclusions can be drawn :

Concentrations of PAH, OPAH and NPAH compounds at the trafficked location BROS were generally higher than at the urban background site EROS, due to the closer proximity to the traffic source. Relative inter-site differences were variable between species and also displayed distinct seasonality. This was attributed to differences in relative rates of atmospheric degradation and relative input from non-traffic sources (such as wood combustion, volatilisation from surfaces and photochemical reactions) for different compounds. The traffic increment (that is BROS – EROS) concentrations of most compounds was reflected in the relative concentrations measured in the Queensway Road Tunnel, suggesting traffic is the dominant source for most compounds at BROS. Concentrations at EROS were correlated with BROS concentrations for most compounds suggesting traffic is the dominant source at EROS also.

Concentrations of most PAH appear to have declined substantially at these sites over the past 10 years. This is broadly consistent with the estimated reduction of PAH emissions over this time,

particularly those associated with urban traffic. However, a number of compounds such as Ret, Ace, Pyr and Flt did not display this trend, suggesting the increased importance of non-traffic sources such as wood combustion at these sites.

Concentrations of PAH, OPAH and NPAH compounds were generally much higher in the Queensway Road Tunnel than observed in the ambient atmosphere, due to the higher volume of traffic and the reduced dilution and chemical reactivity inside the tunnel. However, considerable variation was noted in tunnel/ambient behaviour between compounds, which was attributed to differences in the relative level of input from non-traffic sources and the role of photochemical degradation and/or input for PAHs, OPAHs and NPAHs in the ambient environment. The potential occurrence of OH radical reaction with PAHs in vehicle exhaust was also suggested.

The concentrations of PAH compounds measured inside the Queensway Road Tunnel displayed a substantial decline compared with measurements taken in 1992. This was linked mainly to the introduction of catalytic converters as well as increasingly stringent vehicle emission legislation since the previous studies. In contrast, concentrations of NPAHs in the tunnel were similar to those measured in 1996. These results suggest that the increased numbers and relative proportion of diesel passenger vehicles over this time has impacted on the overall and relative concentrations of PAH and NPAH emissions from vehicles in the UK. These results suggest relative emissions of NPAH from traffic relative to PAHs have increased substantially in the past 20 years.

The observed temporal, seasonal and diurnal patterns of PAH, OPAH and NPAH concentrations, and their inter-site variation between BROS and EROS indicate the potential importance of non-traffic sources affecting the concentrations of a number of compounds at these sites. PMF source apportionment analysis was carried out for some key PAHs and a small number of NPAH and OPAH compounds. The results suggest the potential importance of wood combustion at these sites, consistent with the estimated growth in emissions from this source nationally over the past 10 years. The results also indicate a distinction between PAH source patterns from domestic heating and non-domestic heating combustion activities.

Concentrations for most compounds were higher during the winter months compared to summer. This was mainly associated with colder temperature and the resultant reduction in dispersion rate in winter, as well as lower rate of photochemical degradation. However, seasonal differences were relatively low, especially for LMW PAH compounds. This was attributed to the dominance of a non-seasonal traffic source, relatively low seasonal variation in ambient temperature and possible influence of additional input of compounds from chemical reactions and/or volatilisation from surfaces during summer.

Diurnal patterns derived in this study appear to be dominated for most compounds by a characteristic traffic profile with highest concentrations observed during morning rush hour. However, when concentrations were normalised with traffic marker compound NO_x , the influence of a potential daytime source for LMW compounds was highlighted. It was suggested that temperature-driven volatilisation from soil, vegetation or road surfaces may be the cause of this pattern.

PAHs, OPAHs and NPAHs exhibited characteristic gas-particle partitioning behaviour. It was shown that the proportion of these compounds in the particulate phase is well characterised by different physiochemical properties such as MW, VP, K_{ow} and H. Phase partitioning of PAHs at background site EROS appeared to be approaching equilibrium conditions in contrast to trafficked site BROS, consistent with established partitioning models. However the factors influencing partitioning behaviour of OPAH and NPAH compounds were less clear.

The importance of chemical reactivity as a PAH degradation process was indicated by the relatively large differences in concentration for highly reactive species such as Acy and Ant between trafficked and background sites. The ratio between BROS and EROS concentrations of LMW PAHs was shown to display distinct seasonality and association with measured OH reaction rate coefficients, although this was possibly masked to a degree by input from non-traffic sources.

It was not possible to make a quantitative assessment on the relative contribution of secondary NPAH or OPAH input due to PAH reactivity at these sites. This was due to the relatively short

distance between traffic and background sites. However, the occurrence of photochemical input of NPAH (and OPAH) compounds between BROS and EROS samples was indicated by the inter-site differences and diurnal and seasonality patterns of 2NFlt/1NPyr ratios and product/reactant concentration ratios. It is indicated that OH radical input is dominant over NO₃-related input at these sites.

7.2. Recommendations for future work

The following aspects are identified as potential areas for future investigation :

- i) This investigation presents the first instance of a regular year-long measurement campaign for OPAH and NPAH concentrations in the U.K. It is suggested that there is a requirement for more regular monitoring of NPAHs and OPAHs in the long-term at different locations and better characterisation of their primary sources. This will help establish a longer-term profile for their concentrations and a better understanding of how this is influenced by changes in primary emissions in relation to secondary input from PAH reactivity.
- ii) This investigation highlights the potential for PMF source apportionment to be applied to OPAH and NPAH compounds. A larger scale long-term monitoring of these compounds would allow a relatively large data set to be available for this analysis in future. This would allow a more extensive suite of compounds to be considered and would enhance our understanding of the sources of NPAH and OPAH in the U.K.
- iii) It is clear that more work is required to fully understand the factors influencing the gas-particle partitioning of PAH, OPAH and NPAH. An important pre-requisite for this will be to obtain reliable experimental data for the key physiochemical properties of PAH, OPAH and NPAH compounds that are shown to play an important role in this process. For example, data on specific parameters

such as vapour pressure, octanol-air partitioning coefficient (K_{oa}) and Henry's Law constant, are lacking for many NPAH compounds.

iv) Investigations of PAH, NPAH and OPAH emissions from vehicles often focus solely on particle-phase extracts. The present investigation highlights the need for a better understanding of gas-phase emissions in vehicle exhaust to better understand the relative role of primary traffic emissions vs. secondary atmospheric formation on the observed concentrations of LMW NPAH and OPAH compounds.

v) Measurement of NPAH compounds in the present study indicate the possibility of reactions of PAH with OH radicals occurring in road tunnels. Further investigation of potential PAH + OH reactivity in vehicle exhaust emissions should be investigated to assess if this process can influence the nature and extent of NPAH input in the urban atmosphere.

vi) This investigation also highlights how the concentrations of PAH, OPAH and NPAH compounds have been influenced by changes to vehicle emission control technologies, fuel formation and legislative measures. Future measures imposed to improve air quality e.g. introduction of low emission zones, should be accompanied by concurrent monitoring studies to assess the impact on PAH, OPAH and NPAH concentrations, with particular focus on potentially differing impacts on compounds on primary and secondary origin. Effective emission control measures to reduce NPAH emissions from vehicles should also be further investigated.

vii) The majority of reaction products from PAH photochemical degradation processes remain unidentified. A more comprehensive elucidation of products from the reactions of many PAHs with OH, NO_3 and O_3 in both gas-phase and heterogeneous phases is required. This will allow more specific species to be targeted in air sampling studies to better investigate the role of PAH reactivity in observed atmospheric levels of NPAH and OPAH compounds.

References

- Alam, M. S., Delgado-Saborit, J. M., Stark, C., Harrison, R. M. (2013) Using atmospheric measurements of PAH and quinone compounds at roadside and urban background sites to assess sources and reactivity. *Atmospheric Environment*. **77**, 24-35.
- Alam, M. S., Delgado-Saborit, J. M., Stark, C., Harrison, R. M. (2014) Investigating PAH relative reactivity using congener profiles, quinone measurements and back trajectories. *Atmospheric Chemistry and Physics*. **14**, 2467-2477.
- Albinet, A., Leoz-Garziandia, E., Budzinski, H., Villenave, E. (2006) Simultaneous analysis of oxygenated and nitrated polycyclic aromatic hydrocarbons on standard reference material 1649a (urban dust) and on natural ambient air samples by gas chromatography-mass spectrometry with negative ion chemical ionisation. *Journal of Chromatography A*. **1121**, 106-113.
- Albinet, A., Leoz-Garziandia, E., Budzinski, H., Villenave, E. (2007a) Polycyclic aromatic hydrocarbons (PAHs), nitrated PAHs and oxygenated PAHs in ambient air of the Marseilles area (South of France): Concentrations and sources. *Sci Total Environ*. **384**, 280-292.
- Albinet, A., Leoz-Garziandia, E., Budzinski, H., Villenave, E. (2007b) Sampling precautions for the measurement of nitrated polycyclic aromatic hydrocarbons in ambient air. *Atmospheric Environment*. **41**, 4988-4994.
- Albinet, A., Leoz-Garziandia, E., Budzinski, H., Villenave, E., Jaffrezo, J. L. (2008a) Nitrated and oxygenated derivatives of polycyclic aromatic hydrocarbons in the ambient air of two French alpine valleys - Part 1: Concentrations, sources and gas/particle partitioning. *Atmospheric Environment*. **42**, 43-54.
- Albinet, A., Leoz-Garziandia, E., Budzinski, H., Villenave, E., Jaffrezo, J. L. (2008b) Nitrated and oxygenated derivatives of polycyclic aromatic hydrocarbons in the ambient air of two French alpine valleys - Part 2: Particle size distribution. *Atmospheric Environment*. **42**, 55-64.
- Allen, J. O., Dookeran, N. M., Taghizadeh, K., Lafleur, A. L., Smith, K. A., Sarofim, A. F. (1997) Measurement of oxygenated polycyclic aromatic hydrocarbons associated with a size-segregated urban aerosol. *Environ Sci Technol*. **31**, 2064-2070.
- Ananthula, R., Yamada, T., Taylor, P. H. (2006) Kinetics of OH radical reaction with anthracene and anthracene-d(10). *Journal of Physical Chemistry A*. **110**, 3559-3566.
- Ananthula, R., Yamada, T., Taylor, P. H. (2007) Kinetics of OH radical reaction with phenanthrene: New absolute rate measurements and comparison with other PAHs. *International Journal of Chemical Kinetics*. **39**, 629-637.
- Anderson, J. O., Thundiyil, J. G., Stolbach, A. (2012) Clearing the air: a review of the effects of particulate matter air pollution on human health. *Journal of medical toxicology : official journal of the American College of Medical Toxicology*. **8**, 166-175.
- Andreou, G., Rapsomanikis, S. (2009) Polycyclic aromatic hydrocarbons and their oxygenated derivatives in the urban atmosphere of Athens. *Journal of Hazardous Materials*. **172**, 363-373.
- AQEG. (2005) Particulate matter in the United Kingdom *Defra, London*
- Arce, R., Pino, E. F., Valle, C., Agreda, J. (2008) Photophysics and Photochemistry of 1-Nitropyrene. *Journal of Physical Chemistry A*. **112**, 10294-10304.

- Arey, J., Zielinska, B., Atkinson, R., Winer, A. M., Ramdahl, T., Pitts, J. N. (1986) The formation of nitro-PAH from the gas-phase reactions of fluoranthene and pyrene with the OH radical in the presence of NO_x. *Atmospheric Environment*. **20**, 2339-2345.
- Arey, J., Zielinska, B., Atkinson, R., Winer, A. M. (1987) Polycyclic Aromatic Hydrocarbon and Nitroarene Concentrations in Ambient Air During a Wintertime High-NO_x Episode in the Los Angeles Basin. *Atmospheric Environment*. **21**, 1437-1444.
- Arey, J., Zielinska, B., Atkinson, R., Winer, A. M. (1988) Formation of nitroarenes during ambient high-volume sampling. *Environ Sci Technol*. **22**, 457-462.
- Arey, J., Atkinson, R., Zielinska, B., McElroy, P. A. (1989a) Diurnal concentrations of volatile polycyclic aromatic-hydrocarbons and nitroarenes during a photochemical air-pollution episode in Glendora, California. *Environ Sci Technol*. **23**, 321-327.
- Arey, J., Zielinska, B., Atkinson, R., Aschmann, S. M. (1989b) Nitroarene products from the gas-phase reactions of volatile polycyclic aromatic-hydrocarbons with the OH radical and N₂O₅. *International Journal of Chemical Kinetics*. **21**, 775-799.
- Arey, J., Atkinson, R., Aschmann, S.M., Schuetzle, D. (1990) Experimental investigation of the atmospheric chemistry of and a comparison of predicted nitroarene concentrations with ambient air data. *Polycyclic Aromatic Compounds* **1**, 33-50.
- Atkinson, R., Aschmann, S. M., Pitts, J. N. (1984) Kinetics of the reactions of naphthalene and biphenyl with hydroxyl radicals and with ozone at 294 ± 1 K. *Environ Sci Technol*. **18**, 110-113.
- Atkinson, R., Lloyd, A. C. (1984) Evaluation of kinetic and mechanistic data for modelling of photochemical smog. *Journal of Physical and Chemical Reference Data*. **13**, 315-444.
- Atkinson, R., Aschmann, S. M. (1986) Kinetics of the reactions of naphthalene, 2-methylnaphthalene, and 2,3-dimethylnaphthalene with OH radicals and with O₃ at 295 ± 1 K. *International Journal of Chemical Kinetics*. **18**, 569-573.
- Atkinson, R., Winer, A. M., Pitts, J. N. J. (1986) Estimation of night-time dinitrogen pentoxide concentrations from ambient nitrogen dioxide and nitrogen trioxide radical concentrations and the role of dinitrogen pentoxide in night-time chemistry. *Atmospheric Environment*. **20**, 331-340.
- Atkinson, R., Arey, J., Zielinska, B., Aschmann, S. M. (1987a) Kinetics and products of the gas-phase reactions of OH radicals and N₂O₅ with naphthalene and biphenyl. *Environ Sci Technol*. **21**, 1014-1022.
- Atkinson, R., Arey, J., Zielinska, B., Pitts, J. N., Winer, A. M. (1987b) Evidence for the transformation of polycyclic organic-matter in the atmosphere. *Atmospheric Environment*. **21**, 2261-2262.
- Atkinson, R., Aschmann, S. M. (1987) Kinetics of the gas-phase reactions of alkyl naphthalenes with O₃, N₂O₅ and OH radicals at 298 ± 2 K. *Atmospheric Environment*. **21**, 2323-2326.
- Atkinson, R., Aschmann, S. M. (1988) Kinetics of the reactions of acenaphthene and acenaphthylene and structurally-related aromatic-compounds with OH and NO₃ radicals, N₂O₅ and O₃ at 296 ± 2 K. *International Journal of Chemical Kinetics*. **20**, 513-539.
- Atkinson, R. (1989) Kinetics and mechanisms of the gas-phase reactions of the hydroxyl radical with organic compounds. *J Phys Chem Ref. Data Monograph*, 1-246.

- Atkinson, R., Aschmann, S. M., Arey, J., Zielinska, B., Schuetzle, D. (1989) Gas-phase atmospheric chemistry of 1-nitronaphthalene and 2-nitronaphthalene and 1,4-naphthoquinone. *Atmospheric Environment*. **23**, 2679-2690.
- Atkinson, R., Arey, J., Zielinska, B., Aschmann, S. M. (1990a) Kinetics and nitro-products of the gas-phase OH and NO₃ radical-initiated reactions of naphthalene-d₈, fluoranthene-d₁₀, and pyrene. *International Journal of Chemical Kinetics*. **22**, 999-1014.
- Atkinson, R., Tuazon, E. C., Arey, J. (1990b) Reactions of naphthalene in N₂O₅-NO-NO₂-air mixtures. *International Journal of Chemical Kinetics*. **22**, 1071-1082.
- Atkinson, R. (1991) Kinetics and mechanisms of the gas-phase reactions of the NO₃ radical with organic-compounds. *Journal of Physical and Chemical Reference Data*. **20**, 459-507.
- Atkinson, R. (1994) Gas-phase tropospheric chemistry of organic-compounds. *Journal of Physical and Chemical Reference Data, Monograph No 2*.
- Atkinson, R., Arey, J. (1994) Atmospheric chemistry of gas-phase polycyclic aromatic-hydrocarbons - formation of atmospheric mutagens. *Environmental Health Perspectives*. **102**, 117-126.
- Atkinson, R., Tuazon, E. C., Bridier, I., Arey, J. (1994) Reactions of NO₃-naphthalene adducts with O₂ and NO₂. *International Journal of Chemical Kinetics*. **26**, 605-614.
- Atkinson, R., Arey, J. (2007) Mechanisms of the gas-phase reactions of aromatic hydrocarbons and PAHs with OH and NO₃ radicals. *Polycyclic Aromatic Compounds*. **27**, 15-40.
- Aulinger, A., Matthias, V., Quante, M. (2007) Introducing a partitioning mechanism for PAHs into the Community Multiscale Air Quality modeling system and its application to simulating the transport of benzo(a) pyrene over Europe. *Journal of Applied Meteorology and Climatology*. **46**, 1718-1730.
- Baek, S. O., Goldstone, M. E., Kirk, P. W. W., Lester, J. N., Perry, R. (1991) Phase distribution and particle-size dependency of polycyclic aromatic-hydrocarbons in the urban atmosphere. *Chemosphere*. **22**, 503-520.
- Ball, J. C., Young, W. C. (1992) Evidence for a new class of mutagens in diesel particulate extracts. *Environ Sci Technol*. **26**, 2181-2186.
- Bamford, H. A., Baker, J. E. (2003) Nitro-polycyclic aromatic hydrocarbon concentrations and sources in urban and suburban atmospheres of the Mid-Atlantic region. *Atmospheric Environment*. **37**, 2077-2091.
- Bamford, H. A., Bezabeh, D. Z., Schantz, M. M., Wise, S. A., Baker, J. E. (2003) Determination and comparison of nitrated-polycyclic aromatic hydrocarbons measured in air and diesel particulate reference materials. *Chemosphere*. **50**, 575-587.
- Banceu, C. E., Mihele, C., Lane, D. A., Bunce, N. J. (2001) Reactions of methylated naphthalenes with hydroxyl radicals under simulated atmospheric conditions. *Polycyclic Aromatic Compounds*. **18**, 415-425.
- Barbas, J. T., Sigman, M. E., Dabestani, R. (1996) Photochemical oxidation of phenanthrene sorbed on silica gel. *Environ Sci Technol*. **30**, 1776-1780.

- Bari, M. A., Baumbach, G., Kuch, B., Scheffknecht, G. (2010) Temporal variation and impact of wood smoke pollution on a residential area in southern Germany. *Atmospheric Environment*. **44**, 3823-3832.
- Barrado, A. I., Garcia, S., Barrado, E., Maria Perez, R. (2012) PM2.5-bound PAHs and hydroxy-PAHs in atmospheric aerosol samples: Correlations with season and with physical and chemical factors. *Atmospheric Environment*. **49**, 224-232.
- Bayona, J. M., Casellas, M., Fernandez, P., Solanas, A. M., Albaiges, J. (1994) Sources and seasonal variability of mutagenic-agents in the Barcelona city aerosol. *Chemosphere*. **29**, 441-450.
- Becker, S., Halsall, C. J., Tych, W., Hung, H., Attewell, S., Blanchard, P., et al. (2006) Resolving the long-term trends of polycyclic aromatic hydrocarbons in the Canadian Arctic atmosphere. *Environ Sci Technol*. **40**, 3217-3222.
- Bedjanian, Y., Nguyen, M. L., Le Bras, G. (2010) Kinetics of the reactions of soot surface-bound polycyclic aromatic hydrocarbons with the OH radicals. *Atmospheric Environment*. **44**, 1754-1760.
- Behymer, T. D., Hites, R. A. (1985) Photolysis of polycyclic aromatic-hydrocarbons adsorbed on simulated atmospheric particulates. *Environ Sci Technol*. **19**, 1004-1006.
- Behymer, T. D., Hites, R. A. (1988) Photolysis of polycyclic aromatic-hydrocarbons adsorbed on fly-ash. *Environ Sci Technol*. **22**, 1311-1319.
- Benner, B. A. (1988) Mobile sources of polycyclic aromatic hydrocarbons (PAH) and nitro-PAH: a roadway tunnel study. *PhD thesis, University of Maryland, USA*.
- Benner, B. A., Gordon, G. E., Wise, S. A. (1989) Mobile sources of atmospheric polycyclic aromatic-hydrocarbons - a roadway tunnel study. *Environ Sci Technol*. **23**, 1269-1278.
- Bertram, A. K., Ivanov, A. V., Hunter, M., Molina, L. T., Molina, M. J. (2001) The reaction probability of OH on organic surfaces of tropospheric interest. *Journal of Physical Chemistry A*. **105**, 9415-9421.
- Bethel, H. L., Atkinson, R., Arey, J. (2001) Kinetics and products of the reactions of selected diols with the OH radical. *International Journal of Chemical Kinetics*. **33**, 310-316.
- Bi, X., Simoneit, B. R. T., Sheng, G., Fu, J. (2008) Characterization of molecular markers in smoke from residential coal combustion in China. *Fuel*. **87**, 112-119.
- Bi, X. H., Sheng, G. Y., Chen, Y. J., Tan, J. H., Fu, J. M. (2003) Distribution of N-alkanes and polycyclic aromatic hydrocarbons in the urban atmosphere of Guangzhou, China. *Abstracts of Papers of the American Chemical Society*. **225**, U818-U818.
- Bi, X. H., Sheng, G. Y., Peng, P., Chen, Y. J., Fu, J. M. (2005) Size distribution of n-alkanes and polycyclic aromatic hydrocarbons (PAHs) in urban and rural atmospheres of Guangzhou, China. *Atmospheric Environment*. **39**, 477-487.
- Bidleman, T. F. (1988) Atmospheric processes - wet and dry deposition of organic-compounds are controlled by their vapor particle partitioning. *Environ Sci Technol*. **22**, 361-367.
- Biermann, H. W., Mac Leod, H., Atkinson, R., Winer, A. M., Pitts, J. N. (1985) Kinetics of the gas-phase reactions of the hydroxyl radical with naphthalene, phenanthrene, and anthracene. *Environ Sci Technol*. **19**, 244-248.

Bolton, J. L., Trush, M. A., Penning, T. M., Dryhurst, G., Monks, T. J. (2000) Role of quinones in toxicology. *Chemical Research in Toxicology*. **13**, 135-160.

Bonfanti, L., Careri, M., Mangia, A., Manini, P., Maspero, M. (1996) Simultaneous identification of different classes of hydrocarbons and determination of nitro-polycyclic aromatic hydrocarbons by means of particle beam liquid chromatography mass spectrometry. *Journal of Chromatography A*. **728**, 359-369.

Brorstrom-Lunden, E., Lindskog, A. (1985) Degradation of polycyclic aromatic-hydrocarbons during simulated stack gas sampling. *Environ Sci Technol*. **19**, 313-316.

Brorstrom, E., Grennfelt, P., Lindskog, A. (1983) The effect of nitrogen-dioxide and ozone on the decomposition of particle-associated polycyclic aromatic-hydrocarbons during sampling from the atmosphere. *Atmospheric Environment*. **17**, 601-605.

Brown, A. S., Brown, R. J. C., Coleman, P. J., Conolly, C., Sweetman, A. J., Jones, K. C., et al. (2013) Twenty years of measurement of polycyclic aromatic hydrocarbons (PAHs) in UK ambient air by nationwide air quality networks. *Environmental Science-Processes & Impacts*. **15**, 1199-1215.

Brubaker, W. W., Hites, R. A. (1998) OH reaction kinetics of polycyclic aromatic hydrocarbons and polychlorinated dibenzo-p-dioxins and dibenzofurans. *Journal of Physical Chemistry A*. **102**, 915-921.

Bunce, N. J., Liu, L., Zhu, J., Lane, D. A. (1997) Reaction of naphthalene and its derivatives with hydroxyl radicals in the gas phase. *Environ Sci Technol*. **31**, 2252-2259.

Busby, W. F., Penman, B. W., Crespi, C. L. (1994a) human cell mutagenicity of mononitropyrenes and dinitropyrenes in metabolically competent MCL-5 CELLS. *Mutation Research-Genetic Toxicology*. **322**, 233-242.

Busby, W. F., Smith, H., Bishop, W. W., Thilly, W. G. (1994b) Mutagenicity of mononitropyrenes and dinitropyrenes in the salmonella-typhimurium-TM677 forward mutation assay. *Mutation Research-Genetic Toxicology*. **322**, 221-232.

Busby, W. F., Smith, H., Crespi, C. L., Penman, B. W. (1995) Mutagenicity of benzo a pyrene and dibenzopyrenes in the salmonella-typhimurium TM677 and the MCL-5 human cell forward mutation assays. *Mutation Research-Genetic Toxicology*. **342**, 9-16.

Butler, J. D., Crossley, P. (1979) Appraisal of relative airborne sub-urban concentrations of polycyclic aromatic-hydrocarbons monitored indoors and outdoors. *Sci Total Environ*. **11**, 53-58.

Butler, J. D., Crossley, P. (1981) Reactivity of polycyclic aromatic-hydrocarbons adsorbed on soot particles. *Atmospheric Environment*. **15**, 91-94.

Campbell, R. M., Lee, M. L. (1984) Capillary column gas-chromatographic determination of nitro polycyclic aromatic-compounds in particulate extracts. *Analytical Chemistry*. **56**, 1026-1030.

Cancio, J. A. L., Castellano, A. V., Martin, S. S., Rodriguez, J. F. S. (2004) Size distributions of PAHs in ambient air particles of two areas of Las Palmas de Gran Canaria. *Water Air and Soil Pollution*. **154**, 127-138.

- Castells, P., Santos, F. J., Gaiceran, M. T. (2003) Development of a sequential supercritical fluid extraction method for the analysis of nitrated and oxygenated derivatives of polycyclic aromatic hydrocarbons in urban aerosols. *Journal of Chromatography A*. **1010**, 141-151.
- Cecinato, A. (2003) Nitrated polynuclear aromatic hydrocarbons in ambient air in Italy. A brief overview. *Journal of Separation Science*. **26**, 402-408.
- Chapman, O. L., Heckert, D. C., Reasoner, J. W., Thackabe.S. (1966) Photochemical studies on 9-nitroanthracene. *Journal of the American Chemical Society*. **88**, 5550-&.
- Chen, F., Hu, W., Zhong, Q. (2013) Emissions of particle-phase polycyclic aromatic hydrocarbons (PAHs) in the Fu Gui-shan Tunnel of Nanjing, China. *Atmospheric Research*. **124**, 53-60.
- Chetwittayachan, T., Shimazaki, D., Yamamoto, K. (2002) A comparison of temporal variation of particle-bound polycyclic aromatic hydrocarbons (pPAHs) concentration in different urban environments: Tokyo, Japan, and Bangkok, Thailand. *Atmospheric Environment*. **36**, 2027-2037.
- Cho, A. K., Di Stefano, E., You, Y., Rodriguez, C. E., Schmitz, D. A., Kumagai, Y., et al. (2004) Determination of four quinones in diesel exhaust particles, SRM 1649a, an atmospheric PM2.5. *Aerosol Science and Technology*. **38**, 68-81.
- Choi, H., Harrison, R., Komulainen, H., J.M., D.-S. (2010) Polycyclic aromatic hydrocarbons. *In: WHO guidelines for indoor air quality: selected pollutants, World Health Organization, Copenhagen*
- Chrysikou, L. P., Gemenetzis, P. G., Samara, C. A. (2009) Wintertime size distribution of polycyclic aromatic hydrocarbons (PAHs), polychlorinated biphenyls (PCBs) and organochlorine pesticides (OCPs) in the urban environment: Street- vs rooftop-level measurements. *Atmospheric Environment*. **43**, 290-300.
- Chuang, J. C., Mack, G. A., Kuhlman, M. R., Wilson, N. K. (1991) Polycyclic aromatic-hydrocarbons and their derivatives in indoor and outdoor air in an 8-home study. *Atmospheric Environment Part B-Urban Atmosphere*. **25**, 369-380.
- Chung, M. Y., Lazaro, R. A., Lim, D., Jackson, J., Lyon, J., Rendulic, D., et al. (2006) Aerosol-borne quinones and reactive oxygen species generation by particulate matter extracts. *Environ Sci Technol*. **40**, 4880-4886.
- Ciccioli, P., Cecinato, A., Brancaleoni, E., Draisci, R., Liberti, A. (1989) Evaluation of nitrated polycyclic aromatic-hydrocarbons in anthropogenic emission and air samples - a possible means of detecting reactions of carbonaceous particles in the atmosphere. *Aerosol Science and Technology*. **10**, 296-310.
- Ciccioli, P., Cecinato, A., Brancaleoni, E., Frattoni, M., Zacchei, P., Miguel, A. H., et al. (1996) Formation and transport of 2-nitrofluoranthene and 2-nitropyrene of photochemical origin in the troposphere. *Journal of Geophysical Research-Atmospheres*. **101**, 19567-19581.
- Cochran, R. E., Dongari, N., Jeong, H., Beranek, J., Haddadi, S., Shipp, J., et al. (2012) Determination of polycyclic aromatic hydrocarbons and their oxy-, nitro-, and hydroxy-oxidation products. *Analytica Chimica Acta*. **740**, 93-103.
- Cole, J. A., Bittner, J. D., Longwell, J. P., Howard, J. B. (1984) Formation mechanisms of aromatic-compounds in aliphatic flames. *Combustion and Flame*. **56**, 51-70.
- Coleman, P. J., Lee, R. G. M., Alcock, R. E., Jones, K. C. (1997) Observations on PAH, PCB, and PCDD/F trends in UK urban air, 1991-1995. *Environ Sci Technol*. **31**, 2120-2124.

Collier, A. R., Rhead, M. M., Trier, C. J., Bell, M. A. (1995) Polycyclic aromatic compound profiles from a light-duty direct-injection diesel-engine. *Fuel*. **74**, 362-367.

COMEAP. (2010) The Mortality Effects of Long-Term Exposure to Particulate Air Pollution in the United Kingdom. *A report by Health Protection Agency for the Committee on the Medical Effects of Air Pollutants*.

Cortes, D. R., Basu, I., Sweet, C. W., Hites, R. A. (2000) Temporal trends in and influence of wind on PAH concentrations measured near the Great Lakes. *Environ Sci Technol*. **34**, 356-360.

Cortes, D. R., Hites, R. A. (2000) Detection of statistically significant trends in atmospheric concentrations of semivolatile compounds. *Environ Sci Technol*. **34**, 2826-2829.

Cotham, W. E., Bidleman, T. F. (1995) Polycyclic Aromatic Hydrocarbons and Polychlorinated Biphenyls in Air at an Urban and a Rural Site Near Lake Michigan. *Environ Sci Technol*. **29**, 2782-2789.

Coutant, R. W., Brown, L., Chuang, J. C., Riggan, R. M., Lewis, R. G. (1988) Phase distribution and artifact formation in ambient air sampling for polynuclear aromatic-hydrocarbons. *Atmospheric Environment*. **22**, 403-409.

Dachs, J., Glenn, T. R., Gigliotti, C. L., Brunciak, P., Totten, L. A., Nelson, E. D., et al. (2002) Processes driving the short-term variability of polycyclic aromatic hydrocarbons in the Baltimore and northern Chesapeake Bay atmosphere, USA. *Atmospheric Environment*. **36**, 2281-2295.

Defra. (2007) The Air Quality Strategy for England, Scotland, Wales and Northern Ireland (Volume 2). *Defra, London*.

Defra. (2010) Valuing the overall impacts of air pollution. *Defra, London*.

Delgado-Saborit, J. M., Baker, S. J. (2006) Standard Operating Procedure For The Determination of PAHs by Gas Chromatography Mass Spectrometry University of Birmingham

Delgado-Saborit, J. M., Stark, C., Harrison, R. M. (2011) Carcinogenic potential, levels and sources of polycyclic aromatic hydrocarbon mixtures in indoor and outdoor environments and their implications for air quality standards. *Environment International*. **37**, 383-392.

Delgado-Saborit, J. M., Alam, M. S., Godri Pollitt, K. J., Stark, C., Harrison, R. M. (2013) Analysis of atmospheric concentrations of quinones and polycyclic aromatic hydrocarbons in vapour and particulate phases. *Atmospheric Environment*. **77**, 974-982.

Delgado-Saborit, J. M., Stark, C., Harrison, R. M. (2014) Use of a Versatile High Efficiency Multiparallel Denuder for the Sampling of PAHs in Ambient Air: Gas and Particle Phase Concentrations, Particle Size Distribution and Artifact Formation. *Environ Sci Technol*. **48**, 499-507.

Delhomme, O., Millet, M., Herckes, P. (2008) Determination of oxygenated polycyclic aromatic hydrocarbons in atmospheric aerosol samples by liquid chromatography-tandem mass spectrometry. *Talanta*. **74**, 703-710.

Deutschwenzel, R. P., Brune, H., Grimmer, G., Dettbarn, G., Misfeld, J. (1983) Experimental studies in rat lungs on the carcinogenicity and dose-response relationships of 8 frequently occurring environmental polycyclic aromatic-hydrocarbons. *Journal of the National Cancer Institute*. **71**, 539-544.

Department for Transport. (2014) DfT Vehicle Licensing Statistics : 2013, . *UK Government online resources*

Di Filippo, P., Riccardi, C., Pomata, D., Buiarelli, F. (2010) Concentrations of PAHs, and nitro- and methyl- derivatives associated with a size-segregated urban aerosol. *Atmospheric Environment*. **44**, 2742-2749.

Diamond, M. L., Priemer, D. A., Law, N. L. (2001) Developing a multimedia model of chemical dynamics in an urban area. *Chemosphere*. **44**, 1655-1667.

Dimashki, M., Harrad, S., Harrison, R. M. (2000) Measurements of nitro-PAH in the atmospheres of two cities. *Atmospheric Environment*. **34**, 2459-2469.

Dimashki, M., Lim, L. H., Harrison, R. M., Harrad, S. (2001) Temporal trends, temperature dependence, and relative reactivity of atmospheric polycyclic aromatic hydrocarbons. *Environ Sci Technol*. **35**, 2264-2267.

Ding, X., Wang, X.-M., Xie, Z.-Q., Xiang, C.-H., Mai, B.-X., Sun, L.-G., et al. (2007) Atmospheric polycyclic aromatic hydrocarbons observed over the North Pacific Ocean and the Arctic area: Spatial distribution and source identification. *Atmospheric Environment*. **41**, 2061-2072.

Draper, W. M. (1986) Quantitation of nitropolycyclic and dinitropolycyclic aromatic-hydrocarbons in diesel exhaust particulate matter. *Chemosphere*. **15**, 437-447.

Durant, J. L., Busby, W. F., Lafleur, A. L., Penman, B. W., Crespi, C. L. (1996) Human cell mutagenicity of oxygenated, nitrated and unsubstituted polycyclic aromatic hydrocarbons associated with urban aerosols. *Mutation Research-Genetic Toxicology*. **371**, 123-157.

Durant, J. L., Lafleur, A. L., Plummer, E. F., Taghizadeh, K., Busby, W. F., Thilly, W. G. (1998) Human lymphoblast mutagens in urban airborne particles. *Environ Sci Technol*. **32**, 1894-1906.

EEA. (2012) Air quality in Europe - 2012 report. *EEA, Copenhagen*

Eiguren-Fernandez, A., Miguel, A. H., Jaques, P. A., Sioutas, C. (2003) Evaluation of a denuder-MOUDI-PUF sampling system to measure the size distribution of semi-volatile polycyclic aromatic hydrocarbons in the atmosphere. *Aerosol Science and Technology*. **37**, 201-209.

Eiguren-Fernandez, A., Miguel, A. H., Di Stefano, E., Schmitz, D. A., Cho, A. K., Thuraiatnam, S., et al. (2008a) Atmospheric distribution of gas- and particle-phase quinones in Southern California. *Aerosol Science and Technology*. **42**, 854-861.

Eiguren-Fernandez, A., Miguel, A. H., Lu, R., Purvis, K., Grant, B., Mayo, P., et al. (2008b) Atmospheric formation of 9,10-phenanthraquinone in the Los Angeles air basin. *Atmospheric Environment*. **42**, 2312-2319.

Eiguren-Fernandez, A., Miguel, A. H. (2012) Size-Resolved Polycyclic Aromatic Hydrocarbon Emission Factors from On-Road Gasoline and Diesel Vehicles: Temperature Effect on the Nuclei-Mode. *Environ Sci Technol*. **46**, 2607-2615.

EMEP. (2011) Measurement data online, European Monitoring and Evaluation Programme. *Measurement data online, European Monitoring and Evaluation Programme, Geneva*, 43 <http://www.niluno/projects/ccc/emepdatahtml>.

Enya, T., Suzuki, H., Watanabe, T., Hirayama, T., Hisamatsu, Y. (1997) 3-nitrobenzanthrone, a powerful bacterial mutagen and suspected human carcinogen found in diesel exhaust and airborne particulates. *Environ Sci Technol.* **31**, 2772-2776.

EPAQS. (1999) Expert Panel on Air Quality Standards. Polycyclic Aromatic Hydrocarbons. Report for the Department of the Environment, Transport and the Regions.

Estève, W., Budzinski, H., Villenave, E. (2003) Heterogeneous reactivity of OH radicals with phenanthrene. *Polycyclic Aromatic Compounds.* **23**, 441-456.

Estève, W., Budzinski, H., Villenave, E. (2004) Relative rate constants for the heterogeneous reactions of OH, NO₂ and NO radicals with polycyclic aromatic hydrocarbons adsorbed on carbonaceous particles. Part 1: PAHs adsorbed on 1-2 µm calibrated graphite particles. *Atmospheric Environment.* **38**, 6063-6072.

Estève, W., Budzinski, H., Villenave, E. (2006) Relative rate constants for the heterogeneous reactions of NO₂ and OH radicals with polycyclic aromatic hydrocarbons adsorbed on carbonaceous particles. Part 2: PAHs adsorbed on diesel particulate exhaust SRM 1650a. *Atmospheric Environment.* **40**, 201-211.

Fan, Z. H., Chen, D. H., Birla, P., Kamens, R. M. (1995) Modeling of nitro-polycyclic aromatic hydrocarbon formation and decay in the atmosphere. *Atmospheric Environment.* **29**, 1171-1181.

Fan, Z. H., Kamens, R. M., Hu, J. X., Zhang, J. B., McDow, S. (1996a) Photostability of nitro polycyclic aromatic hydrocarbons on combustion soot particles in sunlight. *Environ Sci Technol.* **30**, 1358-1364.

Fan, Z. H., Kamens, R. M., Zhang, J. B., Hu, J. X. (1996b) Ozone-nitrogen dioxide-NPAH heterogeneous soot particle reactions and modeling NPAH in the atmosphere. *Environ Sci Technol.* **30**, 2821-2827.

Feilberg, A., Kamens, R. M., Strommen, M. R., Nielsen, T. (1999) Modeling the formation, decay, and partitioning of semivolatile nitro-polycyclic aromatic hydrocarbons (nitronaphthalenes) in the atmosphere. *Atmospheric Environment.* **33**, 1231-1243.

Feilberg, A., Nielsen, T. (2000) Effect of aerosol chemical composition on the photodegradation of nitro-polycyclic aromatic hydrocarbons. *Environ Sci Technol.* **34**, 789-797.

Feilberg, A., Poulsen, M. W. B., Nielsen, T., Skov, H. (2001) Occurrence and sources of particulate nitro-polycyclic aromatic hydrocarbons in ambient air in Denmark. *Atmospheric Environment.* **35**, 353-366.

Feilberg, A., Nielsen, T., Binderup, M. L., Skov, H., Poulsen, M. W. B. (2002) Observations of the effect of atmospheric processes on the genotoxic potency of airborne particulate matter. *Atmospheric Environment.* **36**, 4617-4625.

Fernandez, P., Grimalt, J. O., Vilanova, R. M. (2002) Atmospheric gas-particle partitioning of polycyclic aromatic hydrocarbons in high mountain regions of Europe. *Environ Sci Technol.* **36**, 1162-1168.

Fiedler, H., Mücke, W. (1991) Nitro Derivatives of Polycyclic Aromatic Hydrocarbons (NO₂-PAH). In : (Ed Hutzinger, O) *The Handbook of Environmental Chemistry, Volume 3 / 3G, Anthropogenic Compounds* pp 97-137

- Fine, P. M., Cass, G. R., Simoneit, B. R. T. (2002) Chemical characterization of fine particle emissions from the fireplace combustion of woods grown in the southern United States. *Environ Sci Technol.* **36**, 1442-1451.
- Fine, P. M., Chakrabarti, B., Krudysz, M., Schauer, J. J., Sioutas, C. (2004) Diurnal variations of individual organic compound constituents of ultrafine and accumulation mode particulate matter in the Los Angeles basin. *Environ Sci Technol.* **38**, 1296-1304.
- Finlayson-Pitts, B. J., Pitts, J. N. (2000) Airborne Polycyclic Aromatic Hydrocarbons and Their Derivatives: Atmospheric Chemistry and Toxicological Implications. In : Chemistry of the Upper and Lower Atmosphere : Theory, Experiments, Application. *Academic Press, San Diego, USA* 436-546 pp
- Fitzpatrick, E. M., Ross, A. B., Bates, J., Andrews, G., Jones, J. M., Phylaktou, H., et al. (2007) Emission of oxygenated species from the combustion of pine wood and its relation to soot formation. *Process Safety and Environmental Protection.* **85**, 430-440.
- Fraser, M. P., Cass, G. R., Simoneit, B. R. T. (1998a) Gas-phase and particle-phase organic compounds emitted from motor vehicle traffic in a Los Angeles roadway tunnel. *Environ Sci Technol.* **32**, 2051-2060.
- Fraser, M. P., Cass, G. R., Simoneit, B. R. T., Rasmussen, R. A. (1998b) Air quality model evaluation data for organics. 5. C-6-C-22 nonpolar and semipolar aromatic compounds. *Environ Sci Technol.* **32**, 1760-1770.
- Geyer, A., Ackermann, R., Dubois, R., Lohrmann, B., Muller, T., Platt, U. (2001) Long-term observation of nitrate radicals in the continental boundary layer near Berlin. *Atmospheric Environment.* **35**, 3619-3631.
- Geyer, A., Alicke, B., Ackermann, R., Martinez, M., Harder, H., Brune, W., et al. (2003) Direct observations of daytime NO₃: Implications for urban boundary layer chemistry. *Journal of Geophysical Research-Atmospheres.* **108**.
- Gibson, T. L. (1982) Nitro-derivatives of polynuclear aromatic-hydrocarbons in airborne and source particulate matter. *Atmospheric Environment.* **16**, 2037-2040.
- Goriaux, M., Jourdain, B., Temime, B., Besombes, J. L., Marchand, N., Albinet, A., et al. (2006) Field comparison of particulate PAH measurements using a low-flow denuder device and conventional sampling systems. *Environ Sci Technol.* **40**, 6398-6404.
- Gorse, R. A., Riley, T. L., Ferris, F. C., Pero, A. M., Skewes, L. M. (1983) 1-Nitropyrene concentration and bacterial mutagenicity in on-road vehicle particulate-emissions. *Environ Sci Technol.* **17**, 198-202.
- Goulay, F., Rebrion-Rowe, C., Le Garrec, J. L., Le Picard, S. D., Canosa, A., Rowe, B. R. (2005) The reaction of anthracene with OH radicals: An experimental study of the kinetics between 58 and 470 K. *Journal of Chemical Physics.* **122**.
- Graham, R. A., Johnston, H. S. (1978) The photochemistry of NO₃ and the kinetics of the N₂O₅-O₃ system. *Journal of Physical Chemistry* **82**, 254-268.
- Grosjean, D. (1983) The effect of nitrogen-dioxide and ozone on the decomposition of particle-associated polycyclic aromatic-hydrocarbons during sampling from the atmosphere. *Atmospheric Environment.* **17**, 2112-2114.

- Guo, H., Lee, S. C., Ho, K. F., Wang, X. M., Zou, S. C. (2003) Particle-associated polycyclic aromatic hydrocarbons in urban air of Hong Kong. *Atmospheric Environment*. **37**, 5307-5317.
- Guo, Z., Kamens, R. M. (1991) An experimental technique for studying heterogeneous reactions of polyaromatic hydrocarbons on particle surfaces. *Journal of Atmospheric Chemistry*. **12**, 137-151.
- Gupta, P., Harger, W. P., Arey, J. (1996) The contribution of nitro- and methyl nitro-naphthalenes to the vapor-phase mutagenicity of ambient air samples. *Atmospheric Environment*. **30**, 3157-3166.
- Gusev, A., Dutchak, S., Rozovskaya, O., Shatalov, V., Sokovyh, V., Vulykh, N., et al. (2011) Persistent Organic Pollutants in the Environment. EMEP Status Report 3/2011, Meteorological Synthesizing 38 Centre - East, Moscow, Russian Federation, 108 pp. *Persistent Organic Pollutants in the Environment EMEP Status Report 3/2011, Meteorological Synthesizing 38 Centre - East, Moscow, Russian Federation, 108 pp.*
- Halsall, C., Burnett, V., Davis, B., Jones, P., Pettit, C., Jones, K. C. (1993) PCBs and PAHs in U.K. urban air. *Chemosphere*. **26**, 2185-2197.
- Halsall, C. J., Barrie, L. A., Fellin, P., Muir, D. C. G., Billeck, B. N., Lockhart, L., et al. (1997) Spatial and temporal variation of polycyclic aromatic hydrocarbons in the Arctic atmosphere. *Environ Sci Technol*. **31**, 3593-3599.
- Halsall, C. J., Sweetman, A. J., Barrie, L. A., Jones, K. C. (2001) Modelling the behaviour of PAHs during atmospheric transport from the UK to the Arctic. *Atmospheric Environment*. **35**, 255-267.
- Halse, A. K., Schlabach, M., Eckhardt, S., Sweetman, A., Jones, K. C., Breivik, K. (2011) Spatial variability of POPs in European background air. *Atmospheric Chemistry and Physics*. **11**, 1549-1564.
- Hanedar, A., Alp, K., Kaynak, B., Avsar, E. (2014) Toxicity evaluation and source apportionment of Polycyclic Aromatic Hydrocarbons (PAHs) at three stations in Istanbul, Turkey. *Sci Total Environ*. **488**, 439-448.
- Hannigan, M. P., Cass, G. R., Penman, B. W., Crespi, C. L., Lafleur, A. L., Busby, W. F., et al. (1997) Human cell mutagens in Los Angeles air. *Environ Sci Technol*. **31**, 438-447.
- Hannigan, M. P., Cass, G. R., Penman, B. W., Crespi, C. L., Lafleur, A. L., Busby, W. F., et al. (1998) Bioassay directed chemical analysis of Los Angeles airborne particulate matter using a human cell mutagenicity assay. *Environ Sci Technol*. **32**, 3502-3514.
- Harner, T., Bidleman, T. F. (1998) Octanol-air partition coefficient for describing particle/gas partitioning of aromatic compounds in urban air. *Environ Sci Technol*. **32**, 1494-1502.
- Harner, T., Bidleman, T. F., Jantunen, L. M. M., Mackay, D. (2001) Soil-air exchange model of persistent pesticides in the United States cotton belt. *Environmental Toxicology and Chemistry*. **20**, 1612-1621.
- Harrad, S., Hassoun, S., Romero, M. S. C., Harrison, R. M. (2003) Characterisation and source attribution of the semi-volatile organic content of atmospheric particles and associated vapour phase in Birmingham, UK. *Atmospheric Environment*. **37**, 4985-4991.
- Harrad, S., Laurie, L. (2005) Concentrations, sources and temporal trends in atmospheric polycyclic aromatic hydrocarbons in a major conurbation. *Journal of Environmental Monitoring*. **7**, 722-727.

- Harrison, R. M., Smith, D. J. T., Luhana, L. (1996) Source apportionment of atmospheric polycyclic aromatic hydrocarbons collected from an urban location in Birmingham, UK. *Environ Sci Technol.* **30**, 825-832.
- Harrison, R. M., Tilling, R., Romero, M. S. C., Harrad, S., Jarvis, K. (2003) A study of trace metals and polycyclic aromatic hydrocarbons in the roadside environment. *Atmospheric Environment.* **37**, 2391-2402.
- Harrison, R. M., Smith, D. J. T., Kibble, A. J. (2004) What Is Responsible for the Carcinogenicity of PM_{2.5}? *Occupational and Environmental Medicine.* **61**, 799-805.
- Hart, K. M., Pankow, J. F. (1994) High-volume air sampler for particle and gas sampling .2. use of backup filters to correct for the adsorption of gas-phase polycyclic aromatic-hydrocarbons to the front filter. *Environ Sci Technol.* **28**, 655-661.
- Hayakawa, K., Butoh, M., Miyazaki, M. (1992) Determination of dinitropyrenes and nitropyrenes in emission particulates from diesel and gasoline-engine vehicles by liquid-chromatography with chemiluminescence detection after precolumn reduction. *Analytica Chimica Acta.* **266**, 251-256.
- Hayakawa, K., Butoh, M., Hirabayashi, Y., Miyazaki, M. (1994) Determination of 1,3-dinitropyrenes 1,6-dinitropyrenes 1,8-dinitropyrenes and 1-nitropyrene in-vehicle exhaust particulates. *Japanese Journal of Toxicology and Environmental Health.* **40**, 20-25.
- Hayakawa, K., Tang, N., Akutsu, K., Murahashi, T., Kakimoto, H., Kizu, R., et al. (2002) Comparison of polycyclic aromatic hydrocarbons and nitropolycyclic aromatic hydrocarbons in airborne particulates collected in downtown and suburban Kanazawa, Japan. *Atmospheric Environment.* **36**, 5535-5541.
- Hays, M. D., Fine, P. M., Geron, C. D., Kleeman, M. J., Gullett, B. K. (2005) Open burning of agricultural biomass: Physical and chemical properties of particle-phase emissions. *Atmospheric Environment.* **39**, 6747-6764.
- Healy, R. M., Chen, Y., Kourtchev, I., Kalberer, M., O'Shea, D., Wenger, J. C. (2012) Rapid Formation of Secondary Organic Aerosol from the Photolysis of 1-Nitronaphthalene: Role of Naphthoxy Radical Self-reaction. *Environ Sci Technol.* **46**, 11813-11820.
- Helmig, D., Arey, J., Atkinson, R., Harger, W. P., McElroy, P. A. (1992a) Products of the OH radical-initiated gas-phase reaction of fluorene in the presence of NO_x. *Atmospheric Environment Part a-General Topics.* **26**, 1735-1745.
- Helmig, D., Arey, J., Harger, W. P., Atkinson, R., Lopezcancio, J. (1992b) Formation of mutagenic nitrodibenzopyranones and their occurrence in ambient air. *Environ Sci Technol.* **26**, 622-624.
- Helmig, D., Lopezcancio, J., Arey, J., Harger, W. P., Atkinson, R. (1992c) Quantification of Ambient Nitrodibenzopyranones - Further Evidence For Atmospheric Mutagen Formation. *Environ Sci Technol.* **26**, 2207-2213.
- Helmig, D., Harger, W. P. (1994) OH radical-initiated gas-phase reaction-products of phenanthrene. *Sci Total Environ.* **148**, 11-21.
- Hien, T. T., Thanh, L. T., Kameda, T., Takenaka, N., Bandow, H. (2007) Nitro-polycyclic aromatic hydrocarbons and polycyclic aromatic hydrocarbons in particulate matter in an urban area of a tropical region: Ho Chi Minh City, Vietnam. *Atmospheric Environment.* **41**, 7715-7725.

- Ho, K. F., Ho, S. S. H., Lee, S. C., Cheng, Y., Chow, J. C., Watson, J. G., et al. (2009) Emissions of gas- and particle-phase polycyclic aromatic hydrocarbons (PAHs) in the Shing Mun Tunnel, Hong Kong. *Atmospheric Environment*. **43**, 6343-6351.
- Holloway, M. P., Biaglow, M. C., McCoy, E. C., Anders, M., Rosenkranz, H. S., Howard, P. C. (1987) Photochemical instability of 1-nitropyrene, 3-nitrofluoranthene, 1,8-dinitropyrene and their parent polycyclic aromatic-hydrocarbons. *Mutation Research*. **187**, 199-207.
- Holloway, A.M. and Wayne, R.P. (2010) *Atmospheric Chemistry*, RSC Publishing. Royal Society of Chemistry, Cambridge, U.K.
- Holoubek, I., Klanova, J., Jarkovsky, J., Kohoutek, J. (2007) Trends in background levels of persistent organic pollutants at Kosectice observatory, Czech Republic. Part I. Ambient air and wet deposition 1996-2005. *Journal of Environmental Monitoring*. **9**, 557-563.
- Hu, S., Herner, J. D., Robertson, W., Kobayashi, R., Chang, M. C. O., Huang, S.-m., et al. (2013) Emissions of polycyclic aromatic hydrocarbons (PAHs) and nitro-PAHs from heavy-duty diesel vehicles with DPF and SCR. *J Air Waste Manage Assoc*. **63**, 984-996.
- Huang, B., Liu, M., Bi, X., Chaemfa, C., Ren, Z., Wang, X., et al. (2014) Phase distribution, sources and risk assessment of PAHs, NPAHs and OPAHs in a rural site of Pearl River Delta region, China. *Atmospheric Pollution Research*. **5**, 210-218.
- Hung, H., Blanchard, P., Halsall, C. J., Bidleman, T. F., Stern, G. A., Fellin, P., et al. (2005) Temporal and spatial variabilities of atmospheric polychlorinated biphenyls (PCBs), organochlorine (OC) pesticides and polycyclic aromatic hydrocarbons (PAHs) in the Canadian Arctic: Results from a decade of monitoring. *Sci Total Environ*. **342**, 119-144.
- IARC. (1983) International Agency for Research on Cancer, Monographs on the Evaluation of Carcinogenic Risk of Chemicals to Humans, Volume 32 : Polynuclear Aromatic Hydrocarbons, Part 1 : Chemical, Environmental and Experimental Data. IARC, Lyon.
- IARC. (1989) International Agency for Research on Cancer, Monographs on the Evaluation of Carcinogenic Risk of Chemicals to Humans, Volume 46 : Diesel and Gasoline Engine Exhausts and Some Nitroarenes. IARC, Lyon. [URL http://monographsiarcfr/ENG/Monographs/vol46/volume46pdf](http://monographsiarcfr/ENG/Monographs/vol46/volume46pdf)
- IARC (2010) I International Agency for Research on Cancer, Monographs on the Evaluation of Carcinogenic Risk of Chemicals to Humans, Volume 92 : Some Non-heterocyclic Polycyclic Aromatic Hydrocarbons and Some Related Exposures. IARC, Lyon.
- Iinuma, Y., Brüeggemann, E., Gnauk, T., Mueller, K., Andreae, M. O., Helas, G., et al. (2007) Source characterization of biomass burning particles: The combustion of selected European conifers, African hardwood, savanna grass, and German and Indonesian peat. *Journal of Geophysical Research-Atmospheres*. **112**.
- Inazu, K., Kobayashi, T., Hisamatsu, Y. (1997) Formation of 2-nitrofluoranthene in gas-solid heterogeneous photoreaction of fluoranthene supported on oxide particles in the presence of nitrogen dioxide. *Chemosphere*. **35**, 607-622.
- Ioki, Y. (1977) Aryloxy radicals by photorearrangement of nitro-compounds. *Journal of the Chemical Society-Perkin Transactions 2*, 1240-1242.
- Jaffrezo, J. L., Masclat, P., Clain, M. P., Wortham, H., Beyne, S., Cachier, H. (1993) Transfer-function of polycyclic aromatic-hydrocarbons from the atmosphere to the polar ice .1. determination

of atmospheric concentrations at dye-3, greenland. *Atmospheric Environment Part a-General Topics*. **27**, 2781-2785.

Jakober, C. A., Riddle, S. G., Robert, M. A., Destailats, H., Charles, M. J., Green, P. G., et al. (2007) Quinone emissions from gasoline and diesel motor vehicles. *Environ Sci Technol*. **41**, 4548-4554.

Jang, E., Alam, M. S., Harrison, R. M. (2013) Source apportionment of polycyclic aromatic hydrocarbons in urban air using positive matrix factorization and spatial distribution analysis. *Atmospheric Environment*. **79**, 271-285.

Jariyasopit, N., Zimmermann, K., Schrlau, J., Arey, J., Atkinson, R., Massey Simonich, S. L. (2011) Heterogeneous reactions of O₃, OH Radicals and N₂O₅ with Chinese particulate matter to simulate trans-Pacific atmospheric transport. *23rd International Symposium on Polycyclic Aromatic Compounds, Münster, Germany, 4-7 September 2011*.

Jariyasopit, N., Zimmermann, K., Schrlau, J., Arey, J., Atkinson, R., Yu, T.-W., et al. (2014) Heterogeneous Reactions of Particulate Matter-Bound PAHs and NPAHs with NO₃/N₂O₅, OH Radicals, and O₃ under Simulated Long-Range Atmospheric Transport Conditions: Reactivity and Mutagenicity. *Environ Sci Technol*. **48**, 10155-10164.

Jones, K. C., Stratford, J. A., Waterhouse, K. S., Furlong, E. T., Giger, W., Hites, R. A., et al. (1989) Increases in the polynuclear aromatic hydrocarbon content of an agricultural soil over the last century. *Environ Sci Technol*. **23**, 95-101.

Jones, K. C., Sanders, G., Wild, S. R., Burnett, V., Johnston, A. E. (1992) Evidence for a decline of pcbs and pahs in rural vegetation and air in the United-Kingdom. *Nature*. **356**, 137-140.

Jonker, M. T. O., Hawthorne, S. B., Koelmans, A. A. (2005) Extremely slowly desorbing polycyclic aromatic hydrocarbons from soot and soot-like materials: Evidence by supercritical fluid extraction. *Environ Sci Technol*. **39**, 7889-7895.

Kahan, T. F., Kwamena, N. O. A., Donaldson, D. J. (2006) Heterogeneous ozonation kinetics of polycyclic aromatic hydrocarbons on organic films. *Atmospheric Environment*. **40**, 3448-3459.

Kakimoto, H., Kitamura, M., Matsumoto, Y., Sakai, S., Kanoh, F., Murahashi, T., et al. (2000) Comparison of atmospheric polycyclic aromatic hydrocarbons and nitropolycyclic aromatic hydrocarbons in Kanazawa, Sapporo and Tokyo. *Journal of Health Science*. **46**, 5-15.

Kakimoto, H., Yokoe, H., Matsumoto, Y., Sakai, S., Kanoh, F., Murahashi, T., et al. (2001) Considerations of atmospheric behaviors of polycyclic aromatic hydrocarbons, nitropolycyclic aromatic hydrocarbons and inorganic pollutants based on their interrelationships. *Journal of Health Science*. **47**, 385-393.

Kallio, M., Hyotylainen, T., Lehtonen, M., Jussila, M., Hartonen, K., Shimmo, M., et al. (2003) Comprehensive two-dimensional gas chromatography in the analysis of urban aerosols. *Journal of Chromatography A*. **1019**, 251-260.

Kam, W., Liacos, J. W., Schauer, J. J., Delfino, R. J., Sioutas, C. (2012) On-road emission factors of PM pollutants for light-duty vehicles (LDVs) based on urban street driving conditions. *Atmospheric Environment*. **61**, 378-386.

Kameda, T., Inazu, K., Bandow, H., Sanukida, S., Maeda, Y. (2004) Diurnal change of direct-acting mutagenicity of soluble organic fraction of airborne particles collected at Southern Osaka:

correlation between the mutagenicity, particles-associated nitroarenes, and gaseous emission. *Atmospheric Environment*. **38**, 1903-1912.

Kameda, T. (2011) Atmospheric Chemistry of Polycyclic Aromatic Hydrocarbons and Related Compounds. *Journal of Health Science*. **57**, 504-511.

Kamens, R. M., Guo, Z., Fulcher, J. N., Bell, D. A. (1988) Influence of humidity, sunlight, and temperature on the daytime decay of polyaromatic hydrocarbons on atmospheric soot particles. *Environ Sci Technol*. **22**, 103-108.

Kamens, R. M., Karam, H., Guo, J. H., Perry, J. M., Stockburger, L. (1989) The Behavior of Oxygenated Polycyclic Aromatic Hydrocarbons on Atmospheric Soot Particles. *Environ Sci Technol*. **23**, 801-806.

Karagulian, F., Rossi, M. J. (2007) Heterogeneous chemistry of the NO₃ free radical and N₂O₅ on decane flame soot at ambient temperature: Reaction products and kinetics. *Journal of Physical Chemistry A*. **111**, 1914-1926.

Karavalakis, G., Stournas, S., Bakeas, E. (2009) Light vehicle regulated and unregulated emissions from different biodiesels. *Sci Total Environ*. **407**, 3338-3346.

Katz, M., Chan, C., Tosine, H., Sakuma, T. (1979) Relative Rates of Photochemical and Biological Oxidation in Vitro of Polycyclic Aromatic Hydrocarbons. in *Polynuclear Aromatic Hydrocarbons (P W Jones and P Leber, Eds)*, Ann Arbor Science Publishers, Ann Arbor, MI, pp. 171-189.

Kautzman, K. E., Surratt, J. D., Chan, M. N., Chan, A. W. H., Hersey, S. P., Chhabra, P. S., et al. (2010) Chemical Composition of Gas- and Aerosol-Phase Products from the Photooxidation of Naphthalene. *Journal of Physical Chemistry A*. **114**, 913-934.

Kavouras, I. G., Lawrence, J., Koutrakis, P., Stephanou, E. G., Oyola, P. (1999) Measurement of particulate aliphatic and polynuclear aromatic hydrocarbons in Santiago de Chile: source reconciliation and evaluation of sampling artifacts. *Atmospheric Environment*. **33**, 4977-4986.

Kawanaka, Y., Matsumoto, E., Sakamoto, K., Wang, N., Yun, S. J. (2004) Size distributions of mutagenic compounds and mutagenicity in atmospheric particulate matter collected with a low-pressure cascade impactor. *Atmospheric Environment*. **38**, 2125-2132.

Kawanaka, Y., Tsuchiya, Y., Yun, S.-J., Sakamoto, K. (2009) Size Distributions of Polycyclic Aromatic Hydrocarbons in the Atmosphere and Estimation of the Contribution of Ultrafine Particles to Their Lung Deposition. *Environ Sci Technol*. **43**, 6851-6856.

Keller, C. D., Bidleman, T. F. (1984) Collection of airborne polycyclic aromatic-hydrocarbons and other organics with a glass-fiber filter polyurethane foam system. *Atmospheric Environment*. **18**, 837-845.

Keyte, I. J., Wild, E., Dent, J., Jones, K. C. (2009) Investigating the Foliar Uptake and Within-Leaf Migration of Phenanthrene by Moss (*Hypnum Cupressiforme*) Using Two-Photon Excitation Microscopy with Autofluorescence. *Environ Sci Technol*. **43**, 5755-5761.

Keyte, I. J., Harrison, R. M., Lammel, G. (2013) Chemical reactivity and long-range transport potential of polycyclic aromatic hydrocarbons - a review. *Chemical Society Reviews*. **42**, 9333-9391.

- Khalili, N. R., Scheff, P. A., Holsen, T. M. (1995) PAH source fingerprints for coke ovens, diesel and gasoline-engines, highway tunnels, and wood combustion emissions. *Atmospheric Environment*. **29**, 533-542.
- Kim, J. Y., Lee, J. Y., Kim, Y. P., Lee, S. B., Jin, H. C., Bae, G. N. (2012) Seasonal characteristics of the gaseous and particulate PAHs at a roadside station in Seoul, Korea. *Atmospheric Research*. **116**, 142-150.
- Kishikawa, N., Nakao, M., Ohba, Y., Nakashima, K., Kuroda, N. (2006) Concentration and trend of 9,10-phenanthrenequinone in airborne particulates collected in Nagasaki city, Japan. *Chemosphere*. **64**, 834-838.
- Kiss, G., Varga-Puchony, Z., Hlavaj, Z. . (1996) Distribution of polycyclic aromatic hydrocarbons on atmospheric aerosol particles of different size. In: Nucleation and Atmospheric Aerosols, Kulmala, M., Wagner, P.O. (eds.). Elsevier, Kidlington, pp 501–503. *Distribution of polycyclic aromatic hydrocarbons on atmospheric aerosol particles of different size In: Nucleation and Atmospheric Aerosols, Kulmala, M, Wagner, PO (eds) Elsevier, Kidlington, pp 501–503.*
- Klamt, A. (1993) Estimation of gas-phase hydroxyl radical rate constants of organic-compounds from molecular-orbital calculations. *Chemosphere*. **26**, 1273-1289.
- Klanova, J., Cupr, P., Holoubek, I., Boruvkova, J., Pribylova, P., Kares, R., et al. (2009) Monitoring of persistent organic pollutants in Africa. Part 1: Passive air sampling across the continent in 2008. *Journal of Environmental Monitoring*. **11**, 1952-1963.
- Klopffer, W., Frank, R., Kohl, E. G., Haag, F. (1986) Quantitative presentation of photochemical transformation processes in the troposphere. *Chemiker-Zeitung*. **110**, 57-61.
- Kojima, Y., Inazu, K., Hisamatsu, Y., Okochi, H., Baba, T., Nagoya, T. (2010) Changes in Concentration Levels of Polycyclic Aromatic Compounds Associated with Airborne Particulate Matter in Downtown Tokyo after Introducing Government Diesel Vehicle Controls. *Asian Journal of Atmospheric Environment*. **4**, 1-8.
- Korfmacher, W. A., Natusch, D. F. S., Taylor, D. R., Mamantov, G., Wehry, E. L. (1980) Oxidative transformations of polycyclic aromatic-hydrocarbons adsorbed on coal fly-ash. *Science*. **207**, 763-765.
- Krol, M., Lelieveld, J. (2003) Can the variability in tropospheric OH be deduced from measurements of 1,1,1-trichloroethane (methyl chloroform)? *Journal of Geophysical Research-Atmospheres*. **108**.
- Kumagai, Y. (2009) Polycyclic Aromatic Hydrocarbon Quinones as Redox and Electrophilic Chemicals Contaminated in the Atmosphere. *Journal of Health Science*. **55**, 887-894.
- Kwamena, N. O. A., Thornton, J. A., Abbatt, J. P. D. (2004) Kinetics of surface-bound benzo a pyrene and ozone on solid organic and salt aerosols. *Journal of Physical Chemistry A*. **108**, 11626-11634.
- Kwamena, N. O. A., Earp, M. E., Young, C. J., Abbatt, J. P. D. (2006) Kinetic and product yield study of the heterogeneous gas-surface reaction of anthracene and ozone. *Journal of Physical Chemistry A*. **110**, 3638-3646.
- Kwok, E. S. C., Atkinson, R., Arey, J. (1994a) Kinetics and mechanisms of the gas-phase reactions of the NO₃ radical with aromatic-compounds. *International Journal of Chemical Kinetics*. **26**, 511-525.

- Kwok, E. S. C., Harger, W. P., Arey, J., Atkinson, R. (1994b) Reactions of gas-phase phenanthrene under simulated atmospheric conditions. *Environ Sci Technol.* **28**, 521-527.
- Kwok, E. S. C., Atkinson, R., Arey, J. (1995) Rate constants for the gas-phase reactions of the OH radical with dichlorobiphenyls, 1-chlorodibenzo-p-dioxin, 1,2-dimethoxybenzene, and diphenyl ether - estimation of OH radical reaction-rate constants for PCBs, PCDDs AND PCDFs. *Environ Sci Technol.* **29**, 1591-1598.
- Kwok, E. S. C., Atkinson, R., Arey, J. (1997) Kinetics of the gas-phase reactions of indan, indene, fluorene, and 9,10-dihydroanthracene with OH radicals, NO₃ radicals, and O₃. *International Journal of Chemical Kinetics.* **29**, 299-309.
- Lammel, G., Klanova, J., Kohoutek, J., Prokes, R., Ries, L., Stohl, A. (2009) Observation and origin of organochlorine compounds and polycyclic aromatic hydrocarbons in the free troposphere over central Europe. *Environmental Pollution.* **157**, 3264-3271.
- Lammel, G., Novák, J., Landlová, L., Dvorská, A., Klánová, J., Čupr, P., Kohoutek, J., Reimer, E., Škrdlíková, L. (2010) Sources and distributions of polycyclic aromatic hydrocarbons and toxicity of polluted atmosphere aerosols. In: *Urban Airborne Particulate Matter: Origins, Chemistry, Fate and Health Impacts, Zereini F, Wiseman CLS (eds) Springer, Berlin, pp 39-62.*
- Lane, D. A., Katz, M. (1977) The Photomodification of Benzo a pyrene, Benzo b fluoranthene, and Benzo k fluoranthene under Simulated Atmospheric Conditions. in *Fate of Pollutants in the Air and Water Environments, Part 2 (A Suffet, Ed), Wiley-Interscience, New York, pp. 133 -154.*
- Laurie, E. H. (2003) Source apportionment of urban atmospheric polycyclic aromatic hydrocarbons *PhD thesis, University of Birmingham, United Kingdom*
- Lawther, P. J., Waller, R. E. (1976) Coal fires, industrial emissions and motor vehicles as sources of environmental carcinogens. *IARC scientific publications, 27-40.*
- Lee, H. K. (1995) Recent applications of gas and high-performance liquid-chromatographic techniques to the analysis of polycyclic aromatic-hydrocarbons in airborne-particulates. *Journal of Chromatography A.* **710**, 79-92.
- Lee, J., Lane, D. A. (2010) Formation of oxidized products from the reaction of gaseous phenanthrene with the OH radical in a reaction chamber. *Atmospheric Environment.* **44**, 2469-2477.
- Lee, J. Y., Lane, D. A. (2009) Unique products from the reaction of naphthalene with the hydroxyl radical. *Atmospheric Environment.* **43**, 4886-4893.
- Lee, J. Y., Lane, D. A., Heo, J. B., Yi, S.-M., Kim, Y. P. (2012) Quantification and seasonal pattern of atmospheric reaction products of gas phase PAHs in PM_{2.5}. *Atmospheric Environment.* **55**, 17-25.
- Lee, R. G. M., Hung, H., Mackay, D., Jones, K. C. (1998) Measurement and modeling of the diurnal cycling of atmospheric PCBs and PAHs. *Environ Sci Technol.* **32**, 2172-2179.
- Lee, R. G. M., Jones, K. C. (1999) The influence of meteorology and air masses on daily atmospheric PCB and PAH concentrations at a UK location. *Environ Sci Technol.* **33**, 705-712.

- Lee, W., Stevens, P. S., Hites, R. A. (2003) Rate constants for the gas-phase reactions of methylphenanthrenes with OH as a function of temperature. *Journal of Physical Chemistry A*. **107**, 6603-6608.
- Lewis, A. C., Robinson, R. E., Bartle, K. D., Pilling, M. J. (1995) Online coupled lg-gc-itd/ms for the identification of alkylated, oxygenated, and nitrated polycyclic aromatic-compounds in urban air particulate extracts. *Environ Sci Technol*. **29**, 1977-1981.
- Lewtas, J., Chuang, J., Nishioka, M., Petersen, B. (1990) Bioassay-directed fractionation of the organic extract of SRM-1649 urban air particulate matter. *International Journal of Environmental Analytical Chemistry*. **39**, 245-256.
- Liberti, A., Ciccioni, P. (1986) High-resolution chromatographic techniques for the evaluation of atmospheric pollutants. *Journal of High Resolution Chromatography & Chromatography Communications*. **9**, 492-501.
- Ligocki, M. P., Leuenberger, C., Pankow, J. F. (1985) Trace organic-compounds in rain .3. particle scavenging of neutral organic-compounds. *Atmospheric Environment*. **19**, 1619-1626.
- Ligocki, M. P., Pankow, J. F. (1989) Measurements of the gas particle distributions of atmospheric organic-compounds. *Environ Sci Technol*. **23**, 75-83.
- Lim, L. H., Harrison, R. M., Harrad, S. (1999) The contribution of traffic to atmospheric concentrations of polycyclic aromatic hydrocarbons. *Environ Sci Technol*. **33**, 3538-3542.
- Lin, T. C., Chang, F. H., Hsieh, J. H., Chao, H. R., Chao, M. R. (2002) Characteristics of polycyclic aromatic hydrocarbons and total suspended particulate in indoor and outdoor atmosphere of a Taiwanese temple. *Journal of Hazardous Materials*. **95**, 1-12.
- Lindskog, A., Brorstrom-Lunden, E., Sjoedin, A. (1985) Transformations of reactive PAH on particles by exposure to oxidised nitrogen compounds and ozone. *Environment International*. **11**, 125-130.
- Lintelmann, J., Fischer, K., Matuschek, G. (2006) Determination of oxygenated polycyclic aromatic hydrocarbons in particulate matter using high-performance liquid chromatography-tandem mass spectrometry. *Journal of Chromatography A*. **1133**, 241-247.
- Liu, C., Zhang, P., Yang, B., Wang, Y., Shu, J. (2012) Kinetic Studies of Heterogeneous Reactions of Polycyclic Aromatic Hydrocarbon Aerosols with NO₃ Radicals. *Environ Sci Technol*. **46**, 7575-7580.
- Liu, L. B., Liu, Y., Lin, J. M., Tang, N., Hayakawa, K., Maeda, T. (2007) Development of analytical methods for polycyclic aromatic hydrocarbons (PAHs) in airborne particulates: A review. *Journal of Environmental Sciences-China*. **19**, 1-11.
- Liu, Y., Liu, L., Lin, J.-M., Tang, N., Hayakawa, K. (2006a) Distribution and characterization of polycyclic aromatic hydrocarbon compounds in airborne particulates of east asia. *China Particuology*. **4**, 283-292.
- Liu, Y., Sklorz, M., Schnelle-Kreis, J., Orasche, J., Ferge, T., Kettrup, A., et al. (2006b) Oxidant denuder sampling for analysis of polycyclic aromatic hydrocarbons and their oxygenated derivatives in ambient aerosol: Evaluation of sampling artefact. *Chemosphere*. **62**, 1889-1898.

- Lorenz, K., Zellner, R. (1983) Kinetics of the reactions of OH-radicals with benzene, benzene-d6 and naphthalene. *Berichte Der Bunsen-Gesellschaft-Physical Chemistry Chemical Physics*. **87**, 629-636.
- Ma, J., Liu, Y., He, H. (2011) Heterogeneous reactions between NO₂ and anthracene adsorbed on SiO₂ and MgO. *Atmospheric Environment*. **45**, 917-924.
- Magnotta, F., Johnston, H. S. (1980) Photo-dissociation quantum yields for the NO₃ free-radical. *Geophysical Research Letters*. **7**, 769-772.
- Mak, J., Gross, S., Bertram, A. K. (2007) Uptake of NO₃ on soot and pyrene surfaces. *Geophysical Research Letters*. **34**.
- Mari, M., Harrison, R. M., Schuhmacher, M., Domingo, J. L., Pongpiachan, S. (2010) Inferences over the sources and processes affecting polycyclic aromatic hydrocarbons in the atmosphere derived from measured data. *Sci Total Environ*. **408**, 2387-2393.
- Marino, F., Cecinato, A., Siskos, P. A. (2000) Nitro-PAH in ambient particulate matter in the atmosphere of Athens. *Chemosphere*. **40**, 533-537.
- Marinov, D., Dueri, S., Puillat, I., Carafa, R., Jurado, E., Berrojalbiz, N., et al. (2009) Integrated modelling of Polycyclic Aromatic Hydrocarbons in the marine environment: Coupling of hydrodynamic, fate and transport, bioaccumulation and planktonic food-web models. *Marine Pollution Bulletin*. **58**, 1554-1561.
- Marr, L. C., Kirchstetter, T. W., Harley, R. A., Miguel, A. H., Hering, S. V., Hammond, S. K. (1999) Characterization of polycyclic aromatic hydrocarbons in motor vehicle fuels and exhaust emissions. *Environ Sci Technol*. **33**, 3091-3099.
- Mastral, A. M., Callen, M. S., Lopez, J. M., Murillo, R., Garcia, T., Navarro, M. V. (2003a) Critical review on atmospheric PAR Assessment of reported data in the Mediterranean basin. *Fuel Processing Technology*. **80**, 183-193.
- Mastral, A. M., Lopez, J. M., Callen, M. S., Garcia, T., Murillo, R., Navarro, M. V. (2003b) Spatial and temporal PAH concentrations in Zaragoza, Spain. *Sci Total Environ*. **307**, 111-124.
- Matsumoto, Y., Sakai, S., Kato, T., Nakajima, T., Satoh, H. (1998) Long-term trends of particulate mutagenic activity in the atmosphere of Sapporo. 1. Determination of mutagenic activity by the conventional tester strains TA98 and TA100 during an 18-year period (1974-1992). *Environ Sci Technol*. **32**, 2665-2671.
- McDonald, J. D., Zielinska, B., Fujita, E. M., Sagebiel, J. C., Chow, J. C., Watson, J. G. (2000) Fine particle and gaseous emission rates from residential wood combustion. *Environ Sci Technol*. **34**, 2080-2091.
- McDonald, J. D., Zielinska, B., Sagebiel, J. C., McDaniel, M. R. (2002) Characterization of fine particle material in ambient air and personal samples from an underground mine. *Aerosol Science and Technology*. **36**, 1033-1044.
- Meijer, S. N., Sweetman, A. J., Halsall, C. J., Jones, K. C. (2008) Temporal trends of polycyclic aromatic hydrocarbons in the UK atmosphere: 1991-2005. *Environ Sci Technol*. **42**, 3213-3218.
- Miet, K., Budzinski, H., Villenave, E. (2009a) Heterogeneous reactions of OH radicals with particulate-pyrene and 1-nitropyrene of atmospheric interest. *Polycyclic Aromatic Compounds*. **29**, 267-281.

- Miet, K., Le Menach, K., Flaud, P. M., Budzinski, H., Villenave, E. (2009b) Heterogeneous reactions of ozone with pyrene, 1-hydroxypyrene and 1-nitropyrene adsorbed on particles. *Atmospheric Environment*. **43**, 3699-3707.
- Miet, K., Le Menach, K., Flaud, P. M., Budzinski, H., Villenave, E. (2009c) Heterogeneous reactivity of pyrene and 1-nitropyrene with NO₂: Kinetics, product yields and mechanism. *Atmospheric Environment*. **43**, 837-843.
- Miguel, A. H., Pereira, P. A. P. (1989) Benzo(k)fluoranthene, Benzo(ghi)perylene, and Indeno(1,2,3-cd)pyrene: New Tracers of Automotive Emissions in Receptor Modeling. *Aerosol Science and Technology*. **10**, 292-295.
- Miguel, A. H., Kirchstetter, T. W., Harley, R. A., Hering, S. V. (1998) On-road emissions of particulate polycyclic aromatic hydrocarbons and black carbon from gasoline and diesel vehicles. *Environ Sci Technol*. **32**, 450-455.
- Miguel, A. H., Eiguren-Fernandez, A., Jaques, P. A., Froines, J. R., Grant, B. L., Mayo, P. R., et al. (2004) Seasonal variation of the particle size distribution of polycyclic aromatic hydrocarbons and of major aerosol species in Claremont, California. *Atmospheric Environment*. **38**, 3241-3251.
- Mmerekki, B. T., Donaldson, D. J. (2003) Direct observation of the kinetics of an atmospherically important reaction at the air-aqueous interface. *Journal of Physical Chemistry A*. **107**, 11038-11042.
- Mmerekki, B. T., Donaldson, D. J., Gilman, J. B., Eliason, T. L., Vaida, V. (2004) Kinetics and products of the reaction of gas-phase ozone with anthracene adsorbed at the air-aqueous interface. *Atmospheric Environment*. **38**, 6091-6103.
- Murahashi, T., Hayakawa, K. (1997) A sensitive method for the determination of 6-nitrochrysene, 2-nitro-fluoranthene and 1-, 2- and 4-nitropyrenes in airborne particulates using high-performance liquid chromatography with chemiluminescence detection. *Analytica Chimica Acta*. **343**, 251-257.
- Murrells, T. P., Passant, N. R., Thistlethwaite, G., Wagner, A., Li, Y., Bush, T., et al. (2010) UK Emissions of Air Pollutants 1970 to 2008. *AEAT/ENV/R/3036, Defra, London*.
- Nassar, H. F., Tang, N., Kameda, T., Toriba, A., Khoder, M. I., Hayakawa, K. (2011) Atmospheric concentrations of polycyclic aromatic hydrocarbons and selected nitrated derivatives in Greater Cairo, Egypt. *Atmospheric Environment*. **45**, 7352-7359.
- Neususs, C., Pelzing, M., Plewka, A., Herrmann, H. (2000) A new analytical approach for size-resolved speciation of organic compounds in atmospheric aerosol particles: Methods and first results. *Journal of Geophysical Research-Atmospheres*. **105**, 4513-4527.
- Newton, D. L., Erickson, M. D., Tomer, K. B., Pellizzari, E. D., Gentry, P., Zweidinger, R. B. (1982) Identification of nitroaromatics in diesel exhaust particulate using gas-chromatography negative-ion chemical ionization mass-spectrometry and other techniques. *Environ Sci Technol*. **16**, 206-213.
- Nguyen, M. L., Bedjanian, Y., Guilloteau, A. (2009) Kinetics of the reactions of soot surface-bound polycyclic aromatic hydrocarbons with NO₂. *Journal of Atmospheric Chemistry*. **62**, 139-150.
- Nicol, S., Dugay, J., Hennion, M. C. (2001) Determination of oxygenated polycyclic aromatic compounds in airborne particulate organic matter using gas chromatography tandem mass spectrometry. *Chromatographia*. **53**, S464-S469.

- Niederer, M. (1998) Determination of polycyclic aromatic hydrocarbons and substitutes (nitro-, oxy-PAHs) in urban soil and airborne particulate by GC-MS and NCI-MS/MS. *Environmental Science and Pollution Research*. **5**, 209-216.
- Nielsen, T. (1984) Reactivity of polycyclic aromatic-hydrocarbons toward nitrating species. *Environ Sci Technol*. **18**, 157-163.
- Nielsen, T., Seitz, B., Ramdahl, T. (1984) Occurrence of nitro-PAH in the atmosphere in a rural area. *Atmospheric Environment*. **18**, 2159-2165.
- Nielsen, T. (1996) Traffic contribution of polycyclic aromatic hydrocarbons in the center of a large city. *Atmospheric Environment*. **30**, 3481-3490.
- Nielsen, T., Feilberg, A., Binderup, M. L. (1999) The variation of street air levels of PAH and other mutagenic PAC in relation to regulations of traffic emissions and the impact of atmospheric processes. *Environmental Science and Pollution Research*. **6**, 133-137.
- Nikolaou, K., Masclat, P., Mouvier, G. (1984) Sources and chemical-reactivity of polynuclear aromatic-hydrocarbons in the atmosphere - a critical-review. *Sci Total Environ*. **32**, 103-132.
- Nishino, N., Atkinson, R., Arey, J. (2008) Formation of Nitro Products from the Gas-Phase OH Radical-Initiated Reactions of Toluene, Naphthalene, and Biphenyl: Effect of NO₂ Concentration. *Environ Sci Technol*. **42**, 9203-9209.
- Nishioka, M. G., Chuang, C. C., Petersen, B. A., Austin, A., Lewtas, J. (1985) Development and quantitative-evaluation of a compound class fractionation scheme for bioassay-directed characterization of ambient air particulate matter. *Environment International*. **11**, 137-146.
- Niu, J. F., Yang, Z. F., Shen, Z. Y., Long, X. X. (2005) Estimation of photolysis lifetimes of the nitronaphthalenes and methylnitronaphthalenes. *Bulletin of Environmental Contamination and Toxicology*. **75**, 813-819.
- Nizzetto, L., Lohmann, R., Gioia, R., Jahnke, A., Temme, C., Dachs, J., et al. (2008) PAHs in air and seawater along a North-South Atlantic transect: Trends, processes and possible sources. *Environ Sci Technol*. **42**, 1580-1585.
- Oda, J., Maeda, I., Mori, T., Yasuhara, A., Saito, Y. (1998) The relative proportions of polycyclic aromatic hydrocarbons and oxygenated derivatives in accumulated organic particulates as affected by air pollution sources. *Environmental Technology*. **19**, 961-976.
- Oda, J., Nomura, S., Yasuhara, A., Shibamoto, T. (2001) Mobile sources of atmospheric polycyclic aromatic hydrocarbons in a roadway tunnel. *Atmospheric Environment*. **35**, 4819-4827.
- OECD. (2012) Environmental Outlook to 2050 : the consequences of inaction *OECD Publishing*, <http://dxdoiorg/101787/9789264122246-en>.
- Ohura, T., Amagai, T., Sugiyama, T., Fusaya, M., Matsushita, H. (2004) Characteristics of particle matter and associated polycyclic aromatic hydrocarbons in indoor and outdoor air in two cities in Shizuoka, Japan. *Atmospheric Environment*. **38**, 2045-2054.
- Ohura, T., Kitazawa, A., Amagai, T., Makino, M. (2005) Occurrence, profiles, and photostabilities of chlorinated polycyclic aromatic hydrocarbons associated with particulates in urban air. *Environ Sci Technol*. **39**, 85-91.

- Okuda, T., Okamoto, K., Tanaka, S., Shen, Z., Han, Y., Huo, Z. (2010) Measurement and source identification of polycyclic aromatic hydrocarbons (PAHs) in the aerosol in Xi'an, China, by using automated column chromatography and applying positive matrix factorization (PMF). *Sci Total Environ.* **408**, 1909-1914.
- Pankow, J. F. (1987) Review and comparative-analysis of the theories on partitioning between the gas and aerosol particulate phases in the atmosphere. *Atmospheric Environment.* **21**, 2275-2283.
- Pankow, J. F., Bidleman, T. F. (1992) Interdependence of the slopes and intercepts from log log correlations of measured gas particle partitioning and vapor-pressure .1. Theory and analysis of available data. *Atmospheric Environment Part a-General Topics.* **26**, 1071-1080.
- Paputa-Peck, M. C., Marano, R. S., Schuetzle, D., Riley, T. L., Hampton, C. V., Prater, T. J., et al. (1983) Determination of nitrated polynuclear aromatic-hydrocarbons in particulate extracts by capillary column gas-chromatography with nitrogen selective detection. *Analytical Chemistry.* **55**, 1946-1954.
- Park, D., Oh, M., Yoon, Y., Park, E., Lee, K. (2012) Source identification of PM10 pollution in subway passenger cabins using positive matrix factorization. *Atmospheric Environment.* **49**, 180-185.
- Park, E.-J., Kim, D.-S., Park, K. (2008) Monitoring of ambient particles and heavy metals in a residential area of Seoul, Korea. *Environmental Monitoring and Assessment.* **137**, 441-449.
- Park, S. S., Kim, Y. J., Kang, C. H. (2002) Atmospheric polycyclic aromatic hydrocarbons in Seoul, Korea. *Atmospheric Environment.* **36**, 2917-2924.
- Patton, G. W., Walla, M. D., Bidleman, T. F., Barrie, L. A. (1991) Polycyclic aromatic and organochlorine compounds in the atmosphere of Northern Ellesmere-Island, Canada. *Journal of Geophysical Research-Atmospheres.* **96**, 10867-10877.
- Pedersen, D. U., Durant, J. L., Penman, B. W., Crespi, C. L., Hemond, H. F., Lafleur, A. L., et al. (2004) Human-cell mutagens in respirable airborne particles in the northeastern United States. 1. Mutagenicity of fractionated samples. *Environ Sci Technol.* **38**, 682-689.
- Pedersen, D. U., Durant, J. L., Taghizadeh, K., Hemond, H. F., Lafleur, A. L., Cass, G. R. (2005) Human cell mutagens in respirable airborne particles from the Northeastern United States. 2. Quantification of mutagens and other organic compounds. *Environ Sci Technol.* **39**, 9547-9560.
- Pedersen, P. S., Ingwersen, J., Nielsen, T., Larsen, E. (1980) Effects of fuel, lubricant, and engine operating parameters on the emission of polycyclic aromatic-hydrocarbons. *Environ Sci Technol.* **14**, 71-79.
- Peltonen, K., Kuljukka, T. (1995) Air sampling and analysis of polycyclic aromatic-hydrocarbons. *Journal of Chromatography A.* **710**, 93-108.
- Perraudin, E., Budzinski, H., Villenave, E. (2005) Kinetic study of the reactions of NO₂ with polycyclic aromatic hydrocarbons adsorbed on silica particles. *Atmospheric Environment.* **39**, 6557-6567.
- Perraudin, E., Budzinski, H., Villenave, E. (2007a) Identification and quantification of ozonation products of anthracene and phenanthrene adsorbed on silica particles. *Atmospheric Environment.* **41**, 6005-6017.

- Perraudin, E., Budzinski, H., Villenave, E. (2007b) Kinetic study of the reactions of ozone with polycyclic aromatic hydrocarbons adsorbed on atmospheric model particles. *Journal of Atmospheric Chemistry*. **56**, 57-82.
- Perrone, M. G., Carbone, C., Faedo, D., Ferrero, L., Maggioni, A., Sangiorgi, G., et al. (2014) Exhaust emissions of polycyclic aromatic hydrocarbons, n-alkanes and phenols from vehicles coming within different European classes. *Atmospheric Environment*. **82**, 391-400.
- Phouongphouang, P. T., Arey, J. (2002) Rate constants for the gas-phase reactions of a series of alkylnaphthalenes with the OH radical. *Environ Sci Technol*. **36**, 1947-1952.
- Phouongphouang, P. T., Arey, J. (2003a) Rate constants for the photolysis of the nitronaphthalenes and methylnitronaphthalenes. *Journal of Photochemistry and Photobiology a-Chemistry*. **157**, 301-309.
- Phouongphouang, P. T., Arey, J. (2003b) Rate constants for the gas-phase reactions of a series of alkylnaphthalenes with the nitrate radical. *Environ Sci Technol*. **37**, 308-313.
- Phuleria, H. C., Geller, M. D., Fine, P. M., Sioutas, C. (2006) Size-resolved emissions of organic tracers from light-and heavy-duty vehicles measured in a California roadway tunnel. *Environ Sci Technol*. **40**, 4109-4118.
- Pitts, J. N., Grosjean, D., Mischke, T. M., Simmon, V. F., Poole, D. (1977) Mutagenic activity of airborne particulate organic pollutants. *Toxicology Letters*. **1**, 65-70.
- Pitts, J. N., Vancauwenberghe, K. A., Grosjean, D., Schmid, J. P., Fitz, D. R., Belser, W. L., et al. (1978) Atmospheric reactions of polycyclic aromatic-hydrocarbons - facile formation of mutagenic nitro-derivatives. *Science*. **202**, 515-519.
- Pitts, J. N., Lokensgard, D. M., Ripley, P. S., Vancauwenberghe, K. A., Vanvaeck, L., Shaffer, S. D., et al. (1980) Atmospheric epoxidation of benzo alpha pyrene by ozone - formation of the metabolite benzo alpha pyrene-4,5-oxide. *Science*. **210**, 1347-1349.
- Pitts, J. N., Lokensgard, D. M., Harger, W., Fisher, T. S., Mejia, V., Schuler, J. J., et al. 1982. Mutagens in diesel exhaust particulate identification and direct activities of 6-nitrobenzo a pyrene, 9-nitroanthracene, 1-nitropyrene and 5h-phenanthro 4,5-bcd pyran-5-one. *Mutation Research*, **103**, 241-249.
- Pitts, J. N. (1983) Formation and fate of gaseous and particulate mutagens and carcinogens in real and simulated atmospheres. *Environmental Health Perspectives*. **47**, 115-140.
- Pitts, J. N., Atkinson, R., Sweetman, J. A., Zielinska, B. (1985a) The gas-phase reaction of naphthalene with N₂O₅ to form nitronaphthalenes. *Atmospheric Environment*. **19**, 701-705.
- Pitts, J. N., Sweetman, J. A., Zielinska, B., Atkinson, R., Winer, A. M., Harger, W. P. (1985b) Formation of nitroarenes from the reaction of polycyclic aromatic-hydrocarbons with dinitrogen pentoxide. *Environ Sci Technol*. **19**, 1115-1121.
- Pitts, J. N., Zielinska, B., Sweetman, J. A., Atkinson, R., Winer, A. M. (1985c) Reactions of adsorbed pyrene and perylene with gaseous N₂O₅ under simulated atmospheric conditions. *Atmospheric Environment*. **19**, 911-915.
- Pitts, J. N., Paur, H. R., Zielinska, B., Arey, J., Winer, A. M., Ramdahl, T., et al. (1986) Factors influencing the reactivity of polycyclic aromatic-hydrocarbons adsorbed on filters and ambient POM with ozone. *Chemosphere*. **15**, 675-685.

- POST. (2014) Ambient Air Quality *Parliamentary Office of Science and Technology, London*
- Poster, D. L., Schantz, M. M., Sander, L. C., Wise, S. A. (2006) Analysis of polycyclic aromatic hydrocarbons (PAHs) in environmental samples: a critical review of gas chromatographic (GC) methods. *Analytical and Bioanalytical Chemistry*. **386**, 859-881.
- Prevedouros, K., Brorstrom-Lunden, E., Halsall, C. J., Jones, K. C., Lee, R. G. M., Sweetman, A. J. (2004a) Seasonal and long-term trends in atmospheric PAH concentrations: Evidence and implications. *Environmental Pollution*. **128**, 17-27.
- Prevedouros, K., Jones, K. C., Sweetman, A. J. (2004b) Modelling the atmospheric fate and seasonality of polycyclic aromatic hydrocarbons in the UK. *Chemosphere*. **56**, 195-208.
- Primbs, T., Piekarz, A., Wilson, G., Schmedding, D., Higginbotham, C., Field, J., et al. (2008) Influence of Asian and Western United States urban areas and fires on the atmospheric transport of polycyclic aromatic hydrocarbons, polychlorinated biphenyls, and fluorotelomer alcohols in the Western United States. *Environ Sci Technol*. **42**, 6385-6391.
- Prinn, R. G., Huang, J., Weiss, R. F., Cunnold, D. M., Fraser, P. J., Simmonds, P. G., et al. (2005) Evidence for variability of atmospheric hydroxyl radicals over the past quarter century. *Geophysical Research Letters*. **32**.
- Qu, X., Zhang, Q., Wang, W. (2006a) Theoretical study on mechanism for NO₃-initiated atmospheric oxidation of naphthalene. *Chemical Physics Letters*. **432**, 40-49.
- Qu, X., Zhang, Q., Wang, W. (2006b) Mechanism for OH-initiated photooxidation of naphthalene in the presence of O₂ and NO_x: A DFT study. *Chemical Physics Letters*. **429**, 77-85.
- Ramdahl, T. (1983) Retene - a molecular marker of wood combustion in ambient air. *Nature*. **306**, 580-583.
- Ramdahl, T., Bjorseth, A., Lokensgard, D. M., Pitts, J. N. (1984) Nitration of polycyclic aromatic-hydrocarbons adsorbed to different carriers in a fluidized-bed reactor. *Chemosphere*. **13**, 527-534.
- Ramdahl, T., Zielinska, B., Arey, J., Atkinson, R., Winer, A. M., Pitts, J. N. (1986) Ubiquitous occurrence of 2-nitrofluoranthene and 2-nitropyrene in air. *Nature*. **321**, 425-427.
- Rappaport, S. M., Wang, Y. Y., Wei, E. T., Sawyer, R., Watkins, B. E., Rapoport, H. (1980) Isolation and identification of a direct-acting mutagen in diesel-exhaust particulates. *Environ Sci Technol*. **14**, 1505-1509.
- Rappaport, S. M., Jin, Z. L., Xu, X. B. (1982) High-performance liquid-chromatography with reductive electrochemical detection of mutagenic nitro-substituted polynuclear aromatic-hydrocarbons in diesel exhausts. *Journal of Chromatography*. **240**, 145-154.
- Ratcliff, M. A., Dane, A. J., Williams, A., Ireland, J., Luecke, J., McCormick, R. L., et al. (2010) Diesel Particle Filter and Fuel Effects on Heavy-Duty Diesel Engine Emissions. *Environ Sci Technol*. **44**, 8343-8349.
- Ravindra, K., Sokhi, R., Van Grieken, R. (2008) Atmospheric polycyclic aromatic hydrocarbons: Source attribution, emission factors and regulation. *Atmospheric Environment*. **42**, 2895-2921.
- Reff, A., Eberly, S., Bhave, P. V. (2007) Receptor modeling of ambient particulate matter data using positive matrix factorization: Review of existing methods. *J Air Waste Manage Assoc*. **57**, 146-154.

- Reisen, F., Arey, J. (2002) Reactions of hydroxyl radicals and ozone with acenaphthene and acenaphthylene. *Environ Sci Technol.* **36**, 4302-4311.
- Reisen, F., Wheeler, S., Arey, J. (2003) Methyl- and dimethyl-/ethyl-nitronaphthalenes measured in ambient air in Southern California. *Atmospheric Environment.* **37**, 3653-3657.
- Reisen, F., Arey, J. (2005) Atmospheric reactions influence seasonal PAH and nitro-PAH concentrations in the Los Angeles basin. *Environ Sci Technol.* **39**, 64-73.
- Rhead, M. M., Pemberton, R. D. (1996) Sources of naphthalene in diesel exhaust emissions. *Energy & Fuels.* **10**, 837-843.
- Ringuet, J., Albinet, A., Leoz-Garziandia, E., Budzinski, H., Villenave, E. (2012a) Diurnal/nocturnal concentrations and sources of particulate-bound PAHs, OPAHs and NPAHs at traffic and suburban sites in the region of Paris (France). *Sci Total Environ.* **437**, 297-305.
- Ringuet, J., Albinet, A., Leoz-Garziandia, E., Budzinski, H., Villenave, E. (2012b) Reactivity of polycyclic aromatic compounds (PAHs, NPAHs and OPAHs) adsorbed on natural aerosol particles exposed to atmospheric oxidants. *Atmospheric Environment.* **61**, 15-22.
- Ringuet, J., Leoz-Garziandia, E., Budzinski, H., Villenave, E., Albinet, A. (2012c) Particle size distribution of nitrated and oxygenated polycyclic aromatic hydrocarbons (NPAHs and OPAHs) on traffic and suburban sites of a European megacity: Paris (France). *Atmospheric Chemistry and Physics.* **12**, 8877-8887.
- Rogge, W. F., Hildemann, L. M., Mazurek, M. A., Cass, G. R., Simoneit, B. R. T. (1993a) Sources of fine organic aerosol .2. Noncatalyst and catalyst-equipped automobiles and heavy-duty diesel trucks. *Environ Sci Technol.* **27**, 636-651.
- Rogge, W. F., Hildemann, L. M., Mazurek, M. A., Cass, G. R., Simoneit, B. R. T. (1993b) Sources of fine organic aerosol .3. road dust, tire debris, and organometallic brake lining dust - roads as sources and sinks. *Environ Sci Technol.* **27**, 1892-1904.
- Rogge, W. F., Hildemann, L. M., Mazurek, M. A., Cass, G. R., Simoneit, B. R. T. (1993c) Sources of Fine Organic Aerosol. 5. Natural Gas Home Appliances. *Environ Sci Technol.* **27**, 2736-2744.
- Rogge, W. F., Hildemann, L. M., Mazurek, M. A., Cass, G. R., Simoneit, B. R. T. (1998) Sources of fine organic aerosol. 9. Pine, oak and synthetic log combustion in residential fireplaces. *Environ Sci Technol.* **32**, 13-22.
- Romero, R., Sienra, R., Richter, P. (2002) Efficient screening method for determination of polycyclic aromatic hydrocarbons (PAHs) in airborne particles. Application in real samples of Santiago-Chile metropolitan urban area. *Atmospheric Environment.* **36**, 2375-2381.
- Rosenkranz, H. S., Mermelstein, R. (1983) Mutagenicity and genotoxicity of nitroarenes: All nitro-containing chemicals were not created equal. *Mutation Research/Reviews in Genetic Toxicology.* **114**, 217-267.
- Ross, J. A., Nelson, G. B., Wilson, K. H., Rabinowitz, J. R., Galati, A., Stoner, G. D., et al. (1995) Adenomas induced by polycyclic aromatic-hydrocarbons in strain a/j mouse lung correlate with time-integrated dna adduct levels. *Cancer Research.* **55**, 1039-1044.

- Ruehle, P. H., Bosch, L.C., Duncan, W.P. (1985) Synthesis of nitrated polycyclic aromatic hydrocarbons. In: White, CM (Ed), *Nitrated Polycyclic Aromatic Hydrocarbons Huethig, Heidelberg*, pp 170-235.
- Salmeen, I., Durisin, A. M., Prater, T. J., Riley, T., Schuetzle, D. (1982) Contribution of 1-nitropyrene to direct-acting ames assay mutagenicities of diesel particulate extracts. *Mutation Research*. **104**, 17-23.
- Salmeen, I. T., Pero, A. M., Zator, R., Schuetzle, D., Riley, T. L. (1984) Ames assay chromatograms and the identification of mutagens in diesel particle extracts. *Environ Sci Technol*. **18**, 375-382.
- Sasaki, J., Arey, J., Eastmond, D. A., Parks, K. K., Grosovsky, A. J. (1997a) Genotoxicity induced in human lymphoblasts by atmospheric reaction products of naphthalene and phenanthrene. *Mutation Research-Genetic Toxicology and Environmental Mutagenesis*. **393**, 23-35.
- Sasaki, J., Aschmann, S. M., Kwok, E. S. C., Atkinson, R., Arey, J. (1997b) Products of the gas-phase OH and NO₃ radical-initiated reactions of naphthalene. *Environ Sci Technol*. **31**, 3173-3179.
- Sato, S., Ohgaki, H., Takayama, S., Ochiai, M., Tahira, T., Ishizaka, Y., et al. (1986) Carcinogenicity of dinitropyrenes in rats and hamsters. *Developments in toxicology and environmental science*. **13**, 271-277.
- Schauer, C., Niessner, R., Poschl, U. (2003) Polycyclic aromatic hydrocarbons in urban air particulate matter: Decadal and seasonal trends, chemical degradation, and sampling artifacts. *Environ Sci Technol*. **37**, 2861-2868.
- Schauer, J. J., Kleeman, M. J., Cass, G. R., Simoneit, B. R. T. (1999) Measurement of emissions from air pollution sources. 2. C-1 through C-30 organic compounds from medium duty diesel trucks. *Environ Sci Technol*. **33**, 1578-1587.
- Schauer, J. J., Kleeman, M. J., Cass, G. R., Simoneit, B. R. T. (2002) Measurement of emissions from air pollution sources. 5. C-1-C-32 organic compounds from gasoline-powered motor vehicles. *Environ Sci Technol*. **36**, 1169-1180.
- Schnelle-Kreis, E., Sklorz, M., Peters, A., Cyrus, J., Zimmermann, R. (2005) Analysis of particle-associated semi-volatile aromatic and aliphatic hydrocarbons in urban particulate matter on a daily basis. *Atmospheric Environment*. **39**, 7702-7714.
- Schnelle-Kreis, J., Gebefugi, I., Welzl, G., Jaensch, T., Kettrup, A. (2001) Occurrence of particle-associated polycyclic aromatic compounds in ambient air of the city of Munich. *Atmospheric Environment*. **35**, S71-S81.
- Schnelle-Kreis, J., Sklorz, M., Orasche, J., Stoelzel, M., Peters, A., Zimmermann, R. (2007) Semi volatile organic compounds in ambient PM(2.5). Seasonal trends and daily resolved source contributions. *Environ Sci Technol*. **41**, 3821-3828.
- Schnelle, J., Jansch, T., Wolf, K., Gebefugi, I., Kettrup, A. (1995) Particle-size dependent concentrations of polycyclic aromatic-hydrocarbons (PAH) in the outdoor air. *Chemosphere*. **31**, 3119-3127.
- Schuetzle, D., Lee, F. S. C., Prater, T. J., Tejada, S. B. (1981) The identification of polynuclear aromatic hydrocarbon (PAH) derivatives in mutagenic fractions of diesel particulate extracts. *International Journal of Environmental Analytical Chemistry*. **9**, 93-144.

- Schuetzle, D., Riley, T. L., Prater, T. J., Harvey, T. M., Hunt, D. F. (1982) Analysis of nitrated polycyclic aromatic-hydrocarbons in diesel particulates. *Analytical Chemistry*. **54**, 265-271.
- Schuetzle, D., Perez, J. M. (1983) Factors influencing the emissions of nitrated-polynuclear aromatic hydrocarbons(nitro-PAH) from diesel-engines. *Journal of the Air Pollution Control Association*. **33**, 751-755.
- Seinfeld, J. H., Pandis, S. N. (1998) Atmospheric Chemistry and Physics. From Air Pollution to Climate Change. . *John Wiley & Sons, Inc ISBN0-471-17815-2*.
- Sharma, H., Jain, V. K., Khan, Z. H. (2007) Characterization and source identification of polycyclic aromatic hydrocarbons (PAHs) in the urban environment of Delhi. *Chemosphere*. **66**, 302-310.
- Shen, G., Wei, S., Zhang, Y., Wang, R., Wang, B., Li, W., et al. (2012) Emission of oxygenated polycyclic aromatic hydrocarbons from biomass pellet burning in a modern burner for cooking in China. *Atmospheric Environment*. **60**, 234-237.
- Shi, J. P., Harrison, R. M. (1997) Rapid NO₂ formation in diluted petrol-fuelled engine exhaust - A source of NO₂ in winter smog episodes. *Atmospheric Environment*. **31**, 3857-3866.
- Shimada, T. (2006) Xenobiotic-metabolizing enzymes involved in activation and detoxification of carcinogenic polycyclic aromatic hydrocarbons. *Drug Metab Pharmacokinet*. **21**, 257-276.
- Shimmo, M., Adler, H., Hyotylainen, T., Hartonen, K., Kulmala, M., Riekkola, M. L. (2002) Analysis of particulate polycyclic aromatic hydrocarbons by on-line coupled supercritical fluid extraction-liquid chromatography-gas chromatography-mass spectrometry. *Atmospheric Environment*. **36**, 2985-2995.
- Shimmo, M., Anttila, P., Hartonen, K., Hyotylainen, T., Paatero, J., Kulmala, M., et al. (2004a) Identification of organic compounds in atmospheric aerosol particles by on-line supercritical fluid extraction-liquid chromatography-gas chromatography-mass spectrometry. *Journal of Chromatography A*. **1022**, 151-159.
- Shimmo, M., Jantti, J., Aalto, P., Hartonen, K., Hyotylainen, T., Kulmala, M., et al. (2004b) Characterisation of organic compounds in aerosol particles from a Finnish forest by on-line coupled supercritical fluid extraction-liquid chromatography-gas chromatography-mass spectrometry. *Analytical and Bioanalytical Chemistry*. **378**, 1982-1990.
- Sidhu, S., Gullett, B., Striebich, R., Klosterman, J., Contreras, J., DeVito, M. (2005) Endocrine disrupting chemical emissions from combustion sources: diesel particulate emissions and domestic waste open burn emissions. *Atmospheric Environment*. **39**, 801-811.
- Sienra, M. D. (2006) Oxygenated polycyclic aromatic hydrocarbons in urban air particulate matter. *Atmospheric Environment*. **40**, 2374-2384.
- Sienra, M. D., Rosazza, N. G. (2006) Occurrence of nitro-polycyclic aromatic hydrocarbons in urban particulate matter PM₁₀. *Atmospheric Research*. **81**, 265-276.
- Silibello, C., Calori, G., Costa, M. P., Dirodi, M. G., Mircea, M., Radice, P., et al. (2012) Benzo a pyrene modelling over Italy: comparison with experimental data and source apportionment. *Atmospheric Pollution Research*. **3**, 399-407.
- Simcik, M. F., Franz, T. P., Zhang, H. X., Eisenreich, S. J. (1998) Gas-particle partitioning of PCBs and PAHs in the Chicago urban and adjacent coastal atmosphere: States of equilibrium. *Environ Sci Technol*. **32**, 251-257.

Simoneit, B. R. T., Rogge, W. F., Mazurek, M. A., Standley, L. J., Hildemann, L. M., Cass, G. R. (1993) Lignin pyrolysis products, lignans, and resin acids as specific tracers of plant classes in emissions from biomass combustion. *Environ Sci Technol.* **27**, 2533-2541.

Simoneit, B. R. T., Bi, X., Oros, D. R., Medeiros, P. M., Sheng, G., Fu, J. (2007) Phenols and Hydroxy-PAHs (Arylphenols) as tracers for coal smoke particulate matter: Source tests and ambient aerosol assessments. *Environ Sci Technol.* **41**, 7294-7302.

Simonich, S. L., Hites, R. A. (1994) Importance of vegetation in removing polycyclic aromatic-hydrocarbons from the atmosphere. *Nature.* **370**, 49-51.

Sjogren, M., Li, H., Rannug, U., Westerholm, R. (1996) Multivariate analysis of exhaust emissions from heavy-duty diesel fuels. *Environ Sci Technol.* **30**, 38-49.

Sklorz, M., Briede, J.-J., Schnelle-Kreis, J., Liu, Y., Cyrus, J., de Kok, T. M., et al. (2007) Concentration of oxygenated polycyclic aromatic hydrocarbons and oxygen free radical formation from urban particulate matter. *Journal of Toxicology and Environmental Health-Part a-Current Issues.* **70**, 1866-1869.

Skrdlikova, L., Landlova, L., Klanova, J., Lammel, G. (2011) Wet deposition and scavenging efficiency of gaseous and particulate phase polycyclic aromatic compounds at a central European suburban site. *Atmospheric Environment.* **45**, 4305-4312.

Smith, D. J. T., Harrison, R. M. (1996) Concentrations, trends and vehicle source profile of polynuclear aromatic hydrocarbons in the UK atmosphere. *Atmospheric Environment.* **30**, 2513-2525.

Sofowote, U. M., Hung, H., Rastogi, A. K., Westgate, J. N., Deluca, P. F., Su, Y., et al. (2011) Assessing the long-range transport of PAH to a sub-Arctic site using positive matrix factorization and potential source contribution function. *Atmospheric Environment.* **45**, 967-976.

Souza, K. F., Carvalho, L. R. F., Allen, A. G., Cardoso, A. A. (2014) Diurnal and nocturnal measurements of PAH, nitro-PAH, and oxy-PAH compounds in atmospheric particulate matter of a sugar cane burning region. *Atmospheric Environment.* **83**, 193-201.

Stahelin, J., Keller, C., Stahel, W., Schläpfer, K., Wunderli, S. (1998) Emission factors from road traffic from a tunnel study (Gubrist tunnel, Switzerland). Part III: Results of organic compounds, SO₂ and speciation of organic exhaust emission. *Atmospheric Environment.* **32**, 999-1009.

Stark, G., Stauff, J., Miltenburger, H. G., Stummfischer, I. (1985) Photodecomposition of 1-nitropyrene and other direct-acting mutagens extracted from diesel-exhaust particulates. *Mutation Research.* **155**, 27-33.

Strandell, M., Zakrisson, S., Alsberg, T., Westerholm, R., Winquist, L., Rannug, U. (1994) Chemical-analysis and biological testing of a polar fraction of ambient air, diesel-engine, and gasoline-engine particulate extracts. *Environmental Health Perspectives.* **102**, 85-92.

Sun, P., Blanchard, P., Brice, K. A., Hites, R. A. (2006) Trends in polycyclic aromatic hydrocarbon concentrations in the Great Lakes atmosphere. *Environ Sci Technol.* **40**, 6221-6227.

Tancell, P. J., Rhead, M. M., Pemberton, R. D., Braven, J. (1995a) Survival of polycyclic aromatic-hydrocarbons during diesel combustion. *Environ Sci Technol.* **29**, 2871-2876.

- Tancell, P. J., Rhead, M. M., Trier, C. J., Bell, M. A., Fussey, D. E. (1995b) The sources of benzo a pyrene in diesel exhaust emissions. *Sci Total Environ.* **162**, 179-186.
- Tang, N., Tabata, M., Mishukov, V. F., Sergineko, V., Toriba, A., Kizu, R., et al. (2002) Comparison of atmospheric nitropolycyclic aromatic hydrocarbons in Vladivostok, Kanazawa and Toyama. *Journal of Health Science.* **48**, 30-36.
- Tang, N., Hattori, T., Taga, R., Igarashi, K., Yang, X. Y., Tamura, K., et al. (2005) Polycyclic aromatic hydrocarbons and nitropolycyclic aromatic hydrocarbons in urban air particulates and their relationship to emission sources in the Pan-Japan Sea countries. *Atmospheric Environment.* **39**, 5817-5826.
- Tokiwa, H., Nakagawa, R., Morita, K., Ohnishi, Y. (1981) Mutagenicity of nitro-derivatives induced by exposure of aromatic-compounds to nitrogen-dioxide. *Mutation Research.* **85**, 195-205.
- Tokiwa, H., Nakagawa, R., Horikawa, K., Ohkubo, A. (1987) The nature of the mutagenicity and carcinogenicity of nitrated, aromatic-compounds in the environment. *Environmental Health Perspectives.* **73**, 191-199.
- Tsapakis, M., Lagoudaki, E., Stephanou, E. G., Kavouras, I. G., Koutrakis, P., Oyola, P., et al. (2002) The composition and sources of PM_{2.5} organic aerosol in two urban areas of Chile. *Atmospheric Environment.* **36**, 3851-3863.
- Tsapakis, M., Stephanou, E. G. (2003) Collection of gas and particle semi-volatile organic compounds: use of an oxidant denuder to minimize polycyclic aromatic hydrocarbons degradation during high-volume air sampling. *Atmospheric Environment.* **37**, 4935-4944.
- Tsapakis, M., Stephanou, E. G. (2005) Occurrence of gaseous and particulate polycyclic aromatic hydrocarbons in the urban atmosphere: study of sources and ambient temperature effect on the gas/particle concentration and distribution. *Environmental Pollution.* **133**, 147-156.
- Tsapakis, M., Stephanou, E. G. (2007) Diurnal cycle of PAHs, nitro-PAHs, and oxy-PAHs in a high oxidation capacity marine background atmosphere. *Environ Sci Technol.* **41**, 8011-8017.
- Tuominen, J., Salomaa, S., Pyysalo, H., Skytta, E., Tikkanen, L., Nurmela, T., et al. (1988) Polynuclear aromatic-compounds and genotoxicity in particulate and vapor-phases of ambient air - effect of traffic, season, and meteorological conditions. *Environ Sci Technol.* **22**, 1228-1234.
- UKPIA. (2012) Statistical Review, 2012.
- Umbuzeiro, G. A., Franco, A., Martins, M. H., Kummrow, F., Carvalho, L., Schmeiser, H. H., et al. (2008) Mutagenicity and DNA adduct formation of PAH, nitro-PAH, and oxy-PAH fractions of atmospheric particulate matter from Sao Paulo, Brazil. *Mutation Research-Genetic Toxicology and Environmental Mutagenesis.* **652**, 72-80.
- UNECE. (1998) United Nations Economic Commission for Europe, Convention on Long-range Transboundary Air Pollution, Protocol on Persistent Organic Pollutants, Aarhus, Denmark. *United Nations Economic Commission for Europe, Convention on Long-range Transboundary Air Pollution, Protocol on Persistent Organic Pollutants, Aarhus, Denmark.*
- Valavanidis, A., Fiotakis, K., Vlahogianni, T., Papadimitriou, V., Pantikaki, V. (2006) Determination of Selective Quinones and Quinoid Radicals in Airborne Particulate Matter and Vehicular Exhaust Particles *Environmental Chemistry.* **3**, 118-123.

- Valle-Hernandez, B. L., Mugica-Alvarez, V., Salinas-Talavera, E., Amador-Munoz, O., Murillo-Tovar, M. A., Villalobos-Pietrini, R., et al. (2010) Temporal variation of nitro-polycyclic aromatic hydrocarbons in PM(10) and PM(2.5) collected in Northern Mexico City. *Sci Total Environ.* **408**, 5429-5438.
- Van Drooge, B. L., Fernandez, P., Grimalt, J. O., Stuchlik, E., Torres Garcia, C. J., Cuevas, E. (2010) Atmospheric polycyclic aromatic hydrocarbons in remote European and Atlantic sites located above the boundary mixing layer. *Environmental Science and Pollution Research.* **17**, 1207-1216.
- Van Vaeck, L., Van Cauwenberghe, K. (1984) Conversion of poly cyclic aromatic hydro carbons on diesel particulate matter upon exposure to parts-per-million levels of ozone. *Atmospheric Environment.* **18**, 323-328.
- Venkataraman, C., Friedlander, S. K. (1994) Size distributions of polycyclic aromatic-hydrocarbons and elemental carbon .2. ambient measurements and effects of atmospheric processes. *Environ Sci Technol.* **28**, 563-572.
- Vione, D., Maurino, V., Minero, C., Pelizzetti, E., Harrison, M. A. J., Olariu, R. I., et al. (2006) Photochemical reactions in the tropospheric aqueous phase and on particulate matter. *Chemical Society Reviews.* **35**, 441-453.
- Walgraeve, C., Demeestere, K., Dewulf, J., Zimmermann, R., Van Langenhove, H. (2010) Oxygenated polycyclic aromatic hydrocarbons in atmospheric particulate matter: Molecular characterization and occurrence. *Atmospheric Environment.* **44**, 1831-1846.
- Wallington, T. J., Atkinson, R., Winer, A. M., Pitts, J. N. (1987) A study of the reaction $\text{NO}_3 + \text{NO}_2 + \text{M} \rightarrow \text{N}_2\text{O}_5 + \text{M} (\text{M} = \text{N}_2, \text{O}_2)$. *International Journal of Chemical Kinetics.* **19**, 243-249.
- Wang, G., Kawamura, K., Zhao, X., Li, Q., Dai, Z., Niu, H. (2007) Identification, abundance and seasonal variation of anthropogenic organic aerosols from a mega-city in China. *Atmospheric Environment.* **41**, 407-416.
- Wang, H. M., Hasegawa, K., Kagaya, S. (1999) Nitration of pyrene adsorbed on silica particles by nitrogen dioxide under simulated atmospheric conditions. *Chemosphere.* **39**, 1923-1936.
- Wang, H. M., Hasegawa, K., Kagaya, S. (2000) The nitration of pyrene adsorbed on silica particles by nitrogen dioxide. *Chemosphere.* **41**, 1479-1484.
- Wang, L., Atkinson, R., Arey, J. (2007a) Dicarbonyl products of the OH radical-initiated reactions of naphthalene and the C-1- and C-2-alkylnaphthalenes. *Environ Sci Technol.* **41**, 2803-2810.
- Wang, L., Atkinson, R., Arey, J. (2007b) Formation of 9,10-phenanthrenequinone by atmospheric gas-phase reactions of phenanthrene. *Atmospheric Environment.* **41**, 2025-2035.
- Wang, L., Atkinson, R., Arey, J. (2010) Comparison of AlkylNitronaphthalenes Formed in NO_3 and OH Radical-Initiated Chamber Reactions with those Observed in Ambient Air. *Environ Sci Technol.* **44**, 2981-2987.
- Wang, W., Jariyasopit, N., Schrlau, J., Jia, Y., Tao, S., Yu, T.-W., et al. (2011a) Concentration and Photochemistry of PAHs, NPAHs, and OPAHs and Toxicity of PM(2.5) during the Beijing Olympic Games. *Environ Sci Technol.* **45**, 6887-6895.
- Wang, W., Simonich, S., Giri, B., Chang, Y., Zhang, Y., Jia, Y., et al. (2011b) Atmospheric concentrations and air-soil gas exchange of polycyclic aromatic hydrocarbons (PAHs) in remote,

rural village and urban areas of Beijing-Tianjin region, North China. *Sci Total Environ.* **409**, 2942-2950.

Wei, S., Huang, B., Liu, M., Bi, X., Ren, Z., Sheng, G., et al. (2012) Characterization of PM_{2.5}-bound nitrated and oxygenated PAHs in two industrial sites of South China. *Atmospheric Research.* **109**, 76-83.

Wei, S. J. C., Chang, R. L., Bhachech, N., Cui, X. X., Merkler, K. A., Wong, C. Q., et al. (1993) Dose-dependent differences in the profile of mutations induced by (+)-7r,8s-dihydroxy-9,10-epoxy-7,8,9,10-tetrahydrobenzo(a)pyrene in the coding region of the hypoxanthine (guanine) phosphoribosyltransferase gene in chinese-hamster V-79 cells. *Cancer Research.* **53**, 3294-3301.

Wei, Y. L., Bao, L. J., Wu, C. C., He, Z. C., Zeng, E. Y. (2014) Association of soil polycyclic aromatic hydrocarbon levels and anthropogenic impacts in a rapidly urbanizing region: Spatial distribution, soil-air exchange and ecological risk. *Sci Total Environ.* **473**, 676-684.

Westerholm, R., Egebäck, K. E. (1994) Exhaust emissions from light-duty and heavy-duty vehicles - chemical-composition, impact of exhaust after treatment, and fuel parameters. *Environmental Health Perspectives.* **102**, 13-23.

Westerholm, R., Li, H. (1994) A multivariate statistical-analysis of fuel-related polycyclic aromatic hydrocarbon emissions from heavy-duty diesel vehicles. *Environ Sci Technol.* **28**, 965-972.

WHO. (2000) Air Quality Guidelines for Europe, Second Edition. *World Health Organization, Copenhagen*

WHO. (2003) Environmental health criteria for selected nitro- and nitro-oxy-polycyclic aromatic hydrocarbons. *World Health Organization, Geneva*

Wild, E., Dent, J., Thomas, G. O., Jones, K. C. (2006) Visualizing the air-to-leaf transfer and within-leaf movement and distribution of phenanthrene: Further studies utilizing two-photon excitation microscopy. *Environ Sci Technol.* **40**, 907-916.

Wild, E., Dent, J., Thomas, G. O., Jones, K. C. (2007) Use of two-photon excitation microscopy and autofluorescence for visualizing the fate and behavior of semivolatile organic chemicals within living vegetation. *Environmental Toxicology and Chemistry.* **26**, 2486-2493.

Wild, S. R., Jones, K. C. (1995) Polynuclear aromatic-hydrocarbons in the united-kingdom environment - a preliminary source inventory and budget. *Environmental Pollution.* **88**, 91-108.

Williams, M. L. (2001) Atmospheric dispersal of pollutants and the modelling of air pollution. *In: Harrison, RM (Ed), Pollution: Causes, Effects and Control The Royal Society of Chemistry, Cambridge, UK, pp 246-267.*

Williams, P. T., Bartle, K. D., Andrews, G. E. (1986) The relation between polycyclic aromatic compounds in diesel fuels and exhaust particulates. *Fuel.* **65**, 1150-1158.

Williams, P. T., Abbass, M. K., Andrews, G. E., Bartle, K. D. (1989) Diesel particulate emissions: The role of unburned fuel. *Combustion and Flame.* **75**, 1-24.

Wilson, N. K., McCurdy, T. R., Chuang, J. C. (1995) Concentrations and phase distributions of nitrated and oxygenated polycyclic aromatic-hydrocarbons in ambient air. *Atmospheric Environment.* **29**, 2575-2584.

- Wingfors, H., Sjodin, A., Haglund, P., Brorstrom-Lunden, E. (2001) Characterisation and determination of profiles of polycyclic aromatic hydrocarbons in a traffic tunnel in Gothenburg, Sweden. *Atmospheric Environment*. **35**, 6361-6369.
- Wu, S. P., Wang, X. H., Yan, J. M., Zhang, M. M., Hong, H. S. (2010) Diurnal Variations of Particle-bound PAHs at a Traffic Site in Xiamen, China. *Aerosol and Air Quality Research*. **10**, 497-506.
- Xiao, H., Kang, S., Zhang, Q., Han, W., Loewen, M., Wong, F., et al. (2010) Transport of semivolatile organic compounds to the Tibetan Plateau: Monthly resolved air concentrations at Nam Co. *Journal of Geophysical Research-Atmospheres*. **115**.
- Xue, W. L., Warshawsky, D. (2005) Metabolic activation of polycyclic and heterocyclic aromatic hydrocarbons and DNA damage: A review. *Toxicology and Applied Pharmacology*. **206**, 73-93.
- Yaffe, D., Cohen, Y., Arey, J., Grosovsky, A. J. (2001) Multimedia analysis of PAHs and nitro-PAH daughter products in the Los Angeles basin. *Risk Analysis*. **21**, 275-294.
- Yamasaki, H., Kuwata, K., Miyamoto, H. (1982) Effects of ambient-temperature on aspects of airborne polycyclic aromatic-hydrocarbons. *Environ Sci Technol*. **16**, 189-194.
- Yang, P., Gong, B. F., Xiong, Y. (1999) Study of Soxhlet extraction of polycyclic aromatic hydrocarbons on airborne particulate. *Environmental Monitoring in China*. **15**, 16-20.
- Yassaa, N., Meklati, B. Y., Cecinato, A., Marino, F. (2001) Organic aerosols in urban and waste landfill of Algiers metropolitan area: Occurrence and sources. *Environ Sci Technol*. **35**, 306-311.
- Yokley, R. A., Garrison, A. A., Wehry, E. L., Mamantov, G. (1986) Photochemical transformation of pyrene and benzo a pyrene vapor-deposited on 8 coal stack ashes. *Environ Sci Technol*. **20**, 86-90.
- Zhang, Y., Tao, S. (2009) Global atmospheric emission inventory of polycyclic aromatic hydrocarbons (PAHs) for 2004. *Atmospheric Environment*. **43**, 812-819.
- Zhang, Y., Yang, B., Gan, J., Liu, C., Shu, X., Shu, J. (2011) Nitration of particle-associated PAHs and their derivatives (nitro-, oxy-, and hydroxy-PAHs) with NO(3) radicals. *Atmospheric Environment*. **45**, 2515-2521.
- Zhu, J. P., Cao, X. L., Pigeon, R., Mitchell, K. (2003) Comparison of vehicle exhaust emissions from modified diesel fuels. *J Air Waste Manage Assoc*. **53**, 67-76.
- Zielinska, B., Arey, J., Atkinson, R., Ramdahl, T., Winer, A. M., Pitts, J. N. (1986) Reaction of dinitrogen pentoxide with fluoranthene. *Journal of the American Chemical Society*. **108**, 4126-4132.
- Zielinska, B., Arey, J., Atkinson, R., Winer, A. M. (1989) The nitroarenes of molecular weight-247 in ambient particulate samples collected in southern-California. *Atmospheric Environment*. **23**, 223-229.
- Zielinska, B., Sagebiel, J., Arnott, W. P., Rogers, C. F., Kelly, K. E., Wagner, D. A., et al. (2004a) Phase and size distribution of polycyclic aromatic hydrocarbons in diesel and gasoline vehicle emissions. *Environ Sci Technol*. **38**, 2557-2567.
- Zielinska, B., Sagebiel, J., McDonald, J. D., Whitney, K., Lawson, D. R. (2004b) Emission rates and comparative chemical composition from selected in-use diesel and gasoline-fueled vehicles. *J Air Waste Manage Assoc*. **54**, 1138-1150.

Zimmermann, K., Jariyasopit, N., Massey Simonich, S. L., Tao, S., Atkinson, R., Arey, J. (2013) Formation of Nitro-PAHs from the Heterogeneous Reaction of Ambient Particle-Bound PAHs with N₂O₅/NO₃/NO₂. *Environ Sci Technol.* **47**, 8434-8442.

Appendix 1. Reaction kinetics data for gas phase and heterogeneous PAH reactions

The rate coefficients for the reactions of PAHs in both gas-phase and heterogeneous processes with a number of known atmospheric oxidants (e.g. OH, O₃, NO₃/N₂O₅) have been widely investigated in experimental laboratory studies. In the review paper by Keyte *et al.* (2013) these kinetics data for individual PAH compounds were compiled.

Presented here are the tables of derived rate coefficients from these studies. For a more complete discussion of these processes, the reader is directed to the Keyte *et al.* (2013) review paper and the references therein.

The tables included in this section are as follows :

Table A1 – Gas-phase reactions of PAHs with OH radicals

Table A2 – Gas-phase reactions of PAH with NO₃ radicals

Table A3 – Gas-phase reactions of PAH with O₃

Table A4 – Heterogeneous reactions of PAHs with OH, NO₂, O₃ and O₃/N₂O₅

Table A1. Second-order rate coefficients $k^{(2)}$ for gas-phase reactions of PAH with OH radicals (Keyte *et al.*, 2013).

	k_{OH} ($\text{cm}^{-3} \text{ molecules}^{-1} \text{ s}^{-1}$)	Reference	T(K)	Notes
Nap	2.4×10^{-11}	(Phousongphouang and Arey, 2003b)	298 ± 2	RR relative to $k(1,2,3\text{-trimethylbenzene}) = 3.27 \times 10^{-11} \text{ cm}^{-3} \text{ molecules}^{-1} \text{ s}^{-1}$
	2.2×10^{-11}	(Atkinson, 1989)	298	recommended value based on previous data, overall uncertainty of $\pm 30\%$
	2.3×10^{-11}	(Brubaker and Hites, 1998)	298	measured over the temperature range 306-366K
	2.7×10^{-11}	(Klamt, 1993)	n/a	theoretical calculation based on a new molecular orbital based estimation method
	2.4×10^{-11}	(Biermann <i>et al.</i> , 1985)	298 ± 1	RR, relative to $k(\text{propene}) = 2.63 \times 10^{-11} \text{ cm}^{-3} \text{ molecules}^{-1} \text{ s}^{-1}$
	1.9×10^{-11}	(Lorenz and Zellner, 1983)	300	Absolute rate, temperature range 300 - 873 K, extrapolated using Arrhenius parameter
	2.2×10^{-11}	(Klopffer <i>et al.</i> , 1986)	300	RR, relative to $k(\text{ethene}) = 8.44 \times 10^{-12} \text{ cm}^{-3} \text{ molecules}^{-1} \text{ s}^{-1}$
	2.4×10^{-11}	(Atkinson <i>et al.</i> , 1984)	294 ± 1	RR, relative to $k(\text{n-nonane}) = 1.07 \times 10^{-11} \text{ cm}^{-3} \text{ molecules}^{-1} \text{ s}^{-1}$
	2.6×10^{-11}	(Atkinson and Aschmann, 1986)	295 ± 1	RR, relative to $k(2\text{-methyl-1,3-butadiene}) = 1.02 \times 10^{-10} \text{ cm}^{-3} \text{ molecules}^{-1} \text{ s}^{-1}$
1M-Nap	4.1×10^{-11}	(Phousongphouang and Arey, 2002)	298 ± 2	RR, relative to $k(\text{naphthalene}) = 2.39 \times 10^{-11} \text{ cm}^{-3} \text{ molecules}^{-1} \text{ s}^{-1}$, derived from the same work
	5.3×10^{-11}	(Atkinson and Aschmann, 1987)	298 ± 2	RR, 2-methyl-1,3-butadiene used as reference compound, $T = 298 \pm 2$
	6.0×10^{-11}	(Klamt, 1993)	n/a	theoretical calculation based on a new molecular orbital based estimation method
2M-Nap	4.9×10^{-11}	(Phousongphouang and Arey, 2002)	298 ± 2	RR, relative to $k(\text{naphthalene}) = 2.39 \times 10^{-11} \text{ cm}^{-3} \text{ molecules}^{-1} \text{ s}^{-1}$, derived from the same work
	5.2×10^{-11}	(Atkinson and Aschmann, 1986)	295 ± 1	RR, relative to $k(2\text{-methyl-1,3-butadiene}) = 1.02 \times 10^{-10} \text{ cm}^{-3} \text{ molecules}^{-1} \text{ s}^{-1}$
	5.7×10^{-11}	(Klamt, 1993)	n/a	theoretical calculation based on a new molecular orbital based estimation method
1E-Nap	3.6×10^{-11}	(Phousongphouang and Arey, 2002)	298 ± 2	RR, relative to $k(\text{naphthalene}) = 2.39 \times 10^{-11} \text{ cm}^{-3} \text{ molecules}^{-1} \text{ s}^{-1}$, derived from the same work

2E-Nap	4.0×10^{-11}	(Phouongphouang and Arey, 2002)	298 ± 2	RR, relative to k(naphthalene) = $2.39 \times 10^{-11} \text{ cm}^{-3} \text{ molecules}^{-1} \text{ s}^{-1}$, derived from the same work
1,2DM-Nap	6.0×10^{-11}	(Phouongphouang and Arey, 2002)	298 ± 2	RR, relative to k(naphthalene) = $2.39 \times 10^{-11} \text{ cm}^{-3} \text{ molecules}^{-1} \text{ s}^{-1}$, derived from the same work
1,3DM-Nap	2.2×10^{-11}	(Banceu <i>et al.</i> , 2001)	295	RR [relative to k(naphthalene) = $2.39 \times 10^{-11} \text{ cm}^{-3} \text{ molecules}^{-1} \text{ s}^{-1}$
	7.5×10^{-11}	(Phouongphouang and Arey, 2002)	298 ± 2	RR, relative to k(naphthalene) = $2.39 \times 10^{-11} \text{ cm}^{-3} \text{ molecules}^{-1} \text{ s}^{-1}$, derived from the same work
1,4DM-Nap	5.8×10^{-12}	(Klamt, 1993)	n/a	theoretical calculation based on a new molecular orbital based estimation method
	5.8×10^{-11}	(Phouongphouang and Arey, 2002)	298 ± 2	RR, relative to k(naphthalene) = $2.39 \times 10^{-11} \text{ cm}^{-3} \text{ molecules}^{-1} \text{ s}^{-1}$, derived from the same work
1,5DM-Nap	6.0×10^{-11}	(Phouongphouang and Arey, 2002)	298 ± 2	RR, relative to k(naphthalene) = $2.39 \times 10^{-11} \text{ cm}^{-3} \text{ molecules}^{-1} \text{ s}^{-1}$, derived from the same work
1,6DM-Nap	6.3×10^{-11}	(Phouongphouang and Arey, 2002)	298 ± 2	RR, relative to k(naphthalene) = $2.39 \times 10^{-11} \text{ cm}^{-3} \text{ molecules}^{-1} \text{ s}^{-1}$, derived from the same work
1,7DM-Nap	6.8×10^{-11}	(Phouongphouang and Arey, 2002)	298 ± 2	RR, relative to k(naphthalene) = $2.39 \times 10^{-11} \text{ cm}^{-3} \text{ molecules}^{-1} \text{ s}^{-1}$, derived from the same work
1,8DM-Nap	6.3×10^{-11}	(Phouongphouang and Arey, 2002)	298 ± 2	RR, relative to k(naphthalene) = $2.39 \times 10^{-11} \text{ cm}^{-3} \text{ molecules}^{-1} \text{ s}^{-1}$, derived from the same work
2,3DM-Nap	6.2×10^{-11}	(Phouongphouang and Arey, 2002)	298 ± 2	RR, relative to k(naphthalene) = $2.39 \times 10^{-11} \text{ cm}^{-3} \text{ molecules}^{-1} \text{ s}^{-1}$, derived from the same work
	1.0×10^{-10}	(Klamt, 1993)	n/a	theoretical calculation based on a new molecular orbital based estimation method
	7.7×10^{-11}	(Atkinson and Aschmann, 1986)	295 ± 1	RR, relative to k(2-methyl-1,3-butadiene) = $1.02 \times 10^{-10} \text{ cm}^{-3} \text{ molecules}^{-1} \text{ s}^{-1}$
2,6DM-Nap	6.7×10^{-11}	(Phouongphouang and Arey, 2002)	298 ± 2	RR, relative to k(naphthalene) = $2.39 \times 10^{-11} \text{ cm}^{-3} \text{ molecules}^{-1} \text{ s}^{-1}$, derived from the same work
2,7DM-Nap	6.9×10^{-11}	(Phouongphouang and Arey, 2002)	298 ± 2	RR, relative to k(naphthalene) = $2.39 \times 10^{-11} \text{ cm}^{-3} \text{ molecules}^{-1} \text{ s}^{-1}$, derived from the same work
Ace	8.0×10^{-11}	(Reisen and Arey, 2002)	296	RR [relative to k(trans-2-butene) = $6.48 \times 10^{-11} \text{ cm}^{-3} \text{ molecules}^{-1} \text{ s}^{-1}$
	5.8×10^{-11}	(Brubaker and Hites, 1998)	298	measured over the temperature range 325-365K
	1.0×10^{-10}	(Atkinson and Aschmann, 1987)	296 ± 1	RR [relative to k(2,3-dimethyl-2-butene) = $1.11 \times 10^{-10} \text{ cm}^{-3} \text{ molecules}^{-1} \text{ s}^{-1}$
	5.8×10^{-11}	(Klopffer <i>et al.</i> , 1986)	300	RR [relative to k(ethene) = $10^{-12} \text{ cm}^{-3} \text{ molecules}^{-1} \text{ s}^{-1}$
	6.4×10^{-11}	(Banceu <i>et al.</i> , 2001)	295	RR [relative to k(naphthalene) = $2.2 \times 10^{-11} \text{ cm}^{-3} \text{ molecules}^{-1} \text{ s}^{-1}$
	8.0×10^{-11}	(Klamt, 1993)	n/a	theoretical calculation based on a new molecular orbital based estimation method

Acy	1.2×10^{-10}	(Reisen and Arey, 2002)	296	RR [relative to k(trans-2-butene) = $6.48 \times 10^{-11} \text{ cm}^{-3} \text{ molecules}^{-1} \text{ s}^{-1}$
	1.3×10^{-10}	(Banceu <i>et al.</i> , 2001)	295	RR [relative to k(naphthalene) = $2.2 \times 10^{-11} \text{ cm}^{-3} \text{ molecules}^{-1} \text{ s}^{-1}$
	1.1×10^{-10}	(Atkinson and Aschmann, 1987)	296 ± 1	RR [relative to k(2,3-dimethyl-2-butene) = $1.11 \times 10^{-10} \text{ cm}^{-3} \text{ molecules}^{-1} \text{ s}^{-1}$
Fln	1.6×10^{-11}	(Kwok <i>et al.</i> , 1994b)	297	placed on an absolute basis by using $k_2(\text{cyclohexane}) = 7.47 \times 10^{-11} \text{ cm}^{-3} \text{ molecules}^{-1} \text{ s}^{-1}$
	1.3×10^{-11}	(Brubaker and Hites, 1998)	298	measured over the temperature range 326-366K
	9.9×10^{-12}	(Klamt, 1993)	n/a	theoretical calculation based on a new molecular orbital based estimation method
	1.3×10^{-11}	(Klopffer <i>et al.</i> , 1986)	300	RR [relative to k(ethene) = $7.47 \times 10^{-12} \text{ cm}^{-3} \text{ molecules}^{-1} \text{ s}^{-1}$
Phe	3.4×10^{-11}	(Biermann <i>et al.</i> , 1985)	298 ± 1	RR [relative to k(propene) = $4.85 \times 10^{-12} e^{504/T} \text{ cm}^{-3} \text{ molecules}^{-1} \text{ s}^{-1}$
	3.1×10^{-11}	(Atkinson, 1989)	298	recommended value based on previous data, overall uncertainty of $\pm 30\%$
	2.6×10^{-11}	(Klamt, 1993)	n/a	theoretical calculation based on a new molecular orbital based estimation method
	1.6×10^{-11}	(Lorenz and Zellner, 1983)	338	Absolute rate study, measured over a temperature range 338 - 748 K
	1.3×10^{-11}	(Kwok <i>et al.</i> , 1994b)	296	RR [relative to k(propene) = $2.66 \times 10^{-11} \text{ cm}^{-3} \text{ molecules}^{-1} \text{ s}^{-1}$
	2.7×10^{-11}	(Brubaker and Hites, 1998)	298	measured over the temperature range 346-386K, extrapolated using Arrhenius parameters
	3.2×10^{-11}	(Lee <i>et al.</i> , 2003)	298	measured over the temperature range 298-386K, extrapolated using Arrhenius parameters
	$4.98 \pm 2.96 \times 10^{-6} \text{ T}^{-1.97 \pm 0.10}$	(Ananthula <i>et al.</i> , 2006)	373-1000	two-parameter expression to best fit experimental data
1M-Phe	2.9×10^{-11}	(Lee <i>et al.</i> , 2003)	298	measured over the temperature range 363-403K, extrapolated using Arrhenius parameters
2M-Phe	6.5×10^{-11}	(Lee <i>et al.</i> , 2003)	298	measured over the temperature range 338-398K, extrapolated using Arrhenius parameters
3M-Phe	6.6×10^{-11}	(Lee <i>et al.</i> , 2003)	298	measured over the temperature range 353-388K, extrapolated using Arrhenius parameters
9M-Phe	7.6×10^{-11}	(Lee <i>et al.</i> , 2003)	298	measured over the temperature range 333-373K, extrapolated using Arrhenius parameters
Ant	1.1×10^{-10}	(Biermann <i>et al.</i> , 1985)	325 ± 1	RR [relative to k(propene) = $2.29 \times 10^{-11} \text{ cm}^{-3} \text{ molecules}^{-1} \text{ s}^{-1}$
	1.9×10^{-10}	(Brubaker and Hites, 1998)	298	measured over the temperature range 346-365K

	1.3×10^{-11}	(Kwok <i>et al.</i> , 1994b)	296	based on a derived k(anthracene)/k(phenanthrene) value of 1.0 ± 0.5
	2.0×10^{-10}	(Klamt, 1993)	n/a	theoretical calculation based on a new molecular orbital based estimation method
	1.3×10^{-10}	(Atkinson, 1989) ; (Biermann <i>et al.</i> , 1985)	298	recommended value based on previous data, overall uncertainty of $\pm 30\%$
	$1.12 \times 10^{-10} (T/298)^{-0.46}$	(Goulay <i>et al.</i> , 2005)	58-470	two-parameter expression to best fit experimental data
	$8.17 \times 10^{-14} T^{-8.3} e^{(-3171.71/T)}$	(Ananthula <i>et al.</i> , 2006)	373-923	modified Arrhenius equation to best fit experimental data
	$2.18 \times 10^{-11} e^{(-1734.11/T)}$	(Ananthula <i>et al.</i> , 2006)	999-1200	modified Arrhenius equation to best fit experimental data
Flt	1.1×10^{-11}	(Brubaker and Hites, 1998)	298	measured over the temperature range 346-366K
Pyr	5.0×10^{-11}	(Atkinson <i>et al.</i> , 1987a)	296 \pm 2	RR Relative to k(naphthalene) = $3.6 \times 10^{-28} \text{ cm}^{-3} \text{ molecules}^{-1} \text{ s}^{-1}$
1N-Nap	5.4×10^{-11}	(Atkinson, 1989)	298	recommended value
2N-Nap	5.6×10^{-11}	(Atkinson, 1989)	298	recommended value

Table A2. Second-order rate coefficients $k^{(2)}$ for gas-phase reactions of PAH with NO_3 radicals (Keyte *et al.*, 2013).

	k_{NO_3} ($\text{cm}^{-3} \text{ molecules}^{-1} \text{ s}^{-1}$) (x $[\text{NO}_2]$)	k_{NO_3} ($\text{cm}^{-3} \text{ molecules}^{-1} \text{ s}^{-1}$) [NO_2] = 6.91×10^{11} molecule cm^{-3} ^a	Reference	T (K)	Note
Nap	8.5×10^{-28}	1.1×10^{-16}	(Pitts <i>et al.</i> , 1985c)	298±2	RR Relative to $K_5(\text{NO}_3 + \text{NO}_2 - \text{N}_2\text{O}_5) = 3.41 \times 10^{-11} \text{ cm}^{-3} \text{ molecules}^{-1} \text{ s}^{-1}$
	4.8×10^{-28}	6.2×10^{-17}	(Atkinson <i>et al.</i> , 1987b)	298±2	RR Relative to $K_5(\text{NO}_3 + \text{NO}_2 - \text{N}_2\text{O}_5) = 3.41 \times 10^{-11} \text{ cm}^{-3} \text{ molecules}^{-1} \text{ s}^{-1}$
	3.3×10^{-28}	4.3×10^{-17}	(Atkinson and Aschmann, 1988)	296±2	RR Relative to $k(\text{propene}) = 9.45 \times 10^{-15} \text{ cm}^{-3} \text{ molecules}^{-1} \text{ s}^{-1}$
	3.7×10^{-28}	4.7×10^{-17}	(Atkinson <i>et al.</i> , 1990a)	~297	RR Relative to $k(\text{thiophene}) = 9.93 \times 10^{-14} \text{ cm}^{-3} \text{ molecules}^{-1} \text{ s}^{-1}$, Measured over temp range 272-297K
	4.2×10^{-28}	5.5×10^{-17}	(Atkinson <i>et al.</i> , 1990a)	~297	RR Relative to $K_5(\text{NO}_3 + \text{NO}_2 - \text{N}_2\text{O}_5) = 1.26 \times 10^{-27} e^{11275/T} \text{ cm}^{-3} \text{ molecules}^{-1} \text{ s}^{-1}$, Measured over temp range 272-297K
	3.6×10^{-28}	4.6×10^{-17}	(Atkinson, 1991)	298	Recommended value
1M-Nap	8.4×10^{-28}	1.1×10^{-16}	(Atkinson and Aschmann, 1987)	298±2	RR Relative to $k(\text{naphthalene}) = 3.6 \times 10^{-28} \text{ cm}^{-3} \text{ molecules}^{-1} \text{ s}^{-1}$
	7.0×10^{-28}	9.0×10^{-17}	(Atkinson and Aschmann, 1988)	296±2	RR Relative to $k(\text{trans-2-butene}) = 3.89 \times 10^{-13} \text{ cm}^{-3} \text{ molecules}^{-1} \text{ s}^{-1}$
	7.7×10^{-28}	9.9×10^{-17}	(Atkinson, 1991)	298	Recommended value
	7.2×10^{-28}	9.2×10^{-17}	(Phouongphouang and Arey, 2003b)	298±2	RR Relative to $k(\text{naphthalene}) = 3.65 \times 10^{-28} \text{ cm}^{-3} \text{ molecules}^{-1} \text{ s}^{-1}$, derived from the same work
2M-Nap	1.1×10^{-27}	1.4×10^{-16}	(Atkinson and Aschmann, 1987)	298±2	RR Relative to $k(\text{naphthalene}) = 3.6 \times 10^{-28} \text{ cm}^{-3} \text{ molecules}^{-1} \text{ s}^{-1}$
	1.1×10^{-27}	1.4×10^{-16}	(Atkinson and Aschmann, 1988)	296±2	RR Relative to $k(\text{propene}) = 9.45 \times 10^{-15} \text{ cm}^{-3} \text{ molecules}^{-1} \text{ s}^{-1}$
	1.1×10^{-27}	1.4×10^{-16}	(Atkinson, 1991)	298	Recommended value
	1.0×10^{-27}	1.3×10^{-16}	(Phouongphouang and Arey, 2003b)	298±2	RR Relative to $k(\text{naphthalene}) = 3.65 \times 10^{-28} \text{ cm}^{-3} \text{ molecules}^{-1} \text{ s}^{-1}$, derived from the same work

1E-Nap	9.8×10^{-28}	1.3×10^{-16}	(Phousongphouang and Arey, 2003b)	298±2	RR Relative to k(naphthalene) = $3.65 \times 10^{-28} \text{ cm}^3 \text{ molecules}^{-1} \text{ s}^{-1}$, derived from the same work
2E-Nap	8.0×10^{-28}	1.0×10^{-16}	(Phousongphouang and Arey, 2003b)	298±2	RR Relative to k(naphthalene) = $3.65 \times 10^{-28} \text{ cm}^3 \text{ molecules}^{-1} \text{ s}^{-1}$, derived from the same work
1,2DM-Nap	6.4×10^{-27}	8.3×10^{-16}	(Phousongphouang and Arey, 2003b)	298±2	RR Relative to k(2,7-DMN) = $21 \times 10^{-28} \text{ cm}^3 \text{ molecules}^{-1} \text{ s}^{-1}$, derived from the same work
1,3DM-Nap	2.1×10^{-27}	2.7×10^{-16}	(Phousongphouang and Arey, 2003b)	298±2	RR Relative to k(naphthalene) = $3.65 \times 10^{-28} \text{ cm}^3 \text{ molecules}^{-1} \text{ s}^{-1}$, derived from the same work
1,4DM-Nap	1.3×10^{-27}	1.7×10^{-16}	(Phousongphouang and Arey, 2003b)	298±2	RR Relative to k(naphthalene) = $3.65 \times 10^{-28} \text{ cm}^3 \text{ molecules}^{-1} \text{ s}^{-1}$, derived from the same work
1,5DM-Nap	1.4×10^{-27}	1.8×10^{-16}	(Phousongphouang and Arey, 2003b)	298±2	RR Relative to k(naphthalene) = $3.65 \times 10^{-28} \text{ cm}^3 \text{ molecules}^{-1} \text{ s}^{-1}$, derived from the same work
1,6DM-Nap	1.7×10^{-27}	2.1×10^{-16}	(Phousongphouang and Arey, 2003b)	298±2	RR Relative to k(naphthalene) = $3.65 \times 10^{-28} \text{ cm}^3 \text{ molecules}^{-1} \text{ s}^{-1}$, derived from the same work
1,7DM-Nap	1.4×10^{-27}	1.7×10^{-16}	(Phousongphouang and Arey, 2003b)	298±2	RR Relative to k(naphthalene) = $3.65 \times 10^{-28} \text{ cm}^3 \text{ molecules}^{-1} \text{ s}^{-1}$, derived from the same work
1,8DM-Nap	2.1×10^{-26}	2.7×10^{-15}	(Phousongphouang and Arey, 2003b)	298±2	RR Relative to k(2,7-DMN) = $21 \times 10^{-28} \text{ cm}^3 \text{ molecules}^{-1} \text{ s}^{-1}$, derived from the same work
2,3DM-Nap	1.5×10^{-28}	1.9×10^{-17}	(Atkinson and Aschmann, 1987)	298±2	RR Relative to k(naphthalene) = $3.6 \times 10^{-28} \text{ cm}^3 \text{ molecules}^{-1} \text{ s}^{-1}$
	1.6×10^{-27}	2.1×10^{-16}	(Atkinson and Aschmann, 1988)	296±2	RR Relative to k(propene) = $9.45 \times 10^{-15} \text{ cm}^3 \text{ molecules}^{-1} \text{ s}^{-1}$
	1.6×10^{-27}	2.0×10^{-16}	(Atkinson, 1991)	298	Recommended value
	1.5×10^{-27}	2.0×10^{-16}	(Phousongphouang and Arey, 2003b)	298±2	RR Relative to k(naphthalene) = $3.65 \times 10^{-28} \text{ cm}^3 \text{ molecules}^{-1} \text{ s}^{-1}$, derived from the same work
2,6DM-Nap	2.1×10^{-27}	2.7×10^{-16}	(Phousongphouang and Arey, 2003b)	298±2	RR Relative to k(naphthalene) = $3.65 \times 10^{-28} \text{ cm}^3 \text{ molecules}^{-1} \text{ s}^{-1}$, derived from the same work
2,7DM-Nap	2.1×10^{-27}	2.7×10^{-16}	(Phousongphouang and Arey, 2003b)	298±2	RR Relative to k(naphthalene) = $3.65 \times 10^{-28} \text{ cm}^3 \text{ molecules}^{-1} \text{ s}^{-1}$

Ace		$4.6 \times 10^{-13}{}^b$	(Atkinson and Aschmann, 1988)	296±2	RR Relative to $k(\text{trans-2-butene}) = 3.89 \times 10^{-13} \text{ cm}^{-3} \text{ molecules}^{-1} \text{ s}^{-1}$
	1.7×10^{-27}	2.1×10^{-16}	(Atkinson and Aschmann, 1988)	296±2	RR Relative to $k(\text{trans-2-butene}) = 3.89 \times 10^{-13} \text{ cm}^{-3} \text{ molecules}^{-1} \text{ s}^{-1}$
Acy		$5.5 \times 10^{-12}{}^b$	(Atkinson and Aschmann, 1988)	296±2	RR Relative to $k(\text{trans-2-butene}) = 3.89 \times 10^{-13} \text{ cm}^{-3} \text{ molecules}^{-1} \text{ s}^{-1}$
Fln		$3.5 \times 10^{-14}{}^c$	(Kwok <i>et al.</i> , 1997)	297±2	RR Relative to $k(\text{1-butene}) = 1.19 \times 10^{-14} \text{ cm}^{-3} \text{ molecules}^{-1} \text{ s}^{-1}$
Phe		$1.2 \times 10^{-13}{}^d$	(Kwok <i>et al.</i> , 1994a)	296±2	RR Relative to $k(\text{1-butene}) = 1.19 \times 10^{-14} \text{ cm}^{-3} \text{ molecules}^{-1} \text{ s}^{-1}$
Flt	5.1×10^{-28}	6.6×10^{-17}	(Atkinson <i>et al.</i> , 1990a)	296±2	RR Relative to $k(\text{naphthalene}) = 3.6 \times 10^{-28} \text{ cm}^{-3} \text{ molecules}^{-1} \text{ s}^{-1}$
Pyr	1.6×10^{-27}	2.1×10^{-16}	(Atkinson <i>et al.</i> , 1990a)	296±2	RR Relative to $k(\text{naphthalene}) = 3.6 \times 10^{-28} \text{ cm}^{-3} \text{ molecules}^{-1} \text{ s}^{-1}$
1N-Nap	3.0×10^{-28}	3.9×10^{-17}	(Atkinson, 1991)	298	Recommended value
2N-Nap	2.7×10^{-28}	3.5×10^{-17}	(Atkinson, 1991)	298	Recommended value

^a $[\text{NO}_2] = 6.91 \times 10^{11} \text{ molecule cm}^{-3}$; annual average, Harwell, U.K. (2011)

^b $[\text{NO}_2] = <1.2 \times 10^{15} \text{ molecule cm}^{-3}$

^c $[\text{NO}_2] = (7.2\text{-}24) \times 10^{13} \text{ molecule cm}^{-3}$

^d $[\text{NO}_2] = (4.8\text{-}24) \times 10^{13} \text{ molecule cm}^{-3}$

Table A3. Second-order rate coefficients $k^{(2)}$ for gas-phase reactions of PAH with O_3 (Keyte *et al.*, 2013).

	k_{O_3} ($cm^{-3} \text{ molecules}^{-1} s^{-1}$)	Reference	T (K)	Notes
Nap	$<2.0 \times 10^{-19}$	(Atkinson <i>et al.</i> , 1984)	294±1	Upper limit
	$<3.0 \times 10^{-19}$	(Atkinson and Aschmann, 1986)	295±1	Upper limit
1M-Nap	$<1.3 \times 10^{-19}$	(Atkinson and Aschmann, 1987)	298±2	Upper limit
2M-Nap	$<3.0 \times 10^{-19}$	(Atkinson and Aschmann, 1986)	295±1	Upper limit
	$<4.0 \times 10^{-19}$	(Atkinson and Aschmann, 1987)	295±2	Upper limit
Ace	$<5.0 \times 10^{-19}$	(Atkinson and Aschmann, 1988)	296±2	Upper limit
Acy	5.5×10^{-16}	(Atkinson and Aschmann, 1988)	296±2	
	1.6×10^{-16}	(Reisen and Arey, 2002)	296±2	RR, relative to $k(2\text{-methyl-2-butadiene}) = 3.96 \times 10^{-16} \text{ cm}^{-3} \text{ molecules}^{-1} s^{-1}$
2,3DM-Nap	$<4.0 \times 10^{-19}$	(Atkinson and Aschmann, 1986)	295±1	Upper limit
	$<2.0 \times 10^{-19}$	(Kwok <i>et al.</i> , 1994b)	297±2	Upper limit
Phe	4.0×10^{-19}	(Kwok <i>et al.</i> , 1997)	296±2	
1N-Nap	$<6.0 \times 10^{-19}$	(Atkinson, 1994)	298±2	Upper limit
2N-Nap	$<6.0 \times 10^{-19}$	(Atkinson, 1994)	298±2	Upper limit

Table A4. Second-order rate coefficients $k^{(2)}$ for heterogeneous reactions of PAH with OH, NO₂, O₃ and NO₃/N₂O₅ (Keyte et al., 2013).

PAH	OH Reactions			NO ₂ Reactions			O ₃ Reactions			NO ₃ reactions		
	k_{OH} (cm ³ molec ⁻¹ s ⁻¹)	Reference	Notes	k_{NO_2} (cm ³ molec ⁻¹ s ⁻¹)	Reference	Notes	k_{O_3} (cm ³ molec ⁻¹ s ⁻¹)	Reference	Notes	k_{NO_3} (cm ³ molec ⁻¹ s ⁻¹)	Reference	Notes
Nap							$0.9 \times 10^{-18} / (1/c_{O_3} + 10^{-15})$	(Kahan et al., 2006)	Octanol			
Phe	5.0×10^{-12}	(Estève <i>et al.</i> , 2004)	Graphite particles	2.8×10^{-19}	(Perraudin <i>et al.</i> , 2005)	Silica particles	2.4×10^{-17}	(Perraudin <i>et al.</i> , 2007)	Graphite particles			
	3.2×10^{-13}	(Estève <i>et al.</i> , 2006)	Diesel exhaust particles SRM 1650a	3.4×10^{-18}	(Nguyen <i>et al.</i> , 2009)	Kerosene flame soot	2.3×10^{-17}	(Perraudin <i>et al.</i> , 2007)	Silica particles			
				3.5×10^{-17}	(Estève <i>et al.</i> , 2004)	Graphite particles	$2.3 \times 10^{-19} / (1/c_{O_3} + 4.6 \times 10^{-16})$	(Kahan et al., 2006)	Octanol			
				1.1×10^{-17}	(Estève <i>et al.</i> , 2006)	Diesel exhaust particles SRM 1650a	$1.0 \times 10^{-18} / (1/c_{O_3} + 1.4 \times 10^{-16})$	(Kahan et al., 2006)	Ice			
				2.3×10^{-21}	(Butler and Crossley, 1981)	Ethylene flame soot						
Ant	4.4×10^{-12}	(Estève <i>et al.</i> , 2006)	Graphite particles	1.0×10^{-16}	(Perraudin <i>et al.</i> , 2005)	Silica particles	9.8×10^{-17}	(Perraudin <i>et al.</i> , 2007)	Graphite particles			
				3.4×10^{-18}	(Nguyen <i>et al.</i> , 2009)	Kerosene flame soot	1.4×10^{-16}	(Perraudin <i>et al.</i> , 2007)	Silica particles			
				6.9×10^{-17}	(Estève <i>et al.</i> , 2004)	Graphite particles	$5.1 \times 10^{-18} / (1/c_{O_3} + 1.96 \times 10^{-15})$	(Kwamena et al., 2006)	Octanol			

				1.0×10^{-16}	(Ma <i>et al.</i> , 2011)	Silica particles	$1.3 \times 10^{-16} / (1/C_{O_3} + 2.2 \times 10^{-15})$	(Kwamena <i>et al.</i> , 2007)	Azelaic acid (wet)			
				5.3×10^{-17}	(Ma <i>et al.</i> , 2011)	MgO particles	$1.0 \times 10^{-15} / (1/C_{O_3} + 10^{-13})$	(Kwamena <i>et al.</i> , 2007)	Phenylsiloxane oil			
							$1.2 \times 10^{-18} / (1/C_{O_3} + 1.2 \times 10^{-18})$	(Mmereki <i>et al.</i> , 2004)	Water			
Fit	1.4×10^{-14}	(Bedjanian <i>et al.</i> , 2010)	Kerosene flame soot	3.2×10^{-21}	(Perraudin <i>et al.</i> , 2005)	Silica particles	1.9×10^{-17}	(Perraudin <i>et al.</i> , 2007)	Graphite particles			
	3.2×10^{-12}	(Estève <i>et al.</i> , 2004)	Graphite particles	1.0×10^{-19}	(Nguyen <i>et al.</i> , 2009)	Kerosene flame soot	1.5×10^{-17}	(Perraudin <i>et al.</i> , 2007)	Silica particles			
	3.8×10^{-13}	(Estève <i>et al.</i> , 2006)	Diesel exhaust particles SRM 1650a	2.9×10^{-17}	(Estève <i>et al.</i> , 2004)	Graphite particles						
				1.0×10^{-17}	(Estève <i>et al.</i> , 2006)	Diesel exhaust particles SRM 1650a						
				2.5×10^{-21}	(Butler and Crossley, 1981)	Ethylene flame soot						
Pyr	1.6×10^{-14}	(Bedjanian <i>et al.</i> , 2010)	Kerosene flame soot	2.0×10^{-17}	(Perraudin <i>et al.</i> , 2005)	Silica particles	2.5×10^{-17}	(Perraudin <i>et al.</i> , 2007)	Graphite particles	6.4×10^{-12}	(Liu <i>et al.</i> , 2012)	Azelaic acid particles
	3.2×10^{-12}	(Estève <i>et al.</i> , 2004)	Graphite particles	1.0×10^{-19}	(Nguyen <i>et al.</i> , 2009)	Kerosene flame soot	5.9×10^{-17}	(Perraudin <i>et al.</i> , 2007)	Silica particles			
	4.1×10^{-13}	(Estève <i>et al.</i> , 2006)	Diesel exhaust particles SRM 1650a	5.1×10^{-17}	(Estève <i>et al.</i> , 2004)	Graphite particles	9.3×10^{-17}	(Miet <i>et al.</i> , 2009b)	Silica particles			

	2.4×10^{-13}	(Miet <i>et al.</i> , 2009a)	Silica particles	1.5×10^{-17}	(Estéve <i>et al.</i> , 2006)	Diesel exhaust particles SRM 1650a	$2.2 \times 10^{-19} / (1/C_{O_3} + 3.1 \times 10^{-16})$	(Kahan <i>et al.</i> , 2006)	Octanol			
				4.8×10^{-21}	(Butler and Crossley, 1981)	Ethylene flame soot						
				3.2×10^{-16}	Miet <i>et al.</i> ²⁷⁷	Silica particles						
Chr	9.2×10^{-15}	(Bedjanian <i>et al.</i> , 2010)	Kerosene flame soot	6.0×10^{-19}	(Perraudin <i>et al.</i> , 2005)	Silica particles	1.5×10^{-17}	(Perraudin <i>et al.</i> , 2007)	Graphite particles	4.0×10^{-12}	(Liu <i>et al.</i> , 2012)	Azelaic acid particles
	5.0×10^{-12}	(Estéve <i>et al.</i> , 2004)	Graphite particles	1.0×10^{-19}	(Nguyen <i>et al.</i> , 2009)	Kerosene flame soot	3.1×10^{-17}	(Perraudin <i>et al.</i> , 2007)	Silica particles			
	4.4×10^{-13}	(Estéve <i>et al.</i> , 2006)	Diesel exhaust particles SRM 1650a	3.9×10^{-17}	(Estéve <i>et al.</i> , 2004)	Graphite particles						
				1.0×10^{-17}	(Estéve <i>et al.</i> , 2006)	Diesel exhaust particles SRM 1650a						
				2.6×10^{-21}	(Butler and Crossley, 1981)	Ethylene flame soot						
BaA	9.2×10^{-15}	(Bedjanian <i>et al.</i> , 2010)	Kerosene flame soot	6.7×10^{-18}	(Perraudin <i>et al.</i> , 2005)	Silica particles	2.8×10^{-17}	(Perraudin <i>et al.</i> , 2007)	Graphite particles	4.3×10^{-12}	(Liu <i>et al.</i> , 2012)	Azelaic acid particles
	5.6×10^{-13}	(Estéve <i>et al.</i> , 2004)	Graphite particles	1.0×10^{-19}	(Nguyen <i>et al.</i> , 2009)	Kerosene flame soot	8.7×10^{-17}	(Perraudin <i>et al.</i> , 2007)	Silica particles			
	3.2×10^{-13}	(Estéve <i>et al.</i> , 2006)	Diesel exhaust particles SRM 1650a	3.3×10^{-17}	(Estéve <i>et al.</i> , 2004)	Graphite particles						
				1.3×10^{-17}	(Estéve <i>et al.</i> , 2006)	Diesel exhaust particles SRM 1650a						

				6.2×10^{-21}	(Butler and Crossley, 1981)	Ethylene flame soot						
BkF	1.0×10^{-14}	(Bedjanian <i>et al.</i> , 2010)	Kerosene flame soot	2.2×10^{-18}	(Perraudin <i>et al.</i> , 2005)	Silica particles	1.9×10^{-17}	(Perraudin <i>et al.</i> , 2007)	Graphite particles			
	3.5×10^{-12}	(Estève <i>et al.</i> , 2004)	Graphite particles	1.0×10^{-19}	(Nguyen <i>et al.</i> , 2009)	Kerosene flame soot	3.6×10^{-17}	(Perraudin <i>et al.</i> , 2007)	Silica particles			
				2.5×10^{-17}	(Estève <i>et al.</i> , 2004)	Graphite particles						
BaP	1.1×10^{-14}	(Bedjanian <i>et al.</i> , 2010)	Kerosene flame soot	9.3×10^{-16}	(Perraudin <i>et al.</i> , 2005)	Silica particles	5.3×10^{-17}	(Perraudin <i>et al.</i> , 2007)	Graphite particles			
	4.1×10^{-12}	(Estève <i>et al.</i> , 2004)	Graphite particles	1.0×10^{-19}	(Nguyen <i>et al.</i> , 2009)	Kerosene flame soot	1.4×10^{-16}	(Perraudin <i>et al.</i> , 2007)	Silica particles			
	2.9×10^{-13}	(Estève <i>et al.</i> , 2006)	Diesel exhaust particles SRM 1650a	7.8×10^{-17}	(Estève <i>et al.</i> , 2004)	Graphite particles	$2.0 \times 10^{-18} / (1/c_{O_3} + 3.6 \times 10^{-16})$	(Kahan <i>et al.</i> , 2006)	Octanol			
				1.5×10^{-17}	(Estève <i>et al.</i> , 2006)	Diesel exhaust particles SRM 1650a	$<3.8 \times 10^{-18} / (1/c_{O_3} + 10^{-16})$	(Kwamena <i>et al.</i> , 2004, 2006)	NaCl			
				1.0×10^{-20}	(Butler and Crossley, 1981)	Ethylene flame soot	$4.2 \times 10^{-15} / (1/c_{O_3} + 2.8 \times 10^{-13})$	(Kwamena <i>et al.</i> , 2006; Pöschl <i>et al.</i> , 2001)	Soot			
							$1.7 \times 10^{-16} / (1/c_{O_3} + 1.2 \times 10^{-15})$	(Kwamena <i>et al.</i> , 2004)	azelaic acid (wet)			
							$3.0 \times 10^{-16} / (1/c_{O_3} + 9.50 \times 10^{-15})$	(Kwamena <i>et al.</i> , 2006)	Silica particles			
BeP	1.1×10^{-14}	(Bedjanian <i>et al.</i> , 2010)	Kerosene flame soot	2.9×10^{-18}	(Perraudin <i>et al.</i> , 2005)	Silica particles	1.6×10^{-17}	(Perraudin <i>et al.</i> , 2007)	Graphite particles			
	4.7×10^{-12}	(Estève <i>et al.</i> , 2004)	Graphite particles	1.0×10^{-19}	(Nguyen <i>et al.</i> , 2009)	Kerosene flame soot	2.9×10^{-17}	(Perraudin <i>et al.</i> , 2007)	Silica particles			

								2007)				
	4.7×10^{-13}	(Estéve <i>et al.</i> , 2006)	Diesel exhaust particles SRM 1650a	3.5×10^{-17}	(Estéve <i>et al.</i> , 2004)	Graphite particles						
				7.5×10^{-18}	(Estéve <i>et al.</i> 2006)	Diesel exhaust particles SRM 1650a						
				2.8×10^{-21}	(Butler and Crossley, 1981)	Ethylene flame soot						
Per	5.0×10^{-12}	(Estéve <i>et al.</i> , 2004)	Graphite particles	1.1×10^{-16}	(Estéve <i>et al.</i> , 2004)	Graphite particles						
IPy	3.5×10^{-13}	(Estéve <i>et al.</i> , 2006)	Diesel exhaust particles SRM 1650a	6.2×10^{-18}	(Perraudin <i>et al.</i> , 2005)	Silica particles	1.9×10^{-17}	(Perraudin <i>et al.</i> , 2007)	Graphite particles			
				1.0×10^{-19}	(Nguyen <i>et al.</i> , 2009)	Kerosene flame soot	3.8×10^{-17}	(Perraudin <i>et al.</i> , 2007)	Silica particles			
				7.5×10^{-18}	Estéve <i>et al.</i> , 2006	Diesel exhaust particles SRM 1650a						
BgP	5.9×10^{-12}	(Estéve <i>et al.</i> , 2004)	Graphite particles	4.7×10^{-17}	(Perraudin <i>et al.</i> , 2005)	Silica particles						
				1.0×10^{-19}	(Nguyen <i>et al.</i> , 2009)	Kerosene flame soot						
				3.8×10^{-17}	Estéve <i>et al.</i> , 2004	Graphite particles						
				7.9×10^{-21}	(Butler and Crossley, 1981)	Ethylene flame soot						
BgF	8.4×10^{-15}	(Bedjanian <i>et al.</i> , 2010)	Kerosene flame soot	1.0×10^{-19}	(Nguyen <i>et al.</i> , 2009)	Kerosene flame soot						
AcP	1.0×10^{-14}	(Bedjanian	Kerosene flame	1.0×10^{-19}	(Nguyen <i>et</i>	Kerosene flame soot						

		<i>et al.</i> , 2010)	soot		<i>al.</i> , 2009)							
DBahA	1.6×10^{-14}	(Bedjanian <i>et al.</i> , 2010)	Kerosene flame soot	1.0×10^{-19}	(Nguyen <i>et al.</i> , 2009)	Kerosene flame soot						
DBaeP	1.0×10^{-14}	(Bedjanian <i>et al.</i> , 2010)	Kerosene flame soot	1.0×10^{-19}	(Nguyen <i>et al.</i> , 2009)	Kerosene flame soot						
BbF	1.2×10^{-14}	(Bedjanian <i>et al.</i> , 2010)	Kerosene flame soot	1.0×10^{-19}	(Nguyen <i>et al.</i> , 2009)	Kerosene flame soot						
Cor	1.1×10^{-14}	(Bedjanian <i>et al.</i> , 2010)	Kerosene flame soot	1.3×10^{-18}	(Perraudin <i>et al.</i> , 2005)	Silica particles						
				1.0×10^{-19}	(Nguyen <i>et al.</i> , 2009)	Kerosene flame soot						
				2.3×10^{-21}	(Butler and Crossley, 1981)	Ethylene flame soot						
DBalP				1.8×10^{-16}	(Perraudin <i>et al.</i> , 2005)	Silica particles	1.3×10^{-16}	(Perraudin <i>et al.</i> , 2007)	Graphite particles			
							1.3×10^{-16}	(Perraudin <i>et al.</i> , 2007)	Silica particles			
1-NP	1.0×10^{-13}	(Miet <i>et al.</i> , 2009a)	Silica particles	6.2×10^{-18}	(Miet <i>et al.</i> , 2009c)	Silica particles	2.2×10^{-17}	(Miet <i>et al.</i> , 2009b)	Silica particles	1.3×10^{-12}	(Liu <i>et al.</i> , 2012)	Azelaic acid particles

Appendix 2 : Sampler Calibration and total air flow calculation

Sampler flow rates were calibrated according to manufacturer guidelines (Tisch TE-5000 Operations Manual). Sampler calibrations were carried out each time a sampler motor was changed. A Fixed Orifice Calibrator (Tisch Environmental Inc.) was used, utilizing 5 plates of differing resistance to simulate a variation in airflow across the sampler. Flow chart recorder and manometer measurements were taken for each of the five resistances. Actual air flow rates for these readings were calculated according to the formula (Tisch TE-5000 Operations Manual) :

$$Q_a = 1/m[\text{Sqrt}((H_2O)(T_a/P_a))-b] \quad (\text{B1})$$

where:

Q_a = actual flow rate as indicated by the calibrator orifice (m^3/min)

H_2O = orifice manometer reading (inches)

T_a = ambient temperature (K)

P_a = ambient barometric pressure (mm Hg)

m = slope of orifice calibration relationship – *obtained from data sheet provided by manufacturer*

b = intercept of orifice calibration relationship – *obtained from data sheet provided by manufacturer*

Flow recorder readings were corrected to the prevailing meteorological conditions during calibrations using the equation (Tisch TE-5000 Operations Manual) :

$$IC = I[\text{Sqrt}(T_a/P_a)] \quad (\text{B2})$$

where:

IC = flow chart recorder readings corrected to measured Ta and Pa (m³/min)

I = flow recorder reading (m³/min)

Pa = ambient barometric (mm Hg)

Ta = ambient temperature during calibration (K)

A plot of Qa vs. IC forms a 5 point calibration curve for the sampler (see Figure 2.3).

Overall flow rates for each sample were then calculated using the formula (Tisch TE-5000 Operations Manual):

$$Q_s = 1/m((I)[\text{Sqrt}(T_{av}/P_{av})] - b) \quad (\text{B3})$$

where :

Q_s = Sampler flow rate (m³/min)

m = calibration slope

b = calibration intercept

I = average flow chart recording during sampling period (m³/min)

T_{av} = average ambient temperature (K)

P_{av} = average ambient pressure (mm Hg)

Total air flow during each sampler run can then be calculated (Tisch TE-5000 Operations Manual) :

$$Q_T = Q_S \times 60 \times T \quad (\text{B4})$$

where :

Q_T = Total air flow (m³)

Q_S = Sampler flow rate (m³/min)

T = sampler run time (hours)

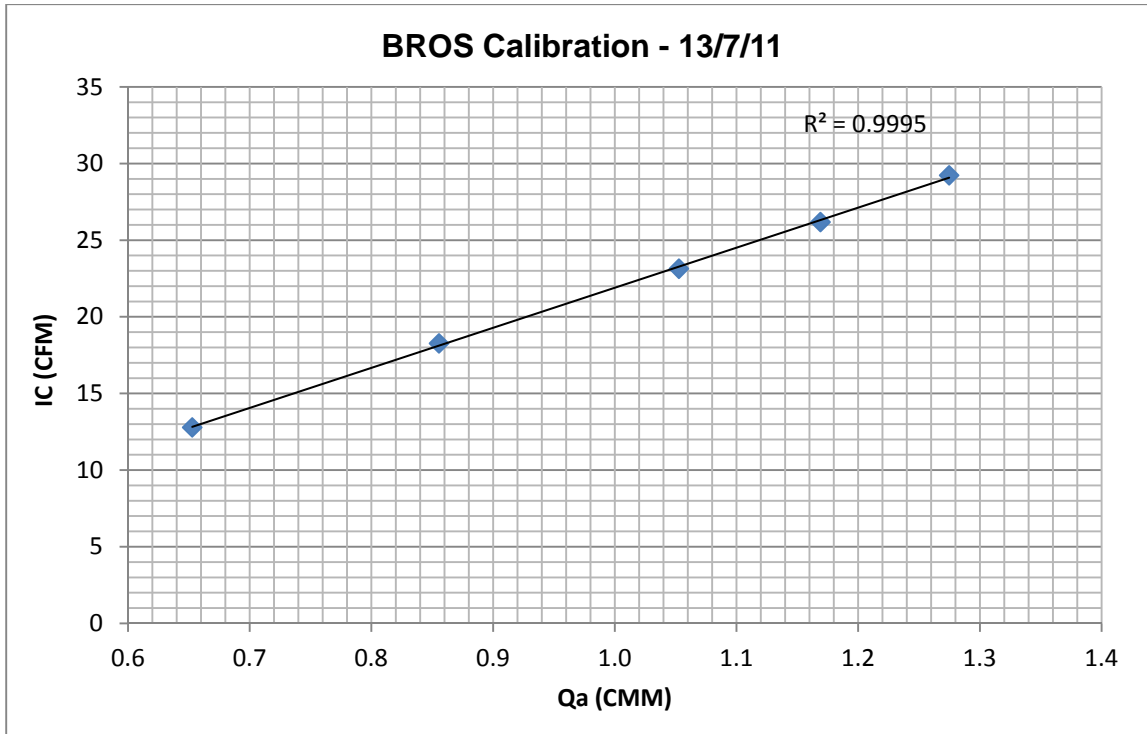


Figure B1. Example calibration curve for high volume samplers

Appendix 3 : PAH, OPAH and NPAH gas chromatograph peaks

Separate GC-MS techniques were used for the analysis of PAH compounds and the analysis of OPAH and NPAH compounds

The gas-chromatograph peaks for all measured PAH compounds and detuerated standards, measured in both sample extracts and internal standards in this study are shown in Figure C1.

The gas-chromatograph peaks for all measured OPAH and NPAH compounds and detuerated standards, measured in samples and internal standards in this study are shown in Figure C2.

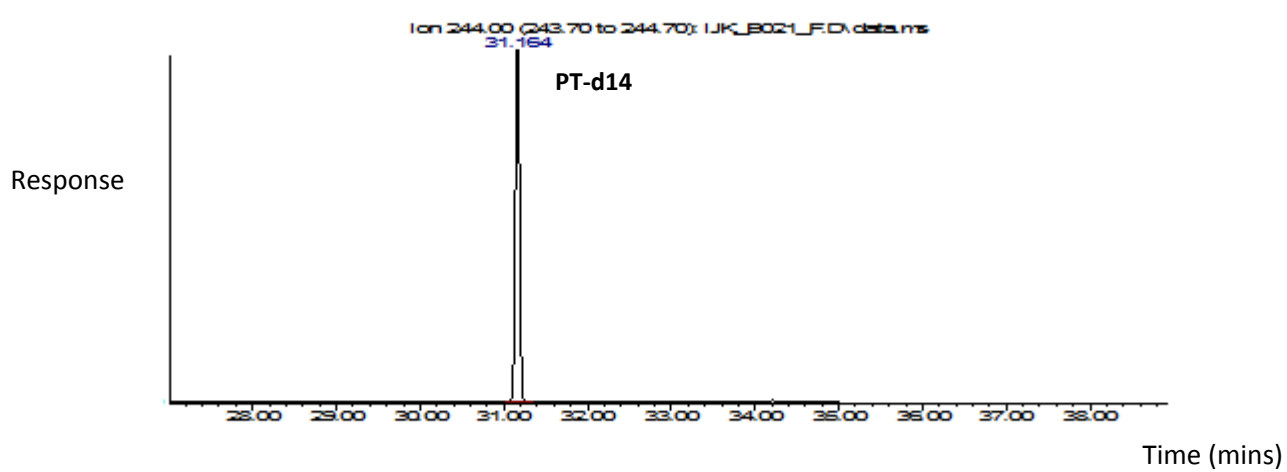
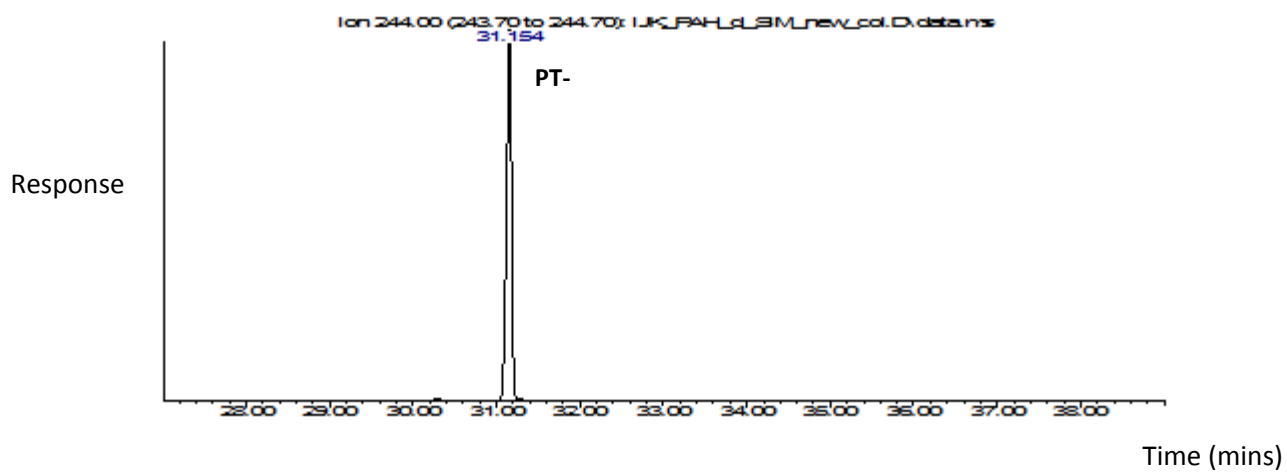


Figure C1a. GC-MS peaks for the recovery standard compound PT-d14 ($M^+ = 244$) in the standard (upper) and sample extract (lower).

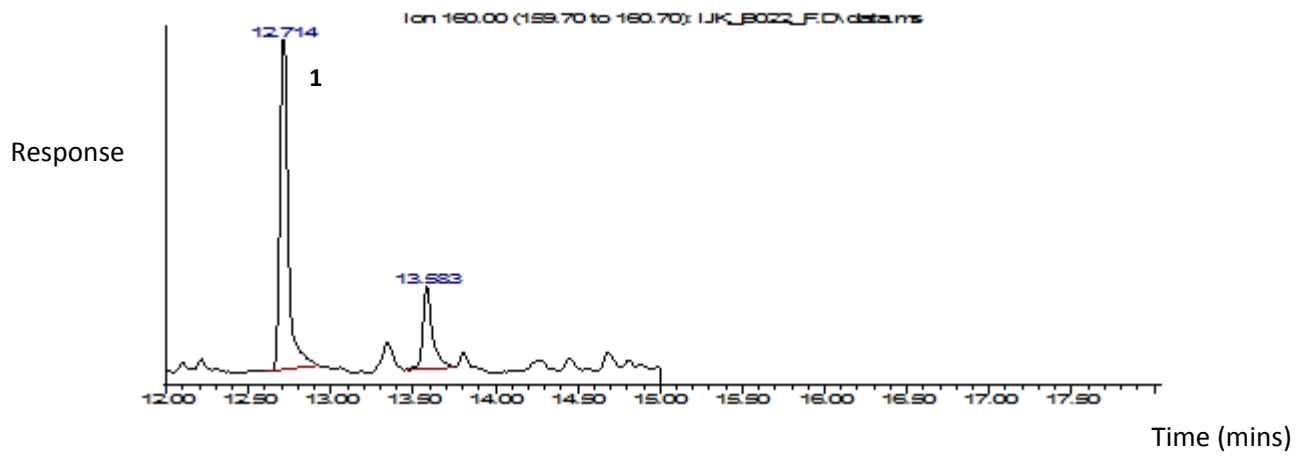
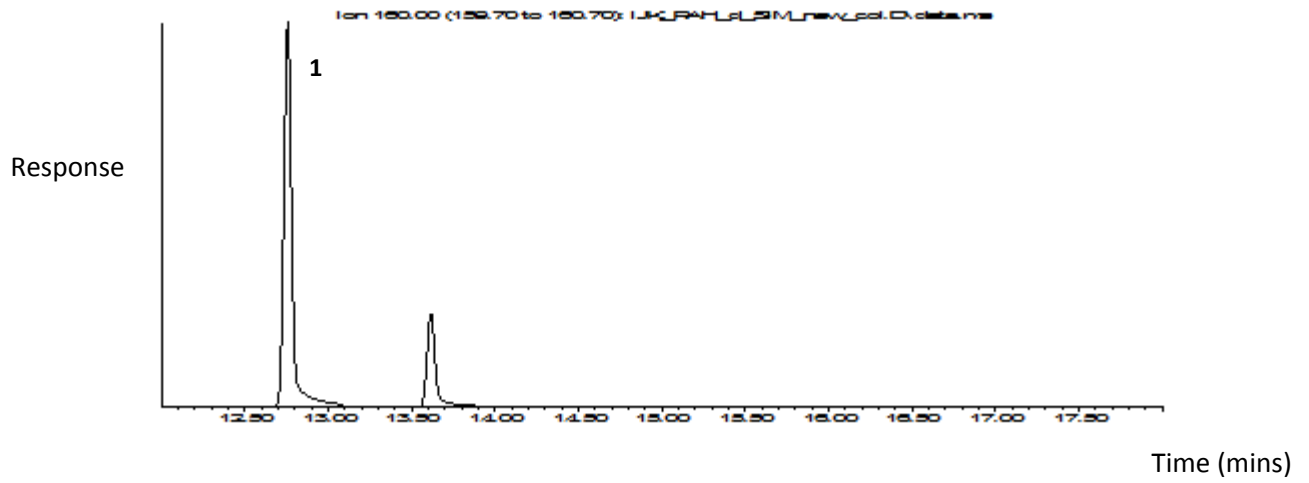


Figure C1b. GC-MS peaks for $M^+ = 160$ in the standard (upper) and sample extract (lower).
1 = Acy-d8.

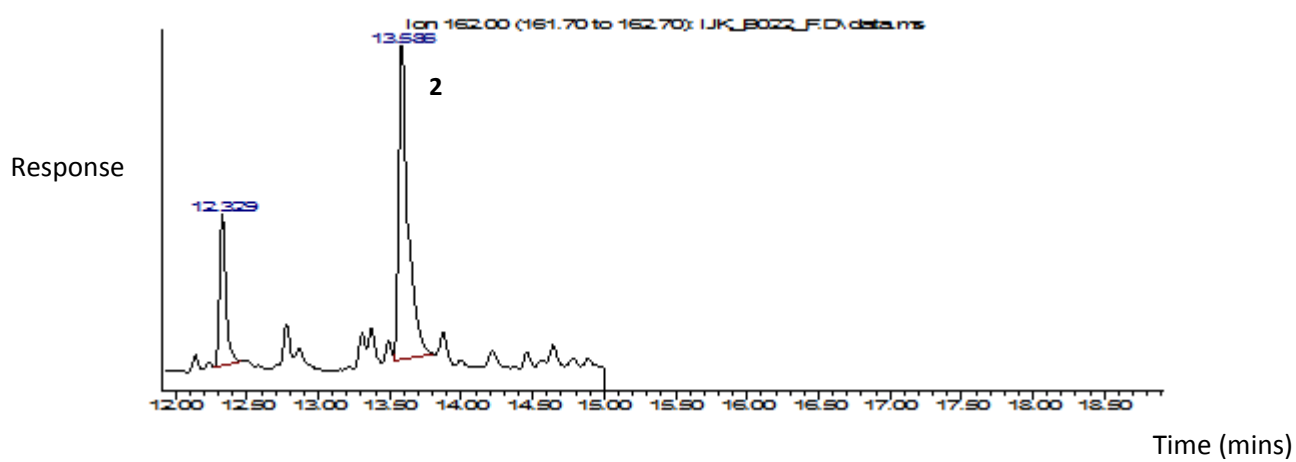
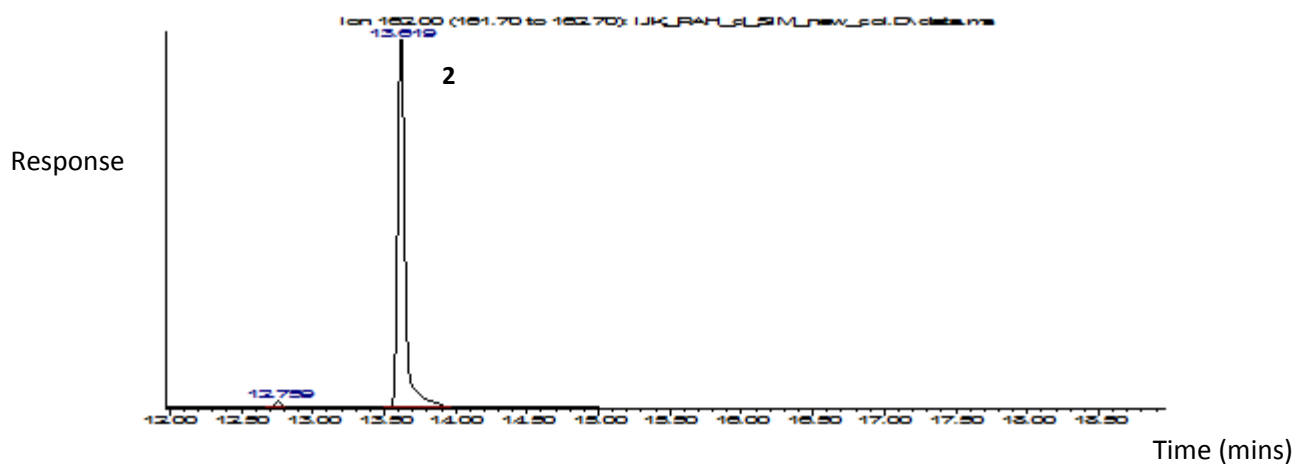


Figure C1c. GC-MS peaks for $M^+ = 162$ in the standard (upper) and sample extract (lower). 2 = Ace-d8.

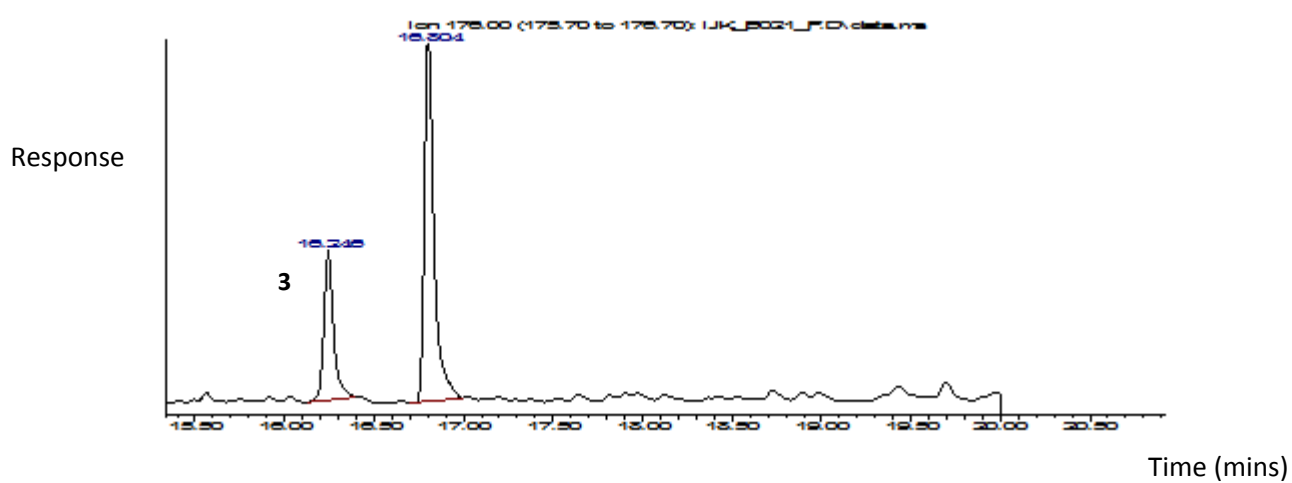
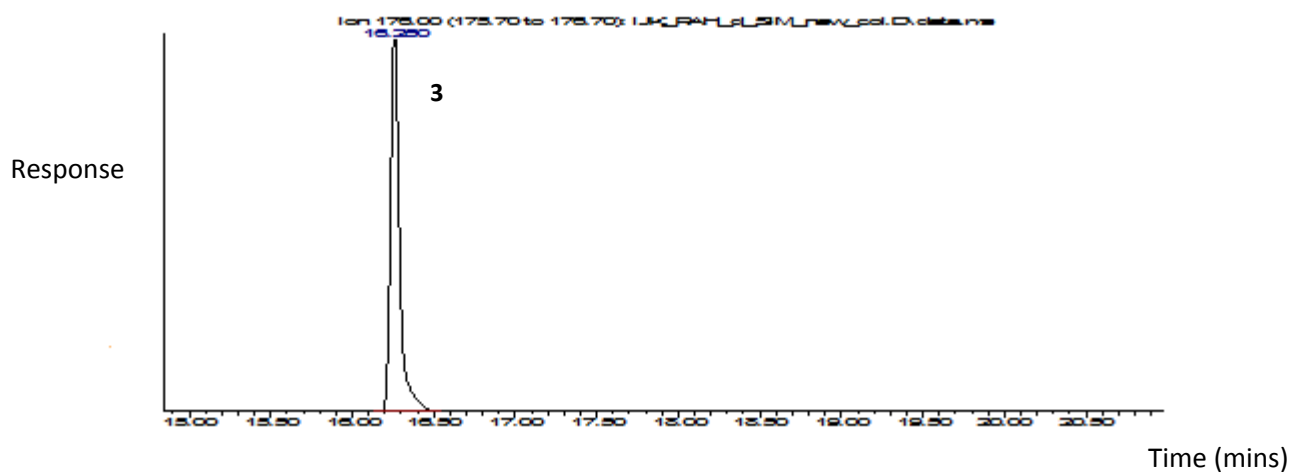


Figure C1d. GC-MS peaks for $M^+ = 176$ in the standard (upper) and sample extract (lower).
3 = Flo-d10.

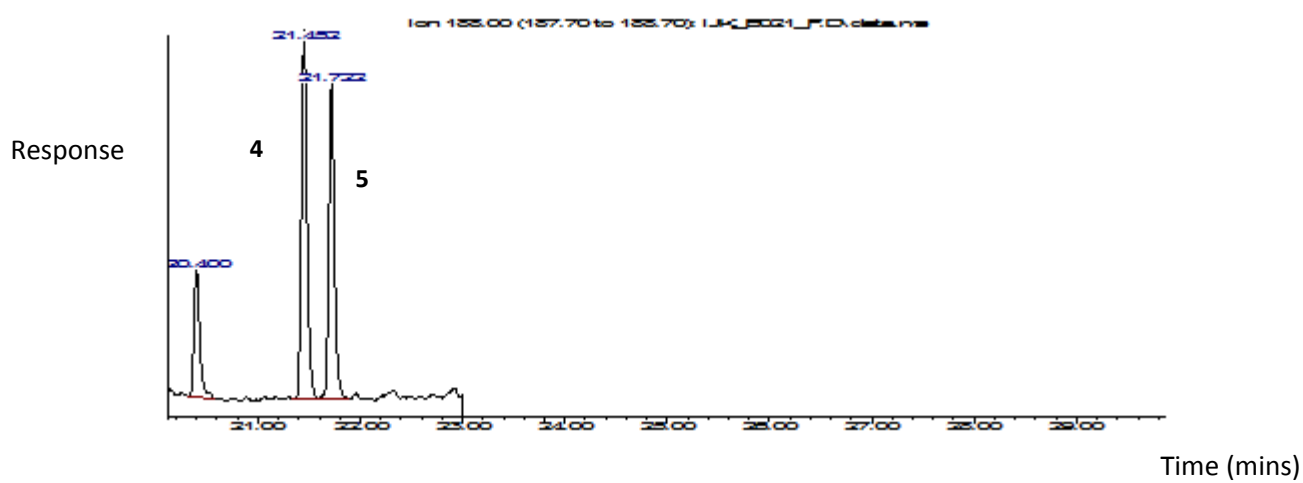
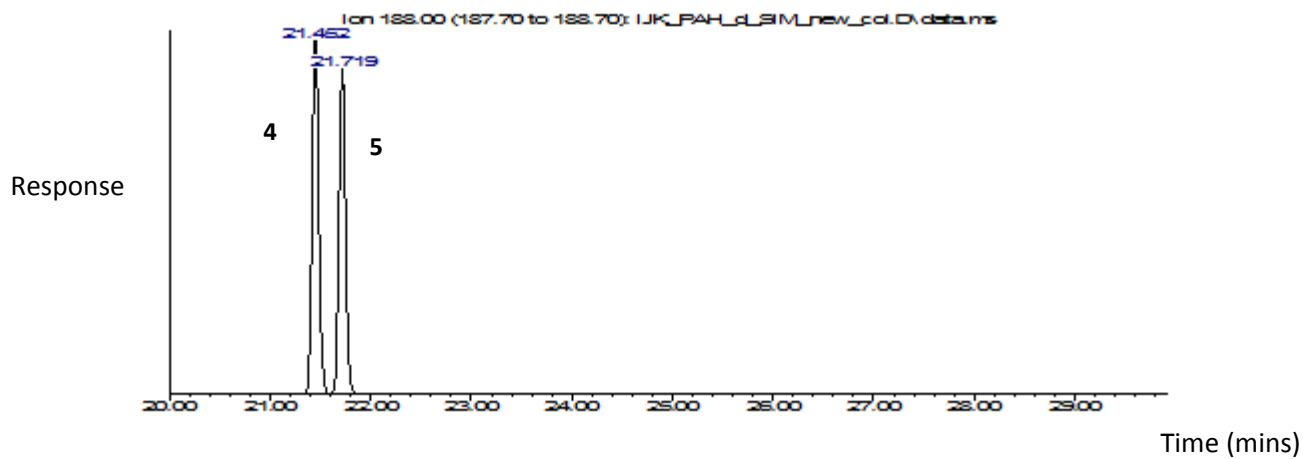


Figure C1e. GC-MS peaks for $M^+ = 188$ in the standard (upper) and sample extract (lower). 4 = Phe-d10, 5 = Ant-d10.

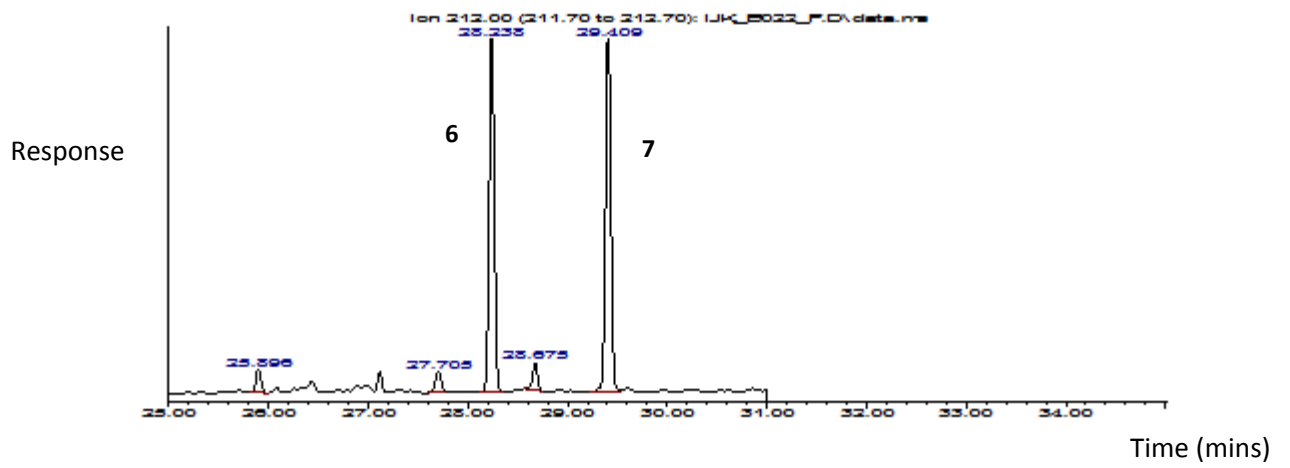
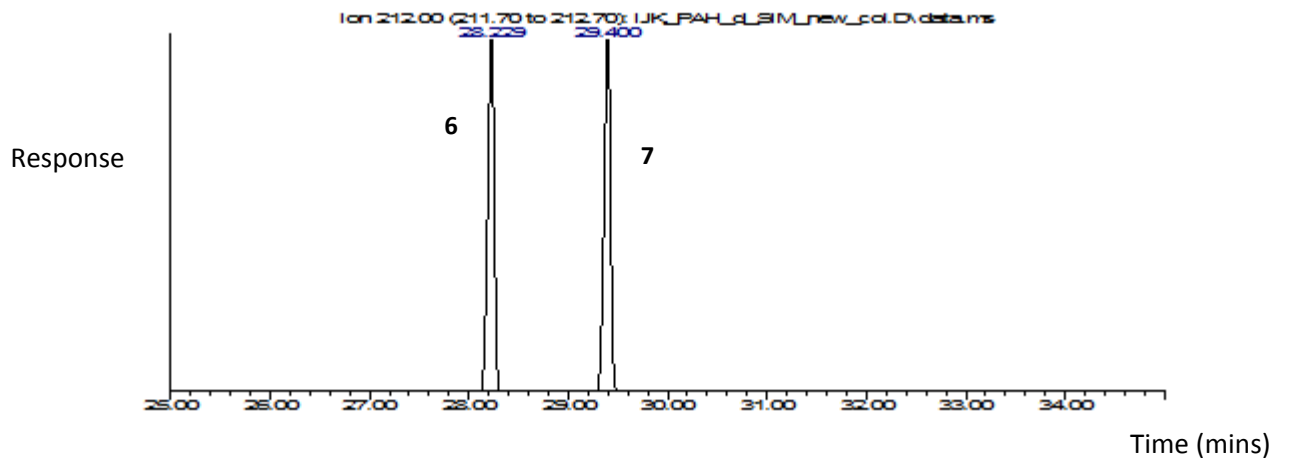


Figure C1f. GC-MS peaks for $M^+ = 212$ in the standard (upper) and sample extract (lower). 6 = Flt-d10, 7 = Pyr-d10.

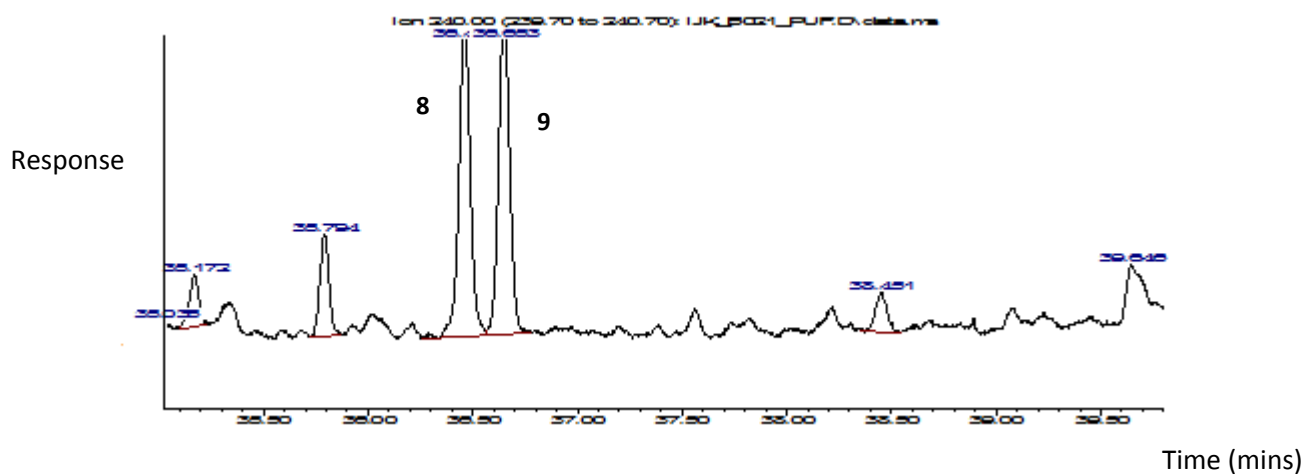
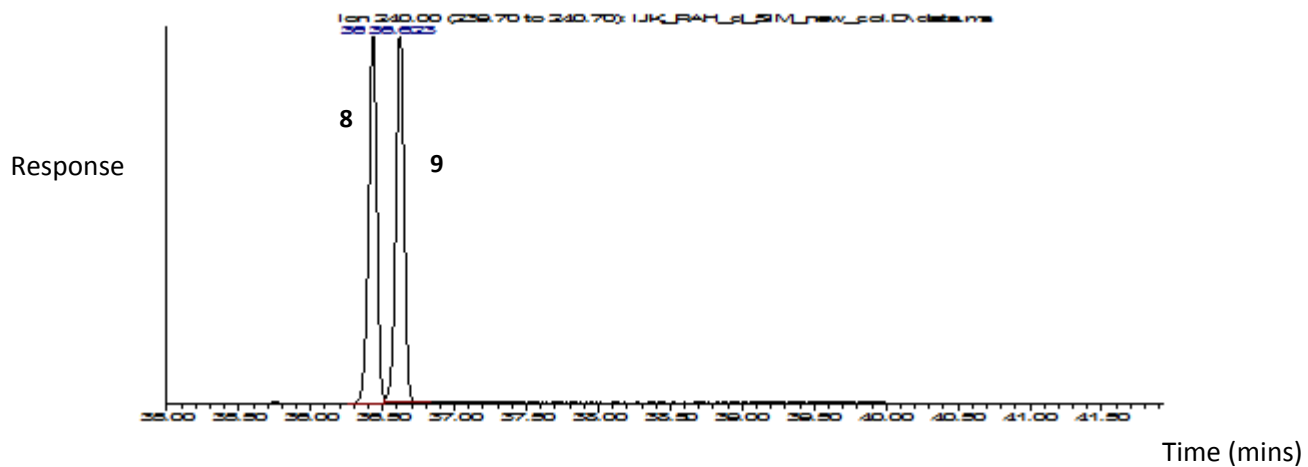


Figure C1g. GC-MS peaks for $M^+ = 240$ in the standard (upper) and sample extract (lower).
 8 = BaA-d12, 9 = Chr-d12.

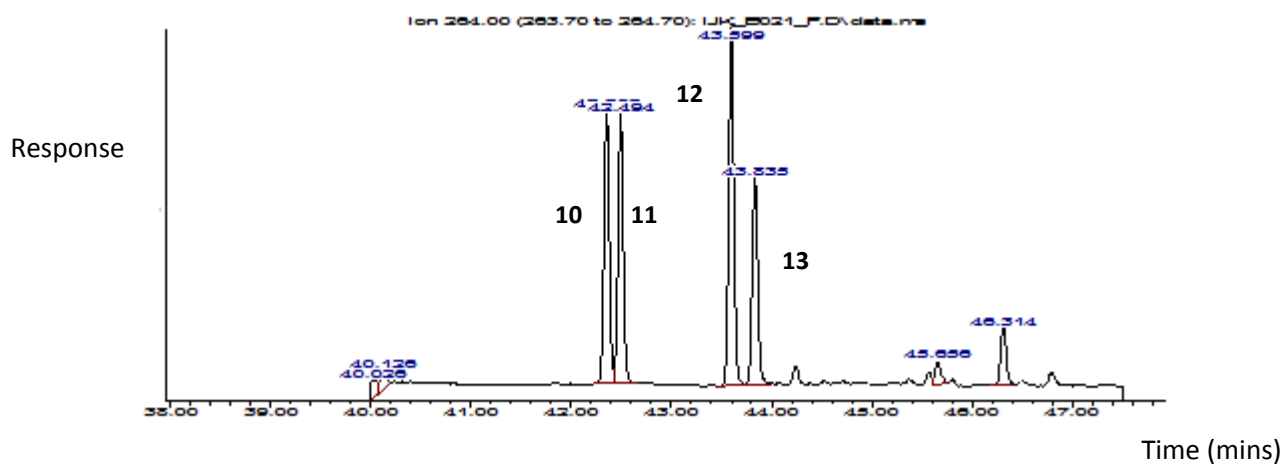
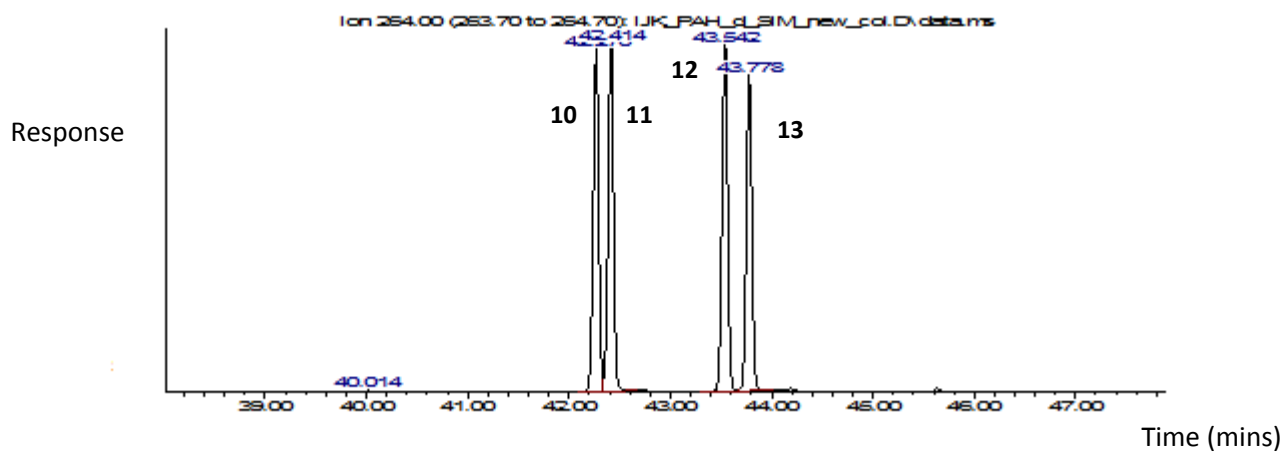


Figure C1h. GC-MS peaks for $M^+ = 264$ in the standard (upper) and sample extract (lower).
 10 = BbF-d12, 11 = BkF-d12, 12 = BeP-d12, 13 = BaP-d12.

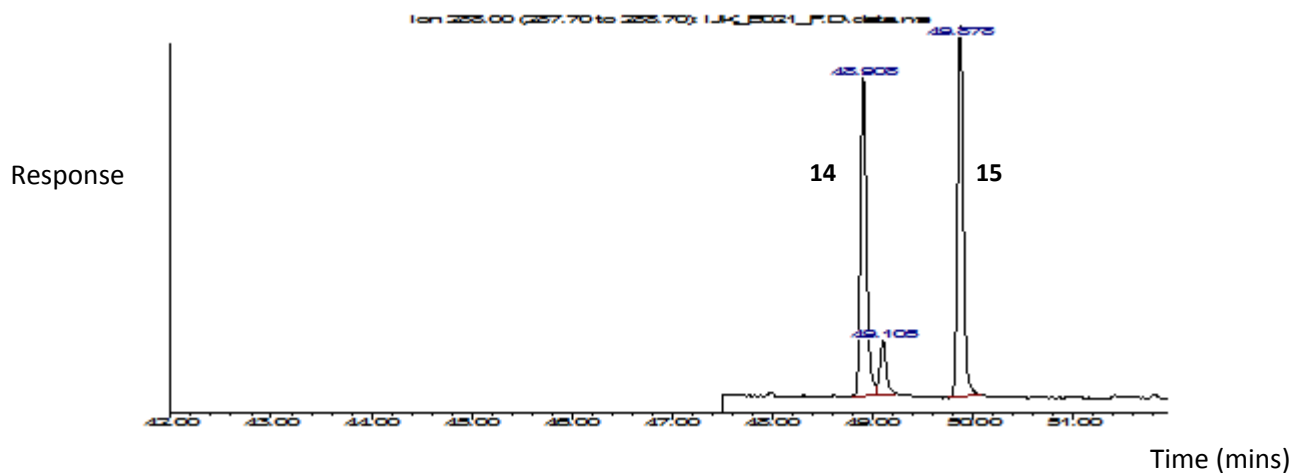
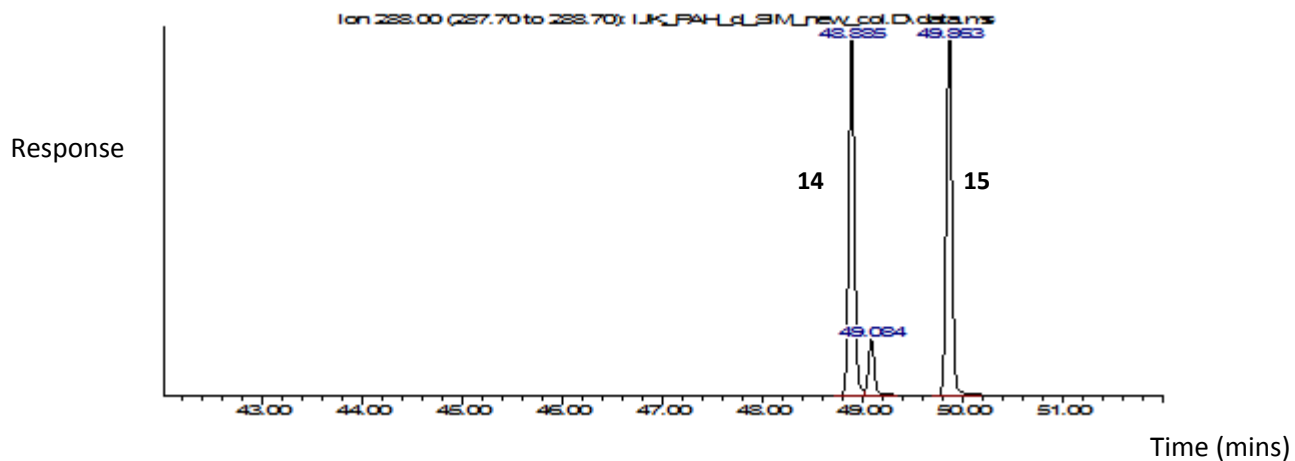


Figure C1i. GC-MS peaks for $M^+ = 288$ in the standard (upper) and sample extract (lower). 14 = IPy-d12, 15 = BPy-d12.

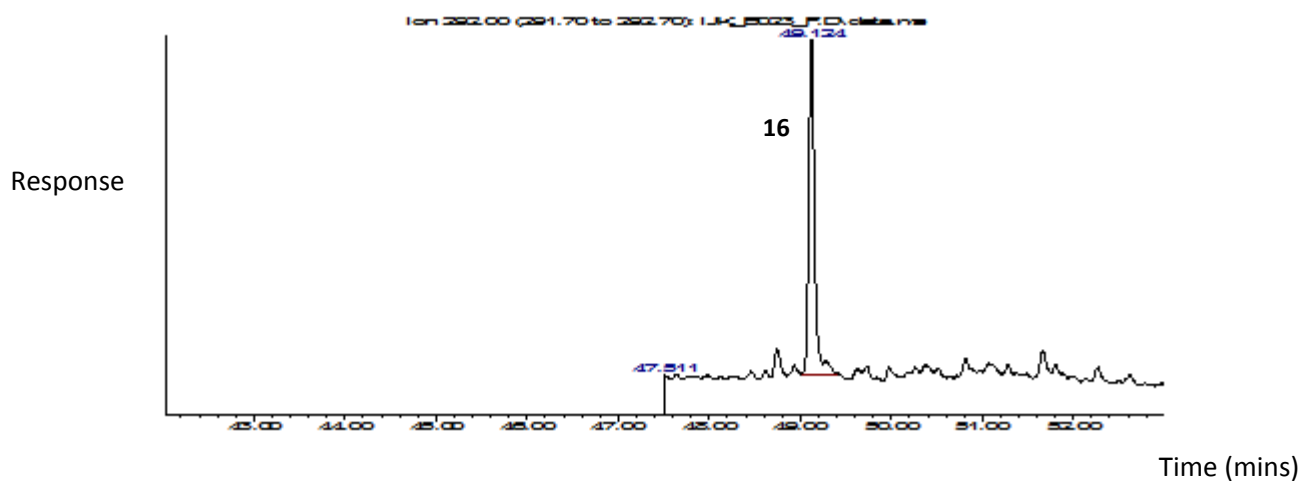
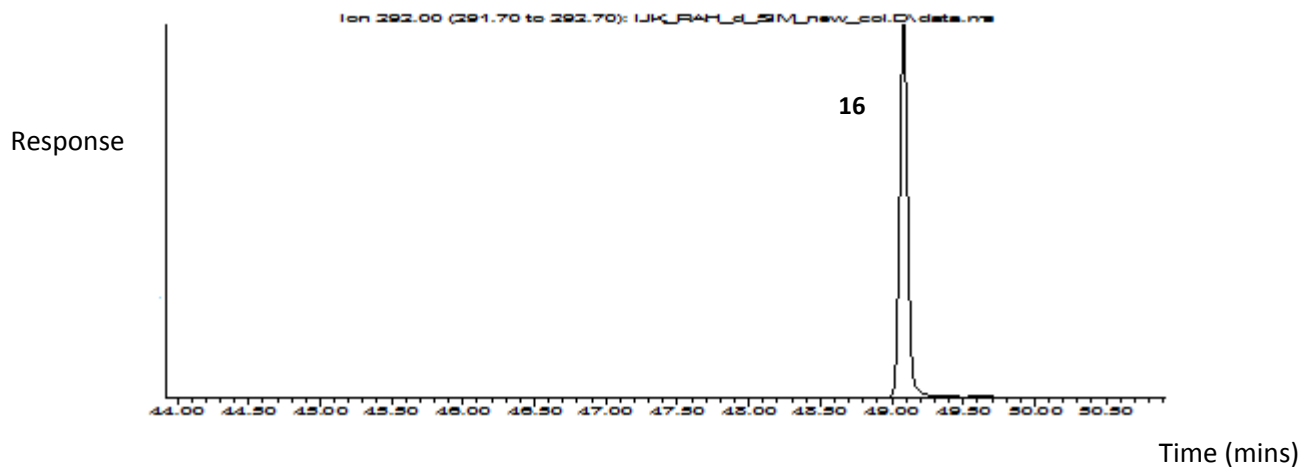


Figure C1j. GC-MS peaks for $M^+ = 292$ in the standard (upper) and sample extract (lower).
16 = DBA-d12.

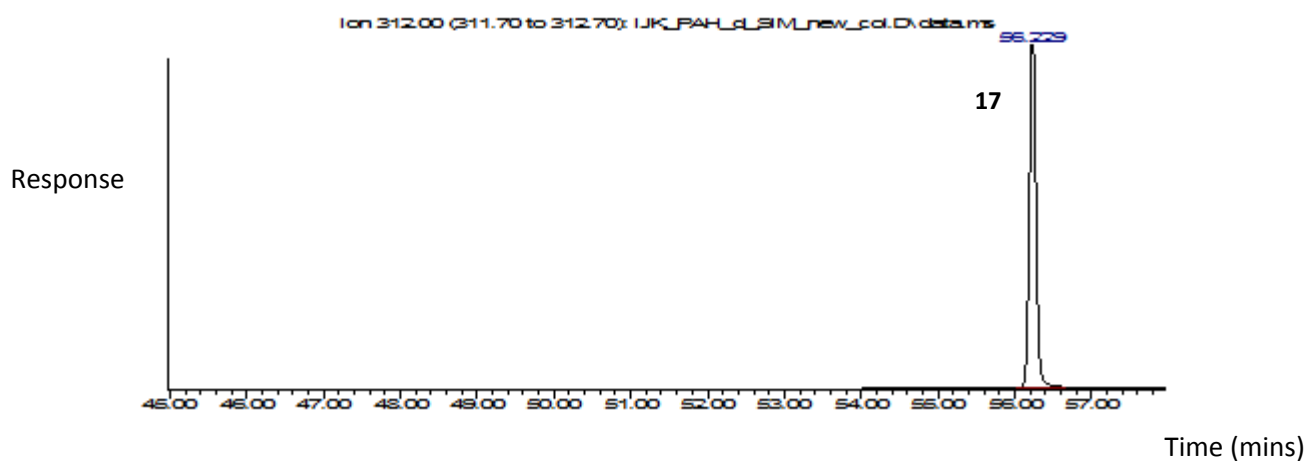
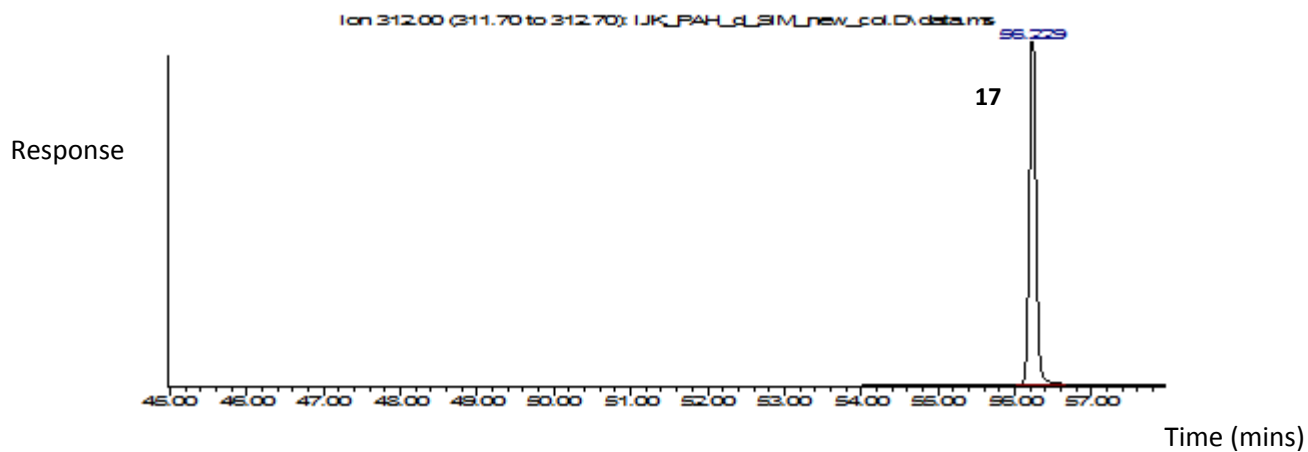


Figure C1k. GC-MS peaks for $M^+ = 312$ in the standard (upper) and sample extract (lower). 17 = Cor-d12.

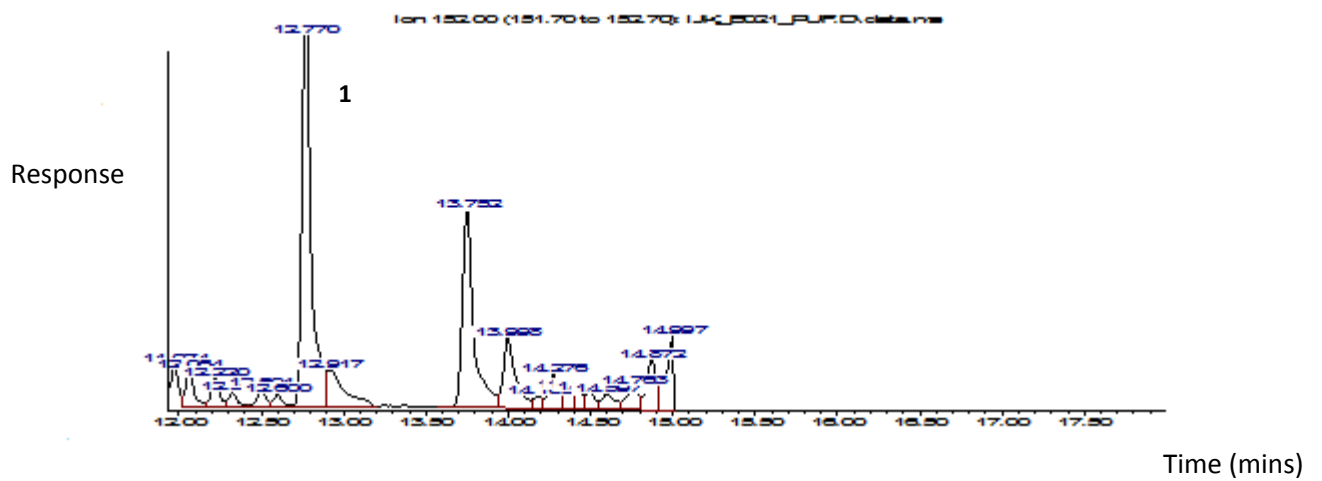
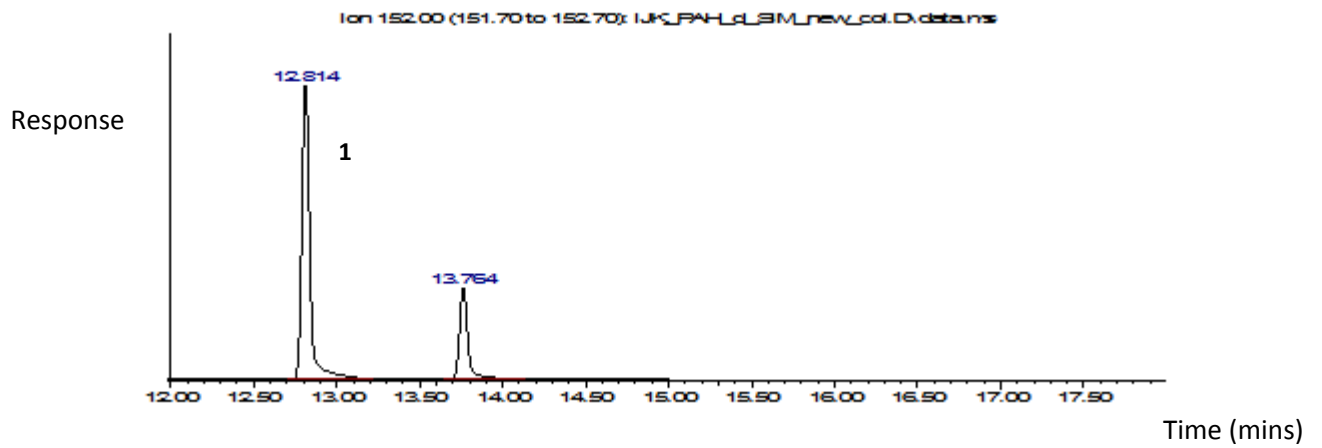


Figure C11. GC-MS peaks for $M^+ = 152$ in the standard (upper) and sample extract (lower). 1 = Ace.

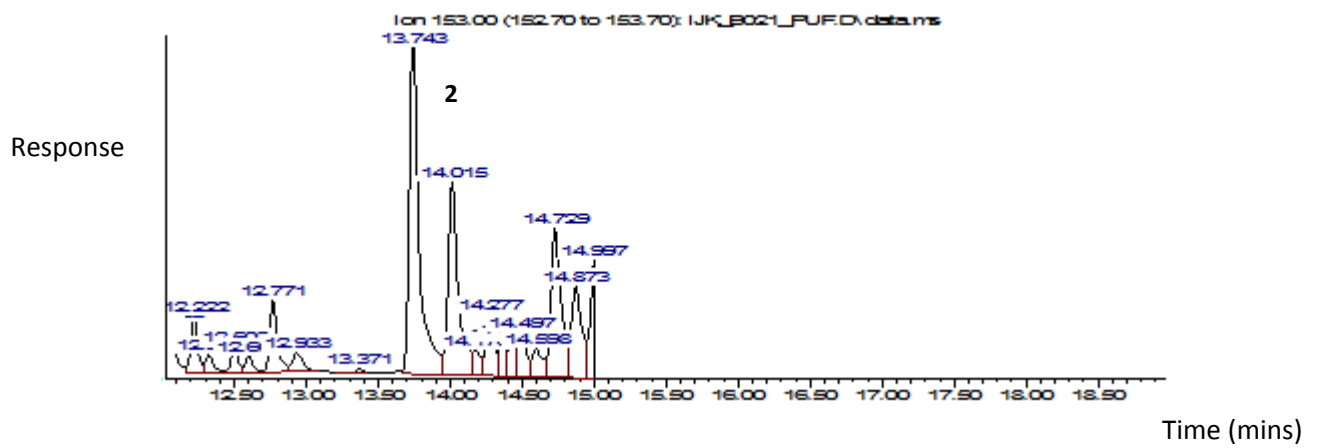
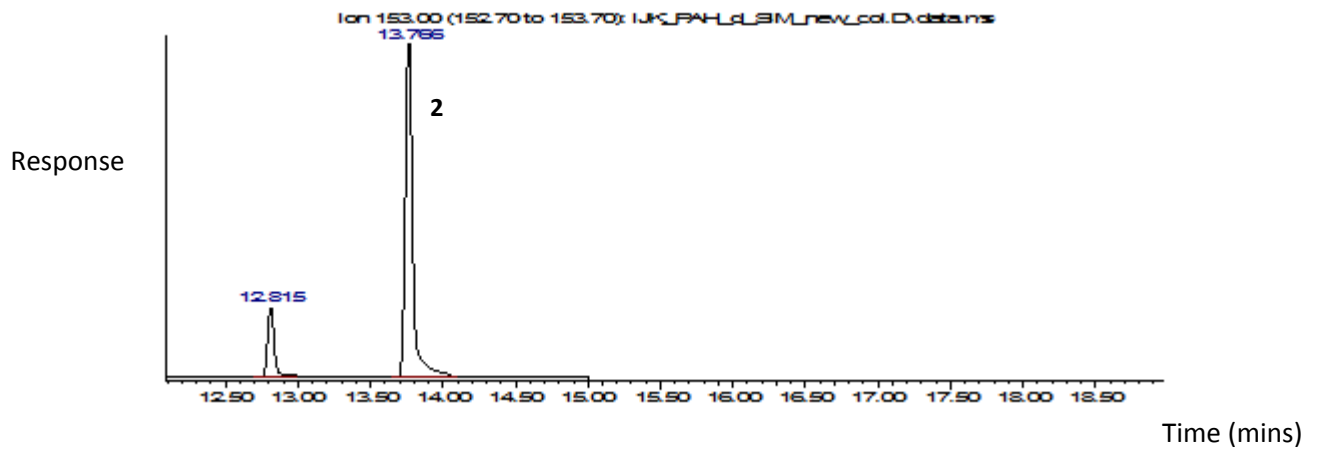


Figure C1m. GC-MS peaks for $M^+ = 153$ in the standard (upper) and sample extract (lower).
2 = Acy.

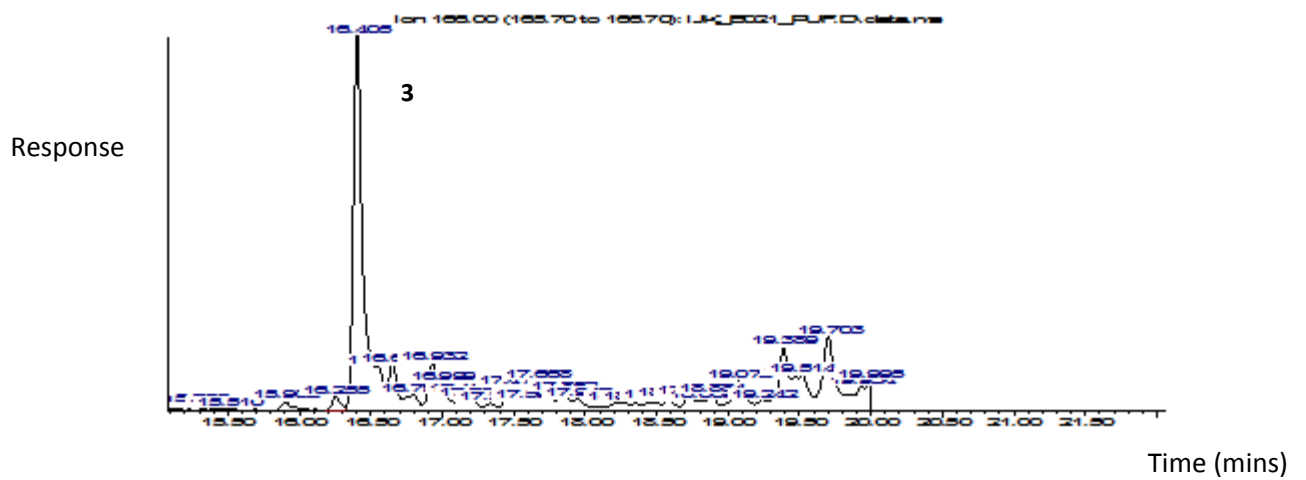
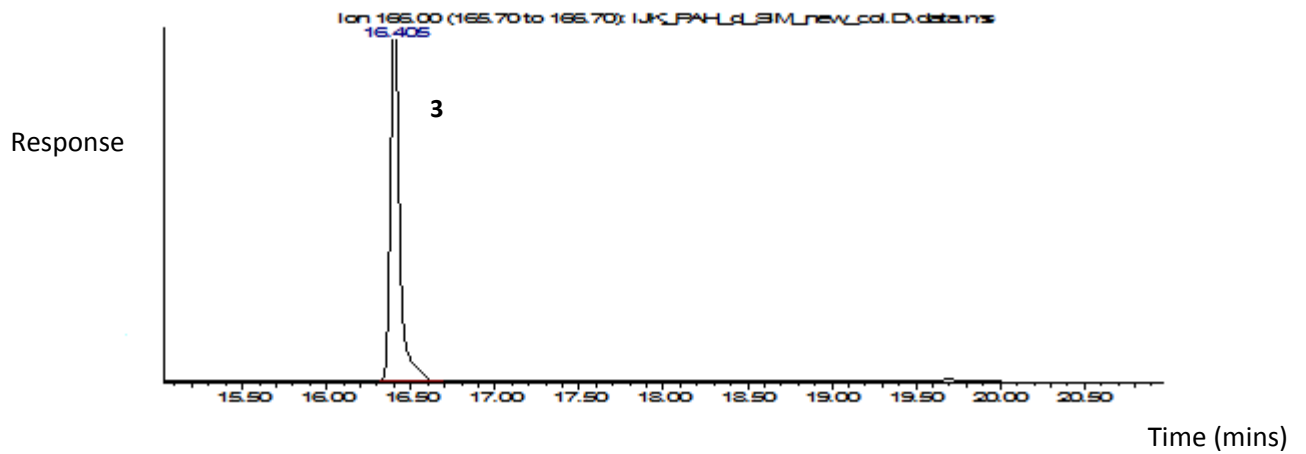


Figure C1n. GC-MS peaks for $M^+ = 166$ in the standard (upper) and sample extract (lower).
3 = Flo.

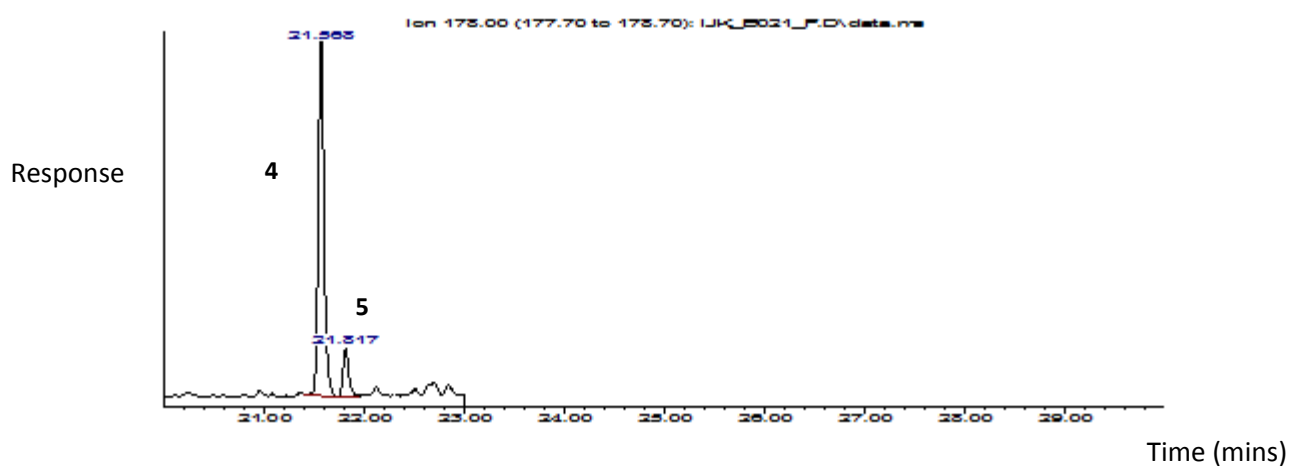
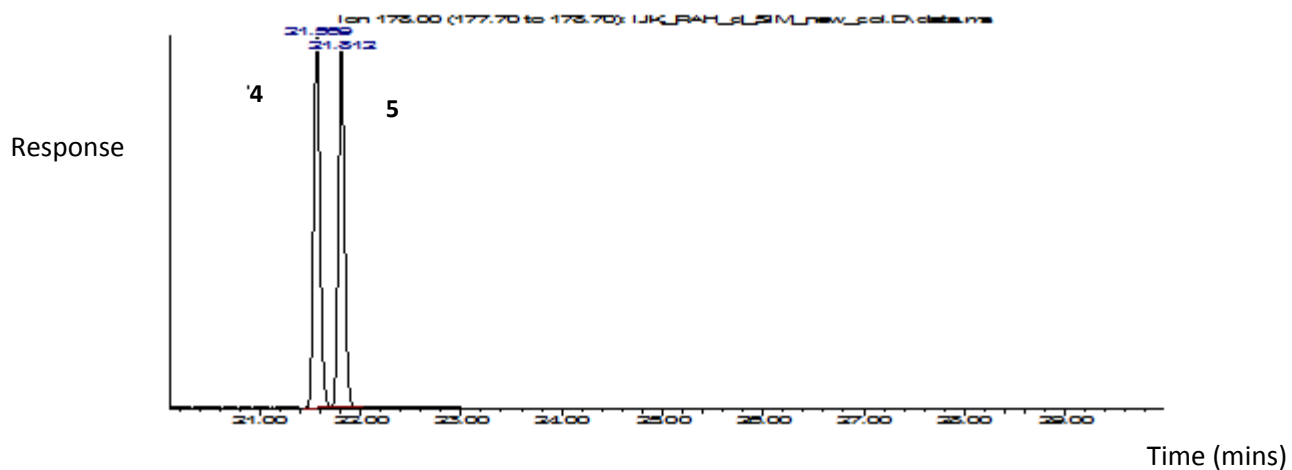


Figure C1o. GC-MS peaks for $M^+ = 178$ in the standard (upper) and sample extract (lower).
4 = Phe, 5 = Ant.

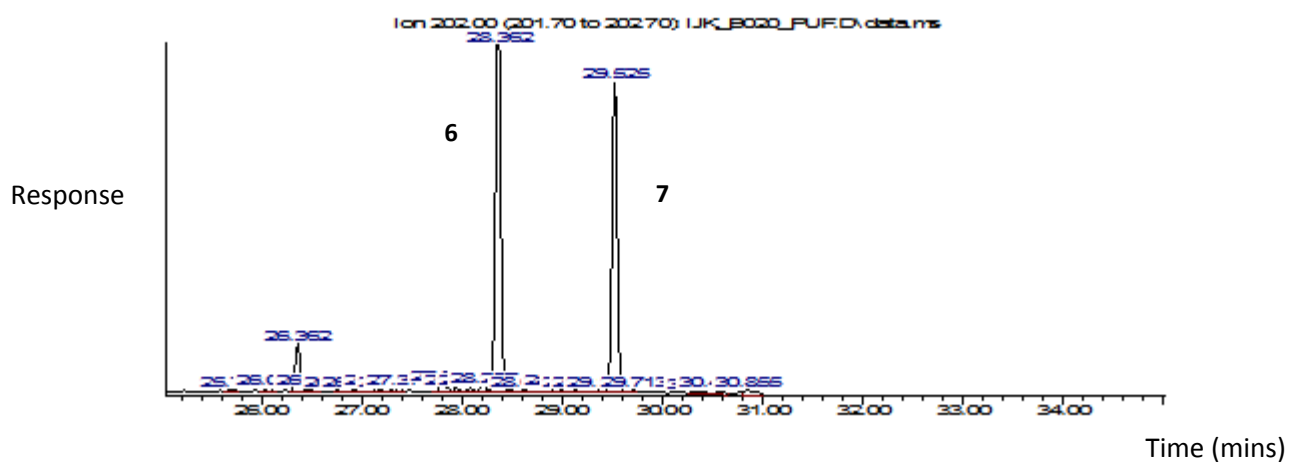
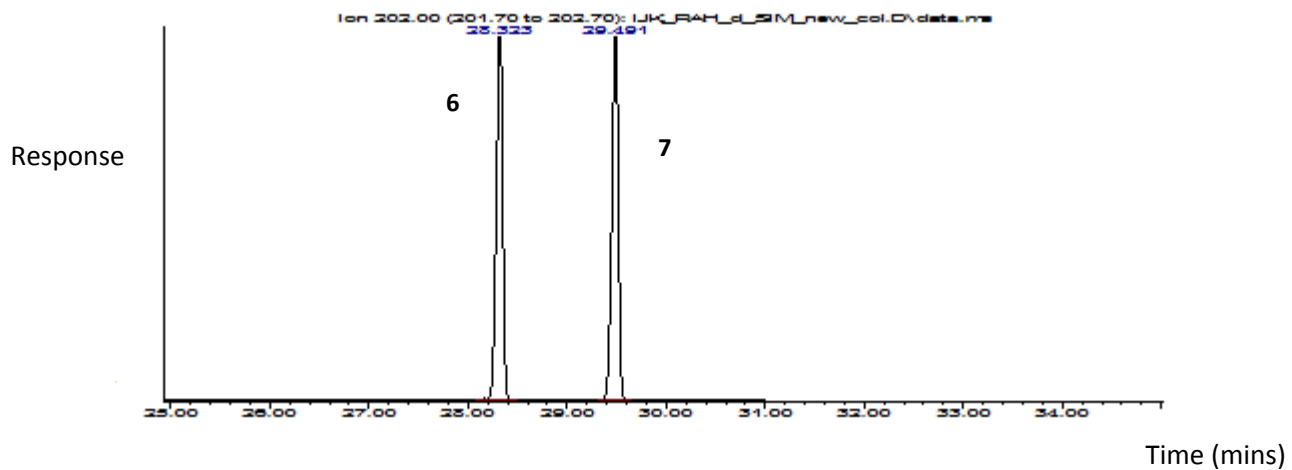


Figure C1p. GC-MS peaks for $M^+ = 202$ in the standard (upper) and sample extract (lower).
6 = Flt, 7 = Pyr.

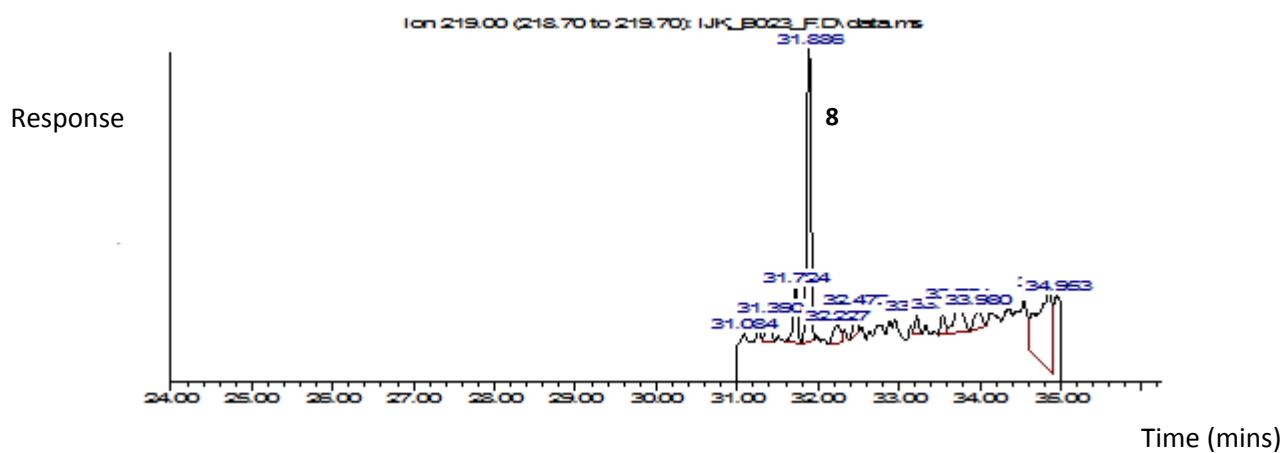
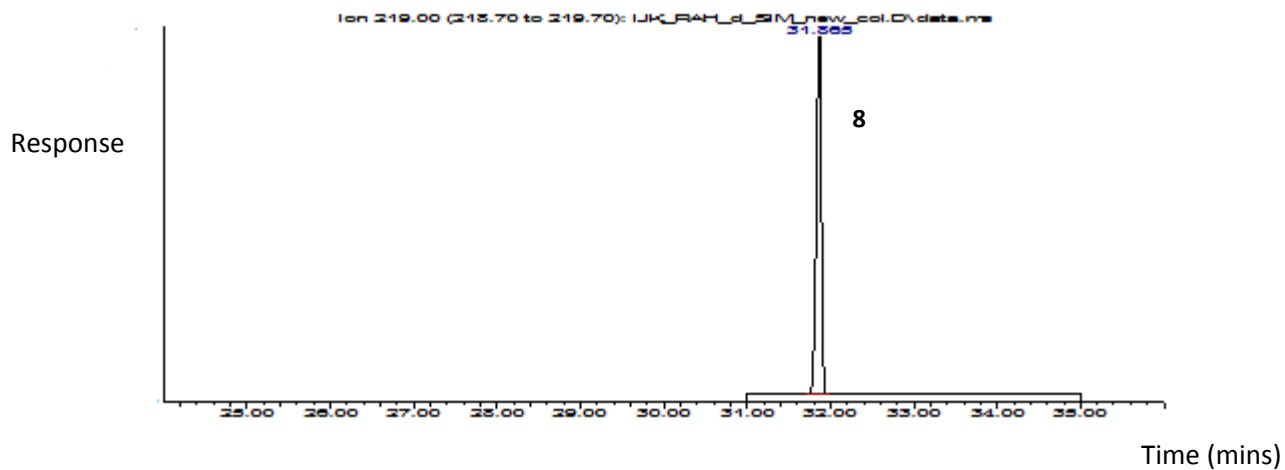


Figure C1q. GC-MS peaks for $M^+ = 219$ in the standard (upper) and sample extract (lower).
8 = Ret.

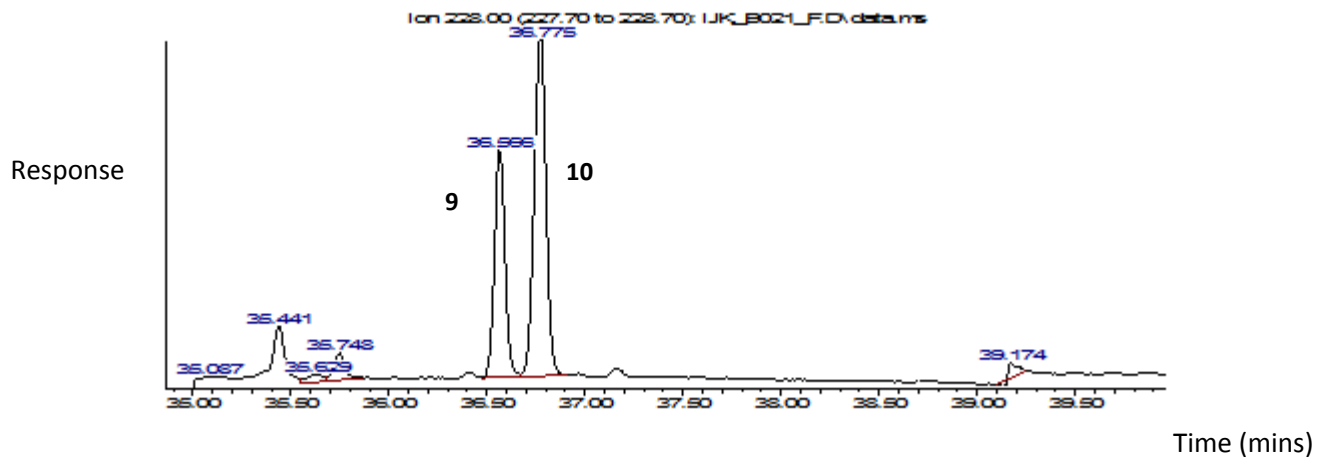
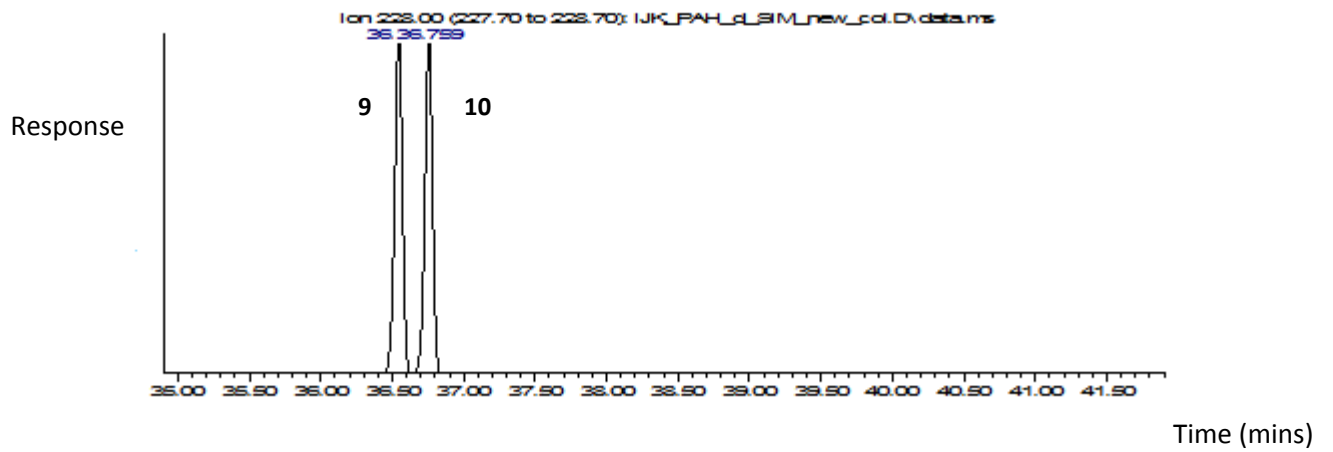


Figure C1r. GC-MS peaks for $M^+ = 228$ in the standard (upper) and sample extract (lower). 9 = BaA, 10 = Chr.

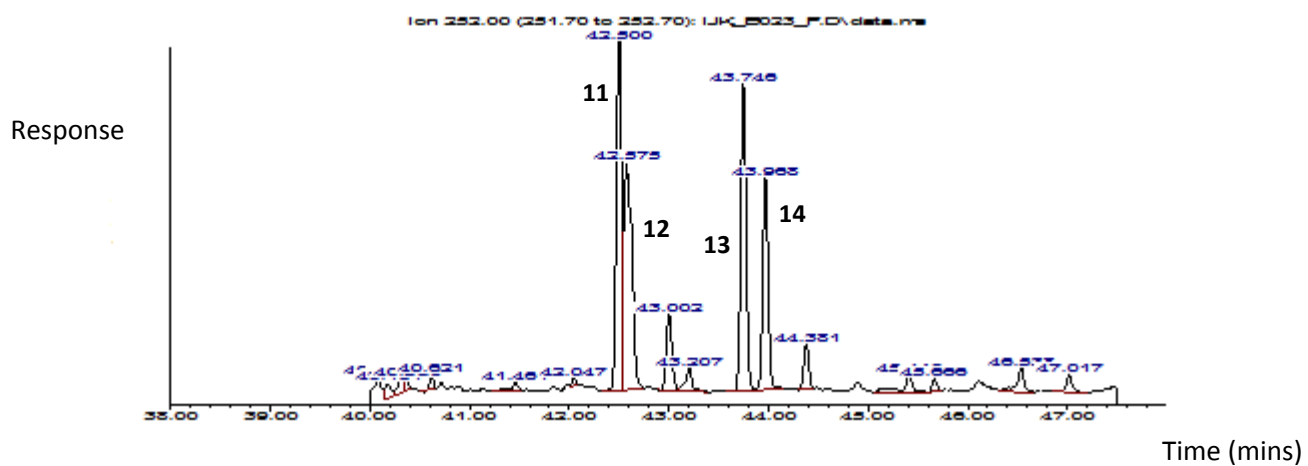
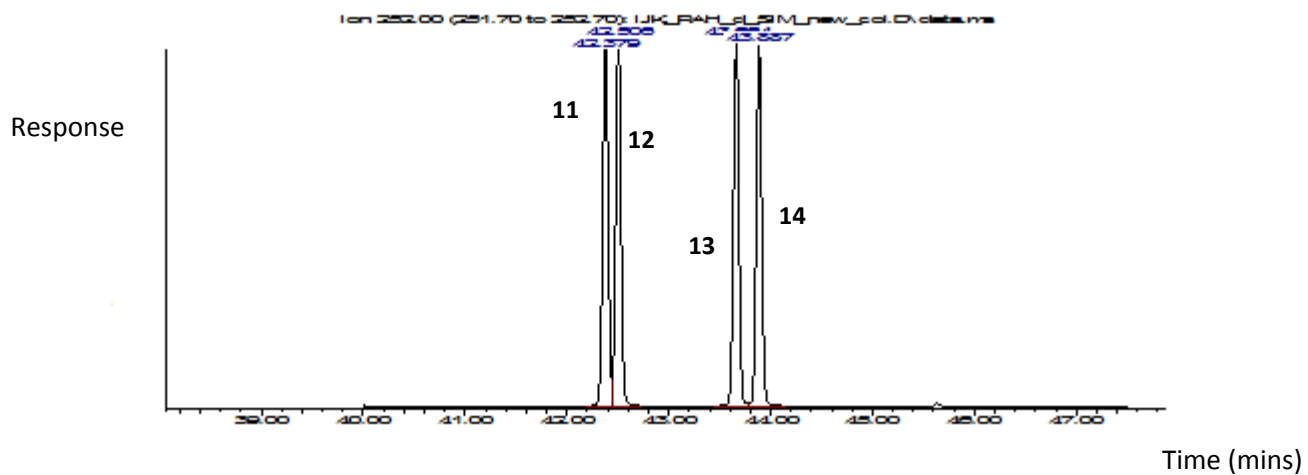


Figure C1s. GC-MS peaks for $M^+ = 252$ in the standard (upper) and sample extract (lower).
 11 = BbF, 12 = BkF, 13=BeP. 14=BaP.

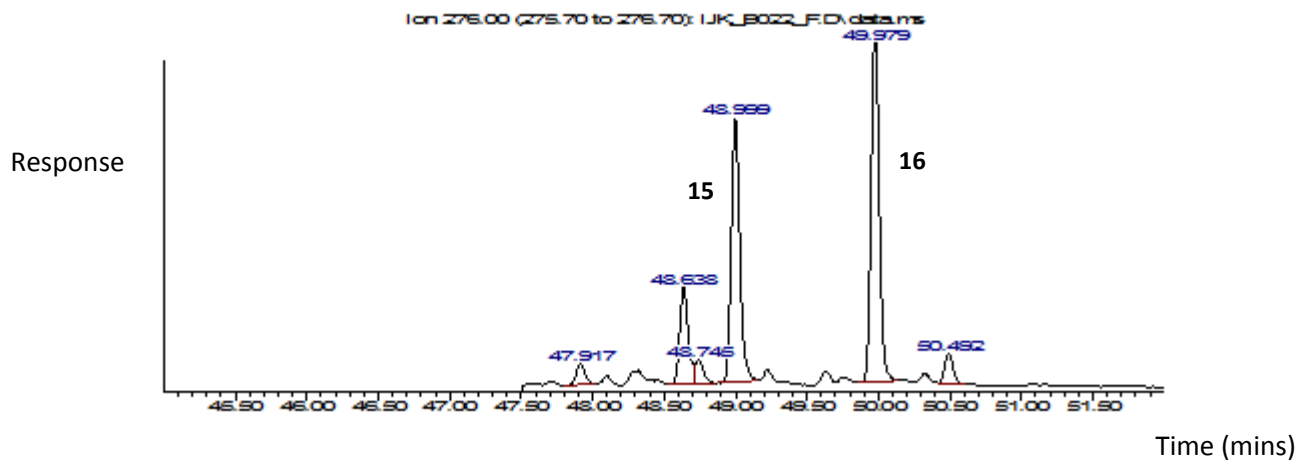
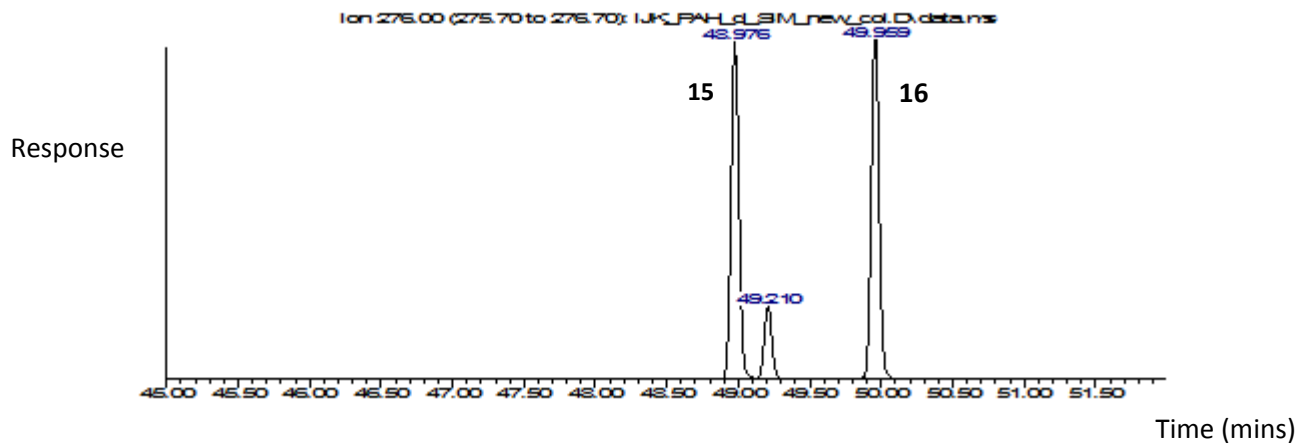


Figure C1t. GC-MS peaks for $M^+ = 276$ in the standard (upper) and sample extract (lower).
15 = IPy, 16 = BPy.

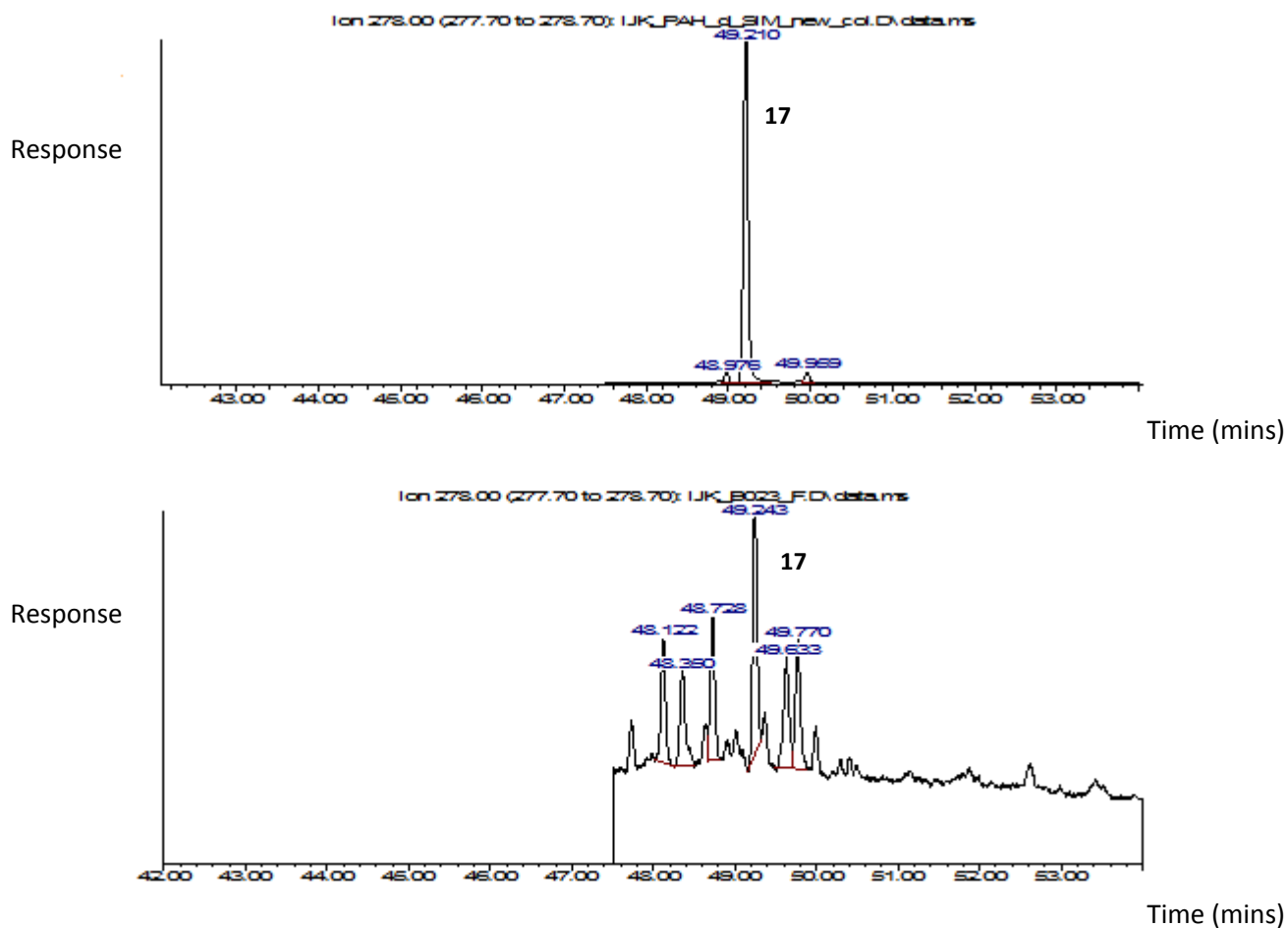


Figure C1u. GC-MS peaks for $M^+ = 278$ in the standard (upper) and sample extract (lower).
17 = DBA.

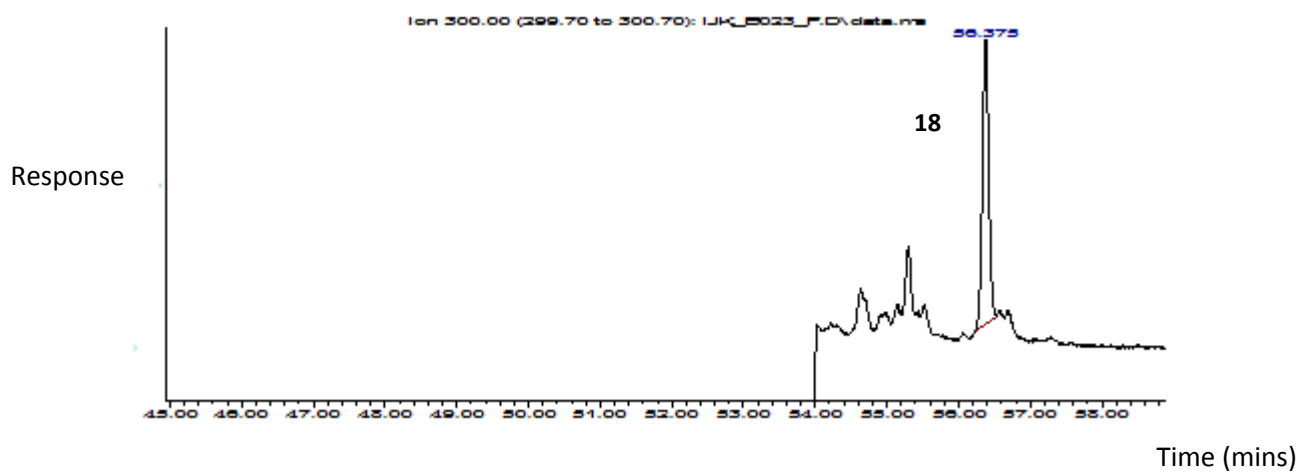
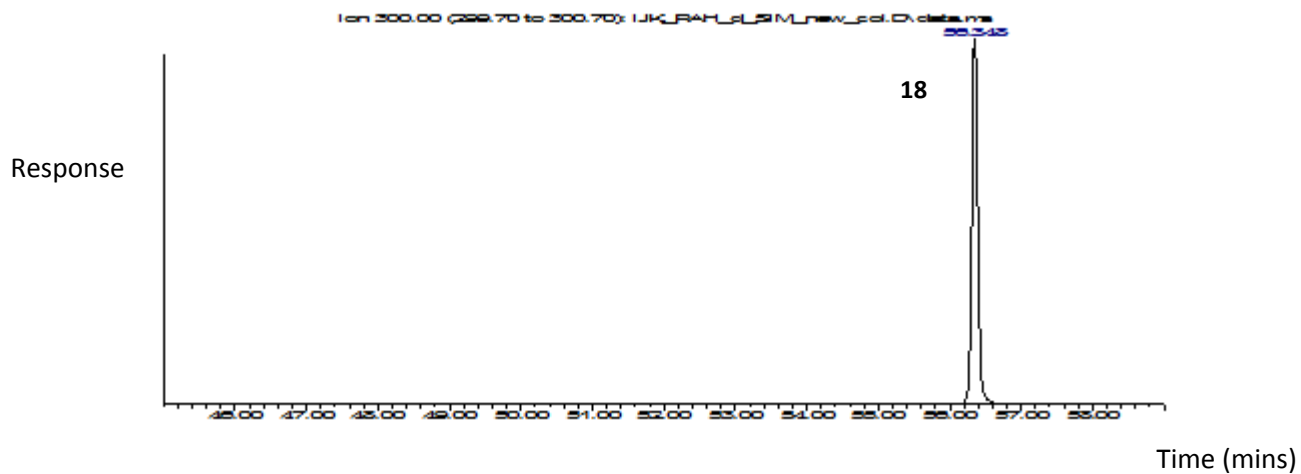


Figure C1v. GC-MS peaks for $M^+ = 300$ in the standard (upper) and sample extract (lower).
18 = Cor.

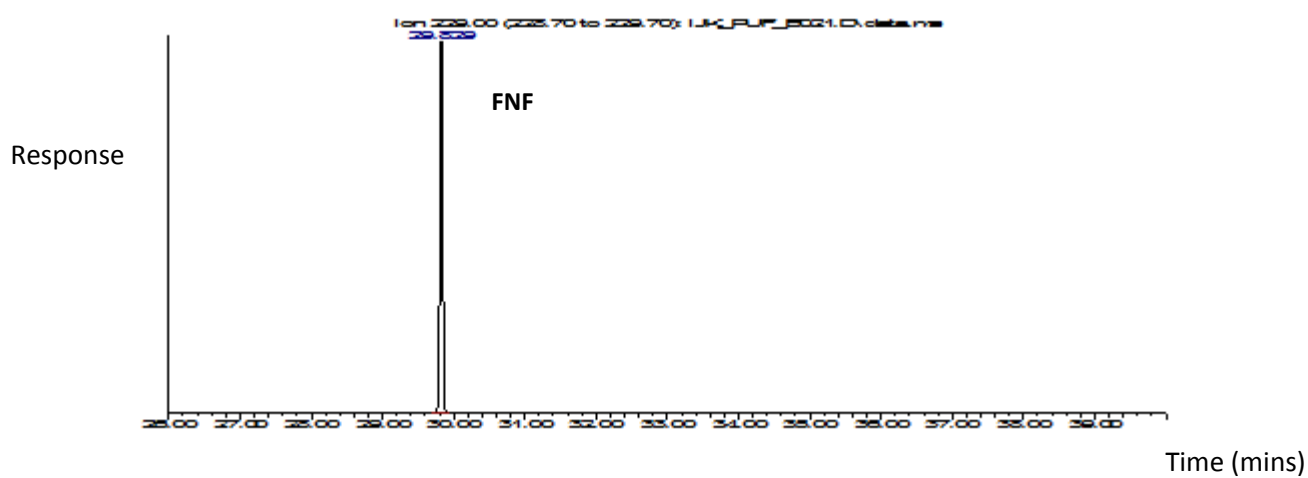
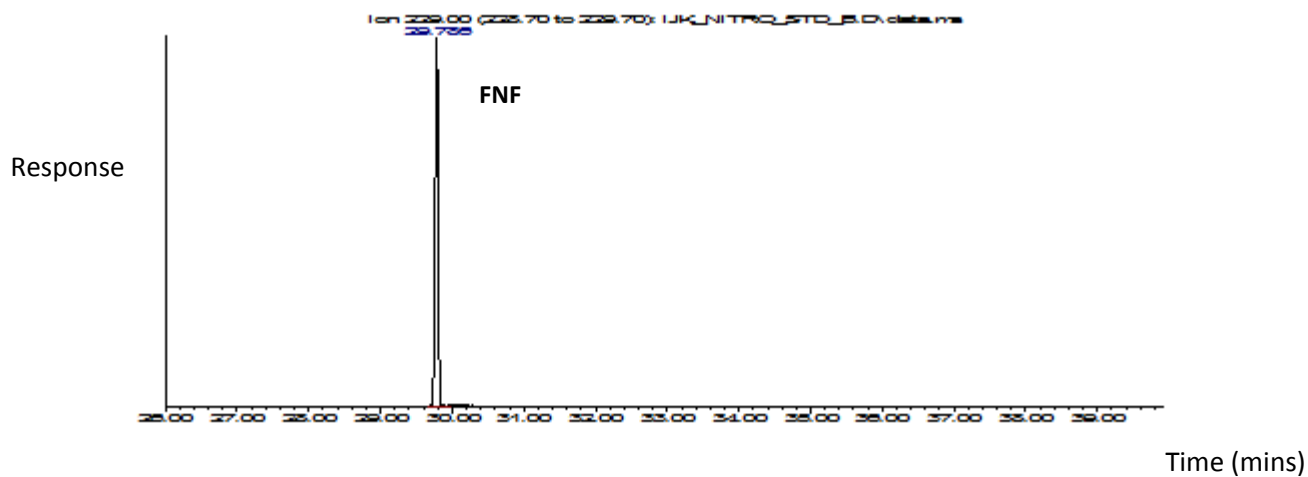


Figure C2a. GC-MS peaks for recovery standard FNN ($M^+ = 229$) observed in the standard (upper) and sample extract (lower).

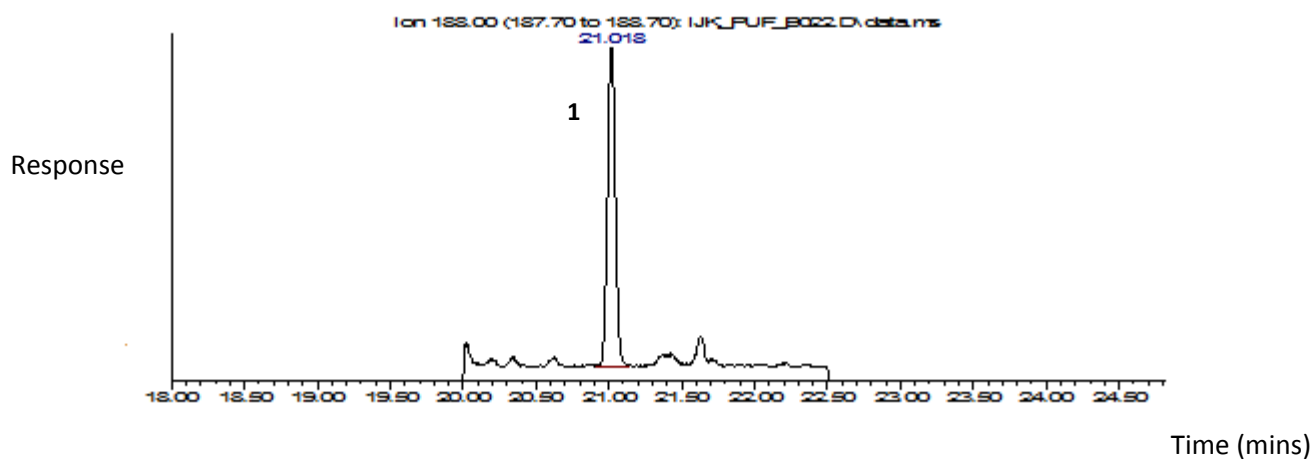
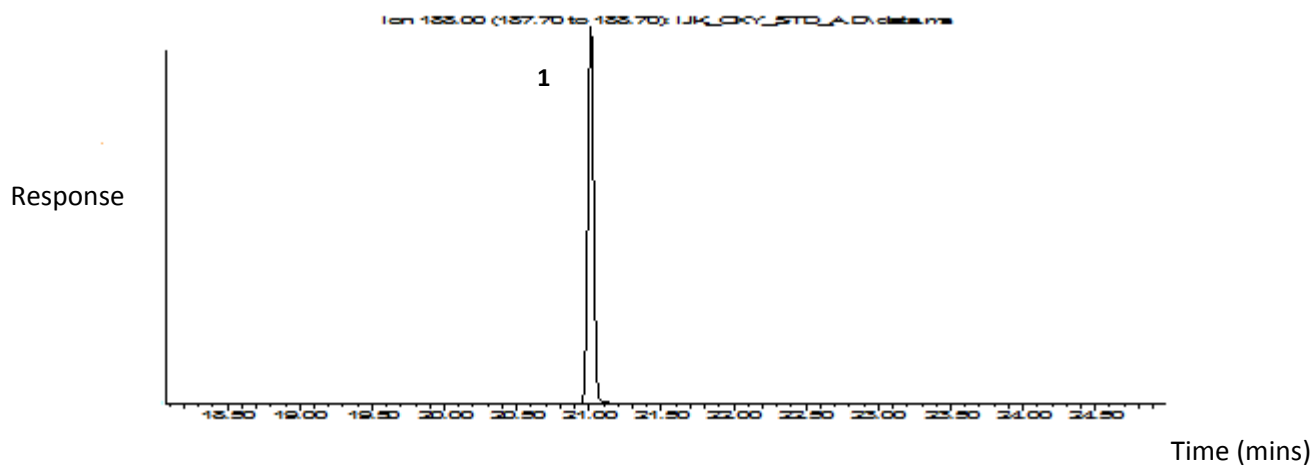


Figure C2b. GC-MS peaks for $M^+ = 188$ in the standard (upper) and sample extract (lower). 1= 9F-d8.

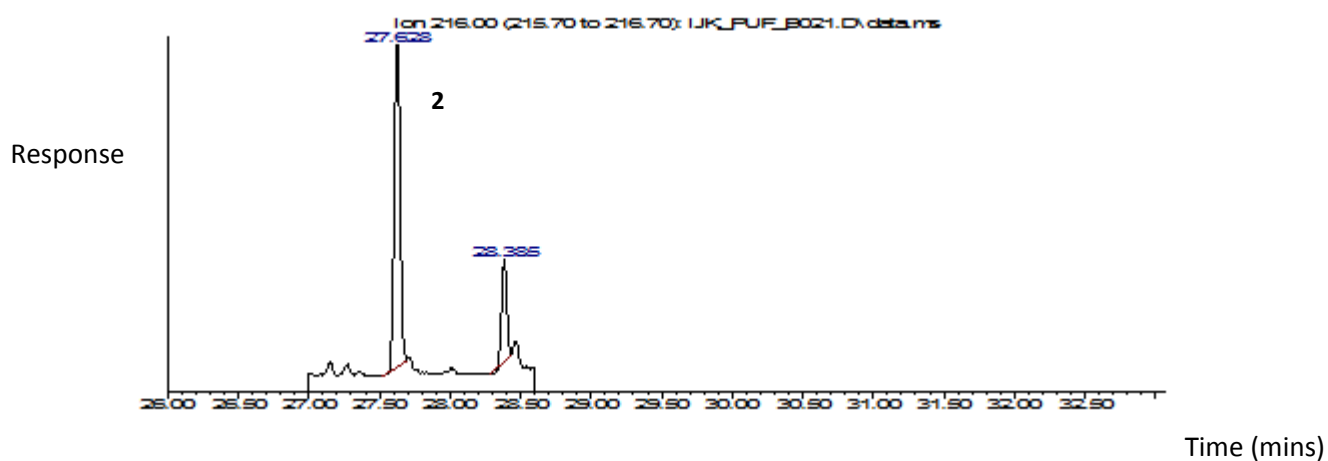
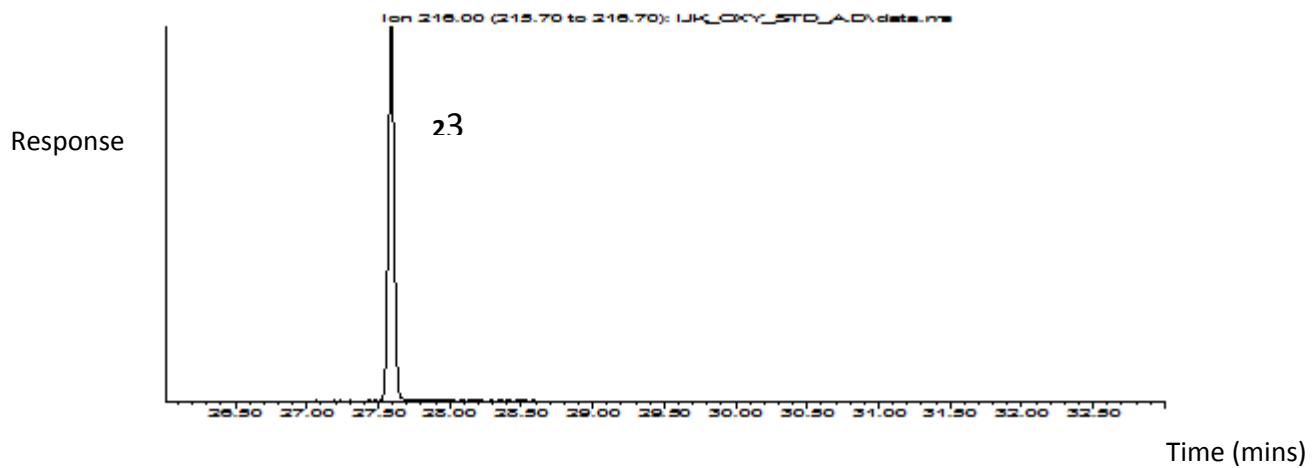


Figure C2c. GC-MS peaks for $M^- = 216$ in the standard (upper) and sample extract (lower).

2= AQ-d8.

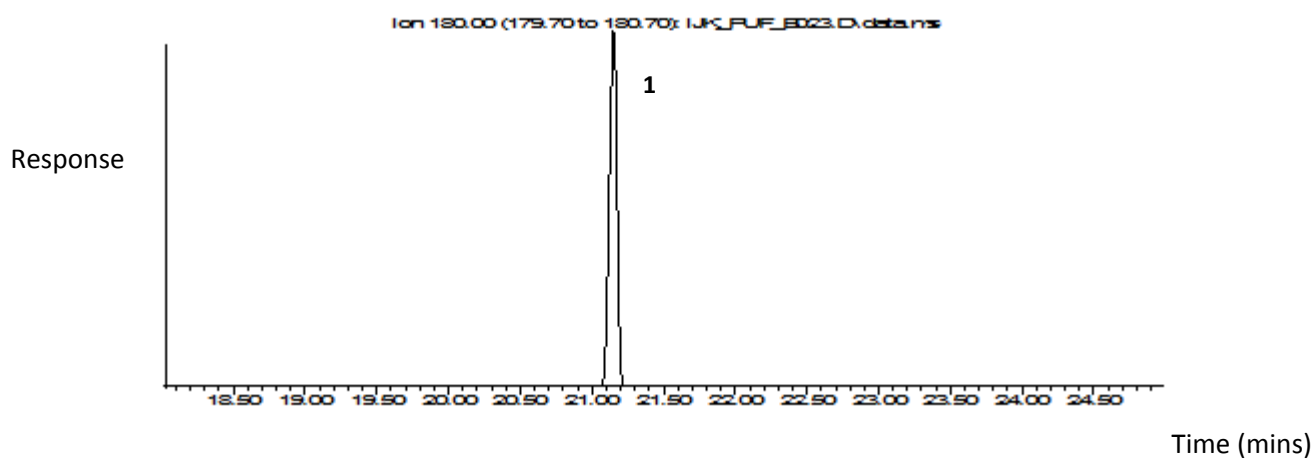
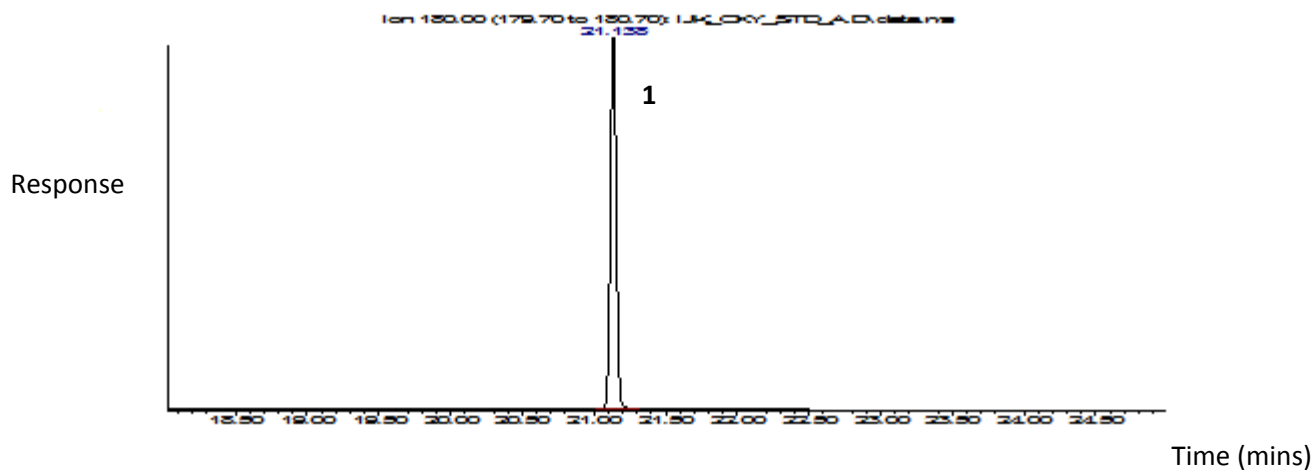


Figure C2d. GC-MS peaks for $M^+ = 180$ in the standard (upper) and sample extract (lower).

1= 9F.

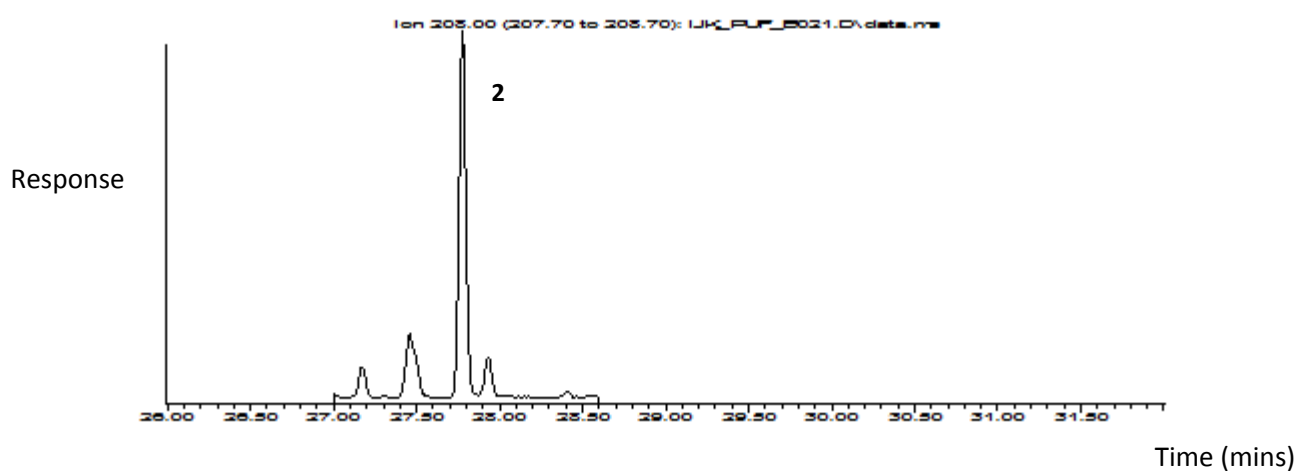
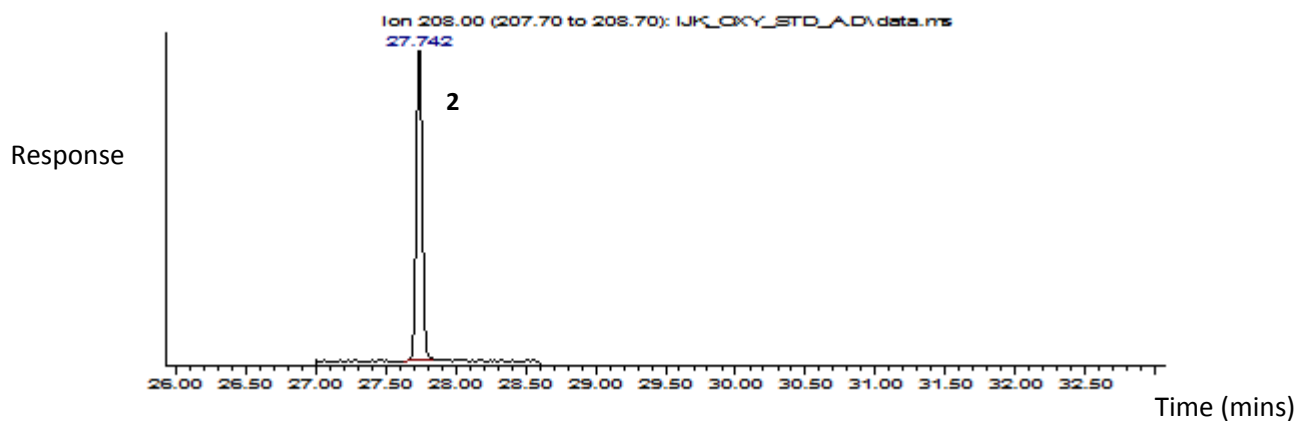


Figure C2e. GC-MS peaks for $M^+ = 208$ in the standard (upper) and sample extract (lower).
2= AQ.

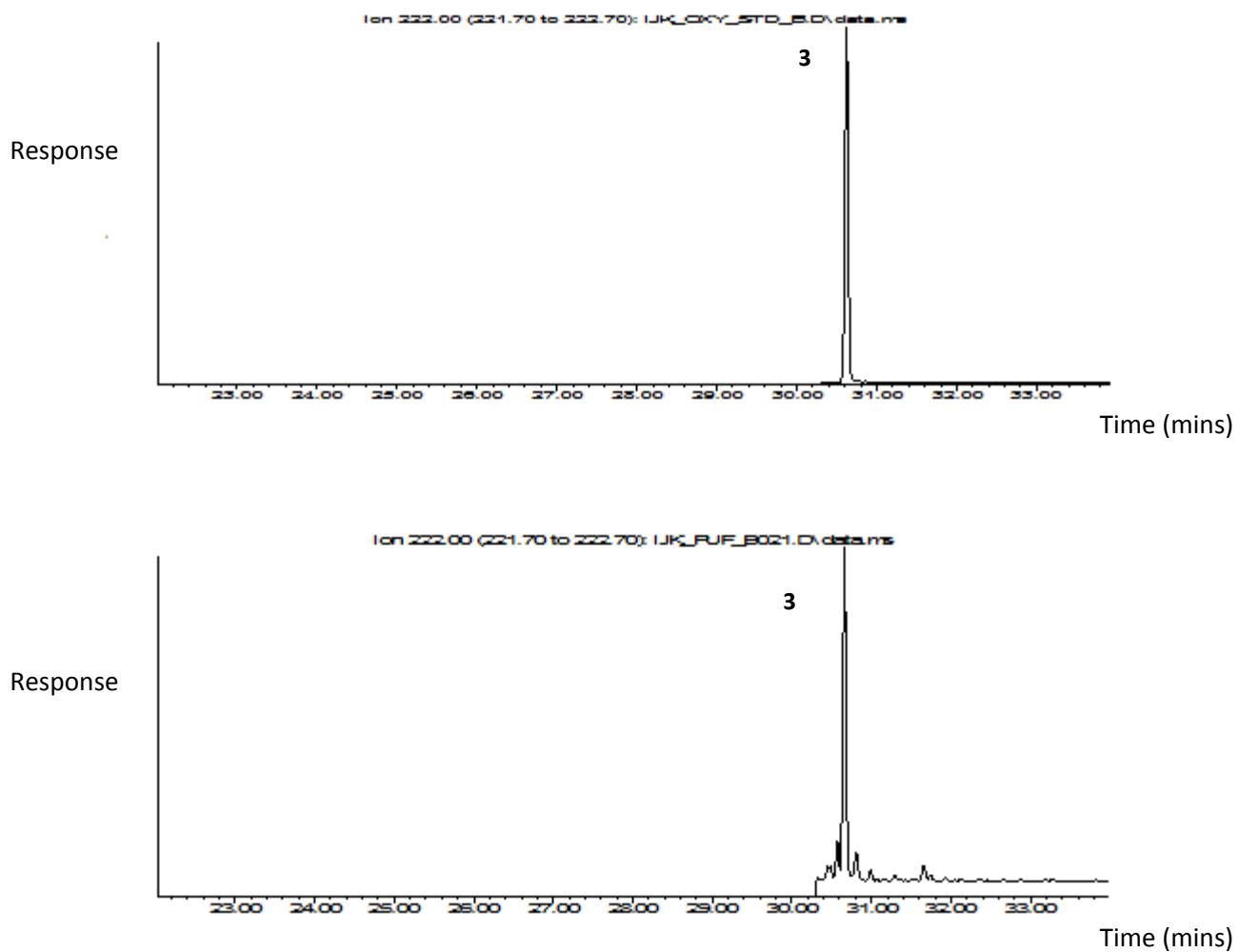


Figure C2f. GC-MS peaks for $M^- = 222$ in the standard (upper) and sample extract (lower).
2= MAQ.

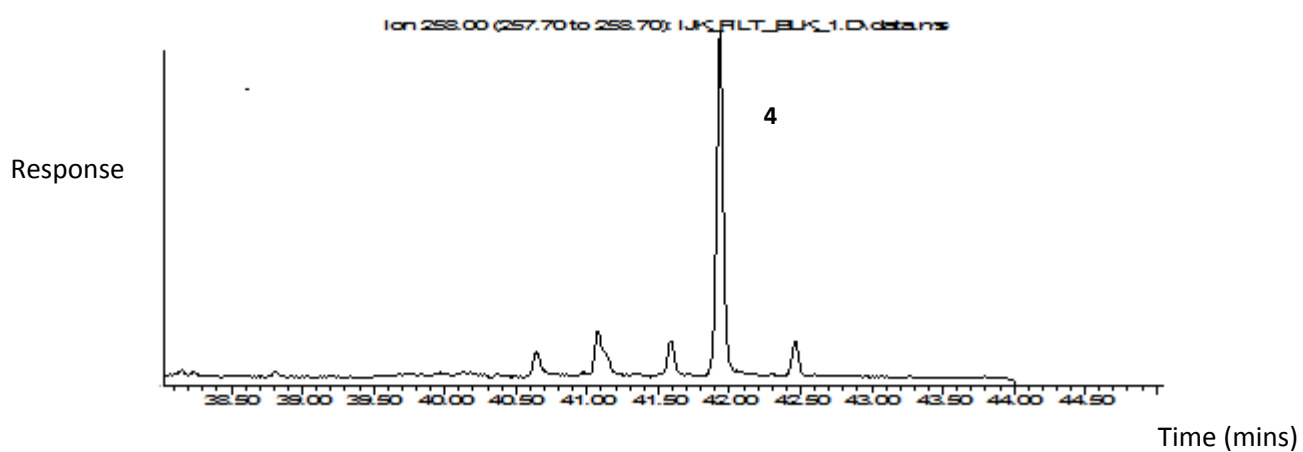
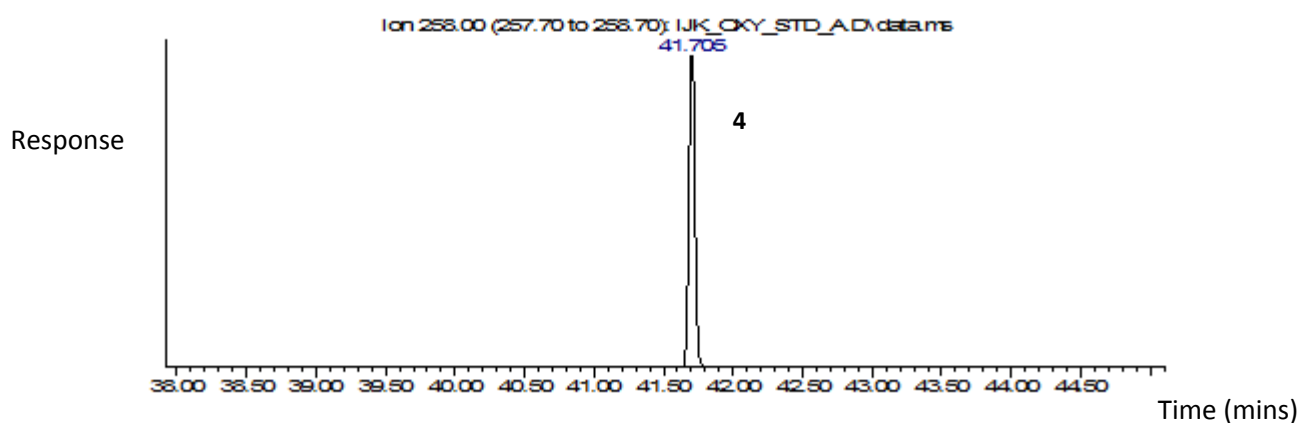


Figure C2g. GC-MS peaks for $M^+ = 258$ in the standard (upper) and sample extract (lower).

4= BaAQ.

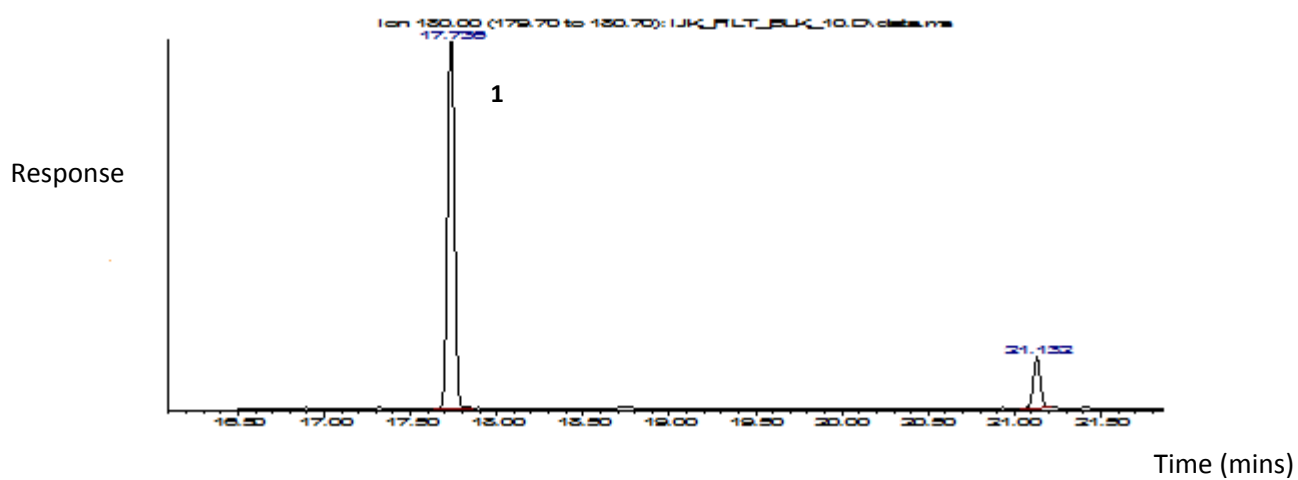
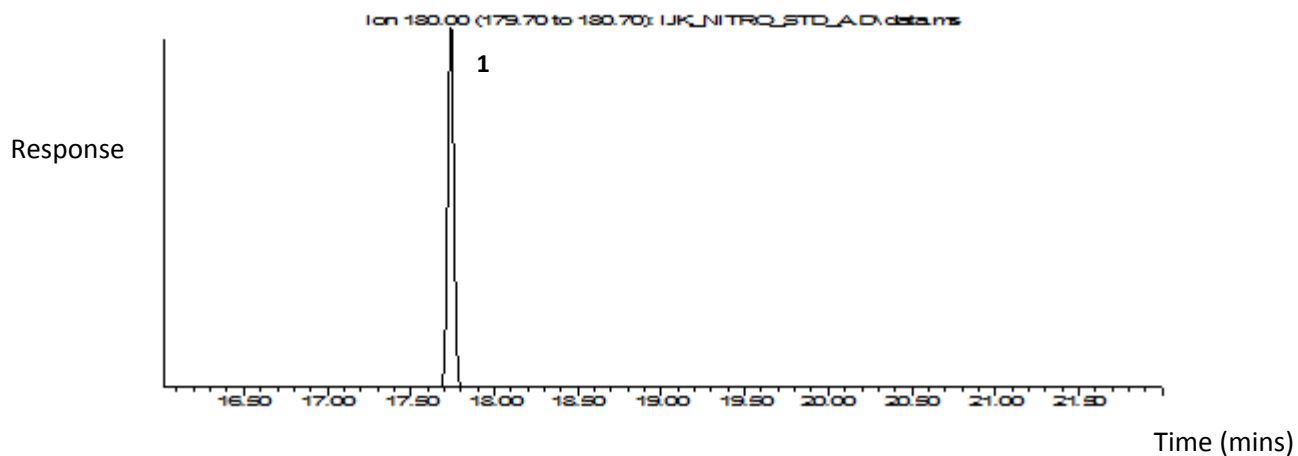


Figure C2h. GC-MS peaks for $M^- = 180$ in the standard (upper) and sample extract (lower).

1 = 1NNap-d7.

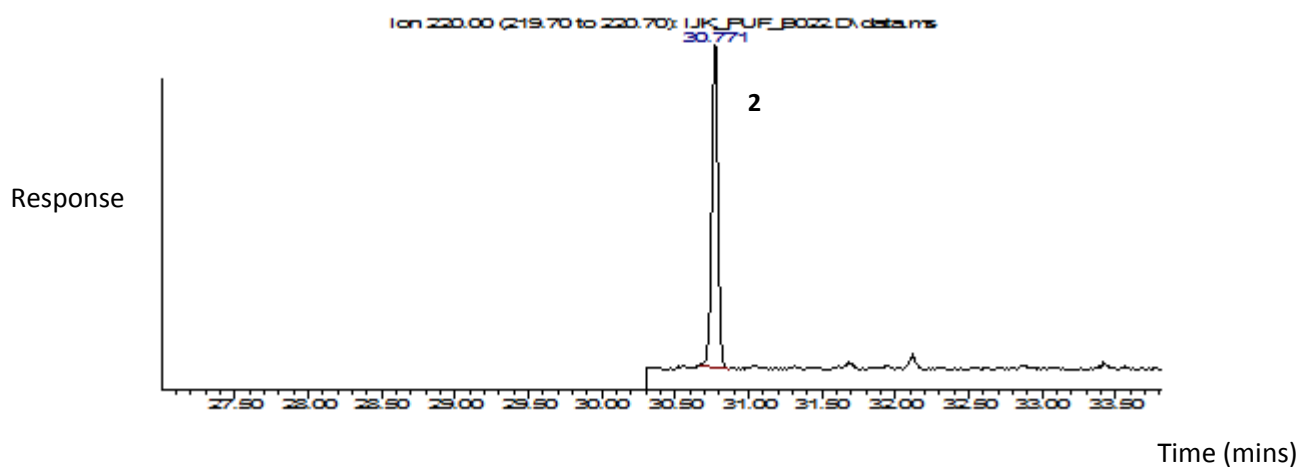
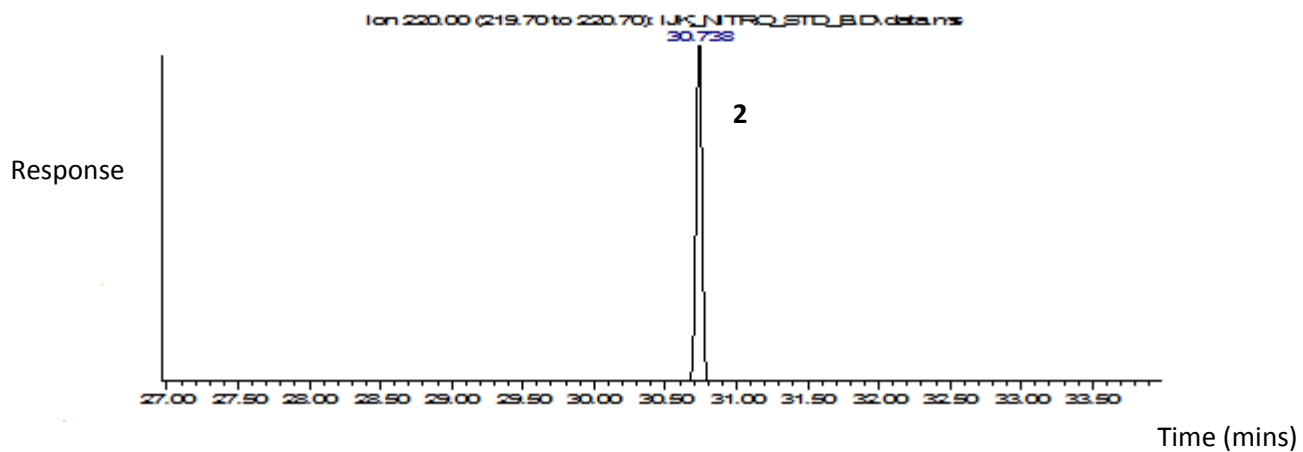


Figure C2i. GC-MS peaks for $M^+ = 220$ in the standard (upper) and sample extract (lower).
2= 2NFlo-d8.

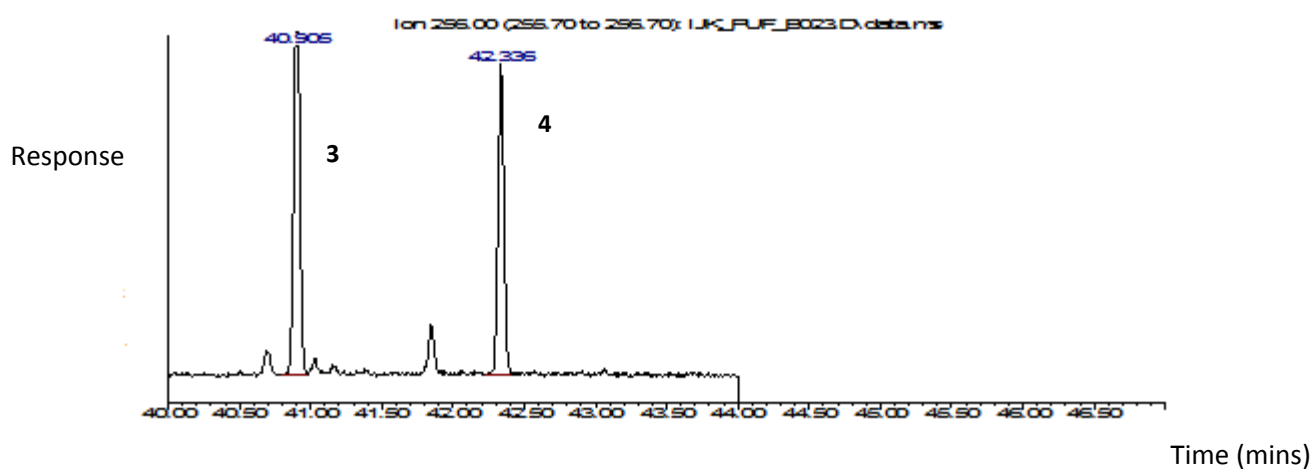
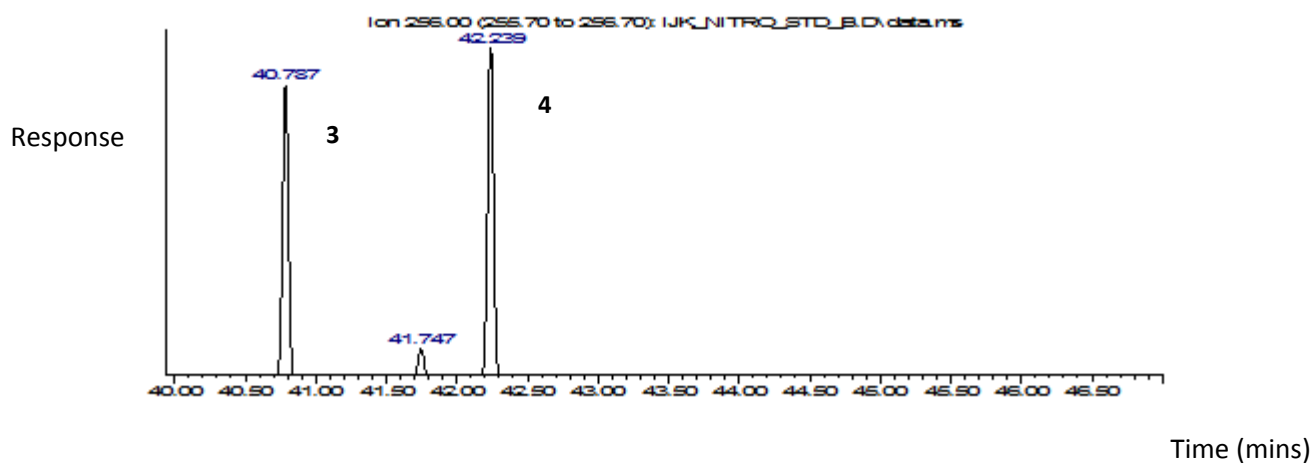


Figure C2j. GC-MS peaks for $M^+ = 256$ in the standard (upper) and sample extract (lower). 3 = 3NFIt-d6, 4 = 1NPyr-d9.

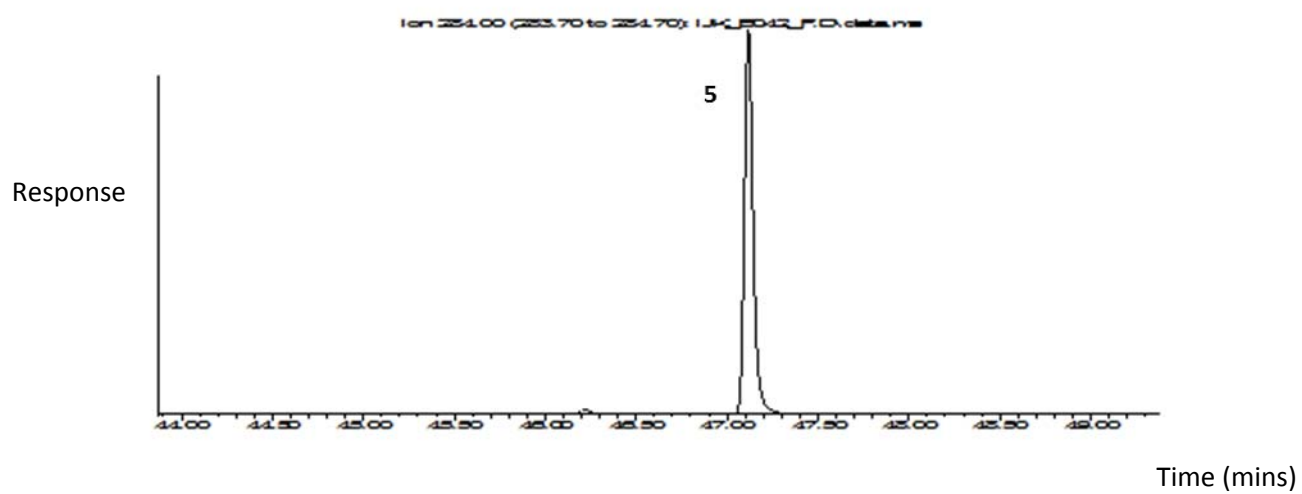
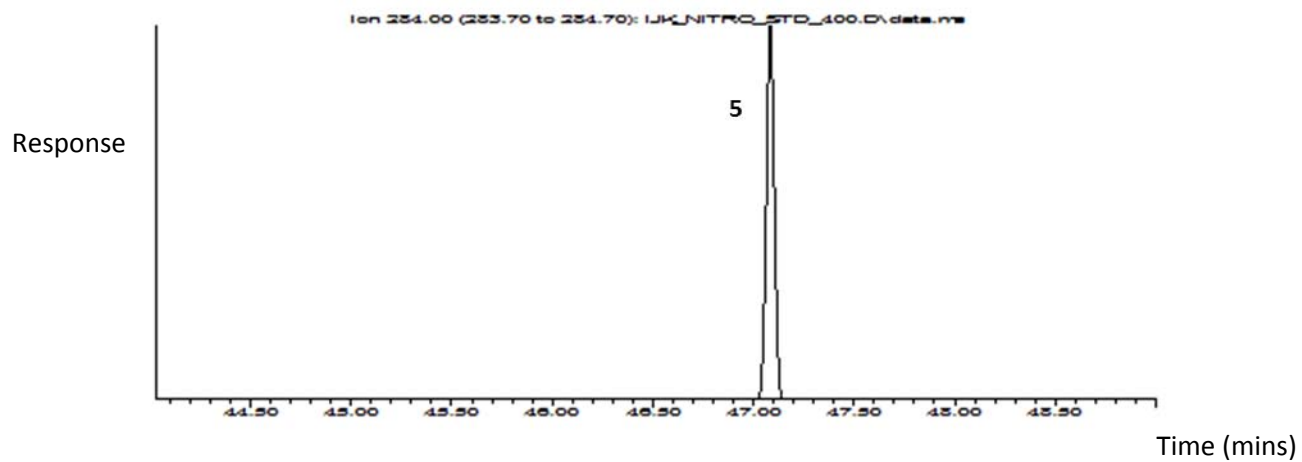


Figure C2k. GC-MS peaks for $M^+ = 284$ in the standard (upper) and sample extract (lower). 5 = 6NChr-d11.

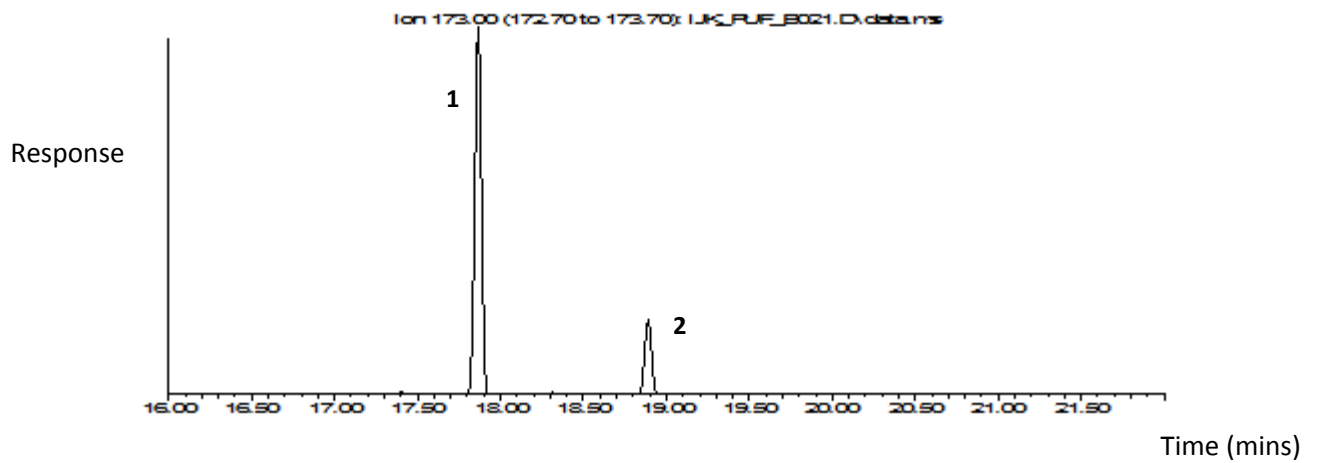
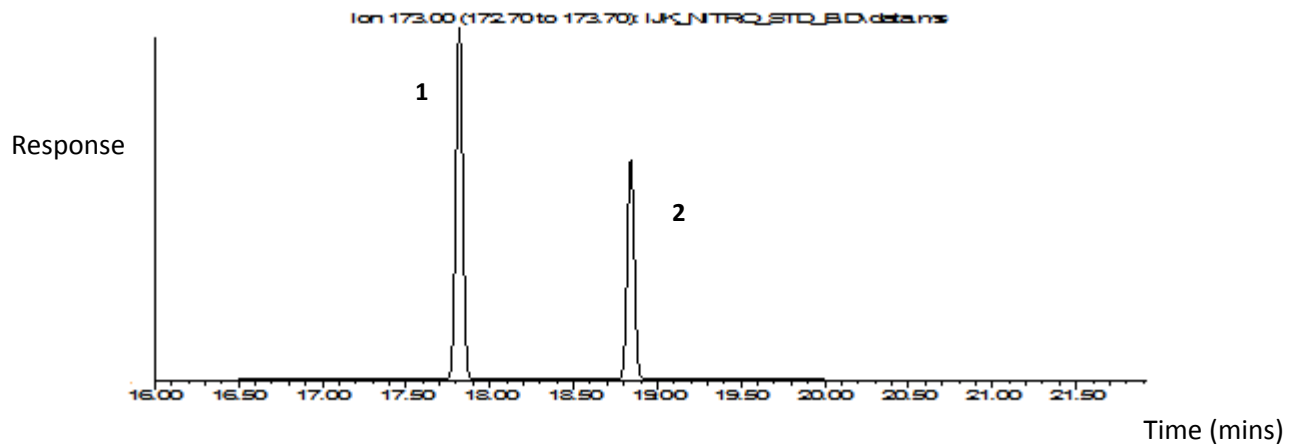


Figure C2I. GC-MS peaks for $M^+ = 173$ in the standard (upper) and sample extract (lower).

1= 1Nnap, 2= 2Nnap.

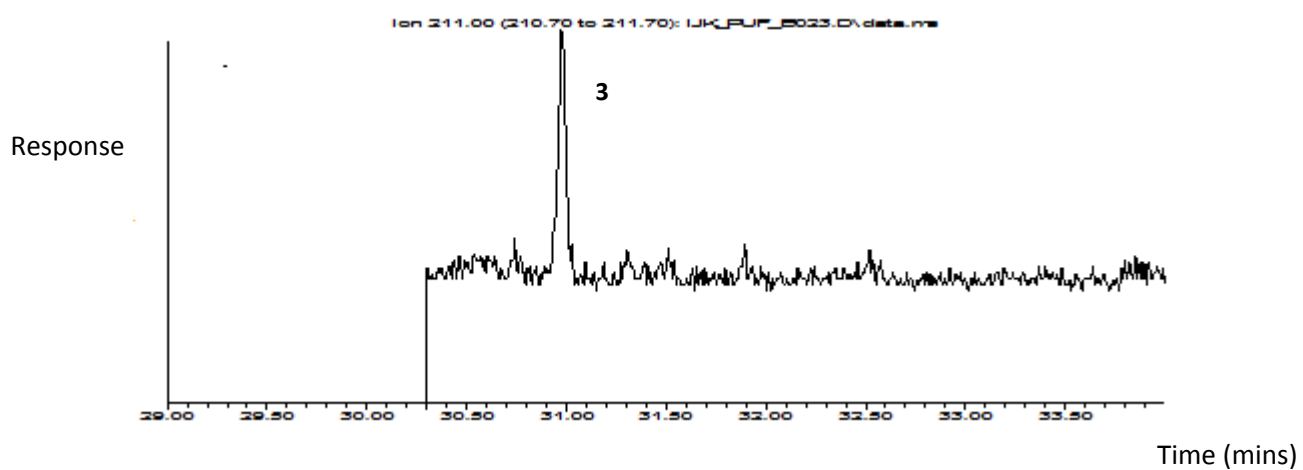
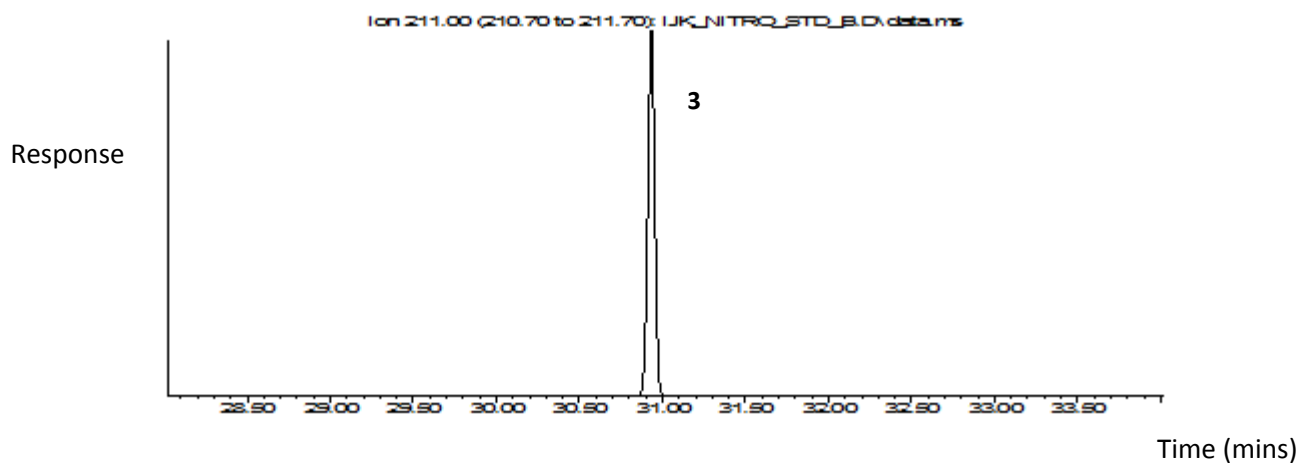


Figure C2m. GC-MS peaks for $M^+ = 211$ in the standard (upper) and sample extract (lower).

3= 2NFlo..

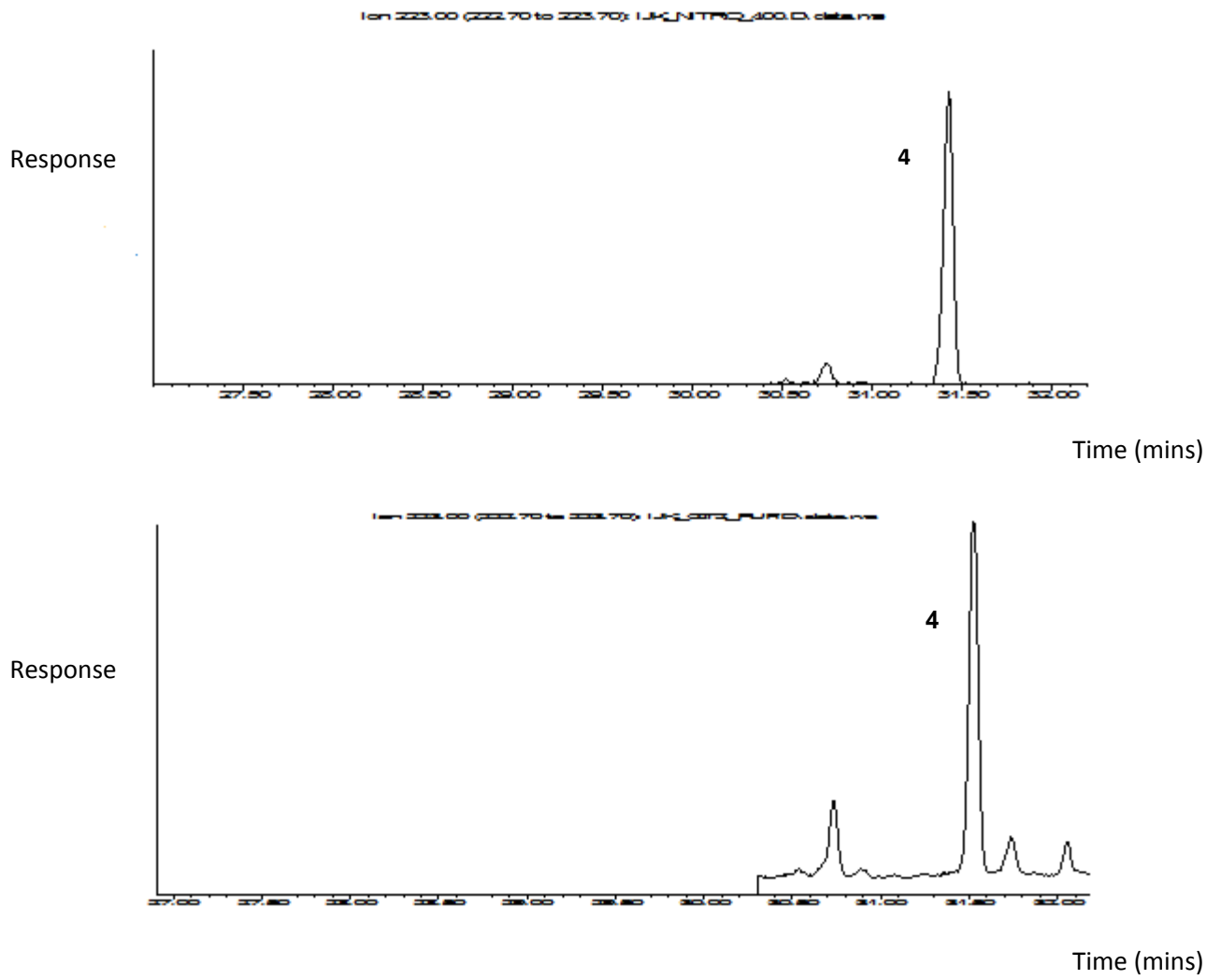


Figure C2n. GC-MS peaks for $M^+ = 223$ in the standard (upper) and sample extract (lower).
4= 9NAnt.

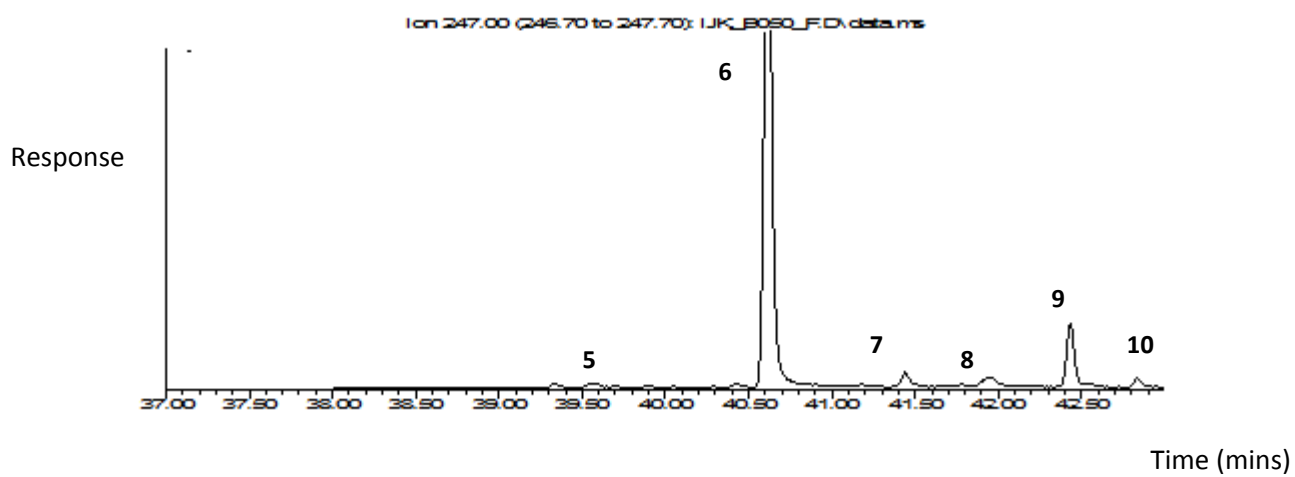
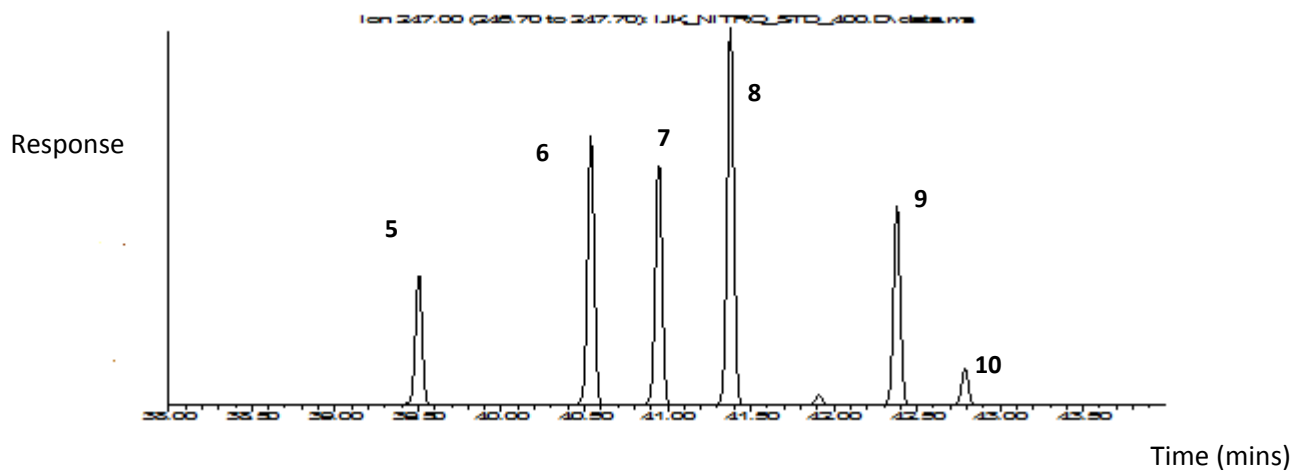


Figure C2o. GC-MS peaks for $M^+ = 247$ in the standard (upper) and sample extract (lower). 5 = 1NFit, 6 = 2NFit, 7 = 3NFit, 8 = 4NPyr, 9 = 1NPyr, 10 = 2NPyr,

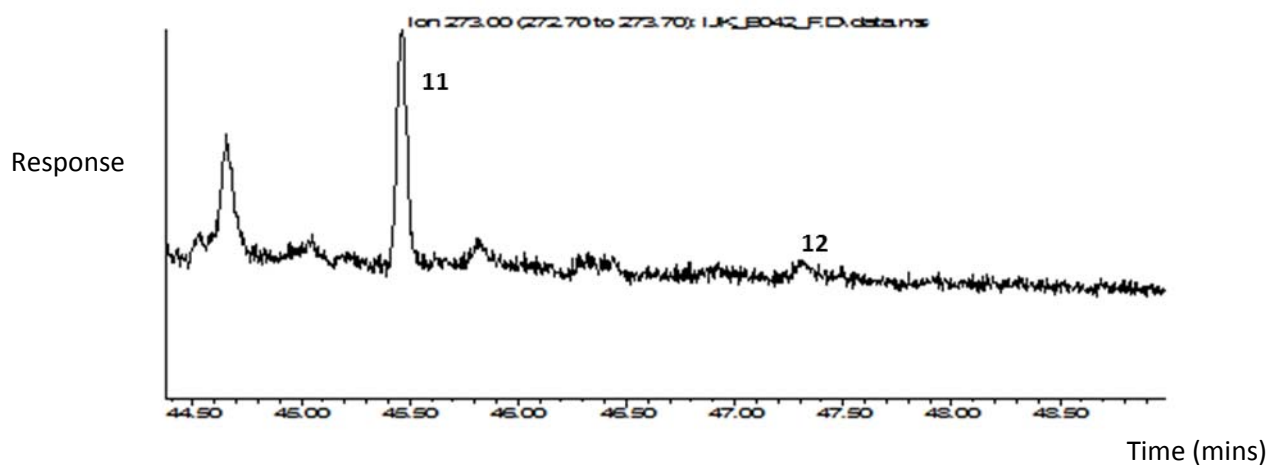
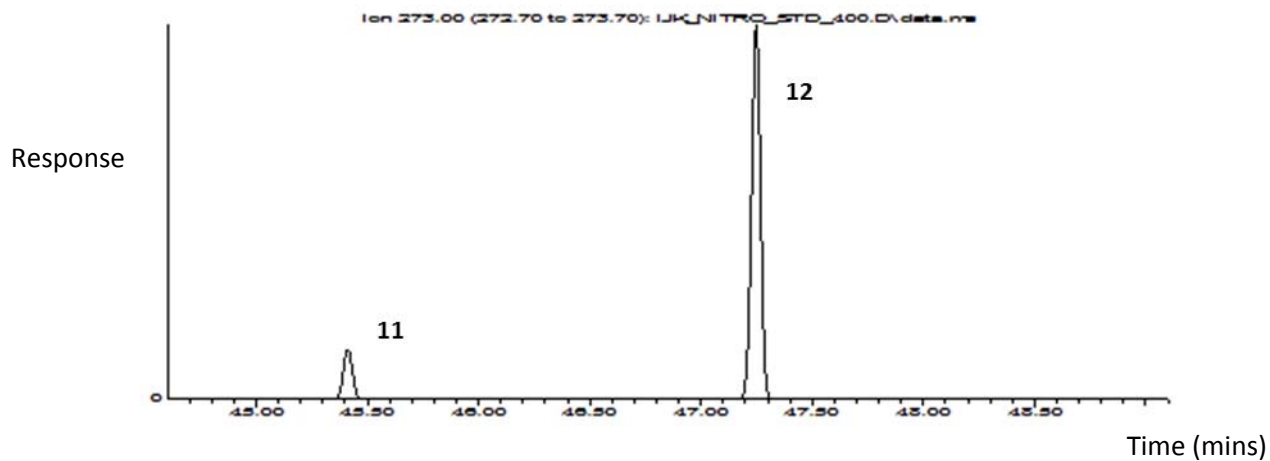


Figure C2p. GC-MS peaks for $M^+ = 273$ in the standard (upper) and sample extract (lower).

11 = 7NBaA, 12 = 6NChr.